



Department of the Army
U.S. Army Corps of Engineers
Washington, DC

Engineer Manual* 1110-2-1914

7 March 2025

CECW-EC

Engineering and Design

Design, Construction, and Maintenance of Relief Wells

FOR THE COMMANDER:

DAMON A. DELAROSA
COL, EN
Chief of Staff

Purpose. This engineer manual covers the design, construction, and maintenance of relief wells, focusing on their use at dams and levees. This manual presents basic principles of implementing relief wells as well as the history of relief wells to enhance understanding of multiple generations of relief well systems. It also covers the analysis of the underseepage conditions and the impact of relief wells on these analyses, reviews risk-informed decision-making for the life cycle of the relief wells, and provides construction and maintenance best practices for relief wells at various points in their life cycle.

Applicability. This manual applies to all Headquarters, United States Army Corps of Engineers commands having responsibilities for the planning, design, analysis, construction, and maintenance of Civil Works projects.

Distribution statement. Approved for public release; distribution is unlimited.

Proponent and exception authority. The proponent of this manual is the Headquarters, United States Army Corps of Engineers, Engineering and Construction Division. The proponent has the authority to approve exceptions or waivers to this manual that are consistent with controlling law and regulations. Only the proponent of a publication or form may modify it by officially revising or rescinding it.

*This manual supersedes EM 1110-2-1914 dated 29 May 1992.

Summary of Change

EM 1110-2-1914

Design, Construction, and Maintenance of Relief Wells

This major revision, dated 7 March 2025, incorporates the following changes:

- All chapters of the new manual were updated to incorporate and discuss current design philosophies and standards for relief wells.
- The following chapters are new and address subject matters that were not previously covered by the manual:
 - Chapter 4 – Risk Considerations for Relief Wells
 - Chapter 9 – Relief Well Pumping Test, Efficiency, and Well Head Loss
- Some equations and methods presented briefly in the original manual were expanded to include a more complete description and moved to the following appendixes:
 - Appendix D – Image Well Theory and Other Analytical Well Solutions.
 - Appendix E – Partial-Penetration Wells and Stratified Aquifers.
- The following appendixes were added to demonstrate use of modern computer software in design and evaluation of relief well systems:
 - Appendix F – 3D Finite Element Modeling of Relief Wells in a Transformed Aquifer.
 - Appendix G – Seepage Analysis Using the Finite Element Method for Relief Wells.
 - Appendix K – Numerical Analyses of Physical Tank Tests.
 - Appendix H - History of Well Factors for an Infinite Line of Partial-Penetration Relief Wells was added to include technical content in support of Chapter 2.
- The following appendixes were added to demonstrate use of content in the manual to both design relief wells and evaluate performance:
 - Appendix I – Example Relief Well Calculations.
 - Appendix J – Application of Pumping Test Data in the Evaluation of Relief Wells.
- Several technical and typographical errors in formulae, a figure, and a table in the existing manual were revised to improve accuracy and usability.
- References were updated.

Contents

Chapter 1 Introduction	1
1-1. Purpose	1
1-2. Distribution statement	1
1-3. References	1
1-4. Records management (recordkeeping) requirements.....	1
1-5. Associated publications	1
1-6. Discussion	1
1-7. Objective and scope	2
1-8. Applicability.....	2
1-9. Project Development Team	2
1-10. General considerations	2
1-11. Applications	3
1-12. Description.....	3
1-13. Relief well components	5
1-14. Definitions	6
1-15. Manual organization	6
Chapter 2 Relief Well History	8
2-1. Introduction	8
2-2. Initial use of relief wells	8
2-3. Relief well research	9
2-4. History of relief well design	11
Chapter 3 General Well System Design Considerations	15
3-1. Relief well application	15
3-2. Collection of relief well discharge.....	19
3-3. Seepage analysis	20
3-4. Site characterization	26
3-5. Relief well penetration.....	33
3-6. Performance monitoring.....	33
Chapter 4 Risk Considerations for Relief Wells	34
4-1. Introduction	34
4-2. Risk assessment methodology	34
4-3. Potential failure modes	35
4-4. Event trees.....	36
4-5. Relief well purpose	39
4-6. Well-specific potential failure modes leading to breach	41
4-7. Evaluation factors	46
4-8. Long-term considerations	48
4-9. Collector system issues	48
4-10. Operation and maintenance considerations.....	48

4-11. Relief well effect on sand boil activity	54
Chapter 5 Analysis and Design of an Infinite Line of Wells	57
5-1. Applicability of method	57
5-2. Analysis parameters	58
5-3. Uplift factors	62
5-4. Conceptual approach	69
5-5. General design approach	70
5-6. Computer programs for well design	71
Chapter 6 Analysis and Design of a Finite Line of Wells	72
6-1. Finite well line conditions	72
6-2. 3D finite-element or finite-difference models	72
6-3. 2D plan view finite element method	74
6-4. Procedure to adjust infinite line solution	76
6-5. Image Well Method	81
Chapter 7 Design of Well Components and Calculation of Head Loss	86
7-1. Well components	86
7-2. Drilled hole	88
7-3. Well diameter	88
7-4. Well materials	88
7-5. Well screen	90
7-6. Filter	94
7-7. Pre-packed well screens	95
7-8. Backfill	95
7-9. Well head loss used in design	97
Chapter 8 Relief Well Installation	111
8-1. General requirements	111
8-2. Drilling plans	111
8-3. Requirements for the well borehole	111
8-4. Drilling methods	111
8-5. Installation of well screen and riser pipe	120
8-6. Development	123
8-7. Sand infiltration testing	127
8-8. Initial pumping test	128
8-9. Backfilling	128
8-10. Disinfection	128
8-11. Video inspection	129
8-12. Records	129
8-13. Abandonment of non-well boreholes	129
8-14. Well abandonment	130
Chapter 9 Well Efficiency, Specific Capacity Ratio, and Relief Well Pumping Tests	131
9-1. Introduction	131

9-2.	Specific capacity	131
9-3.	Well efficiency	132
9-4.	Specific capacity (<i>SC</i>) and efficiency (<i>E</i>)	139
9-5.	Monitoring of well condition	142
9-6.	Pumping test	145
9-7.	Driscoll parameter, <i>Lp</i>	154
9-8.	New relief wells – evaluation of <i>SC</i> and <i>E</i>	154
9-9.	Existing wells – specific capacity and efficiency evaluation	157
Chapter 10 Relief Well Collection Systems		159
10-1.	General	159
10-2.	Passive relief well systems	159
10-3.	Active relief well systems	159
10-4.	Relief well types	159
10-5.	Below-grade discharge	162
10-6.	Relief well collector ditches	162
10-7.	Tailwater	163
10-8.	Relief well housing	163
10-9.	Collector pipes	164
10-10.	Check valves	167
10-11.	Outlet pipe	169
10-12.	Standpipes	169
10-13.	Inspections	169
10-14.	Maintenance	169
10-15.	Ice removal	169
10-16.	Groundwater contamination	170
Chapter 11 Operation and Maintenance for Well Systems		171
11-1.	General maintenance	171
11-2.	Applicable regulations	171
11-3.	Records	171
11-4.	Inspections	171
11-5.	Pump testing of relief wells	173
11-6.	Evaluation	174
11-7.	Causes for decreased well performance over time	177
11-8.	Rehabilitation	179
11-9.	Combined treatment	182
Appendixes		
Appendix A References		187
Appendix B List of Symbols		203
Appendix C Mathematical Analysis of Underseepage and Substratum Pressure		207
Appendix D Image Well Theory and Other Analytical Well Solutions		215

Appendix E Partial-Penetration Wells and Stratified Aquifers	222
Appendix F Three-Dimensional, Finite Element Modeling of Relief Wells in a Transformed Aquifer.....	233
Appendix G Seepage Analysis Using the Finite Element Method for Relief Wells.....	315
Appendix H History of Well Factors for an Infinite Line of Partial-Penetration Relief Wells.....	333
Appendix I Example Relief Well Calculations.....	355
Appendix J Application of Pumping Test Data for Relief Well Evaluation.....	397
Appendix K Numeric Analyses of Physical Tank Tests.....	416

Table List

Table 3–1 Indicators of corrosive and encrusting waters (from U.S. Army 1983).....	26
Table 5–1 Theoretical uplift factor solutions developed by Barron (1978).....	65
Table 7–1 Properties of continuous wire-wrapped stainless-steel screens (Type 304) commonly used in relief wells (based on: https://johnsonscreens.com (2021)).....	91
Table 8–1 Comparison of major drilling methods used for relief wells	114
Table 9–1 Well condition based on well loss coefficient C (after Kasenow 2001 and Walton 1962).....	137
Table 9–2 Efficiency and SCR calculation for four assumed wells, each with different aquifer losses and increasing well losses during subsequent pumping tests (values of sa , sw and st are in feet)	141
Table 9–3 Components of total drawdown of partial-penetration well and efficiency estimation.....	156
Table 11–1 Quantities of various chlorine compounds required to provide as much available chlorine as 1 pound of chlorine gas (Driscoll 1986)	182
Table A–1 Measurement conversion table	202
Table C–1 Factors involved in Blanket Theory seepage analyses	209
Table C–2 Additional factors to include in a Blanket Theory seepage analysis for an infinite line of relief wells	214
Table E–1 Partial-penetration well function, $G(T)$ (Harr 1962)	223
Table E–2 Calculation of effective well penetration for Model B-a in Figure E–4	228
Table E–3 Comparison of results, Blanket Theory, and physical model, Model B-a ...	231
Table F–1 Modeled stratigraphy (Models #1 and #2).....	235
Table F–2 Relief well screen elevations at various penetrations.....	236
Table F–3 Transformed relief well screen elevations	239
Table F–4 Model results of mid-well head and relief well flow.....	241
Table F–5 Mid-well head as percent of net head ($\%H$) and relief well flow results from Technical Memorandum 3-304, Blanket Theory, and Numerical Models #2 and #2a	247

Table F–6 Comparison of mid-well head and relief well flow, Numerical Models #2 and #2a	248
Table F–7 Mid-well head as percent of net head (%H) and relief well flow results from Technical Memorandum 3-304, Blanket Theory, and Numerical Models #2, #2b, #2c, and #2d	249
Table F–8 Comparison of mid-well head and relief well flow, Numerical Models #2, #2b, #2c, and #2d	251
Table F–9 Mid-well head as percent of net head (%H) and relief well flow results from Technical Memorandum 3-304, Blanket Theory, and Numerical Models #1 and #3	254
Table F–10 Comparison of mid-well head and relief well flow, Numerical Models #1 and #3	255
Table F–11 Three-dimensional model simulated relief well flow in gallons per minute 80% versus 100% efficiency.....	258
Table F–12 Mid-well head summary – 80% versus 100% efficiency.....	258
Table F–13 Mid-well head summary – relief wells with and without a 10-foot blank section of screen	260
Table F–14 Relief well flow in gallons per minute; relief wells with and without a 10-foot blank section of screen	261
Table F–15 Defect surface area	263
Table F–16 Defect flow (87-foot well spacing)	264
Table F–17 Horizontal gradient computed over 5 feet from center of defect (87-foot well spacing)	267
Table F–18 Vertical gradient computed across 10-foot depth of defect (87-foot well spacing)	267
Table F–19 Relief well flow in gallons per minute for simulations including a blanket defect (87-foot well spacing).....	267
Table F–20 Defect B flow – 80% versus 100% relief well efficiency (87-foot well spacing)	268
Table F–21 Gradient summary (Defect B) – 80% versus 100% relief well efficiency (87-foot well spacing)	269
Table F–22 Relief well flow in gallons per minute – 80% versus 100% relief well efficiency (87-foot well spacing)	271
Table F–23 Defect B flow – relief wells with and without a 10-foot blank section of screen (87-foot well spacing)	272
Table F–24 Gradient summary (Defect B) – relief wells with and without a 10-foot blank section of screen (87-foot well spacing)	273
Table F–25 Relief well flow in gallons per minute – relief wells with and without a 10-foot blank section of screen (87-foot well spacing)	275
Table F–26 Defect B flow – 261-foot relief well spacing; relief wells with and without a 10-foot blank section of screen	276
Table F–27 Gradient summary (Defect B) – 261-foot relief well spacing; relief wells with and without a 10-foot blank section of screen.....	277
Table F–28 Relief well flow in gallons per minute – 261-foot relief well spacing; relief wells with and without a 10-foot blank section of screen	279

Table F–29 Transformed relief well screen elevations	280
Table F–30 Mid-well head in feet	281
Table F–31 Mid-well head in percent of net head ($%H$)	281
Table F–32 Relief well flow in gallons per minute	283
Table F–33 Summary of numerical model features.....	285
Table F–34 Flow and gradient for Case 2c with 261-foot relief well spacing and a sand boil at defect location “B”	291
Table F–35 Comparison of Blanket Theory, Physical Model, 2D, and 3D model results	292
Table F–36 Summary of mid-well head results in percent of net head ($%H$).....	310
Table F–37 Summary of mid-well head results in feet.....	311
Table F–38 Difference between numerical model and Blanket Theory calculated mid-well heads (in feet)	312
Table F–39 Summary of relief well flow results in gallons per minute	313
Table F–40 Percent difference between numerical model and Blanket Theory calculated relief well flow.....	314
Table G–1 Results of generalized levee comparison	325
Table G–2 Flow passing the well line comparison	326
Table H–1 Modern notation for relief well design equations.....	347
Table I–1 Observed piezometer readings compared with prediction using the Image Well Method with Blanket Theory adaptation	364
Table I–2 Saturated permeability values for general levee example	370
Table I–3 Example calculations for $FSvg$	372
Table I–4 Iterative relief well head loss calculations with 150-foot well spacing.....	375
Table I–5 Blanket theory parameters and results without wells.....	379
Table I–6 Blanket theory parameters and results with an infinite line of wells every 150 feet.....	379
Table I–7 Blanket theory parameters and results for Case 3 with an infinite line of wells every 170 feet	379
Table I–8 Blanket Theory parameters and results from Huntington District spreadsheet with no wells – Huntington District spreadsheet	382
Table I–9 Blanket Theory parameters and results with wells and no well losses (150-foot spacing) – Huntington District spreadsheet	382
Table I–10 Blanket Theory parameters and results with wells and well losses (150-foot spacing) – Huntington District spreadsheet.....	382
Table I–11 Blanket theory parameters and results with an infinite line of wells every 150 feet and well factors based on a transformed aquifer thickness of $D = 342$ feet.....	386
Table I–12 Blanket theory parameters and results with an infinite line of wells every 150 feet with a transformed aquifer thickness of $D = 342$ feet and $Hw = 0$	386
Table I–13 Interpolation of Chapter 6 figures to determine theta values for five wells	387
Table I–14 Interpolation of Chapter 6 figures to determine theta values for 20 wells ..	387
Table I–15 Results with five wells at 170-foot spacing for Case 3.....	388

Table I–16 Results with 20 wells at 170-foot spacing for Case 3	388
Table I–17 Image Well Method with Blanket Theory adaptation analysis results for 5-well and 20-well systems with 170-foot spacing for 100% and 61.6% penetration	394
Table J–1 Levee District No. 1 constant rate pumping test results.....	399
Table J–2 Levee District No. 1 step-drawdown pumping test data.....	402
Table J–3 Relation of well loss coefficient to well condition (from Kasenow 2001)	404
Table J–4 Distance-drawdown measurements: Relief Well 1	408
Table J–5 Summary of factors of safety (Example 5).....	411
Table J–6 Summary of factors of safety (Example 6).....	413

Figure List

Figure 1–1. Typical relief well.....	4
Figure 1–2. Typical line of relief wells at the toe of a dam or levee	5
Figure 1–3. Line of wells at Upper Wood River Levee District (USACE 1956b).....	5
Figure 2–1. Electrical analogy (USACE 1939b)	9
Figure 2–2. Foundation profile with intermediate silty sand stratum (USACE 2002)	13
Figure 3–1. Illustration of excess head: the top diagram shows the landside ground surface as the base elevation for measuring head; the bottom diagram shows tailwater as the base elevation	16
Figure 3–2. Illustration of aquifer transmissivity for a stratified foundation	18
Figure 3–3. Example of sand boil, East St. Louis, 2016 New Year’s Day flood.....	19
Figure 3–4. Profile of typical design reaches for relief well analysis (from EM 1110- 2-1901).....	21
Figure 3–5. Projection of observed piezometer levels to design pool for successive high-pool events for Piezometer 32-1. Piezometric head increases with time are a result of relief well biofouling. Perry Dam, Kansas City District.....	22
Figure 3–6. Evaluation of 2010 high pool piezometric levels for seepage vertical gradient safety factor, stations 27+00 to 31+00 (exaggerated scale); Perry Dam, Kansas City District	23
Figure 3–7. Relief well pump test data, combined with geologic information, along a levee profile.....	24
Figure 3–8. Graphical depiction of how localized topographical defects, or low areas, are typically accounted for in 2D analysis	28
Figure 3–9. Permeability and effective grain size of individual sand strata, example from Well FC-105	29
Figure 3–10. Seepage through point bar deposits	30
Figure 4–1. Internal erosion of the levee foundation materials due to underseepage (adapted from van Beek et al. 2010).....	35
Figure 4–2. Backward erosion failure mode event tree (USBR and USACE 2019).....	38
Figure 4–3. Event tree for potential failure mode-1, relief well collapse	45
Figure 4–4. Location of Harrisonville example levee reach	51
Figure 4–5. Comparison of extrapolated piezometer readings with design factor of safety values	52

Figure 4–6. Comparison of measured well flow with design and pumping test data	52
Figure 4–7. Harrisonville example combining geomorphology, design, and performance information	53
Figure 4–8. Cross section from Technical Memorandum 3-304 used in WASH123D model (USACE 1949).....	55
Figure 4–9. Adaptive meshing to represent backward erosion piping in the plan view with and without wells (adapted from Robbins and Griffiths 2022).....	56
Figure 5–1. Infinite artesian relief well line (located along landward levee toe) with design notation and parameters: conceptual plan view (a), section X-X' (b), and section Y-Y' (c).....	61
Figure 5–2. General plan view flow nets of a full-penetration infinite well line (top) and a full-penetration drainage slot (bottom); flow is from a line source located a distance S from the well or drainage slot (also Figure G–1 in Appendix G)	63
Figure 5–3. Cross-sectional view of a flow net to a partial-penetration drainage slot....	64
Figure 5–4. Nomogram for determining values of average and mid-well uplift factors (USACE 1955; Bennett and Barron 1957).....	66
Figure 5–5. Relief well design nomogram for average (a) and mid-well (b) uplift factor values (Keffer and Guy 2022)	67
Figure 5–6. Relief well design nomogram for providing landward uplift factor values at $x3a = 5$ (a) and $x3a = 50$ (b) (Keffer and Guy 2022)	68
Figure 6–1. An area of seepage concern in Upper Wood River (USACE 2016)	73
Figure 6–2. A WASH123D model including relief wells and cutoff (USACE 2016); black and red dots indicate existing and proposed new wells, respectively	74
Figure 6–3. Plan view of typical finite element analyses and measurement locations, infinite well lines (a) and finite lines with 2 (b), 4 (c), and 10 (d) wells ($a/rw = 100$, $D/a = 1$, $W/D = 100\%$) (Keffer et al. 2023)	75
Figure 6–4. Profile of excess head along the well lines of various lengths from Figure 6–3 (a, section A-A'), and perpendicular to the middle (b, section B-B') and end (c, section C-C') (Keffer et al. 2023).....	76
Figure 6–5. θmm for finite well lines for the infinite line cases when $\theta m = 0.29$ (a), 1.92 (b), and 3.49 (c) (Keffer et al. 2023)	78
Figure 6–6. θme for finite well lines for the infinite line cases when $\theta m = 0.29$ (a), 1.92 (b), and 3.49 (c) (Keffer et al. 2023)	79
Figure 6–7. θdm for finite well lines for the infinite line cases when $\theta av = 0.18$ (a), 1.93 (b), and 3.84 (c) (Keffer et al. 2023)	80
Figure 6–8. θde for finite well lines for the infinite line cases when $\theta av = 0.18$ (a), 1.93 (b), and 3.84 (c) (Keffer et al. 2023)	81
Figure 6–9. Hydraulic grade line (HGL) used in Image Well Method with Blanket Theory adaptation	83
Figure 7–1. Typical relief well installation	87
Figure 7–2. Typical design of a well-graded filter and slot size for relief well	93
Figure 7–3. Typical below-grade discharge well detail with filter pack monitoring tubes, Kansas City District	97

Figure 7–4. Trends in entrance velocity with variation in flow rate, screen diameter, slot size, and degree of screen obstruction; calculated values are based on a full-penetration well	99
Figure 7–5. Entrance losses versus inflow for 8-inch inner diameter, slotted-wood well screens in St. Louis (after USACE 1972); best-fit equations shown for the newly constructed well entrance losses for inflow per foot of screen	101
Figure 7–6. Friction head losses in screen and riser sections.....	102
Figure 7–7. Discharge curves for measurement of flow from vertical standard pipes and calculated velocity head; the curves are based on data from experiments by Lawrence and Braunworth in 1906 (USBR 2001).....	103
Figure 7–8. Diagram of well, inflow through screen, well flow in screen, and definition of head losses (from USACE 1952).....	105
Figure 7–9. Head loss in wells for both pumping and natural flow conditions (from USACE 1952).....	106
Figure 7–10. Components of head loss for a 6-inch diameter relief well.....	107
Figure 7–11. Components of head loss for an 8-inch diameter relief well.....	108
Figure 7–12. Components of head loss for a 10-inch diameter relief well.....	109
Figure 7–13. Components of head loss for a 12-inch diameter relief well.....	110
Figure 8–1. Schematic diagram of circulatory system (after EM 1110-2-1913); an excavated pit may be used for a fluid reservoir in place of an above-ground tub (see text)	115
Figure 8–2. Side (top) and top (bottom) views of centralizer/tremie guide	122
Figure 8–3. Surge block used to mechanically develop wells	124
Figure 8–4. Schematic of four-nozzle jetting tool	126
Figure 8–5. Well development by high-velocity jetting	127
Figure 9–1. Components of head loss in a pumped well (adapted from Driscoll 1986).....	135
Figure 9–2. Plot of specific drawdown versus pumping rate from step-drawdown data (modified from Guy et al. 2014, RW-85 before and after rehabilitation).	137
Figure 9–3. Partial-penetration flow path convergence (after Houben 2015)	138
Figure 9–4. Efficiency and SCR comparison for hypothetical wells with assumed constant aquifer losses and increasing well losses with time.....	142
Figure 9–5. Example well performance loss with observed performance during floods, Harrisonville Levee	144
Figure 9–6. Example of effect of underdevelopment on specific capacity over time; Wilson Dam (Kansas City District) Relief Well 6A	145
Figure 9–7. Typical drawdown and recovery curves of a pumped well and then allowed to rebound (after U.S. Army 1983)	150
Figure 9–8. Step-drawdown test results: before and after rehabilitation of 3-inch diameter perforated well.....	151
Figure 9–9. Transmissivity estimation from constant rate data using Jacobs method (modified from Kyle 2015)	153
Figure 9–10. Transmissivity and storativity estimation from distance-drawdown test with flow rate of 25 gallons per minute (modified from Kyle 2015)	153

Figure 9–11. An example application of the straight-line method of Cooper and Jacob (1946) and Jacob (1950) to <i>SC</i> data. A value of $\Delta st - t$ is determined from the graph and <i>T</i> is then calculated from equation 9–13 (Sid Simpson Flood Protection Project, Beardstown, Illinois)	155
Figure 9–12. Distance versus drawdown plot from a test well.....	157
Figure 10–1. D-type relief well reach (photo courtesy of Memphis District).....	160
Figure 10–2. Typical relief well components for (a) D-type and (b) T-type	161
Figure 10–3. T-type relief well (South River Drainage District) (photo courtesy of Rock Island District)	162
Figure 10–4. Example of backup water in the housing (left) and full outlet pipe (right).....	163
Figure 10–5. Example of relief well collector pipe system	166
Figure 10–6. Typical detail of well top and check valve for D-type well.....	168
Figure 10–7. Detail of well top, check valve, and outlet for navigation lock application (from Lock and Dam No. 18, USACE Rock Island District)	168
Figure 11–1. Example images from video inspections performed on RW 68A, Milford Dam, Junction City, Kansas. Both images are from the location of the same screen-riser joint. The 2011 image (left) was obtained immediately after well rejuvenation, as indicated by a visibly clean screen. The 2020 image (right) was obtained prior to well rejuvenation, and shows the well screen blocked by biofouling.....	176
Figure 11–2. BCHTTM setup at a USACE project; major system components shown consist of heating units (a), water tank (b), boom (c), and acid (d) (North Branch Kokosing River Lake 2019)	186
Figure C–1. Illustration of symbols used in Appendix C	208
Figure C–2. The eight cases covered by the Blanket Theory	211
Figure C–3. Illustration of change in pressure due to line of relief wells	213
Figure D–1. Artesian flow to a single well with a circular source	216
Figure D–2. Artesian flow to multiple wells with a circular source (adapted from U.S. Army 1983).....	217
Figure D–3. Artesian flow to a single well with a finite line source	218
Figure D–4. Artesian flow to a single well with an infinite line source and variables to calculate head at point of interest, <i>P</i>	219
Figure D–5. Artesian flow to multiple wells with an infinite line source with variables shown for calculating head at point of interest, <i>P</i>	220
Figure E–1. Flow to partial-penetration well (<i>W/D</i> versus <i>Gp</i>) with circular source (after Harr 1962).....	223
Figure E–2. Comparison of actual and effective well penetration.....	224
Figure E–3. Schematic of physical model test with a uniform sand aquifer.....	226
Figure E–4. Schematic of physical model test with a stratified sand aquifer	226
Figure E–5. Effective and actual well penetration versus observed pressure relief for Model A-a-1 and B-a (from Technical Memorandum 3-304).....	230
Figure E–6. Blanket Theory input parameters for the 10^{-10} cm/second blanket condition.....	230

Figure E–7. Comparison of mid-well head, Blanket Theory versus physical model, Model B-a.....	232
Figure F–1. Model cross sections; (a) schematic of physical model B-a from Technical Memorandum 3-304 (USACE 1949) and (b) cross section of WASH123D numerical seepage model.....	234
Figure F–2. Plan view of numerical model; (a) 29-foot well spacing, (b) 58-foot well spacing, (c) 87-foot well spacing, and (d) 174-foot well spacing	235
Figure F–3. Modeled relief well penetration	236
Figure F–4. Numerical Model #1 computational mesh, plan view	237
Figure F–5. Numerical Model #2 and Model #3 computational mesh, plan view.....	237
Figure F–6. Cross-sectional view of transformed aquifer model; vertical magnification = 4x horizontal.....	238
Figure F–7. Comparison of mid-well head from the physical model, Blanket Theory, and Model #1	242
Figure F–8. Comparison of mid-well head from the physical model, Blanket Theory, and Model #1	242
Figure F–9. Comparison of equipotential lines in percent of net head from Physical Model B-a (USACE 1949, Figure 30) and Numerical Model #1 for 29-foot well spacing and (a) 100% well penetration or (b) 25% penetration.....	244
Figure F–10. Plan view of total head contours at the top of the fine sand aquifer for full-penetration wells every 174 feet. The top image shows results from Model #1 (downstream boundary located 400 feet from relief wells), and the bottom image shows results from Model #2 (downstream boundary located 4,800 feet from relief wells)	245
Figure F–11. Plan view of total head contours at the top of the fine sand aquifer for relief wells every 29 feet penetrating 10% (2.5% effective) of the aquifer. The top image shows results from Model #1 (downstream boundary located 400 feet from relief wells), and the bottom image shows results from Model #2 (downstream boundary located 4,800 feet from relief wells)	245
Figure F–12. Comparison of mid-well head from the physical model, Blanket Theory, and Model #3	256
Figure F–13. Comparison of relief well flow from the physical model, Blanket Theory, and Model #3	257
Figure F–14. Head computed mid-way between relief wells for 80% and 100% efficiency	259
Figure F–15. Screen intervals with a 10-foot blank section at top of fine sand for penetrations of 25, 50, 70 and 100%	260
Figure F–16. Head computed mid-way between wells at the top of the aquifer/base of the blanket; relief wells with and without a 10-foot blank section of screen are compared.....	261
Figure F–17. Relief well flow with and without a 10-foot blank section of screen	262
Figure F–18. Blanket defect model setup (full model domain not pictured).....	263
Figure F–19. Flow from defects to ground surface in (a) gallons per minute and (b) gallons per minute per square foot (87-foot well spacing).....	265

Figure F–20. Horizontal gradients computed from the center of each defect (87-foot well spacing)	266
Figure F–21. Defect B flow – 80% efficiency versus 100% efficiency (87-foot well spacing)	268
Figure F–22. Gradient summary (Defect B) – 80% well efficiency (87-foot well spacing): (a) horizontal gradient computed 5 feet from center of Defect B and vertical gradients across the defect, and (b) horizontal gradient computed from center of Defect B for simulations assuming relief well efficiency of 80% ...	270
Figure F–23. Relief well flow – 80% versus 100% relief well efficiency (87-foot well spacing)	271
Figure F–24. Defect flow (location B) – relief wells with and without a 10-foot blank section of screen (87-foot well spacing)	272
Figure F–25. Gradient summary (Defect B) – relief wells with 10-foot blank section of screen (87-foot well screen): (a) horizontal gradient computed 5 feet from center of Defect B and vertical gradients across the defect, (b) horizontal gradient computed from center of Defect B for simulations including 10-foot blank section of screen	274
Figure F–26. Relief well flow – relief wells with and without a 10-foot blank section of screen (87-foot well spacing)	275
Figure F–27. Defect B flow – 261-foot relief well spacing.....	276
Figure F–28. Gradient summary – 261-foot relief well spacing: (a) horizontal gradient computed 5 feet from center of Defect B and vertical gradients across the defect; (b) horizontal gradient computed from center of Defect B, relief wells every 261 feet, no blank section of screen; and (c) horizontal gradient computed from center of Defect B, relief wells every 261 feet, blank section at top 10 feet of relief well screens	278
Figure F–29. Relief well flow – 261-foot well spacing.....	279
Figure F–30. Comparison of mid-well head calculated by the numerical model and Blanket Theory for an anisotropic aquifer: (a) results from Model #2, and (b) results from Model #2b.....	282
Figure F–31. Comparison of relief well flow calculated by the numerical model and Blanket Theory for an anisotropic aquifer: (a) results from Model #2, and (b) results from Model #2b.....	284
Figure F–32. Total head beneath the landside blanket without wells	288
Figure F–33. Model #1 total head results, top of fine sand 100% relief well penetration (100% effective)	293
Figure F–34. Model #1 total head results, cross section through center relief well, 100% relief well penetration (100% effective)	294
Figure F–35. Model #1 total head results, cross section through relief well line, 100% relief well penetration (100% effective)	295
Figure F–36. Model #1 total head results contoured from 410 feet to 416.5 feet, cross section through relief well line, 100% relief well penetration (100% effective)	296
Figure F–37. Model #1 total head results, top of fine sand, 70% relief well penetration (51% effective)	297

Figure F–38. Model #1 total head results, cross section through center relief well, 70% relief well penetration (51% effective)	298
Figure F–39. Model #1 total head results, cross section through relief well line, 70% relief well penetration (51% effective)	299
Figure F–40. Model #1 total head results contoured from 410 feet to 420 feet, cross section through relief well line, 70% relief well penetration (51% effective)	300
Figure F–41. Model #1 total head results, top of fine sand, 50% relief well penetration (19% effective)	301
Figure F–42. Model #1 total head results, cross section through center relief well, 50% relief well penetration (19% effective)	302
Figure F–43. Model #1 total head results, cross section through relief well line, 50% relief well penetration (19% effective)	303
Figure F–44. Model #1 total head results, top of fine sand, 25% relief well penetration (6.2% effective)	304
Figure F–45. Model #1 total head results, cross section through center relief well, 25% relief well penetration (6.2% effective)	305
Figure F–46. Model #1 total head results, cross section through relief well line, 25% relief well penetration (6.2% effective)	306
Figure F–47. Model #1 total head results, top of fine sand, 10% relief well penetration (2.5% effective)	307
Figure F–48. Model #1 total head results, cross section through center relief well, 10% relief well penetration (2.5% effective)	308
Figure F–49. Model #1 total head results, cross section through relief well line, 10% relief well penetration (2.5% effective)	309
Figure G–1. General plan view flow net of a full-penetration infinite well line and a full-penetration drainage slot; flow is from a line source located a distance L from the well or drainage slot	317
Figure G–2. General total head profile along the well line at the base of an impervious blanket; $h\Delta M$, $h\Delta L$, and hw are shown to demonstrate the comparison between the variables.....	319
Figure G–3. Generalized levee; seepage analysis cross section (not to scale). Ground surface elevation is assumed to be Elevation 0.	324
Figure G–4. Generalized levee; plan view analysis section (not to scale).....	325
Figure G–5. Total head at the case of the impervious blanket for line perpendicular to the well line through the well	327
Figure G–6. Total head at the base of the impervious blanket for line perpendicular to the well line through the midpoint between wells	328
Figure G–7. Total head at the case of the impervious blanket along well for a finite well line and an infinite well line	329
Figure G–8. Well flows for a finite and an infinite well line.....	330
Figure H–1. Relief well design nomogram from Middlebrooks and Jervis (1947).....	335
Figure H–2. Drawdown for well between infinite line source and downstream sink (after Barron 1948).....	336

Figure H–3. Infinite line of full-penetration wells, combined gravity, and artesian flow.....	337
Figure H–4. Relief well design nomogram from USACE (1955).....	338
Figure H–5. Theoretical values of average uplift factor (after Barron 1978–1982).....	340
Figure H–6. Theoretical values of mid-well uplift factor (after Barron 1978–1982).....	341
Figure H–7. Well factor determined from various methods (figure adapted from Keffer et al. 2019).....	342
Figure H–8. Ratio of head midway between relief wells at center of a finite well system to head midway between wells in an infinite system (after USACE 1956a).....	344
Figure H–9. Example uplift factor solutions (for $W/D = 50\%$ and different D/a values) using the USACE design nomogram.....	351
Figure H–10. Comparison of uplift factor solutions from the Sharma analytical approach and the USACE nomogram (Figure H–9).....	352
Figure H–11. Uplift factor solutions obtained using the Sharma analytical approach for the full range of the USACE design nomogram (Figure H–9) input parameters.....	353
Figure I–1. Design data and calculations for first iteration of relief well example.....	357
Figure I–2. Hm for each well reach compared with original design and field measurement.....	360
Figure I–3. Qw compared with original design and field measurement.....	361
Figure I–4. Qw factored for performance loss (80%) compared with original design and field measurement (Note: Reaches 2 and 5 have no well flow information).....	362
Figure I–5. Example of Image Well Method compared with Infinite Well Approach (Chapter 5).....	363
Figure I–6. Generalized levee cross section (adapted from USACE 1956a as shown in Manseur et al. (2000)).....	365
Figure I–7. Comparison of vertical gradient through a landside confining layer with observed performance (adapted from USACE 1956a).....	366
Figure I–8. SeepW model based on cross section in Figure I–6.....	369
Figure I–9. Output total head contours, flow, and the excess head and gradient at location where $FSvg$ is measured.....	371
Figure I–10. Landside levee toe and points used to assess various measures of vertical gradient and to calculate vertical gradient factors of safety.....	371
Figure I–11. $FSvg$ versus relief well spacing to achieve target value of $FSvg = 1.6$...	376
Figure I–12. Total head pressure contours, total flow, well flow, and flow lines for the case with a line of relief wells at 150-foot spacing.....	376
Figure I–13. Screen shot of input in Huntington District spreadsheet for Case 3.....	380
Figure I–14. Screenshot of output in Huntington District spreadsheet for Case 3.....	383
Figure I–15a. Image Well Method with Blanket Theory adaptation inputs for analysis, results for well flow, and results for heads around five-well system with well spacing of 170 feet, partial-penetration wells.....	390

Figure I–15b. Image Well Method with Blanket Theory adaptation inputs for analysis, results for well flow, and results for heads around five-well system with well spacing of 170 feet, partial-penetration wells.....	391
Figure I–16. Calculation tables to support results shown in Figure I–15 (a and b)	392
Figure I–17. Image Well Method with Blanket Theory adaptation analysis results for heads around 20-well system with well spacing of 170 feet, partial-penetration (61.6%) wells.....	393
Figure I–18. Boundaries used in plan view model of the generalized levee cross section.....	394
Figure I–19. Total head contours in a plan view model of the generalized levee cross section	395
Figure I–20. Total head determined from node midway between wells.....	395
Figure I–21. Flux through a boundary used to determine flow to the well	396
Figure J–1. Illustration of specific capacity variables.....	398
Figure J–2. Illustration of variables for step-drawdown testing.....	400
Figure J–3. Simplified head loss components	401
Figure J–4. Example step-drawdown base data	402
Figure J–5. Example step-drawdown base data with <i>B-C</i> relationship trendline	403
Figure J–6. Typical cross section for Example 3	406
Figure J–7. Illustration of distance-drawdown method	408
Figure J–8. Distance-drawdown plot	409
Figure J–9. Typical cross section – Upper Mississippi levee example	410
Figure J–10. Factor of safety (heave) versus well efficiency (Example 5).....	411
Figure J–11. South Beardstown typical section.....	412
Figure J–12. Factor of safety (vertical gradient) versus well efficiency (Example 6) ...	413
Figure K–1. Tank used for relief well tests per Technical Memorandum TM 3-341 (USACE 1952)	418
Figure K–2. Tank used for relief well tests per Technical Memorandum TM 3-341 (USACE 1952)	418
Figure K–3. Testing apparatus (Mitronovas 1968)	419
Figure K–4. Testing apparatus showing piezometer elevations (Hadj-Hamou et al. 1990).....	420
Figure K–5. Plan view of Mitronovas (1968) model used in the finite element model .	422
Figure K–6. Axisymmetric view of Mitronovas (1968) model used in the finite element model.....	422
Figure K–7. Axisymmetric model mesh for Mitronovas (1968)	423
Figure K–8. Axisymmetric model results for Mitronovas (1968)	424
Figure K–9. Input and output of simple plan view model of Mitronovas (1968) Test 1	425
Figure K–10. SeepW results for the Mitronovas (1968) test plotted with lab results ...	426
Figure K–11. SeepW results for the Hadj-Hamou et al. (1990) test plotted with lab results	427
Figure K–12. Axisymmetric SeepW model with discrete slots through a low permeability screen	428

Figure K–13. Axisymmetric SeepW model with discrete slots through a low permeability screen, increased detail	429
Figure K–14. Nodal velocity measured along five vertical lines outside of screen slot	429
Figure K–15. Approximation for estimating reduction in permeability for turbulent flow (adapted from EM 1110-2-1901).....	430
Figure K–16. Nodal gradient measured along five vertical lines outside of screen slot	431
Figure K–17. Approximate reduction in permeability for turbulent flow (from EM 1110-2-1901).....	431
Figure K–18. Screen included in the model as a no-flow boundary, with free-drainage boundaries at every slot	432
Figure K–19. Separate regions created along contours of high x-y gradient.....	433
Figure K–20. Lower permeability assigned to regions around one of the slots	433

Glossary of Terms

Chapter 1 Introduction

1-1. Purpose

This engineer manual covers the design, construction, and maintenance of relief wells, focusing on their use at dams and levees. This manual presents basic principles of implementing relief wells as well as the history of relief wells to enhance understanding of multiple generations of relief well systems. It also covers the analysis of the underseepage conditions and the impact of relief wells on these analyses, reviews risk-informed decision-making for the life cycle of the relief wells, and provides construction and maintenance best practices for relief wells at various points in their life cycle.

1-2. Distribution statement

Approved for public release; distribution is unlimited.

1-3. References

See Appendix A.

1-4. Records management (recordkeeping) requirements

The records management requirement for all record numbers, associated forms, and reports required by this publication are addressed in the Army Records Retention Schedule. Detailed information for all related record numbers is located on the U.S. Army Corps of Engineers (USACE) Records Management Site <https://usace.dps.mil/sites/INTRA-CIOG6/SitePages/Records-Management.aspx>. If any record numbers, forms, and reports are not current, addressed, and/or published correctly, see DA Pam 25-403 for guidance. Specific records requirements are described in paragraphs 8-12 and 11-3.

1-5. Associated publications

Policy and/or procedures associated with this manual are found in ER 1110-2-1942, which describes the inspection, monitoring, and maintenance of relief wells; ER 1110-2-1156, which describes continuing evaluation inspections for USACE dams; and EC 1165-2-218 or its successor regulation, which describes evaluations and inspections at USACE levees.

1-6. Discussion

This manual updates EM 1110-2-1914, dated 29 May 1992, and is intended for designers and operators of relief wells. Relief wells, as used in this manual, are vertical wells installed to reduce pore-water pressure in dam and levee embankments and foundation strata. Without an avenue of release, this pressure can cause surface

saturation, pin boils, heave and uplift, material transport, internal erosion, and potential failure. Relief wells are typically placed on the downstream toe of a dam or levee or adjacent to hydraulic structures.

1-7. Objective and scope

This manual provides guidance and information on the design, construction, and maintenance of pressure relief wells. It focuses on wells installed to relieve subsurface hydrostatic pressures that may develop in the pervious foundations of dams, levees, and hydraulic structures.

1-8. Applicability

This manual is applicable to all USACE Divisions and Districts responsible for seepage control at dams, levees, and hydraulic structures.

1-9. Project Development Team

The Project Development Team (PDT) responsible for this manual includes USACE engineers, geologists, and modelers drawn mainly from the Mississippi River, Northwestern, Great Lakes, and Ohio River Divisions. These divisions include the Mississippi, Ohio, and Missouri River valleys where the majority of USACE relief wells are located. Additional PDT and Agency Technical Review (ATR) members belong to the North Atlantic, South Pacific, Southwest, and Pacific Ocean Divisions.

1-10. General considerations

All water retention structures are subject to seepage through their foundations and abutments. In many cases, seepage coincides with excess hydrostatic or uplift pressures beneath elements of the structure or landward strata. Relief wells are designed to reduce foundation pressures to a safe level, preventing the movement of foundation materials. Controlled seepage release prevents the buildup of pressures that might otherwise endanger the stability of the structure.

a. Performance monitoring. Relief wells require a minimum amount of real estate compared with other measures such as seepage berms. Unlike seepage berms, however, wells require periodic maintenance to prevent a decrease in performance over time. These decreases can be due to clogging of well screens by muddy surface waters, bacterial growth, or mineral encrustation. Eventually, relief wells may need to be replaced if their performance cannot be maintained above threshold levels. The proper design, installation, and maintenance of relief wells are essential elements in ensuring their effectiveness and the integrity of the protected feature. Adequate systems of piezometers and flow-measuring devices must be installed according to EM 1110-2-1908 to monitor the performance of relief well systems.

b. Seepage collection. Relief wells divert underseepage to near-surface locations where it must be collected and disposed (Turnbull and Mansur 1954). Collection

systems convey seepage away from the area of concern and safely discharge it to storm sewers or surface water bodies.

1–11. Applications

a. Pressure reduction. Relief wells are used extensively to relieve excess hydrostatic pressures in pervious foundation strata covered by more impervious top strata. These conditions often exist landward of levees and downstream of dams. Pressure relief wells have also been used beneath the stilling basins of spillways, outlet channels of dams and navigation locks, and other hydraulic structures. Often, wells incorporated in structures rely on a system of collector pipes and manholes to safely discharge seepage volumes. Unlike relief well systems in embankments, these systems are often placed in locations not readily accessible under normal conditions. Thus, inspection, cleaning, and maintenance cannot be performed unless the structures are dewatered.

b. Seepage control. Relief well systems are flexible as a seepage control measure. Additional wells can easily be added if the initial system is not adequate or if conditions change. If needed, the discharge rate from individual wells can be increased by pumping to further reduce pore pressures. Other underseepage control measures can be used in conjunction with relief wells. These include upstream blankets, downstream seepage berms, and cut-off walls to help control the seepage flow path and prevent uplift.

1–12. Description

Typical relief wells consist of a screen surrounded by a compatible aggregate filter material to prevent migration of foundation materials into the well. The well screens can be placed at varying depths to encompass permeable layers as determined by exploratory borings. Relief wells are typically sized to accommodate the maximum design flow without excessive head loss. A typical relief well is shown in Figure 1–1. Wells can be singular or designed as a system to ensure pressure relief is obtained where needed. A schematic of a series of wells installed in a line along the landside toe of a levee or dam is shown in Figure 1–2. Figure 1–3 is a photo taken during construction at Upper Wood River Levee and is typical of how a line of relief wells housings appear in the field.

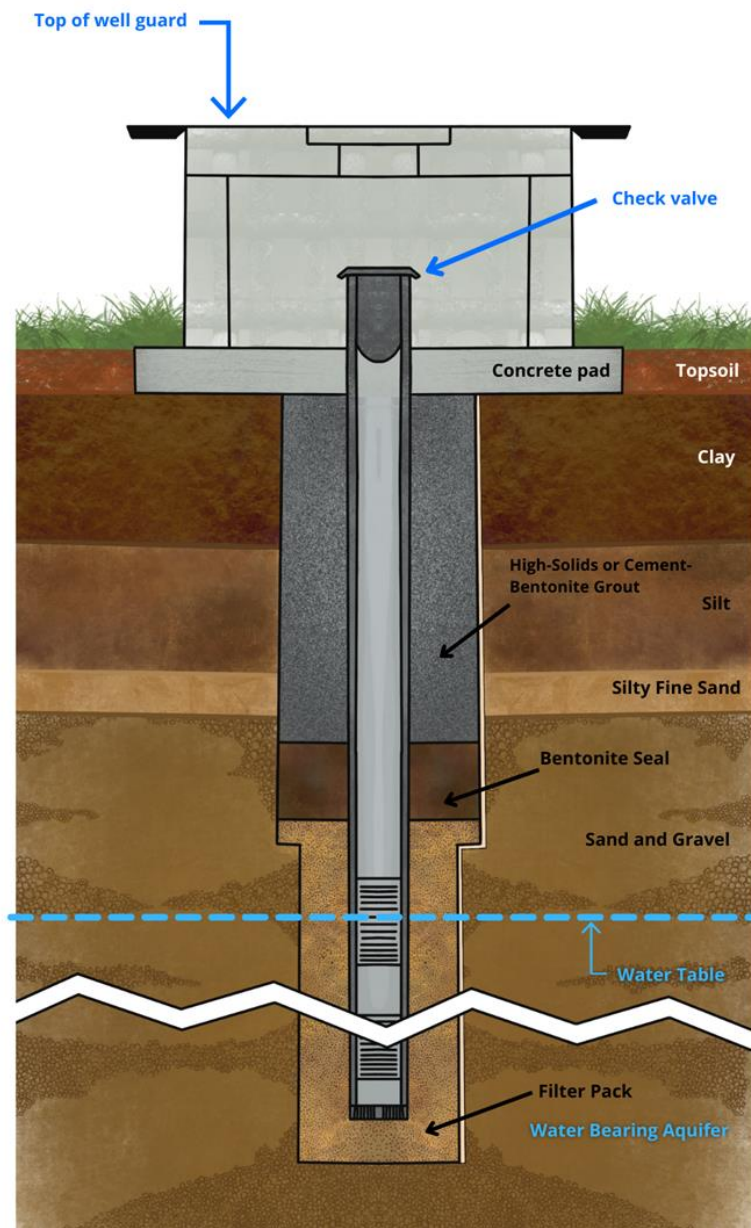


Figure 1-1. Typical relief well

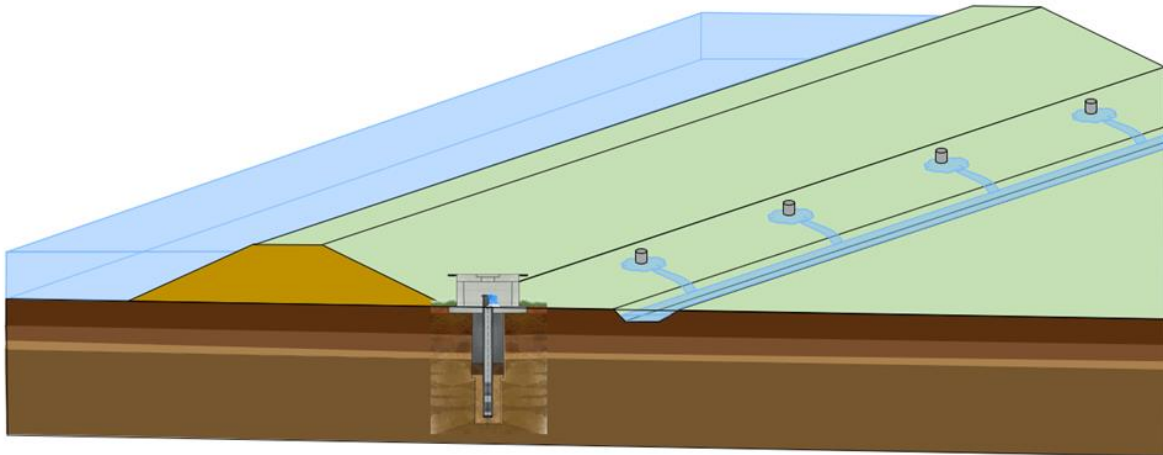


Figure 1–2. Typical line of relief wells at the toe of a dam or levee



Figure 1–3. Line of wells at Upper Wood River Levee District (USACE 1956b)

1–13. Relief well components

Slotted, wood-stave wells were used in the earliest relief wells and are still in existence at many locations. Although polyvinyl chloride (PVC) and other materials have been used over time, current practice is to use a wire-wrapped, stainless-steel screen and riser. The screen and riser pipe have inside diameters typically between 6 and 18 inches. Generally, the filter gravel pack around the screen is capped with an impervious material such as bentonite. A grout or concrete plug is placed above the seal to encase

the riser pipe to the ground surface. The following components are described in further detail in Chapter 7.

a. *Screen*. A filtering element that allows water but not sediment to enter the well. The screen also provides structural support for the surrounding soil.

b. *Riser pipe*. Blank pipe above the screen that conveys water to the surface and supports the surrounding soil.

c. *Well guard*. A protective device at the ground surface that prevents damage to the well while allowing flow from the well to exit.

d. *Filter pack*. Sand or gravel placed between the screen and the borehole wall to prevent foundation soils from entering the well.

e. *Check valve*. A plate that seals against the top of the riser to prevent backflow of surface water into the well.

f. *Seal* (also called plug). An impermeable material in the annulus of the well that provides a bond between the riser pipe and the surrounding soil.

1–14. Definitions

See the Glossary of Terms for a list of terms and definitions.

1–15. Manual organization

This manual presents basic principles related to the implementation and evaluation of relief wells. The manual is organized into three parts: (1) general considerations and background; (2) analysis, design, and evaluation; and (3) construction, operation, and maintenance. Appendixes are provided to supplement content in the main chapters, including methodology, background, and examples. Some of the appendixes are technically extensive, and the ordinary practitioner is not expected to replicate all of the analysis.

a. *General considerations and background*. The beginning of this manual includes general considerations and background. Chapter 1 presents the purpose and function of relief wells, defines general terms, and provides a layout of the manual. The history of relief wells used to relieve substratum pressure at dams, levees, and other structures is presented in Chapter 2. Chapter 3 considers overarching engineering and geologic considerations critical for well system design.

b. *Analysis, design, and evaluation*. The middle portion of the manual considers the analysis, design, and evaluation of relief well systems.

(1) Chapter 4 addresses how relief wells impact risk due to poor project performance. Chapter 5 presents the traditional design approach used to select the depth, capacity, and spacing of relief wells. It assumes an infinite line of wells spaced a

uniform distance apart. This method has been used for most relief wells installed in USACE since the 1950s. The history of infinite well theory is included in Appendix H to enhance understanding of multiple generations of relief well systems.

(2) Chapter 6 explains how the theoretical approach in Chapter 5 is adapted for the finite length of well systems used in practice. Chapter 6 also describes image well theory, which has been used to design systems that are either limited in number or have irregular spacing. Modern 3D seepage analyses are presented in Chapter 6, with examples in appendixes to handle complex geometry and foundation conditions. Chapter 7 details the design of the physical well to be installed and describes components of head loss in the well.

c. *Construction, operation, and maintenance.* The final portion of the manual covers construction, implementation, and maintenance of the relief wells and collection systems. Construction and maintenance best practices are provided for relief wells at various points in their life cycle. Chapter 8 provides guidance on installation. Chapter 9 covers pumping tests, which are an integral part of in situ analysis. Chapter 10 covers the relief well collector system, and Chapter 11 provides best practices for operating and maintaining wells.

Chapter 2 Relief Well History

2–1. Introduction

Thousands of relief wells installed over the last century at USACE dams, levees, and other structures are still in use. During this time, design practices have evolved. The historic use and development of design methodology for relief wells in USACE is important to this manual and summarized in this chapter. A more detailed history of relief well uses and current USACE practices are provided in Walshire et al. (2020). Methods of analysis for relief wells were co-opted from the oil and gas industry and validated against field experiments and laboratory models. As a result of these research investigations, conservative, safe, and economical methods of pressure relief were developed and are still in use.

2–2. Initial use of relief wells

a. *Early well use.* Wells have been used for centuries to control agricultural seepage (Johnstone 1797; French 1859). Later, the value of wells was recognized for reducing uplift pressures on hydraulic structures (Khosla 1930), and for construction dewatering (Terzaghi 1927). Many of these early wells did not extend the full depth of the aquifer and thus fit the definition of “partial penetration.” Relief wells can be either partial or full penetration. Although analysis is more complex, partial-penetration wells sometimes offer technical or economic advantages.

b. *Initial use in an existing structure.* In 1942 to 1943, the Omaha District became the first USACE entity to use relief wells for controlling uplift pressure. This occurred at Fort Peck Dam, Montana, along the Missouri River (Slichter 1945; Middlebrooks 1948). The action was taken to address excess head of 45 feet in piezometers tipped in the pervious foundation at the downstream toe. As an emergency measure, ordinary steel pipe was used in various arrangements to relieve the pressure. When this proved unsuccessful, well casings were slotted with a cutting torch. Twenty-one wells were installed between July 1942 and September 1943. The excess head at the downstream toe was reduced from 45 to 5 feet. Total flow from the 21 wells averaged about 4,500 gallons per minute (gpm). The wells quickly became severely corroded and were replaced with wooden wells in 1946.

c. *Initial use in a new structure.* Relief wells were first incorporated in the original design of a dam in 1943 by the USACE Vicksburg District. The foundation stratum at Arkabutla Dam consisted of 30 feet of relatively impervious loess underlain by a pervious stratum of sand and gravel. A line of 250, 2-inch brass relief wells was installed along the downstream toe and spaced at 25-foot intervals. The system was effective for many years (USACE 1958), but their small size precluded any maintenance. Today, these wells are being grouted and replaced with 52 modern wells spaced 40 to 200 feet apart.

2–3. Relief well research

a. *Initial research.* Historic floods along the Mississippi River during the late 19th to early 20th centuries were highly destructive. These events caused detrimental underseepage, sand boils, and at least six levee failures due to internal erosion (Fatherree 2006). After floods in the 1920s and 1930s, USACE initiated research programs to understand seepage mechanics and countermeasures, including pressure relief wells. This research was performed by the Mississippi River Commission, the USACE Vicksburg Engineer District, and the U.S. Waterways Experiment Station (WES). (WES is now known as the Engineer Research and Development Center [ERDC]). Exact mathematical solutions for underseepage were not available at the time. Instead, research methods consisted of electrical analog models, physical sand models, and theoretical studies.

b. *1930s electrical analogy modeling.* ERDC developed models using electrical current as a substitute for seepage flow (Figure 2–1). Calculations for seepage gradient and flow quantity were derived from voltage drop measurements and used to analyze effects of partial well penetration. An analytical procedure was developed to predict underseepage quantity, aquifer pressure, and vertical gradient across the top blanket.

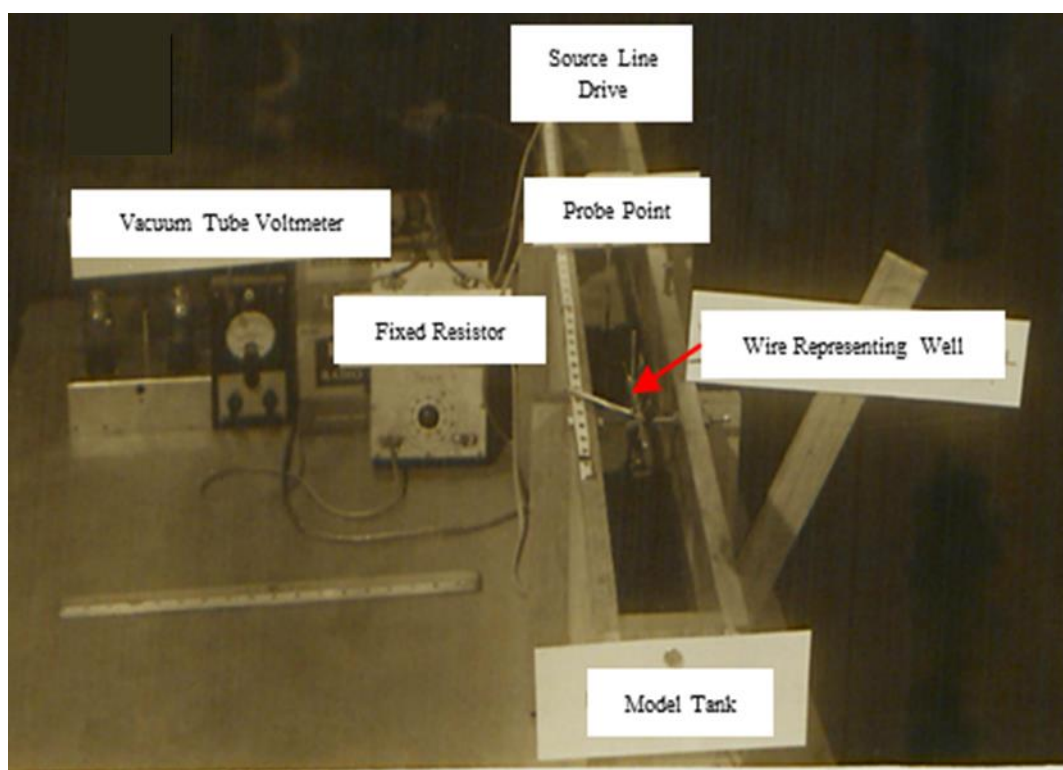


Figure 2–1. Electrical analogy (USACE 1939b)

c. *Black Bayou Levee.* The Vicksburg District performed seepage studies at the Black Bayou Levee along the Mississippi River. This research was used to confirm the usefulness, economy, and practicality of using pressure relief wells (USACE 1939b).

Muskat (1937) had previously developed mathematical solutions for effective spacing of oil wells. These solutions were successfully applied to the relief well spacing at Black Bayou (USACE 1939b). Design curves by Muskat were also validated against both physical and electrical models of relief wells. Curves were developed for both full- and partial-penetration wells at Black Bayou.

d. Underseepage studies. In September 1940, the Mississippi River Commission initiated a general study of underseepage along Lower Mississippi River levees. This began with a review and compilation of all underseepage reports related to the 1937 flood. Also included were exploration and geological studies of numerous sites where underseepage was a serious problem in 1937. Piezometers were installed at selected sites to measure substratum pressures beneath and landward of levees. Field pumping tests were performed to determine the permeability of the sand aquifer at certain sites. In addition, theoretical, electrical-analogy, and sand model studies were done. Prototype studies of relief wells, partial cutoffs, and landside berms for the control of underseepage were conducted. The effort was still underway in 1950 when observation and measurement of natural seepage was performed at certain locations during high water.

e. Technical Memorandum 3-304 (USACE 1949). The 1940s model studies are summarized in this document. A number of sand models were constructed to study the phenomenon of underseepage and its control using relief wells. The studies represented conditions commonly encountered in the Lower Mississippi River Valley. These models investigated seepage flow and landward substratum pressure with and without relief wells. Relief wells with proper spacing and penetration effectively reduced excess hydrostatic pressure landward of levees underlain by a pervious foundation. This was demonstrated for a wide range of seepage entrances, foundation conditions, and landward top strata.

f. Experimental relief wells. In 1942 to 1943, lines of experimental relief wells were installed at four sites where underseepage had caused problems in 1937. Foundation conditions were known, and piezometers were already present at these sites (Commerce, Trotters 51, and Trotters 54, Mississippi; and Wilson Point, Louisiana). The experimental systems operated during the high water in 1943. Unfortunately, the wells proved too small in diameter to handle the flows, which were greater than anticipated. The large flows were attributed to a more pervious foundation than had been assumed. The seepage entrance on the river side of the levee may also have been closer than assumed. The wells were subsequently plugged or pulled. Despite the setbacks, valuable information was obtained from these early field tests. This included insights on permeability of the foundations, well flow, and pressure reduction.

g. Pumping tests. Field pumping tests were conducted at Commerce and Trotters 54 in 1943 to 1944 to measure overall permeability of the pervious substratum. The Trotters 54 tests also determined flow for various drawdowns in the well and head loss through the filter and well screen. These early tests helped establish field pumping tests as an integral part of relief well design. Later, more comprehensive pumping tests were

conducted on wells installed along the levees in the St. Louis District. These tests are documented in Technical Memorandum (TM) 3-430 (USACE 1956b).

h. Larger experimental relief wells. In 1950, a new, larger capacity relief well system and additional piezometers were installed at Trotters 54. Piezometer readings and seepage observations made during high-water events in 1951 and 1952 indicated that the system performed as designed. The well system reduced substratum hydrostatic pressures landward of the levee to a small fraction of the head on the levee. The system also intercepted a large portion of natural seepage that otherwise would have emerged landward of the levee. An analysis of this system, including 1951 and 1952 high-water events, was reported in TM 3-341 (USACE 1952).

2–4. History of relief well design

A full chronology of the development of USACE relief well design methods is discussed in Appendix H.

a. Full-penetration relief wells. The historic Mississippi River floods of the 1920s and 1930s ignited research on underseepage. This included determining the causes of, and treatments for, underseepage in a pervious stratum. Field studies in the late 1920s (Long and U.S. Army WES 1931) and adaptation of approaches from the petroleum industry resulted in a design method. These methods assume a homogeneous, isotropic (either natural or transformed) pervious foundation with various limiting boundary conditions. An initial solution for flow and pressure along a line of full-penetration foundation wells was developed.

b. Partial-penetration relief wells. Mathematical formulation for an infinite line of wells, parallel to a line source, did not exist in the 1930s. Also lacking at the time was an analytical method for modeling partial-penetration wells. The reduced flow due to partial-penetration wells was understood, but there was no means to determine substratum pressure. Additional model and theoretical work (USACE 1939a, b, c) eventually led to developing a solution for partial-penetration relief well systems. The theoretical infinite full-penetration well line solution was combined with electric analog-based, partial-penetration solutions developed by USACE. This design process is sometimes referred to as the “Muskat-Jervis” approach.

c. Extra length and head factors. Analytic and model studies performed by USACE in the 1940s and 1950s resulted in further advancement of numerical methods for seepage analysis and relief well design. Piezometers measured foundation pressure and were configured at varying depths and spacing for partial-penetration simulation. The “extra length” and “head” factor concepts were derived from these experiments and published in 1946 (Middlebrooks and Jervis). These concepts are covered in Chapter 5 of this manual.

d. Blanket Theory. Bennett (1946) developed what is known as Blanket Theory (BT). The theory provided a solution for steady-state, two-dimensional (2D) flow through a semi-pervious top layer and pervious bottom layer. Bennett assumed vertical flow

through the top layer and horizontal flow through a bottom layer. The horizontal permeability of the bottom layer was assumed to be at least 10 times greater than the vertical permeability of the top layer. BT allowed pressure relief in an aquifer due to flow through a confining top stratum. Barron (1948) derived closed-form solutions to also incorporate pressure relief due to flow from wells in these analyses. These concepts and assumptions eventually led to the design equations in use today.

e. *Relief well guidance.* Historical evolution of relief well guidance in USACE is also summarized in Walshire et al. (2020). The first USACE engineer manual to identify relief wells as a seepage control measure was published in 1952 as part of a comprehensive soil mechanics design manual. A Civil Works Engineer Bulletin in 1955 (USACE 1955) represents a turning point in relief well design. That bulletin covered topics still pertinent to well design that are contained in this manual. Included was an updated design chart for an infinite line of wells.

f. *Technical Memorandum 3-424 (USACE 1956a).* TM 3-424 is a valuable resource for designing relief wells. This report represents a comprehensive summary of almost two decades of research described in the previous paragraphs. The document has become the foundation of seepage analysis, evaluation, and design of seepage control measures for dams and levees across USACE. TM 3-424 demonstrates how to apply Civil Works Engineer Bulletin 55-11. These procedures carried over to several EMs (1110-2-1901, -1905, -1913, and -1914).

g. *Technical Memorandum 3-430 (USACE 1956b).* TM 3-430 is the companion report to TM 3-424. It documents relief wells installed in the early 1950s along river levees in the St. Louis District. In October 1952, WES was authorized to assist with the investigation and to design the required seepage control measures. TM 3-430 presents the results of that investigation, and includes all field, laboratory, and design studies made during the project. This included geological studies of the alluvial valley and construction procedures for installing and testing relief wells and piezometers. In addition, the report contained as-built information on relief wells and piezometers and a description of required maintenance.

h. *Miscellaneous Paper S-72-21 (USACE 1972).* The purpose of this paper was to quantify loss of well efficiency over time and examine the causes. Step-drawdown pumping tests were performed on target wells selected in the 1950s to represent typical wells for this type of study. These target wells are surrounded by an array of piezometers that extend both parallel and perpendicular to the levee alignment. The report demonstrates how to evaluate well condition and estimate head losses.

i. *Performance of Underseepage Controls During the 1973 Flood (USACE 1976).* This report documented areas along levees in the Alton to Gale system where the design approach may have been deficient. These areas included the inside of bends in levee alignment where seepage was concentrated. Another issue was how to analyze foundations with a thin clay blanket underlain by a thick layer of sandy silt or silty very fine sands. This sandy silt layer is often located between the blanket and foundation, as

shown in Figure 2–2. Well screens are traditionally not installed in these transition layers because the sand is too fine.

j. *Engineer Research and Development Center/Geotechnical and Structures Laboratory Technical Report 02-19 (USACE 2002)*. This ERDC/GSL report was completed in 1986 and published in 2002. It summarizes what was learned from observing several floods during the 20-year period from 1966 through 1986. Performance of control measures was evaluated using wellpoint piezometers installed at numerous locations along the Alton to Gale levees. This report highlighted three-dimensional (3D) seepage effects on the inside bends of alignments. It also reiterated analytical problems with fine sands often present between the aquifer and blanket. The intermediate silty sand shown in Figure 2–2 is not properly accounted for in BT. In practice, this layer is often not screened when relief wells are installed because it requires a very small slot size. Unfortunately, uniform fine sands often found in the intermediate layer are susceptible to backward erosion piping (BEP).

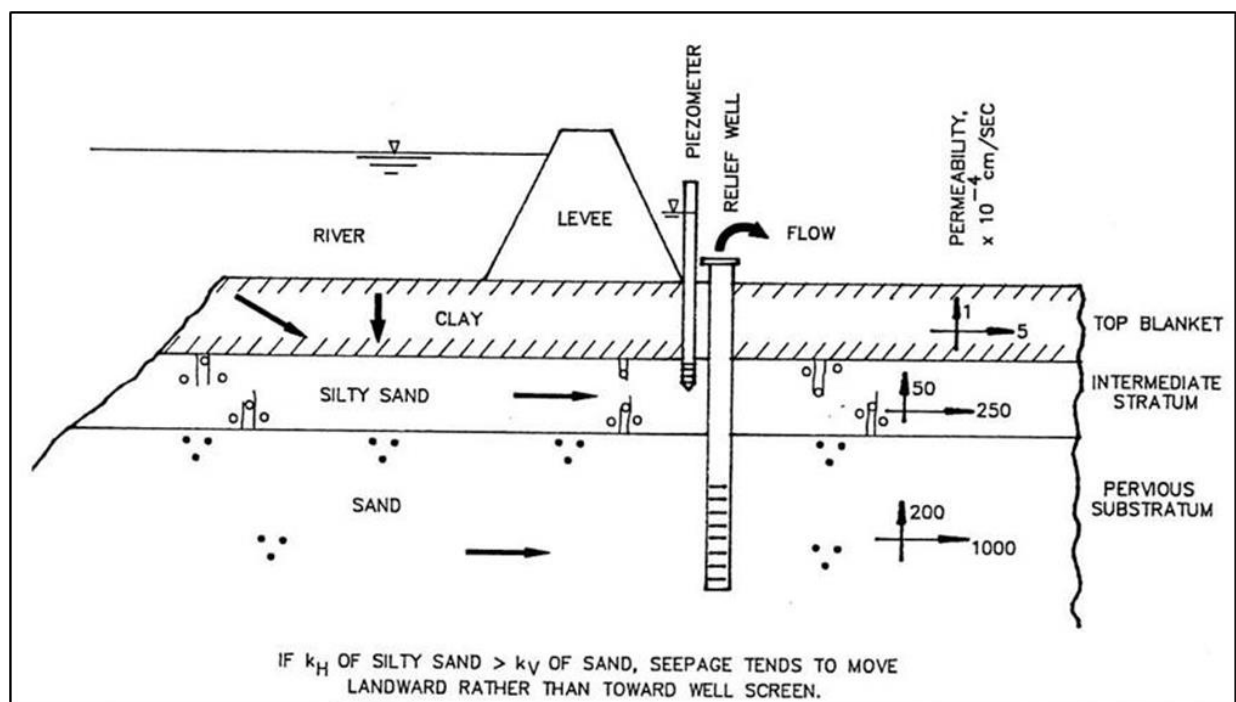


Figure 2–2. Foundation profile with intermediate silty sand stratum (USACE 2002)

k. *1970s and 1980s – analytical approaches*. Sharma (1974) developed well discharge and drawdown expressions for partial-penetration wells. During this period, Barron (1978–1982) further documented the theoretical basis behind the USACE (1955) nomogram. The 1992 version of this manual contains comparisons of “more theoretically exact” uplift factor solutions developed by Barron and verified by electrical analogy tests. Uplift factors calculated using Sharma (1974), Barron’s electrical analogy and analytical work, and USACE (1955) nomogram differ by less than 5%. Therefore, all approaches should yield similar practical design results.

l. 1980s to 2020s (present) – modeling. Advancements in modeling, including finite element method (FEM) and 3D, have been developed and continue to progress through the 21st century. This manual describes modeling studies applied to finite lines of wells, partial-penetration design, and an update to the 1955 nomogram.

m. Original publication of EM 1110-2-1914. The application of wells for water-retention structures eventually resulted in the development of the 1992 version of this manual. This 1992 version of the manual standardized the analysis methods and has remained in use until the publication of this updated version. The 2D approach using BT was later adapted to 2D FEM models as described in Appendix G of this current manual. The design approach for an infinite line of wells is given in Chapter 5, and the development of this approach is described in Appendix H. These simple methods supplement more rigorous 3D FEM that are described in Chapter 6.

n. Performance of Relief Well Systems Along Mississippi River Levees. This paper (Mansur et al. 2000) describes the successful performance of relief wells that were installed in the 1950s during the 1993 flood. The paper compares design values with field performance of 2,480 relief wells during a flood event that exceeded design levels.

Chapter 3 General Well System Design Considerations

3–1. Relief well application

Relief wells are best suited for seepage control where a fine-grained top stratum (blanket) overlies a more pervious stratum (aquifer). This is particularly true when the blanket is of insufficient thickness to resist potentially destructive seepage pressures. Relief wells can also be used to capture seepage through deep, pervious lenses in an otherwise less pervious stratum (glacial till, etc.). In some cases, an overlying confining layer is absent on the dry side of the structure. Under these conditions, relief wells have little impact on seepage pressures in thick pervious strata. However, even in the absence of confinement, wells can still capture flow that would otherwise exit on the dry side of the structure.

a. *Excess head.*

(1) Whenever water is confined in pervious deposits beneath a structure, potentially damaging pressures can exist beneath and downstream of the structure. The seepage pressures in the pervious deposits are often referred to in terms of total hydraulic head. The head, generally expressed in feet, is the water level above a given base elevation. Pressures are considered artesian when water levels in wells or piezometers screened in these deposits rise above the top of the pervious layer.

(2) When water levels in wells rise above the landside ground surface, or above tailwater, it is often referred to as excess head. Excess head at the landside toe of the embankment, without any relief wells, is typically designated as h_o . Numerous illustrations and examples in this manual use the landside ground surface as the base elevation for defining head, thus any positive value of head is excess head (see Figure 3–1). Pressure relief wells protect structures by reducing the excess head to an allowable head, discussed in paragraph 3–1c.

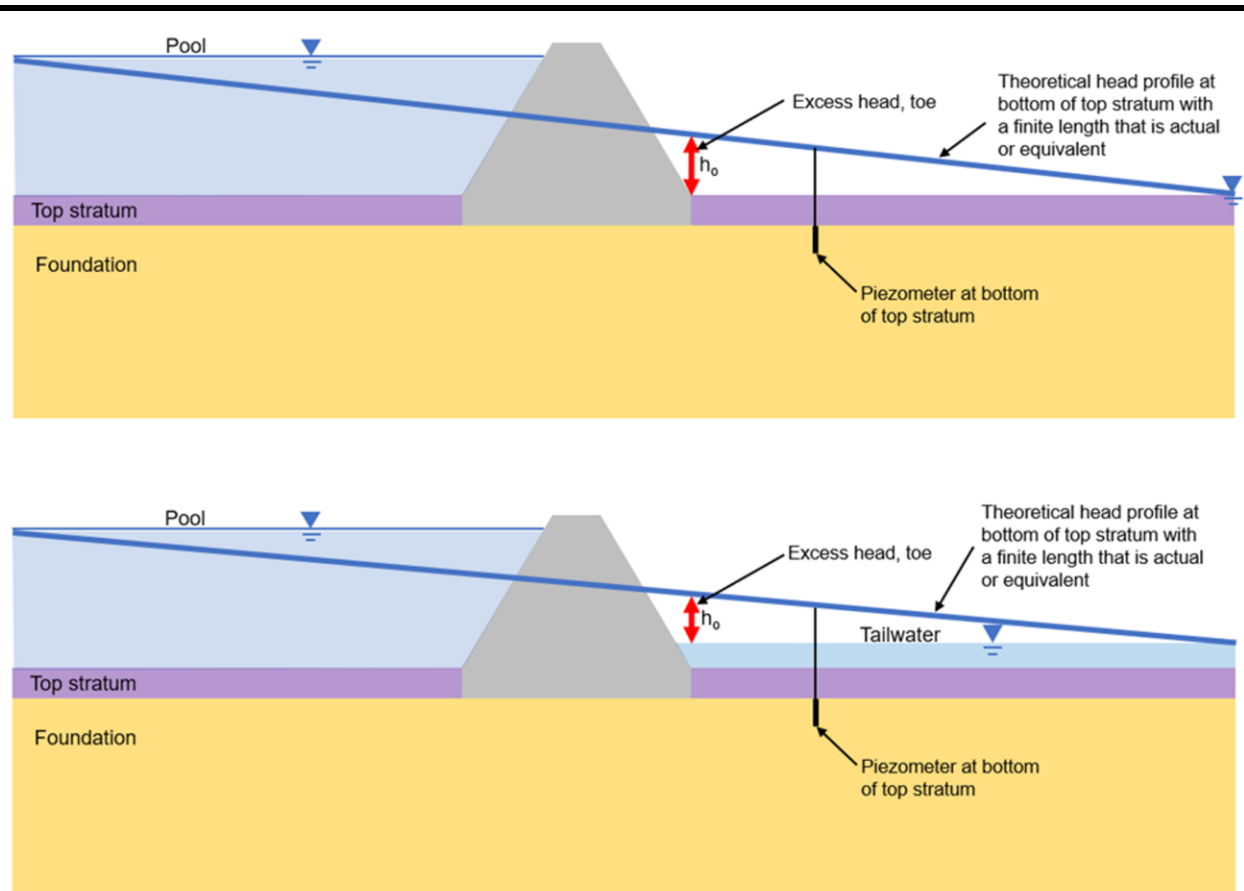


Figure 3–1. Illustration of excess head: the top diagram shows the landside ground surface as the base elevation for measuring head; the bottom diagram shows tailwater as the base elevation

b. *Factor of safety.* Minimum required factors of safety for dams are given in EM 1110-2-1901. For levees, this information is given in EM 1110-2-1913. The factor of safety calculation is commonly presented as the vertical gradient factor of safety (FS_{vg}). Historically, gradients have been used directly to specify seepage design criteria. More recently, the criteria have been normalized for material of any unit weight. Inherent in the calculation of vertical gradient factor of safety is that the material is saturated. The FS_{vg} is calculated as shown in equation 3–1:

$$FS_{vg} = \frac{i_{cv}}{i_v} = \frac{\gamma' z_t}{\gamma_w h_x} \quad (3-1)$$

where:

FS_{vg} = factor of safety based on vertical gradient

i_{cv} = critical vertical gradient = γ' / γ_w

i_v = vertical gradient at point of interest = h_o / z_t , typically the embankment toe

z_t = vertical distance to surface, typically the landside blanket thickness, z_{bl}

h_x = excess head (above hydrostatic) at the point of interest, typically bottom of blanket

- γ' = average effective (or buoyant) unit weight of overlying soil = $\gamma_{sat} - \gamma_w$
- γ_{sat} = total, or saturated, unit weight of overlying soil
- γ_w = unit weight of water

c. *Allowable heads.* In most cases, allowable head (h_a) is the value of excess head that provides an acceptable factor of safety based on vertical gradient through the top stratum, as defined in equation 3–3. However, h_a may be driven by other failure modes or design criteria where seepage pressures are relevant. For example, h_a could be defined to reduce uplift on a structure or reduce foundation pressures to improve embankment slope stability. The h_a might also be defined to ensure a structure is stable during dewatering. Allowable heads may also be dictated by horizontal gradients in the pervious strata that could lead to progression of BEP. This applies to areas on the dry side of the structure with a known defect. The h_a may also be based on preventing any seepage from reaching the ground surface on the dry side of a structure. Relief wells can be used to achieve h_a for many of the above design objectives.

$$h_a = \frac{i_{cv} \times Z_t}{FS_{vg} - min} \quad (3-2)$$

where:

h_a = the maximum allowable excess head at a point, typically at the base of the blanket

$FS_{vg} - min$ = minimum allowable factor of safety based on vertical gradient

d. *Permeability.* Permeability (k) is a measure of how easily a fluid moves through a porous medium. In this manual and many other engineering applications, k is expressed in dimensions of Length/Time (such as feet per day) and is synonymous with hydraulic conductivity (K). This is appropriate for flow to relief wells at USACE projects, where fresh water is generally the only fluid of concern. In other applications, fluid properties are variable. Examples include aquifers where water may be of variable salinity, or when pore space is filled with oil, water, and/or gas. In such cases, k is a property of the porous medium only, and is expressed in dimensions of length squared (L^2).

e. *Anisotropy.*

(1) If a geologic layer is equally permeable in all directions, it is referred to as isotropic. If a layer has a different value of horizontal permeability (k_h) relative to its vertical permeability (k_v), the layer is referred to as anisotropic. The ratio k_h / k_v is typically greater than unity for sedimentary layers, such as those formed in alluvial or glacial environments. These types of materials are common at USACE projects.

(2) Anisotropic layers can be mathematically converted to isotropic layers through an aquifer transformation. This process uses k_h and k_v to calculate an effective permeability (k_e) that applies to flow in all directions (see paragraph 3–4g and Appendix E). Designers should be aware that, if not transformed, a series of isotropic layers will behave as a single anisotropic layer with $k_h > k_v$ (Freeze and Cherry 1979). FEMs can

incorporate anisotropy directly. The design implications of permeability and anisotropy are discussed in more detail in paragraph 3–4f.

f. *Transmissivity.* The transmissivity (T) is a measure of aquifer productivity. It is the numerical product of k and aquifer thickness (b), having units of L^2/Time (for example, square feet per day). Figure 3–2 illustrates the concept of T . T can also be defined as the rate of groundwater flow through a unit width of a fully saturated aquifer thickness under a hydraulic gradient of 1. This parameter has historically been an important consideration for water supply wells because it determines well yield. For a stratified aquifer, each layer has an associated T . The total T for the aquifer is the sum of T for the individual layers (see paragraph 3–4g(3)). Relief wells are most effective in a stratified aquifer when the screen is in contact with the most transmissive layers. For alluvial aquifers, this is typically the bottom layers.

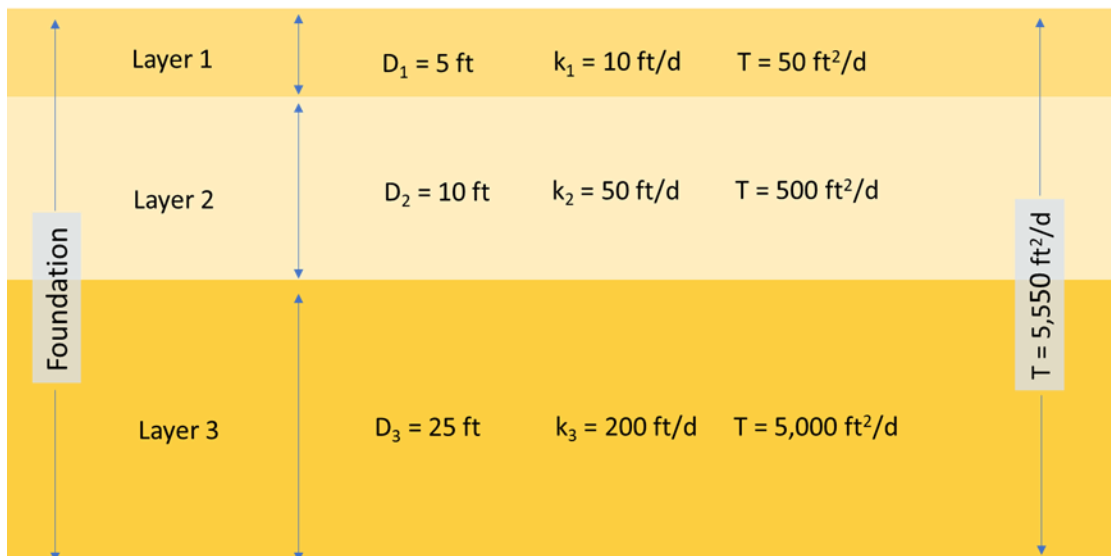


Figure 3–2. Illustration of aquifer transmissivity for a stratified foundation

g. *Storativity.* When heads decrease in an aquifer, as during the transient stage of pumping, a volume of water is released elastically. This results from expansion of the water and compression of the aquifer skeleton. Storativity (S_t) is a measure of the volume released per unit area per unit change in hydraulic head (Freeze and Cherry 1979). In practice, S_t is not of great importance to relief well analysis as most evaluations consider steady-state conditions only.

h. *Areas with pre-existing boils.*

(1) Sand boils occur when excessive head causes sand to flow to the surface through defects in the confining layer. The defects could be pre-existing or the result of exceeding the FS_{vg} . Sand boils resemble a volcano-like cone feature at the ground surface where the water-saturated sediment has broken through the confining layer (see Figure 3–3). The process also creates a zone of higher k in the subsurface.

(2) Flow-through boils or other flaws in the confining layer complicates design or evaluation of relief wells. In such cases, seepage models should account for the increased k of the blanket when evaluating existing or proposed relief well systems. This results in lower calculated vertical gradients through the blanket compared to an intact blanket. However, once a defect exists, the vertical gradient required to move underlying sand to the ground surface is decreased because the boil is an unfiltered exit. Evaluation of these conditions is explained further in Chapter 4.



Figure 3–3. Example of sand boil, East St. Louis, 2016 New Year’s Day flood

i. Relief wells and pre-existing boils.

(1) A relief well system by itself may not be able to mitigate potential distress conditions from pre-existing piping or concentrated seepage. In such cases, a relief well placed at the toe of a seepage berm may be appropriate as a secondary mitigation measure. If there are pre-existing boils, placing relief wells between the seepage source and the boil locations is recommended when practical. This placement of wells may further reduce the likelihood of progression because horizontal gradients may be reduced near the pre-existing boils.

(2) Appendix F documents sensitivity studies, using 3D modeling, to evaluate the interaction of a system of relief wells and a defect in the blanket. The location of the defect was modeled both upstream and downstream of the relief well line. The results indicated that regardless of defect location, the relief wells reduced the amount of flow through the defect. See Appendix F for more detailed study results.

3–2. Collection of relief well discharge

a. Relief well discharge. Relief well discharge can be collected at or below the landside ground surface. This discharge can be actively pumped or allowed to drain by gravity away from the wells. Gravity flow to an at-grade discharge point is the simplest

type of collection system. Unfortunately, various site conditions can require elaborate collection and pumping systems. Relief well flow collection systems are discussed further in Chapter 10.

b. Groundwater contamination. Relief well discharge from wells in areas of known groundwater contamination, either man-made or naturally occurring, may be subject to state or federal regulation. Consultation with state and federal regulations is required if there is groundwater contamination in the area of proposed relief wells. Installation of relief wells in areas with known contamination may require discharge permits or treatment of relief well flows prior to discharge.

3–3. Seepage analysis

There are many methods to analyze seepage, determine if relief wells are needed, and what design parameters might apply. Methods include, but are not limited to, hand-drawn flow nets, BT calculations, and both 2D and 3D FEM. Selecting an appropriate analysis method is important. However, the thought and care used to characterize the foundation of the structure is much more important in the design process. This also applies to definition of the reaches used in the analysis (see paragraph 3–3f). It is recommended to perform the seepage analysis with the simplest method that will reasonably represent the analysis reach. Complex boundary conditions or geologic features may be difficult to directly analyze using BT or 2D modeling.

a. Blanket Theory. BT is an analytical approach based on a simple, graphical representation of subsurface pressure that is used to evaluate underseepage. With BT, the stratigraphy can be represented as a pervious substratum (aquifer) underlying a less pervious top stratum (blanket). BT is appropriate where conditions can be approximated by relatively consistent layer thicknesses. Appendix C includes some of the basic elements of BT to help the reader understand relief well design and evaluation as presented in this manual. BT is described in detail in EM 1110-2-1913.

b. Finite element modeling. Two-dimensional FEM is appropriate when there are long distances along the levee alignment, but conditions are too complex for BT. Appendix G describes an approach to include an infinite line of wells in a 2D plane-strain FEM model. Chapter 6 discusses how full-penetration wells can be included in a 2D plan view FEM model, as well as 3D FEM that can model even the most complex problems. FEM is described in detail in EM 1110-2-1901.

c. Wells in two-dimensional, plane-strain seepage models. Chapter 5 describes analysis of seepage to an infinite line of relief wells along the landside toe of a dam or levee. However, many well systems do not have continuous reaches long enough to be considered infinite, which is generally 1,300 to 1,500 feet. As such, shorter well system designs with infinite line methods are unconservative with calculated heads lower than actual heads. Further, the ends of well systems have higher heads than the middle of well systems, regardless of system length. Chapter 6 describes how a finite line of relief wells along the landside toe of a dam or levee are included in seepage analyses. This type of analysis considers system length and end effects.

d. *Design water surface for seepage analysis.* Seepage analysis should be performed with water at the design water surface elevation (DWSE) as specified in EM 1110-2-1913 or EM 1110-2-1901. The DWSE is the highest elevation at which water is expected to be retained by the structure. For levees, the DWSE is the top-of-structure elevation. This excludes portions of the structure that are designed to accommodate future settlement or wave run-up. Some levees have designated overtopping areas with freeboard. In such cases, the water surface profile at overtopping may be considered the DWSE. For dams, the DWSE is commonly the top of the structure. Alternatively, the DWSE may be the top of the flood control pool or the elevation of highest sustained hydraulic loading.

e. *Effective well radius.* The effective well radius to be used in design computations is calculated as the outside radius of the well screen plus one-half the thickness of the filter.

f. *Development of reaches for seepage analysis.* The structure alignment is generally partitioned into distinct reaches for seepage analysis. Each reach has similar characteristics that are identified during the site characterization, as discussed in paragraph 3–4. Figure 3–4 illustrates a profile divided into a series of design reaches.

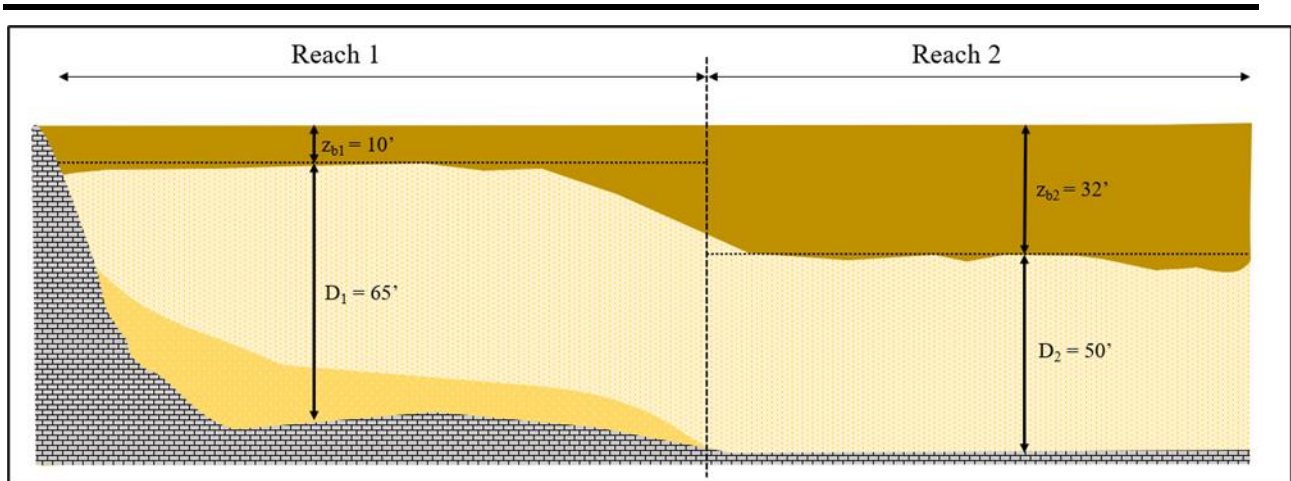


Figure 3–4. Profile of typical design reaches for relief well analysis (from EM 1110-2-1901)

g. *Using performance data and observations for seepage analysis.* Existing performance data and physical observations during loading are important indicators of relief well system performance. On structures where piezometric and relief well data are available, seepage analyses can be refined and uncertainty reduced from evaluating such data.

(1) *Piezometric data.* These data can be used to extrapolate observed performance to the project flood conditions and compared to performance thresholds as shown in Figure 3–5. The figure shows piezometric head in the foundation increasing with time because of relief well biofouling. Despite this trend, the observed heads remain well below thresholds for the design pool elevation. Uncertainty in projected

piezometric levels increases as the extrapolations become far outside the limits of the experienced loading conditions, and care should be exercised in large extrapolations. Piezometric projections from individual instruments can be shown along cross sections or profiles with several instruments. The piezometric projections from the instrument in Figure 3–5 are shown on a cross section with other instruments near the same embankment station in Figure 3–6.

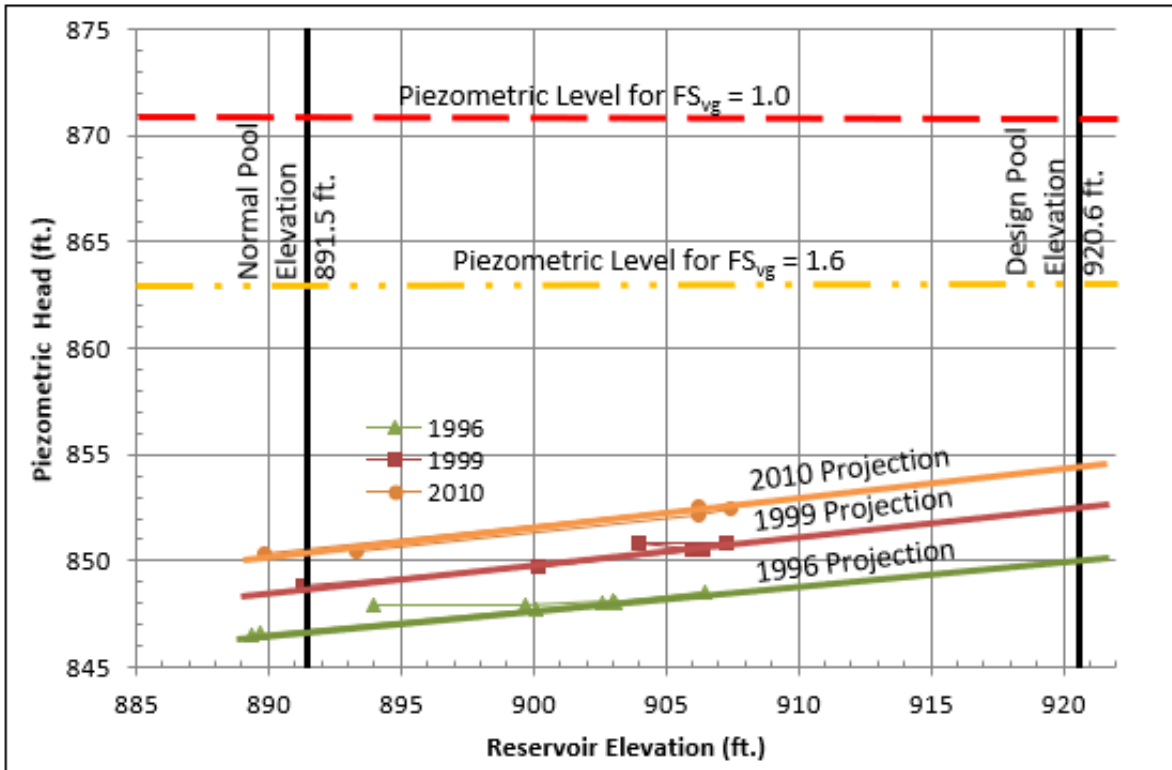


Figure 3–5. Projection of observed piezometer levels to design pool for successive high-pool events for Piezometer 32-1. Piezometric head increases with time are a result of relief well biofouling. Perry Dam, Kansas City District

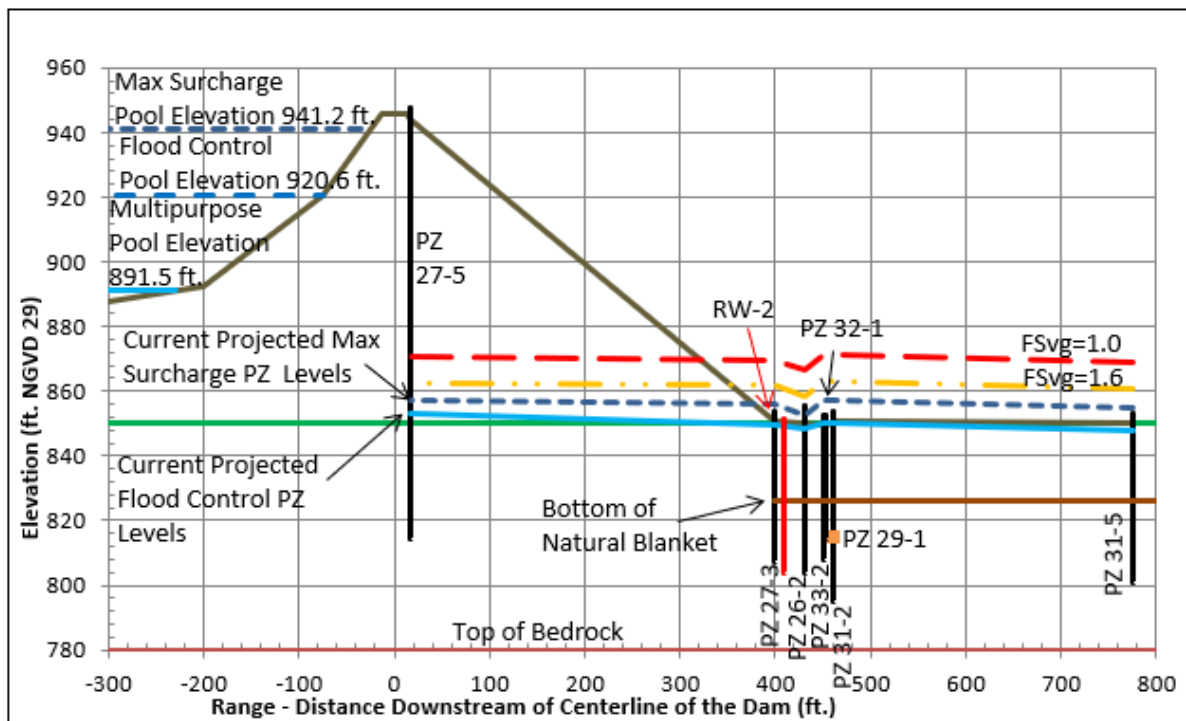


Figure 3–6. Evaluation of 2010 high pool piezometric levels for seepage vertical gradient safety factor, stations 27+00 to 31+00 (exaggerated scale); Perry Dam, Kansas City District

(2) *Physical observation.* If no instrumentation data is available, physical observations can be used to inform seepage analysis. For example, the total head differential acting on a structure might be known from flood events. This could potentially be correlated with observations of sand boil development. The known differential head at this time would approximate a condition where the FS_{vg} is equal to unity. From a known FS_{vg} , the performance of existing relief wells can be estimated. Or, if well performance is known through pumping test evaluations, this information can be used to refine subsurface and boundary condition assumptions. Well flow rates can also be compared to historical flow rates during similar loadings or design flow rates expected under full loading. Well flow rate can be estimated based on the water column height above the well riser top as described in Chapter 7.

(3) *Pumping test data.* Some relief well systems are not instrumented or only flow infrequently. This limits opportunities to collect piezometric data or make physical observations. In these situations, only pump test data may be available to analyze seepage and evaluate the well system. Figure 3–7 shows relief well pump test data, combined with geologic information, along a levee profile. The changes in specific capacity or efficiency over time can be correlated to changes in relief well drawdown and flow. This information can be used to update seepage analysis and estimate performance under hydraulic loading. Using pump test data in relief well evaluation and design is further discussed in Chapter 9, Chapter 11, and Appendix I, with examples included in Appendix J.

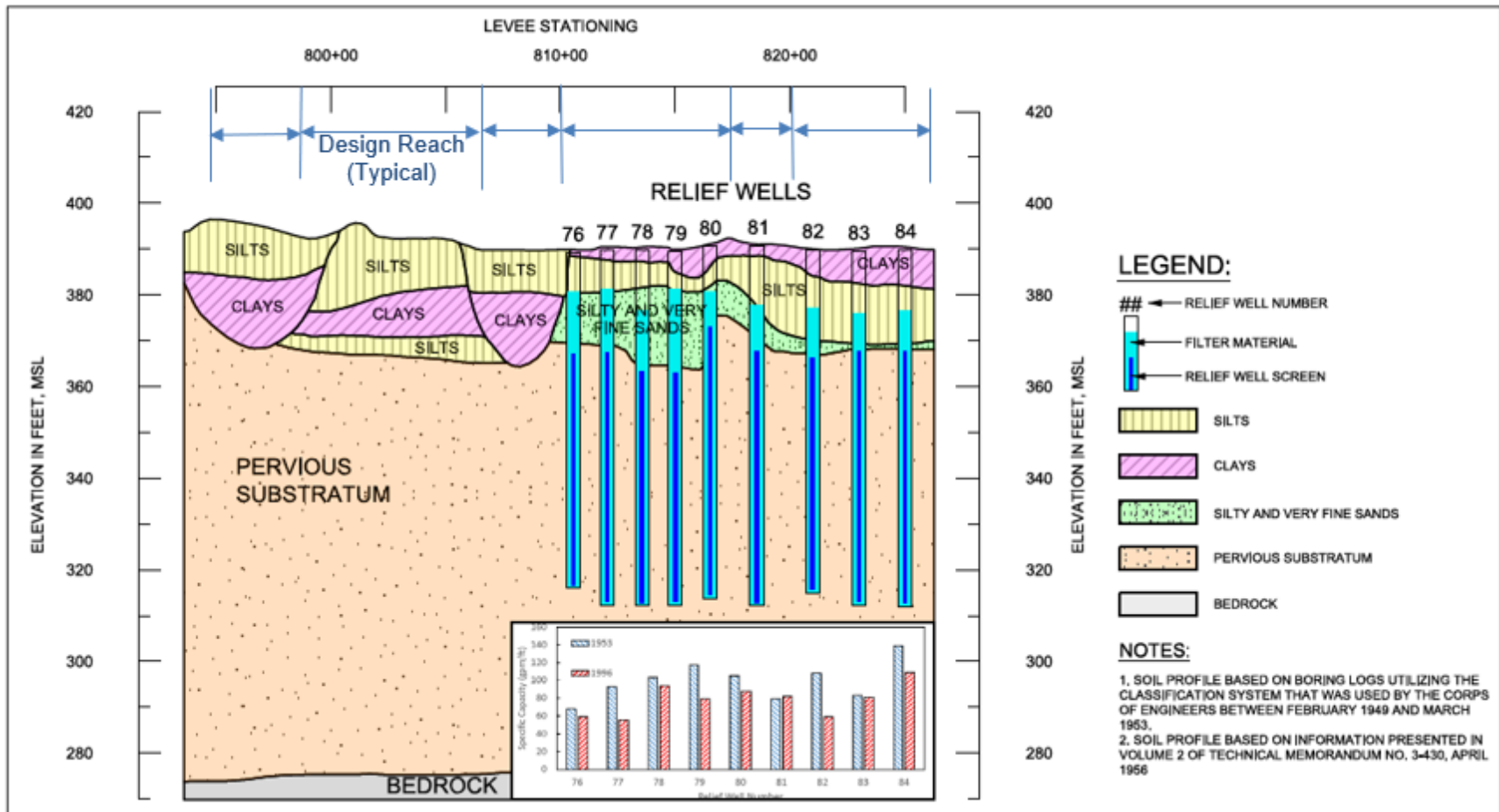


Figure 3-7. Relief well pump test data, combined with geologic information, along a levee profile

h. Relief well biofouling and mineralization.

(1) Future well losses from biofouling, mineralization, etc., should be accounted for during relief well system design. This allows declining well performance over time while still achieving design goals. A common historical practice in USACE has been to design well systems that provide the desired pressure relief assuming a performance loss of 20%. This is accomplished by ensuring that 80% of the initially projected drawdown will meet required safety factors. Alternatively, 80% of the initially calculated flow can be used to calculate the drawdown required to meet required safety factors. Both practices are consistent with the recommendation for well rejuvenation after an observed performance loss of 20%.

(2) A project-specific decline in well performance other than 20% can be developed based on a risk-informed approach. More information on determining well performance and selecting proper well performance levels for design are included in Chapter 9 and Appendix J. Biofouling impacts and relief well maintenance is covered in Chapter 11.

i. Chemical compositions of groundwaters.

(1) Some groundwaters are acidic and highly corrosive to relief wells. In other environments, groundwater may contain dissolved minerals or carbonates that can encrust the well screen. Both conditions can cause clogging and reduced efficiency of the well. For these reasons, the chemical composition of the groundwater should be determined as part of the foundation investigation. This includes chemical characterization of river or reservoir supply waters.

(2) Wisconsin Department of Natural Resources (DNR) (1996) and U.S. Department of Agriculture (USDA) (2012) describe procedures for collecting groundwater and surface water samples, respectively. U.S. Environmental Protection Agency (EPA) (1983) gives approved methods for chemical analysis of groundwater and wastewater. Indications of corrosive and encrusting waters are given in Table 3–1. Degradation of relief well screens and filter packs due to chemical factors is described in Chapter 11. As with biofouling, it is important to consider reduced efficiency if corrosion or chemical encrustation is anticipated.

Table 3–1
Indicators of corrosive and encrusting waters (from U.S. Army 1983)

Indicators of Corrosive Water	Indicators of Encrusting Water
1. A pH less than 7	1. A pH greater than 7
2. Dissolved oxygen in excess of 2 ppm*	2. Total iron (Fe) in excess of 2 ppm
3. Hydrogen sulfide (H ₂ S) in excess of 1 ppm detected by a rotten egg odor	3. Total manganese in excess of a 1 ppm in conjunction with a high pH and the presence of oxygen
4. Total dissolved solids in excess of 1,000 ppm indicates an ability to conduct electric current great enough to cause serious electrolytic corrosion	4. Total carbonate hardness in excess of 300 ppm
5. Carbon dioxide (CO ₂) in excess of 50 ppm	
6. Chlorides (CL) in excess of 500 ppm	

Note:

*ppm = parts per million

3–4. Site characterization

a. *Topography.* The ground surface elevation on the dry side of the embankment is an important variable in seepage analysis. The difference between this elevation and the water level on the waterside is the net head across the embankment. Often, the landside ground surface is assumed to be horizontal (constant elevation) to simplify calculations.

(1) *Topographical anomalies.* Localized low areas, drainage ditches, and sloping dry-side ground surfaces are all critical features in relief well design. These features may be sites of concentrated seepage and need to be considered in the analysis. BT or 2D finite-element cross-section models do not allow direct evaluation of localized topographic features.

(2) *Topographic design assumptions.* The total head in the pervious strata should be calculated by assuming the prevailing landside ground elevation is uniform, ignoring the anomaly. The vertical gradient should be calculated by applying this total head to areas where the blanket is thinner (topographic lows). Figure 3–8 depicts how localized topographical anomalies can be accounted for in BT or 2D finite-element models. This assumption is conservative because it ignores additional pressure relief in these areas. These topographic low areas can be directly included in 3D FEM. Ditches parallel to the line of relief wells can be included in 2D FEM. Where these features can be included, lower values of *k* should be assumed for the bottom of ditches or other localized thin spots. This conservative assumption means the analysis does not over-rely on pressure relief in those areas.

b. *Foundation investigations.* Thorough field and geologic studies conducted according to EM 1110-1-1804 are an essential requirement for proper relief well design. Geophysical exploration methods should be conducted according to EM 1110-1-1802. Borings performed on an existing dam or levee may also be subject to ER 1110-2-1807. Chapter 8 discusses drilling methods.

(1) *Purpose of foundation investigations.*

(a) The number, location, and depth of exploratory borings should be sufficient to define the seepage entrance and exit conditions. The borings should allow determination of the depths, thicknesses, and physical characteristics of the top stratum and underlying pervious strata. This applies to both the wet and dry sides of the structure. It is necessary to drill completely through the pervious strata to determine their thickness. Bedrock is often at the base of the pervious strata. However, cobbles, boulders, or float blocks within the pervious strata can give a false impression of true bedrock. It is imperative to core through these features to ensure that the thickness of the aquifer is not underestimated for relief well design.

(b) Figure 3–9 shows k and grain size data from a foundation investigation plotted on a boring log. An example of a generalized soil profile for relief well design along an embankment profile developed from a foundation investigation is shown in Figure 3–4.

(2) *Unique geologic features.*

(a) Subsurface layers or zones with significantly different physical properties than adjacent materials are sometimes referred to as geologic heterogeneities. Foundation investigations should identify and define any heterogeneities that will impact seepage pressures and the performance of a relief well system. In alluvial deposits, these can include buried channels, clay-filled swales, and pervious abutments. In glacial till and outwash deposits, such features may be more pervious zones in an otherwise less pervious matrix.

(b) If interconnected, these zones can transmit, concentrate, or divert significant seepage. Typically, unique geologic features will need to be defined and evaluated in a 3D model. Otherwise, it will be difficult or impossible to directly evaluate them analytically. An alternative approach is to perform sensitivity analyses on a variety of different simplifications using BT or 2D FEM analysis. In some instances, additional relief wells, along with future performance monitoring, is the best strategy to account for these features. An example of a clay-filled swale that concentrates seepage is shown in Figure 3–10.

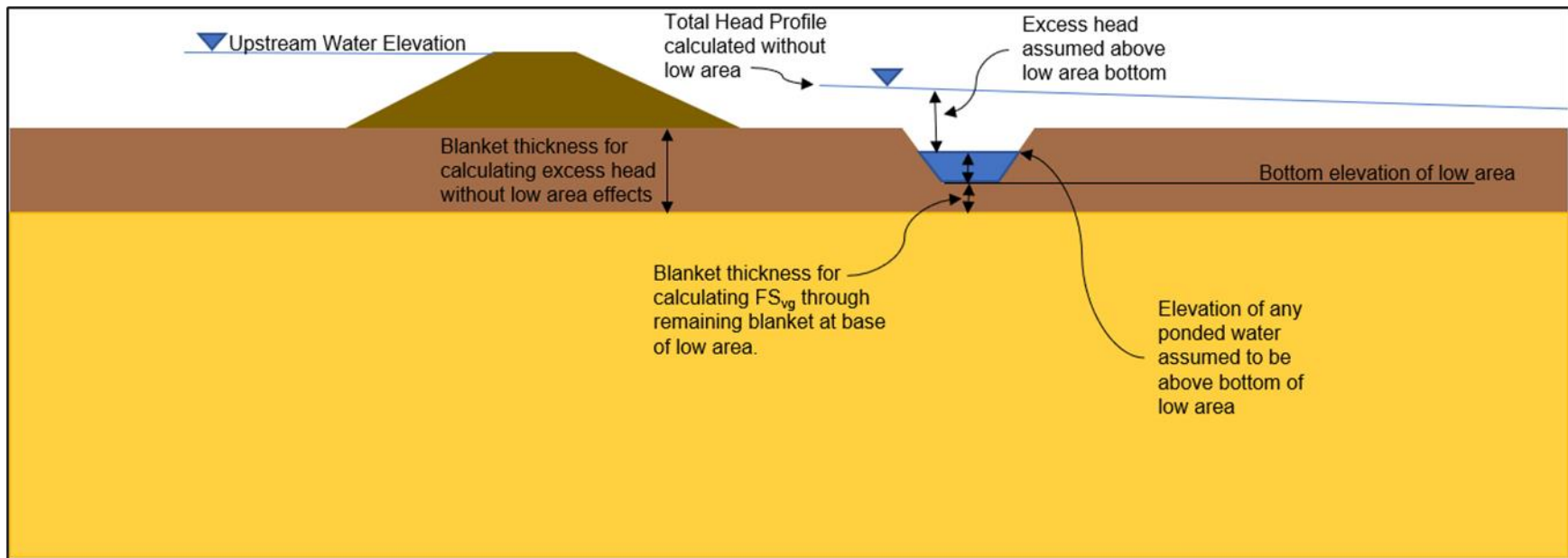


Figure 3–8. Graphical depiction of how localized topographical defects, or low areas, are typically accounted for in 2D analysis

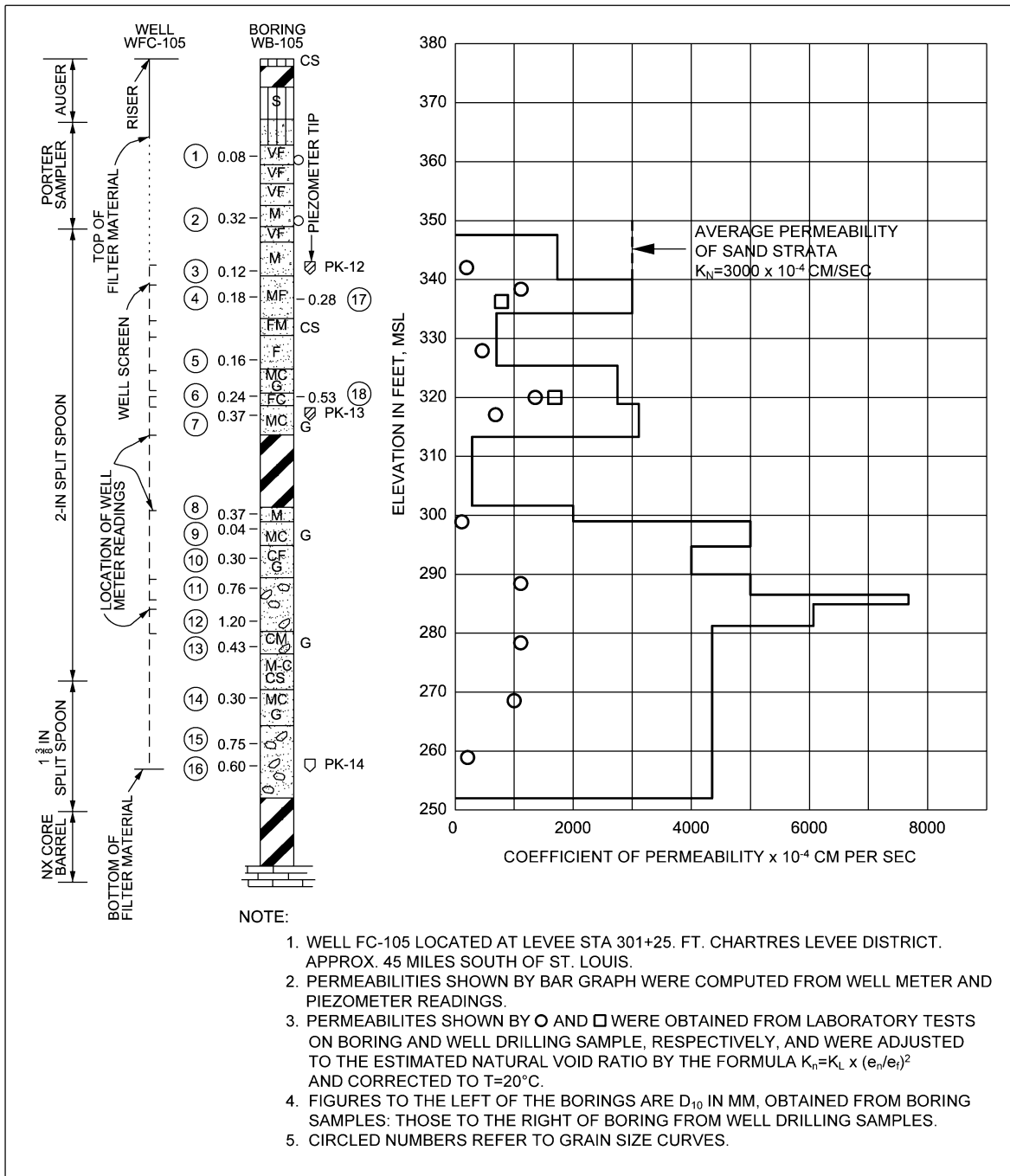


Figure 3-9. Permeability and effective grain size of individual sand strata, example from Well FC-105

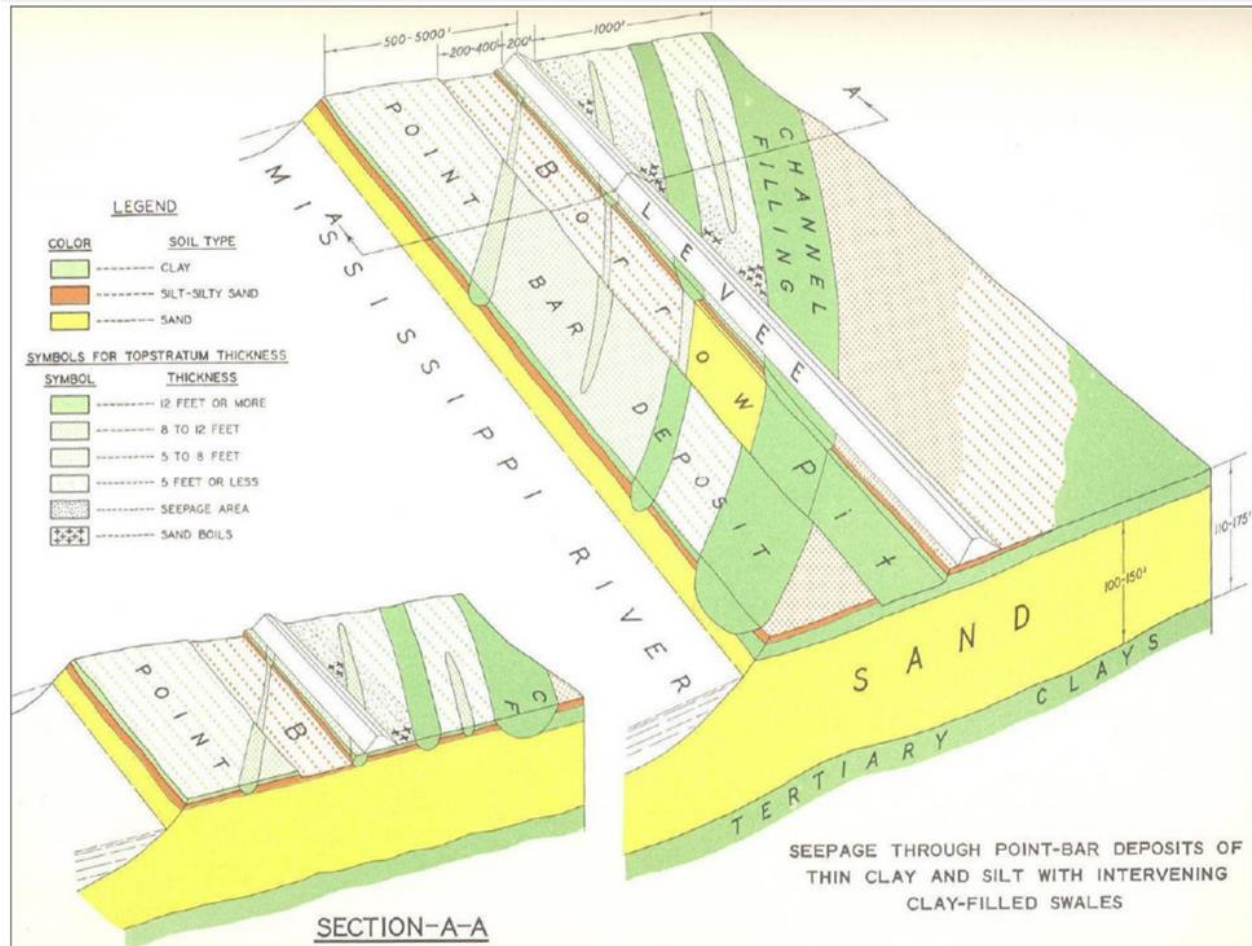


Figure 3-10. Seepage through point bar deposits

(3) *Pilot holes.*

(a) Before installation of a relief well system, pilot holes are typically drilled within 5 feet of each well location. These holes are usually sampled continuously or at frequent intervals (< 3 feet). Pilot holes are used to verify foundation conditions used for seepage analysis and relief well design. The holes also serve as a check on the design of the relief well filter pack, screen/slot sizes, and screened/blank intervals. Selected pilot holes should be extended into the layer underneath the aquifer to ensure that the thickness and characterization of the aquifer is understood. This is important for both full- and partial-penetration well designs.

(b) Pilot holes can be drilled during the pre-construction engineering and design phase. In this case, information from the pilot holes is included in the subsequent construction documents. Alternatively, pilot holes can be drilled during the construction phase with the final well design performed during well construction.

(4) *Reducing number of pilot holes.* A best practice is to drill pilot holes at all relief well locations. However, where there is high confidence in subsurface conditions,

risk-informed decision-making can reduce the number of pilot holes. Such cases include sites with extremely uniform geology, a high density of previous borings, and in areas adjacent to existing relief wells. Requirements and risk relating to using pilot holes should be addressed in the project design documentation.

c. *Entrance conditions.* The seepage entrance for a levee is often the river or riverside borrow pits and is normally simple to determine. The seepage entrance for a dam may not be as readily determined, depending on waterside borrow areas, presence of old channels, and the like. The effective entrance condition can be calculated as demonstrated in Appendix C for new projects or existing structures without performance or instrumentation data. On completed structures, the entrance condition can be estimated by extrapolating piezometric data to the project flood levels. Considering scour potential that could shorten the entrance condition is warranted in some cases.

d. *Exit conditions.* The landside top stratum is generally assumed to extend infinitely in the landward direction. An effective exit distance can be calculated using the methods described in Appendix C. Exceptions to the infinite case include evidence of a seepage block. For example, a bedrock high may block flow through the pervious layer and force seepage to exit through the blanket. Another finite case is a seepage exit (for example, a landside oxbow lake).

e. *Blanket characteristics.* The thickness and composition of the top stratum is a critical factor for determining seepage pressures in the pervious strata. Generally, flow through the top stratum is considered vertical and k_v is used for BT calculations. Transformations for a layered blanket are described in EM 1110-2-1913. Different permeabilities for horizontal and vertical flow in the blanket (anisotropy) can be directly accounted for in 2D FEM cross-section modeling.

f. *Blanket permeability.*

(1) The micro-level k of the blanket materials can be determined by laboratory tests on undisturbed samples. Field tests used for this purpose include cone penetrometer dissipation tests and sealed ring infiltration tests. Laboratory and field tests often indicate permeabilities up to several orders of magnitude lower than macro-level (“bulk”) k in the floodplain. The latter is influenced by natural defects such as pervious seams, previous sand boil activity, ground penetrations, small burrows, roots, etc.

(2) Macro-level k measured for Missouri and Mississippi river floodplains were several orders of magnitude higher than the micro-level k (USACE 1956a; USACE 1962). Macro-level k is measured at the scale appropriate to a relief well system. When micro-level values are used in analysis, they result in calculated heads higher than actual heads. The corresponding design results in more relief wells than may be required. The selection of appropriate blanket k values is further discussed in EM 1110-2-1913.

g. *Aquifer characteristics.* The thickness and k of the pervious (foundation) strata are critical factors in relief well design. Flow rate through the aquifer and well flow rates

depend on thickness and permeability of the aquifer. The flow magnitude, in turn, will influence the sizing of any collection systems and pump stations that are part of a design. Reducing uncertainty in foundation k can lower construction costs if wells and flow collection systems do not have to be over-designed. Chapter 9 further discusses the use of pump tests to determine aquifer characteristics.

(1) *Determining permeability.* Foundation k is best determined directly from aquifer pumping tests. An example of data derived from field pumping tests is shown in Figure 3–7. Field pumping test procedures for steady-state and transient flow conditions are given in United Facilities Criteria (UFC) 3-220-05 (which superseded U.S. Army 1983), Appendix C, and are further discussed in Chapter 9 of this manual. Additional information is given in EM 1110-2-1901. The k_v of aquifer materials can be measured in laboratory tests on undisturbed samples or field pumping tests (Mansur and Dietrich 1965). If a pumping test is not feasible, regional data for a formation (such as state publications) can be applied to the project site. Alternatively, aquifer k can be estimated from laboratory tests or correlations with grain size as described in EM 1110-2-1901 and EM 1110-2-1913. As noted in paragraph 3–4f above, these small-scale tests often underestimate the field-scale k .

(2) *Permeability assumptions.* Most analytical methods for relief well system design assume a uniform, isotropic aquifer. For full-penetration relief wells, this assumption does not result in substantially different results than for a layered aquifer. In both cases, flow to the wells is horizontal. However, for partial-penetration relief wells, aquifer stratification and anisotropy are critical considerations. The lower relative k_v values can have a significant impact on flow and head distribution around partial-penetration wells. Significant differences between k_h and k_v can be directly accounted for in FEM cross-section or 3D modeling. For a layered aquifer where absolute k values are uncertain, the designer should accurately estimate the relative k of the different layers. A reasonable assumption will usually result in calculated well spacing that achieves adequate factors of safety.

(3) *Stratified aquifers.* Many USACE projects are located on alluvial deposits, which are typically layered. These materials commonly grade coarser and become more permeable with depth. Pervious strata in glacial deposits can also have varying k with depth. In both cases the result is a stratified aquifer. Aquifer stratification should not be discounted in the design of partial-penetration wells until a sensitivity analysis is performed. The analysis should determine the differences between effective and actual well penetration, as discussed in Appendix D, for a range of reasonable strata permeabilities. The effects of stratification in the formation will be more pronounced for smaller well penetrations. The ability of different layers to transmit more or less flow relates to the aquifer transmissivity (Figure 3–2).

(4) *Aquifer transformation.* A stratified aquifer can be transformed into an equivalent uniform aquifer for relief well design. The total T of the actual and transformed aquifer is the same. The process also requires changing actual well penetration in the stratified aquifer into the equivalent effective well penetration in the transformed aquifer. Designers need to be aware that not using a proper transformation

provides extremely unconservative results for partial-penetration relief wells. This is discussed further in paragraph 3–5 and Appendix E.

3–5. Relief well penetration

USACE WES (currently ERDC) evaluated the effects of relief well penetration in uniform and stratified aquifers using physical models. These model studies are discussed in TM 3-430 (USACE 1956b). Key points are summarized in paragraph 3–5a. Relief well penetration can be iterated during system design to develop the most cost-effective system to balance number and depth of wells. Cost comparisons between a smaller number of deeper wells and a greater number of shallower wells can be made.

a. Relief well penetration in non-stratified aquifers. The physical model studies described in TM 3-304 showed that 50% penetrating wells in a uniform aquifer are nearly as effective as 100% penetrating wells. This implies that the additional pressure relief provided by deeper wells may not be as cost effective as additional shallow wells. However, a system of deeper wells may prove more resilient to biofouling and the resulting well losses. This is because there is typically more well screen in contact with the aquifer. To reduce well performance a given amount, more biofouling per foot of well screen is required in a deeper well.

b. Relief well penetration in stratified aquifers. TM 3-304 model studies and other field studies indicate that relief wells must penetrate the main water-bearing strata in the aquifer to be most effective. The goal should be installing wells that penetrate at least 50% of the stratum with the highest T . These wells will be nearly as effective as wells that penetrate 100% of this stratum. Design analysis using a transformed aquifer must also incorporate the actual well penetration, as discussed above and in Appendix E.

3–6. Performance monitoring

Monitoring the performance of relief well systems is critical to ensuring the system will provide the intended pressure relief. The ideal condition for monitoring is when the structure is retaining water. Piezometers and flow monitoring are typically the best ways to monitor performance. Piezometers should be located near the middle and ends of the relief well system. Individual piezometers can be screened in shallow or deeper zones of the aquifer, depending on aquifer stratification and zones of interest by the analyst. Flow monitoring may be performed at individual wells with a flow meter or overflow weir. Combined relief well system flow can be monitored with weirs and flumes on collector ditches or pipes.

Chapter 4

Risk Considerations for Relief Wells

4–1. Introduction

a. USACE has adopted a risk-informed approach for new designs and/or modifications to its dam and levee systems. This approach does not replace the need for deterministic design requirements. Instead, a risk-informed approach supplements these requirements by identifying, evaluating, and effectively reducing risks associated with the project. Although formal risk assessment is relatively recent in well design, good practice has always included many of the risk considerations presented in this chapter.

b. Evaluation of relief well design using performance measurements during high-water events does not require a formal risk assessment. Comparison of relief well flow and piezometer readings with design values should be a routine activity after every high-water event. The same is true for making observations of sand boils after such events. Paragraph 4–10b includes an example of how to extrapolate well flow and piezometer measurements to the design elevation as recommended in ER 1110-2-1942.

c. USACE calculates the risk associated with the presence of a dam or levee as the function of three distinct quantitative components:

- (1) The probability that a certain water level (pool or flood) will occur (the hazard);
- (2) How the dam or levee will respond to the event—the likelihood of project failure (the performance); and
- (3) The loss of life, economic losses, and environmental impacts that could occur as a result of inundation (the consequences).

d. It is not the intent of this chapter to explain the risk quantification process for any of these three components; instead, guidance and recommendations are provided on how relief wells influence risk.

4–2. Risk assessment methodology

a. The Risk Management Center (RMC) is a center of expertise in USACE. The RMC is responsible for developing, disseminating, and training of risk assessment methodology used in the Dam and Levee Safety Programs. A description of the risk analysis process can be found in Best Practices in Dam and Levee Safety Risk Analysis (U.S. Bureau of Reclamation [USBR] and USACE 2019), and ER 1110-2-1156. Additional information is given in the latest Dam and Levee Safety Program guidance documents.

b. Including risk assessment in the design phase allows risk drivers to be identified and risks (structural and non-structural) to be reduced efficiently. Identifying high-risk projects in the design phase also allows designs to incorporate higher safety factors.

c. This chapter provides information on how risk is incorporated into the design and evaluation of relief well systems. Risk considerations are also addressed throughout this manual regarding design, installation, operation, and maintenance of wells.

4–3. Potential failure modes

a. *Overview.* Potential failure mode (PFM) is defined in ER 1110-2-1156. A failure can lead to uncontrolled release of water from a dam or levee resulting in life loss or economic/environmental damages. The word “failure” as used in PFM refers to a system failure, which is broader than only catastrophic breaches of dams or levees. USACE also considers failure to include those cases in which inundation resulted in consequences even though no breach occurred. Alternately, failure can result in loss of service for navigation and other structures where wells may be used to reduce uplift. Flooding due to levee overtopping or dam spillway flow is not related to relief wells, and is therefore outside the scope of this manual.

b. *Applicability.* Multiple USACE Districts are responsible for the design, evaluation, construction, inspection, or modifications of relief wells. These Districts should develop an understanding of related PFMs and how the probability of failure can be reduced.

c. *Backward erosion piping.* The purpose of relief wells is to relieve uplift pressure acting on a structure or to reduce the likelihood of uncontrolled seepage beneath a dam or levee. If not controlled, excess pressure can lead to breach due to internal erosion. A common internal erosion failure mode for dams and levees is BEP. This failure mode initiates by heaving of the blanket and transportation of underlying sand to breach the embankment. Figure 4–1 illustrates BEP. The specific and differing aspects of internal erosion are not covered in this manual. See the comprehensive discussion of this topic in Best Practices in Dam and Levee Safety Risk Analysis (USBR and USACE 2019).

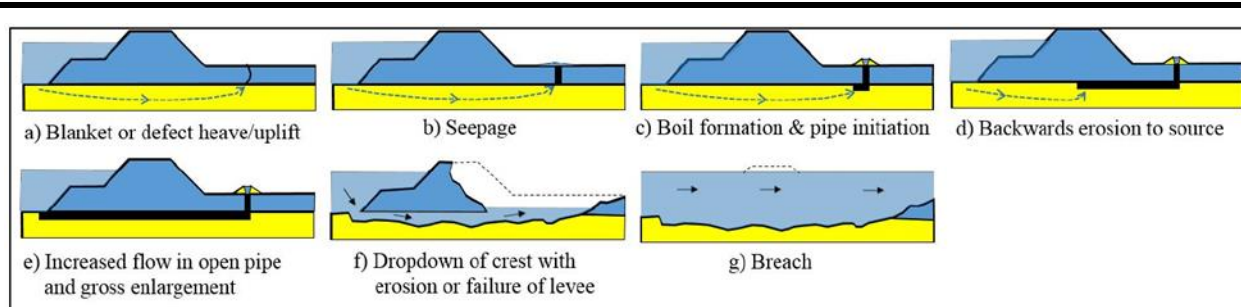


Figure 4–1. Internal erosion of the levee foundation materials due to underseepage (adapted from van Beek et al. 2010)

d. Detection and intervention. If developing failure modes are detected before progression is complete, it may be possible to intervene and prevent the failure or limit the breach. However, it is preferable to use a risk-informed process to reduce the risk associated with a dam or levee over time.

e. Failure mode descriptions. Failure mode descriptions contain an overview of the load, failure mechanism, and consequences that are specific to that site. The general PFM descriptions explain the failure path from initiation of load to breach of the dam or levee. Also included with the general failure modes are some aspects of design performance that are not failure modes themselves but can contribute to the PFMs.

f. Relief well specific failure modes. Most internal erosion PFMs that pertain to a dam or levee system are applicable either with or without the presence of wells. Additional relief well-related failure modes include mechanisms that result in removal of surrounding foundation soil into the well. This can include collapse of a well, a defective seal, improper filter design, and the like. Progression of such failure modes can lead to a collapse of the embankment crest or collapse of a floodwall monolith(s). A well system failure that does not result in breach may still inundate areas with an uncontrolled release of water. In addition, improperly designed or constructed collector systems have rendered a series of wells inoperable during a flood event.

g. General potential failure modes. A few general PFMs are provided in this chapter. These general PFMs are provided as a guide and do not present an all-inclusive list. They are intended to describe the general failure modes that are addressed by the guidance in this manual. For a particular project, critical loadings and failure mechanisms should be developed and included as part of each PFM description.

h. Potential failure mode analysis. A potential failure mode analysis (PFMA) will be performed as part of any risk assessment. In the absence of a risk assessment, a PFMA should be performed as part of the design process for all projects. The level of the PFMA can be scaled to the project. All PFMs must be addressed in the design. As the design develops, it should be continuously reviewed to assure that all PFMs are being addressed.

4-4. Event trees

a. In their most basic form, breaching PFMs must have at least three elements present:

- (1) A load must be applied, such as water during a flood or reservoir impoundment;
- (2) A flaw or defect must be present or develop over time; and
- (3) The flaw must be able to initiate and progress to breach.

b. Each PFM potentially leads from a flaw to a breach or inundation. It is helpful to expand the basic elements into an “event tree” comprised of several detailed steps. Non-breaching PFMs are similar but do not result in failure of a dam or levee.

c. Figure 4–2 illustrates an example of a failure mode event tree developed for the common BEP failure mode described above. This example event tree is provided to illustrate the following discussions and should not be considered a standard. The project’s risk assessment team should develop a project/site-specific failure mode event tree to ensure project and site-specific issues are considered.

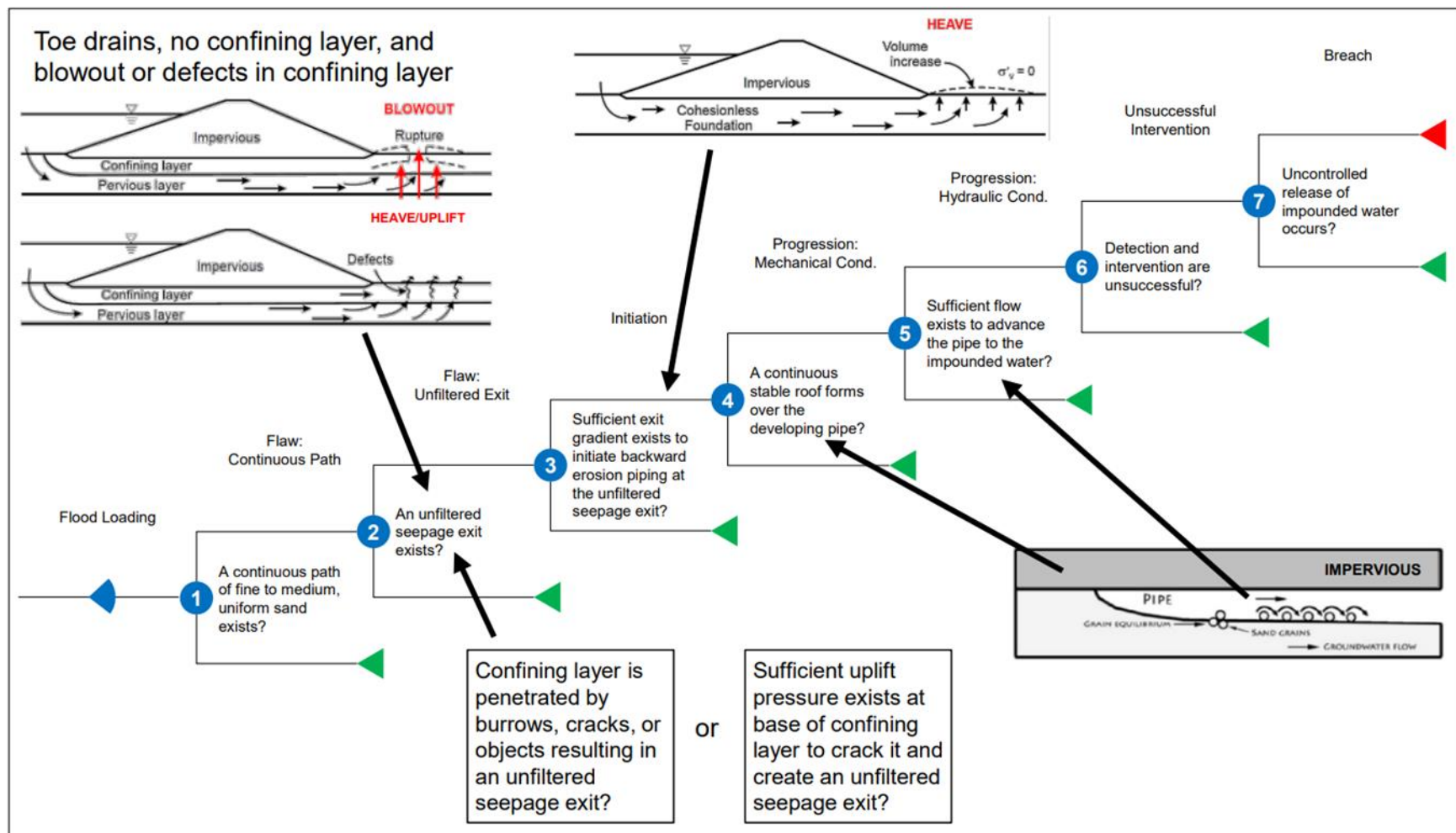


Figure 4–2. Backward erosion failure mode event tree (USBR and USACE 2019)

4–5. Relief well purpose

a. *Overview.* The primary purpose of relief wells is to reduce seepage uplift pressure and hence, vertical gradients in the foundation. This, in turn, reduces the probability of initiation (Node 3 in Figure 4–2) and progression (Node 5). The relief well may also reduce or eliminate an unfiltered exit (Node 2). This is due to the majority of seepage flowing to the well screen and surrounding filter pack at depth. However, proper design and construction is critically important because of the large flow and gradient toward the well. These large gradients increase the potential for BEP if a defect occurs and the well itself becomes an unfiltered exit. Screening wells at some distance below a surficial blanket layer may reduce risk associated with a roof layer if a flaw develops in the screen (Node 4). Well systems can also reduce risk through detection and intervention (Node 6).

b. *Node 1 – Flaw: Continuous Path.* The probability that a continuous, cohesionless, pipeable layer exists is independent of the presence of a relief well system. However, such a feature may be verified by site-specific exploration and testing associated with well installation.

c. *Node 2 – Flaw: Unfiltered Exit.* Where excess gradients exist at the landside levee toe or downstream dam toe, heave/blowout of the foundation can occur with subsequent creation of an unfiltered exit. In a properly designed relief well system, most of the seepage flow exits the foundation through the filter pack into the well screen. This reduces the probability of excess gradient and development of an unfiltered exit through the blanket. It is important to employ the best practices for well development outlined in Chapter 8 of this manual. This ensures the filter pack and well screen is stressed beyond levels that the well will experience during normal operations. A properly designed filter pack that has been successfully developed will perform as a filtered exit for the life of the well.

d. *Node 3 – Initiation.* The relief well design process reduces the vertical seepage gradient through the landside blanket. The critical location is typically midway between relief wells. Reducing the vertical seepage gradient at the downstream dam toe or landside levee toe reduces risk related to Node 2 and/or Node 3. The extent of the risk reduction depends on the geotechnical characteristics of the substratum, the relief well spacing, and water level loading on the embankment. The current relief well design process can be adapted to the first-order second-moment (FOSM) analyses technique to capture the variability of the probabilistic factors used in the well analyses. This technique determines the probability the critical gradient will be exceeded midway between the wells for a given well spacing. An example of the FOSM analysis for relief wells is included in Guy et al. (2010).

e. *Node 4 – Progression: Mechanical Condition.* An advancing pipe may either clog or self-heal. The probability that a continuous, stable roof exists is due to site geology and independent of the presence of wells. Paragraph 3–1 mentions that relief wells are typically used where there is a fine-grained top stratum landside of the

embankment. If a surficial clay blanket exists from riverside to landside of the levee toe or dam, the probability of this node typically remains high for all elicitations.

f. Node 5 – Progression: Hydraulic Condition. There may be some type of flow-limiting feature in the foundation or topography. However, in most cases, progression of a backward-eroding pipe to the source is limited only by the hydraulic condition. For most instances where relief wells are considered, this node becomes whether the aquifer will supply sufficient flow for BEP to continue.

(1) *Evaluation.* The value for this node depends on many site-specific variables, including the site’s geologic and anthropologic history. Also relevant are geometry (levee width, effective seepage entrance, aquifer thickness, seepage exit, etc.), and the nature of the foundation materials. Aquifer stratigraphy, permeability and anisotropy, topographic conditions, hydrology, flood history, and previous seepage and sand boils have impacts as well.

(2) *Use of wells.* Relief wells are traditionally designed to reduce piezometric head under, and reduce vertical gradient through, the landside blanket. Relief wells rely on artesian conditions to function passively. Relief wells provide limited flow and pressure relief where no landside blanket is present, or where the blanket is thin and compromised. If wells are pumped or discharge at a low elevation, they may be effective when located between the source and known problem areas that have little to no confinement. Generally, other alternatives are more appropriate than relief wells when there is not adequate confinement. Mitigation alternatives when relief wells are not appropriate are provided in EMs 1110-2-1901 and 1110-2-1913.

(3) *Horizontal gradient.* For Node 5, the probability of backward erosion progression is estimated using empirical methods from USACE’s RMC Best Practice documents. These techniques incorporate the uncertainty in the horizontal gradient within the layer where backward erosion progression occurs. Modeling and research in this area continue to improve. The change in local horizontal gradient due to relief wells are not yet included in Best Practices in Dam and Levee Safety Risk Analysis (USBR and USACE 2019). Detailed 2D or 3D seepage analyses may be required to estimate localized gradients in the foundation when BEP is assumed to have initiated. Example seepage models with boils between wells are included in paragraph 4–8.

g. Node 6 – Unsuccessful Intervention. Although represented as a single node immediately before breach, intervention can occur anywhere in the BEP process. Intervention at any stage requires both detection and a response.

(1) *Detection of need for intervention.* Relief wells may fail to prevent heave/blowout of the blanket. This node is generally elicited as if the wells were not present. However, the presence of the relief wells may increase the frequency of flood fight inspections compared to a non-well reach. If the blanket has heaved with attendant sand boils or if the well filter pack has failed, sand may be visible at the surface. If the well is producing observable amounts of sand due to failure of its filter pack (a “sander”), it must be prevented from flowing. This action will raise uplift pressure and

increase the probability that foundation heave/blowout will occur. However, a potential heave failure is generally preferable to allowing a known filter pack failure to progress.

(2) *Action taken for intervention.* Relief wells provide an opportunity to install mechanical pumping systems and further reduce seepage uplift pressure. Wells can be pumped by air lifting, submersible pumps, or a suction header system. In all cases, pumping the relief wells reduces the probability of heave/blowout.

h. Node 7 – Breach. The probability that a levee or dam breach will occur is independent of the relief well system. Instead, it depends on the materials used to construct the levee/dam and the foundation materials underlying the structure. This is informed by site specific exploration and testing.

i. Design. All nodes in the event tree should be evaluated for various relief well spacings and screened intervals. Well spacing can be optimized for a series of factors of safety and cost parameters. Relief wells are required to be designed to provide a minimum vertical gradient factor of safety (FS_{vg}) at the levee or dam toe, generally including consideration or allowance for future performance degradation. This criterion is provided in EM 1110-2-1901 for dams and in EM 1110-2-1913 for levees, as described in paragraph 3–1b.

j. Loading. The hydrologic event trees developed for the baseline risk assessment should be used to calculate total risk. This applies for each design alternative for each effected node. The elicited PFM scenario system responses for each alternative described are input into the event tree to calculate total risk. There should be no changes to economic or life loss consequences from the baseline condition. The estimated annual probability of failure and annualized incremental life loss for each design alternative should then be summarized. This is necessary to see the overall effectiveness of each design alternative.

4–6. Well-specific potential failure modes leading to breach

a. PFM-1 – Well Collapse.

(1) *Failure mode description.* Inferior material selection and improper installation result in a damaged relief well screen. Pool or river rises result in a critical head differential across the dam or levee. There exists a layer of pipeable soil underneath the embankment. The damaged portion of the well becomes an unfiltered exit. A continuous stable roof is formed by the base of the compacted embankment. Alternatively, there are sufficient fines in the waterside or landside soils along the erosion pathway outside the embankment footprint that can support a roof. Material in the foundation fails to clog the pipe. Horizontal flow and gradient are sufficient to continuously transport eroded soil particles to the exit. The pipe advances to the waterside. Detection and intervention are unsuccessful. The pipe enlarges and the embankment collapses leading to breach due to uncontrolled flow over the collapsed dam or levee.

(2) *Event tree.* The example event tree for PFM-1 in Figure 4–3 illustrates the dissection of the failure mode into discrete steps. Note that although intervention is shown near the end of some examples, the failure process may be interrupted earlier. Persons responsible for the selection, design, installation, inspection, maintenance, repair, rehabilitation, and abandonment of relief wells should be trained to understand well-related PFMs. This includes the sequence of events as visualized in an event tree. This understanding can be applied to lower the probability of poor performance and/or failure over the life of the well.

(3) *Relief well materials.* Relief wells manufactured of wooden components were installed throughout the USACE Mississippi and Missouri River Valleys in the 1950s. Many of these wells have served successfully for nearly 70 years, although many others have been replaced over time. High sanding rates or other signs of distress have raised concerns of structural failure of the wooden well screen or wooden riser pipe. This can lead to an unfiltered exit at the well. Stainless-steel wells, first installed widely in the early 1970s, are stronger and should provide longer service lives than their wooden predecessors. Plastics and other materials inferior to stainless steel are sometimes considered due to their lower initial cost but are more likely to collapse.

(4) *Dissimilar materials.* Dissimilar materials such as stainless screens joined with carbon steel risers or blank sections may lead to corrosion of the carbon steel and defects in the well.

(5) *Nodes 1 and 2.* High water acting across the embankment and a continuous layer of erodible soils are conditions that do not change with the presence of the relief well.

(6) *Node 3.* A defect in the well screen, casing, or seal allows the unfiltered movement of soil either into the well or to the ground surface.

(7) *Node 4.* The likelihood of a continuous roof is unchanged by the presence of a defective well seal. Such a condition allows movement of soil to the ground surface. For the case of well collapse, the defect may be a distance below the base of the blanket. A failure mechanism involving a deeper failure path may have a lower probability than directly beneath blanket.

(8) *Node 5.* The likelihood of clogging is unchanged by the presence of a defective well seal. For the case of well collapse, the well may fill up with material rather than flush to the surface. After the volume of eroded material reaches the elevation of the defect, this failure mode would stop. However, in this condition the well will no longer provides the intended pressure relief. Another consideration is if the eroded sand is very fine, there could be adequate flow to flush this material to the ground surface.

(9) *Node 6.* The likelihood of progression from the source to the well differs from the no-well scenario. The same is true for progression from the well to the ground surface. Considerations listed in paragraph 4–5h are affected by the presence of the well and failure mode.

(10) *Node 7.* Detection and intervention differs from the no-well scenario. Wells should be inspected during high-water events for foundation material deposited around the well.

(11) *Node 8.* The flow from deeper portions of the well could contribute to gross enlargement of a pipe to an improper seal. Pipe enlargement may be limited for failure modes that include defects into the well.

b. PFM-2 – Finer Fraction of Filter Suffuses and Clogs Collection System.

(1) Failure mode description.

(a) Pool or river rises for several loading cycles or for a long duration. The smaller or finer fraction of the filter pack suffuses out due to high localized gradients adjacent to the well screen. This material is finer than the slot size of the well screen and enters the well and into the collection system. Sand pack material continues to enter the well and fill the well and move into the collection system limiting its effectiveness. The collection system is unable to freely discharge and provide pressure relief. Localized pressure gradients near the relief well are enough to heave the surficial soils and create an unfiltered exit. Finer soils particles migrate out the exit under the high exit gradients as backward erosion and piping progresses within the foundation working back beneath the embankment or structure.

(b) If the relief well has surface discharge ports, sediment may be visibly seen transporting out with discharging groundwater during flow events. Sediment transport continues, and a pipe forms within the substrate undermining the embankment or structure until it connects to the pool. Gross enlargement occurs causing a rapid increase in sediment transport, velocity, and pipe enlargement eventually causing foundation settlement leading to overtopping and breach.”

(2) Detection. Routine soundings of relief wells and maintenance of the collection system, if employed, are an effective early detection measure to reduce the likelihood of this failure mode.

(3) Design and installation. A properly designed and constructed well according to Chapters 7 and 8 of this manual should not experience this type of failure.

c. PFM-3 – Finer Fraction of Foundation Suffuses and Leads to Loss of Foundation Soil.

(1) Failure mode description.

(a) Pool or river rises several loading cycles or for a long duration. A finer sediment matrix that supports larger grained material in the formation is present. The smaller or finer fraction suffuses out due to high localized gradients adjacent to the well screen. The filter is either too coarse or has a gap that allows this material to reach the screen. Insufficient well development can lead to later settlement of the filter pack resulting in a gap below the plug. The fines are smaller than the slot size of the well screen and

enters the well. Foundation material continues to enter the well and fill the well and then starts to accumulate in the collection system reducing the effectiveness of the relief well system in and around this well point.

(b) As the collection system fills, sediment may start discharging out the surface discharge pipes with groundwater. Localized pressure gradients increase due to the relief wells ineffectiveness and surficial soil material heaves creating an unfiltered exit with high exit gradients that transports foundation soils as backward erosion develops and progresses. Sediment transport continues forming a pipe that migrates back beneath the embankment or structure toward the pool. When the pipe connects to the pool, gross enlargement occurs with rapidly increasing velocities and sediment transport until the foundation settles, causing the structure to overturn or the embankment structure to overtop and breach causing an uncontrolled release of the pool.”

(2) *Detection.* Routine soundings of relief wells are an effective early detection measure to reduce the likelihood of this failure mode.

(3) *Design and installation.* A properly designed and constructed well according to Chapters 7 and 8 of this manual should not experience this type of failure.

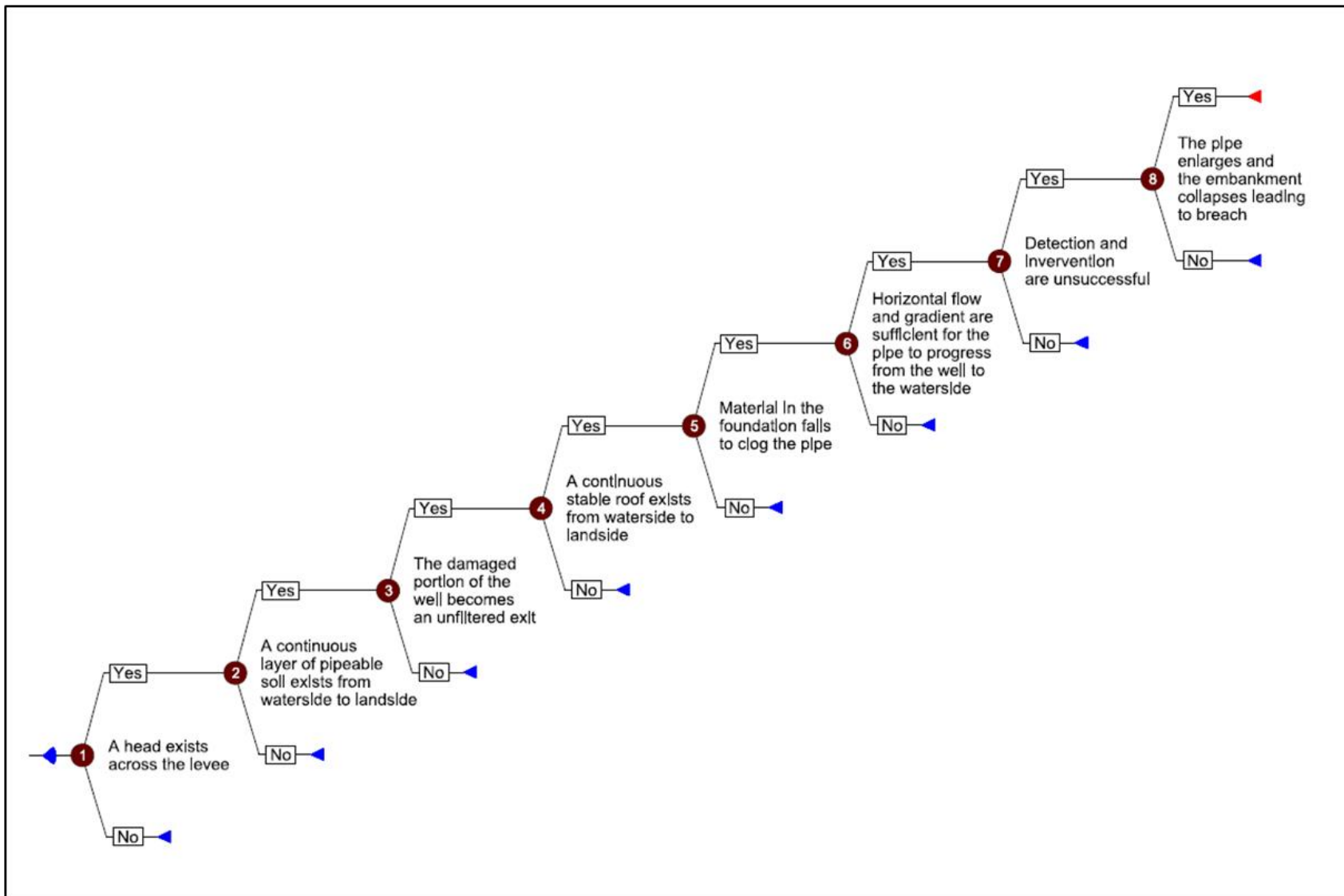


Figure 4-3. Event tree for potential failure mode-1, relief well collapse

4-7. Evaluation factors

a. Excess hydrostatic pressures can develop in pervious foundation strata overlain by less pervious top strata. Relief wells have been used extensively since 1942 at USACE structures to relieve such pressures. Relief wells may be used in combination with other underseepage control measures, such as upstream blankets, downstream seepage berms, cutoffs, and grouting. Relief well systems require a minimum of additional real estate as compared with other seepage control measures such as berms and blankets. Relief wells provide a flexible control measure as the systems can later be expanded within that real estate footprint. Any comparison of alternatives should consider the following factors when evaluating estimates of risk reduction:

- (1) Robustness;
- (2) Redundancy;
- (3) Resiliency; and
- (4) "Do no harm."

b. While the above factors are described in ER 1110-2-1156, other factors include:

- (1) Completeness and effectiveness;
- (2) Efficiency; and
- (3) Acceptability.

c. The last three factors are described in ER 1105-2-103. Designability, constructability, and long-term operation and maintenance should also be considered as evaluation factors for any seepage mitigation alternative. The future without action condition is also included as an alternative for comparison.

(1) **Robustness:** The ability of a system to continue to operate correctly across a wide range of operational conditions with minimal damage, alteration, or loss of functionality. Relief well systems commonly fit this definition. Relief wells routinely provide seepage control at hydraulic load levels less than the maximum design level. To increase capacity, relief wells have been pumped or airlifted and surface-discharged, if needed. Robustness in a relief well system can be improved by reducing well spacing and adding wells.

(2) **Redundancy:** Duplication of critical components of a system with the intention of increasing reliability of the system. This is usually accomplished with a backup or failsafe. Redundancy in seepage control means employing more than one method to remediate more than one node of the BEP event tree. For example, redundancy can be achieved by using relief wells in conjunction with seepage berms and/or filter blankets. Relief wells reduce the likelihood of heave (unfiltered exit). Berms and/or filter blankets elongate the seepage path and add weight to the landside levee toe or the downstream

dam toe. This limits the possibility of initiation and lowers the possibility of piping progression.

(3) **Resiliency:** The ability to avoid, minimize, withstand, and recover from the effects of adversity, whether natural or man-made, under all circumstances of use. Paragraph 7–9 describes the reduction in well efficiency over time, and resilient well designs account for this loss. Relief wells also exhibit resiliency if the filter pack and screen are sized correctly and remain in place for hydraulic loads in excess of the design load. Relief wells with subsurface outlets are resilient when they can overflow and surface-discharge if the subsurface outlet and/or conveyance systems are overwhelmed. To increase capacity, relief wells can be pumped and surface discharged, if needed. Care should be taken to prevent collapse of the well during pumping, which could lead to PFM-1 as described in paragraph 4–6a. Wells can be designed to accommodate pumping and use stronger screen and riser materials.

(4) **Do no harm:** The principle of “do no harm” must underpin all actions intended to reduce dam safety risk (ER 1110-2-1156). Relief wells meet the objectives of “do no harm” when the wells are installed according to ER 1110-1-1807 and follow the design, construction, operation, and maintenance guidance in this manual.

(5) **Completeness:** The extent to which a risk and management plan accounts for all investments or actions required to meet risk objectives. Relief wells typically meet this definition because they can be designed and constructed to withstand assumed adverse effects existent at the project. In addition, they are resilient in their ability to perform during hydraulic loads in excess of the design life. Finally, if properly operated, maintained, and rehabilitated, they will be sustainable longer than the wood-stave wells installed in the 1950s. Many of those wells are still in use today.

(6) **Effectiveness:** The degree to which the alternative contributes to achieving the planning objectives. Relief wells are an effective alternative for flood risk reduction projects because they reduce the life safety risk prior to overtopping. Relief wells reduce the probability of breach due to various failure modes that are worsened by excessive seepage or uplift pressure.

(7) **Efficiency:** The extent to which an alternative plan is the most cost-effective means of achieving the objectives. The relief well filter packs and screen opening size can be designed against the in situ formation soils to further increase performance. To remain efficient, relief wells require periodic maintenance to address clogged screens, bacterial growth, or carbonate encrustation. The maintenance and scheduled replacement add to the long-term costs.

(8) **Acceptability:** The extent to which the alternative plans are acceptable in terms of applicable laws, regulations, and public policies. Relief wells are generally acceptable to all federal, state, and local policies. However, local sponsors may not consider relief wells acceptable due to technical or financial limitations in completing required maintenance. Robustness, redundancy, resiliency, and effectiveness depend on routine

and proper maintenance. Defects need to be identified and corrected as part of maintenance. Corrections during loading are generally very difficult or not possible.

(9) Relief well durability and performance have substantially increased since 1980. This is due to the widespread acceptance of corrosion-resistant, stainless-steel well screens, risers, and surface housings. Stainless steel remains physically and economically serviceable much longer than common materials used in the past. These include wood stave construction, punctured iron pipe, and saw-cut PVC. High quality, non-carbonate filter materials used as filter packs will remain serviceable unless clogged by biofouling.

d. For example, TM 3-424 (USACE 1956a) evaluated several seepage mitigation alternatives: wells, berms, relief trenches, cutoffs, and upstream fill. As the tools in the following section continue to improve, they should be considered in these types of comparisons.

4–8. Long-term considerations

Consideration should be given to the following regarding long-term relief well risk management: reduction of flow capacity, well screen failure, filter failure, impeded discharge, and collector system issues.

a. Reduction of flow capacity: biofouling, encrustation, and products with low open area (such as saw-cut PVC).

b. Well screen failure: rusting of ferrous screens, splitting of wood screens, crushing, and damage during development or rehab.

c. Filter failure: flawed design (such as stability criteria) and construction problems (such as borehole sloughing, partial collapse, borehole gouged by equipment).

d. Impeded discharge: surface housing damaged (mowers, future construction, etc.), malicious tampering or vandalism, and clogging of discharge conveyance (such as collector ditch overgrown, collector pipes silted in or collapsed).

4–9. Collector system issues

Subterranean discharge and collection systems do not allow direct observation of relief well flow to observe for either reduced flow conditions or the discharge of sediment indicating failure of a well component. Additionally, EM 1110-2-2902 describes the inherent risk that buried pipe could have a defect that leads to dam or levee breach.

4–10. Operation and maintenance considerations

a. Background. Operation and maintenance of relief wells is described in Chapter 11. The importance of proper operation and long-term maintenance for relief wells is documented in TM 3-424 (USACE 1956a) and TM 3-430 (USACE 1956b). The recommendations in those documents have changed little over time. The guidance

assumed a reduced well efficiency of 80% of the installed specific capacity as determined by pumping tests. Pumping tests were recommended for 15% of wells annually so that every well is tested every 5 to 8 years. Subsequent pumping tests of “target wells” over the following decades validated those assumptions.

b. Evaluation of well condition on system performance. Any reduction in efficiency beyond the value assumed in design results in a factor of safety lower than the threshold value. The reduction in well efficiency should be considered when evaluating Node 3 in paragraph 4–5d. The following section includes an example to visually represent data in a manner to support the requirement in ER 1110-2-1942: “The values obtained from measurement of piezometric levels and flow quantities should be extrapolated to predict the values that would be produced by a maximum design reservoir level or river stage.”

c. Harrisonville example consolidation of well and performance data. Figure 3–1 in this manual shows a half-mile reach of the Harrisonville Levee District. The figure has been adapted from USACE 1956b. The figure demonstrates the importance of geomorphology in the design and location of relief wells. TM 3-430 Vol. 2 (USACE 1956b) design plates combine a profile along the landside levee toe with geomorphology, boring, piezometer, seepage berm and relief well information.

(1) *Location.* The reach of Harrisonville Levee for this example is depicted on the map in Figure 4–4. Figure 3–1 is a subset of one of several design plates for this levee system in TM 3-430 Vol 2 (USACE 1956b). This levee system is one of several systems along the Middle Mississippi River in that design document. This synthesis of information compiled for over 200 miles of levee improvements is useful for the evaluation of levee system performance data.

(2) *Foundation conditions.* These original design plates include a profile along the levee toe, showing the composition of blanket soils and underlying pervious substratum. The blanket soils for this reach are shown in Figure 4–5, and it is apparent the blanket along this reach includes two abandoned sloughs filled with clay. The clay-filled sloughs that cross under the levees do not allow seepage and pressure relief, and sand boils are often found adjacent to these features. Relief wells are frequently located along this boundary between the clay-filled sloughs and surrounding sand, where the overlying blanket soil is thin.

(3) *Intermediate fine sand layer.* The composition of the green “silty and very fine sand” shown in this profile is of particular concern. TM 1-184 (1941) states in paragraph 39: “When there is enough pressure and the supply of water from the pervious strata (shallow or deep) is sufficient, piping will develop through the fine sands lying immediately under the impervious surface stratum.” This sand is often too fine to screen, explaining why these relief wells have blank sections through this upper portion of these wells (indicated by black dots in Figure 4–5). The intermediate sand layer is described in Chapter 2 as a historical topic of concern (USACE 2002).

(4) *Piezometer readings.* BT design calculations summarized in TM 3-430 (USACE 1956b) include the design river and tailwater that should be compared to any high-water piezometer measurements. The red line in Figure 4–5 indicates the $FS_{vg} = 1.0$ condition and the green line indicates the design threshold of $FS_{vg} = 1.3$. Piezometer readings from the 1973 flood (green squares), the 1993 flood (blue diamonds), and the 1995 flood (orange circles) have been extrapolated to the design river elevation and included in this figure.

(5) *Sand boils and observed seepage distress.* Also depicted in Figure 4–5 are locations where sand boils have been observed (yellow circles). USACE continues to improve data collection during high-water events. This information is typically not used to great benefit beyond flood-fight activities until a full risk assessment is performed. The evaluation of performance data should be included in any evaluation of relief wells. The size, color, and symbols used could be varied to depict the type and severity of observed distress.

(6) *Well flow and pumping test data.* Like piezometer data, well flow data from high-water events should be extrapolated to the design flood or reservoir pool. This is shown in Figure 4–6 using the same symbols used for piezometer measurements; 1973 flood (green squares), the 1993 flood (blue diamonds), and the 1995 flood (orange circles). The blue line is the design flow for wells at these locations. The specific capacity ratio (SCR) is often used as indication of well efficiency and discussed further in Chapter 9. Also shown in Figure 4–6 is the ratio of the most recent specific capacity to the original, along with the design threshold of $SCR = 80\%$.

(7) *Consolidation of performance and observation data.* Levee performance evaluation requires an understanding of all available design, condition, and performance information. Using the format pioneered by TM 3-430 (USACE 1956b), pumping test data can be shown at each well location, as is shown for Harrisonville in Figure 4–7. This figure also includes (as shown from bottom to top) the percentage of original specific capacity, measured well flows, and piezometer data. Piezometer and well flow data is extrapolated to the design river elevation to compare with design values. The piezometer levels are plotted along with the factor of safety (FS) = 1 (red) and the original design target value $FS = 1.3$ (green). The figure also includes observed sand boil locations, along with design river elevation (brown) and assumed tailwater (blue).

(8) *Data synthesis.* Although Figure 4–7 includes several sources of information, there is great benefit to consolidating into a single image. Similar images would then be created for every reach in the levee system. The analyst can rapidly compare observed piezometer and well flow data with design values, well condition, and areas of noted poor performance. These types of figures could be automated to provide information on the full Alton to Gale system, which would support flood-fight activities and post-flood assessment.

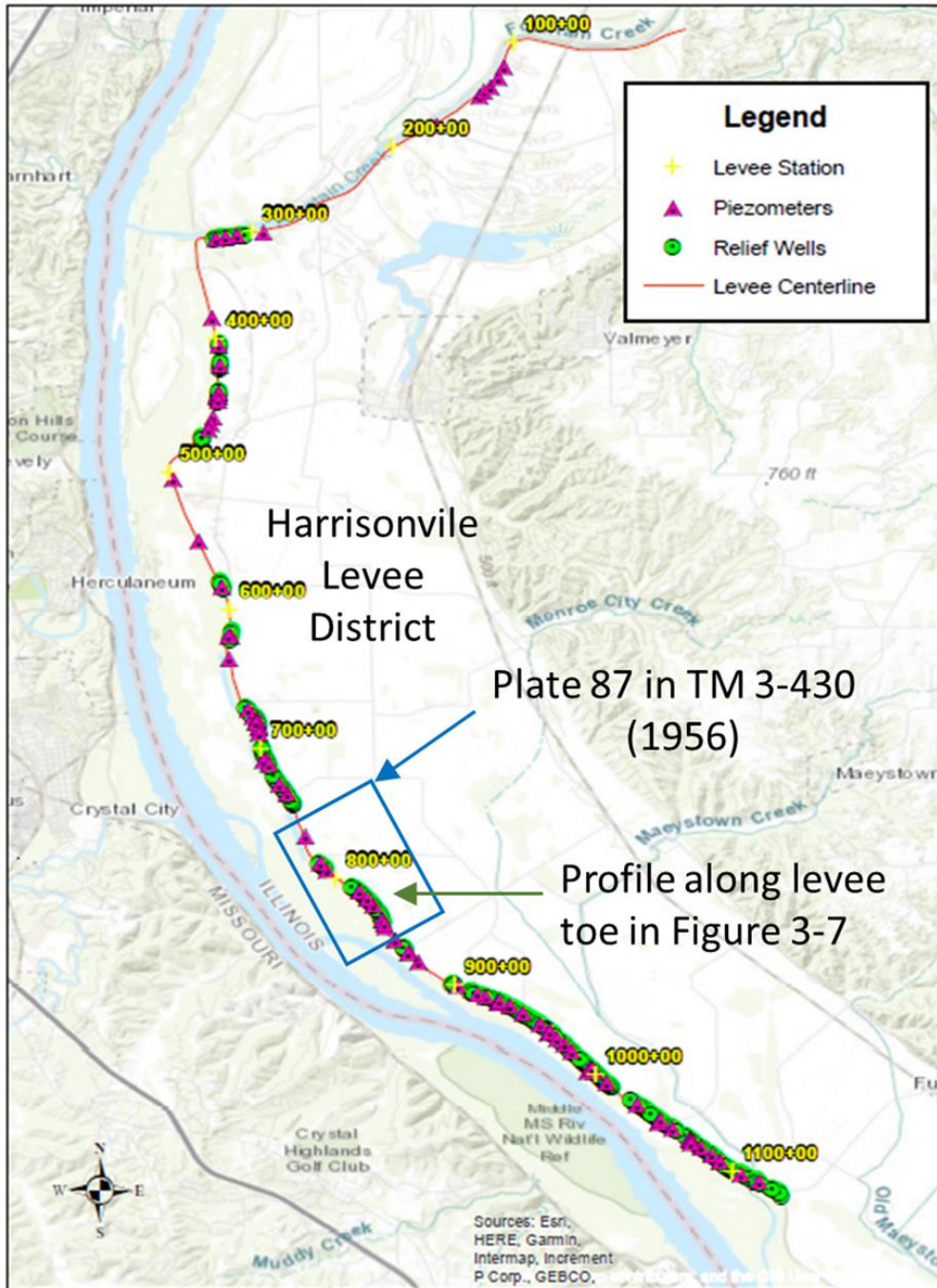


Figure 4-4. Location of Harrisonville example levee reach

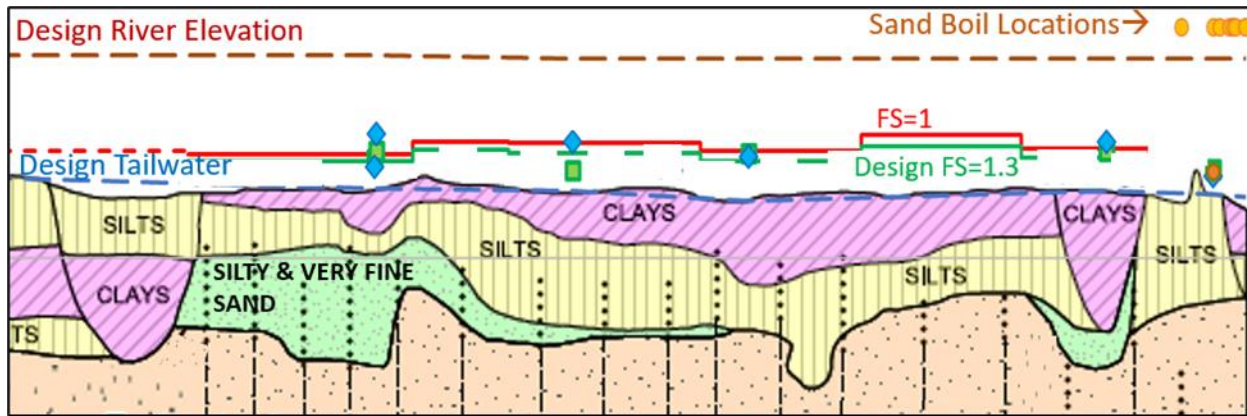


Figure 4-5. Comparison of extrapolated piezometer readings with design factor of safety values

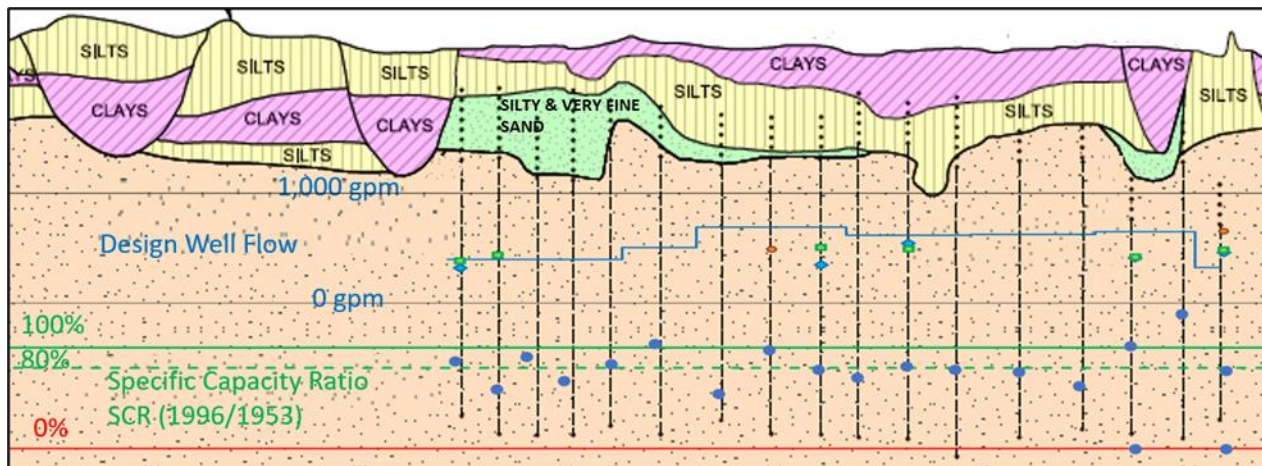


Figure 4-6. Comparison of measured well flow with design and pumping test data

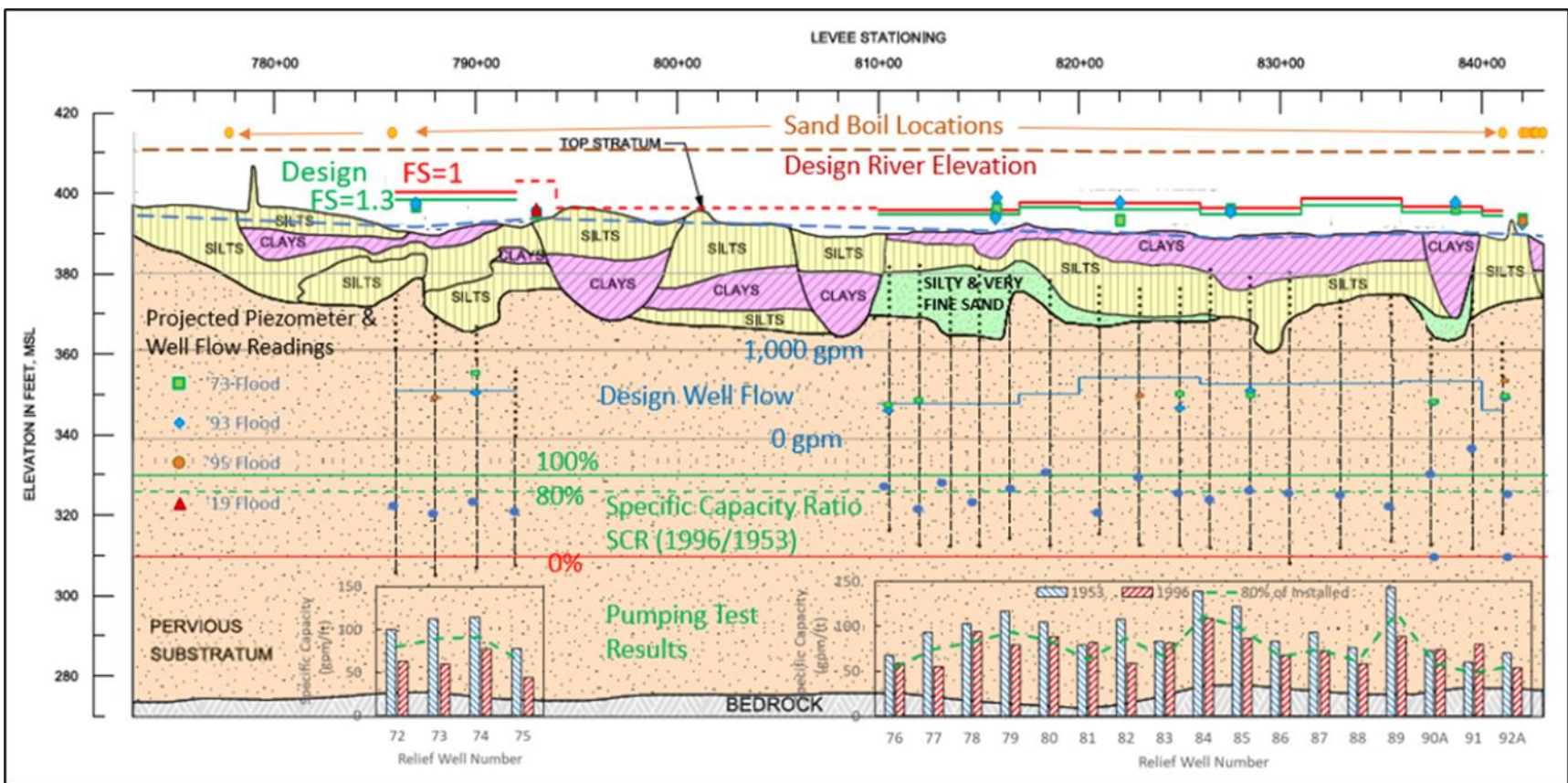


Figure 4-7. Harrisonville example combining geomorphology, design, and performance information

4–11. Relief well effect on sand boil activity

Relief wells provide a filtered exit for flow to safely discharge and reduce seepage pressure in the foundation. Paragraph 10–11 describes standpipes that are used to restrict relief well flow during periods of low water. During periods of high water, standpipes are removed to allow the wells to flow freely. This increase in well flow has been observed to reduce flow and soil movement emanating from active sand boils located near relief wells. Wells are sometimes pumped to draw down the piezometric level to address unwanted seepage and sand boil activity, similar to a dewatering system.

a. Legacy sand boils. In many cases, there will be remnants of old sand boils in areas where relief wells are being considered. Sometimes referred to as “legacy sand boils,” these old sand boils represent fissures, seams, or other anomalies in the blanket and aquifer that could provide a preferential seepage path during future floods. Piping defects can remain open for an extended time and require little excess head to discharge again. As such, the existence and location of legacy sand boils must be accounted for during the risk assessment to discern if and how relief wells should be installed.

b. Evaluation of BEP progression with and without wells. Risk assessment tools that are part of Best Practices in Dam and Levee Safety Risk Analysis (USBR and USACE 2019) continue to develop. The likelihood of BEP progression with wells nearby is complex and difficult to estimate with tools that are currently available. Relief wells increase the average global horizontal gradient across the structure, which suggests well flow could increase the likelihood of progression. However, relief wells redirect water from a sand boil or an advancing BEP erosion pipe, which can greatly reduce the likelihood of progression. The consensus is that relief wells improve the condition when sand boils are landside of the well line.

c. 3D seepage model with pre-existing boils. Sensitivity studies described further in Appendix F were performed using WASH123D, a type of finite difference model. These studies replicated a series physical model tests performed at WES that are depicted in Figure 4–8. Models in Appendix F included a high-permeability region in a vertical 18-inch diameter column through the blanket. The sand-filled column represents a sand boil and was placed midway between wells at a range of distances from the levee toe. The results show not only improvement from wells with respect to heave and vertical gradient, but also greatly reduce horizontal gradient around a sand boil. The filtered flow through the well screen reduces flow through defects in the blanket that, in turn, reduces further erosion in and around any boils.

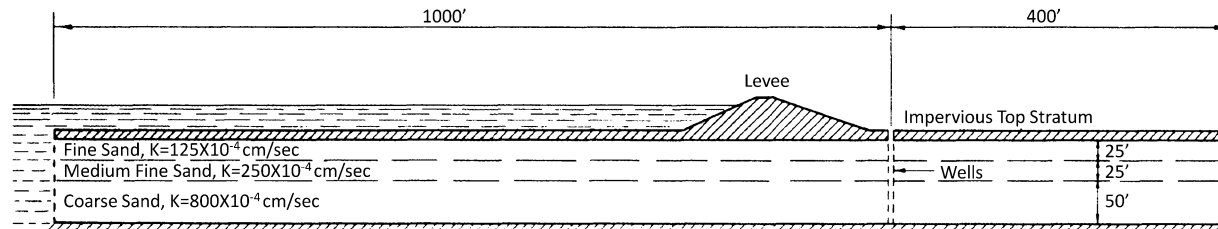


Figure 4–8. Cross section from Technical Memorandum 3-304 used in WASH123D model (USACE 1949)

d. *Adaptive finite element analysis.* Robbins and Griffiths (2022) also investigated the effect wells have on internal erosion progression where a landside defect exists. Figure 4–9 shows an example of the use of adaptive meshing to estimate BEP pipe progression. Figure 4–9(a) depicts the progression of an erosion path upstream from a sand boil toward the source. There are several criteria that need to be satisfied for this type of progression to occur. The mesh is adapted to include a pipe when flow and velocity exceed thresholds to maintain BEP as shown in Figure 4–9(b). This field of research and these types of numerical models will continue to evolve to better incorporate these various phenomena. The risk assessment process is well suited to incorporate that improvement in understanding over time.

(1) *Alternatives.* Various seepage mitigation alternatives were considered in this simple 2D plan view model: a cut-off wall with limited horizontal extent, relief wells upstream of the boil, and relief wells downstream of the boil. A pair of relief wells downstream of the boil location are shown in Figure 4–9(c).

(2) *Results.* All the alternatives considered resulted in a higher differential head for piping to progress upstream. It is generally agreed relief wells upstream of the boil location reduce the likelihood of progression. Indeed, critical head needed to be increased by 30% for the pipe to progress with wells located upstream of the boil. Less expected, critical head needed to be increased by 11% for the pipe to progress with wells located downstream of the boil. These findings contrast with what some of the simple heuristics commonly used for risk assessments may suggest. The models depicted in Figure 4–9 demonstrate that BEP is less likely to progress with the presence of wells. The wells attract flow that would otherwise worsen the condition even after a boil has formed.

e. *Assessing overall performance.* Any of these occurrences will affect the overall performance of the relief well. Some may lead to development of an unfiltered exit for a BEP failure mode. As such, these considerations should be considered when assessing overall relief well performance during routine maintenance and continued risk assessment.

f. *Reassessing design assumptions.* High-water events should trigger a reassessment of design assumptions. Vertical and horizontal gradients, and the localized gradient at assumed backward erosion pipes, should be reanalyzed with new

well performance data. Relief well systems may need to be replaced based on the considerations listed above and updated factor of safety calculations. Eventually wells will clog or deteriorate, and pumping tests described in Chapter 9 are critical to monitor performance when flood performance data is not available. The risk assessment process can be used to determine a schedule for rehabilitation or replacement.

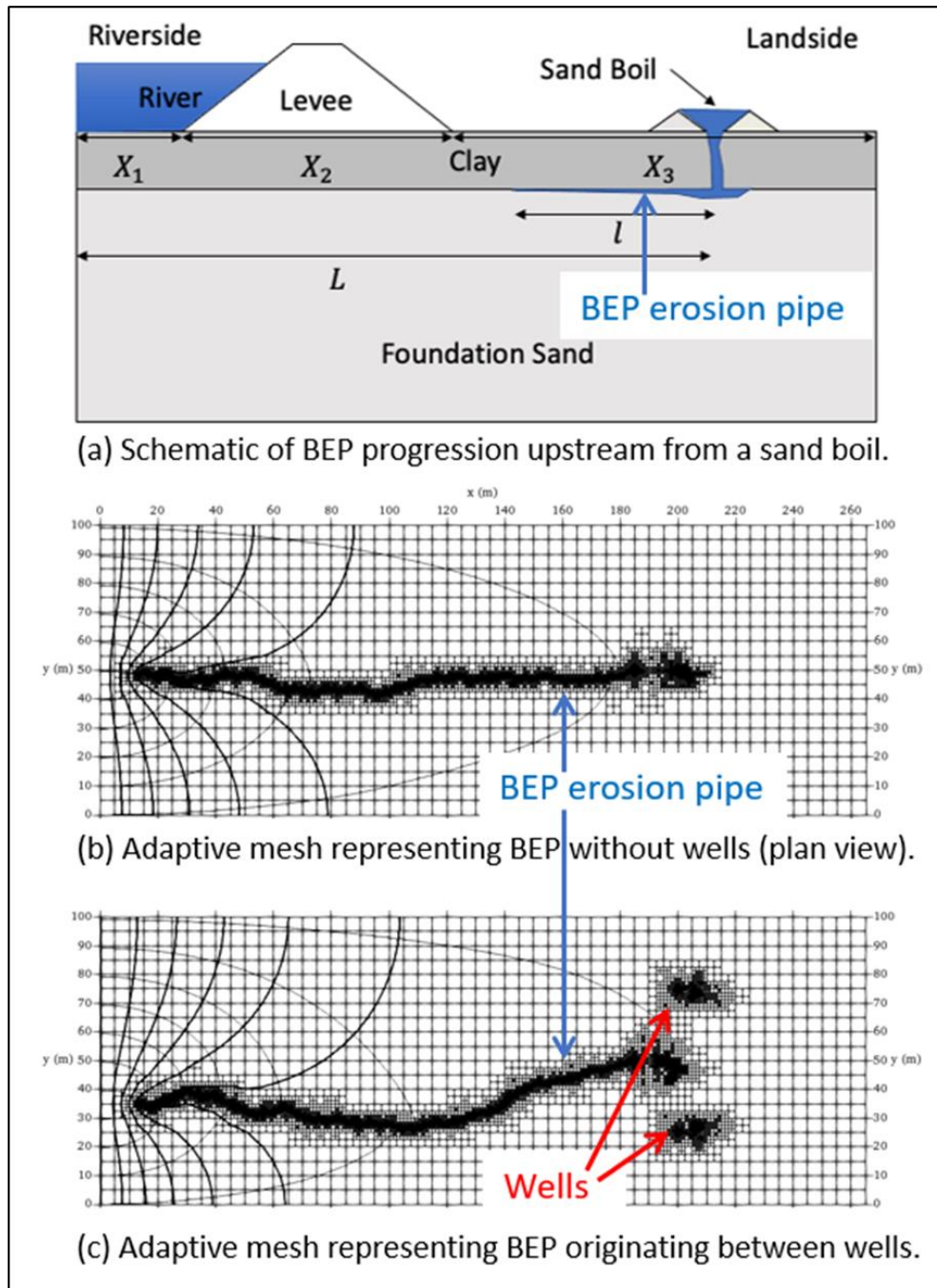


Figure 4-9. Adaptive meshing to represent backward erosion piping in the plan view with and without wells (adapted from Robbins and Griffiths 2022)

Chapter 5 Analysis and Design of an Infinite Line of Wells

5–1. Applicability of method

The following procedure can be applied where both a source and well system can be approximated as linear, infinite in extent, and parallel to each other. The wells are assumed to be uniformly spaced and identical, so they result in an equal quantity of flow. The term infinite is applied because the system may be analyzed mathematically by assuming an infinite length, thus an infinite number of wells.

a. History. The infinite line approach to relief well design has remained largely unchanged since 1955. This method has been used to design thousands of relief wells throughout USACE. The approach is based on the use of BT, presented in Appendix C. The development of the approach and the well factors used to calculate pressure and well flow are presented in Appendix H. More recently, the approach has been incorporated into 2D FEM seepage models as described in Appendix G.

b. Assumptions. The procedures in this chapter are formulated for an infinite line of wells that approximately conform to a set of idealized conditions. The equations are established based on the assumed conditions listed below. The geology and relief well systems at some projects satisfy these conditions better than others.

(1) First, the wells are equally spaced and have identical dimensions.

(2) Second, the pervious foundation stratum (the aquifer) is of uniform depth and permeability along the entire length of the system.

(3) Third, the effective source of flow and the effective landside exit, or block, are parallel to the well line. The waterside and landside boundaries are assumed to extend infinitely, parallel to the well line.

(4) Fourth, the boundaries normal to the line of the wells are impervious. These impervious boundaries are at a distance of one-half the well spacing beyond the end of the well system. One example is a well system for a dam on a pervious foundation within a bedrock valley that forms the abutments. Therefore, all flow is perpendicular to the line of wells and there is no flow across planes centered between wells, normal to the line such that overall flow is perpendicular to the well line.

(5) Fifth, the flow to each well and pressure distribution around each well in the line is assumed to be equal.

c. Adjustments. In many cases, the assumptions for an infinite well line are not met. In practice, adjustments to foundation characterization by either calculation or judgment enable the use of infinite line methods for a wider range of relief well systems.

(1) *Finite well lines.*

(a) System length and end effects need to be considered where the well system does not extend to an impervious boundary. In a finite line of wells, the heads will likely exceed those heads predicted by the infinite line design method. Modifications to the methods presented in this chapter to account for finite length effects are discussed in Chapter 6. These include an approach to estimate head at locations between wells and landward of the well line (at both the middle and end of that line). Other methods in Chapter 6, including 3D FEM, 2D FEM plan view models, and image well methods can also consider system length and end effects of finite well lines.

(b) In practice, well systems are generally extended, spacing is reduced near the ends of the system, or partial-penetration wells are extended deeper near the ends of the system to account for end effects. However, no universal rule is available at this time to help revise the infinite well system design to account for end effects or well system length.

(2) *Aquifer transformation.* If the foundation is composed of discrete layers, a mathematical transformation can be applied. Appendix E includes an approach to transform a stratified foundation with multiple pervious layers into a single layer with uniform depth and permeability. The transformation will result in effective values of thickness (\bar{D}), permeability (\bar{k}_e), and well screen length (\bar{W}). This procedure is valid for both full- and partial-penetration well systems. The transformed aquifer meets the requirement stated in paragraph 5–1b(2) and thus allows BT to be used for the analysis of a stratified foundation.

(3) *Semipervious blanket.* The equations are presented as though an impervious top stratum of finite length terminates at prescribed distances from the well line. If the top stratum is semipervious, it can be transformed to an equivalent length of impervious material using the methods in Appendix C.

(4) *Blanket transformation.* The transformation of a multi-layered blanket into a single blanket with uniform thickness and permeability is discussed in EM 1110-2-1913.

5–2. Analysis parameters

a. *Formula and notation.* The key formulas and notation for analysis of an infinite line of relief wells are included in Figure 5–1. Some inputs define the site geology, and these are often determined using BT and informed by piezometer readings, if available. These include distances to the effective seepage entrance (S) and exit (x_3) and thickness of the pervious foundation (D). Other inputs define the well system geometry: well screen length (W), well spacing (a), and effective well radius (r_w). Outputs for the analysis include head (h_{av} , h_m , and h_d) and discharge (Q_w) for each well along the well line.

b. *Boundary conditions.*

(1) The infinite line method uses assumed boundary conditions. These are fixed for each analysis and thus establish steady-state flow through the system. Total head boundary conditions are used for the waterside and landside vertical edges of the model. The landside boundary BT condition is generally equal to the landside/downstream ground surface elevation. The net head loading (H in Figure 5–1) is the difference between the waterside river or pool elevation and this landside boundary. The relief well can be conceptually represented by a total head boundary (such a boundary is actually used in numerical models) with elevation equal to the well's discharge elevation.

(2) This conceptual boundary for the well should be adjusted (increase the effective discharge elevation) to incorporate well losses as described in Chapter 7. This boundary should also account for any extension of the well riser above landside ground or ponding elevation. Chapter 3 includes considerations for landside, waterside, and relief well elevations assumed in design.

(3) The top stratum thickness, permeability, and lateral extent have a pronounced effect on well performance and must be specified in any seepage analysis. Theoretical solutions are available for an impervious top stratum extending landward to infinity. However, this condition is rarely realized in practice. A more generalized condition occurs when the impervious top stratum extends landward a finite distance terminating at a line sink. A semipervious top stratum can be converted to an equivalent length of impervious top stratum using BT. The resulting impervious blanket of finite length is illustrated in Figure 5–1.

(4) BT is used to calculate two distances from the well line: the effective seepage entrance (S) and the effective seepage exit (x_3). Both these distances are shown in Figure 5–1. The method for determining S and x_3 is summarized in Appendix C, which includes reference to more detailed procedures. USACE (1956a) contains a method of using piezometer data to estimate S and x_3 , which can refine the mathematical BT method of estimation.

c. *Resulting pressure in the substratum.* Figure 5–1 shows head distributions with and without relief wells, including the effects of well losses. Three values of head with wells are determined using the infinite line approach: an average excess head along the well line, h_{av} , excess head midway between wells, h_m , and maximum excess head landward of the wells, h_d . These values are combined with well head loss, H_w , to determine average excess head along the well line with losses, H_{av} , head midway between wells with losses, H_m , and maximum excess head landward of the wells with losses, H_d . Also shown conceptually is head through the location of each well.

d. *Well flow.* Flow from a single well in an infinite line (Q_w) is computed using equation 5–1 or equation 5–2. Flow from a line of wells is equal to ΣQ_w multiplied by the number of wells installed. Calculating Q_w uses the difference in slopes of the hydraulic

grade lines riverward and landward of the well line (ΔM) and the net head loading the well system corrected for losses (h).

$$Q_w = (a)(\Delta M)(\bar{k}_e)(\bar{D}) \quad (5-1)$$

$$Q_w = \frac{(\bar{k}_e)(\bar{D})(h)}{\left(\frac{S}{a}\right) + \theta_{av}\left(\frac{S + x_3}{x_3}\right)} \quad (5-2)$$

e. *Seepage calculations.* The presence of relief wells tends to increase the total quantity of seepage beneath a levee or dam (Q_s). As presented in Appendix C, the seepage per foot of structure with no wells is estimated using equation 5-3. The seepage for a reach with wells is equal to flow from the well system plus the seepage beyond the well system. Seepage landside of the well system (Q_{sw}) is computed by equation 5-4.

$$Q_s = \frac{\bar{k}_e \times \bar{D} \times H}{S + x_3} \quad (5-3)$$

$$Q_{sw} = \frac{\bar{k}_e \times \bar{D} \times H_{av}}{x_3} \quad (5-4)$$

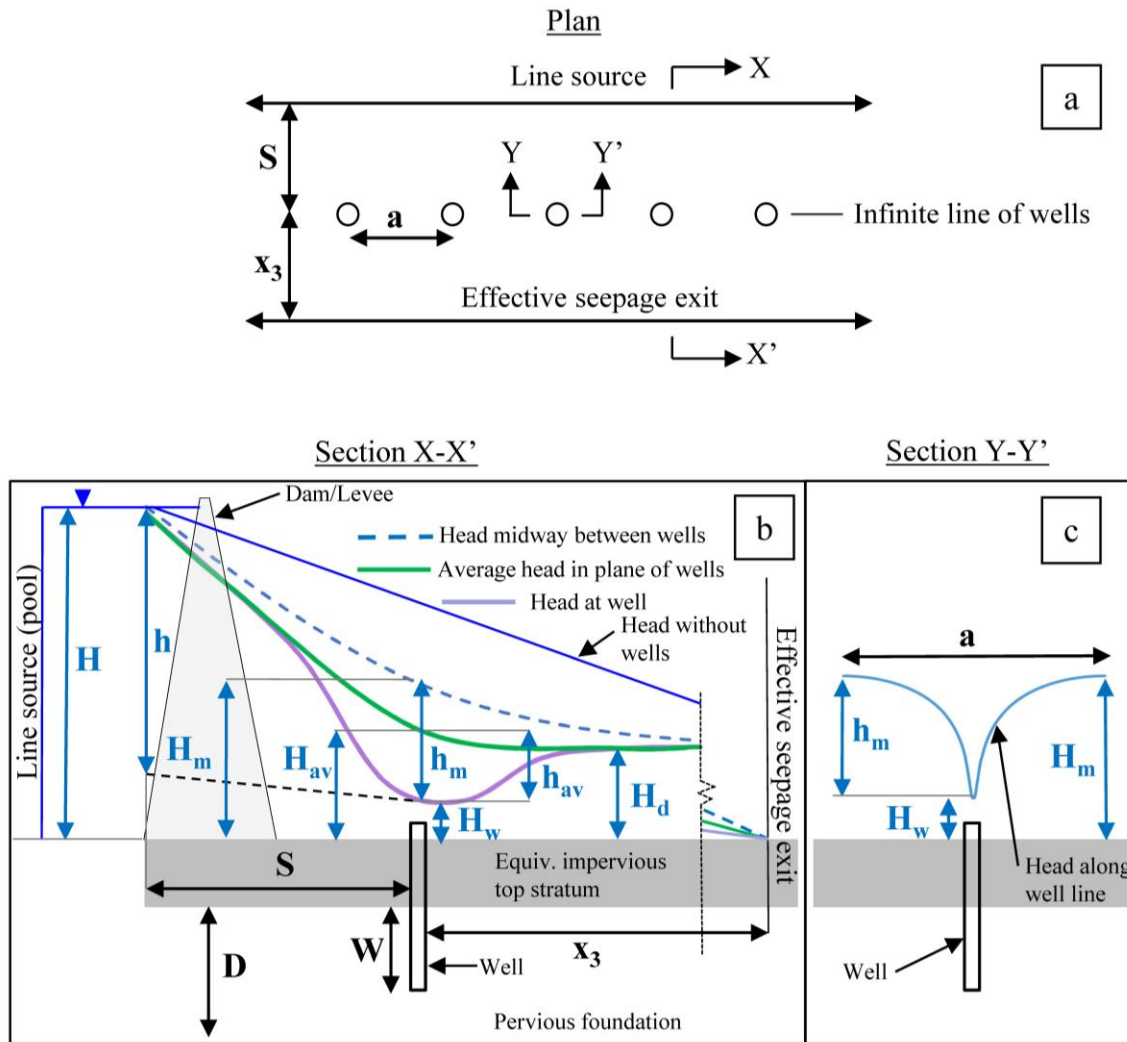


Figure 5-1. Infinite artesian relief well line (located along landward levee toe) with design notation and parameters: conceptual plan view (a), section X-X' (b), and section Y-Y' (c)

(1) *Formulas.*

$$h = H - H_w \left(\frac{S + x_3}{x_3} \right) \quad (5-5)$$

$$H_m = H_w + h_m \quad (5-6)$$

$$h_{av} = \frac{h \times \theta_{av}}{\frac{S}{a} + \theta_{av} \left(\frac{S + x_3}{x_3} \right)} \quad (5-7)$$

$$\Delta M = \frac{H - H_{av}}{S} - \frac{H_{av}}{x_3} \quad (5-8)$$

$$H_{av} = H_w + h_{av} \quad (5-9)$$

$$h_{av} = a(\Delta M)(\theta_{av}) \quad (5-10)$$

$$h_m = h_{av} \left(\frac{\theta_m}{\theta_{av}} \right) = \frac{h \times \theta_m}{\frac{S}{a} + \theta_{av} \left(\frac{S + x_3}{x_3} \right)} \quad (5-11)$$

$$h_m = a(\Delta M)(\theta_m) \quad (5-12)$$

$$h_d = \frac{h \times \theta_d}{\frac{S}{a} + \theta_{av} \left(\frac{S + x_3}{x_3} \right)} \quad (5-13)$$

$$h_d = (a)(\Delta M)(\theta_d) \quad (5-14)$$

$$H_d = H_w + h_d \quad (5-15)$$

(2) *Notation.*

h = Net head on the well system corrected for well losses

ΔM = Net seepage gradient toward the well line

H = Total net head on well system

S = Distance from effective source of seepage entry into foundation to the landside embankment toe

H_w = Total well losses (elevation and efficiency)

x_3 = Distance from landside embankment toe to effective seepage exit

h_{av} = Average net head in plane of wells corrected for total well losses

D = Foundation thickness

H_{av} = Average net head in plane of wells

W = Screen length of well in foundation strata

h_m = Net head midway between wells corrected for total well losses

a = Well spacing

H_m = Net head midway between wells

θ_{av} = Average uplift factor

H_d = Maximum net head landward of wells

θ_m = Mid-well uplift factor

5-3. Uplift factors

Mathematical analysis of flow into an infinite line of discrete wells is more complex than flow toward a continuous slot. This is resolved using uplift factors θ_{av} , θ_m and θ_d . The θ_{av} is the "extra length" or average uplift factor, θ_m is the mid-well uplift factor, and θ_d is the landward uplift factor.

a. *Basis of analysis.* Computations for an infinite line of wells in 2D are based on flow toward a continuous drainage slot. Flow to an infinite line of discrete relief wells is then adjusted to account for the increased length of groundwater flow paths to well

locations relative to the slot. This increase in length results in additional head losses, reduced discharge, and greater pressures in the aquifer for a well relative to a slot. Jervis (USACE 1939b) identified these additional head losses as the “extra length” and incorporated it into relief well design for both full- and partial-penetration wells. Figure 5–2 (top) shows a plan view of flow to a well that is uniformly spaced at distance a from identical wells. The bottom part of the figure, also a plan view, shows flow to a drainage slot.

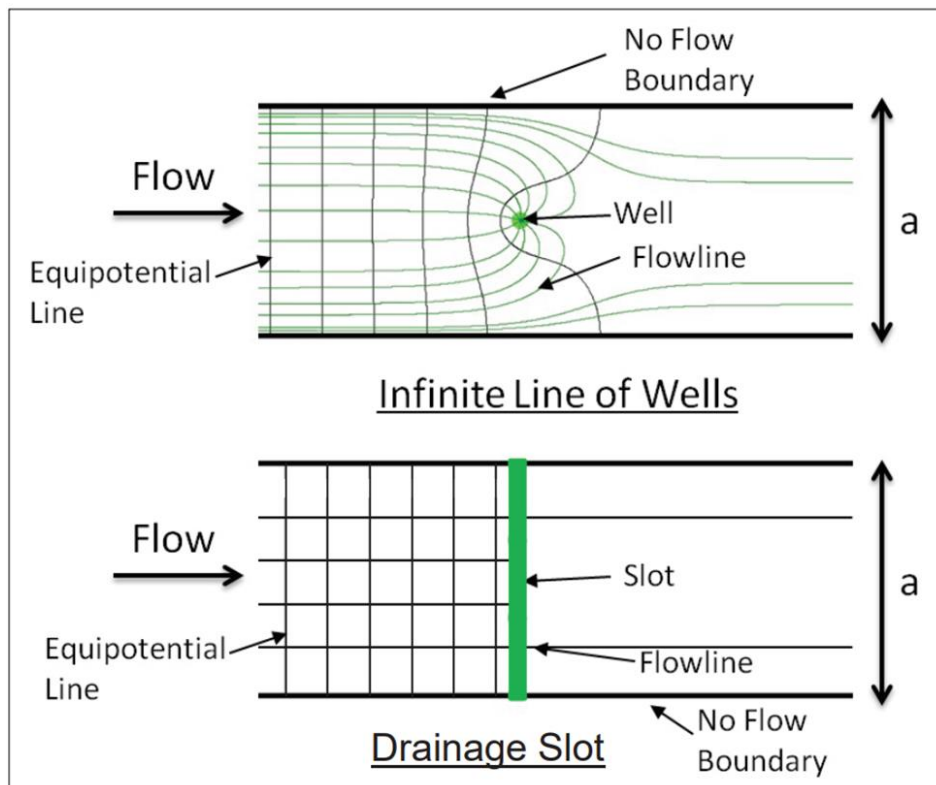


Figure 5–2. General plan view flow nets of a full-penetration infinite well line (top) and a full-penetration drainage slot (bottom); flow is from a line source located a distance S from the well or drainage slot (also Figure G–1 in Appendix G)

b. Parameters for uplift factor estimation. Longer flow paths to a well result in increased resistance to flow. This is accounted for during design with the dimensionless uplift factors. The uplift factors are based on effective penetration (\bar{W}/\bar{D}), well spacing (a), effective radius (r_w), and effective foundation thickness (\bar{D}). The parameter θ_d , as developed by Keffer and Guy (2019), uses another parameter based on x_3 / a .

c. Application of uplift factors. The average uplift factor, θ_{av} , is used to compute the average net foundation head in the plane of the wells (h_{av}). The θ_{av} is also used to compute the net seepage gradient toward the well line (ΔM), and the well discharge (Q_w). The θ_m is used to compute the net head midway between the wells (h_m). The θ_d is used to calculate the maximum net head landward of the wells (h_d). Multiple methods can be used to calculate the uplift factors.

(1) *Full-penetration wells.* For full-penetration wells, θ_{av} and θ_m can be calculated directly using equations 5–16 and 5–17.

$$\theta_{av} = \frac{1}{2\pi} \ln \left(\frac{a}{2\pi r_w} \right) \quad (5-16)$$

$$\theta_m = \frac{1}{2\pi} \ln \left(\frac{a}{\pi r_w} \right) \quad (5-17)$$

(2) *Partial-penetration wells.* Figure 5–3 illustrates a convergence of flow in cross-sectional view that occurs due to partial penetration for either a slot or a line of wells. For partial-penetration wells, θ_{av} and θ_m may be calculated using Table 5–1 (Barron 1978–1982) in conjunction with $\Delta\theta$ and equations 5–18 and 5–19. The following section and Appendix H describe other methods used to determine these well factor parameters.

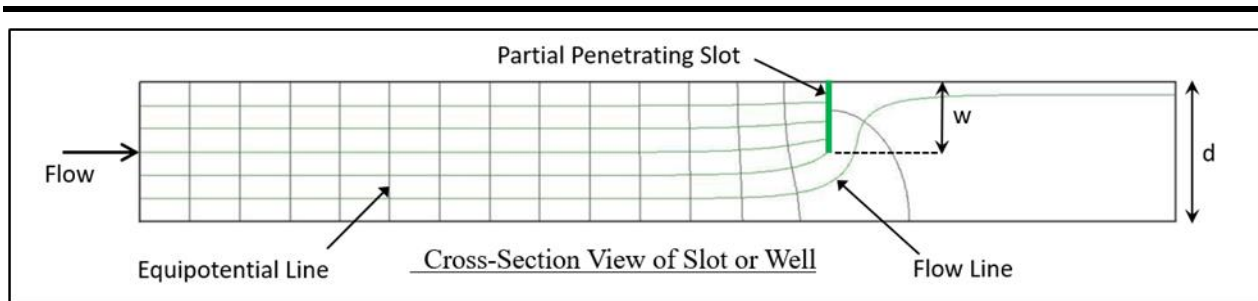


Figure 5–3. Cross-sectional view of a flow net to a partial-penetration drainage slot

$$\theta_{av} = \theta_{av} \left(\frac{a}{r_w} = 100 \right) + \Delta\theta \left(\log \left(\frac{a}{r_w} \right) - 2 \right) \quad (5-18)$$

$$\theta_m = \theta_m \left(\frac{a}{r_w} = 100 \right) + \Delta\theta \left(\log \left(\frac{a}{r_w} \right) - 2 \right) \quad (5-19)$$

d. Methods. Various approaches were used to develop uplift factor computation methods between the 1930s and 1950s. These include electric analogy models, physical models, and analytical/mathematical solutions. Nomograms were often used to apply these methods. The nomogram in Figure 5–4 (USACE 1955; Bennett and Barron 1957) can be used to determine values of θ_{av} and θ_m . Keffer et al. (2019) verified that finite element modeling solutions are practically equivalent to these other approaches. Figure 5–5 can also be used to determine θ_{av} and θ_m . The values of θ_{av} and θ_m rise rapidly as well penetration falls below 25%. Due to this, 25% aquifer penetration has historically been recommended as the minimum for dewatering and relief well design. The value of θ_d determined from Figure 5–6 can be used to compute the maximum head landward of the well. The θ_{av} has been used historically to provide a conservative estimate of head landward of the well (Keffer and Guy 2022).

Table 5-1
Theoretical uplift factor solutions developed by Barron (1978)

Theoretical values of θ_{av} and θ_m

W/D	D/a	a/r_w	θ_{av}	θ_m	$\Delta\theta$
100%	All Values	100	0.440	0.550	0.3665
75%	0.25	100	0.523	0.633	0.480
	0.5		0.563	0.667	
	1		0.606	0.681	
	2		0.578	0.682	
	3		0.748	0.682	
	4		0.818	0.682	
50%	0.25	100	0.742	0.851	0.733
	0.5		0.857	0.955	
	1		0.983	1.012	
	2		1.175	1.024	
	3		1.361	1.024	
	4		1.547	1.024	
25%	0.25	100	1.225	1.335	1.466
	0.5		1.569	1.622	
	1		1.926	1.908	
	2		2.390	2.024	
	3		2.798	2.047	
	4		3.199	2.075	
15%	0.25	100	1.662	1.722	2.077
	0.5		2.310	2.401	
	1		2.970	2.938	
	2		3.747	3.293	
	4		4.941	3.432	
	10%		0.25	100	
0.5		2.934	3.025		
1		3.977	3.941		
2		5.139	4.649		
4		6.814	5.071		
5%		0.25	100		1.778
	0.5	3.879		3.969	
	1	6.063		6.021	
	2	8.377		7.864	
	4	11.144		9.283	

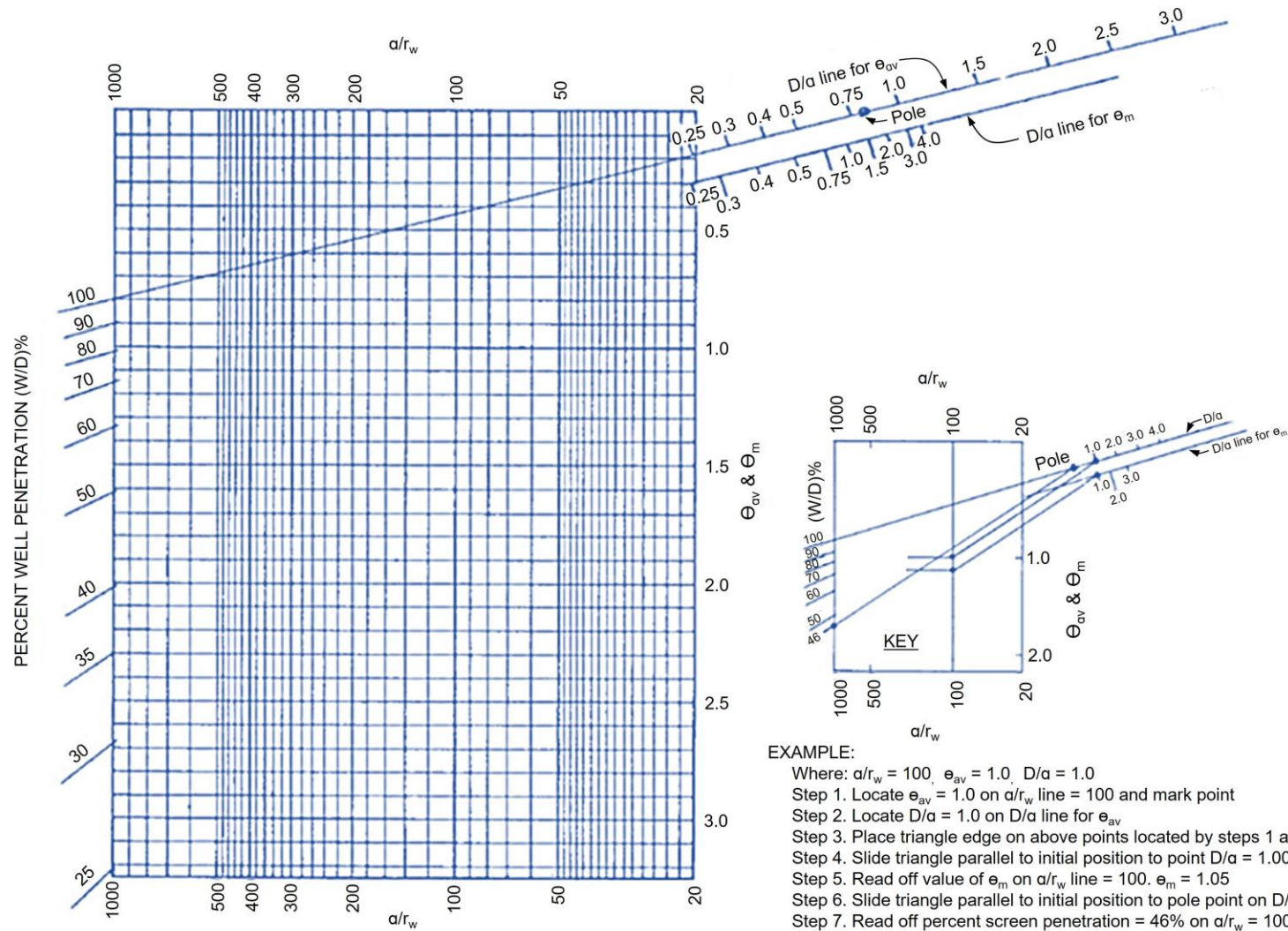


Figure 5-4. Nomogram for determining values of average and mid-well uplift factors (USACE 1955; Bennett and Barron 1957)

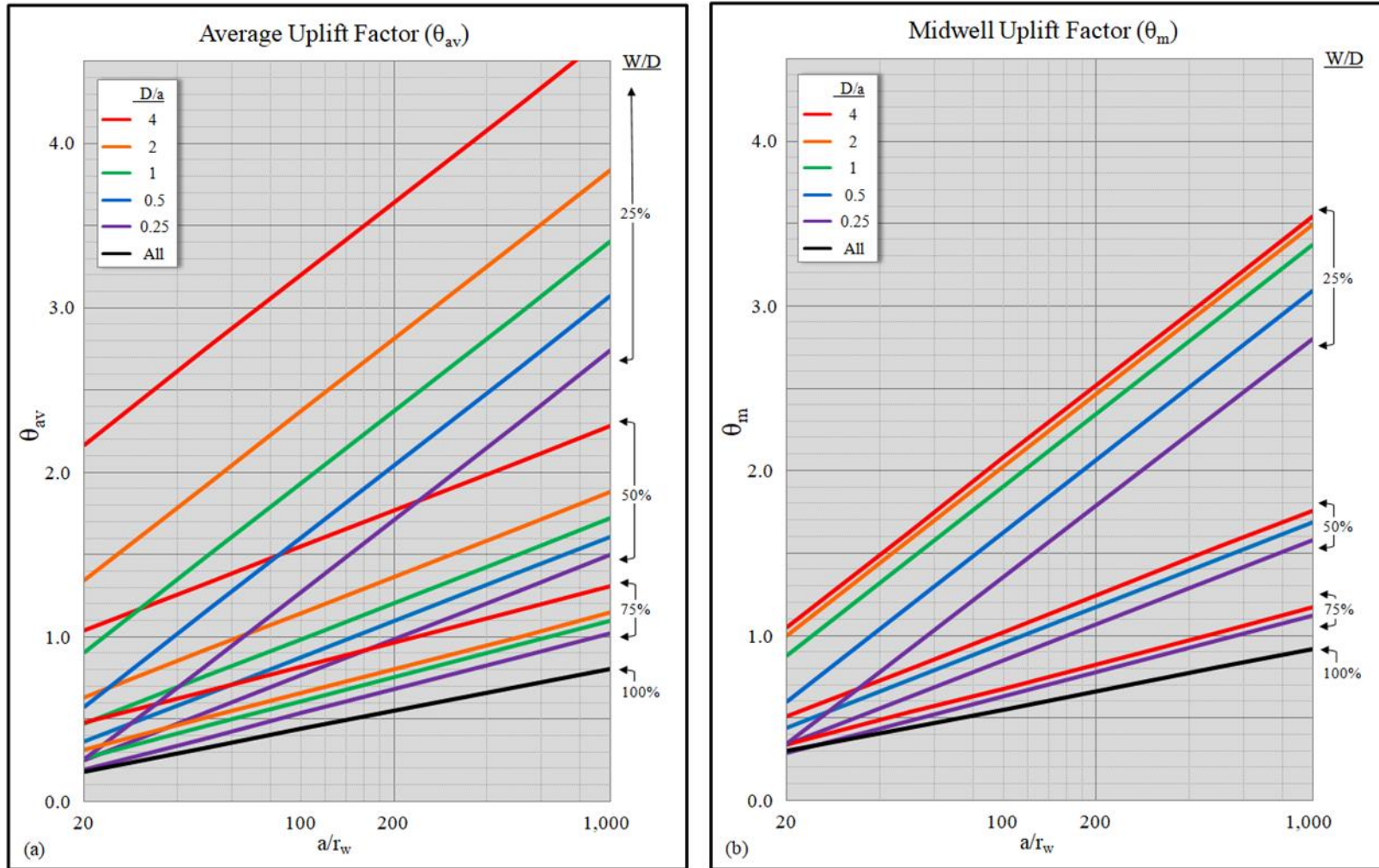


Figure 5-5. Relief well design nomogram for average (a) and mid-well (b) uplift factor values (Keffer and Guy 2022)

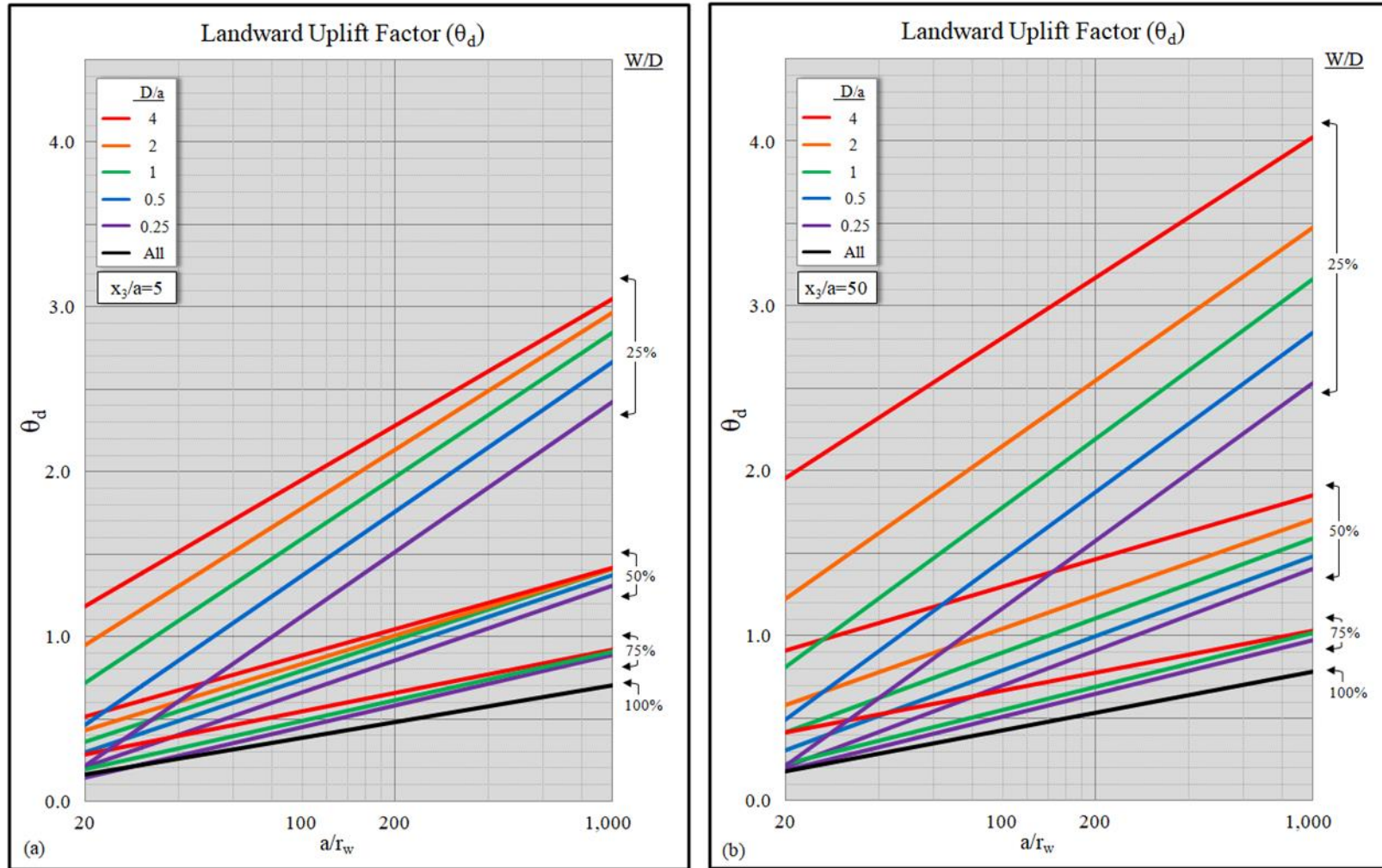


Figure 5–6. Relief well design nomogram for providing landward uplift factor values at $x_3/a = 5$ (a) and $x_3/a = 50$ (b) (Keffer and Guy 2022)

5–4. Conceptual approach

As described in the previous section, much of the complexity for the analysis of an infinite line of wells is handled by well factors.

a. *Approach.* Two sets of equations presented in paragraph 5–2 (differentiated by the use of ΔM) are used to perform calculations to determine pressure and flow using those well factors. Two general approaches are used in practice, and both should begin by calculating excess head at the levee toe without wells (h_o), which is discussed in Appendix C. They also make an initial assumption that $H_w = 0$ foot. After Q_w and excess heads are computed without losses, H_w should be estimated, and its effects extrapolated back to the seepage entrance to reduce the effective loading on the system (h). This extrapolation of H_w to find h is accomplished by equation 5–5 and demonstrated in Figure 5–1. Expected excess heads are then increased based on the reduced Q_w caused by H_w . Excess heads including losses (H_m , H_d , H_{av}) are computed with equations in Figure 5–1.

b. *Spreadsheet formulation.* Appendix C includes a simple approach to calculate flow and substratum pressure for an infinite line of wells using equations on the right side of Figure 5–1. Although it can be used to design wells and results in the same values as the more complex formulation presented in paragraph 5–5, it is included primarily for illustrative purposes to demonstrate the approach. Well designers are encouraged to replicate those calculations by hand or by creating a simple spreadsheet. The design approach described in the following section has been coded into spreadsheet that is available online for USACE employees. A few additional considerations are listed below.

c. *Maximum head downstream of the well line.* When W/D is less than 50% and x_3 is an order of magnitude larger than well spacing, a , the head downstream of the well line may be larger than the head midway between wells. In those cases, H_d and θ_d should be checked in addition to H_m and θ_m using equation 5–15 and Figure 5–6.

d. *Discharge below ground surface.* In many installations, the well outlets are located below the ground surface or in a ditch. Under this condition, there is assumed to be no upward flow through the landside blanket. Without pressure relief due to seepage through the top stratum, the corresponding condition is to set $x_3 = \infty$ for the equations in Figure 5–1. Solutions are obtained by incrementally increasing x_3 by an order of magnitude until further increases do not change the result. The elevation component of H_w (H_{el}) is set as a negative number equal to the depth of the well discharge. Discharge capacity of the collector system must be considered to account for backflooding of the well system. If this occurs, there will be an effective increase in discharge elevation that can affect long-term performance.

5–5. General design approach

The purpose of a relief well system is to reduce excess head landward of a dam or levee (H_m , H_d , or H_{av}). A successful design will lower the excess head to the allowable value (h_a). Since H_{av} has been used historically in the design process, it may be calculated with equation 5–9 and used to evaluate FS_{vg} along with H_m and H_d in the below design approach. However, it should be understood as a value that is likely an overestimation of H_d . The designer determines the values of r_w , a , and \bar{W}/\bar{D} necessary to meet this requirement. For given boundary conditions and the same h_a , there are different combinations of r_w , a , and \bar{W}/\bar{D} that will suffice. The final selected r_w , a , and \bar{W}/\bar{D} will be based on technical acceptability and cost effectiveness. Consideration should also be given to natural topographic features that will influence the elevation of relief well outlets.

a. The design steps in paragraph 5–5a(1) through 5–5a(10) use equations and concepts from Figure 5–1 to calculate the excess head along and landward of an infinite well line and the discharge from each well. They are favorable for incorporation in a computer spreadsheet so that the effects of varying input parameters can be quickly evaluated. The spreadsheet from Guy et al. (2010) was used to analyze an example levee in Appendix I. Each design step begins with a brief explanation of its intent.

(1) Determine excess head (difference between piezometer reading at the bottom of the top stratum and the greater of the ground surface or landside water elevation) at the levee toe without wells to evaluate the need for relief wells if the factor of safety is too low. Calculate h_o from equation C–3 and base condition FS_{vg} from equation 3–2.

(2) Calculate h_a based on a target design FS_{vg} . Set FS_{vg} equal to the target value, and solve equation 3–2 for h_a instead of h_o .

(3) Parameters for well system geometry must be selected by the designer. Select a trial a , r_w , and \bar{W}/\bar{D} .

(4) Parameters a , r_w , and \bar{W}/\bar{D} are represented by theta uplift factors. Determine θ_{av} , θ_m , and θ_d from Table 5–1, Figure 5–5, Figure 5–6, or the Sharma (1974) approach from Appendix H.

(5) Adjust well system geometry to achieve acceptable excess heads with perfectly efficient wells. Assume no well losses ($H_w = 0$ foot and $h = H$) and calculate h_m with equation 5–11 and h_d with equation 5–13. If the greater of the two is above h_a , adjust a , r_w , or \bar{W}/\bar{D} and repeat the steps in paragraphs 5–5a(1) through 5–a(5).

(6) Determine the greatest expected well discharge, for wells without any consideration of performance loss, for a conservative design of a collector system. Calculate Q_w from equation 5–2. This is the value used to size relief well system discharge capacity.

(7) Consider well performance losses at installation and in the future. Well losses can be estimated based on reduced flow rate, pumping tests, or experimental data that are presented in Chapter 7. Use paragraph 7–9 to estimate H_w based on the Q_w that was calculated in paragraph 5–5a(6). H_w may include losses at installation and estimated future losses (such as biofouling).

(8) Extrapolate the effects of well losses to the seepage entrance to reduce the effective loading on the well system (H is reduced to h). Calculate h from equation 5–5, then h_m with equation 5–11 and h_d with equation 5–14.

(9) Incorporate well loss effects on excess heads resulting from the inefficient well system (increase the expected excess heads because well discharge was decreased by losses). Calculate H_m with equation 5–6 and H_d with equation 5–15. If the greater of the two is above h_a , adjust a , r_w , or \bar{W}/\bar{D} and repeat the steps in paragraphs 5–5a(3) through 5–5a(9).

(10) Compute the actual expected discharge from a well with losses. Calculate Q_w from equation 5–2.

b. It is recommended that this process be completed for a range of a , r_w , and \bar{W}/\bar{D} values to find the most economical balance between the number of wells and the depth of each well.

5–6. Computer programs for well design

There are multiple design computer programs used in various districts throughout the USACE to perform infinite line well calculations. These programs have been tested for certain conditions but not all possible conditions have been tested; therefore, the user should not accept any results without adequate comparative analysis. The examples in Appendix I provide a means to compare any program with the equations and methods presented in this manual.

Chapter 6 Analysis and Design of a Finite Line of Wells

6–1. Finite well line conditions

USACE has historically assumed an infinite line of wells for design of relief wells and made any adjustments to the solution for finite well lines. Infinite well lines terminate at impervious boundaries and are described in Chapter 5. However, relief well systems may not satisfy the infinite condition and finite line effects need to be considered in such cases.

a. End effects. The presence of seepage flow that is not perpendicular to the well line may be a significant difference for finite well systems. Such flow results in a non-uniform distribution of uplift pressure and well discharge. Both parameters may be significantly increased compared to an infinite well line.

b. Unique boundary or design conditions. Relief wells are sometimes considered where gaps (windows) are present in a seepage barrier. Wells have been used along landside ditches orientated perpendicular to the levee alignment and are common around pump stations to reduce uplift. Other non-linear well arrays, or a linear well array with variable well spacing, are also sometimes required.

c. Approach. Common approaches for designing finite well systems are described in this chapter. These include 3D FEM, 2D plan view FEM, adjusting the infinite line solution, and the Image Well Method (IWM).

6–2. 3D finite-element or finite-difference models

Geologic and site-specific factors may impose conditions that are difficult to simulate using simpler approaches. Finite-element or finite-difference models may be used when subsurface conditions are non-uniform. This includes variable aquifer thickness, zones of different permeability, significant vertical flow, or unusual boundary conditions. These modern tools build on the flow net analyses and electrical analogy tests used to analyze many USACE projects for generations. Mansur and Kaufman (1962) described the use of flow nets for the design of well systems. USACE (1963), USACE (1965), and McAnear and Trahan (1972) described methods for conducting 3D electrical analogy tests. The concepts in these early references are also applicable to modern FEM analyses.

a. 3D modeling approach. The WASH123D model included in Appendix F was created to support the update of this manual. The use of this finite-difference code is included to both validate the simpler approaches and to help the reader better understand 3D modeling efforts. The analyst should consider replicating these types of simple models before applying their 3D approach to model complex field conditions.

b. Example use of 3D modeling.

(1) Figure 6–1 shows the location of a large boil that formed at an inside bend of the Upper Wood Levee during the 1993 flood. A full-penetration cut-off wall was installed beneath the levee centerline but not under the interstate highway that runs through the project. The discontinuous wall created conditions too complex for conventional analytical methods. Therefore, a WASH123D model of this reach was created to simulate flow to relief wells. The model is described in Seepage and Piping through Levees and Dikes Using 2D and 3D Modeling Codes (USACE 2016).

(2) Results shown in Figure 6–2 demonstrate how 3D models incorporate wells situated in complex locations. Section A-A' through the center of the proposed line of wells is an example of how total head contours are presented for any location of interest. Best practice includes evaluating a slice through the gap or outside the edge of the wall for potential BEP using the risk assessment methods described in Chapter 4.

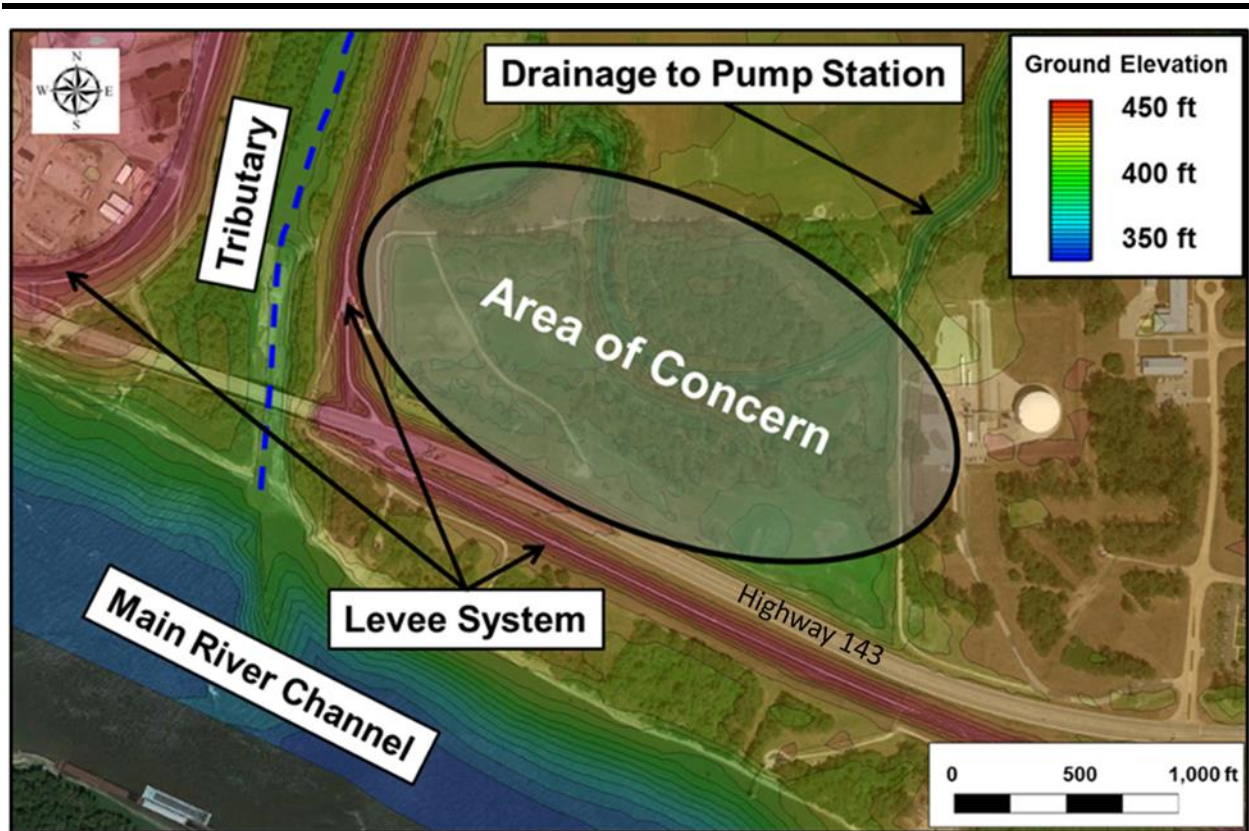


Figure 6–1. An area of seepage concern in Upper Wood River (USACE 2016)

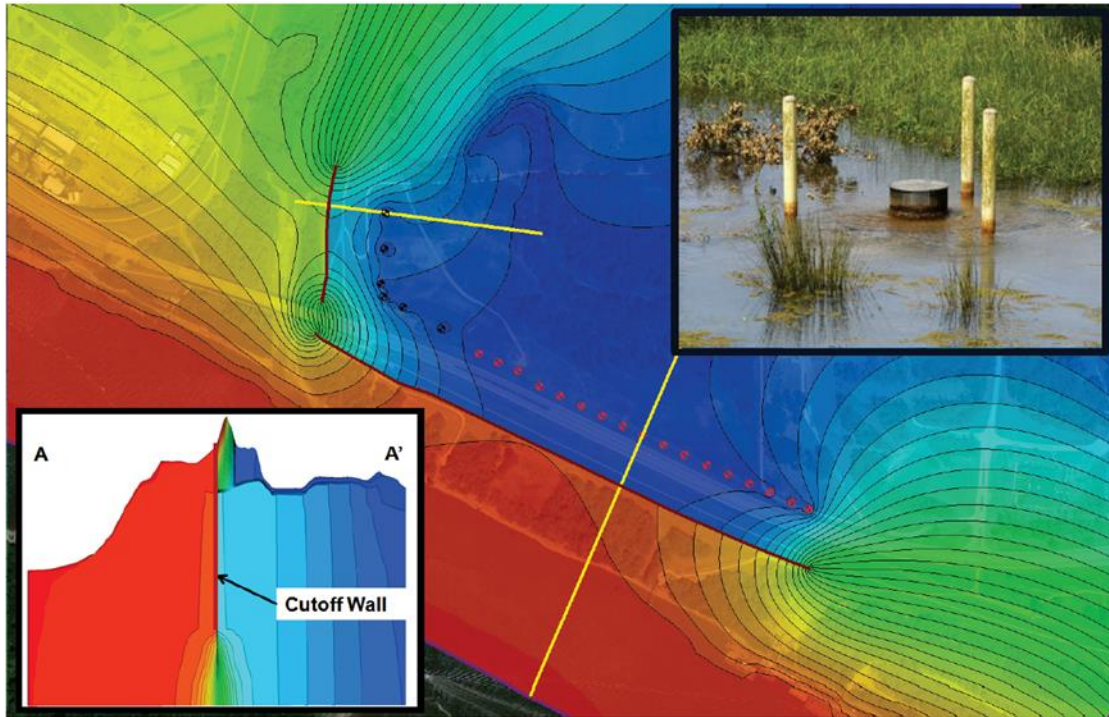


Figure 6–2. A WASH123D model including relief wells and cutoff (USACE 2016); black and red dots indicate existing and proposed new wells, respectively

6–3. 2D plan view finite element method

a. 2D finite element analyses can be used in cases where the substratum can be approximated by a single, permeable artesian layer and wells are full-penetration, and the flow in the permeable layer is confined. These simple models have been used to design finite well systems using concepts from BT described in Appendix C. The boundaries of the model are set equal to the calculated effective entrance (full pool elevation) and effective exit (tailwater elevation). BT provides a means to calculate this distance to account for leakage through the confining layer.

b. Figure 6–3(a) includes the arrangement that is directly analogous to the infinite well condition in Chapter 5. Figure 6–3(b), (c), and (d) represent finite well arrangements with 2, 4, and 10 wells, respectively. However, variable well spacing or non-linear well arrays can be assessed with 2D finite element analyses.

c. The no-flow boundaries indicated on each of these figures mirror the wells, along with everything else in the model. Figure 6–4 compares excess head for infinite and finite well systems in profile. Some of the design parameters included in these figures are explained in the following section. As shown in Figure 6–4, finite well systems have higher heads near the ends of the systems and shorter well systems have higher heads than longer well systems. Plan view FEM can also be used to consider flow around seepage barriers and are not limited to straight levee alignments.

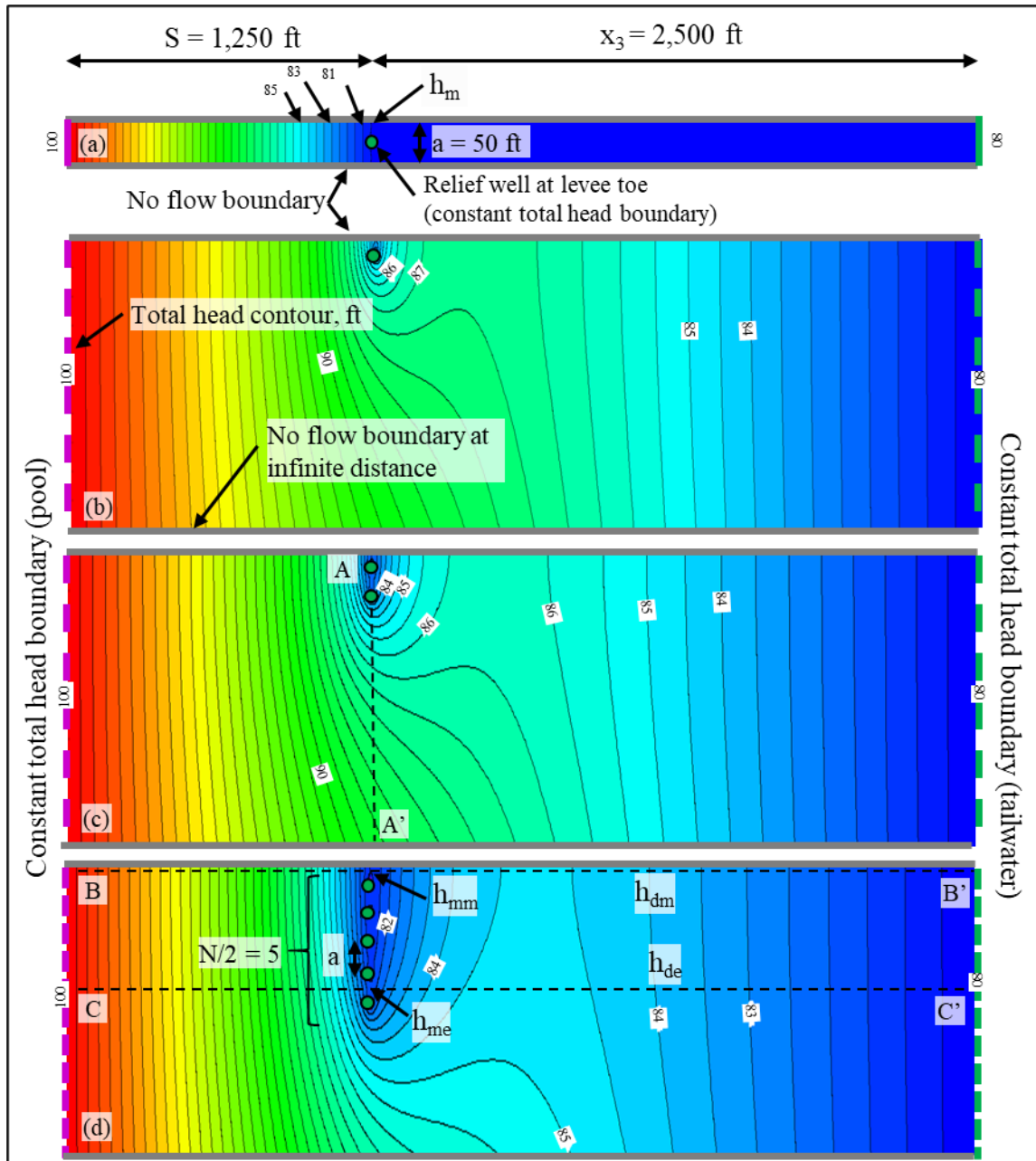


Figure 6-3. Plan view of typical finite element analyses and measurement locations, infinite well lines (a) and finite lines with 2 (b), 4 (c), and 10 (d) wells ($ar_w = 100$, $D/a = 1$, $W/D = 100\%$) (Keffer et al. 2023)

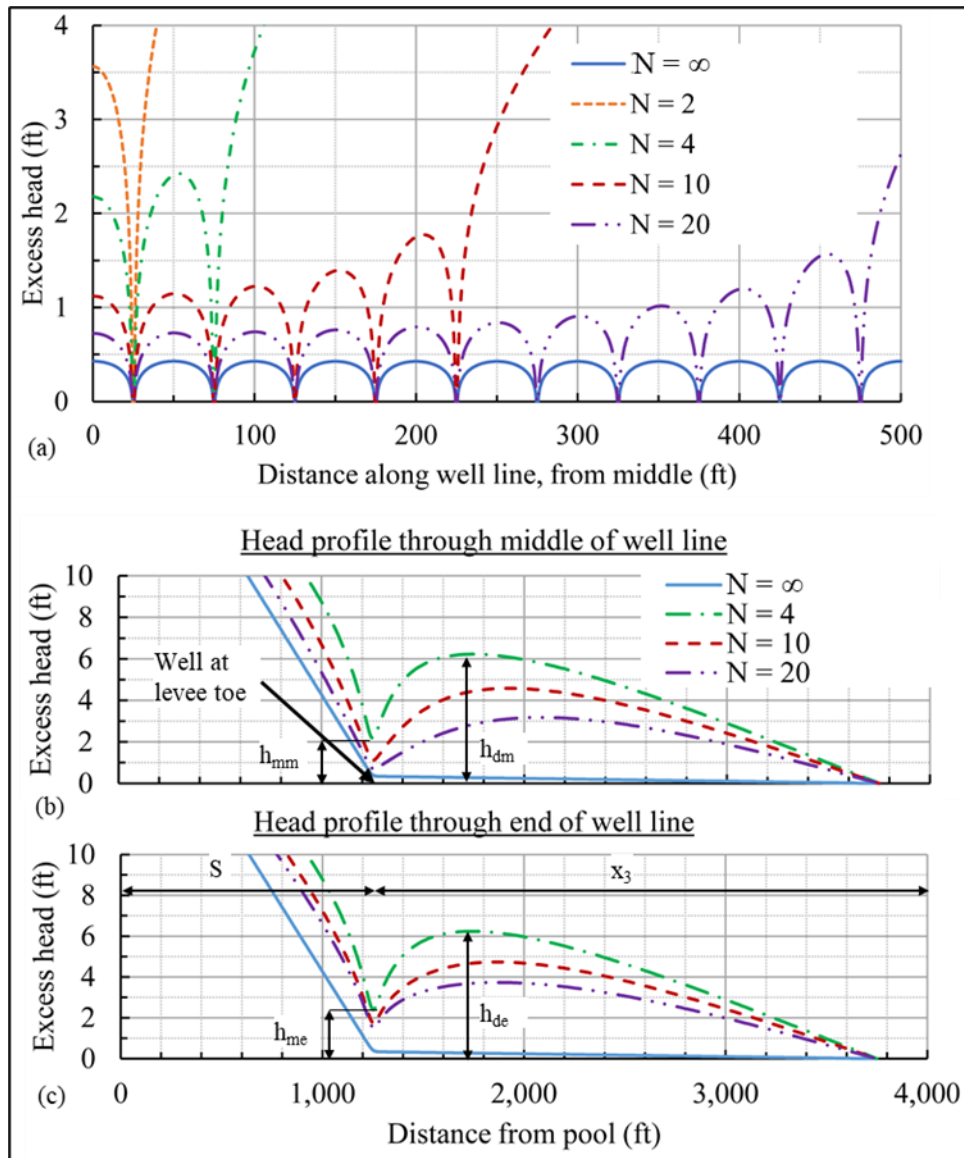


Figure 6-4. Profile of excess head along the well lines of various lengths from Figure 6-3 (a, section A-A'), and perpendicular to the middle (b, section B-B') and end (c, section C-C') (Keffer et al. 2023)

6-4. Procedure to adjust infinite line solution

a. *Prior finite line method.* USACE (1963) presented a method to compute excess heads along, but not landward of, a finite well line using similar BT input parameters and number of wells. It also used electric analog models in its development. However, it requires the use of more than 100 tables with extensive plotting and interpolation, and is impractical for most engineering applications. For some finite line scenarios, head landward of the well line exceeds head between wells, so it needs to be considered.

b. *Finite line parameters.*

(1) Most of the parameters for a finite well system are the same as for an infinite system. The exception is that the number of wells must be considered for a finite system. Chapter 5 describes how BT-based calculations are used to compute excess head values for infinite well lines. The resulting values are h_m , h_{av} , and h_d . Input parameters for these calculations are S , x_3 , a , θ_{av} , θ_m , and θ_d .

(2) Keffer et al. (2023) developed a method for determining excess head for finite well lines from the excess head for infinite well lines. Infinite parameters are used to find new finite parameters, so that excess head can be calculated at four key locations: excess head at the middle (h_{mm}) and at the end (h_{me}) of a well line between the last two wells, and maximum landward of the middle (h_{dm}), and maximum landward of the end (h_{de}) of a finite well line. The locations of these head values are illustrated in Figure 6–3 and Figure 6–4.

c. *Finite line design charts and equations.* Figure 6–5 through Figure 6–8 are used in this process. These figures use inputs of θ_{av} , θ_m , S/a , x_3/a , and the number of wells in the finite line (N). From these figures, the finite line uplift factors (θ_{mm} , θ_{me} , θ_{dm} , and θ_{de}) can be determined. Each finite uplift factor is then substituted for θ_{xx} in equations 6–1 or 6–2 to solve for h_{xx} (excess head for each uplift factor). θ_{mm} and θ_{me} are used to solve for h_{mm} and h_{me} . θ_{dm} and θ_{de} are used to solve for h_{dm} and h_{de} .

$$h_{xx} = \frac{h \times \theta_{xx}}{\frac{S}{a} + \theta_{av} \left(\frac{S + x_3}{x_3} \right)} \quad (6-1)$$

$$h_{xx} = a \times \Delta M \times \theta_{xx} \quad (6-2)$$

d. *Using the design charts.* Figure 6–5 through Figure 6–8 are based on N , S/a , x_3/a , and the infinite line uplift factors. Inputs are θ_m , S/a , and x_3/a from an infinite line design (Chapter 5), which appears to satisfy h_a . However, since the line is finite, N must also be considered, which could increase the expected excess head. From these values, θ_{mm} is determined from Figure 6–5 and θ_{me} from Figure 6–6. The values for θ_{av} , S/a , x_3/a , and N then are used to determine θ_{dm} (Figure 6–7) and θ_{de} (Figure 6–8). If excess heads for the finite line exceed h_a , then decrease a , increase (\bar{W}/\bar{D}) , or increase N , and repeat the infinite and finite line analyses until they are acceptable.

e. *Interpolation to designer values.* The user's values for θ_m , or θ_{av} virtually always fall between the plotted values on the figures ($\theta_m = 0.29; 1.92; \text{ or } 3.49$ or $\theta_{av} = 0.18; 1.93; \text{ or } 3.84$). If so, the designer should solve for finite uplift factors at the two given infinite uplift factors above and below the designer's value. Then, linear interpolation should be used to find the finite uplift factor at the needed infinite uplift factors. In these interpolations, θ_m or θ_{av} are the independent variables, and θ_{mm} , θ_{me} , θ_{dm} , or θ_{de} are the dependent variables.

Uplift factor for middle of finite well line (θ_{mm})

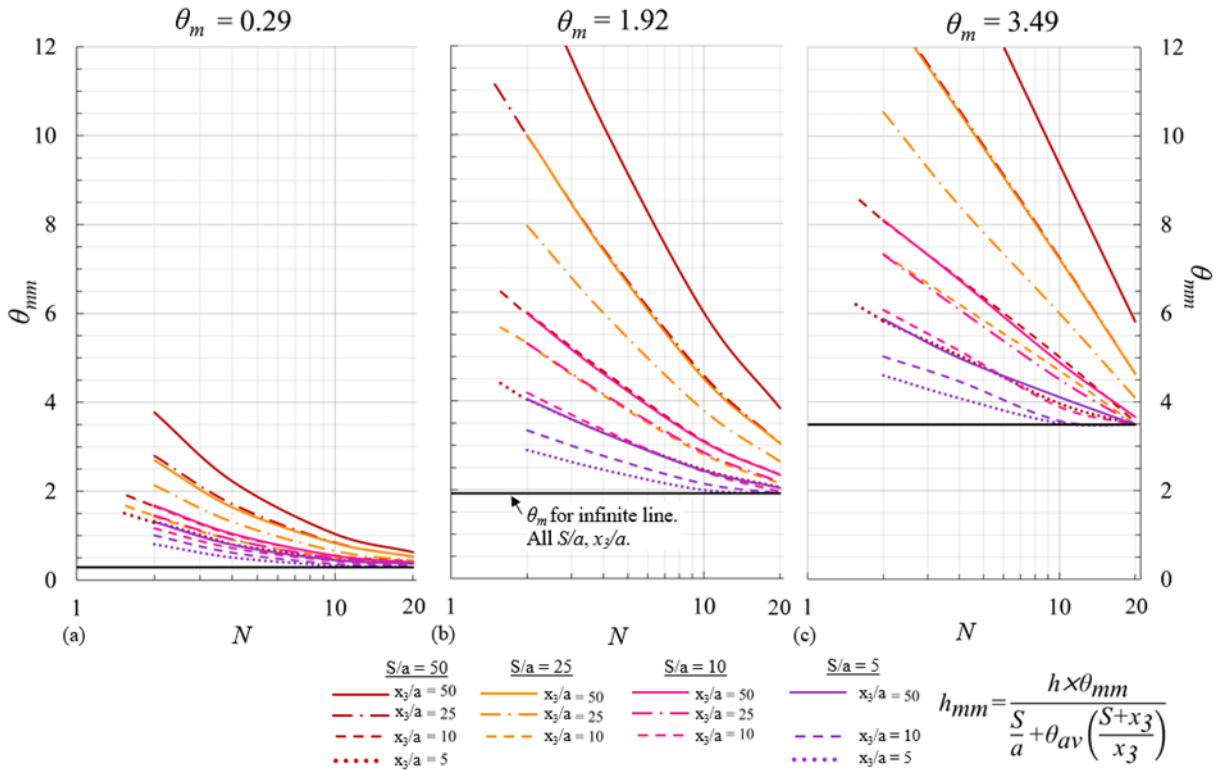


Figure 6–5. θ_{mm} for finite well lines for the infinite line cases when $\theta_m = 0.29$ (a), 1.92 (b), and 3.49 (c) (Keffer et al. 2023)

Uplift factor for end of finite well line (θ_{me})

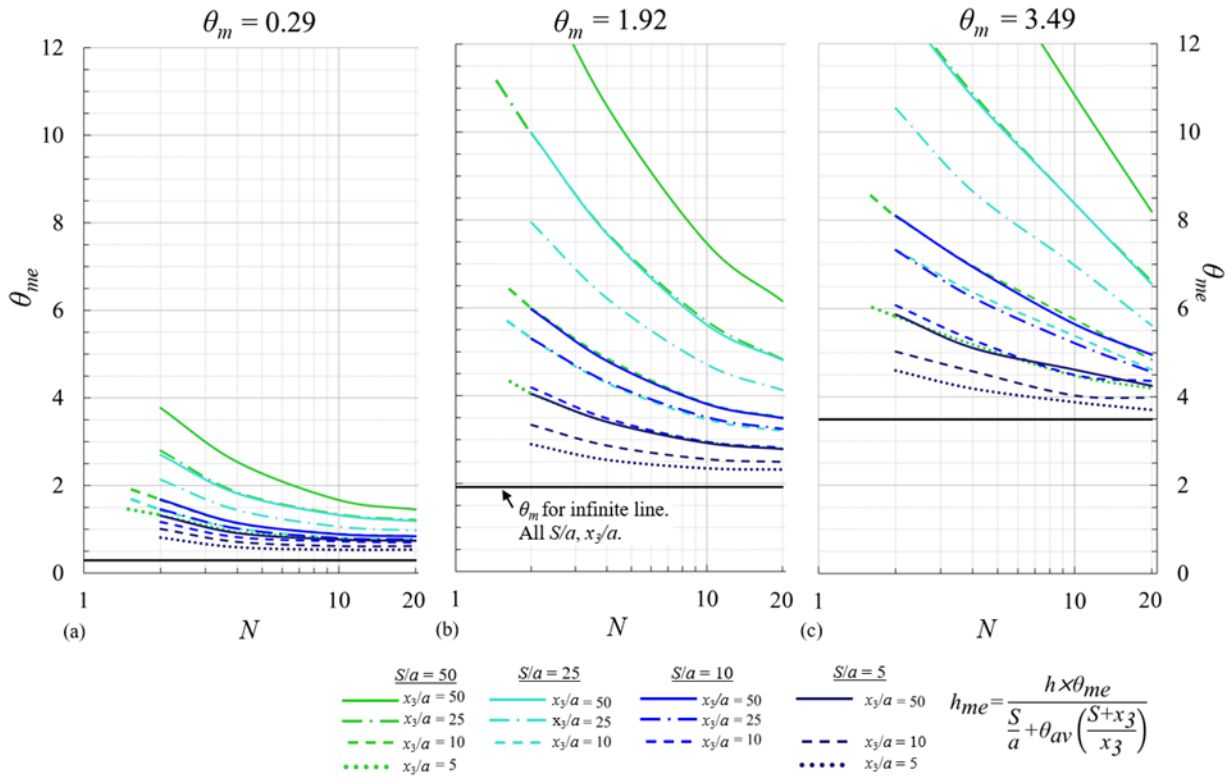


Figure 6–6. θ_{me} for finite well lines for the infinite line cases when $\theta_m = 0.29$ (a), 1.92 (b), and 3.49 (c) (Keffer et al. 2023)

Landward maximum uplift factor for middle of finite well line (θ_{dm})

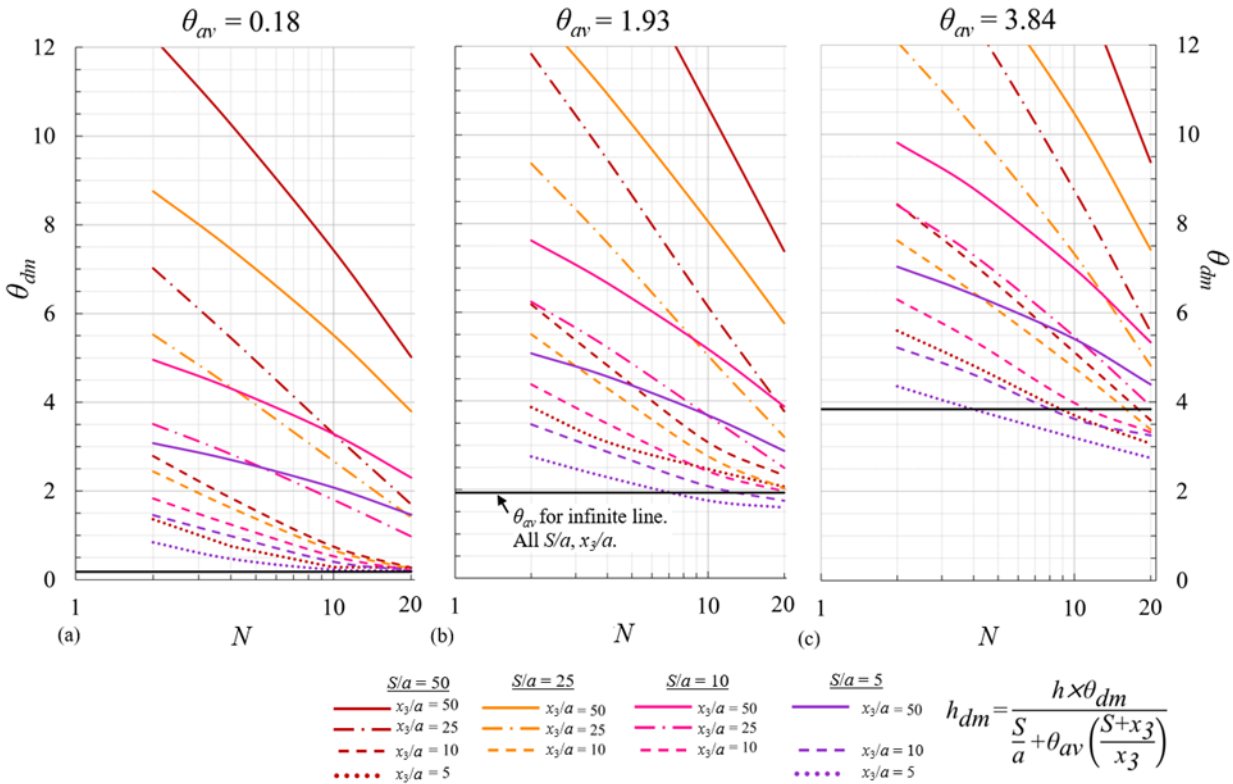


Figure 6–7. θ_{dm} for finite well lines for the infinite line cases when $\theta_{av} = 0.18$ (a), 1.93 (b), and 3.84 (c) (Keffer et al. 2023)

Landward maximum uplift factor for end of finite well line (θ_{de})

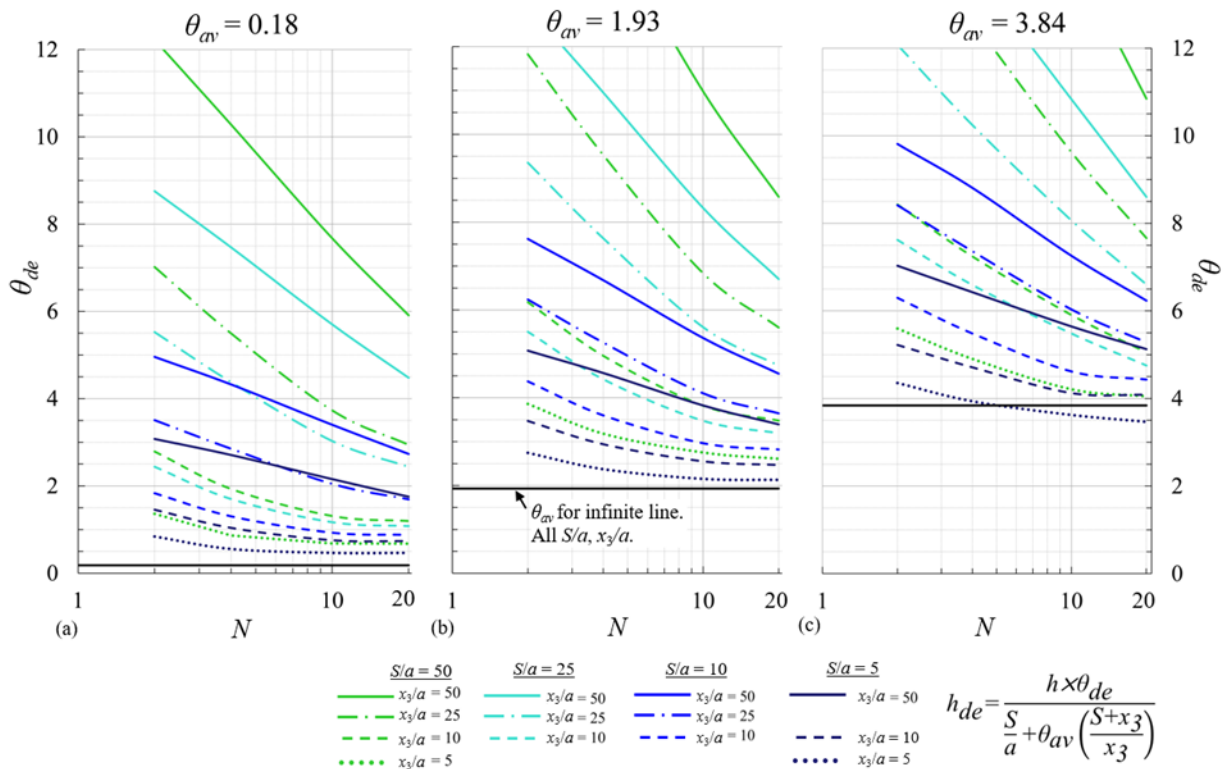


Figure 6–8. θ_{de} for finite well lines for the infinite line cases when $\theta_{av} = 0.18$ (a), 1.93 (b), and 3.84 (c) (Keffer et al. 2023)

6–5. Image Well Method

The analysis of multiple well systems using superposition theory and image wells is presented in detail in Appendix D. One method discussed in Appendix D is the IWM for an infinite line source and an impervious blanket. This can be adapted using BT to incorporate a semi-pervious blanket, a practical modification applicable to many wells. An infinite line source and a finite well system is a common design assumption for most levees and some dams. Several examples of the IWM with the BT adaption are presented in Appendix I. This adaptation results in well solutions that are in good agreement with heads calculated by the other well analysis methods discussed in this manual.

a. Discussion of method.

(1) The benefit of IWM with the BT adaptation is that well system geometry and boundary conditions can be quickly varied to evaluate the effect on well system effectiveness. Key design variables include well spacing, discharge elevation, and the level of performance loss over time (described in Chapter 9). Other parameters, including hydraulic loading on the structure, can also be easily adjusted. End effects are directly accounted for in the solution. Relief wells can be placed in any arrangement,

with the location referenced from the landward toe of the structure. A common application for this method would be wells located along a ditch perpendicular to the levee. Wells are often needed for ditches around gravity structures and pump stations to reduce uplift.

(2) This adaptation results in well solutions that are in good agreement with heads calculated by the other well analysis methods discussed in this manual. However, the calculated flows from the IWM and BT adaptation are often less than those calculated by the other well analysis methods. It is common practice to assign aquifer permeability based on the most pervious layers in the aquifer, which helps offset well flow that tends to be underestimated in this calculation method. Using the higher permeability of the deeper aquifer layers in the well analysis can counteract the underestimated well flows.

b. Assumptions of method. The source and levee are assumed to be parallel, linear, and infinitely long. Other assumptions listed in Appendix C for BT and Appendix D for IWM also apply. The semi-pervious blanket overlying the aquifer is assumed to be infinite in extent for the BT equations presented in this manual. EM 1110-2-1913 includes BT adjustments for other boundary conditions not discussed in Appendix C.

c. Computations. IWM with the BT adaptation is more computationally intense than the infinite line of wells solution described in Chapter 5. This approach typically uses a spreadsheet or other software because hand calculation would be difficult to execute. The calculation to determine well flow is iterative when flow is used to estimate well losses. This process is repeated until the assumed and calculated well losses converge. Well system design using this method is also iterative to locate wells to provide adequate drawdown. Trial well locations and losses are assumed, flows calculated, well losses calculated based on those flows, heads are calculated at points of interest, and well locations are adjusted until gradient safety factors are acceptable at all points of interest. The IWM is adapted to BT for the case of an infinite line source and infinite semi-pervious blanket using the steps described below.

(1) *Excess head at any point from Blanket Theory.* The excess head along the landside toe is calculated using BT with the appropriate equations (Appendix C and EM 1110-2-1913). This calculation ignores the effects of any wells. The head at any distance riverward from the landside toe is calculated assuming a linear head loss between the full head at the effective entrance and BT head at the landside toe. The excess head at any distance landward from the landside toe is calculated using BT equation 6–3.

$$h_x = h_o e^{-cx} \quad (6-3)$$

where:

h_x = excess head at location x

h_o = excess head calculated at landside toe

x = distance landward between landside toe and location x

c = landward factor for calculating effective seepage exit distance, $c = 1/x_3$ for an infinite landward blanket

(2) *Hydraulic grade line.*

(a) The hydraulic grade line, or *HGL*, represents the total head acting along the base of the semi-pervious blanket, and is determined by adding the excess head, calculated as described in paragraph 6–5c(1), to the assumed landside ground surface elevation. The *HGL* includes pressure relief caused by seepage through the semi-pervious blanket and extends from the effective seepage entrance to an infinite distance landward as shown in Figure 6–9. The excess head without wells at each proposed well location is used to calculate flow for that well. This is because the flow with wells is proportional to the head without wells at the well location.

(b) In turn, flow from each well is used to calculate drawdown at a point of interest. The drawdown is then subtracted from the *HGL* to calculate the head with wells, at the location of the point of interest. That head is then used to calculate FS_{vg} at the point of interest. In summary, the *HGL* also serves as the baseline from which drawdown due to well flow is subtracted to calculate FS_{vg} at points of interest.

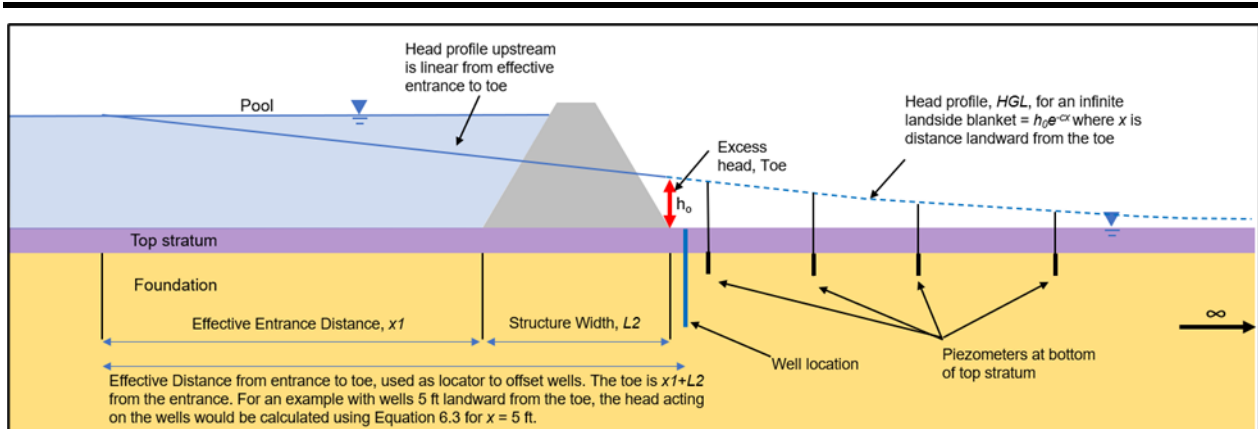


Figure 6–9. Hydraulic grade line (*HGL*) used in Image Well Method with Blanket Theory adaptation

(3) *Trial well system.* An initial well system is assumed. Typically, it is easiest to start with a uniform well spacing. Thereafter the exact spacing and/or well locations can be adjusted near the ends of the line to account for end effects.

(4) *Calculating flow from wells.*

(a) The head at each well location is assumed to be the *HGL* minus the well discharge elevation plus well losses. The flow from each well, Q_w , can be determined for wells 1 through n using a modified version of equation D–12 in Appendix D (included here as equation 6–4). The calculated flow is for a full-penetration well and does not introduce significant error for full-penetration wells. However, this is an important consideration for partial penetration as needed. Partial-penetration wells are discussed in paragraph 6–5c(5).

(b) The image well theory using superposition principles considers the impact of adjacent wells. Therefore, well flows are variable along a finite well line. Wells nearer the ends of the system flow more than wells nearer the middle of the system. Wells in adjacent sub-reaches should be included in the analysis of a specific reach to avoid undue conservatism in determining well spacing. The calculation becomes more complex as the number of wells increase and must be iterative because H_w is a function of Q_w . Excel spreadsheets can automatically perform iterative calculations until convergence.

$$Q_w = \frac{2\pi kD(H_{HGL} - W_D + H_w)}{\sum_{j=1}^n \frac{r'_j}{r_j}} \quad (6-4)$$

where:

k, D, r'_j, r_j are as defined in Appendix D

H_{HGL} = the HGL elevation without wells

W_D = well discharge elevation

H_w = well losses

(5) *Aquifer transformation and well penetration.* Aquifer transformation and well penetration are important considerations for partial-penetration wells and are discussed in detail in Appendix E. The aquifer layers with different permeabilities are transformed to an equivalent depth of homogeneous aquifer to determine the effective well penetration. Ignoring aquifer transformation and using actual well penetration does not introduce significant error for full-penetration wells. If full-penetration wells are to be used, a representative permeability value for the more permeable portions of the aquifer is adequate to calculate well flows.

(6) *Partial-penetration wells.* Flows calculated for full-penetration wells must be adjusted if partial-penetration wells are used. The Kozeny equation (equation E-3 in Appendix E) can calculate a partial-penetration factor to adjust the calculated flow for full-penetration wells. Those reduced flows are then used to calculate the head at points of interest. Since flow and head losses are calculated iteratively until convergence, the calculated head losses account for the reduced flow from partial penetration. This method has shown reasonable agreement when comparing calculated heads and observed field data.

(7) *Reduced performance with time.* Flow from wells may also be adjusted for assumed performance loss over time due to biofouling or other well degradation as described in Chapter 9. For example, if an 80% reduction in well performance is assumed to occur over the life of the well, 80% of the calculated flow should be used to calculate heads. By assuming a reduced flow rate, the system design will have resilience to some level of degradation. The appropriate reduction in flow for a well system design over time depends on several factors. These include the gradient without

wells and the threshold gradient safety factor for well rehabilitation. Also, the anticipated rate and magnitude of biofouling should be assessed, as discussed in Chapter 9.

(8) *Calculation of drawdown.* The adjusted flows from each well are used to calculate the head at points of interest. The drawdown is subtracted from the *HGL* without wells to determine the head acting at the base of the semi-pervious blanket. Locations of interest are typically along the landside toe and midway between relief wells. However, the heads can be calculated at any location of interest, such as along a landside ditch or around an isolated feature. The head at a point of interest, h_p , is calculated using a modified version of equation D–10 in Appendix D (here equation 6–5), with all terms previously defined. The calculation becomes more complex as the number of wells and number of interest points increase. A calculation table, or tables, can be pre-configured to facilitate calculating heads at points of interest, such as points along a line parallel to the well system or a line perpendicular to the well system.

$$h_p = H_{HGL} + H_w - \frac{1}{2\pi kD} \sum_{j=1}^{j=n} Q_{w_j} \ln\left(\frac{r'_j}{r_j}\right) \quad (6-5)$$

(9) *Gradient safety factor.* Finally, the vertical gradient through the blanket is calculated at points of interest using h_p . Then the FS_{vg} is calculated at the points of interest and compared to the desired vertical gradient safety factor. The well locations are then adjusted as necessary to achieve the desired gradient safety factor and to economize the design to the extent practical. In practice this usually means modifying well locations to meet the desired safety factor at all points of interest. This process typically results in tighter well spacing at the ends of the system. The design must also consider site constraints such as difficulty in accessing one or more of the proposed well locations, with well locations adjusted as needed.

Chapter 7

Design of Well Components and Calculation of Head Loss

7–1. Well components

There are several components of relief wells, each of which have the potential to contribute to head loss in the well system. The well head loss needs to be estimated and accounted for in design. While the materials, dimensions, and methods of installations differ, all relief wells share the same basic elements:

- a. Drilled hole to facilitate the installation;
 - b. Screen or slotted pipe section to allow entrance of groundwater;
 - c. Riser to conduct the water from the screen to the ground surface;
 - d. Sump and bottom plate;
 - e. Granular filter around screen to prevent entrance and ultimate loss of foundation material;
 - f. Check-valve to prevent backflooding and foreign material from entering the discharge point;
 - g. Backfill and seal above screened interval to prevent entry of surface water; and
 - h. Protective cover to prevent vandalism and/or damage to the top of the well by maintenance crews, livestock, etc. The cover may require a lock in some instances.
- Figure 7–1 shows a typical relief well installation.

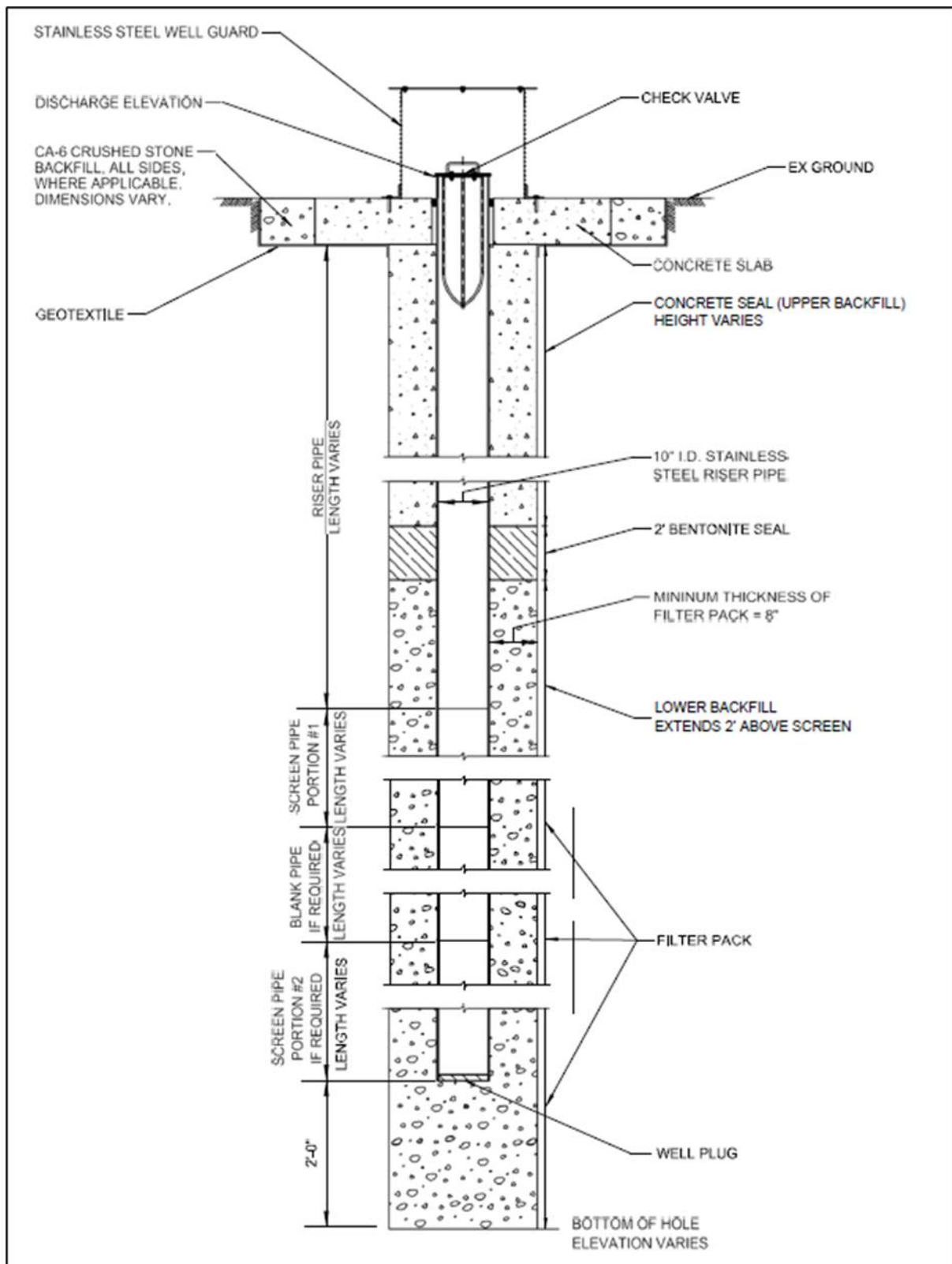


Figure 7-1. Typical relief well installation

7-2. Drilled hole

The size of the borehole for a relief well depends on the well diameter plus a minimum filter thickness of 4 to 8 inches. The hole is drilled to a large enough diameter to provide for filter material that may become segregated during placement. This is described in paragraph 7-6a(2). The diameter of the borehole also depends on the size of tremie pipe used for filter placement.

7-3. Well diameter

The well diameter must be large enough to conduct the maximum anticipated flow to the ground surface. The diameter must also allow testing and servicing of the well after installation and for the lifespan of the project. Such testing and servicing can include using brushes, instrumentation, and submersible pumps. Anticipated head loss should also be considered.

7-4. Well materials

Commercially available well screens and riser pipes are fabricated from a variety of materials, including black iron, galvanized iron, stainless steel, brass, bronze, fiberglass, and PVC. Pressure relief wells are designed and installed to protect the foundations of structures. Therefore, selection of materials for the wells should be based on costs and performance over the life of these structures.

a. Recommended well materials. Stainless steel is a very stable material in most environments. Although the up-front cost is relatively expensive, stainless steel can generally be maintained successfully for the life of a project. It is recommended for permanent well installations in most situations. Other materials can experience significant degradation over these time spans or be unable to withstand aggressive rejuvenation techniques. Types 304 and 316 stainless steel have excellent corrosion resistance, whereas Type 403 stainless steel has moderate corrosion resistance. Types 304 and 316 contains some nickel, which makes them more expensive than Type 403. Couplings and the bottom plate for the well screen should be constructed of the same material as the well. These are glued, threaded, or welded to the well.

b. Less commonly used well materials.

(1) Low-carbon or other types of steel wire-wrapped screen may appear economical in many instances. However, these materials are susceptible to corrosion and are not well suited to permanent installations.

(2) PVC is chemically stable, relatively inexpensive, and easy to handle and install. However, it is relatively weak, easily damaged, unable to withstand heat treatment, and not well suited to permanent installations.

(3) Iron has also been used for relief well screens and riser pipes. The life of iron wells can be extended by galvanizing, but iron will corrode sooner than stainless steel. Primarily for this reason, iron relief wells have been largely discontinued.

(4) Some older wells are constructed of wood, which has proven to be very stable in most environments if continuously submerged in water. However, wood wells are not able to withstand aggressive rejuvenation. Wood well screens and risers are no longer commercially available and are not used in new well construction.

(5) Porous concrete well screen was also used in some USACE relief wells installed prior to 1950 but is not considered suitable for new wells.

(6) Brass and bronze are extremely expensive and are not completely stable in some acid environments.

c. Material selection criteria. How well a material performs with time depends on several factors, including its strength, resistance to damage from servicing, and resistance to chemical constituents in the groundwater. Generally, the choice of well material depends on three factors: (1) water quality, (2) presence of iron bacteria, and (3) strength. A water quality analysis will determine the chemical nature of the groundwater and indicate whether it is corrosive and/or encrusting (see Table 3–1). In most cases, stainless steel and wire-wrapped screen are generally the best choice for relief wells. Other materials such as PVC or carbon steel may be appropriate for temporary wells or when selected in a risk-informed, decision-making framework.

(1) *Chemical considerations.* Enlargement of screen openings due to corrosion can allow progressive movement of fines into the well. Therefore, the well screen must be fabricated from corrosion-resistant material if corrosive waters are expected. Groundwater chemistry also can facilitate mineral encrustation of the well screen. Bacteria may also be present. In either case acid, heat, and/or chemical treatments may be required (see Chapter 11). The well material must be able to withstand such treatments. Ferrous and non-ferrous metals should never be placed in direct contact with each other. An example is a brass screen and a steel riser. The direct contact of these dissimilar metals may induce electrolysis and a resultant deterioration of the material.

(2) *Strength considerations.* The strength of the well screen is usually not a major factor when commercial well screens designed for deeper well installations are employed. The screen sections should be able to withstand maximum compression and tensile forces during installation operations as well as horizontal forces, which may develop during installation and possibly later because of lateral earth movements. The recommended hang weight and collapse strength can frequently be obtained from the manufacturer. Stainless steel screens are more amenable to aggressive redevelopment than other material types that may release contaminants or melt. Screened sections can be susceptible to damage during pump testing. This is especially true if the pump intake is located in the well screen and sudden suction is applied.

(3) *Riser, blank sections, and sump.* The material chosen for the screened intervals should generally be used for the well riser, blank sections, and sump. The riser extends above the screened intervals to the ground surface. Blank sections are included between changes in the screen/filter pack or to exclude fine grained layers

from exposure to the filter pack. Filter packs should overlap the blank interval to provide at least 2 feet of allowance for filter pack settlement during development. A sump is included at the bottom of the well to allow space for materials to settle and to allow better tool access during well development and future rejuvenation. The sump should be at least 2-feet deep, with a bottom plate of the same material.

7–5. Well screen

a. *Slot type.* Different screen types are available in a variety of materials, including continuous-slot (wire-wrap) screens and slotted plastic pipe.

(1) *Continuous slot.* These screens consist of a skeleton of vertical rods wrapped with a continuous spiral of wire. Continuous-slot, wire-wrapped screens are the dominant screen type used in the water well industry. They are commercially fabricated, typically of carbon, galvanized carbon, or Type 304 or 316 stainless steel. These screens can also be made of thermoplastic materials, mainly PVC and acrylonitrile-butadiene-styrene (ABS), or alloys of these materials. Wire-wrapped screen is strong and has a high percentage of open area, which reduces entrance velocities and makes wells more efficient. The wire wrap is typically V-shaped in cross section with slots progressively larger toward the inside of the screen. This shape allows any filter gravel that enters the slot to fall into the well rather than clog the screen.

(2) *Slotted plastic pipe.* PVC screens with open slots of varying dimensions, consisting of a series of saw cuts. Machine-cut slots typically have jagged edges that facilitate the attachment of iron bacteria and make treatment more difficult. These screens also have less open area than continuous-slot screen for an equivalent slot width.

b. *Slot size.*

The size of the slots is a factor in the open area of the screen. The slot size also must be compatible with the filter pack.

(1) *Slot size and open area.* The slot size, well diameter, and length of the screen determine the open area available for water flow. The open area and flow rate, in turn, determines the entrance velocity, v_e , of water moving through the screen. Larger entrance losses, greater than the entrance losses depicted in this chapter, would need to be considered for entrance velocities larger than 0.1 feet per second (fps). The slot size is determined after the filter is sized to meet retention and permeability requirements for the aquifer. Well diameter and screen length are then adjusted to achieve the necessary open area. Representative areas and maximum well capacities for various well diameters with different continuous slot sizes are shown in Table 7–1. Well screen manufacturers should be consulted for more specific information.

Table 7--1

Properties of continuous wire-wrapped stainless-steel screens (Type 304) commonly used in relief wells (based on: <https://johnsonscreens.com> (2021))

Size Nominal (in)	Max. Depth (ft)	Out. Diam. (in)	Inside Diam. (in)	Weight (lbs/ft)	Hanging Wt. ¹ (lbs)	Collapse St. ² (psi)	Intake Area ³ (in ² /ft) Slot Size (thousandths of an inch)							
							10	20	30	40	50	60	80	100
6	100	6.6	6.1	4.5	4,315	83	36	62	83	100	113	124	142	156
6	250	6.7	6.1	4.8	4,315	187	20	37	52	65	76	86	103	117
8	250	8.7	7.9	8.0	12,118	130	26	48	67	84	98	111	133	151
8	600	8.7	7.9	10.0	11,444	487	21	39	55	69	82	94	114	131
10	600	10.7	9.9	12.5	14,566	173	25	48	68	85	101	116	141	162
12	250	12.7	11.8	14.7	16,646	104	30	57	80	101	120	137	167	192
12	600	12.7	11.8	16.2	16,646	138	30	57	80	101	120	137	167	192
14	250	14.0	13.0	15.5	16,126	79	33	62	88	111	132	151	183	211
14	600	14.1	13.0	28.5	16,126	249	35	66	93	117	138	158	192	220

Notes:

¹ Hanging weight is given as 50% of the calculated tensile strength.

² Collapse strength based on 0.030-in slot size.

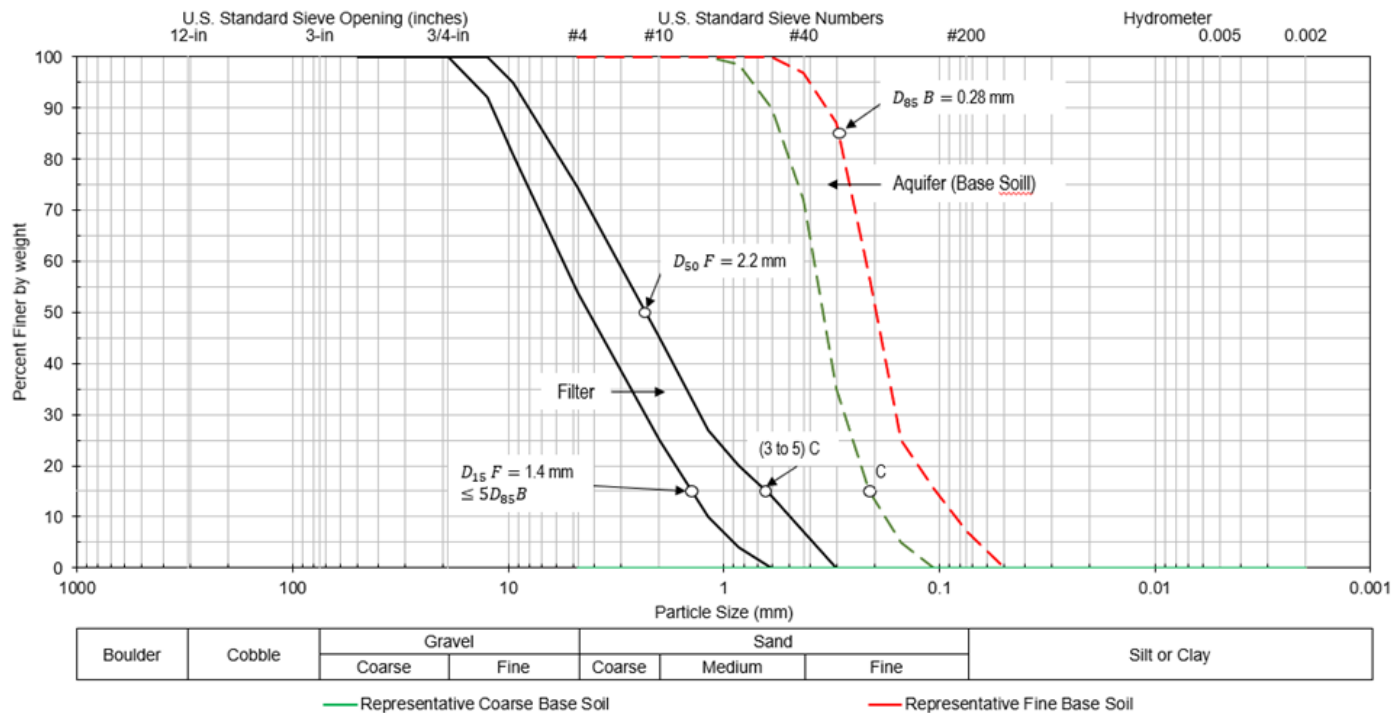
³ Transmitting capacity (gpm/ft) = 0.31 x intake area (assumes entrance velocity of 0.1 ft/s).

(2) *Matching slot size and filter.*

(a) The size of the slots in a well screen should be as wide as possible to allow maximum flow and minimal entrance velocity. Larger slot size also provides resiliency against possible long-term clogging or encrustation. At the same time, the slots must be sufficiently small to minimize entrance of filter materials. For well-graded filters, the slot width should be equal to or less than the 50% size (D_{50}) of the finest gradation of adjacent filter pack material. Application of this criterion is demonstrated in Figure 7–2.

(b) Hadj-Hamou et al. (1990) demonstrated the 50% size criterion was sufficient for the well-graded filters that USACE commonly used at that time. This slot size provided reasonable assurance against in-wash of filter materials during well development and surging. Hadj-Hamou et al. (1990) also tested a uniform filter with screen slot width based on the D_{10} size of the filter. Screen entrance losses were negligible and there was practically no loss of filter material during and after surging.

(c) Some USACE Districts have successfully used uniform filter gradations with screens set at 10 to 15% passing criterion. Talbot and Pabst (2006) explain that the USDA Natural Resources Conservation Service requires screens to be set at 15% passing criterion for critical drains with surging or reverse gradient, which is the case for relief wells.



General Procedures for Sand and Gravel Aquifers with < 15% Fines (Category 4 Base Soil):

1. Identify the maximum and minimum gradation curves that characterize the aquifer or “base” material.
2. Determine minimum $D_{85}B$ on band of grain size curves for aquifer.
3. Determine maximum $D_{15}F$ for filter material based on the stability criterion.
4. Maximum $D_{15}F < (4 \text{ to } 5) \times \text{Minimum } D_{85}B$ (Category 4 base soil).
5. Select a widely graded or uniform filter material meeting the above criteria.
6. Establish a reasonable grain size band for the filter, in particular a sufficient spread between minimum and maximum $D_{15}F$.
7. Check to ensure that permeability criterion is satisfied, that is, the minimum D_{15} size of the filter band is 3 to 5 times greater than the maximum D_{15} size of the aquifer band.
8. Select a maximum screen slot size equal to the minimum D_{50} size of the fine curve of the filter band.

$$(D_{15}F - D_{15} \text{ size of the filter}; D_{85}B - D_{85} \text{ of the base soil}; D_{50}F - D_{50} \text{ size of the filter})$$

Figure 7-2. Typical design of a well-graded filter and slot size for relief well

7-6. Filter

A properly designed filter prevents infiltration of foundation material. It also has sufficient permeability to allow the design flow at a minimal v_e . To function as designed, the filter should consist of durable and stable material and not be subject to segregation during placement. The filter should extend at least 2 feet above the top of screen.

a. *Grading.* Either well-graded or uniform filter materials may be used for the filter pack as long as the screen is chosen appropriately. A specially blended material may be required to meet all the gradation requirements for uniform filters. However, these blends are generally more expensive.

(1) *Uniformly graded filters.*

(a) A uniform filter has a coefficient of uniformity, C_u , of less than 2.5, where C_u is defined as equation 7-1.

$$C_u = D_{60} / D_{10} \quad (7-1)$$

where:

D_{60} = grain size at which 60 percent by weight of sample is finer

D_{10} = grain size at which 10 percent by weight of sample is finer

(b) The annular thickness of uniform filters can be in the range of 4 to 6 inches, as these materials are not subject to segregation during handling and placement.

(2) *Well-graded filters.* Used with proper well development procedures, well-graded filters increase efficiency and permit the use of larger slot sizes. This also results in relatively large openings in the filter pack. Such spaces can minimize the effects of encrustations and blockages, which may develop during the life of the well. The C_u of well-graded filter materials should be between 2.5 and 6 to minimize segregation during placement. The grain sizes should be reasonably well distributed over the specified range (not gap-graded). Well-graded filters should have an annular thickness of 6 to 8 inches to allow some segregation.

b. *Stability criteria.* The filter gradation is typically sized to prevent infiltration of foundation sands through the filter. This means the maximum 15% size (D_{15}) of the filter is no greater than 5 times the minimum 85% size (D_{85}) of the base soil. As shown in Figure 7-2, the design should be based on the finest gradation of the foundation materials. Blank screen can be used in zones of unusually fine foundation materials. If the screen will penetrate foundation strata with different grain size bands, different filter gradations should be designed for each band.

c. *Permeability criteria.* Each filter gradation must also meet permeability criteria. This typically means the minimum D_{15} of the filter should be 3 to 5 times the maximum D_{15} of foundation sands.

d. Filter composition. The filter should consist of natural material made of hard durable particles. It should not contain organic matter or soft, friable, thin, or elongated particles. Crushed carbonate aggregates should be avoided because they tend to break down, resulting in a loss in permeability. They will also tend to dissolve if the wells require acid treatment as part of rehabilitation. The American Water Well Association (AWWA) (2016) standard test AWWA B100 can be used to determine the acid solubility of potential filter materials. Relief well designers typically specify filters with a minimum of 85 or 90% silica content.

7-7. Pre-packed well screens

a. Pre-packed well screens are available that consist of a riser and screen, with the filter included in the assembly. The filter annular thickness is generally very small compared to a traditionally constructed well. Pre-packed well screens have not been used widely for new installations but have been used successfully in retrofit applications. One application is where an existing well screen/riser has a defect or a well filter is not retaining the foundation soils. In these instances, pre-packed well screens may be placed inside the compromised screens to allow the wells to function. The smaller diameter screen and riser of a retrofit application should be re-evaluated for increased well losses. Another use of a pre-packed well screen may be a temporary or emergency relief well installation.

b. The advantage of a pre-packed well screen is that a smaller diameter bore hole is required. Disadvantages include the ability to incorporate mid-screen blank sections or multiple screen/filter sizes in the same well installation.

7-8. Backfill

The lower backfill fills the annular space around the riser pipe immediately below the bentonite seal. Its only function is to prevent collapse of the boring. This backfill normally consists of concrete sand or otherwise excess filter material. These granular materials are easily placed and require minimal compaction. The level of backfill should be brought at least 5 feet above the top of the filter.

a. Bentonite seal. An impermeable seal composed of either bentonite chips or a 30% high-solids grout is placed above the lower backfill. The seal serves multiple purposes, including preventing vertical flow of surface water down the outside of the well into the aquifer. This is particularly important if the aquifer is used for water supply. Relief wells relieve uplift pressure by allowing filtered flow of groundwater to the surface. The seal prevents flow from bypassing the well and filter and initiating erosion along the contact with the confining blanket. The seal also must resist the excess pressure head acting on the underside of the confining blanket. The bentonite seal should extend at least 2 feet above the top of the lower backfill.

b. Concrete seal. An upper backfill is placed in the annular space remaining above the bentonite seal and ground surface. This material should consist of a cement-

bentonite grout resistant to cracking. Design considerations for cold climates should incorporate measures to help alleviate frost jacking of the seal.

c. Filter pack monitoring tubes.

(1) If the well has been developed properly, there should not be any consolidation or settlement of the filter pack after placement of the bentonite seal and cement-bentonite backfill. However, it is sometimes desirable to monitor the filter pack level during relief well operation or rehabilitation. For example, consolidation or settlement of the filter pack can occur over time as well defects develop.

(2) Monitoring tubes (consisting of small PVC pipes, 2 to 3-inch in diameter) can be extended from the top of the well to the top of the filter pack. Once the tubes are installed, the seal and backfill can be placed. The tubes can be left unfilled and sounded to monitor levels or they can be filled with filter pack material so that any filter pack settlement is immediately filled with material to avoid formation of a void. Tubes filled with filter pack can be rodded or flushed with water to ensure that the material is not bridging in the pipe during routine observations. Figure 7–3 shows a typical well detail with filter pack monitoring tubes.

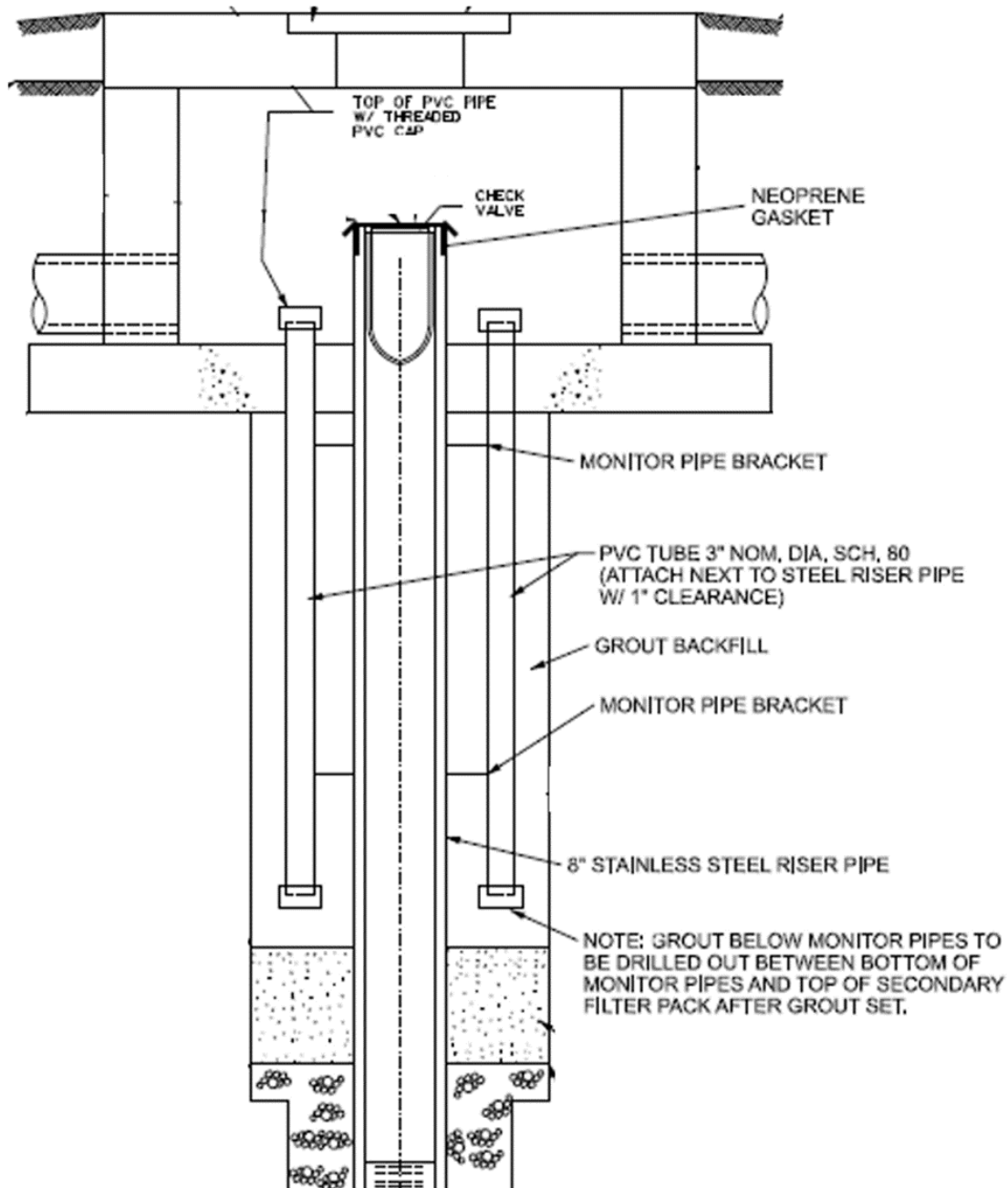


Figure 7-3. Typical below-grade discharge well detail with filter pack monitoring tubes, Kansas City District

7-9. Well head loss used in design

Relief well design must account for head losses that occur as water moves from the foundation into filters and screens and exits the relief well. Well efficiency (E) of a new well can be approximated by estimating total well losses (H_w) as described in this section. An assumed loss in E or SCR over time should be included in the relief well

design effort to align with operations and maintenance requirements. This can either be incorporated by increasing H_w , reducing the calculated drawdown by SCR or E -ratio, or by using well flow rates reduced by SCR or E - ratio to calculate drawdown. Further discussion of SCR and E - ratio and how to incorporate this into well design is included in Chapter 9 with examples in Appendix I

a. *Definition.* Head losses represent the decreased energy level of water as it flows through the relief well system or other resistances to flow leaving the well discharge point. These losses are expressed in units of length (for example, feet). There are three general components of head loss. The first is entrance head loss, which develops across the screen and filter (H_e). The second is friction head losses arising from flow in the screen, riser, and connections (H_f). The third is velocity head (H_v). The total loss (H_w) is given by equation 7-2.

$$H_w = H_e + H_f + H_v \quad (7-2)$$

b. *Entrance head loss.* The entrance loss (H_e) for a properly designed and developed screen and filter will generally be relatively small for a new well. Installation techniques resulting in smear or undue disturbance of the drill hole walls, however, can result in larger values of H_e .

(1) *Entrance velocity.*

(a) The average entrance velocity (v_e) is calculated by dividing the estimated flow rate of a well by the total area of the screen openings. Lower values of v_e promote laminar flow and minimize head loss. A well design that maximizes open area not only reduces entrance velocity but also allows better development and more effective well rehabilitation (Driscoll 1986). Past research (Driscoll 1986) has suggested that v_e should not exceed 0.1 fps. Many USACE districts have historically used 0.1 fps as the maximum allowable v_e for well designs. More recent sources allow higher entrance velocities; for example 1.5 fps (American Society of Civil Engineers [ASCE] 2014).

(b) Figure 7-4 shows that for a large range in flow rates (screen diameters and slot sizes typical for relief wells) a v_e of less than 0.1 fps is readily achievable. The figure also shows that these designs are conservative, as in most cases, v_e remains below 0.1 fps even when the screens become 50% obstructed. If the v_e calculated during the design is greater than desired, the screen length and/or diameter can be increased accordingly to increase open area.

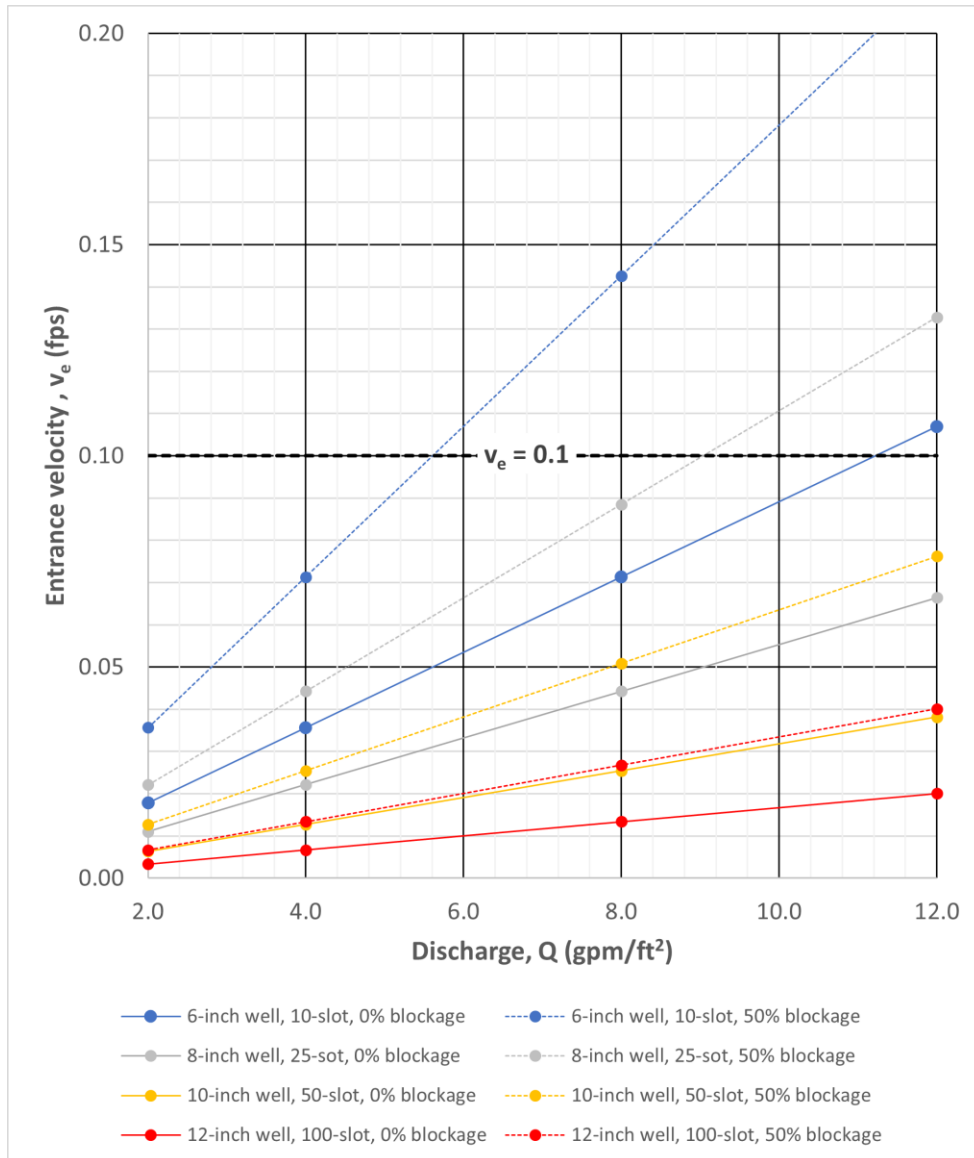


Figure 7-4. Trends in entrance velocity with variation in flow rate, screen diameter, slot size, and degree of screen obstruction; calculated values are based on a full-penetration well

(2) *Increase in H_e .* Entrance loss can be expected to increase with time for a variety of reasons, as discussed in Chapter 11. For example, consider a case where measurements of H_e were made for 8-inch, slotted-wood well screens. H_e was determined at the time of well installation and then determined at later times during subsequent pumping tests. H_e increased from less than 0.5 foot to over 1 foot with time because of biofouling and screen encrustation. The long-term value of H_e is difficult to predict without site-specific results such as this.

(3) H_e for design of wells.

(a) The H_e of a new well can be estimated using equation 7–3, which is based on wells 105 and 185 from Figure 7–5. This is likely a conservative estimate of H_e , as it is based on wood well screens, whereas wire-wrapped, stainless-steel screens are more prevalent for newer wells.

$$H_e = 0.02 \times (Q/\text{screen length}) \quad (7-3)$$

where:

H_e is measured in feet

Q is measured in gpm

Screen length is measured in feet

(b) As previously noted, H_e is expected to increase with time because of biofouling. The increase in H_e is the reason reduced well performance is generally assumed during design of new wells. As long as reduced well performance has been accounted for in design, and operation and maintenance is performed to ensure the performance threshold is never exceeded, the design should perform adequately with a design H_e assumed to be that of a newly constructed well. If information regarding the increase in H_e is available for a specific location is available, an increased H_e may be used instead of reduced well performance assumption in the design of a well. It is overly conservative to assume both a decreased well performance and an increased H_e during design of a well.

c. *Friction head loss.*

(1) Values of H_f in the screen (H_{f-s}) and riser (H_{f-r}) sections may be estimated from the Hazen-Williams relationship shown on Figure 7–6. The head loss in the screen section should be computed for one-half the screen length. The head loss in the riser is computed for the full length of riser. This estimate of friction loss is simple and generally adequate for relief well design.

(2) However, friction loss can be calculated more accurately with the Darcy-Weisbach formula as described in EM 1110-2-1602. The resistance coefficient in the formula is solved by the Colebrook-White equation, also given in EM 1110-2-1602. This equation requires the input of an effective roughness parameter for the material comprising the well screen and riser pipe.

(3) Losses due to elbow connections, flap gates, check valves, or other features that add resistance to flow should be added to values of calculated H_f as applicable to the discharge configuration of the well.

d. *Velocity head.* Flow velocity up the well riser is equal to the well flow rate divided by the riser area. The velocity head can be calculated using equation 7–4. At the top of the well riser, the velocity head causes the discharge water to swell above the top of the riser. This volume of water above the top of riser effectively raises the

discharge elevation of the well. Measurements of the fountain height are slightly higher than calculated with equation 7-4, and that additional height of water would resist well flow. Although velocity head is generally used for relief well system design, other methods to estimate the water fountain height could conservatively be used instead.

$$H_v = \frac{v^2}{2g} \tag{7-4}$$

where:

- v = velocity of water in the riser pipe
- g = acceleration due to gravity

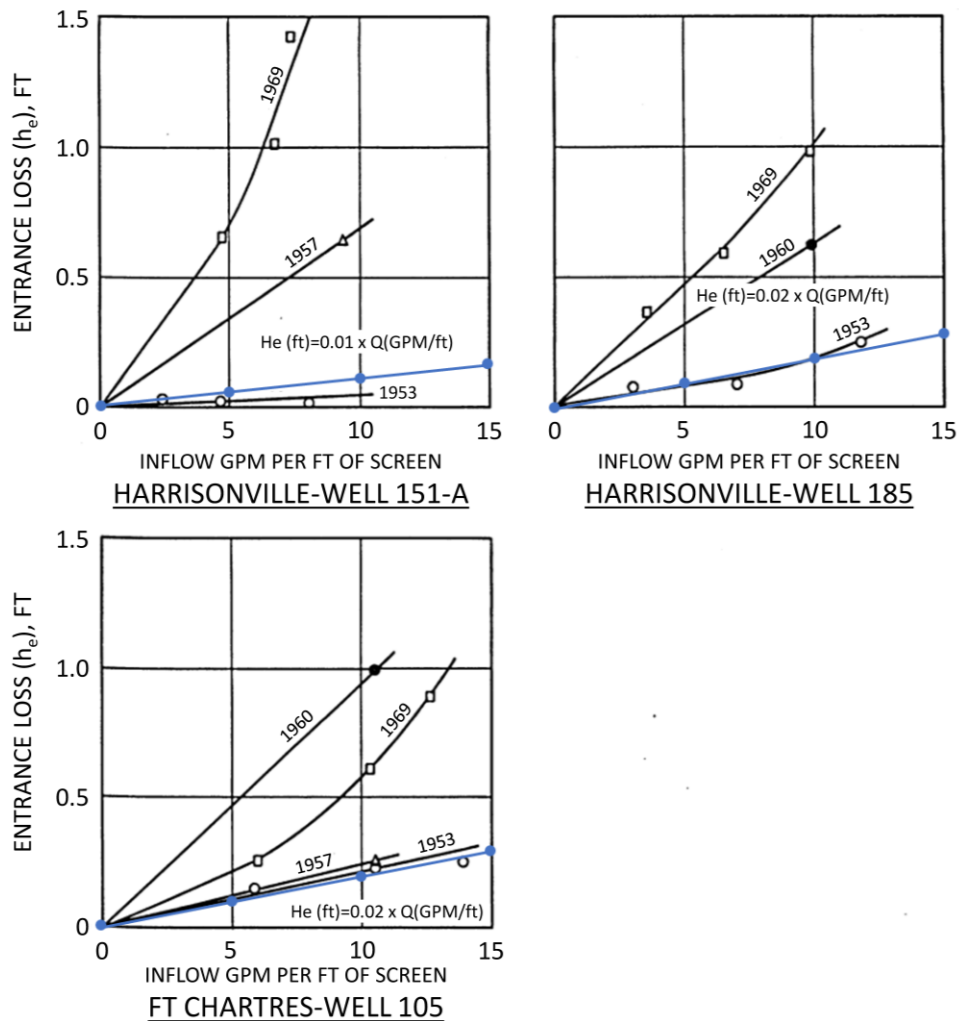


Figure 7-5. Entrance losses versus inflow for 8-inch inner diameter, slotted-wood well screens in St. Louis (after USACE 1972); best-fit equations shown for the newly constructed well entrance losses for inflow per foot of screen

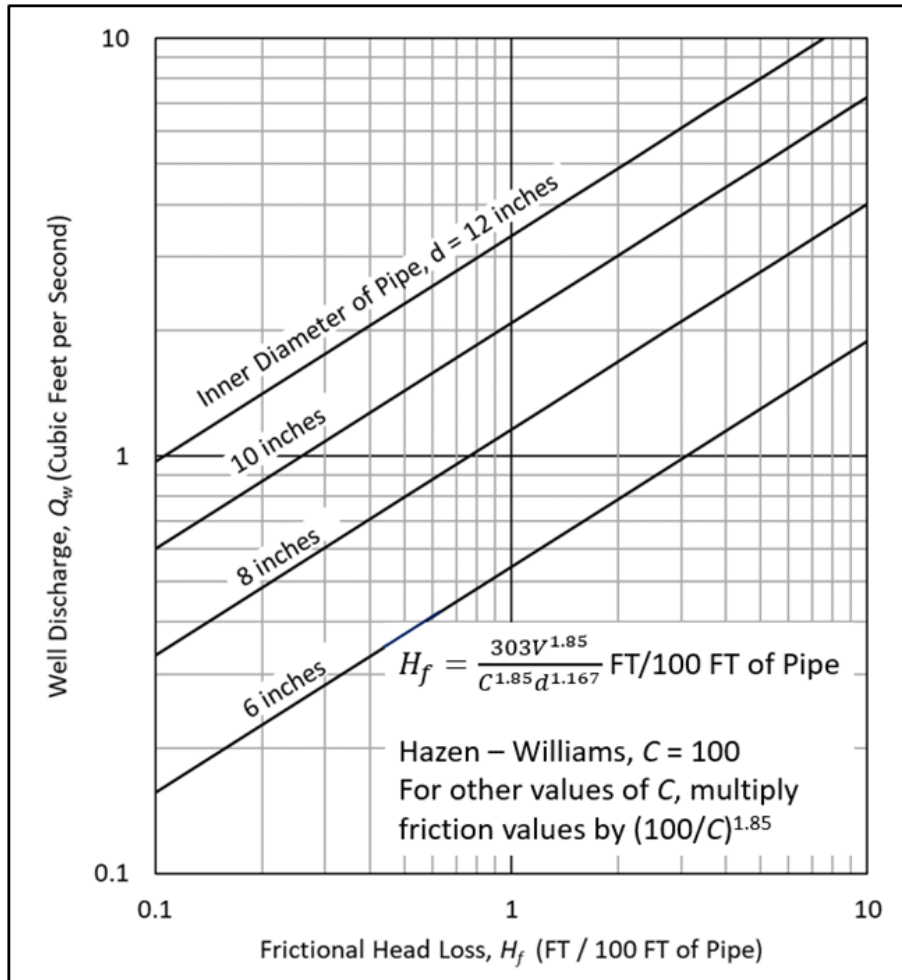


Figure 7–6. Friction head losses in screen and riser sections

(1) *Methods to estimate water fountain height.*

(a) Lower flow rates from a vertical pipe are analogous to circular weir flow, while higher flow rates from a vertical pipe are analogous to jetting, with a transition zone in between. Methods that include this range of flow behavior are available to estimate the water fountain height exiting a vertical pipe. Several of these methods are described in the Water Measurement Manual (USBR 2001). These methods provide either water fountain height or a water fountain height to pipe diameter ratio as a function of flow rate and pipe diameter, with varying degrees of reported accuracy.

(b) Figure 7–7 is one of those methods to relate water fountain height (solid lines) to flow for a range of pipe diameter based on published experiments. Equations for the solid lines in Figure 7–7 were presented by Lawrence and Braunworth in 1906 (USBR 2001) based on sighting rod measurements. Very similar results were measured using a pitot tube. These relationships between flow and fountain height are also useful to estimate flow from relief wells in the field.

(2) *Comparison between measured fountain height and velocity head.* The calculated velocity head (dashed lines) for common relief well diameters has been superimposed in Figure 7–7 for comparison. The upper-right quadrant of Figure 7–7 shows that as flow increases into the jetting zone, the water fountain height approximates the velocity head. The lower-left quadrant of Figure 7–7 shows that circular weir flow is the controlling behavior at lower flow rates and results in slightly higher estimates of water fountain height compared to velocity head. In the range of typical relief well scenarios, with well diameters from 6 to 12 inches and flows from 450 to 1,000 gpm, the difference between the experimentally observed water column height and calculated velocity head is generally less than 3 inches.

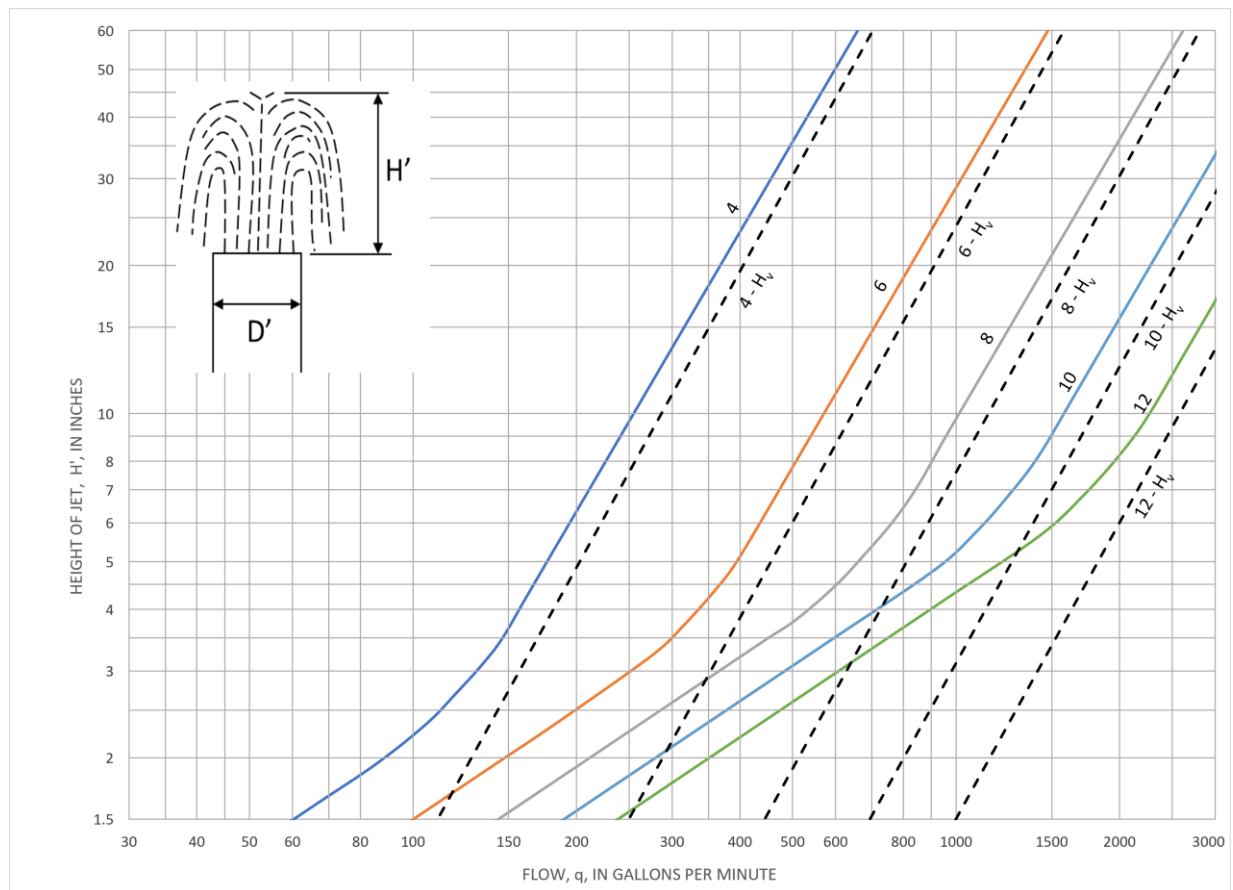


Figure 7–7. Discharge curves for measurement of flow from vertical standard pipes and calculated velocity head; the curves are based on data from experiments by Lawrence and Braunworth in 1906 (USBR 2001)

e. *Comparison of head loss from pumping tests and natural flow.*

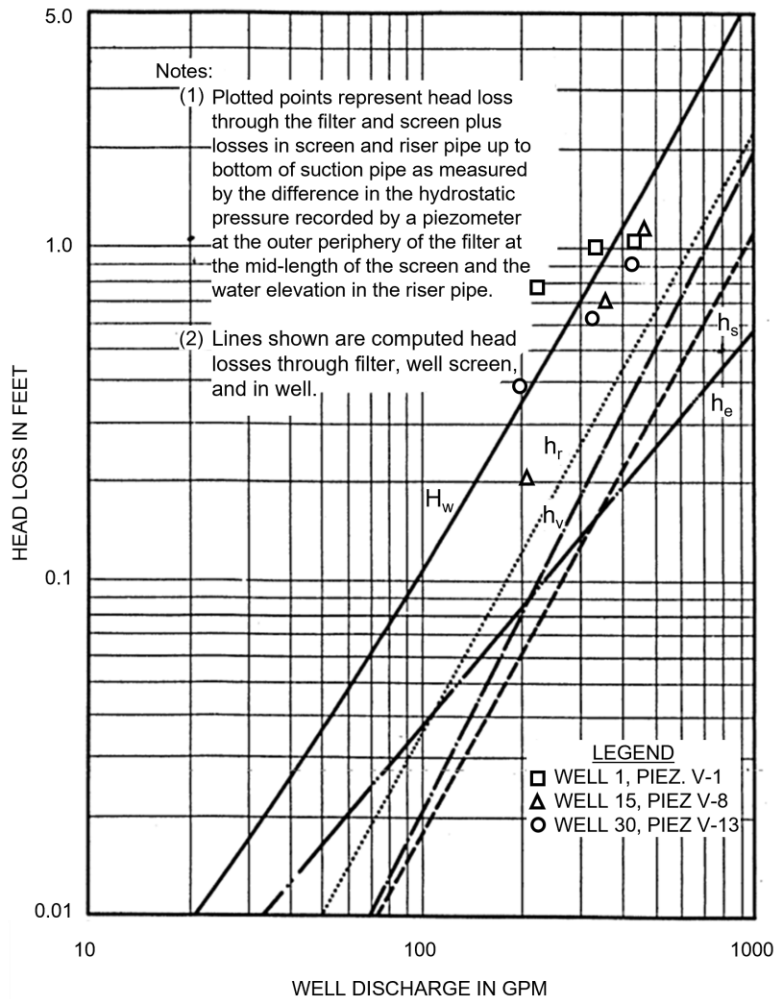
(1) This chapter covers determining well head losses from wells flowing under artesian flow applicable to well system design. The increase in entrance loss is illustrated in Figure 7–5 and results from biofouling or other screen blockages.

(2) Chapter 9 discusses well pumping tests used to monitor change in well head loss over time. Some individual components of well head losses differ between pumping tests and naturally flowing relief wells under artesian conditions. This is important to understand when evaluating individual head loss components from pumping tests. These head loss components for artesian flow that are used to design wells were studied and validated with field testing in USACE (1952) and related to well discharge as shown in Figure 7–8 and Figure 7–9. The velocity and entrance head losses are generally the same for a pumped or artesian condition. However, the friction losses are different between the two conditions because of the differences in discharge and pump configuration.

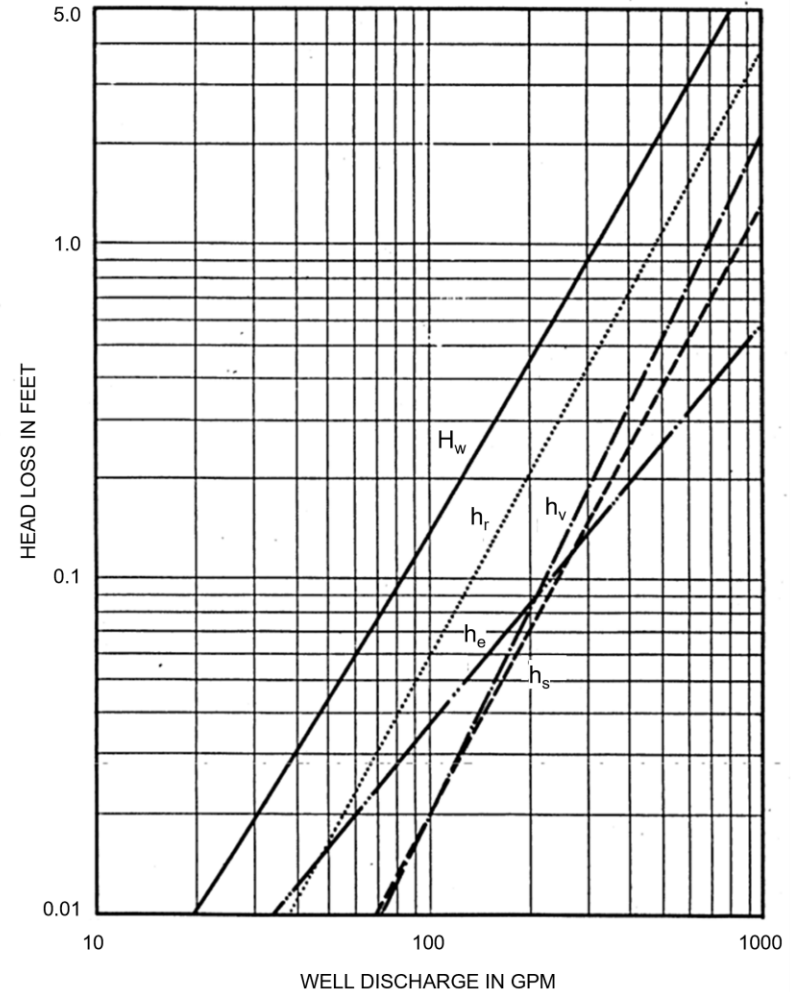
(3) For example, Figure 7–9a is for pumped wells and Figure 7–9b is for naturally flowing wells. The basis for the difference is explained in Figure 7–8. Pumping tests are normally used to monitor well performance. Therefore, comparing results from a baseline test to a subsequent test conducted under similar conditions makes any differences between pumped and artesian flow irrelevant. If pumping tests are being used to estimate well losses in the design of new wells, these differences should be considered.

f. Summary charts and tables. The equations and methods presented above are summarized in Figure 7–10 through Figure 7–13 for wells flowing under artesian conditions over a range of well flows, diameters, screen lengths, and riser lengths.

g. Example. A new 8-inch diameter well with a 20-foot riser, 80-foot screen, and calculated flow of 450 gpm would have, per Figure 7–11, 0.084 foot of riser friction losses and 0.55 foot of other well losses (screen friction, velocity, entrance) for a total well loss of 0.634 foot. Other combinations of diameter, riser length, screen, length, and calculated flow can be obtained from the charts or tabulated values in Figure 7–10 through Figure 7–13 for expedient determinations of well losses.



(a) HYDRAULIC HEAD LOSSES IN WELLS FOR PUMPIN CONDITION



(b) COMPUTED HEAD LOSSES IN WELLS FOR NATURAL FLOW CONDITION

Figure 7-9. Head loss in wells for both pumping and natural flow conditions (from USACE 1952)

Initial Well Head Loss, H_w , in Feet for properly constructed new well screen - 6 inch well																
Well Screen Portion Length	20 feet				40 feet				60 feet				80 feet			
Well Flow (gpm)	$\Sigma H_e+v+f-s$	H_e	H_v	H_f-s	$\Sigma H_e+v+f-s$	H_e	H_v	H_f-s	$\Sigma H_e+v+f-s$	H_e	H_v	H_f-s	$\Sigma H_e+v+f-s$	H_e	H_v	H_f-s
113	0.16	0.11	0.03	0.01	0.13	0.06	0.03	0.03	0.13	0.04	0.04	0.03	0.15	0.03	0.03	0.05
225	0.41	0.23	0.10	0.05	0.38	0.11	0.10	0.09	0.43	0.08	0.14	0.12	0.50	0.06	0.10	0.19
338	0.75	0.34	0.23	0.10	0.76	0.17	0.23	0.20	0.88	0.11	0.30	0.25	1.04	0.08	0.23	0.40
450	1.16	0.45	0.40	0.17	1.25	0.23	0.40	0.34	1.48	0.15	0.51	0.42	1.75	0.11	0.40	0.68
675	2.24	0.68	0.91	0.36	2.56	0.34	0.91	0.72	3.10	0.23	1.08	0.89	3.70	0.17	0.91	1.44
900	3.63	0.90	1.61	0.61	4.29	0.45	1.61	1.22	5.26	0.30	1.84	1.51	6.30	0.23	1.61	2.45
1125	5.33	1.13	2.52	0.92	6.45	0.56	2.52	1.85	7.95	0.38	2.77	2.28	9.55	0.28	2.52	3.70
1350	7.34	1.35	3.62	1.30	9.03	0.68	3.62	2.59	11.17	0.45	3.89	3.20	13.42	0.34	3.62	5.18
1575	9.65	1.58	4.93	1.72	12.01	0.79	4.93	3.45	14.89	0.53	5.17	4.25	17.90	0.39	4.93	6.89
1800	12.27	1.80	6.44	2.21	15.39	0.90	6.44	4.41	19.12	0.60	6.62	5.45	22.99	0.45	6.44	8.83
2025	15.19	2.03	8.16	2.74	19.18	1.01	8.16	5.49	23.84	0.68	8.23	6.77	28.68	0.51	8.16	10.97
2250	18.40	2.25	10.07	3.33	23.36	1.13	10.07	6.67	29.06	0.75	10.00	8.23	34.96	0.56	10.07	13.34

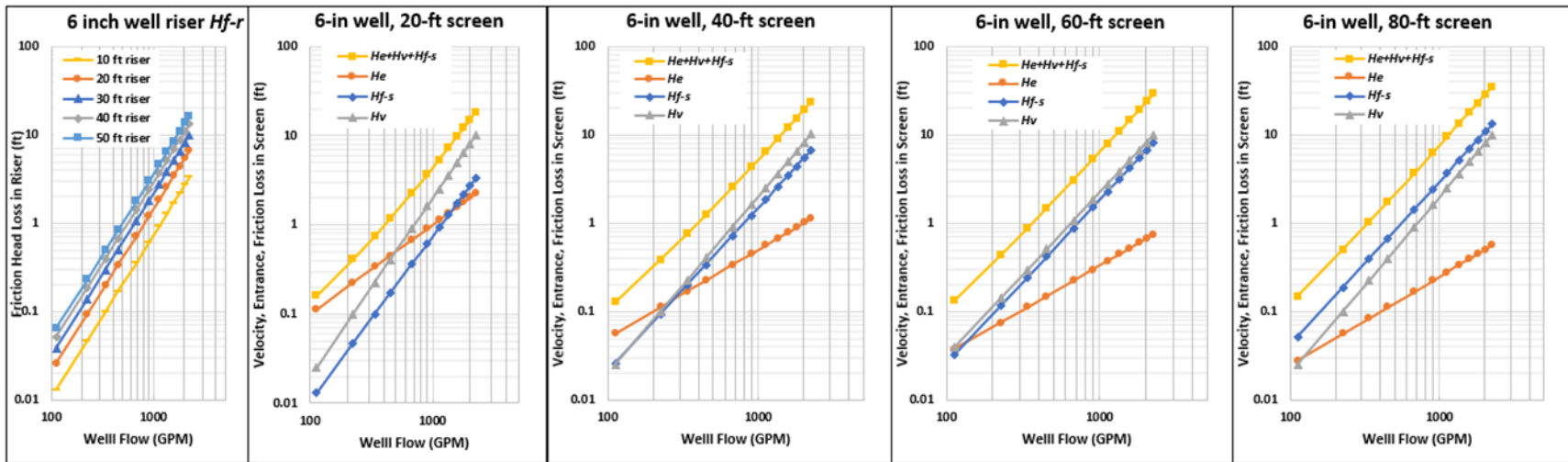


Figure 7–10. Components of head loss for a 6-inch diameter relief well

Initial Well H_w , Head Loss in Feet for properly constructed new well screen - 8 inch well																
Well Screen Portion Length	20 feet				40 feet				60 feet				80 feet			
Well Flow (gpm)	$\Sigma H_{e+v+f-s}$	H_e	H_v	H_{f-s}	$\Sigma H_{e+v+f-s}$	H_e	H_v	H_{f-s}	$\Sigma H_{e+v+f-s}$	H_e	H_v	H_{f-s}	$\Sigma H_{e+v+f-s}$	H_e	H_v	H_{f-s}
113	0.13	0.11	0.01	0.00	0.08	0.06	0.01	0.01	0.06	0.04	0.01	0.01	0.06	0.03	0.01	0.01
225	0.28	0.23	0.03	0.01	0.19	0.11	0.03	0.02	0.17	0.08	0.03	0.03	0.17	0.06	0.03	0.05
338	0.45	0.34	0.07	0.02	0.33	0.17	0.07	0.05	0.32	0.11	0.07	0.07	0.34	0.08	0.07	0.10
450	0.65	0.45	0.13	0.04	0.51	0.23	0.13	0.08	0.51	0.15	0.13	0.13	0.55	0.11	0.13	0.17
675	1.12	0.68	0.29	0.09	0.95	0.34	0.29	0.18	1.00	0.23	0.29	0.27	1.10	0.17	0.29	0.35
900	1.69	0.90	0.51	0.15	1.51	0.45	0.51	0.30	1.64	0.30	0.51	0.45	1.84	0.23	0.51	0.60
1125	2.34	1.13	0.80	0.23	2.19	0.56	0.80	0.46	2.42	0.38	0.80	0.68	2.74	0.28	0.80	0.91
1350	3.08	1.35	1.15	0.32	2.99	0.68	1.15	0.64	3.35	0.45	1.15	0.96	3.82	0.34	1.15	1.28
1575	3.91	1.58	1.56	0.42	3.90	0.79	1.56	0.85	4.41	0.53	1.56	1.27	5.06	0.39	1.56	1.70
1800	4.83	1.80	2.04	0.54	4.92	0.90	2.04	1.09	5.62	0.60	2.04	1.63	6.46	0.45	2.04	2.18
2025	5.84	2.03	2.58	0.68	6.06	1.01	2.58	1.35	6.96	0.68	2.58	2.03	8.02	0.51	2.58	2.71
2250	6.94	2.25	3.19	0.82	7.31	1.13	3.19	1.64	8.43	0.75	3.19	2.47	9.75	0.56	3.19	3.29

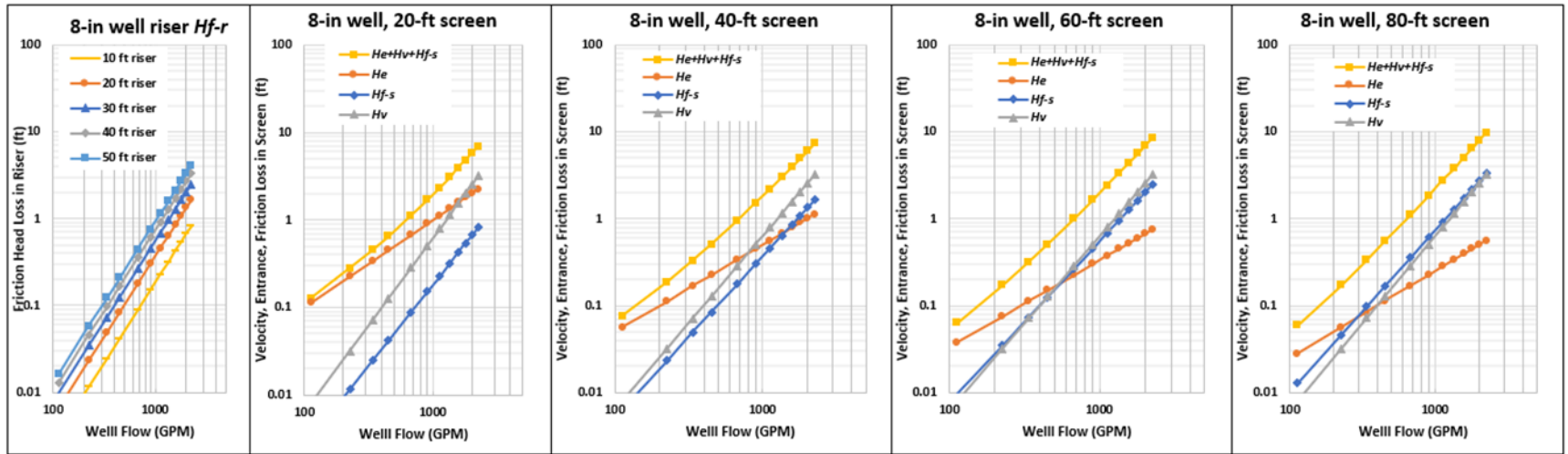


Figure 7-11. Components of head loss for an 8-inch diameter relief well

Initial Well H_w , Head Loss in Feet for properly constructed new well screen - 10 inch well																
Well Screen Portion Length	20 feet				40 feet				60 feet				80 feet			
Well Flow (gpm)	$\Sigma H_e+v+f-s$	H_e	H_v	H_f-s	$\Sigma H_e+v+f-s$	H_e	H_v	H_f-s	$\Sigma H_e+v+f-s$	H_e	H_v	H_f-s	$\Sigma H_e+v+f-s$	H_e	H_v	H_f-s
113	0.12	0.11	0.00	0.00	0.06	0.06	0.00	0.00	0.05	0.04	0.00	0.00	0.04	0.03	0.00	0.00
225	0.25	0.23	0.01	0.00	0.14	0.11	0.01	0.01	0.11	0.08	0.01	0.01	0.10	0.06	0.01	0.02
338	0.38	0.34	0.03	0.01	0.23	0.17	0.03	0.02	0.19	0.11	0.03	0.02	0.17	0.08	0.03	0.03
450	0.53	0.45	0.05	0.01	0.33	0.23	0.05	0.03	0.28	0.15	0.05	0.04	0.27	0.11	0.05	0.06
675	0.85	0.68	0.12	0.03	0.56	0.34	0.12	0.06	0.51	0.23	0.12	0.09	0.50	0.17	0.12	0.12
900	1.20	0.90	0.21	0.05	0.84	0.45	0.21	0.10	0.79	0.30	0.21	0.15	0.81	0.23	0.21	0.20
1125	1.59	1.13	0.33	0.08	1.17	0.56	0.33	0.15	1.12	0.38	0.33	0.23	1.17	0.28	0.33	0.31
1350	2.02	1.35	0.47	0.11	1.54	0.68	0.47	0.22	1.51	0.45	0.47	0.32	1.59	0.34	0.47	0.43
1575	2.48	1.58	0.64	0.14	1.95	0.79	0.64	0.29	1.95	0.53	0.64	0.43	2.08	0.39	0.64	0.57
1800	2.97	1.80	0.84	0.18	2.41	0.90	0.84	0.37	2.44	0.60	0.84	0.55	2.62	0.45	0.84	0.73
2025	3.50	2.03	1.06	0.23	2.90	1.01	1.06	0.46	2.98	0.68	1.06	0.68	3.23	0.51	1.06	0.91
2250	4.06	2.25	1.30	0.28	3.44	1.13	1.30	0.55	3.57	0.75	1.30	0.83	3.89	0.56	1.30	1.11

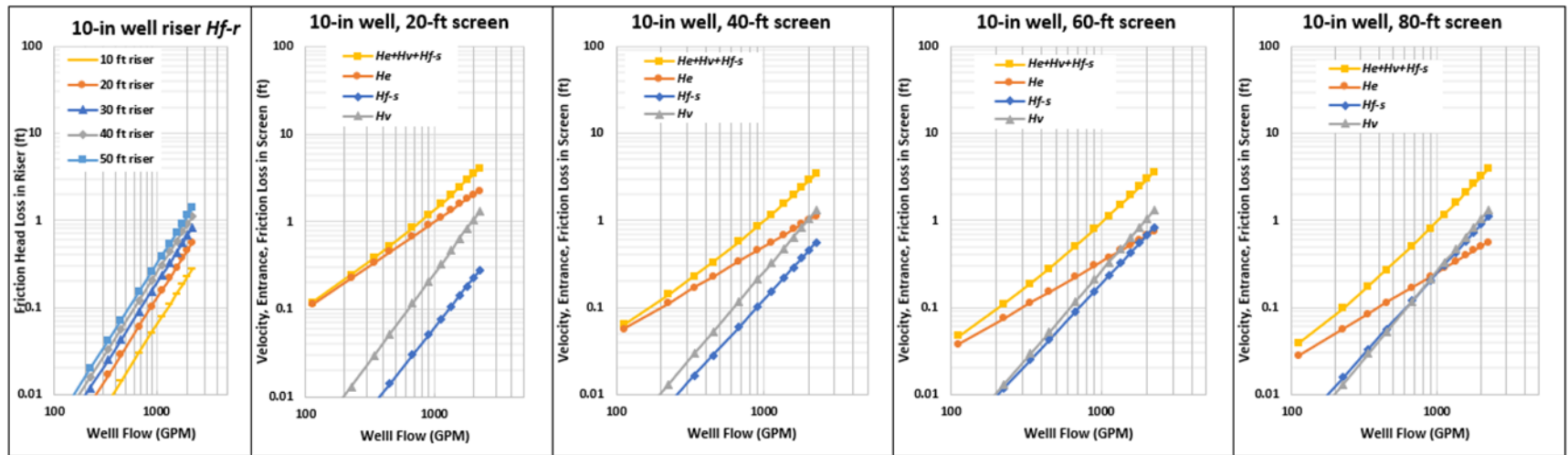


Figure 7-12. Components of head loss for a 10-inch diameter relief well

Initial Well H_w , Head Loss in Feet for properly constructed new well screen - 12 inch well																
Well Screen Portion Length	20 feet				40 feet				60 feet				80 feet			
Well Flow (gpm)	$\Sigma H_e+v+f-s$	H_e	H_v	H_f-s	$\Sigma H_e+v+f-s$	H_e	H_v	H_f-s	$\Sigma H_e+v+f-s$	H_e	H_v	H_f-s	$\Sigma H_e+v+f-s$	H_e	H_v	H_f-s
113	0.11	0.11	0.00	0.00	0.06	0.06	0.00	0.00	0.04	0.04	0.00	0.00	0.03	0.03	0.00	0.00
225	0.23	0.23	0.01	0.00	0.12	0.11	0.01	0.01	0.09	0.08	0.01	0.01	0.07	0.06	0.01	0.01
338	0.36	0.34	0.01	0.01	0.19	0.17	0.01	0.01	0.14	0.11	0.01	0.02	0.12	0.08	0.01	0.02
450	0.48	0.45	0.03	0.01	0.27	0.23	0.03	0.02	0.20	0.15	0.03	0.03	0.18	0.11	0.03	0.04
675	0.75	0.68	0.06	0.02	0.43	0.34	0.06	0.04	0.34	0.23	0.06	0.06	0.31	0.17	0.06	0.08
900	1.03	0.90	0.10	0.03	0.62	0.45	0.10	0.07	0.50	0.30	0.10	0.10	0.46	0.23	0.10	0.14
1125	1.33	1.13	0.16	0.05	0.82	0.56	0.16	0.10	0.69	0.38	0.16	0.15	0.64	0.28	0.16	0.21
1350	1.65	1.35	0.23	0.07	1.05	0.68	0.23	0.14	0.89	0.45	0.23	0.22	0.85	0.34	0.23	0.29
1575	1.98	1.58	0.31	0.10	1.29	0.79	0.31	0.19	1.12	0.53	0.31	0.29	1.09	0.39	0.31	0.38
1800	2.33	1.80	0.40	0.12	1.55	0.90	0.40	0.25	1.37	0.60	0.40	0.37	1.34	0.45	0.40	0.49
2025	2.69	2.03	0.51	0.15	1.83	1.01	0.51	0.31	1.64	0.68	0.51	0.46	1.63	0.51	0.51	0.61
2250	3.06	2.25	0.63	0.19	2.13	1.13	0.63	0.37	1.94	0.75	0.63	0.56	1.93	0.56	0.63	0.74

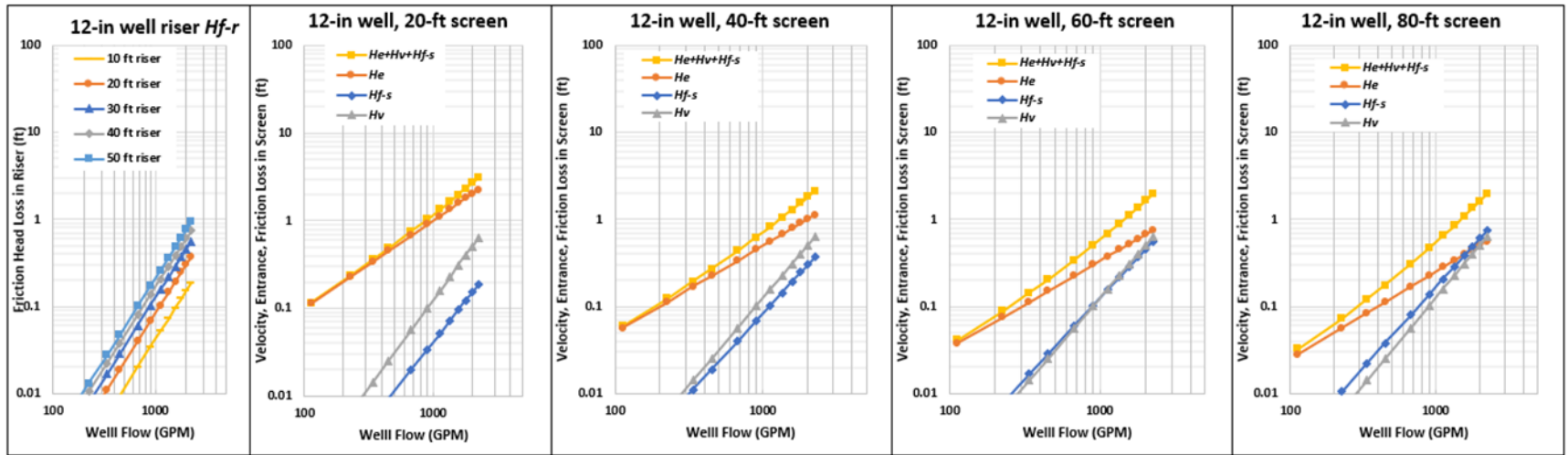


Figure 7–13. Components of head loss for a 12-inch diameter relief well

Chapter 8

Relief Well Installation

8–1. General requirements

Proper installation of relief wells is essential for successful operation of the structures they are designed to protect. There are several actions recommended before installation begins. These will ensure new relief wells are installed cost effectively and according to specifications. All materials required for well completion should be on hand at the worksite. The well screen and riser should be checked for proper material, length, diameter, and slot openings. The filter material should be inspected and checked against gradation specifications. Well drilling and development equipment and all downhole tools should arrive on site clean and decontaminated.

8–2. Drilling plans

All personnel involved with relief well installation should be aware that drilling activities can potentially damage embankments and their foundations. ER 1110-1-1807 specifically addresses drilling in earth embankment dams and levees and/or their earth and rock foundations. An approved Drilling and Invasive Program Plan (DIPP) is required prior to any drilling, grouting, in situ testing, or subsurface exploration at USACE project sites. This includes section drawings showing existing subsurface information and the locations and depths of proposed drill holes and well installations. If drilling fluids will be used, the DIPP must explain how potential risks associated with their use will be managed. Specific requirements for a DIPP are given in Appendix B of ER 1110-1-1807.

8–3. Requirements for the well borehole

It is imperative that the well drilling contractor be prepared to complete the well borehole according to the design specifications. The driller must be able to manage subsurface obstacles that could prevent installing the well at the design depth. These include cobbles, boulders, or other geologic features. The hole diameter must be large enough for the well and filter pack. The drilled hole also must be vertical so that the screen and riser may be installed straight and plumb. Borehole stability must be maintained at all times. Both sidewall and bottom stability is particularly important anytime drilling occurs below the water table, even when the sidewall is supported by casing.

8–4. Drilling methods

a. General. The designer must specify a drilling method for any project involving installation of relief wells. The method should be selected based on previous experience and consultation with the contractor. Geology and site conditions, along with well diameter and depth, are major factors that determine the appropriate drilling method. Relief wells typically vary from 6 to 18 inches in diameter. Boreholes are normally drilled 8 to 12 inches larger than the well diameter to accommodate filter packs.

Large-diameter water wells such as this are normally drilled using a hydraulic rotary (standard or reverse) or cable tool method (ASCE 2014). Hollow-stem augers (HSAs) are another method commonly used to install relief wells.

b. Appropriate methods. These and other methods considered appropriate for permanent relief wells are discussed in the following paragraphs. A comparison of the most common methods is presented in Table 8–1. Driscoll (1986) and ASCE (2014) are standard references on water well drilling that can be consulted for additional information.

c. Cable-tool method. This method is the oldest and most versatile drilling method for water wells (Driscoll 1986). The cable-tool method uses a heavy weight that is dropped repeatedly to crush and loosen soil and sediment in the geologic formation being drilled. As these materials become mixed with water, they form a slurry. A bailer is used to remove the slurry from the borehole for every 5 to 10 feet that the hole is advanced. The cable-tool method does not require a drilling fluid. Therefore, this method is especially useful for drilling coarser-grained formations where fluid circulation cannot be maintained. A common application is in loose, unconsolidated, granular materials. Although drilling progress is generally sure and steady, the frequent bailing causes the operation to proceed significantly more slowly than other drilling methods (ASCE 2014).

(1) *Equipment.* Cable-tool rigs are simpler, smaller, require less maintenance, and are less expensive to operate than other types of rigs. The drill string consists of the bit, stem, jars, swivel socket, and cable. The drill bit is designed to crush material. For this reason, it is massive and can weigh over 1,000 pounds. Cutting edges are welded to the bit. These are typically hard-faced and may have tungsten carbide inserts for use in harder geologic formations. The cable passes over the top of the mast and is wound around the drilling drum. The drum rotates to lift and drop the string and bit. A bailer assembly and sand pump are two types of bailers commonly used to remove cuttings. The bailer is operated on a wire line (ASCE 2014).

(2) *Casing.* With the cable-tool method, steel casing must be advanced to maintain the borehole in loose, unconsolidated formations. Granular formations create significant frictional resistance to advance of the casing. The casing is thick-walled and heavy to sustain driving and should be flush-joint or welded-joint steel pipe. This requires a drill rig that can handle a sizable load as well as a wire line hoist and driving capability. The driving process can densify loose foundation materials, particularly in fine sand formations, thus reducing their hydraulic conductivity. Pre-drilling ahead of the casing and using telescoping casing reduces disturbance to the formation and the borehole walls. During well installation, the casing is gradually pulled back as the filter is placed. A vibratory hammer is sometimes used to pull back large-diameter casing with cable-tool rigs, although this is generally not recommended for relief well installation.

(3) *Effect of fine-grained layers.* The cable-tool method is less effective in drilling finer-grained materials because they are more difficult to bail. To avoid this problem, augers are often used to drill through fine-grained overburden before switching to the

cable-tool method. This is not an option when significant finer grained layers are present in the foundation layer. In such cases, driving casing in the fine-grained layers may result in smearing of the borehole walls. However, this is generally less of a problem with the cable-tool method than with HSAs. Regardless of method, smearing increases the time and effort required to develop a well.

Table 8–1
Comparison of major drilling methods used for relief wells

Cable Tool

Pros

- Drilling fluid not required
- Borehole remains stable
- Formations with voids can be drilled
- Rigs are simple, economical
- Less well development required compared to standard rotary method

Cons

- Low penetration rates
 - Efficiency declines with depth
 - Fine-grained formations can be problematic
-

Standard (Direct) Rotary

Pros

- High penetration rates
- Ability to maintain open borehole without casing facilitates well and filter pack installation (surface casing recommended for USACE relief well installation)

Cons

- Drilling mud required, can cause plugging, “balling” of bit, etc.
 - Rigs are large, expensive, and complex; high transportation and daily operating costs
 - Requires significant water supply
 - Management of drilling fluid requires specialized expertise and experience
 - Mud pits in blanket require careful backfilling, compaction, and reseedling
-

Reverse Rotary

Pros

- High penetration rates
- Few or no drilling additives required
- Ability to maintain open borehole without casing facilitates well and filter pack installation
- Less well development required compared to standard rotary
- Ability to maintain open borehole without casing facilitates well and filter pack installation (surface casing recommended for USACE relief well installation)
- Less well development required compared to standard rotary

Cons

- Large rig size limits site accessibility
 - Requires significant water supply
 - Requires 15 vertical feet of fluid in borehole to initiate air-lift system
 - Not suited for drilling prolific aquifers and/or materials where loss of circulation is a concern
 - Difficulty drilling in cobbles or boulders
 - Mud pits in blanket require careful backfilling, compaction, and reseedling
-

Hollow-Stem Augering

Pros

- Rigs simple and economical
- Drilling mud not required
- Borehole remains stable
- Penetration rates fast when using bottom plug
- Less well development required compared to methods using drilling fluid additive

Cons

- Augers can smear formation with clays from overlying layers
 - Augers must be pulled back while filter material is placed; progress can be slow
 - Larger augers can get “locked” in saturated sand layers
 - Larger augers generate high volume of cuttings
-

d. *Rotary methods using a drilling fluid.*

(1) *Rotary drilling.* With rotary drilling, a rotating bit chews and loosens material in the geologic formation being drilled. A drilling fluid is required and can be air, water, or drilling mud. (Air-rotary drilling is used for drilling in rock and is therefore not used to install relief wells). A reliable water supply is needed for water-based fluids. The fluid is circulated through the bit and annular space. This stabilizes the borehole, cools and cleans the drill bit, and carries cuttings to the surface. The drilling fluid must be of sufficient viscosity and density to carry the cuttings to the surface. Higher viscosity fluids (“muds”) may be required for larger boreholes because the fluid circulates at a slower rate. Drilling muds are formed by mixing silty soil, or a commercial fluid additive, with water (see below). Figure 8–1 shows a schematic of the rotary drilling methods.

(2) *Water and drilling muds.* For water and drilling muds, it is recommended to maintain the fluid level in the hole at least 10 feet above the static water level. This ensures sufficient hydraulic head to counteract pore pressure in the aquifer and prevent sloughing of the borehole walls. Such collapse can result in unwanted pockets of aquifer material in the filter pack. High static groundwater levels may make it difficult to maintain a 10-foot differential. In these situations, casing can be extended above grade to provide additional height. Compressed air has also been used to pressurize the inside of the casing and compensate for lack of a 10-foot elevation difference.

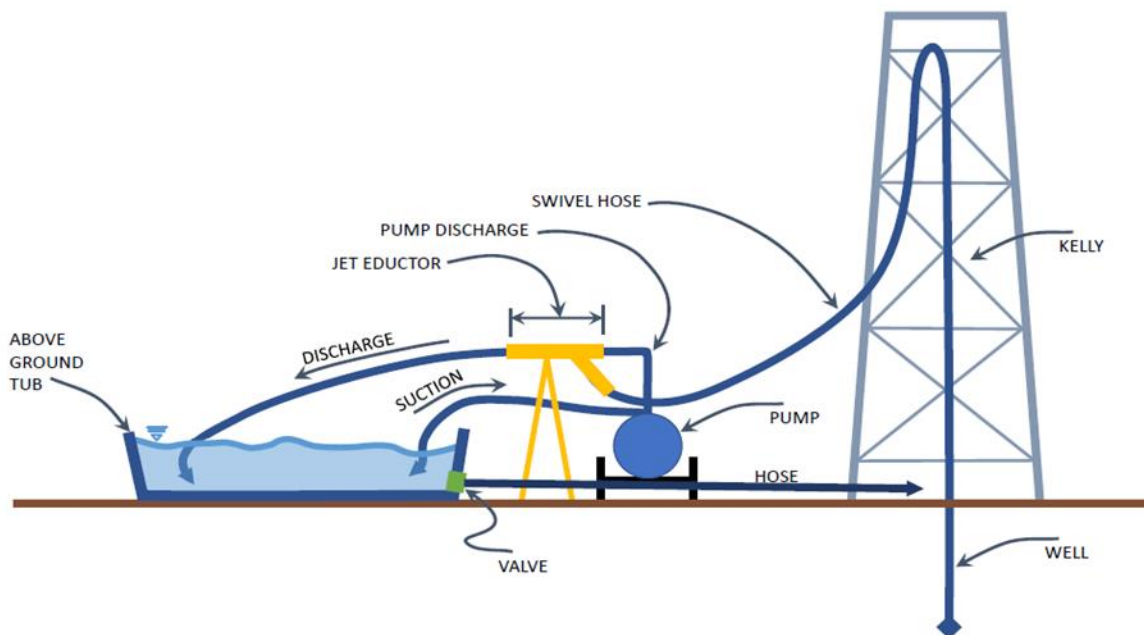


Figure 8–1. Schematic diagram of circulatory system (after EM 1110-2-1913); an excavated pit may be used for a fluid reservoir in place of an above-ground tub (see text)

(3) *Standard rotary method.*

(a) This method is also known as the direct or mud rotary method. It is versatile and suitable for drilling consolidated, semi-consolidated, or alluvial materials (ASCE 2014). It normally progresses more rapidly than cable-tool drilling, but generally is limited to boreholes of 26 inches or less.

(b) The method consists of rotating a cutter bit, often a tri-cone type, while circulating a fluid down the drill pipe. The drilling fluid returns to the surface through the annular space between the drill pipe and borehole wall. Water is the preferred drilling fluid for installing relief wells. However, if the hole is drilled in clean sands or gravels, excessive water may be lost through the borehole walls. This can destabilize the borehole. In such cases, some silty soil or a fluid additive (see paragraph 8–4d(7)), may need to be mixed with the drilling water. Enough additive is used to increase the fluid density to a degree sufficient to reduce fluid loss and stabilize the borehole.

(c) Too great a fluid density caused by excessive mud weight or drilling clay-rich layers in the formation can be problematic. This can result in “balling up” of the bit, which can cause the bit to fail if it is not being lubricated and cooled (ASCE 2014). The same conditions can form “mud rings,” which can result in lack of circulation. “Sidewall sticking” can occur when the drill pipe stops rotating and sticks to the wall cake. The drill then can become stuck if there is not enough torque to resume rotation.

(4) *Reverse-rotary method.*

(a) The reverse-rotary method uses a similar cutting process to standard rotary drilling. The difference between the two methods is that with reverse-rotary, the drilling fluid and cuttings are pulled up through the drill pipe. This is accomplished by vacuum or air lifting the fluid. A minimum of 15 feet of fluid in the borehole is necessary to begin the air-lift process. If the static water level is too deep, casing can be driven to seal the borehole. Water is then added to provide the necessary head to begin the air lift. Alternatively, water and drilling additive can be used to seal the hole and provide the necessary head. The fluid pulled up through the drill stem circulates through the sump and re-enters the top of the open boring by gravity. Reverse-rotary generally provides a stable drill hole.

(b) This method is especially well suited for wells in soft sedimentary rocks and unconsolidated sand and gravel formations (ASCE 2014). The fluid moves through the drill pipe at a relatively high velocity. This generally eliminates the need for a high-viscosity fluid, thus the need for drilling additives. Since the boring’s cross-sectional area is many times larger than that of the drill pipe, the slow downward velocity of the fluid tends to not erode the borehole walls. Pump capacities normally limit the up-hole velocity of the fluid, thus the ability to efficiently remove cuttings from larger boreholes. Therefore, borehole diameters with the reverse-rotary method are usually limited to a maximum of 24 inches.

(5) *Equipment.* A rotary-type drill rig must possess substantial hoisting and torque capacity. As a result, rigs tend to be large, complex, and expensive to have on site. A reverse-rotary rig will also be equipped with air compressors to air-lift the drilling fluid. The size of a reverse-rotary rig can limit its ability to access some drilling locations. A mud pump and reservoir are also normally required for a rotary drilling operation (see below). Drill bits vary. In alluvial deposits, a drag-type bit is sufficient. Roller-type bits are required in consolidated deposits or in gravel- or cobble-rich zones. The drill pipe should be as large as practical to provide sufficient volume of the drilling fluid. Drill pipe and hoses should be of constant inside diameter throughout the system to ensure complete circulation of material.

(6) *Hydraulic fracturing.*

(a) The standard and reverse-rotary methods both require using a drilling fluid. This presents a potential risk of hydraulic fracturing at levees and dams. Low-stress zones under and within embankments can be subject to fracturing from pressures exerted by drilling fluids. This is especially true if the return path for fluid circulation becomes obstructed. Evidence for fluid loss during drilling should be monitored closely at existing project sites. This includes loss of fluid circulation in the borehole, blowouts into nearby borings, and fluid seepage on the adjacent ground surface.

(b) The potential for hydraulic fracturing is greatest at locations where there are abrupt changes in embankment geometry. These include areas near and over abutments, adjacent to buried structures or conduits, and in narrow valleys. Drilling fluid can also cause damage if it seeps into internal drainage features. Dry drilling methods, which do not require fluids, may be considered if the risks of using fluids is deemed unacceptable. Examples of such methods include hollow-stem augering and cable-tool (ER 1110-1-1807). Sonic drilling also can normally be conducted without using drilling fluids (U.S. Geological Survey [USGS] 1997).

(7) *Drilling fluids.* USACE recommends water as the first choice for a drilling fluid. If a heavier fluid is required, a liquid polymer emulsion (LPE) is recommended as an additive. These products, available from multiple manufacturers, stabilize boreholes and increase fluid viscosity. Wells may have to be treated with sodium hypochlorite (bleach) during development to break down LPE. Conventional bentonite drilling mud should be approved only if necessary. In such cases, the well drilling statement of work should include additional development time. Biodegradable drilling fluid additives (BFA) should be avoided. Although BFAs break down naturally in the formation, they also contain nutrients that can promote biofouling. In addition, BFAs are not approved by the National Sanitation Foundation and are prohibited in some states for use in drilling water wells.

(8) *Circulation and sump pit.*

(a) Drilling fluid used with the standard or reverse-rotary methods is circulated by a centrifugal or jet-eductor pump. The fluid returning from the borehole is delivered to a reservoir (see Figure 8–1). The cuttings settle out in the reservoir, often with the aid of

baffles, shaker tables, and de-sanding cones (ASCE 2014). The muddy water then flows through a pipe from the sump back into the drill hole.

(b) Excavating a pit for a reservoir introduces the risk of compromising the blanket near an embankment dam or levee toe (ER 1110-1-1807). Portable aboveground tanks or tubs can be used as an alternative to excavation, although these lack the volume of a typical sump pit. If a pit is excavated, the drilling contractor should be required to pump the pit completely dry immediately after drilling. This should be followed by backfilling and compacting to match the surrounding blanket soil. The compaction ensures a lower permeability for the blanket. This should be followed by reseeding.

(c) A large-volume reservoir helps ensure an adequate supply of water. The capacity of the reservoir is generally reduced as cuttings accumulate. Therefore, a capacity at least three times the anticipated volume of the completed boring is recommended. Insufficient reservoir capacity can result in incursion of aquifer sands into the borehole if the fluid level in the reservoir drops suddenly.

e. *Hollow stem augers.*

(1) This method is appropriate for drilling a variety of unconsolidated materials. It is generally fast and efficient, especially for smaller diameter wells installed at moderate depths. HSAs allow the borehole to be advanced while also serving as temporary casing to maintain the hole. This eliminates the need to drive casing or use a drilling fluid to stabilize the borehole walls. A plug is inserted into the hollow center of the cutter head to prevent soil from coming up inside the auger. When the hole is completed, the plug is removed to install the well.

(2) The HSAs serve as temporary casing during well installation. The augers are gradually pulled back as the filter pack is added through the hollow stem and fills the annular space around the well. HSAs can be used in combination with a rotary method to install relief wells. HSAs are used to drill through the blanket. A rotary method is then used to advance the hole to the desired depth in the foundation layer(s).

(3) The auger flights are welded onto larger diameter pipe with a cutter head mounted at the bottom. Hollow-stem augers with outside diameters (OD) ranging from 6.25 to 22 inches (2.5 to 13 inches inner diameter [ID]) have been used for water wells, with 6.25 to 13 inches OD (2.5 to 6 inches ID) being the most common. Auger flights are commonly 5 feet in length but on larger rigs may be 10 feet. Holes as deep as 300 feet have been drilled with 6.25 ID HSAs and 100 feet with 12-inch ID HSAs. Deeper holes and larger diameter augers demand a drill rig capable of providing the necessary power and torque to turn the augers.

(4) Some geologic formations can be problematic with HSAs.

(a) Fine saturated sands can settle around the augers and lock them in place. This is particularly true with larger augers, deeper holes, and smaller drill rigs. Water typically must be used to offset “heaving” of formation sands when the plug is removed for sampling or well installation. A knock-out plug can be used to prevent sand from

entering the augers while the well is lowered into place. However, the plug must be removed to install the well.

(b) Where thick clay layers overlay thin sand layers, the auger flights can carry clay downward and smear the borehole walls adjacent to the sand. This can increase development time. An HSA is also not practical when large cobbles or boulders are present. When encountered at depth, these materials can sometimes be ground up and penetrated using the direct rotary method. The bit and drill stem are passed through the HSAs and water used as the drilling fluid. The augers can then be advanced or temporary casing driven inside the augers to maintain the borehole.

f. Dual rotary.

(1) This method is distinct from the standard and reverse-rotary methods discussed earlier. Dual rotary is appropriate for drilling unconsolidated materials. This method results in a stable borehole, although the depth and diameter of the hole is limited. Using a drilling fluid other than water to suppress heaving sands is unnecessary with this method.

(2) Dual rotary refers to two drives on the drill rig. A hydraulic top drive rotates the drill string. The drill can be tooled with a downhole hammer, drag bit, polycrystalline diamond bit, or rolling cone bit. The lower rotary drive rotates steel casing. A casing shoe with cutting edge is welded to the first piece of casing. Rotating the casing to advance it rather than driving minimizes stress on the casing joints and does not compact the formation. Dual-rotary drilling uses large amounts of compressed air, which requires expensive equipment. The method also has the potential for heaving of formation materials within the casing.

g. Bucket auger. This method is also known as rotary-bucket drilling. The bucket rig is a form of the dual-rotary drill rig. It uses mechanical or hydraulic drive to rotate a Kelly bar, which is attached to a cylindrical bucket with cutting teeth. The bucket has a hinged bottom that is used to scoop and lift sediments from the borehole. A bucket rig can be equipped to drill holes from 10 to 36 inches in diameter. The method is well suited for drilling clay-rich overburden to set surface casing. The borehole can then be continued with the rotary method. Sand formations can also be drilled with the bucket-auger method. However, this may require a large water supply to keep the borehole full. Fluid additives may be required in some cases. This method is not well suited for drilling in sediments that include cobbles and boulders. These must be picked out of the borehole individually, which slows the operation.

h. Other drilling methods.

(1) This chapter covers the most commonly used drilling methods used to install relief wells. However, in some cases, other drilling methods may be suitable. One such category is vibratory drilling, also referred to as sonic or rotasonic drilling (USGS 1997). This method uses a hydraulic drill that transmits high-frequency vibrations through a steel pipe to create a cutting action at the bit face (U.S. Department of Energy 1993).

Casing is advanced to maintain the borehole. Sonic drilling is a good alternative to HSAs for smaller diameter boreholes, like pilot holes or smaller relief wells.

(2) The sonic method is faster and can go deeper than HSAs and allows retrieval of continuous core. A distinct advantage of the method is no mud, air, or water is required to drill unconsolidated materials. This method is typically limited to boreholes 12 inches in diameter and wells no larger than 6 or 8 inches in diameter. Sonic drilling has been used to install wells at USACE locks and dams on the Mississippi River. For example, dewatering wells were installed at Lock and Dam 25, and relief wells at Locks 11 and 18. A 16-inch diameter cutting head was used to install the wells at Lock 18.

8–5. Installation of well screen and riser pipe

Once the boring is completed and the tools withdrawn, the boring should be sounded to assure an open hole to the proper depth. All screen and riser to be installed should be laid out. These materials are obtained in standard lengths (such as 10 feet) or fabricated in varying lengths. When non-standard lengths are required, it is advantageous to have screen and blank sections prefabricated to length by the manufacturer. This is especially important when using stainless screens, due to the difficulty of cutting and welding stainless steel in the field. In either case, all screen and riser must be measured prior to installation to determine its total made-up length. This information should be part of the well construction record. The bottom joint of the well screen should be fitted with a sump or bottom cap.

a. Screen installation.

(1) The lengths of screen are connected as they are lowered into the hole. The method of connecting the lengths of screen and riser vary. Metal screen and riser have threaded or welded joints. Plastic and fiberglass screens usually have either mechanical or glued joints. Each joint should be made secure to prevent separation of the well during installation and servicing. Care must be taken to keep the well centered and plumb in the borehole during installation.

(2) Centering devices should be used, and the well should not be allowed to rest on the bottom of the borehole. This allows placement of a continuous filter with uniform thickness around the well screen. A centered and plumb installation also facilitates servicing and testing later in the life of the well. Immediately after installation of the well screen and riser, the total depth inside the well should be sounded. This information is valuable in assessing whether damage to the well occurs during development and servicing.

b. Blank sections. Riser pipe or blank sections of screen may be used between screened intervals to block off finer materials in the formation. This helps prevent potential piping of foundation materials into the well. Additional information on using blank screen sections is provided in paragraph 7–6b.

c. *Filter placement.* This is a critical step in relief well installation. Improper installation of the well filter can negate proper design, manufacture, and handling of filter materials.

(1) *Preventing segregation.* Widely graded filters, when placed in increments, tend to segregate as they pass through water, with coarse particles falling faster than fine particles. To guard against this, a tremie should be used to maintain a continuous flow of material. The tremie pipe is lowered to the bottom of the open drill hole, outside the well screen and riser pipe. The tremie pipe ideally should be at least 2 inches in diameter, although 1-inch pipe is acceptable for some gradations. The pipe should be perforated with slots 1/16 to 3/32 inches wide and about 6 inches long. The slots allow the filter material to become air-saturated, thereby breaking any surface tension and preventing “bulking” of the filter in the tremie. One or two slots per linear foot of tremie is generally sufficient. The tremie should also have flush internal screws or other type of flush joints to prevent particles hanging up inside the pipe.

(2) *Installing the filter.*

(a) The presence of centering devices may interfere with the proper use of the tremie. This issue can be addressed using dual, diametrically opposed tremie pipes. These are connected to a centralizer ring that slides over the outside of the screen (see Figure 8–2). The pipes should be lowered to the bottom of the hole, then filled with filter material. The pipes are then slowly raised to allow the filter to fall out the bottom. At the same time, filter material should be added to the tops to always maintain full pipes. The level of filter material in the annular space should be brought to at least 2 feet above the top of the screen. This allows some settlement.

(b) Drilling fluid or water in the hole should be kept at least 10 feet above the natural groundwater level until all the filter material is placed. This is to ensure that the borehole walls do not slough material into the filter pack. If casing or HSAs are used, they should be pulled as the filter material is placed. During this process, the level of filter material should remain at least 2 feet above the bottom of the HSAs. Temporary casing is a larger diameter than HSAs and is less likely to cause bridging or locking of filter material. In this case, the level of filter material should remain approximately 10 feet above the bottom of the casing. Regardless of method, filter material should flow smoothly into the annular space without any sloughing of the borehole walls.

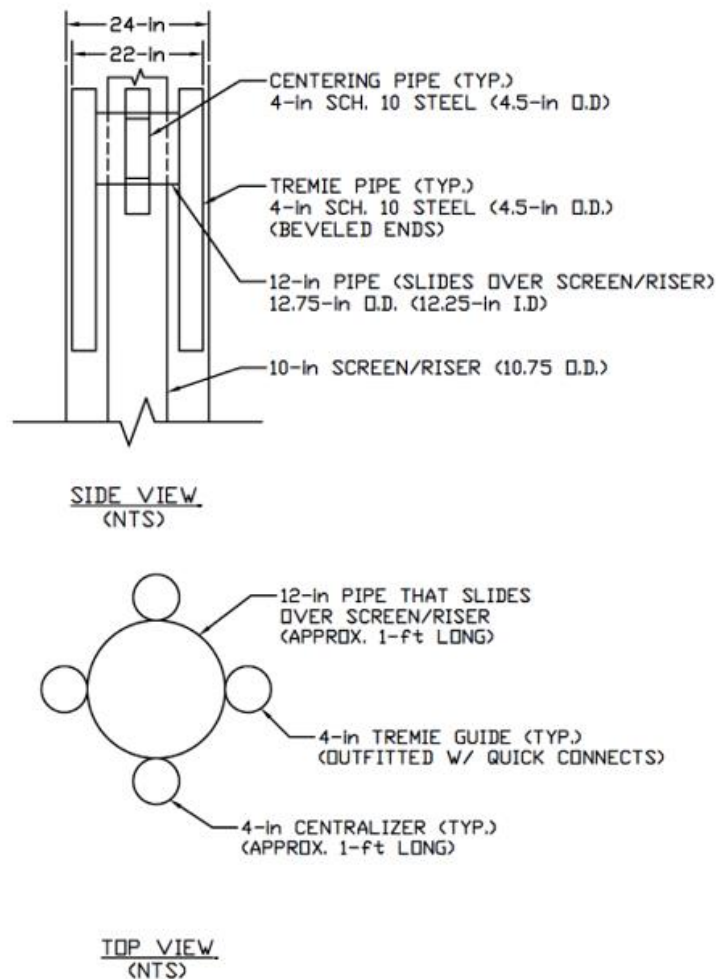


Figure 8–2. Side (top) and top (bottom) views of centralizer/tremie guide

(3) *Ensuring a stable borehole.* The borehole above the filter pack must remain cased until the well has been sealed and grouted. This ensures that water moving through the filter during pre-development, development, and pump-testing does not result in sloughing of the borehole walls. For cable-tool and HSA drilling, the casing or augers are pulled back only enough to install the filter. This ensures the borehole above the filter is stabilized. For standard or reverse-rotary drilling, surface casing should be driven to the top of the filter pack. In such cases, some contractors recommend using a bucket-auger rig to drive the casing. Once casing is in place, the rotary rig can be mobilized to drill the borehole to its total depth.

(4) *Pre-development.* Settlement of the filter pack can occur because of incomplete packing around the well screen. Pre-development pumping should be performed after initial placement of the filter to allow settlement. Additional filter can then be added to bring the level of the filter to the design level. The final top of the filter should also

terminate below the bottom of the overlying impervious top stratum if this layer is present.

8–6. Development

A relief well cannot function properly until developed. Development maximizes well yield and efficiency, and results in relatively sand-free discharge (ASCE 2014). The process should begin as soon as practicable after the hole has been drilled and the well installed. This is particularly true when drilling muds have been used to establish the borehole. Development can begin immediately after pre-development pumping has been completed. Five days is considered the maximum time that should be allowed between well installation and development. Additional delay may prevent a well from functioning at the efficiency assumed in design. Wells may also be redeveloped as part of well rehabilitation, as described in Chapter 11. Development procedures include both chemical and mechanical processes, which are described below.

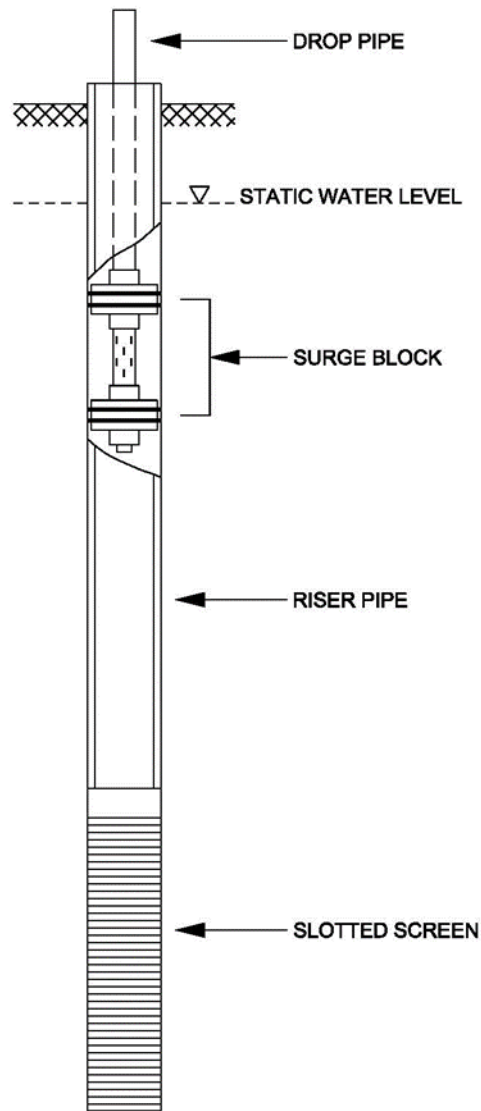
a. Development duration. Many factors affect the time required to fully develop a well. These include the texture of foundation materials, drilling and development methods, screen slot size, and filter characteristics. There is no firm time limit for well development (ASCE 2014) However, a typical newly installed relief well should be developed for a minimum of 4 hours. This includes mechanical development and pumping to remove solids. The well is then pumped again, and sand infiltration is measured to ensure that development is complete, as described below. If chemical treatment is included as part of development, it will require additional time. A typical chemical treatment runs approximately 8 hours, plus intermittent agitation at intervals over the next several days (see below).

b. Mechanical development. The purpose of mechanical development is to remove any fine-grained material from the walls of the drilled hole. It is also meant to set the filter immediately adjacent to the screen. In addition, it is desirable to create grading of the filter particles, from coarsest to finest, extending away from the screen. Both goals can be accomplished by aggressive movement of water through the screen. The result will be an increase in well efficiency and effective well radius. In addition, entrance velocity and sand infiltration will be reduced. Three common methods of mechanical development are discussed below. These methods can be used individually or sequentially.

(1) *Surging.*

(a) This method consists of inducing flow in and out of the screen with the up-and-down motion of a surge block. A surge block is a plunger consisting of one or more stiff rubber or leather discs attached to a heavy shaft (Figure 8–3). The discs should be about 1 inch smaller in diameter than the inner diameter of the screen. The well should always be pumped or bailed before surging to ensure a relatively free inflow of water.

(b) Surging should begin with a slow and gentle motion above the well screen. This is continued with increasing vigor from the top of screen downward. The surge block should be moved at a rate of approximately 2 fps. Surging is particularly effective with screen slots that are widely separated and/or louvered. Moving the surge block up and down the well screen is known as a round trip. For recordkeeping, it is convenient to count 15 round trips as one cycle. At the completion of each cycle, the thickness of sediment in the bottom of the well should be measured.



AFTER DRISCOLL (1986)

Figure 8-3. Surge block used to mechanically develop wells

(c) Surging should continue until the accumulation of material in any one cycle is less than about 0.2 foot. This may not be achievable with surging alone. In these cases, the well screen should be bailed or air-lifted to remove the additional material. Material

bailed from the well also should also be inspected to ensure that no foundation sand is passing through the filter. If so, this should be documented and surging discontinued. Surging may also induce filter material to move through the screen and into the well. The depth to the top of the filter should be measured and recorded after each surging cycle. If necessary, filter material should be added to the annular space to maintain the proper level. A final round of bailing should be performed after surging is completed.

(2) *Air lifting.* This method involves inserting a pipe in the well and forcing compressed air through the pipe into the well. The pipe should be submerged at least 30 to 50% below the static water level in the well. The compressed air aerates the water and causes it to move upward in the well. The static water level and/or depth of the well may not allow sufficient submergence of the pipe. In these cases, the water column must be physically blown out of the well, which requires a larger air supply. Air lifting is especially effective when alternated with surging. Drill rigs must be equipped with a walking beam to perform air lifting. Otherwise, a separate service rig is required. Using compressed air at USACE project sites requires that hydraulic fracturing be considered. This was addressed in paragraph 8–4d in connection with drilling fluids used in the rotary drilling methods (see ER 1110-1-1807).

(3) *Water jetting.*

(a) A water jet allows water to be forced under pressure out through the screen. The jet consists of a series of small nozzles at the end of a pipe. The pipe is lowered into the well screen where water is pumped down and out through the nozzles at high velocity. A typical water jet is shown in Figure 8–4. Nozzles are directed toward the screen slots in small, concentrated areas, as shown in Figure 8–5. The size and number of nozzles must be consistent with the pipe’s size and length. This ensures a high-pressure and high-velocity jetting action. The lowest effective nozzle velocity for water jetting is about 100 fps. Better results are obtained with pumps capable of providing nozzle velocities between 150 and 300 fps.

(b) Care should be exercised to not use too much pressure during jetting. This can displace the filter pack and lead to sanding of the well. Water jetting normally proceeds from the bottom of the well upward. The jet is kept at one depth and rotated until the discharging water is clear. A period of 30 minutes is generally adequate for this purpose. The jet then is raised in increments of approximately 0.5 foot and the process is repeated. The jetting process dislodges fine material, which can then be removed by pumping or air lifting. The jetting tool should be kept in continuous motion to prevent localized erosion of the filter.

(4) *Pumping.* Pumping can be used to successfully develop a well but is generally less effective and more time-consuming than other methods. Submersible pumps can also be damaged if there is significant sand being pumped. The well should be pumped at a rate sufficient to effect maximum drawdown in the well. The size and type of pump required depends on the size of the well, desired yield, and anticipated drawdown. Repeatedly starting and stopping a pump produces a surging effect in the well screen that may make development more effective.

c. *Chemical development.* Chemical treatment in addition to mechanical development may be required of a newly installed well. This applies when drilling fluid additives such as LPE have been used to drill the well (see above). Chemicals such as sodium hypochlorite (bleach) are injected into the well to help dissolve residual drilling fluid in the filter. The chemicals should be of a type and concentration recommended by the manufacturer of the drilling fluid. They should be dispersed throughout the entire screen length by slowly raising and lowering the injection pipe. After the chemicals have been dispersed, the well should be pumped, and the effluent checked to ensure that the drilling fluid has completely broken down.

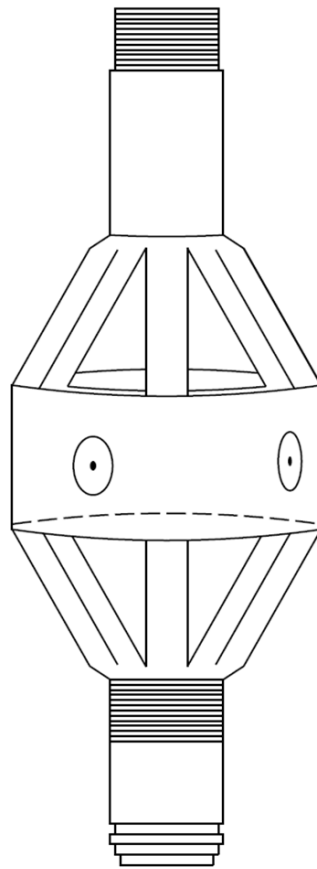


Figure 8-4. Schematic of four-nozzle jetting tool

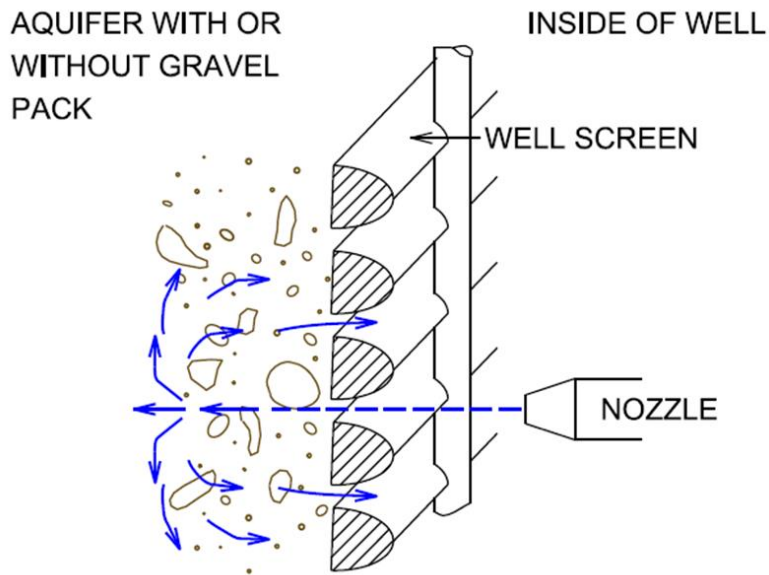


Figure 8-5. Well development by high-velocity jetting

8-7. Sand infiltration testing

A properly developed well will not produce an appreciable amount of sand. The degree of sand infiltration is assessed during a pumping test following development.

a. Pumping parameters. The pump should be set a few feet above the top of the uppermost screen. The well should be pumped as close to the design flow rate as possible while maintaining optimal drawdown. The pumping water level is recommended to be at least 5 feet, and preferably 10 feet or more, above the top of the screen. Pumping should be continued for 120 minutes.

b. Sand infiltration. According to Driscoll (1986) sand-free water can be defined as less than 8 milligrams per liter (mg/L) of sand. Wells producing sand in excess of 15 mg/L risk removing excessive aquifer/foundation materials (Driscoll 1986). USACE specifications commonly require that a fully developed relief well not produce sand in excess of 5 mg/L by the end of a 2-hour pumping test. Sand concentration should be measured with a Rossum Sand Tester (RST) or equivalent centrifugal sand separator. An RST is easy to operate, inexpensive, reliable, and is widely used by USACE and the water well industry. In all cases, discharging water should be visibly free of sand before a well is considered fully developed.

c. Failed sand test. If the above criteria for sand infiltration are not met, the well should be developed further and re-pumped. Wells that continue to produce excessive amounts of sand after 4 to 8 hours of surging or pumping should be abandoned and properly sealed as described below. An alternative to abandonment is to install a small-diameter screen with a pre-packed filter inside the original screen.

8–8. Initial pumping test

Pumping tests are performed to verify relief wells have been properly installed and developed. They serve as a baseline for evaluating a well's performance and loss of efficiency with time. A step-drawdown test with a minimum of three stages is strongly recommended as the best method to assess baseline well performance. A detailed description of the methodology and analysis of pumping tests performed on relief wells is provided in Chapter 9.

8–9. Backfilling

a. After completion of the well testing, at least 12 inches of concrete sand or excess filter material should be placed on top of the filter. The annular space above the top of the filter pack then should be filled with bentonite chips or pellets to form an impermeable seal at least 2 feet thick. Sealing prevents surface water and any potential chemical constituents from migrating down the borehole to the aquifer. It also helps maintain confined conditions in the aquifer.

b. Some situations may prevent successful placement of bentonite chips or pellets, for example in a water-filled borehole. In these cases, a high-solids (30 to 40%) bentonite grout can be pumped into place to form a seal. The remaining annular space above the seal should be filled with a cement-bentonite grout. A tremie pipe is advisable for placing this material. A tremie equipped with a slide deflector will prevent jetting a hole in the seal. The use of grout at USACE project sites requires that hydraulic fracturing be considered. This was addressed earlier in paragraph 8–4d in connection with drilling fluids used in the rotary-drilling methods (see ER 1110-1-1807). Figure 7–1 shows a typical relief well installation.

8–10. Disinfection

a. Relief wells are not drinking water wells. However, sanitizing newly installed relief wells may be advisable for some projects. This may apply to sites where biofouling of relief wells is known to be a problem. Disinfectant will not kill naturally occurring bacteria in the aquifer but may delay biofouling of the well, at least temporarily. Also, USACE should be good stewards of any aquifers known or potentially used for drinking water supply near to the project. If relief wells are installed in such formations, sanitization of new wells is recommended. This is primarily to ensure killing any coliform bacteria introduced by the well materials or filter. The disinfectant should consist of a chlorine solution mixed to a concentration of 200 parts per million (ppm).

b. The volume of the well should be determined assuming that the well diameter includes the filter pack. A volume of disinfectant equal to three times the well volume should then be prepared and injected with a jetting tool. The tool should be slowly raised and lowered within the well's screened interval(s) to disperse the chlorine. After the disinfectant is fully introduced, the well should be gently agitated at approximately 10 minutes every 2 hours. This process should be continued for the first 8 hours. After 8 hours, the well should be agitated at 8-hour intervals for at least the next 24 hours.

The chlorine concentration in the well should be periodically checked. If it falls below 200 ppm, additional chlorine compound should be added.

8–11. Video inspection

A downhole video inspection is recommended soon after installation of a new relief well. The inspection verifies that the well and screen have been installed to the design depths. The video also allows detection of any damage done to the well during installation.

8–12. Records

Detailed and accurate observations of all aspects of relief well installation should be documented on site in a timely manner. This includes drilling, installation, development, testing and, if applicable, disinfection. Records management requirements are described in paragraph 1–4.

a. These records become permanent and are used for future evaluation and testing. Information should include well material, method of drilling, type, length, and size of well screen, and slot size. The filter should be defined as to grain-size characteristics, depth, and thickness. Elevation of the top of the well and the ground surface should be recorded. The depth to granular material, the thickness of that material, and the percent penetration of the well should also be clearly identified.

b. Development data should include the method, the amount of effort, and sand infiltration. The records should show the final sounded depth of the well. (This may differ from the depth to the bottom of the well if sediment has settled). The pumping test data should include pumping rate, drawdown, length of test, and the amount of sand infiltration. USACE Engineer Forms (ENG Forms) 6316 and 6318 are prescribed for recording data from installation, construction, and development of relief wells. ENG Forms 6317 and 6319 are prescribed for pumping and sand testing. ENG Form 1836 is prescribed for recording data from geologic logging during any type of drilling.

c. Forms should be filled in completely at the time each operation is completed, and any additional observations should be recorded in a “remarks” section. Determination of aquifer parameters and well efficiency requires detailed time versus drawdown data for all phases of the test. It is therefore recommended that digital data be acquired for all pumping tests and archived on a secure server.

8–13. Abandonment of non-well boreholes

a. *Reasons for sealing.* All boreholes not being used for a permanent well installation should be sealed after completion. This includes exploration and pilot holes drilled prior to relief well installation.

(1) “Sealing” means the complete filling of an abandoned well with grout or other approved materials. There are a number of reasons for sealing an abandoned borehole. First, sealing ensures the borehole does not pose a physical hazard to people or

animals. It also prevents surface water and any potential chemical constituents originating at the surface from migrating down the borehole to an aquifer. In addition, sealing helps maintain confined conditions in the aquifer and intermixing of water between pervious zones.

(2) Abandonment should comply with all reporting and procedures required by local, state, or federal regulatory agencies. In addition, ER 1110-1-1807 governs borehole abandonment in and around USACE embankment dams. In such cases, sealing ensures that an abandoned borehole does not become a defect that can act as an unfiltered exit for seepage.

b. Procedures for sealing. Boreholes should be sealed by tremie-grouting with a 20 to 30% high-solids cement-bentonite grout or the equivalent. Backfilling a hole with drill cuttings is not an acceptable method of sealing. The use of grout at USACE project sites requires that the risk of hydraulic fracturing be considered, per ER 1110-1-1807. This was addressed earlier in paragraph 8–4d(6) in connection with drilling fluids used in the rotary drilling methods. If a borehole penetrates a drainage or filter zone in an embankment, ER 1110-1-1807 stipulates backfilling these intervals with granular materials. The purpose is to maintain the functionality of these zones within the embankment.

8–14. Well abandonment

Wells may not perform as designed for a variety of reasons. A well that cannot be rehabilitated or retrofitted should be abandoned by sealing. The reasons for sealing are discussed in paragraph 8–7c. Abandonment should comply with all reporting and procedures required by local, state, or federal regulatory agencies. Sealing materials should consist of 20 to 30% high-solids cement-bentonite grout placed from the bottom of the well to the surface. If the well casing is removed, the original well boring will need to be over-drilled prior to grouting. The use of grout at USACE project sites requires hydraulic fracturing be considered. This was addressed earlier in paragraph 8–4d(6) in connection with drilling fluids used in the rotary drilling methods (see ER 1110-1-1807).

Chapter 9

Well Efficiency, Specific Capacity Ratio, and Relief Well Pumping Tests

9–1. Introduction

The performance and productivity of relief wells gradually declines over time due to multiple processes. As a result, wells should be designed for optimal efficiency by minimizing well losses. Adequately performing relief wells reduce seepage uplift pressures between wells, which translates into reduced risk to dam and levee safety structures. Initial well performance is affected by entrance losses from water entering the screen; friction losses in the well screen, riser, discharge pipes, and conduits; and discharge velocity. Other factors include drilling damage, effective well penetration being less than assumed in design, and improper well development. Over time, well performance is largely affected by lack of maintenance and biological fouling. Relief wells should be located where they can be accessed by a drill rig for pumping tests and cleaning.

9–2. Specific capacity

Historically, USACE has used specific capacity (SC) to monitor performance of relief wells. The SC is the pumping rate, Q , divided by the total drawdown in the well, s_t , (equation 9–1). This parameter is a measure of well productivity. The s_t will increase, then stabilize after some time, for a given Q . Therefore, SC should be measured only after the drawdown reaches equilibrium for a given pumping rate. The SC of a well tends to decline with increasing flow rate, as the relationship between Q and s_t is not linear. This is due to increasing turbulence, which is typically assumed to be in the wellbore but can also occur in the formation. In some cases, SC may remain constant or increase slightly with increasing Q . Generally, if the SC remains constant, then laminar flow can be inferred. If SC increases with increasing Q , it may indicate the well is under-developed.

$$SC = Q/s_t \quad (9-1)$$

where:

SC = specific capacity

Q = pumping rate

s_t = total drawdown

a. *Baseline specific capacity.*

(1) The baseline SC should be determined for all newly constructed wells. This enables comparison with future pumping tests to monitor well performance. For such comparisons to be valid, future testing must be conducted under similar conditions to prior tests. These include ensuring the aquifer remains confined throughout the test and the well is pumped at similar rates. In addition, all tests should be of similar duration and subject to similar boundary conditions (such as river or reservoir pool and tail elevations).

(2) The baseline SC should be determined at several flow rates using a step-drawdown pumping test to provide flexibility for flow rates during subsequent tests. In most cases, the baseline SC is determined in the initial pumping test at the time of well installation. If a baseline has not been established at the time of well construction, SC cannot readily be used to evaluate the well performance over time. Where the aquifer is not confined at the time of installation or it is later determined the well was not fully developed during the initial pumping test, the baseline should be determined based on a later pumping test.

b. Specific capacity ratio. The SC determined from subsequent pumping tests should be compared to the baseline SC at a similar flow rate. The ratio of the current SC to the baseline value is the specific capacity ratio, SCR (equation 9–2). The use of SCR to monitor well performance assumes that all aquifer and well parameters, except for well losses, remain constant and there are no changes in boundary conditions. The SCR represents the simplest and most economical method of tracking well performance over the lifetime of a well if a baseline was established at the time of construction.

$$SCR = \frac{SC_{\text{current}}}{SC_{\text{baseline}}} \times 100 \quad (9-2)$$

where:

- SCR = specific capacity ratio
- SC_{current} = current specific capacity
- SC_{baseline} = baseline specific capacity

9–3. Well efficiency

Well efficiency (E) is a relative measure of well and aquifer head loss and is another means of monitoring well performance over time. This parameter has been used in the water well industry and by some USACE Districts to evaluate relief wells. E is a measure of well productivity that compares the current well performance to an ideal well. It can be used to monitor well performance in instances of uncertain or varying aquifer and well parameters with time. A decrease in E with time indicates that relief well performance is decreasing with time. The E considers the ratio of theoretical aquifer loss, or drawdown caused by aquifer loss, to the total measured, drawdown in a given well (equation 9–3). The total drawdown is the sum of the theoretical aquifer loss and losses associated with the well. The ratio is typically expressed as a percentage:

$$Efficiency = E(\%) = \frac{s_a}{s_t} \times (100\%) = \frac{s_a}{s_a + s_w} \times (100\%) \quad (9-3)$$

where:

- s_a = drawdown in an ideal well subject only to aquifer losses
- s_w = drawdown due to well losses
- s_t = total drawdown in a well subject to all aquifer and well losses

a. *Efficiency ratio.* The ratio of the efficiency measured at a given time in the life of the well ($E_{current}$) to the baseline efficiency ($E_{baseline}$) is the efficiency ratio, *E-ratio* (equation 9–4). The *E-ratio* can be determined for all pumping tests subsequent to the baseline test. The *E-ratio* is identical to the *SCR* if aquifer losses remain constant with time and there are no changes in boundary conditions.

$$E - ratio = \frac{E_{current}}{E_{baseline}} \times 100 \quad (9-4)$$

b. *Determining efficiency.* For each well, E can be calculated based on results from the baseline pumping test ($E_{baseline}$) and all subsequent pumping tests. Step-drawdown pumping tests with piezometer arrays or monitoring points around the tested well are used to measure aquifer and well losses to determine efficiency. These components account for non-linear (turbulent) and linear (laminar) well losses and aquifer losses and are used to compute efficiency. New wells will not have 100% efficiency because there are always well losses. However, tests performed on new wells will determine initial well losses that can be compared to assumed losses for the newly constructed well. Subsequent efficiency measurements can be used to monitor the increase in losses, or loss of efficiency, with time caused by biofouling.

c. *Wellbore skin.* Wellbore skin describes the zone with altered permeability between the well and the aquifer immediately outside the well. A positive skin zone represents reduced permeability, indicating damage to the zone. A negative skin indicates a zone of increased permeability. This term is also often used to describe well losses associated with water entering the damaged aquifer, filter pack, and well screen.

d. *Well loss components.*

(1) If there were no losses in the aquifer or well when a well is pumped, the water level inside the riser would remain unchanged from the static condition. However, the water level inside the well riser does drop (drawdown) when the well is pumped.

(2) Generally, the total drawdown in a pumped well consists of two components: aquifer losses and well losses. Aquifer losses are considered constant with time at steady-state flow and their variation is assumed to be linear with Q . Well losses include both linear and non-linear head losses. The total linear well loss is comprised of losses occurring in the wellbore skin (disturbed aquifer), filter, and well screen. Linear well losses may also include effects attributable to partial well penetration. Nonlinear well loss consists of friction losses inside the well housing and losses due to turbulent flow in the vicinity of the pump intake. To determine these components individually, drawdown must be monitored at discrete locations in and around the pumped well.

e. *Well loss coefficients.*

(1) Due to the elaborate pumping test requirements to determine individual well loss components, well loss coefficients can be used to estimate aggregate well loss

components. The concept of well loss coefficients was proposed by Jacob (1947) to include a linear aquifer-loss coefficient and both linear and non-linear, well-loss coefficients. Although flow is assumed to be laminar in the soil around the well, there is some concern that very high flow rates could result in turbulence in a coarse aquifer. This would impact estimates of well efficiency using well-loss coefficients.

(2) The concept of turbulence outside the well screen is explored in Appendix K based on laboratory tank tests that were an integral part of the evolution of USACE well design described in Appendix H and Chapter 2. Figure K–15 provides a reference for analysts to evaluate whether turbulent flow could be a factor for a particular situation. Those tank test results show flow outside the well screen to be laminar for typical aquifer sand and flow rates where relief wells are commonly used.

(3) Jacob proposed the drawdown in a pumped well could be described by the second-degree polynomial shown in equation 9–5 using the well coefficients B and C . (See Figure 9–1 for the components of head losses in a pumped well).

$$s_t = BQ + CQ^2 \quad (9-5)$$

where:

s_t = total drawdown in the well

B = summation of B_1 , B_2 , and B_3 ($\sum_{i=1}^3 B_i$), where:

B_1 = linear aquifer-loss coefficient caused by head losses in the aquifer

B_2 = linear well-loss coefficient caused by drilling damage to aquifer, drilling mud plugging the aquifer, and losses in the gravel pack and well screen (wellbore “skin”)

B_3 = partial-penetration loss coefficient

C = non-linear well loss coefficient generally caused by friction losses inside the well housing and losses due to turbulent flow in the vicinity of the pump intake

Q = flow rate out of the well

(4) The quantity B_1Q is equal to s_a . For a full-penetration well, this relationship can be used as the numerator in equation 9–3 and equation 9–5 substituted as the denominator. The resulting equation, equation 9–6, is another way to express well efficiency.

$$Efficiency (E\%) = \frac{B_1Q}{BQ + CQ^2} \times 100 \quad (9-6)$$

(5) For a partial-penetration well, equation 9–6 becomes equation 9–7.

$$E\% = \frac{B_1Q + B_3Q}{BQ + CQ^2} \times 100 \quad (9-7)$$

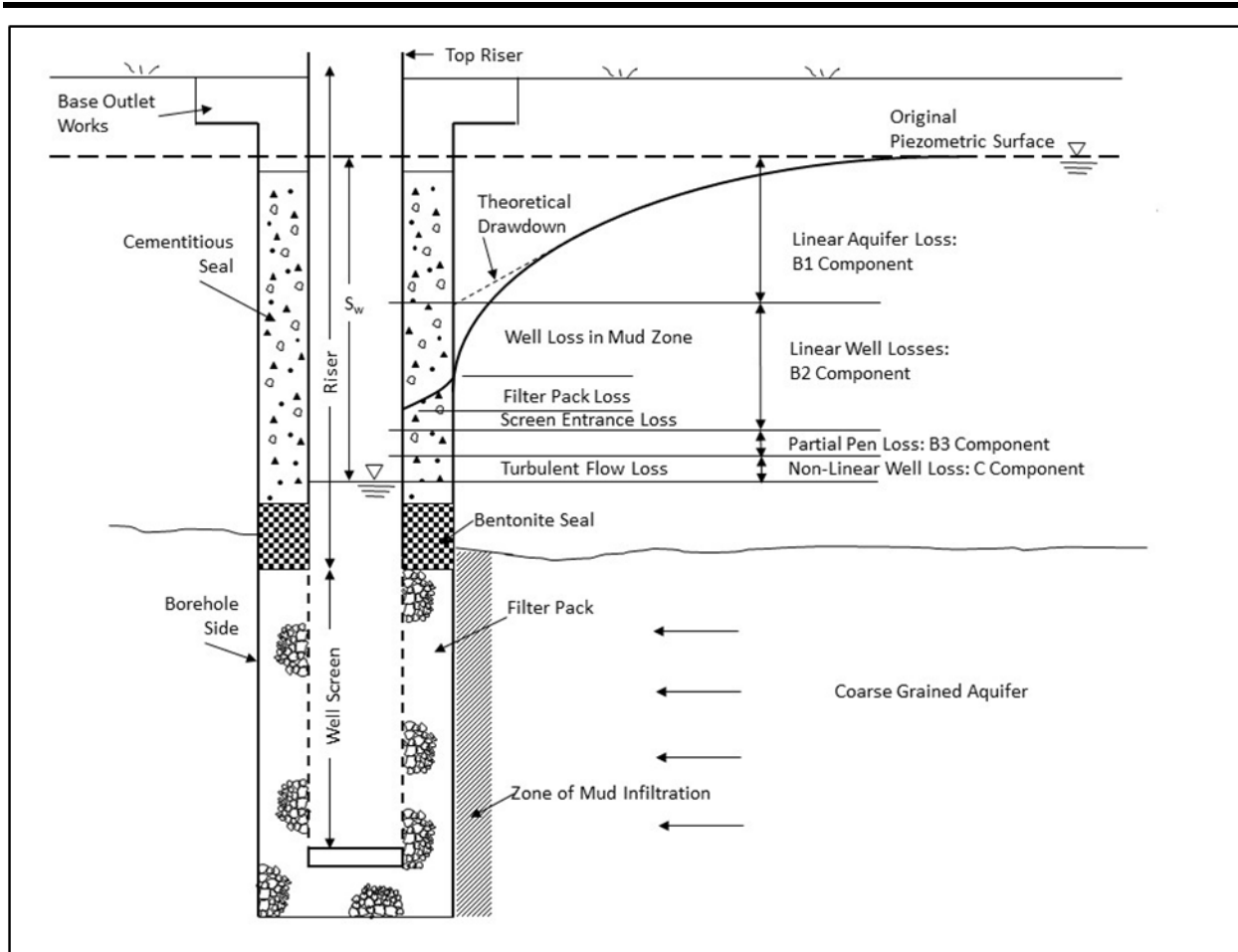


Figure 9–1. Components of head loss in a pumped well (adapted from Driscoll 1986)

f. *The B and C coefficients.*

(1) Aquifer losses described by the B_1 coefficient are a function of aquifer properties and Q . They are independent of well performance, generally constant with time, and always present. The losses described by the B_2 coefficient have been recognized in both pumped (active) and relief (passive) wells and are well documented. The B_2 coefficient is often referred to as the wellbore skin factor. The drawdown attributable to skin is usually due to factors affecting the permeability near or at the relief well screen. These include blockages that result from debris, biofilm, scale, and encrustation. Such defects can be minimized by following best practices of well installation and development (see Chapter 8). Proper design of well screens and filter packs will also minimize B_2 .

(2) Losses due to the B_3 coefficient are always present in partial-penetration wells and must be accounted for in design. Wells cannot be rehabilitated to reduce the B_3 coefficient. Likewise, some degree of turbulent losses implied by the C coefficient are always present and must be recognized.

(3) The B_2 and C coefficients change with time because of well biofouling, mineralization, and the like. Periodic well maintenance is required to remove these materials and maintain B_2 and C at acceptable levels for well performance.

g. Determining B and C directly from pumping tests. Data from a step-drawdown pump test can be used to calculate the relative proportion of laminar and turbulent flow occurring at the various pumping rates. Methods to estimate the B and C coefficients from these data are outlined in Kruseman and de Ridder (2000). When there are no linear well losses ($B_2 = 0$), as may be true of a new, properly installed well, and no partial penetration ($B_3 = 0$), then $B = B_1$. In this case, B can be estimated from the aquifer T and S_t as shown in equation 9–8 for a homogenous aquifer and full-penetration well (Cooper and Jacob 1946; Kasenow 2001; Houben and Kenrick 2022). B_1 can also be calculated when s_a is determined from distance-drawdown data (see example in paragraph 9–8f). For a full-penetration well, ($B_3 = 0$), B_2 can be determined from the s_t in excess of that attributable to B_1 .

$$B = \frac{2.3}{4\pi T} \log \left[\frac{2.25Tt}{r_w^2 S_t} \right] \quad (9-8)$$

where:

- T = transmissivity
- S_t = storativity
- r_w = well radius
- t = time since pumping initiated

h. Determining B and C using specific drawdown. The coefficients B and C can be determined by plotting the specific drawdown (s_t/Q) versus Q , where s_t is the total stabilized drawdown at the end of each step and Q is the pumping rate. This generally results in a straight line with positive slope as shown in Figure 9–2. The straight line is extended to the y-axis. Equation 9–9 will indicate the slope of the line to be C and the y-intercept to be B . The coefficients cannot be determined if the plot results in a negative slope. With the values of B and C known, equation 9–9 can be rearranged to predict s_t for any magnitude of Q .

$$\frac{S_t}{Q} = B + CQ \quad (9-9)$$

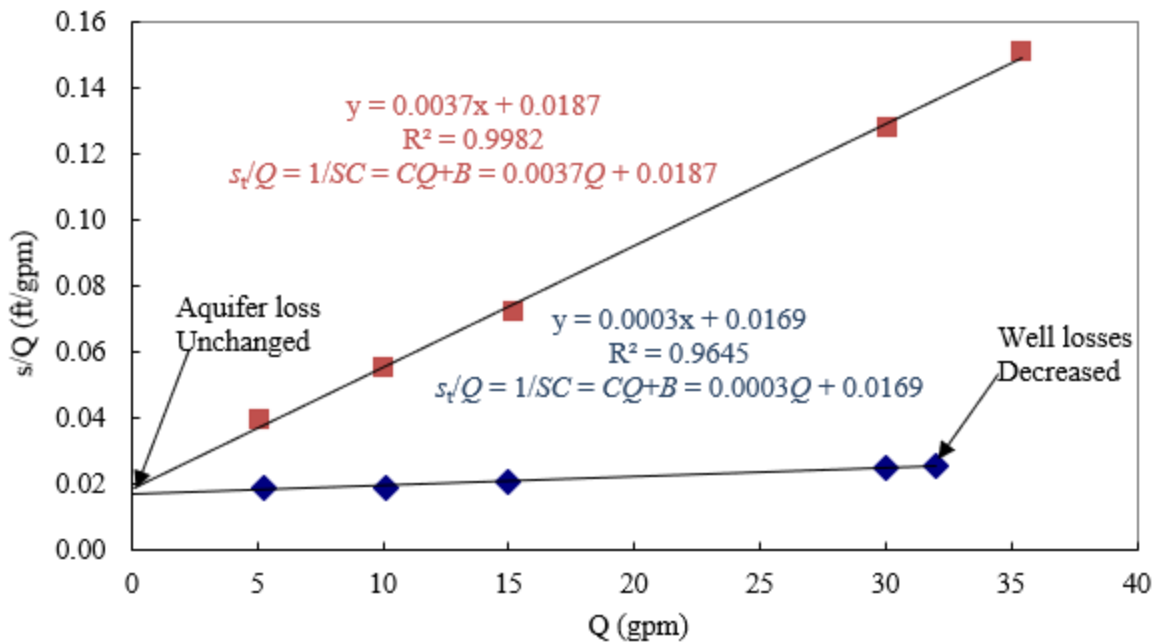


Figure 9–2. Plot of specific drawdown versus pumping rate from step-drawdown data (modified from Guy et al. 2014, RW-85 before and after rehabilitation).

i. *Meaning of C.* The C coefficient can be used to assess the degree of deterioration of the well using the criteria in Walton (1962) and Kasenow (2001). The criteria are shown in Table 9–1. The C coefficient is determined from a step-drawdown test as shown in paragraph 9–3h. Experience in USACE has been mixed regarding the use of C to evaluate the condition of relief wells. For this reason, using the C coefficient as an indicator of a well’s condition should be done in conjunction with other evaluation methods.

Table 9–1
Well condition based on well loss coefficient C (after Kasenow 2001 and Walton 1962)

C (min ² /m ⁵)	C (sec ² /ft ⁵)	C (ft/gpm ²)	Condition of Well
< 0.5	< 5	< 0.000025	Properly constructed and developed
0.5 to 1.0	5 to 10	0.000025 to 0.000050	Mild deterioration or clogging
1.0 to 4.0	10 to 40	0.000050 to 0.00020	Severe clogging or deterioration
> 4.0	> 40	> 0.00020	Difficult to restore to original yield

j. *Well coefficients for partial-penetration wells.* As described in Chapter 5, partial penetration introduces vertical flow components in the area immediately surrounding the well. This results in higher flow velocity near the limits of the screened zone and, in turn, greater losses compared with full-penetration wells for the same flow rate and aquifer characteristics. Figure 9–3 illustrates how flow to a partial-penetration well distorts flowlines as compared to a full-penetration well. Additionally, vertical flow typically follows lower permeability pathways, resulting in greater well losses.

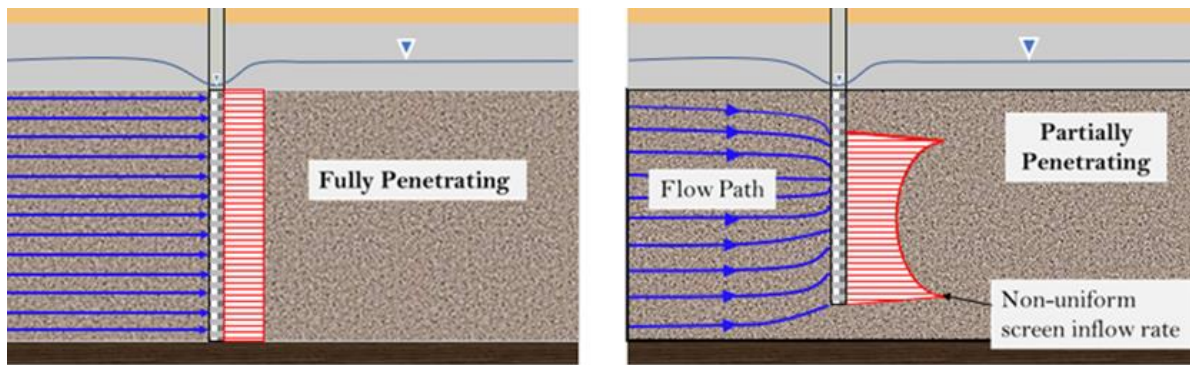


Figure 9–3. Partial-penetration flow path convergence (after Houben 2015)

(1) *Estimating B_2 for partial-penetration wells.* As stated in paragraph 9–3g, B_2 can be calculated or reasonably estimated for a full-penetration well because $B_3 = 0$. For a partial-penetration well, B_2 can be estimated by modeling methods that account for the partial penetration. It is also recommended to use models that can estimate the wellbore skin components.

(2) *Estimating B_3 for partial-penetration wells.* The partial-penetration component (B_3) can be estimated by computer modeling/simulations and/or by the Kozeny method (see paragraph 9–3j(3)) or the Huisman relationship (see paragraph 9–3j(4)).

(3) *Kozeny method.* The Kozeny method (Kozeny 1933 and Houben 2015) is given by equation 9–10. This equation is normally used assuming the percent penetration is equal or less than 50. The equation still gives a reasonable estimate for percent penetrations greater than 50.

$$s_{pp} = \frac{s_{fp}}{\alpha \left[1 + 7 \sqrt{\frac{r_{we}}{2 \alpha b}} \cos \left(\frac{\alpha \pi}{2} \right) \right]} \quad (9-10)$$

where:

$\alpha = L/b \times 100$ (percent penetration, equivalent to $W/D \times 100$)

$b =$ the aquifer thickness (equivalent to D)

$r_{we} =$ effective well radius

$L =$ screen length (equivalent to W)

$s_{pp} =$ drawdown in partial-penetration well

$s_{fp} =$ drawdown in full-penetration well

The difference between s_{fp} and s_{pp} is equal to the $B_3 Q$ term in equation 9–4.

(4) *Huisman method.* The relationship developed by Huisman (Huisman 1972; Kruseman and de Ridder 2000; and Houben 2015) to estimate the partial-penetration drawdown (s_{pp}) is expressed in equation 9–11. This equation requires prior

measurement or estimation of the hydraulic conductivity and effective thickness of the aquifer.

$$s_{pp} = \frac{Q_n}{2\pi kb} \frac{\left(1 - \frac{L}{b}\right)}{\left(\frac{L}{b}\right)} \ln \left[\frac{\left(1 - \frac{L}{b}\right)L}{r_{we}} \right] \quad (9-11)$$

where:

- Q_n = pumped well flow rate at step n
- L = screen length (equivalent to W)
- b = aquifer thickness (equivalent to D)
- k = permeability
- r_{we} = effective well radius

The difference between s_{fp} and s_{pp} is equal to the B_3Q term in equation 9–7.

(5) *Computer modeling/simulations.* Computer simulations or modeling software such as AQTESOLV can be used to simulate pumping tests and estimate s_{fp} and s_{pp} . When simulations include both full- and partial-penetration wells, the ratio between the two can be used in conjunction with hand calculations as a check.

9–4. Specific capacity (SC) and efficiency (E)

SC and E are not the same thing, but they are similar and both can be used to monitor well performance. For each well, E can be calculated based on results from the baseline pumping test ($E_{baseline}$), but SCR cannot be determined until there has been a second pumping test. Determining E is more complex and expensive than measuring the SC . However, E allows a more detailed accounting of various parameters that affect well performance. For SC tests, only s_t is generally known unless drawdown is also measured in at least two observation wells located at different radii from the pumping well, which allows an estimate of s_a .

a. Example comparison between SC and E .

(1) Table 9–2 and Figure 9–4 show how SCR and E are related for four hypothetical wells, each with a different assumed aquifer loss, s_a . Each scenario has a baseline pumping test (Test #1) and four subsequent pumping tests (Test #2, Test #3, etc.) conducted at various times. For actual projects, the subsequent pumping tests typically are 5 years apart. For each well, s_a remains constant because the aquifer is assumed to be unchanging and the boundary conditions are assumed to have not changed. Therefore, well losses, s_w , are responsible for all of the increased drawdown measured during subsequent pumping tests.

(2) The increases in s_w assumed for this example could likely be attributed to biofouling and other mechanisms that decrease well performance over time. All pumping tests are assumed to have been conducted at identical values of Q . As a

result, SCR (equation 9–2) becomes the ratio of $s_{t-current}$ to $s_{t-baseline}$. Plotted data points on Figure 9–4 represent E and SCR determined for each well over time. All values of E for the different assumptions of s_a plot on the same line because there is a 1:1 ratio between x-axis and y-axis values. Both SCR and E decrease as the well losses, s_w , increase over time.

(3) While E and SCR follow similar trends and do not significantly diverge from each other, E is always less than SCR . This is because no well is 100% efficient at the time of installation, but the SCR can be 100% if well performance does not deteriorate. The example presented here assumes that s_w and s_a are known from all tests, when, in most cases of measuring SC , only s_t is measured. If there are additional drawdown monitoring points besides the pumping well location, the theoretical drawdown (s_a) can be determined graphically (see example in paragraph 9–8f) and s_w is then the difference between s_t and s_a . The value of s_a is generally assumed to be a constant with time for all subsequent tests conducted in the same aquifer at the same pumping rate. The value of s_a varies linearly for different pumping rates (see equations 9–12 through 9–14).

b. *Determining $E_{baseline}$ from subsequent pumping tests and SCR .* It may be of interest to estimate $E_{baseline}$, even if it was not determined during the baseline pumping tests. $E_{baseline}$ can be estimated by dividing E from a subsequent pumping test by SCR from the same subsequent pumping test. For example, pumping test #4 for Well 2 has an $E_{current}$ of 50% and an SCR of 55%. If the Well 2 $E_{baseline}$ had not been determined during the baseline pumping test, the $E_{baseline}$ could be estimated by $E_{current} / SCR = 50\% / 55\% = 0.91$ or 91%.

Table 9–2
Efficiency and SCR calculation for four assumed wells, each with different aquifer losses and increasing well losses during subsequent pumping tests (values of s_a , s_w and s_t are in feet)

Well 1							
Pumping Test	s_a	s_w	s_t	$s_w/(s_a+s_w)$	E	E -ratio	SCR
#1 (Baseline)	3	0.5	3.5	0.14	86%	–	–
#2	3	1.5	4.5	0.33	67%	78%	78%
#3	3	3	6	0.50	50%	58%	58%
#4	3	5	8	0.63	38%	44%	44%
#5	3	7	10	0.70	30%	35%	35%
Well 2							
Pumping Test	s_a	s_w	s_t	$s_w/(s_a+s_w)$	E	E -ratio	SCR
# 1 (Baseline)	5	0.5	5.5	0.09	91%	–	–
#2	5	1.5	6.5	0.23	77%	85%	85%
#3	5	3	8	0.38	63%	69%	69%
#4	5	5	10	0.50	50%	55%	55%
#5	5	7	12	0.58	42%	46%	46%
Well 3							
Pumping Test	s_a	s_w	s_t	$s_w/(s_a+s_w)$	E	E -ratio	SCR
#1 (Baseline)	7.5	0.5	8	0.06	94%	–	–
#2	7.5	1.5	9	0.17	83%	89%	89%
#3	7.5	3	10.5	0.29	71%	76%	76%
#4	7.5	5	12.5	0.40	60%	64%	64%
#5	7.5	7	14.5	0.48	52%	55%	55%
Well 4							
Pumping Test	s_a	s_w	s_t	$s_w/(s_a+s_w)$	E	E -ratio	SCR
#1 (Baseline)	10	0.5	10.5	0.05	95%	–	–
#2	10	1.5	11.5	0.13	87%	91%	91%
#3	10	3	13	0.23	77%	81%	81%
#4	10	5	15	0.33	67%	70%	70%
#5	10	7	17	0.41	59%	62%	62%

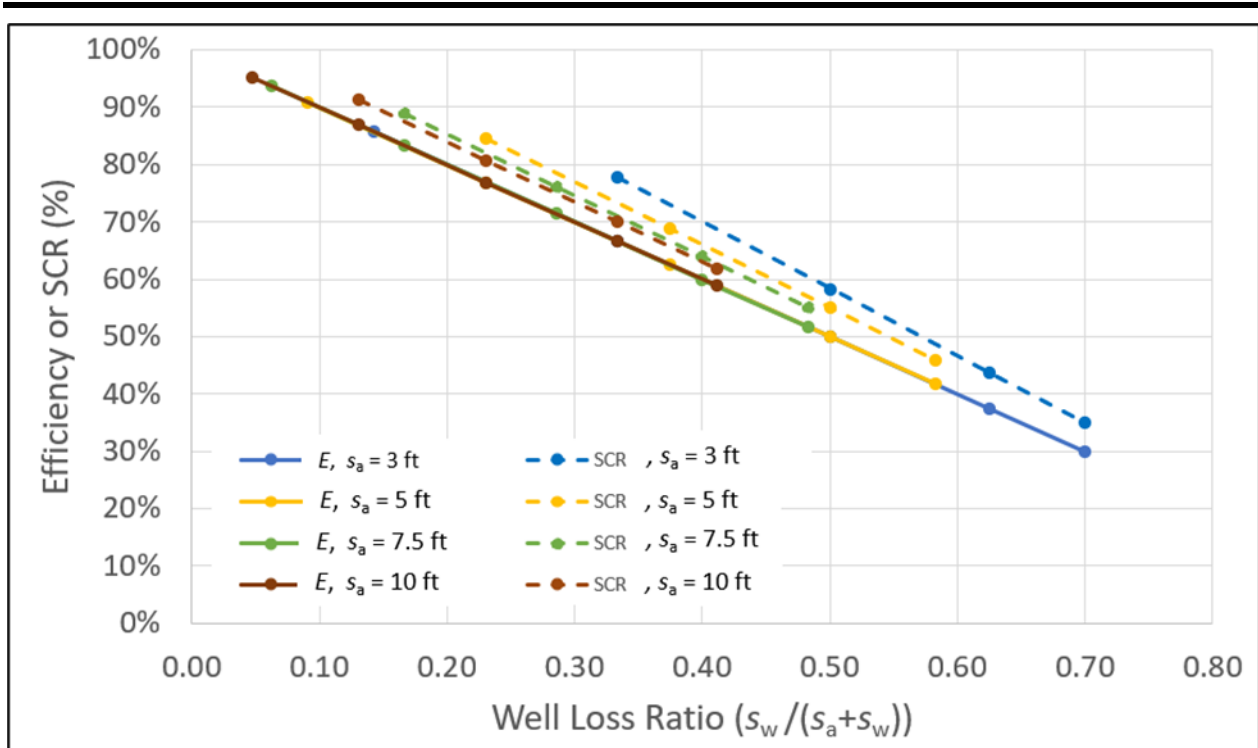


Figure 9-4. Efficiency and SCR comparison for hypothetical wells with assumed constant aquifer losses and increasing well losses with time

9-5. Monitoring of well condition

Reduced well performance results in hydrostatic heads greater than those anticipated in the design, thus potentially leading to unsatisfactory performance. It is critical that wells perform within limits associated with reasonable predictions of satisfactory performance. Relief wells should be evaluated using the results from pumping tests, in conjunction with downhole video inspection and field observations where possible. Guidelines for evaluating and improving well performance are further described in this chapter and Chapter 11.

a. *Monitoring during high water.* Risk to a structure is elevated during high-water events due to higher loading on the structure. Where a structure is equipped with a sufficient level of instrumentation, this risk can be evaluated as described in Chapter 4 and Appendix J. Piezometric levels and flow quantities are typically measured at lower river stages. These can be extrapolated to predict the values that would be produced by a maximum design reservoir level or river stage.

b. *Evaluation using pumping tests.* *SCR* and *E* are two ways to quantitatively express well performance. A historically common threshold for triggering well maintenance efforts was whether *SCR*, or *E-ratio*, had declined to less than 80%. From Figure 9-4, an *SCR* of 80% is analogous to an *E* in the range of 67 to 77% for the assumed scenarios. Another way to evaluate well system performance is to use the increase in drawdown from the baseline pumping test, at the design flow rate, to

increase H_w and calculate the expected FS_{vg} for the current condition and compare to the design criteria.

c. *Decline in SC and E over time.* A decline in future well performance can be accounted for by reducing calculated well flow or drawdown by the assumed percentage of performance reduction. For example, well spacing would be determined by applying a factor of 0.8 to calculated well flow or drawdown if the future assumed condition was $SCR = 80\%$. Alternatively, well losses can be assumed to be higher than calculated or measured for a new well during a pumping test. The increase in drawdown from a pump test at the design flow rate can be applied as an increase in well losses to monitor performance with time. Assuming a reduction in future performance during design improves the resiliency of the system for future loading.

d. *Determining well performance thresholds.*

(1) It may be appropriate to use a risk-informed approach when establishing critical relief well performance loss. Depending on the specific project details and consequences of failure, a performance threshold higher or lower than 80% SCR may be justified.

(2) An example of evaluating likelihood of boils and well performance losses is shown in Figure 9–5 for the initial Harrisonville Levee designs and the subsequently observed performance under different SCR s observed in different well systems along the levee. The original design was for a FS_{vg} of 1.25 with wells that produce 80% of the calculated drawdown ($SCR = 80\%$), which provided a FS_{vg} of 1.55 with 100% of the calculated drawdown. Two different reaches with varying observed loss of well performance, as evaluated using SCR , are shown.

(3) The relationship between measured SCR , predicted FS_{vg} with the measured SCR , FS_{vg} without wells, and observation of boils during flood loading are all in good agreement. This type of assessment could be used to determine the appropriate well performance threshold for a project. Where wells fall below a threshold limit, additional investigations and evaluations should be performed. The studies should determine the cause of the inadequacies and an appropriate rehabilitation program. Further discussion on risk-informed assessment of relief wells is included in Appendix J.

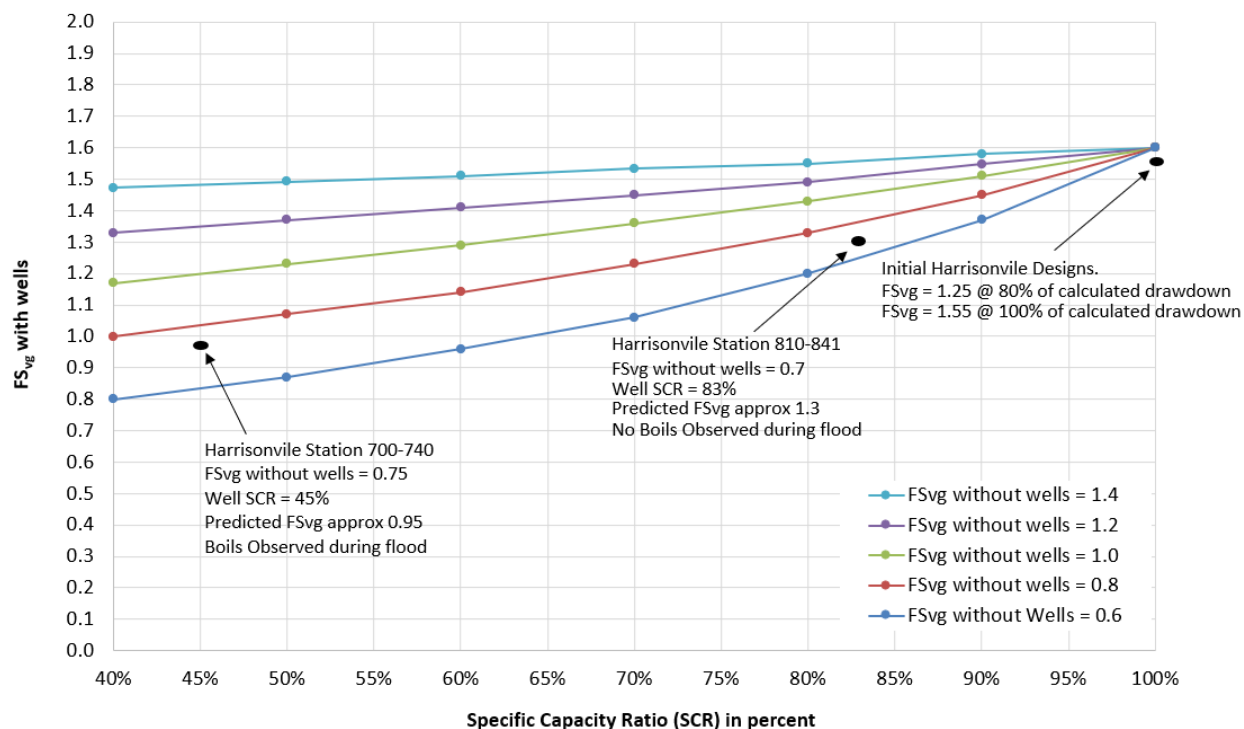


Figure 9-5. Example well performance loss with observed performance during floods, Harrisonville Levee

e. *SCR and E-ratio greater than 100%.*

(1) In some instances, the calculated *SCR* is greater than 100%. This is often due to an uncertain baseline test condition and/or the well not being fully developed following installation. When the well is not tested under conditions similar to the baseline, the calculated *SC* could be higher than the original *SC*. If the *SC* of the well increases during testing, it usually suggests the well was previously underdeveloped. Further development and removal of fines occurs during testing, resulting in a higher *SCR*. The well loss parameters cannot be obtained from the data when a relief well is underdeveloped.

(2) An example of potential well underdevelopment is presented in Figure 9-6. The figure shows *SC* data from a relief well installed and tested in 1992 and retested on four subsequent occasions. Comparison of tests conducted after installation and during the first assessment (10 years later in 2001) shows an increase in *SC*. This outcome is highly unlikely under normal conditions and suggests initial underdevelopment. After 2012, *SC* for the well decreases with time, as is expected. When *SC* results imply that development is occurring during testing, the peak *SC* should be used as the baseline. For the example in Figure 9-6, the appropriate baseline would be the 2001 pumping test.

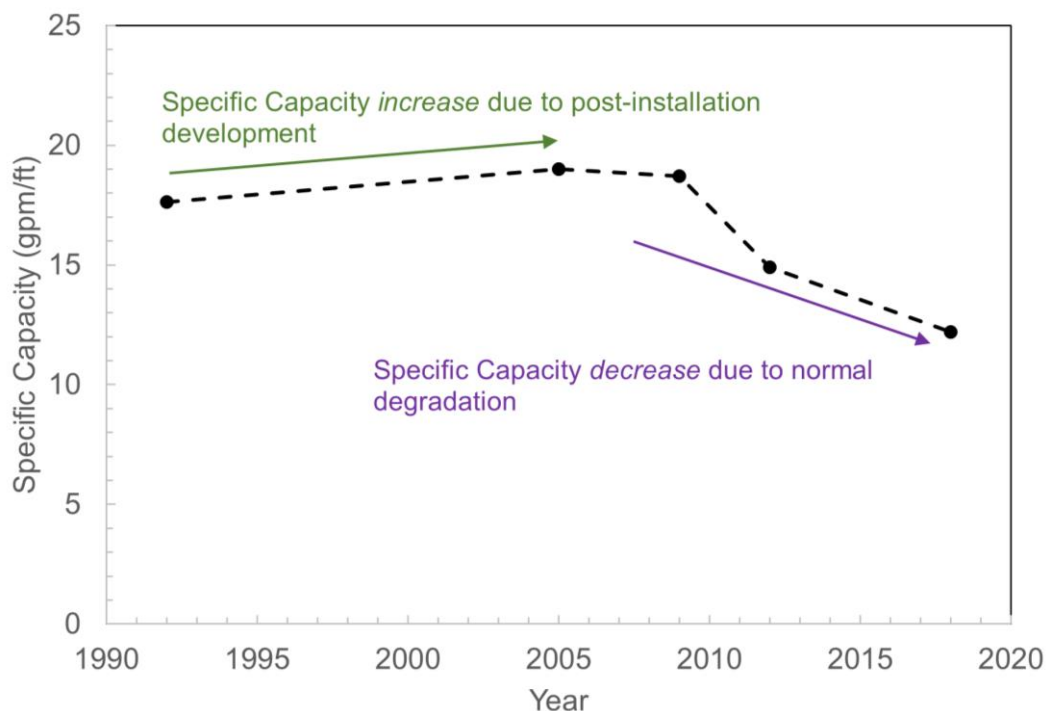


Figure 9–6. Example of effect of underdevelopment on specific capacity over time; Wilson Dam (Kansas City District) Relief Well 6A

9–6. Pumping test

Both E and SCR are determined through pumping tests. The pumping test is a common field test in which a well is pumped at a controlled rate. The corresponding water level response (drawdown) is measured in the pumping well and/or observation wells. Pumping tests are used to estimate aquifer properties and evaluate the condition or performance of wells. Data from pumping tests can be used to monitor changes to SC and E over time. There are also methods to estimate components of well loss from pumping tests described in this chapter. Two types of pumping tests commonly used for relief well evaluation are the constant rate test and the step-drawdown test. There are different levels of complexity associated with each type of test. Relief well evaluators should consider the information needed to assess well performance and specify pumping tests accordingly.

a. Constant rate tests.

(1) The constant rate test is the most common and simplest type of pumping test used for relief wells. The SC can be determined from a constant rate test simply by knowing the pumping rate and drawdown in the pumping well (see paragraphs 9–2 and 9–2a). The aquifer transmissivity (T) can also be measured from these data (see paragraph 9–6g(3)). By measuring drawdown at observation points at some distances from the pumping well (see paragraph 9–6c), a constant rate test allows the determination of both T and S_t by type curve matching or straight-line methods (see

paragraphs 9–6g(1) and 9–6g(2)). T and S_t are aquifer constants and generally will not need to be re-measured during future assessments of well performance.

(2) For a given pumping rate and distance from the pumping well, drawdown will stabilize at some time value. A common assumption is that the radius of influence of the pumping well does not intersect an aquifer boundary. If the radius does intersect an aquifer boundary, additional analysis of the test results may be needed. Constant rate tests are well suited for monitoring the performance over time of existing wells. However, such tests should not be used to establish the performance baseline of new wells.

b. Step-drawdown tests.

(1) The step-drawdown pumping test is a commonly performed test that uses multiple flow rates, or “steps,” to assess a single relief well. Like the constant rate test, flow and drawdown are measured during a step-drawdown test. Also like the constant rate test, these data can be used to determine aquifer parameters (see paragraph 9–6.a).

(2) The advantage of a step-drawdown test is the use of multiple flow rates allows determination of additional well parameters. These include values of SC and E at multiple flow rates and a relief well’s loss coefficients. Well loss coefficients are described in paragraph 9–3e. Step-drawdown tests are recommended for baseline testing of new wells. This allows comparison of SC and E at different flow rates for future tests to monitor well performance. Measurement of the well coefficients can also lead to better assessments of well performance. Step-drawdown tests should cover a range of flows below and above the expected well flow under maximum loading on the structure.

c. Monitoring network.

(1) Pumping tests ideally include observation wells. However, the number and location of observation wells required depend on the type of tests and desired accuracy. For baseline testing, observation wells are highly recommended. The drawdown data collected from these wells allow aquifer parameters to be determined by multiple methods, as described below in paragraph 9–6g.

(2) In addition, multiple observation wells allow determination of s_a and well losses, as described above in paragraph 9–3. Aquifer parameters and s_a are constants and do not need to be re-measured in subsequent tests. Observation wells can include existing piezometers and/or adjacent relief wells. The observation wells should be located multiple directions and distances from the pumping well. Their locations should also account for known/assumed geologic features and hydraulic boundary conditions that could impact the groundwater flow. Ideally, at least one observation well should be located outside of the radius of influence of the pumping well to measure background hydraulic head.

d. *Equipment.* The following sections outline the basic equipment needed to conduct a pumping test. All equipment used should be appropriately sized for the well being tested and conditions present during the tests. Pumps should be able to provide the necessary flow rate, fit inside the well screen, and discharge such that no damage is caused to adjacent wells or the surrounding area.

(1) *Pump.* The pump capacity should be sufficient to produce the desired flows. If only a constant rate pumping test is being performed, it is recommended to pump the well near the expected design well flow. If the static groundwater level is more than 18 to 20 feet from the top of the well outlet, a deep-well pump may be required. Pumps should be able to maintain a constant flow for up to 2 hours. A butterfly valve should be present to avoid over-pumping and allow flow adjustment. A shielded intake should be used to reduce potential damage to the well. The pump and intake should be set in the riser pipe rather than the well screen where possible.

(2) *Flow meter.* A flow meter(s) compatible with the pump and discharge lines should be used to measure total outflow during the pumping test. The flow meter(s) should be calibrated prior to use during the test. The pump rating alone is not a sufficient means of monitoring outflows. In addition to measuring total outflow, a downhole well flow meter is desirable to measure flow in the well. The flow meter can be placed at various depths to help define high-permeability zones.

(3) *Water level measuring device.* Water levels during the pumping test should be monitored with either an electronic water level indicator or deployable sensor (such as a pressure transducer). All devices used to measure water levels should be calibrated prior to use. Pressure transducer data should be checked periodically against manual measurements to verify the accuracy of automated measurements.

e. *Pumping test procedure.* Procedures and general considerations for constant rate and step-drawdown tests are outlined below in paragraphs 9–6e(1) and 9–6e(2), respectively.

(1) *Constant rate test.*

(a) Prior to a pumping test, the well should be sounded and the depth compared to the as-built depth. If sounding the well indicates there is more than minor sedimentation in the well bottom, it is recommended to remove the sediment and perform a camera inspection of the well prior to performing a pumping test to search for well defects that are allowing intrusion of filter pack and foundation materials. Ensure that static water level in the relief well has recovered to within 0.1 foot of the ambient condition if sequentially testing a line or array of wells. No adjacent wells within a relief well's zone of influence should be pumped during a pumping test.

(b) Continuously pump the well until s_t has stabilized. This should take between approximately 15 minutes and 2 hours. Historical data indicate that 30 minutes is typically an adequate duration to achieve steady-state drawdown in generally

homogeneous confined aquifers. The time for s_t to stabilize in any observation wells depends on their distance(s) from the pumping well.

(c) While the well is being pumped, measure and record Q and s_t . The stage or elevation of adjacent bodies of water, including rivers, streams, creeks, landside areas, and ditches should also be monitored and recorded. This is important for comparison of boundary conditions during subsequent tests. Measurements of s_t in the pumping well and any observation wells should be made to the nearest 0.01 foot. Multiple readings should be taken in the first 15 minutes of pumping and at least every 15 minutes thereafter.

(d) It is highly recommended that water levels also be measured during the recovery period. Readings should be taken at 5-minute intervals from the time the pump is shut off. This should continue until the groundwater level recovers to within 10% of the pre-test static level. The analysis is used as an independent check on the pumping test data. The time-drawdown data from a recovery test is more reliable than that collected from the pumping test if the pumping rate is not constant. This is because the groundwater level recovers at a constant rate during recovery period (USACE 1983 and Kruseman and de Ridder 2000). Residual drawdown is the difference between the water level prior to pumping and the water level at a time t , after the pump is shut off (Figure 9–7).

(e) The pumping water level should not be allowed to fall below the top of the aquifer or pervious strata. This will ensure that confined conditions are maintained throughout all steps. The pumping rate can be decreased to prevent loss of confined aquifer conditions.

(f) If the test is being conducted on an existing well, Q should match one of the flow rates from the baseline test. The elevation of the loading source (the river or lake) during the pumping test should also be monitored. This elevation should be as close as practical to what was measured during any previous tests.

(2) *Step-drawdown test.*

(a) Prior to a pumping test, the well should be sounded and the depth compared to the as-built depth. If sounding the well indicates there is more than minor sedimentation in the well bottom, it is recommended to remove the sediment and perform a camera inspection of the well prior to performing a pumping test to search for well defects that are allowing intrusion of filter pack and foundation materials. Ensure that static water level in the relief well has recovered to within 0.1 foot of the ambient condition if sequentially test testing a line or array of wells. No adjacent wells within a relief well's zone of influence should be pumped during a pumping test.

(b) Continuously pump the well until drawdown has stabilized. A minimum of three values of Q are recommended, and five are ideal. Figure 9–8 shows test results of five different steps.

(c) Pumping should be held constant at each flowrate for at least one hour. Readings should be taken at short intervals (2, 4, 8, 10, 15, 20, 30, 45, and 60 minutes) at each flow rate.

(d) While the well is being pumped, measure and record Q and s_t , as described above for the constant rate test. This includes the stage or elevation of adjacent bodies of water. The observed drawdown in the well is plotted with time. The example in Figure 9–8 shows five different steps.

(e) Measure water levels during the recovery period, as described above for the constant rate test.

(f) The pumping water level should not be allowed to fall below the top of the aquifer or pervious strata. This applies to all steps.

(g) As described above for the constant rate test, the pumping rate and loading conditions should be as close as practical to the baseline test.

f. Sand infiltration. Sufficient measurements are necessary to establish an infiltration rate for each hour of the pumping test. For most properly developed wells, the amount of sand deposited in the well will be negligible. In these cases, sand infiltration can be recorded in terms of ppm as measured with a centrifugal sand tester (Driscoll 1986). The infiltration rate during the last 15 minutes of the pumping test should be 5 ppm or less. If not, the well should be re-surfed by manipulation of the test pump for 15 minutes. Then the pumping should be resumed until the infiltration rate is less than 5 ppm. After 6 hours of pumping, if the rate is more than 5 ppm, the well should be abandoned as described in paragraph 8–13. Additional discussion of the sand infiltration test is given in paragraph 8–7.

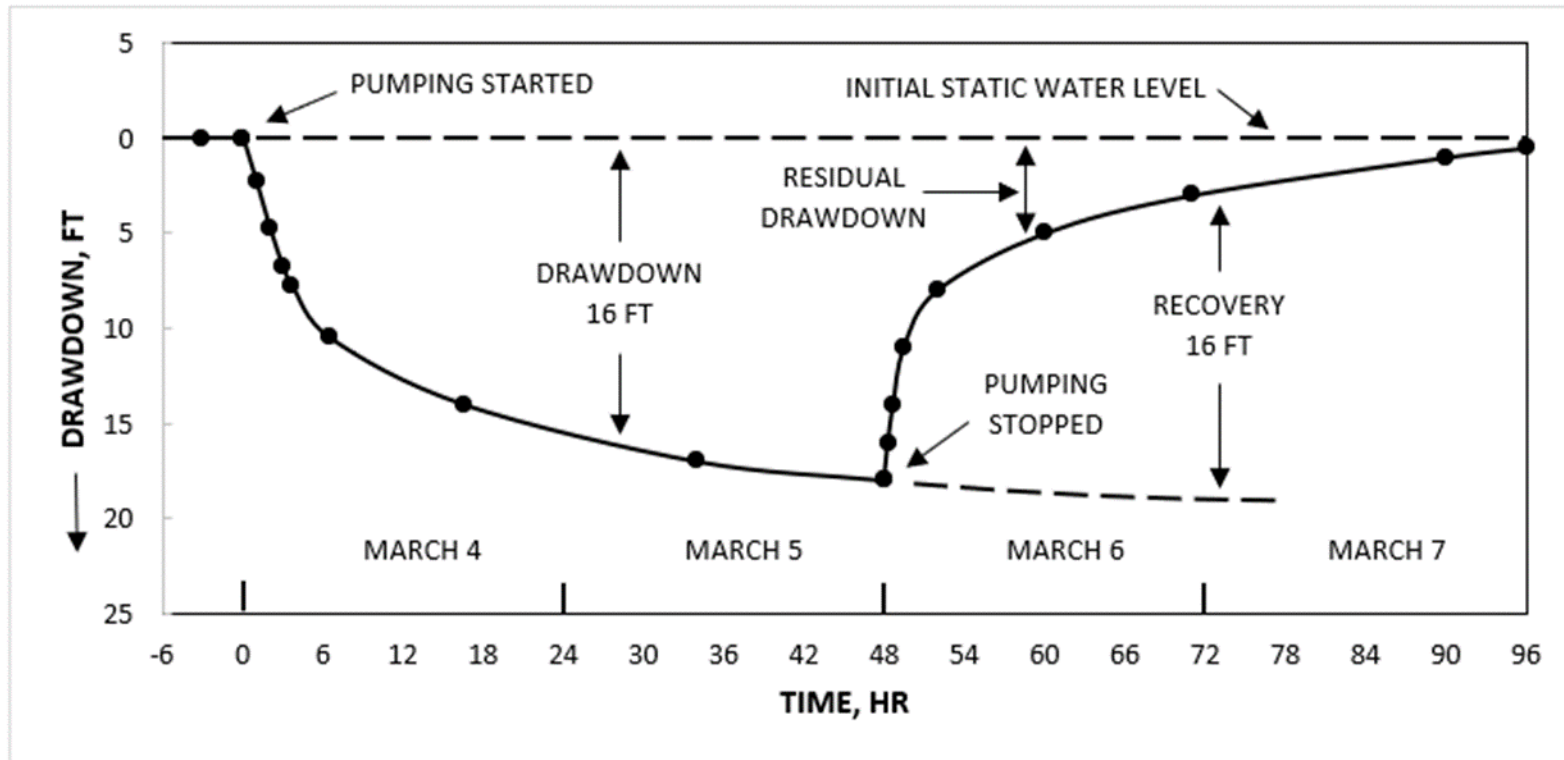


Figure 9-7. Typical drawdown and recovery curves of a pumped well and then allowed to rebound (after U.S. Army 1983)

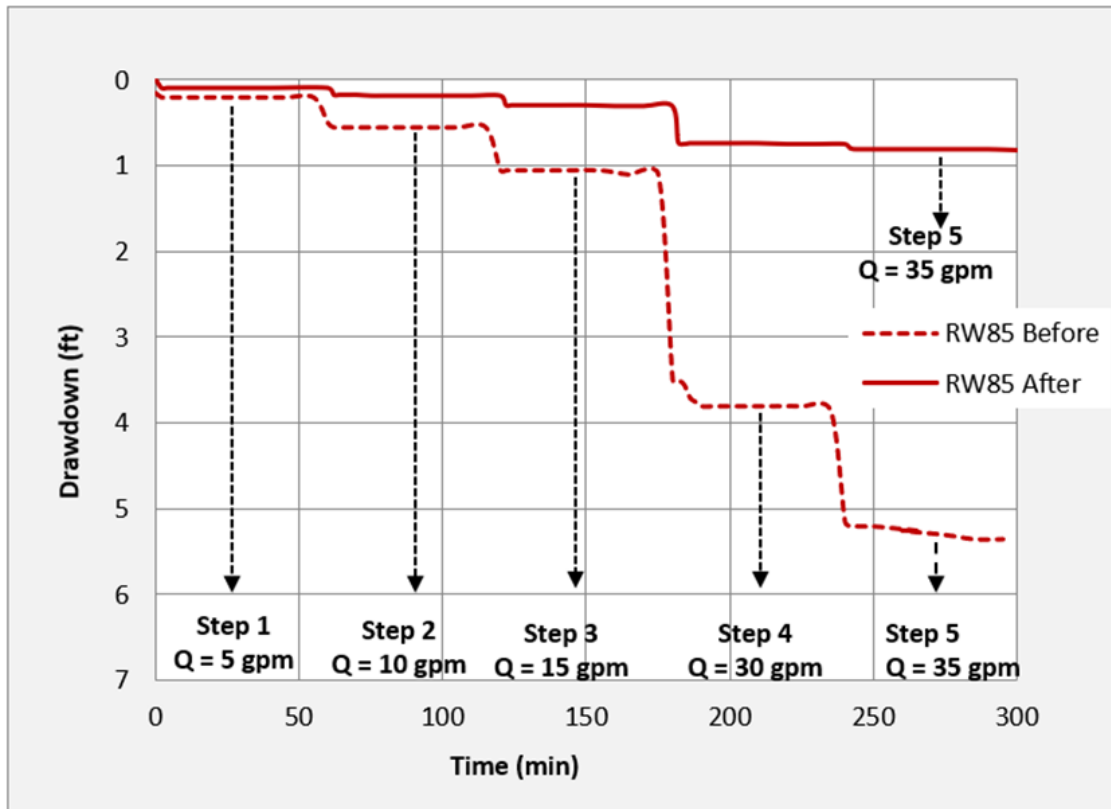


Figure 9-8. Step-drawdown test results: before and after rehabilitation of 3-inch diameter perforated well

g. *Determination of aquifer parameters.* The aquifer constants T and S_t are determined from time-drawdown data collected from either a constant rate or step-drawdown test.

(1) *Determination of transmissivity.*

(a) Transmissivity (T) is the product of hydraulic conductivity (K) and the saturated aquifer thickness (equation 9-12). T can be determined from equation 9-13 by applying the Theis (1935) method to pumping test data.

$$T = kb \tag{9-12}$$

$$T = \frac{Q \times W(u)}{4 \pi s_t} \tag{9-13}$$

$$T = \frac{2.3Q}{4\pi\Delta s_{t-t}} \tag{9-14}$$

$$T = \frac{2.3Q}{2\pi\Delta s_{t-d}} \tag{9-15}$$

where:

- T = as previously defined
- Q = pumping rate
- Δs_{t-t} = drawdown over one log cycle of time
- Δs_{t-d} = drawdown over one log cycle of radial distance
- b = saturated thickness (equivalent to D)
- $W(u)$ = value of the well function
- s_t = drawdown in the observation well after pumping for time interval t
- u = argument of the well function
- r = distance between observation and pumping well

(b) The test data are plotted in log-log format and matched to the Theis-type curve, which is in the form of $W(u)$ versus u . $W(u)$ is based on the exponential integral, which is well known in mathematics. In the context of pumping tests, $W(u)$ is defined as the well function (Freeze and Cherry 1979). A match point is selected that yields values of $W(u)$, u , r and s_t . The $W(u)$ and s_t values are then substituted into equation 9–13 to obtain T . The Theis method can be applied manually, or more commonly, by spreadsheet or specialized software such as AQTESOLV. Straight-line approximations to the Theis solution, derived by Cooper and Jacob (1946) and Jacob (1950), can also be used to determine T .

(c) Figure 9–9 shows s_t (in feet, linear scale) plotted as a function of time (minutes, log scale). Figure 9–10 shows s_t (in feet, linear scale) plotted as a function of radial distance from the pumping well (feet, log scale). Each plot yields a value of Δs_t (feet), which is defined as the drawdown over one log cycle of either time (Δs_{t-t}) or distance (Δs_{t-d}). The values of Δs_{t-t} and Δs_{t-d} are then used in equations 9–14 and 9–15, respectively, to calculate T for confined aquifers. Solutions for determining T from time-drawdown data are also available for leaky, confined aquifers (Walton 1960–1962) and unconfined aquifers (Neuman 1975).

(2) *Determination of storativity.* The Theis (1935) method is a common means of determining storativity (S_t), as shown in equation 9–16. The S_t can also be determined from distance-drawdown data using equation 9–17. The value of r_0 in this equation is effectively the radius of influence. This is illustrated in Figure 9–10 as the radial distance at which the straight line intersects the x-axis at a value of zero drawdown.

$$S_t = \frac{4 T t u}{r^2} \quad (9-16)$$

$$S_t = \frac{2.25 T t}{r_0^2} \quad (9-17)$$

where:

- S_t and u , as previously defined
- T , as determined from equation 9–12.

- t = value of t from match point (equation 9–16), or time at which drawdown measurements are taken (equation 9–17)
- r = distance between pumping well and observation well where drawdown is measured
- r_0 = radius of influence

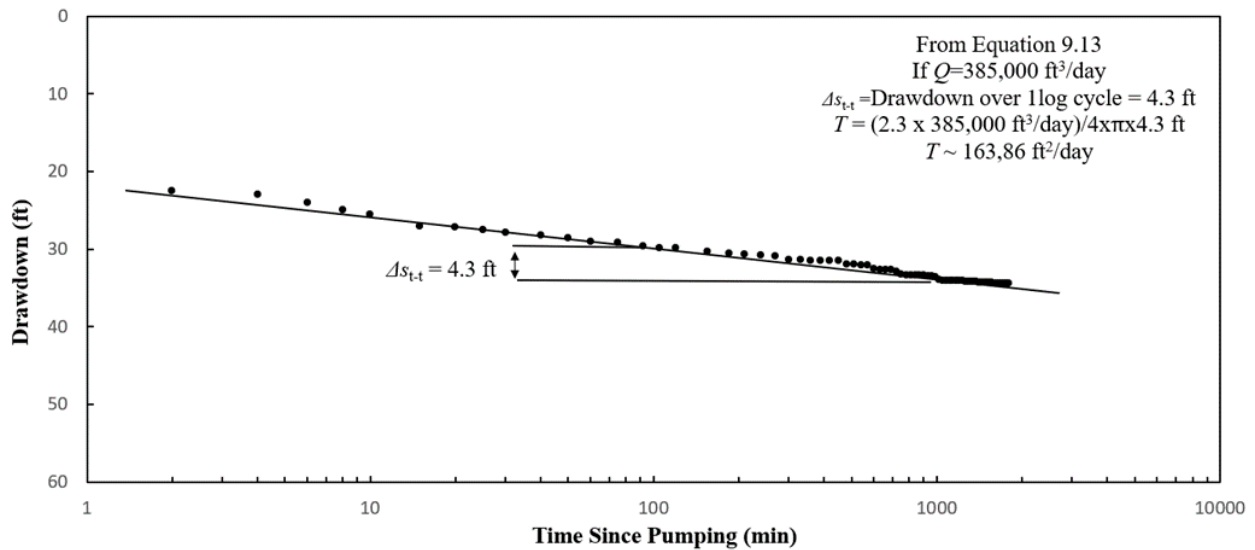


Figure 9–9. Transmissivity estimation from constant rate data using Jacobs method (modified from Kyle 2015)

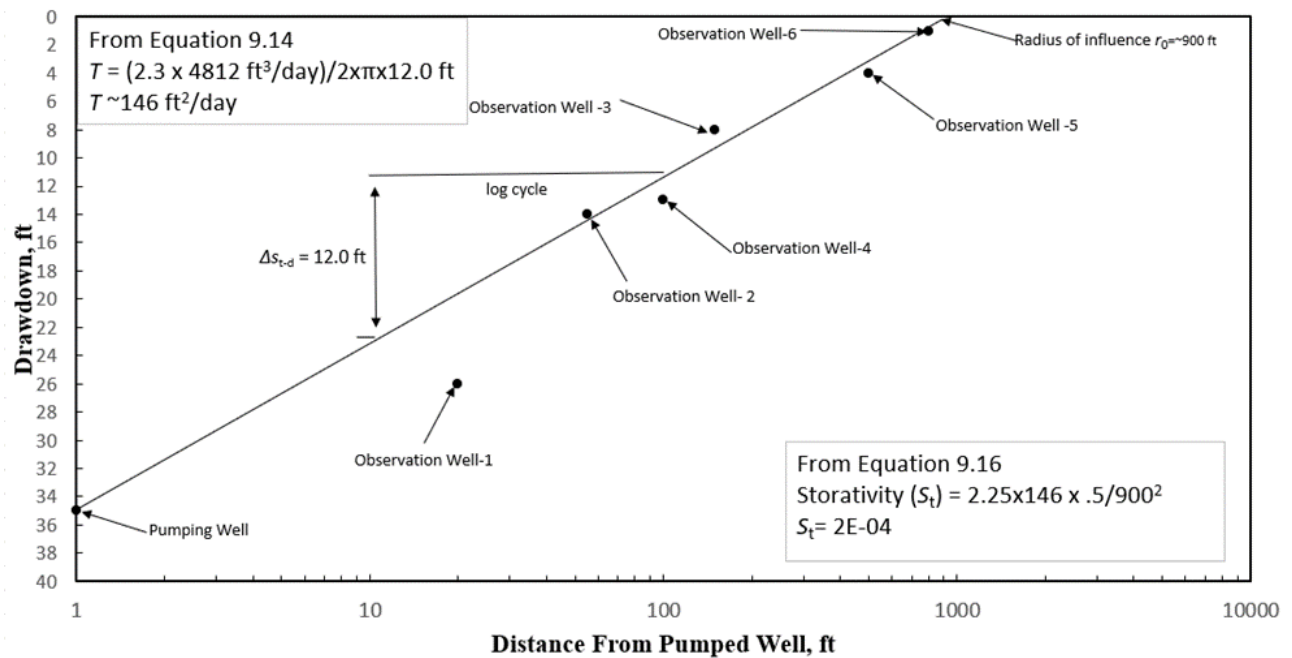


Figure 9–10. Transmissivity and storativity estimation from distance-drawdown test with flow rate of 25 gallons per minute (modified from Kyle 2015)

(3) *Estimating T from SC test data.*

(a) Tests of *SC* are a means of measuring well performance. However, time-drawdown data from these tests can also be used to estimate the aquifer *T*. This can be accomplished using the Cooper and Jacob (1946) and Jacob (1950) technique, as described in paragraph 9–6g(1). The *T* calculated by this technique depends on the rate of drawdown as measured through the Δs_{t-t} parameter. Thus, well losses reflected in the absolute drawdown measured in the pumping well do not affect the calculation.

(b) An example from a USACE project is provided below in Figure 9–11. The well is pumped at 270 gpm (5.2×10^3 ft³/day). Beginning at 5 minutes, the data approximates a straight line. The straight line is extended to determine Δs_{t-t} graphically between 5 and 50 minutes. A *T* of approximately 7,300 ft²/day is calculated using equation 9–14. If the aquifer thickness is known, *K* can be calculated using equation 9–12.

h. Frequency of testing. As described in Chapter 11, pumping tests should be performed on wells at intervals no greater than 5 years.

9–7. Driscoll parameter, L_p

a. If the individual linear well loss coefficients cannot be reliably determined, an apparent efficiency can be estimated using L_p parameter of Driscoll (1986). The L_p parameter represents the ratio of the linear head loss to total head loss (equation 9–18):

$$L_p = \frac{BQ}{BQ + CQ^2} \times 100 \quad (9-18)$$

b. While L_p can be a useful indicator of well performance, it usually overestimates the well efficiency as calculated in equation 9–18. This is due to the inclusion of all the *B* coefficients in the numerator of equation 9–6.

9–8. New relief wells – evaluation of *SC* and *E*

To determine $E_{baseline}$ for new relief wells, the following basic testing and data acquisition are recommended:

a. Conduct a baseline step-drawdown test on each new relief well. Five steps are recommended, but no less than three steps should be used (approximately 8 hours of pumping, assuming 100 minutes per step). Conduct constant rate pumping tests on a small percentage of newly constructed relief wells with measured drawdown in observation wells to estimate aquifer parameters *T* and S_t .

b. From these test data, determine the baseline *E* and/or *SC* of the new wells, depending on the level of instrumentation or observation points around the well system. The baseline *SC* should be calculated using a pumping rate within the design range.

c. Calculate a partial-penetration factor, if applicable.

(1) An example of how much of the measured drawdown is attributable to partial penetration is shown in Table 9–3. The data comes from a 2009 condition assessment of a partial-penetration relief well at the Bolivar Dam project in Huntingdon District (LRH). Table 9–3 indicates that approximately 31% of the total drawdown is attributable to partial penetration as compared to 7% of the well loss. Approximately 58% of the total drawdown is attributed to theoretical aquifer loss while less than 5% is credited to skin effect or linear well loss.

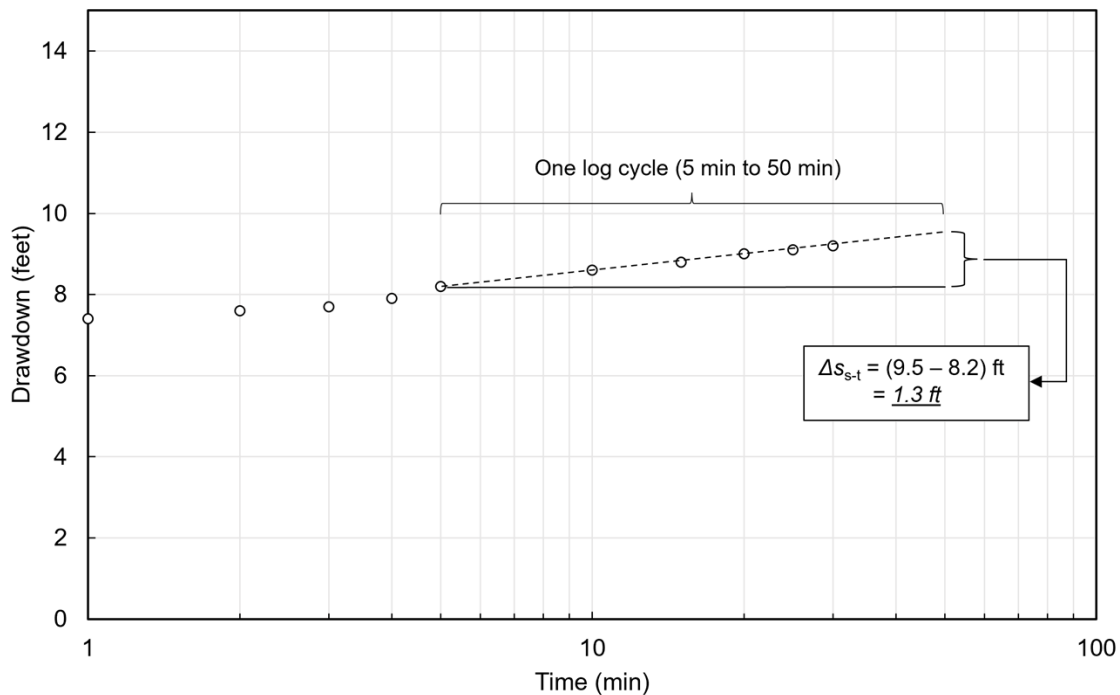


Figure 9–11. An example application of the straight-line method of Cooper and Jacob (1946) and Jacob (1950) to SC data. A value of Δs_{s-t} is determined from the graph and T is then calculated from equation 9–13 (Sid Simpson Flood Protection Project, Beardstown, Illinois)

(2) From this data, three measures of well performance are calculated and included in Table 9–3: L_p , E and a modified efficiency, E_m . The table indicates that the L_p overestimates the condition of the well relative to E . When a modified efficiency (E_m) is defined that includes drawdown attributable to partial penetration, an even lower percentage is calculated. Partial-penetration effects do not reduce E as defined in equation 9–7. However, this example, and the value of E_m , illustrate that partial-penetration wells dramatically underperform relative to full-penetration wells.

Table 9–3
Components of total drawdown of partial-penetration well and efficiency estimation

Head Loss Components (feet)								
Q (gpm)	s_w	s_{pp}	s_a	s_{skin}	s_t	$L_p(\%) = \frac{BQ}{s_t}$	$E(\%) = \frac{s_a}{s_t}$	$E_m(\%) = (s_a + s_{pp})/s_t$
388	0.61	2.69	5.00	0.38	8.64	93	58%	89%
447	1.18	3.11	5.77	0.42	10.06	92	57%	88%
500	1.49	3.88	5.98	0.54	11.35	92	53%	87%
707	2.59	5.34	8.68	0.69	16.61	89	52%	84%
1001	4.67	6.99	12.98	0.85	24.64	85	53%	81%

Note: $B = 0.0208$ ft/gpm; $C = 0.00000381$ ft/gpm²; $BQ = s_a + s_{skin} + s_{pp}$

- d. Calculate SC for each pumping step for each well tested.
- e. Assume laminar flow if the SC measured during the step test is constant as Q increases, assume turbulent flow if the SC decreases as Q increases.
- f. Figure 9–12 shows a plot of log-distance versus drawdown in multiple observation wells. The data was obtained from a pumping test on an 8-inch diameter, full-penetration well installed in beach sands. The Q used during the test, 55 gpm, was determined from a prior short-duration, step-drawdown test. This flow rate ensured the aquifer stayed in the confined condition. The linear trends on the plot can be extrapolated to the pumping well radius. Drawdown in the observation wells is assumed to be unaffected by well losses. The intercept thus provides an estimate of the theoretical drawdown (s_a) in the aquifer. The measured drawdown inside the well is equal to the total head loss (s_t). The values determined from the plot allow calculation of E from equation 9–3. Assuming a 1-foot radius, E varies between 82% and 85%.
- g. Based on Figure 9–12, s_t is 15.5 feet and s_a ranges from 12.8 to 13.2 feet depending on the observation wells used. Using $s_a = 13.2$ in the example below gives:

$$E = \frac{s_a}{s_t} \times 100 = \frac{13.2}{15.5} \times 100 = 85\%$$

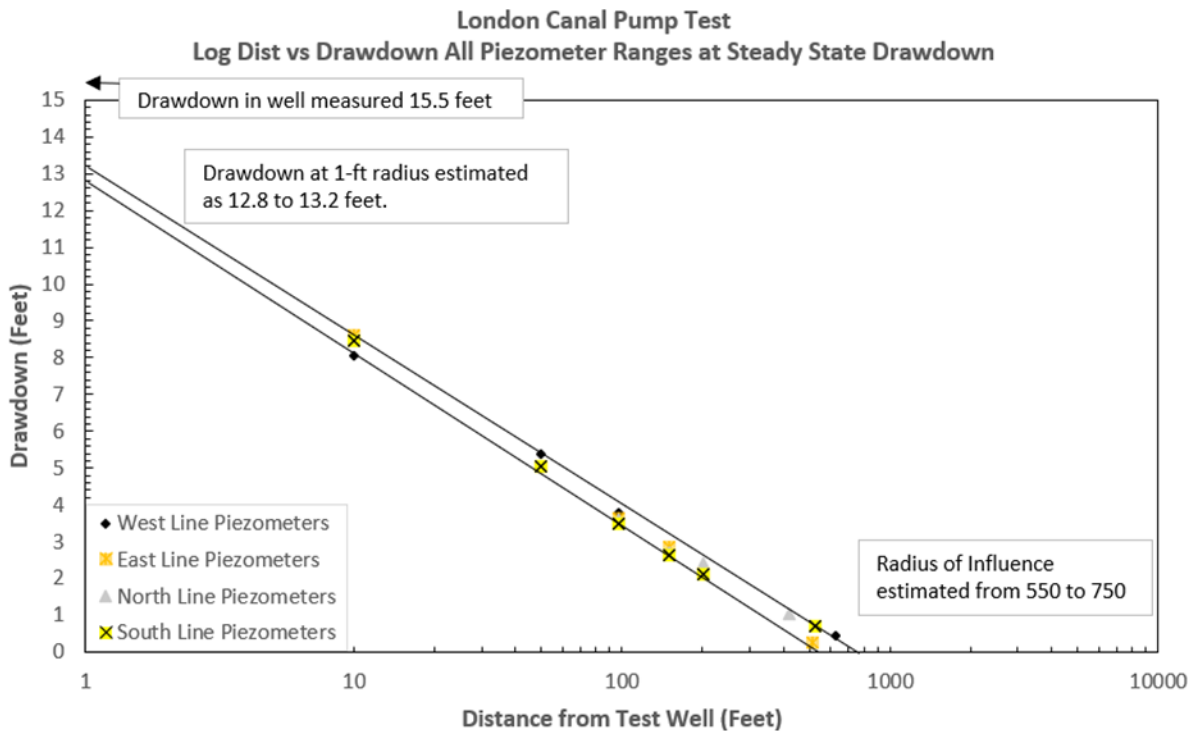


Figure 9–12. Distance versus drawdown plot from a test well

9–9. Existing wells – specific capacity and efficiency evaluation

Evaluation of SC and E for existing relief wells depends on existing testing and performance data. The following items should be considered when evaluating existing relief wells:

a. If no baseline test (installation test) exists for the relief well, conduct step-drawdown tests on a the well to determine E . SCR -based assessment cannot be conducted without reliable baseline data. A simple SCR -based assessment cannot be conducted for a relief well if there is no reliable baseline test (installation test). Step-drawdown tests can be used to determine E without baseline data. A condition assessment based on the calculated E can then serve as a baseline for subsequent tests. The change in SCR can then be monitored over time using constant rate pumping tests at any flow rate from the step-drawdown test. Decreases in E and SCR are proportional over time as shown in Figure 9–4.

b. Within the well array, complete at least one constant rate pumping test with external drawdown measurements for aquifer parameter estimation and pumping test results verification. There should be high confidence that the pumped well is properly developed and performing satisfactorily when executing this recommendation.

c. If installation pumping test data exists for existing relief wells and the relief wells provide the necessary level of pressure relief based on piezometric data or evaluations,

the constant rate pumping test can be used as a reliable proxy for condition assessment.

d. If preliminary testing or past performance indicates the existing relief wells do not provide the necessary level of pressure relief, re-develop the wells. Conduct an additional constant rate pumping test after re-development to determine if the well(s) have been restored to an acceptable level of pressure relief (as estimated by *SCR* or *E*).

e. If the re-developed wells remain deficient, consider performing a step-drawdown pumping test. The data from the pump test will help identify well losses and can assist in diagnosing the source(s) of problems.

f. Based on the results of pumping tests, field observation, and performance history, conduct well rehabilitation suitable for the identified causes of poor performance. See Chapter 11 for further discussion on relief well rehabilitation.

g. If rehabilitation is not successful, abandon or replace the inefficient wells. Abandonment should be conducted according to local regulatory requirements.

h. Wells should be video inspected before and after pump tests and before and after rehabilitation. Video inspection logs should be kept by USACE and the local sponsor for comparison to past and future inspections.

i. Systems with a large number of relief wells may need to focus efforts on a reduced but representative number of wells. See Chapter 11 for discussion on testing of systems with a large number of relief wells.

Chapter 10

Relief Well Collection Systems

10–1. General

Collection systems are designed to safely route relief well discharge away from the structure and prevent accumulation of tailwater above the discharge elevation. Collection systems typically consist of some combination of relief well housings, connector pipes, manholes, collector pipes, outfall pipes, and ditches. The capacity of relief well collection systems should be adequate to transmit the calculated relief well flows from newly constructed wells, without considering future performance losses. The sensitivity of total system flow and the required pipe or pumping capacity to aquifer permeability should be evaluated. When warranted, an additional safety factor may be applied to the calculated relief well flows to ensure that collection system has a low likelihood of being overwhelmed.

10–2. Passive relief well systems

Passive relief well systems do not require any external action for the system to perform as designed. Passive systems do not rely on pumping of well discharge, operation of gates and valves, or any other actions. Flow from passive relief wells is entirely artesian and the flow from the well discharges is gravity flow. Due to their operational simplicity, passive systems should be used whenever possible.

10–3. Active relief well systems

Active relief well systems require operating pump stations, portable pumps, and/or gates and valves. Flow from active relief wells is the result of a combination of pumping and artesian flow. Active relief well systems will not provide their intended pressure relief without operational pumps of adequate capacity. In such cases where pump stations are required to operate active well systems, EM 1110-2-3105 requires considering standby pumping capacity and reliability of the power source.

10–4. Relief well types

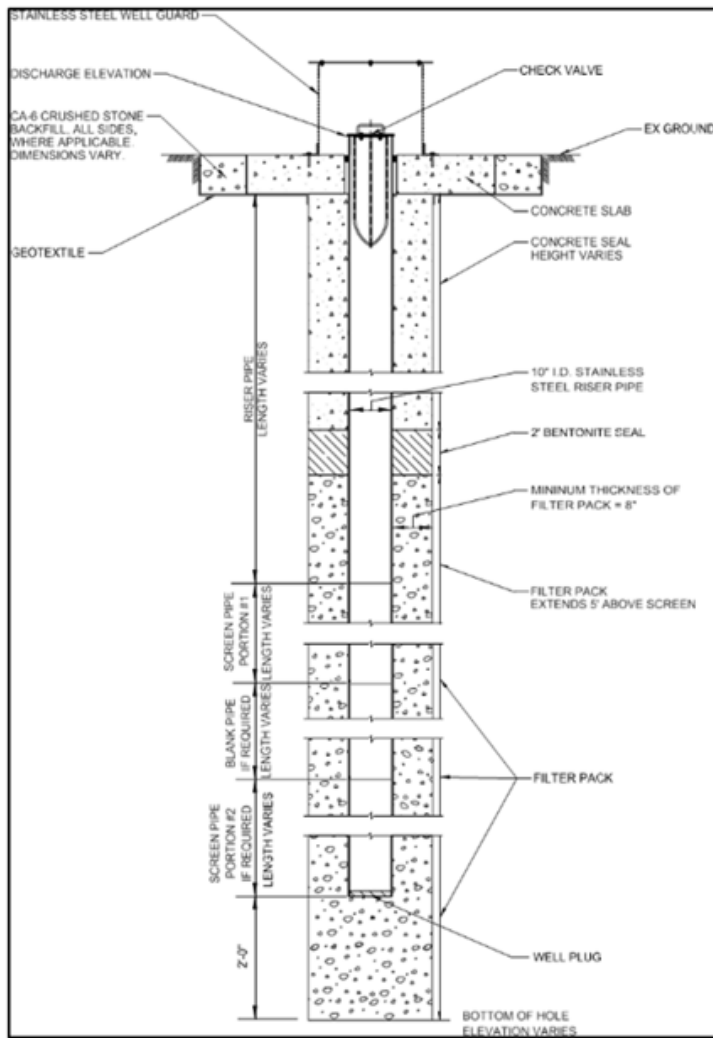
Relief wells can be categorized as either D-type or T-type. The well type depends on the relief well discharge location. D-type relief wells discharge from the top of the well riser at the ground surface. T-type relief wells discharge from a lateral tee extending from the well riser. The tee typically empties into a buried collection system or leads to a surface discharge point at an elevation below the well riser.

a. D-type relief wells. D-type relief wells discharge flow to the natural landside surface exit and are common for long, linear relief well systems. These well systems often drain to a collection ditch. Figure 10–1 shows an example of a reach of D-type relief wells at the landside toe of a levee segment. Figure 10–2(a) shows a typical design detail for a D-type relief well.

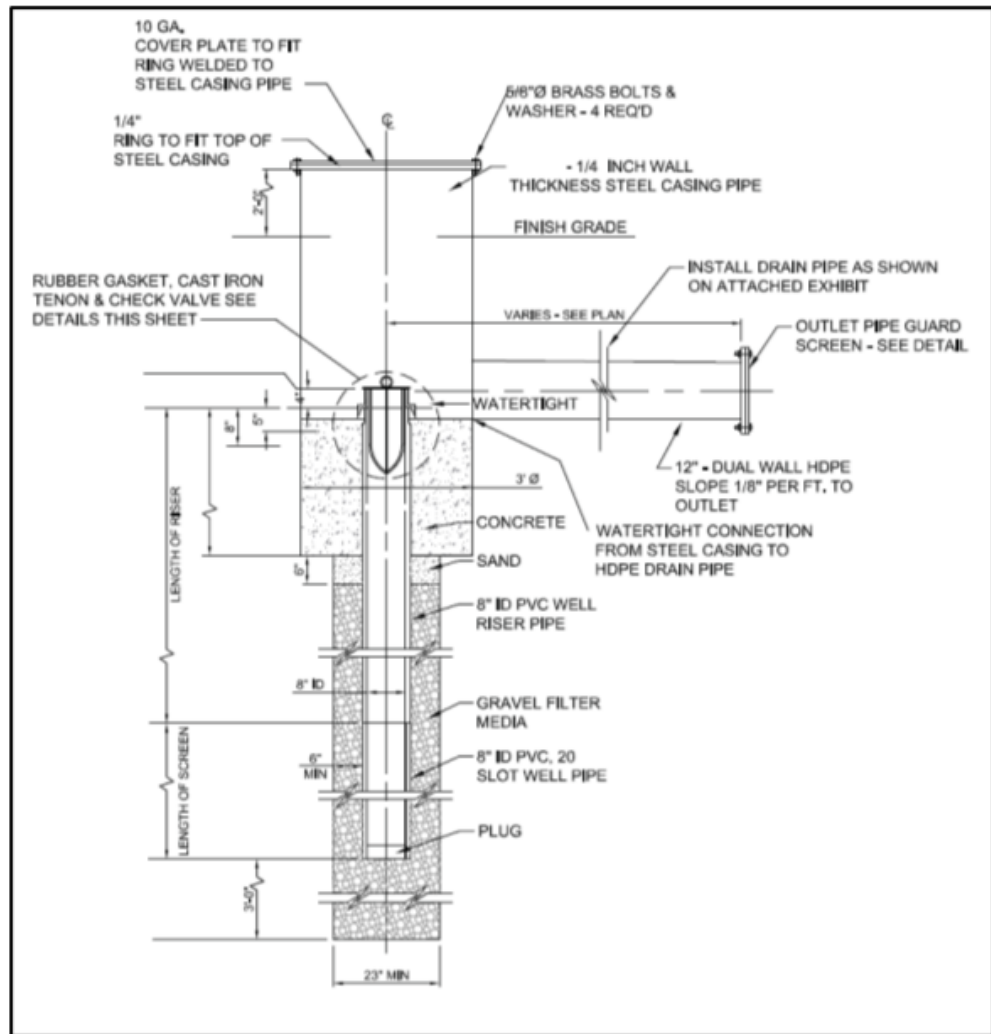
b. *T-type relief wells.* T-type relief wells discharge at a design elevation, usually below the ground surface. These wells are common at projects where a natural landside exit may be too high to adequately relieve pressures. For T-type relief well systems, the well outlets often exit horizontally through a wall or cut-slope feature, or into a buried collection system. Figure 10–2(b) and Figure 10–3 show a detail and example of a T-type relief well, respectively.



Figure 10–1. D-type relief well reach (photo courtesy of Memphis District)



(a)



(b)

Figure 10-2. Typical relief well components for (a) D-type and (b) T-type



**Figure 10–3. T-type relief well (South River Drainage District)
(photo courtesy of Rock Island District)**

10–5. Below-grade discharge

Below-grade discharge is required if seepage cannot be permitted to exit at the landside ground surface of the structure. Below-grade discharge may also be required to achieve an acceptable design where a very thin top stratum (confining blanket) exists. Below-grade discharge may be assumed for a passive system design if there is gravity drainage away from the wells. In this case, pumping is not required to prevent water from pooling above the well discharge points. Below-grade discharge is transmitted through a system of relief well collector pipes to the eventual exit or collection point. Head losses in the collection system should be evaluated to ensure that the relief well discharge elevations are maintained.

10–6. Relief well collector ditches

If relief well discharge is collected in open ditches, the vertical gradient through the bottom of the ditch must be evaluated. Generally, the ditch should be assumed to be in a dry condition. This assumption is not required if there is a high assurance that water will always be held in the ditch. Water can be held in ditches through a system of weirs, wet wells, pump shutoffs, etc. If ditches are lined with concrete, designers should consider impacts of the ditch being impermeable. Impermeable (concrete) ditches may require features such as weep holes to mitigate build-up of hydrostatic pressures. When designing these features, the potential for weep holes to act as initiation points for internal erosion should be carefully evaluated.

10-7. Tailwater

Tailwater elevation is an important consideration in designing the collection system. A relief well collection system should be designed such that tailwater does not pond above the relief well discharge elevation or cause backup water in the well. Figure 10-4 shows examples of water backup in vertically and horizontally discharging wells. Pooling of tailwater above relief well discharge point may reduce the effectiveness of the well. Consistent ponding above the relief well outlet elevation may lead to siltation of the relief well and/or collector pipes. Pipe used in the collection system should be sized correctly to reduce backflow and avoid pressurization. Pipe design should ensure positive drainage.



Figure 10-4. Example of backup water in the housing (left) and full outlet pipe (right)

10-8. Relief well housing

Relief wells should be permanently protected by an individual housing. Relief well housings should be adequately secured to deter vandalism, but readily removable if needed for monitoring flows during flood events. For wells discharging at ground surface, the tops of the wells should be provided with a metal screen. Details of a conventional metal well housing are shown in Figure 10-2(a) and Figure 10-2(b) for D-type and T-type relief wells, respectively. A suitable alternative consists of a section of stainless-steel, wire-wound screen.

a. Housing materials. Alternative housing materials include corrugated metal pipes, concrete, HDPE (high-density polyethylene), and wire mesh. In some instances, T-type relief wells are constructed where the top of the riser pipe is more than 5 feet below ground. In such cases, the depth and diameter of the well housing must be designed to ensure safe access to the well head. Note that head loss associated with the outlet elevation of D-type wells must be considered in the evaluation of H_w .

b. Sizing of housing. Housing for the wells should be adequately sized to minimize water elevation in the riser pipe. Housings and outlets should be designed to minimize

maintenance and protect against contamination and/or siltation from backflooding, damage from floating debris, and vandalism.

c. *Flooding of housing.* Where the well riser is located below the ground surface, the housing should be designed to avoid flooding. In such cases, flooding of the housing prevents water from exiting the well at the elevation of the riser. This reduces the pressure relief benefits of the wells.

10–9. Collector pipes

Collector pipes transmit combined seepage flow from connected relief wells to the system's downstream outlet pipe(s). Depending on the number of relief wells and their locations relative to tailwater, there may be a network of interconnected collector pipes. Like toe and trench drain systems, collector pipes must be capable of discharging significant quantities of seepage flow quickly and without overwhelming the system with excess seepage forces and hydrostatic pressure (Cedergren 1989). EM 1110-2-2902 allows any viable pipe material for use as relief well collectors. Specific materials may be required depending on operating environment.

a. *Pipe design.* Collector pipes should be designed as non-pressurized pipes with relief well discharge entering the collector pipe at an elevation higher than the assumed maximum flow elevation. The pipes should be constructed to avoid deflections, displacement of joints, and/or breakages. An example of a relief well collector system is shown in Figure 10–5.

b. *Sizing of collector pipe.*

(1) Several factors must be considered when sizing relief well collector pipes, such as expected relief well discharge flows and pipe foundation conditions. Uncertainties in aquifer permeability and pipe foundation material strength and consistency are critical components of collector pipe sizing. In general, relief well collector pipes should be sized such that the depth of water in the pipe is no more than 50% of the inside diameter of the pipe for the maximum expected discharge flow where site conditions are well understood.

(2) Where aquifer permeability is not well understood, or uncertainty is not clearly accounted for in relief well design flow computations, it may be practical to reduce the maximum flow depth to 25 to 33% of the inside diameter of the pipe for maximum discharge. Where collector pipes are to be founded on soft or highly heterogeneous soils susceptible to differential settlement, a maximum flow depth of 25% of the inside diameter of the pipe for maximum discharge conditions may be practical to account for pipe sagging. As with all designs, the feasibility of implementing these recommendations should be considered on a case-by-case basis, accounting for cost, constructability, and the degree of redundancy provided.

c. *Collector pipe accessibility.* Relief well collector systems should be designed such that inspection and maintenance of long reaches of collector pipe is possible. A minimum collector pipe inside diameter of 8 inches is recommended for all applications

to allow for commonly available video inspection methods such as remotely operated vehicles. Collector pipes should be designed such that manholes and/or cleanout locations are located no more than 300 feet apart to facilitate maintenance and inspection (EM 1110-2-1902).

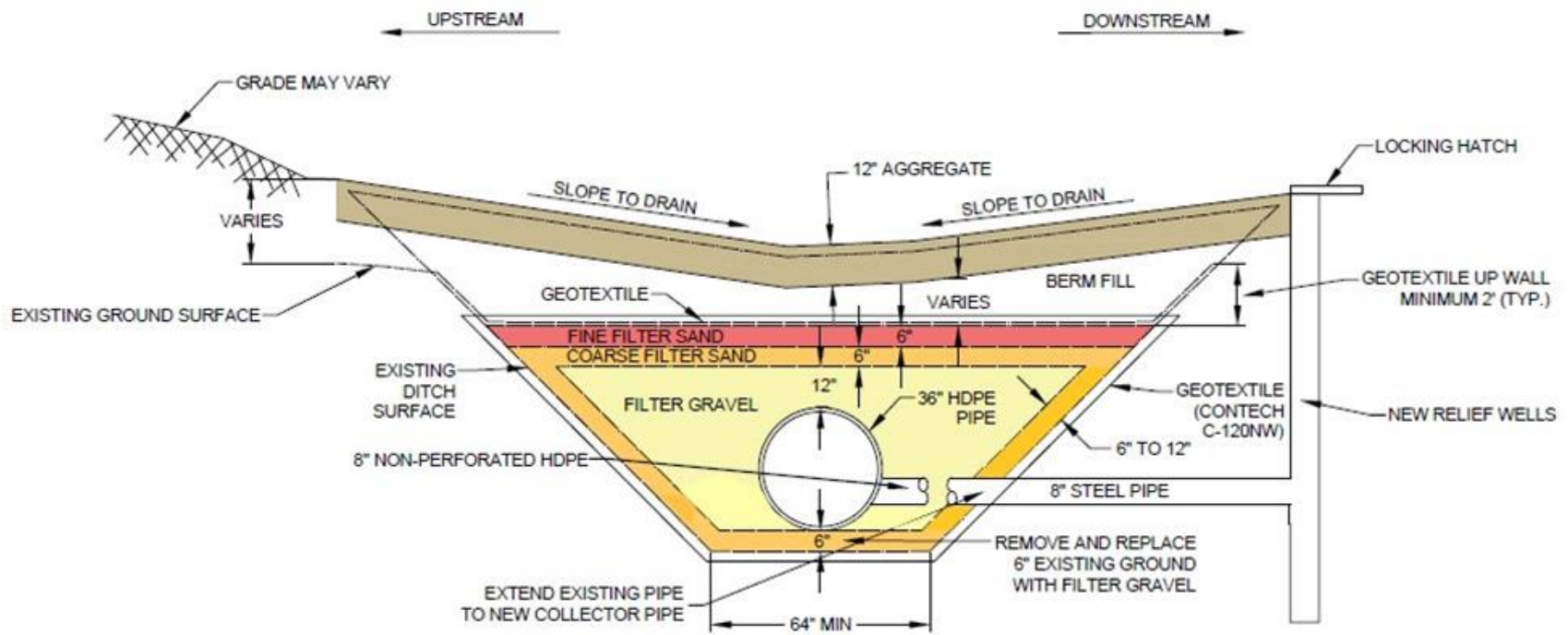


Figure 10-5. Example of relief well collector pipe system

d. Collector pipe performance observation.

(1) Collector pipe performance is a critical aspect of overall relief well system performance. Collector pipe function should be observed, where possible, for both new and existing systems. Flow measurements from within the collector pipe and at the exit of the outlet pipe(s) help determine if collector pipes are functioning properly. Flow can be measured in the collector pipe at various locations by using a flowmeter, measuring flow depth, or with in-line flumes. Flow can be measured at the outlet pipe exit by using horizontal pipe discharge methods. The measured flow can be compared to design flows to determine if the well system is collectively flowing as expected. Flow measurements should occur, at minimum, during high-water events.

(2) If flows are less than expected, potential causes typically include undersized piping, pipe deformation, sedimentation, or higher than expected tailwater over the system discharge. Sedimentation can be related to several issues. The most critical of these are defects in relief well components or the collector pipe, which allow infiltration of foundation material. However, sedimentation can also occur when outlet pipes become inundated because of animals or for other reasons. Overall risk associated with collector pipe performance related PFMs and required operation and maintenance activities are further described in EM 1110-2-2902.

10–10. Check valves

Check valves prevent contamination of the well screen from surface water, grass clippings, etc., that can cause a decrease in well performance. They also control backflooding, which can significantly affect well efficiency. Flat-type check valves constructed of aluminum are recommended for surface discharge applications, as shown in Figure 10–6. The check valve is supported by a soft rubber gasket that fits snugly over the top of the riser or cast iron tenon. Alternate styles of check valves may be used. Alternate styles of check valves should be appropriate for the application and should be field tested. One example is shown in Figure 10–7, where a low-profile, high strength well head is used with horizontal check valves for a navigation lock floor application.

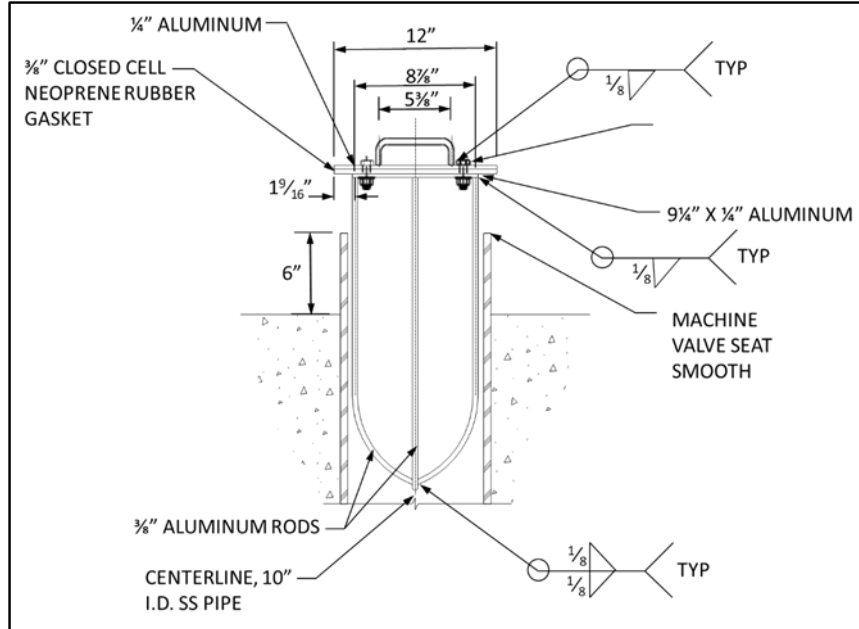


Figure 10-6. Typical detail of well top and check valve for D-type well

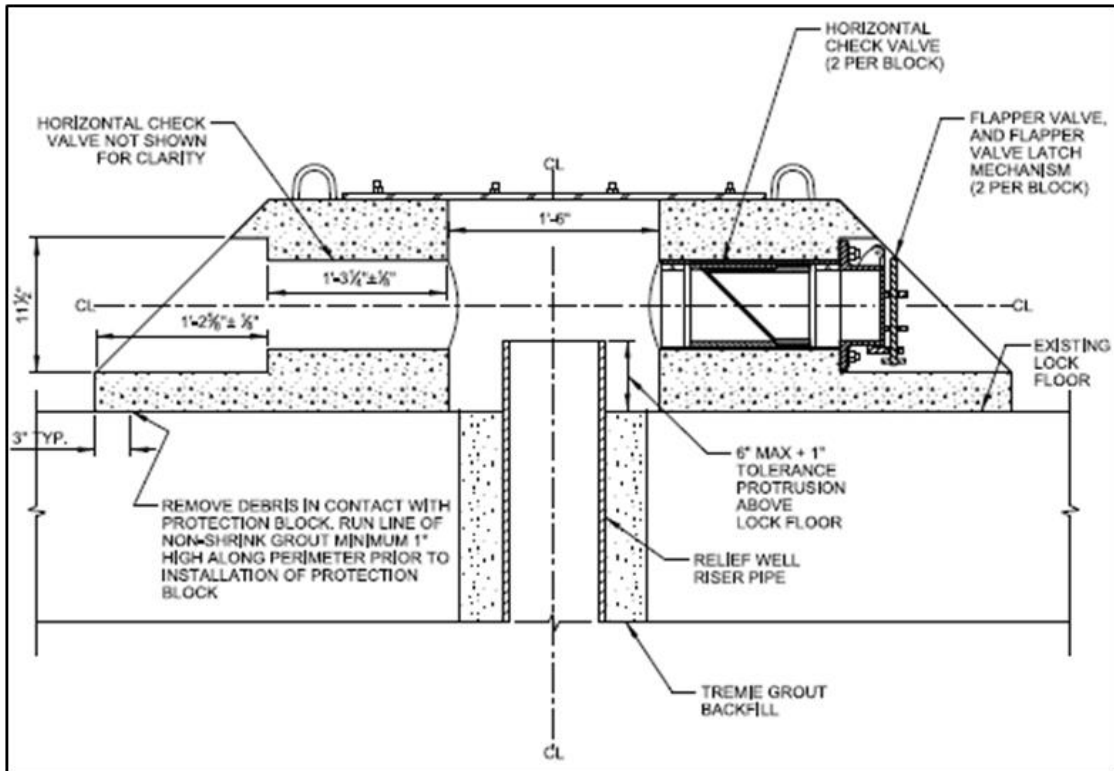


Figure 10-7. Detail of well top, check valve, and outlet for navigation lock application (from Lock and Dam No. 18, USACE Rock Island District)

10–11. Outlet pipe

The outlet pipe transports water from the collector pipes to the tailwater. The pipe should be designed to reduce the influence of tailwater and debris. A guard screen consisting of a wire mesh with 1-inch-square openings may be installed at the end of the outlet pipe. Outlet pipes should be protected against corrosion. A flat-type check valve should be installed on the well riser with a flap gate on the end of the horizontal pipe.

10–12. Standpipes

Relief wells installed to control underseepage at levees may cause excess seepage flow at relatively low river stages. The additional seepage may be considered a nuisance, especially in agricultural areas. As a compromise between designers and stakeholders, wells can be provided with a plastic sleeve, called a standpipe, that is typically 1.0 or 1.5 feet in length. This will raise the discharge elevation of the well accordingly. The sleeves prevent well flow at low river stages when no pressure relief is necessary. At higher river stages, or when substratum pressures become elevated, water may begin to spill over the top of the standpipes. When this occurs, or there are signs of distress surrounding the well, the sleeves must be removed so that the wells can function as intended. The project operation and maintenance manual should contain appropriate guidance if standpipes are used.

10–13. Inspections

Procedures to inspect and maintain pipes, including relief well collectors, can be found in EM 1110-2-2902. Newly constructed collector systems should be fully inspected to evaluate and develop baseline structural condition of the system. This includes deformation of the pipe walls, condition of joints and pipe walls, breakages, separations, etc. Existing systems should also be camera inspected at intervals no less than every 5 years.

10–14. Maintenance

Relief well collection systems deteriorate with time. However, routine maintenance can extend the life of the system. The most common maintenance activity is removal of debris. Less frequent maintenance includes pipe repairs, pipe lining, and/or pipe replacement. Ensuring that collector system outlets remain unobstructed by vegetation or other encroachments aids in reducing likelihood of debris buildup and pipe damage.

10–15. Ice removal

In cold regions or extreme cold weather, ice can form in the collection system. The ice buildup could reduce the system capacity. Frost jacking could also be problematic. Steam, hot water flushing, and electric heaters are methods for removing ice from pipes or gate structures. EM 1110-2-2902 provides additional details on ice removal.

10–16. Groundwater contamination

Relief wells may be proposed in areas where groundwater contamination is present or believed to be present. Relief well discharge may need to be treated before being discharged into the environment. All applicable state and federal laws should be followed.

Chapter 11

Operation and Maintenance for Well Systems

11–1. General maintenance

a. Well maintenance is necessary to ensure relief wells function as designed. It cannot be overemphasized that such maintenance is far preferable to, and less costly than, well replacement. Routine maintenance should include prompt removal of any trash or obstruction that may have entered the well or well guard. Sand or other material that may have accumulated in and around well discharge areas should be removed. Outfall ditches, bank slopes, or berms should be properly maintained in a free-flowing condition. The area around the well should be kept free from weeds, trash, and debris. Mowing and weed spraying should include the area immediately around the wells and a radius of at least 5 feet outward. The ground should be maintained to allow inspecting and servicing the well.

b. The different types of inspections performed on relief wells are discussed in paragraph 11–4. Pumping tests are generally recommended at 5-year intervals to evaluate well performance, as described in paragraph 11–5.

11–2. Applicable regulations

ER 1110-2-1942 describes the inspection, monitoring, and maintenance of relief wells. Other regulations may apply to relief wells depending on their application. ER 1110-2-1156 describes continuing evaluation inspections for USACE dams. EC 1165-2-218 or its successor regulation describes evaluations and inspections at USACE levees.

11–3. Records

Records should be kept of all inspections, maintenance, and rehabilitation performed on a relief well. The records also should include all pumping test data, well flows, and relevant piezometric data. Records management requirements are described in paragraph 1–4.

11–4. Inspections

There are several types of inspections.

a. *Scheduled.* The first group type includes scheduled inspections, which are required at recurring intervals. This includes inspections performed by multi-disciplinary teams and described in applicable regulations (see paragraph 11–4a(1)). Another type of inspection is frequent, less formal, and performed by the operational staff responsible for the project (see paragraph 11–4a(2)). Scheduled inspections also include data collection during normal water (see paragraph 11–4a(3)).

(1) *Scheduled inspections.* These are recurrent engineering inspections of structures or features whose failure or partial failure could have major consequences.

These impacts include jeopardizing the operational integrity of the project, endangering the lives and safety of the public, or substantial property damage. These inspections are typically performed at 5-year intervals in conjunction with pumping tests (described below). Downhole video inspections of relief wells are also recommended at 5-year intervals.

(2) *Operational inspections.* Relief wells that flow continuously should be inspected weekly. Wet spots on the ground around the wells and structures should be noted. Also of interest is evidence of sloughing or piping, or indications of discharge of sand or other materials from the wells. Signs of vandalism, theft, damage, or unauthorized use of the wells also should be noted. Valves, gaskets, well guards, cover plates, flap gates on tee outlets, and other appurtenances all should be regularly inspected. Malfunctioning or damaged items should be repaired or replaced.

(3) *Normal water data collection.* Reading instruments such as piezometers and flow monitors should be performed at intervals commensurate with the loading on the structure. Piezometric levels and flow quantities should be measured at least annually. These parameters are often measured more frequently for actively flowing relief well systems. All relief wells should be sounded at least annually to determine if sand or other material has accumulated in the well. Where relief wells penetrate two or more aquifers, piezometric levels should be monitored in all aquifers. For such cases, flow at various depths also should be measured if possible. Normal water data should be collected before high-water seasons.

b. Unscheduled. The second group type includes unscheduled inspections. These may be required after a flood event, seismic event, or because of vandalism or other unexpected damage to wells. Unscheduled inspections may or may not be described in applicable regulations. However, all requirements, flood levels, or other events that trigger unscheduled inspections should be included in the project's operation and maintenance manual. Unscheduled inspections should follow the same procedures used for scheduled inspections. Some relief wells are in locations where inspections are difficult to perform and cannot be inspected on a typical inspection cycle (see paragraph 11-4b(2)).

(1) *High-water data collection.* Piezometric levels and relief well flow quantities should be measured more frequently during high-river or reservoir events. These measurements should be made before, during, and after the water peak and continue until the water returns to normal levels. Relief wells should be sounded periodically throughout the high water, especially if sudden changes in piezometric levels or relief well flows are observed. High-water data activities may suggest that out-of-cycle testing of relief wells is required based on piezometric level measurements or flow quantities taken during the high-water event. Tailwater changes during high-water events should be noted, as they will affect piezometric levels and relief well flows.

(2) *Inspection in relatively inaccessible locations.* Wells in relatively inaccessible locations cannot be inspected as frequently as other wells. Such wells typically include those installed for special cases (such as dewatering) where the well outlets are below

a normally elevated water surface. Examples are wells located in stilling basins and navigation lock chambers. These wells should be inspected whenever the structure is dewatered, for a general maintenance inspection, or when there are signs of decreased performance as described in paragraph 11–4a.

11–5. Pump testing of relief wells

All relief wells should be pump-tested every 5 years. However, some exceptions may be considered, as noted in paragraph 11–5b. The tests should be performed using procedures described in Chapter 9 to determine a well’s *SCR*, efficiency, or change in the entrance head loss (H_e). Best practice is to perform pumping tests under similar pool, tailwater, and flow conditions to any prior tests in the same wells. In this way, results from different tests on the same well(s) can be directly compared and the *SCR* is more reliable. The amount of sediment in the wells should be measured before and after pumping tests. Wells requiring sediment removal should be cleaned prior to pump testing. If sediment in wells has suddenly increased, there may be defects in the riser or well screen, as described in paragraph 11–6d.

a. Well performance over time. Pumping tests are a direct measure of relief well performance. Performance often decreases with time because of biofouling, mineral encrustation, and other factors that increase well head losses. If pumping tests indicate that the performance is less than assumed during design, the evaluation methods described in paragraph 11–7a should be conducted. The results of the evaluation may indicate the need for well rehabilitation. If rehabilitation is unsuccessful in restoring wells to their design performance level, abandoning and replacing the wells may be required.

b. Less frequent testing. Scenarios where relief wells may not require pumping tests every 5 years include the following:

(1) Wells where recent flow and surrounding piezometer data indicate the well system is meeting performance goals. That is, mid-well head and well flow data from realized flood conditions can be extrapolated to the design condition and adequately assessed.

(2) Inaccessible wells, such as those that can be tested only when a structure is dewatered (see paragraph 11–4b(2)). Not testing inaccessible wells may be justified, particularly if such wells are performing satisfactorily. Piezometers are often used in these situations for critical structures.

(3) The following paragraphs discuss systems with a large numbers of relief wells.

(a) Testing in large systems can potentially be reduced by designating “test wells” within typical reaches of the well system. All wells in the system will have initial baseline pumping tests performed, but subsequent pumping tests to monitor well condition will only be performed on the test wells. Test wells should be selected to ensure adequate coverage of the well systems. The selected wells should allow observation of a general decline in well performance of the system, or portions of the system. For example, test

wells should not be separated to the degree that poor performance of several adjacent wells would be undetected.

(b) In addition, test wells should not be separated by more than two wells that are not routinely tested. A sensitivity analysis should be conducted to determine if using test wells is acceptable and, if so, the appropriate spacing. Typically, the test well approach is difficult to justify in systems of less than 20 wells. Performance of the untested wells is less certain when employing the test well approach rather than testing every well. This increased uncertainty must be accounted for when making risk-informed decisions associated with the relief well system.

(4) *Stabilized wells.*

(a) When wells experience screen/riser damage, often a replacement well cannot be installed immediately. In those instances, the damaged well can be stabilized but still allow some pressure relief by installing a smaller diameter screen and a filter pack between the smaller diameter screen and the original screen, or simply filling the wells with filter pack with a perforated cap placed over the riser. The stabilized wells with a smaller screen usually cannot be pump tested because of the small screen diameter, but they can be visually inspected with downhole video. If an entire well system is being replaced, the original well system can be stabilized as an alternative to abandonment.

(b) Although the new well system would not be designed with consideration of the pressure relief still provided by the stabilized system, the stabilized wells provide some redundancy to the new well system. One concern with stabilized wells is their existence can complicate back-analysis of well system performance based on piezometric data, because the stabilized wells will be difficult to account for in most modeling methods as they will have an unknown E or SCR .

11-6. Evaluation

A number of metrics can be used to evaluate the condition of relief wells. Observations discussed in the following paragraphs may indicate the need for well rejuvenation or further assessment of the relief well system.

a. *Decrease in measured well performance.*

(1) Replacement costs generally outweigh maintenance costs over the lifetime of a typical well. Therefore, timely maintenance that prevents a decline in well performance is a cost-effective strategy (Williams 1985). SCR is the most common method used by USACE to evaluate well performance, but well efficiency, E , can also be used. Both methods, and the relative merits of each, are described in detail in Chapter 9. Historically, USACE has considered an SCR of 80% or less as an indication that well rejuvenation should be completed. Other indicators of the need for well rejuvenation can be used. These include a well efficiency loss of 20% relative to the baseline efficiency.

(2) An additional criterion is if well losses cause drawdown in a pumping test to be 20% less than the design value. Exceptions to these general rules are projects with

alternative criteria contained in design or operation and maintenance documentation. Underperforming wells should be further assessed to determine the cause(s) and the proper corrective action(s).

b. Decreases in well flow or increases in piezometric levels.

(1) Well discharges can be measured with flow meters in individual wells, in flumes at collection locations of multiple wells, or can be estimated by the height of the water column above the riser (Chapter 7). A reduction in relief well discharge accompanied by an increase in piezometric levels generally indicates clogging or obstruction of the wells. Clogging or obstruction requires immediate remedial action if projected piezometric levels are above design intent. Other trends in well flow and piezometric levels may be unrelated to the well condition but still problematic.

(2) One such trend is a reduction in well discharge accompanied by a fall in piezometric levels in downstream areas. The cause could be siltation in the reservoir, riverbed areas, or riverside borrow pits. This situation is a favorable condition, as it indicates less seepage. However, another cause could be erosion or excavation of an impervious top stratum at a point downstream of the line of wells. This unfavorable condition permits the unfiltered exit of seepage and increases the potential for piping.

c. Extrapolation to design loading. Measured piezometric levels and relief well flows can be extrapolated to predict the values at the maximum design reservoir or river elevation. Predicted piezometric levels should be compared to those for which the structure was designed. If the predicted levels are above design values, it may be a sign that well rejuvenation is necessary. If available, piezometric levels can be used to evaluate well systems if operation and maintenance records, including pumping test results, are unavailable.

d. Sediment influx. Excess sediment in a relief well may indicate defects in the riser or well screen. The well defects may be serving as a conduit for removal of foundation material. Wells should be sounded at least annually as part of normal water inspections (see paragraph 11–4b(1)) to determine if sand or other material has accumulated in the well. However, sounding of wells can also be done on an ad hoc basis to assess well condition if there are other indications of reduced performance.

e. Video inspection. Downhole video inspections are a valuable tool for assessing and documenting well screen and riser pipe condition (see Figure 11–1). Video can be used to establish riser length, screen elevations, and the location of any blank sections for wells that are missing critical installation information.

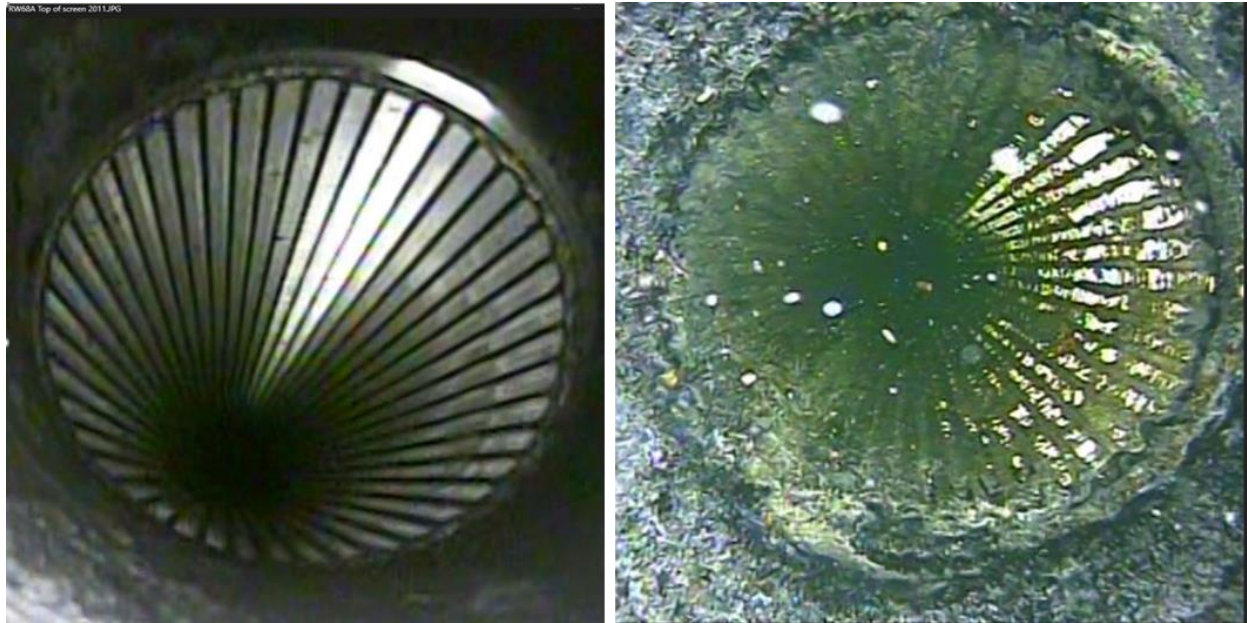


Figure 11–1. Example images from video inspections performed on RW 68A, Milford Dam, Junction City, Kansas. Both images are from the location of the same screen-riser joint. The 2011 image (left) was obtained immediately after well rejuvenation, as indicated by a visibly clean screen. The 2020 image (right) was obtained prior to well rejuvenation, and shows the well screen blocked by biofouling.

(1) *Purpose of video inspections.* Video assessment of all relief wells is recommended every 5 years as part of scheduled inspections (see paragraph 11–4a(1)). Often, downhole video inspections are conducted along with pump-testing of relief wells, which also is required at 5-year intervals. However, video inspections can also be done on an ad hoc basis to assess well condition if there are other indications of reduced performance. Results of a video inspection may indicate the need for pump testing if performed out-of-cycle with scheduled pump testing.

(2) *Video procedures.* The camera should be advanced slowly to minimize sidewall disturbance and enhance visibility. Rapid camera descent may cause the camera view to be blurry due to induced turbidity from sudden displacement of still water. A typical video session will likely take 30 to 60 minutes for each well. The camera should not be allowed to descend into sediment at the bottom of the well. During video inspection, any outfall pipes or collector systems should also be video inspected as described in EM 1110-2-2902 to ensure the well flows can be adequately conveyed.

f. Inclinator readings. Inclinatorometers in the vicinity of wells can provide information on the condition of the wells. Any horizontal movement of the foundation could potentially disrupt well screens or risers. Such movement warrants downhole video inspection to determine if the well is damaged and requires repair.

g. Wells without operation and maintenance records.

(1) Some existing well systems have little or no operation and maintenance records or pumping test results available. The evaluation of well systems without records are more uncertain than properly documented well systems. If there are no design or construction records indicating well depths or screened intervals, well soundings and camera inspections can be used to determine this information.

(2) More complex pumping tests and analysis combined with piezometric and well flow data during high-water events reduce uncertainty of future performance. Absent initial pumping test data, a step-drawdown test can be used to determine well efficiency, E , as described in Chapter 9. Analyses described in Chapters 5 and 6 calculate piezometric head at critical locations, which are adjusted to account for well head loss using methods in Chapter 7.

(3) An estimate of efficiency determined from performance during high-water events and/or pumping tests is used to reduce the benefit of the relief well system. Appendix I includes examples of common approaches to increase head loss by decreasing either drawdown or well flow to include the deterioration of well performance that occurs over time. Example 6 in Appendix J compares the calculated safety factor including the measured efficiency to the original design safety factor for an evaluation of expected well system performance under design loading.

11–7. Causes for decreased well performance over time

a. Mechanical. Relief wells can undergo some loss in performance due to the slow movement of foundation fines into the filter pack. These fines reduce the permeability of the filter pack. The process occurs most commonly in wells with poorly designed or improperly placed filter packs, improper screen selection, or insufficient well development. Backflooding of muddy surface waters can also clog the well and surrounding filter pack. Check valves should be installed at the well outlet to prevent backflooding. However, these valves may not function as intended if not properly designed and maintained.

b. Chemical. Mineral encrustation of the well screen, filter pack, and surrounding formation soils is a major cause of reduced well performance. Mineral precipitates forming within the screen openings reduce their effective open area and cause increased head loss. Deposits in the filter pack and surrounding soils reduce their permeability and increase head losses. Precipitation of minerals in groundwater is determined chiefly by water chemistry. The type and amount of dissolved minerals and gases in water entering the well determine if mineral encrustation occurs. The major forms of mineral encrustation include: (1) calcium and magnesium carbonates or their sulfates, and (2) iron and manganese minerals, primarily their hydroxides or hydrated oxides.

(1) *Causes of carbonate encrustations.* Two factors determine whether calcium carbonate will stay dissolved in water. The first is the concentration of dissolved

calcium, which cannot be too high. The second is the partial pressure of CO₂, which cannot be too low. A pressure reduction occurs as a well discharges from a confined aquifer. As CO₂ is released from the water as gas, some of the calcium carbonate will precipitate. Magnesium carbonate may precipitate from magnesium-rich groundwater in the same manner. The precipitation tends to be concentrated at the well screen and surrounding filter pack, where the maximum pressure reduction occurs. Generally, encrustation from this mechanism is not a problem in relief wells. This is because it occurs only when a well is flowing and at high levels of calcium and/or magnesium carbonate concentration.

(2) *Causes of iron and manganese encrustations.* Many acidic and/or anoxic groundwaters contain dissolved iron and manganese. Well flow can cause pressure changes, resulting in loss of CO₂ and an elevation in pH. Disturbances can oxygenate groundwater, increasing oxidation-reduction (Eh) potential. Increased pH or Eh can lead to deposition of insoluble iron and manganese hydroxides. The hydroxides initially have the consistency of a gel but eventually harden into scale deposits. Depending on the extent of oxygenation, ferrous, ferric, or manganese oxides can precipitate. Ferric oxide is a reddish-brown deposit like rust, whereas the ferrous oxide has the consistency of black sludge. Manganese oxide is usually black or dark brown in color. The iron and manganese deposits are usually found with calcium carbonate and magnesium carbonate scale.

c. *Biological encrustation.* Iron bacteria are a major and costly source of well screen and filter pack contamination (“biofouling”). These organisms thrive by assimilating or dissimilating iron, cycling ferric, and ferrous iron between dissolved and precipitated phases. Rapid growth of the bacteria and iron precipitation can quickly reduce well performance.

(1) *Identification.* Brownish, red, or orange stains usually indicate the presence of iron bacteria in well collector pipes or ditches. Odors are variously described as sulfurous, swampy, oily, or musty, or smelling like rotten vegetables. The deposits can appear as sticky brown, yellow, or grey slime, or sometimes as filamentous growths (Minnesota Department of Health [MDOH] 2021). Video and photographic surveys can pinpoint the locations of screen encrustations. Samples of the encrustations can be obtained using a small bucket-shaped container. Many states have a drinking-water laboratory as part of their Department of Environmental Quality (DEQ), EPA, or Department of Health (DoH) that can analyze these samples for identification. Some private firms familiar with iron bacteria can also provide this service. Correct identification may assist in the selection of a more effective treatment method.

(2) *Minimization.* Biofouling of wells occurs because of iron bacteria that occur naturally in the groundwater. For this reason, disinfection of downhole tools is not necessary at every relief well location. As discussed in Chapter 8, disinfection may be appropriate to kill coliform bacteria in cases where an aquifer is a known drinking water source. Disinfection is best done with a chlorine solution (200 ppm).

11–8. Rehabilitation

If significant reductions in well performance are noted, rehabilitation of the well is needed. A wide range of mechanical, chemical, and heat treatments have been used with mixed success. The preferred approach is to start with mechanical treatment and then progress to more rigorous methods if needed. Chemical treatment is most effective when combined with mechanical treatment. The mechanical forcing of water and chemicals through the screen maximizes the area and volume of material that is affected. More information on treatment of water wells can be found in Driscoll (1986), Houben and Treskatis (2007), and Smith (1998–2015).

a. State regulations. State regulations for water wells are tailored to drinking or potable water supply wells. However, chemical treatments used for relief wells may be subject to various state requirements. This may require National Sanitation Foundation (NSF International) or equivalent approval for any chemicals used. Purge water treatment and disposal may also be regulated (Smith 1998–2015). Prior to treating any well, check with the state DoH, EPA, or DEQ. These state agencies continually update their websites with information pertinent to well treatment.

b. Forms. All data generated during the treatment and subsequent pump test should be recorded on forms. As mentioned in paragraph 11–3, records management requirements are described in paragraph 1–4.

c. Mechanical treatment. Mechanical redevelopment should be the first step in well rejuvenation. This process is the same as that used to develop a new well (see Chapter 8). Air lifting, surging, horizontal jetting devices, and brushing are among the available methods. Overpumping or pumping the well at the highest rate attainable is also generally advantageous. These methods normally do not induce high pore pressure in the foundation that could result in hydraulic fracturing described in paragraph 8–4d(6). The engineer must consider ER 1110-1-1807 prior to rehabilitating or rejuvenating the relief well. Hydraulic fracturing calculations and a DIPP are required for any activities that could potentially increase pore pressure in the foundation.

d. Chemical treatments.

(1) Used to disinfect wells since the 19th century (Smith 1998–2015), chlorine is the most common chemical used to treat water wells (MDOH 2021). A range of chemical treatments in addition to chlorine have been used to clean wells since the end of World War II. During this period, using chlorination to treat wells has become more restrictive in parts of North America. Due to this, and because shock chlorination is seldom the most effective biofouling control treatment, other forms of treatment may be appropriate in many cases (Smith 1998–2015).

(2) Relief wells are not drinking water wells. However, many of the chemical treatments described below have been developed for rejuvenating drinking water wells. The following sections discuss a variety of chemical treatment options. Regardless of

the treatment used, chemicals should always be applied with a physical process to push them from the well bore into the aquifer.

(a) *Chlorine*. The most common chemical used to treat wells is chlorine in the form of household laundry bleach (MDOH 2021). It is used primarily to oxidize organic matter such as biofilms. The chlorine concentration used in a well should not exceed 200 ppm. Higher concentrations are no more effective (MDOH 2021), are more costly, and may leave unwanted residue.

(b) *Hydrogen peroxide*. Like ozone and halogens, aqueous hydrogen peroxide (H_2O_2) is a powerful disinfectant and oxidant. It has been used to treat biofouling in both water supply and environmental wells. Hydrogen peroxide is particularly effective in removing sulfide. (Chlorine is not advised for this purpose). Metal sulfides can form under reducing conditions where sulfate-reducing bacteria thrives, converting sulfate to sulfides. H_2O_2 can enhance microbial growth away from the well as it breaks down to form water (H_2O) and oxygen (O_2). H_2O_2 is also strongly reactive with combustible mixtures (Smith 1998–2015).

(c) *Brominated compounds*. Brominated (Br) compounds are most commonly recommended for maintenance treatment. They are available for well use as NSF-listed hypobromous acid or in solid form as hypobromite (or hypobromate). Brominated compounds in solid form have a longer effective shelf life than in aqueous form. The solids also dissolve better in alkaline groundwaters with significant calcium hardness. Brominated compounds react and dissipate rather quickly, and many combined Br compounds such as bromamines are also disinfecting. Continuous treatment of wells with halogens is not recommended unless other reasonable alternatives are not viable (Smith 1998–2015).

(d) *Acid treatments*.

1. A strong acid solution can chemically dissolve encrusting materials so they can be pumped from the well. The water well industry has also increasingly abandoned chlorine in favor of certain organic acids in well cleaning and preventive maintenance (Smith 1998–2015). Acids most commonly used in well rehabilitation are hydrochloric acid (HCl), sulfamic acid, and hydroxyacetic (glycolic) acid. HCl is a strong acid, and at a high concentration it dissolves iron sulfide (FeS). Acid treatment should be used with caution on wooden well screens as the acid can cause damage the wood. Due to safety issues, acid treatment should be performed only by experienced personnel with specialized equipment.

2. Chelating organic acids such as acetic, or more particularly glycolic acid, have both antibacterial effects and serve to remove oxidized iron products. The microflora is not extensively disrupted, but their clogging products are removed. Glacial acetic is less expensive, but glycolic is a stronger acid and can be used in lower concentration and smells better (Smith 1998–2015). It is available in blends listed by NSF.

(e) *Chemicals to avoid.* It is possible that muriatic acid (industrial-grade hydrochloric acid) may disappear from the list of suitable water well treatment chemicals in North America. Good quality HCl, with its high H^+/Cl^- ionization constant, will likely remain in wide use, particularly for iron sulfide removal. However, glycolic acid, with its high chelating ability with iron, is a safer, more versatile alternative to HCl for most other uses. Phosphorous-based acids (such as phosphoric or phosphonic) leave behind phosphorus (P) on minerals or residual iron and manganese hydroxides. When oxidized to phosphate, for example, when chlorinating, they can provide nutrients for microbial regrowth. The risk of providing unwanted nutrients also exists if polyphosphates are used to alleviate mechanical plugging of screens. For these reasons, adding any P-containing chemicals to a relief well is not recommended.

e. *Treatments for bacterial encrustation.* Encrustation of wells by iron bacteria is best controlled by mechanical, followed by chemical, treatment. Heat treatment is also used, often in addition to chemicals, or in place of chemicals if they are disallowed for environmental reasons.

(1) *Chemical treatments.* There are three groups of chemicals generally used to treat bacterial fouling of wells: disinfectants, surfactants, and acids. Disinfectants, usually chlorine in the form of bleach, are the most commonly used (MDOH 2021). Chlorine gas is used in the restoration of commercial wells. However, safety and experience requirements limit its general application. A more convenient alternative is the use of hypochlorite or other chlorine products (see Table 11–1).

(2) *Heat treatment.*

(a) Applying heat to treat biofouling originally gained favor in the 1990s. The technique is commonly described in well rehabilitation literature from that period (Alford and Cullimore 1998). Typically, the injected fluid extends several feet from the well bore. However, the intent of the heat treatment is not to heat large areas of the aquifer matrix. Rather, the goal is to introduce heated chemical to the encrusted precipitates and any biomass in the filter pack and adjacent aquifer matrix. These are areas where encrustations and biomass likely are limiting flow to the well.

(b) Experience has shown that if a well has never been treated, plugging can be expected to extend into the filter pack and formation. The heat can loosen and remove this material. Heat is normally recommended as a part of a blended chemical-heat treatment (BCHTTM) (Smith 1998–2015). A detailed example of a blended treatment is given in paragraph 11–9c.

Table 11–1
Quantities of various chlorine compounds required to provide as much available chlorine as 1 pound of chlorine gas (Driscoll 1986)

Chemical	% Available Chlorine	Number of lb Equivalent to 1 lb Cl ₂
Chlorine gas	100	1.0
Calcium hypochlorite	65	1.54
Lithium hypochlorite	36	2.78
Sodium hypochlorite	12.5	8.0
Trichlorisocyanuric acid ¹	90	1.11
Sodium dichloroisocyanurate ¹	63	1.59
Potassium dichloroisocyanurate ¹	60	1.67
Chlorine dioxide	4	25.0
Chlorine dioxide	2	50.0

Note:

¹ Chlorine compounds that incorporate isocyanuric acid stabilize the chlorine against degradation from sunlight. Except for storage, the advantage offered by the addition of isocyanuric acid is less valuable in water wells.

11–9. Combined treatment

Clogging of relief well screens and filter materials is often caused by a combination of mechanical, chemical, and biological encrustation. In these cases, a multi-step procedure has been employed to rejuvenate wells. The initial step involves mechanical agitation by scrubbing, surging, and air lifting. This may then be followed by one or more of the following: heat, chlorine, or acid treatment. The heat loosens and dissolves materials. The chlorine compound attacks the organic material, and the strong acid dissolves the mineral deposits. The final step is pumping to remove accumulated material, monitor sand production, and reassess well efficiency.

a. Example of a heat-chlorine treatment. Detailed steps of a combined heat-chemical treatment conducted at the USACE Milford (Kansas) Dam in 2020 are as follows.

(1) Perform a pre-treatment video inspection as described in paragraph 11–6e(2). Results from the inspection may suggest changes to the treatment regimen and should be shared and discussed with senior personnel before proceeding.

(2) Record pool elevation and sound each well for initial depth.

(3) Video inspection may have revealed evidence of bacterial material in the screened zone. If so, the well screen should be scrubbed with a cylindrical brush for a minimum of 5 minutes. This will free the material for removal.

(4) Sound the well again, then use an eductor pipe to air-lift material loosened during the previous step.

(5) Scrub the inside of the well with a cylindrical brush from top to bottom. Allow approximately 15 minutes per well for brushing. Do not raise and lower the brush too quickly and do not bump the bottom of the well. Air lift the well again.

(6) Surge the well with a loose-fitting surge block (the size of the block should be 1 inch less than the diameter of the well). Surge for at least 15 minutes, starting at the top of the screened interval and working down to the bottom of the well in 2 to 3 feet increments at a rate of 2 fps. Sound the well and record the depth after surging.

(7) Carefully remove material in the bottom of the well by air lifting with an eductor pipe for 20 minutes. Collect all air-lifted material and estimate the quantity; collect a representative pint jar sample and record the new depth. Allow the well to flow, or to stand if not flowing, for 10 minutes before performing the next step.

(8) Initiate the heat treatment. Install a packer in the outfall pipe of each well to prevent flow. Do not pack adjacent wells at the same time. Place a jetting tool/packer assembly in the well with the jet openings 1 foot above the bottom of the well. Connect the jet assembly to the heating system so that hot water can be injected into the well.

(9) Install the remote temperature probe just below the packer plate assembly. Treat 5 or 10 feet of the well at a time with the hot water jet, starting at the bottom of the well. Continue until the assembly is several feet above the screen.

(10) Inject hot water from the heater into the well and monitor the water temperature. Once a temperature of 130 °F is attained, inject 1.0 gallons of 5% sodium hypochlorite solution (laundry bleach) into the well through the jet pipe. Continue to heat the 10-foot section for 10 minutes before moving up to the next 10-foot section of well. Treat the entire well in 10-foot increments.

(11) If, after 30 minutes, the 10-foot section of the well being treated does not reach a temperature of 130 °F, remove the jetting tool. Reduce the jetting tool's packer interval to 5 feet and use only 0.5 gallons of laundry bleach per 5-foot interval. A bottom packer also aids in attaining the desired temperature.

(12) At least 12 hours after heat treatment, sound the well for depth of accumulated material. Repeat the scrubbing and surging regimen if more than 0.5 foot of material is present.

(13) Prepare to perform a post-treatment pump test. Do not pump more than one well at a time. Sound the well to be pumped as well as adjacent wells and piezometers to be monitored during the test.

(14) If the well is flowing, inflate a packer/rubber plug inside the outfall pipe and allow the well to reach static. Do not pack adjacent wells. If necessary, install an

extension pipe above the riser pipe to maintain a static water level. The static level is obtained when variation in reading is less than 0.1 foot after 10 minutes.

(15) Ensure that the pumped water is not discharged into the collector system. This may cause flow into adjacent wells that have previously been rejuvenated and/or are being used to monitor drawdown. Instead, discharge should be directed into the flume of the drainage ditch associated with the well being pumped or to another area removed from the well. Do not allow the pump to discharge water in a manner that causes erosion at the discharge point, ditch linings, or ditch bottoms.

(16) Place the submersible pump in the well a few feet above top of screen. Perform the test for at least 30 minutes at a rate as close as possible to the original pumping rate. Use a backpressure valve if needed to maintain a constant pumping rate. If the target pumping rate cannot be achieved, reduce the rate to 75% of the target or the maximum that can be sustained for a 30-minute test.

(17) Measure and record the water level in the pumping well every minute for the first 10 minutes, and every 5 minutes for remainder of test. Also monitor and record levels in adjacent wells and/or piezometers at approximately the same time intervals.

(18) Use an RST and in-line flow meter, and record pump rate and flow frequently during testing. Record type and amount of sediment collected in the RST over the duration of measurement and whether sand content is being measured in ppm or milliliters (ml).

(19) Continue the test for a full hour if, after 30 minutes, the drawdown has not reached the pump intake. Do not end a test until 60 minutes has elapsed unless maximum drawdown is achieved prior to this.

(20) Following the pump test, record the recovery at the same time intervals used during the pumping phase of the test. Monitor recovery until the water level in the well fluctuates no more than 0.1 foot over a 10-minute interval.

b. Example of an acid-chlorine treatment. In this procedure, the chlorine compound is injected to attack the organic material and the strong acid is added to dissolve the mineral deposits. After performing the video inspection (paragraph 11–6e(2)) and mechanical treatment (paragraph 11–8b), follow the steps below:

(1) Inject a mixture of acid, inhibitor, and wetting agent to bring the pH of the well water to below 3. An inhibitor is needed only if the well screen is metal. During treatment, the pH should not be allowed to rise above 3, as iron may precipitate and clog the well screen. Therefore, a chelating agent such as hydroxyacetic acid also may be added. The amount of acid should typically be 1.5 to 2.0 times the volume of the well screen. The pH should be monitored throughout the acid treatment, even if a chelating agent is used.

(2) Gently agitate the solution with a jetting tool at 10-minute intervals for a period of 1 to 2 hours.

- (3) Pump out a volume of solution equal to the volume of the well.
- (4) Determine the pH of solution removed from the well. If the pH is more than 3, repeat steps 11–9b(1) to 11–9b(3).
- (5) Allow the acid to remain in the well for a minimum of 12 hours and then pump to waste.
- (6) Inject a mixture of chlorine and one or more chloric-stable surfactants (detergents and wetting agents, for example). The concentration should be 5% sodium hypochlorite solution (laundry bleach).
- (7) Between each treatment, pump the well to ensure that chlorine and acid are not in the well at the same time.
- (8) At least 12 hours after the acid/chlorine treatment, sound the well for depth of accumulated material. Repeat scrubbing and surging regimen if more than 0.5 foot of material is present.

c. *Example of a blended chemical-heat treatment.* A particularly effective method of BCHTTM is known as blended chemical-heat treatment. It was originally designed under sponsorship by ERDC specifically for relief wells. The procedure involves injecting a blend of chemicals into a well at high temperature and pressure. Aggressive mechanical methods are then employed to force the heat and chemicals into the screen, filter pack, and adjacent formation. The objective is to establish turbulence, improve entry into the formation, and establish a convection process that penetrates the formation. The general steps in the treatment are given in paragraphs 11–9c(3) through 11–9c(7). Figure 11–2 shows a BCHTTM system in operation at a USACE project.

(1) *History of method.* USACE began development of BCHTTM in the 1980s, and substantial testing was conducted at Huntington District projects (such as Leesville, Beach City, Bolivar, Senecaville, Beach Fork, Mohawk, Alum, and Dillon Dams, and Zoar Levee). The Huntington District adopted BCHTTM as a standard treatment method for relief wells in 2005 and continues to use the method today.

(2) *Documented results.* BCHTTM has proven very effective at restoring biofouled wells in unconsolidated alluvial aquifers. Alford and Cullimore (1998) reported a success ratio of 80% on over 1,750 wells. The Huntington District's contractors have successfully treated over 300 wells, including nearly 100 for the District. In 2005, BCHTTM resulted in increases of 280% and 1,530% in specific capacity (*SC*) at Alum Creek and Dillon Dam, respectively. Linear well loss coefficients were decreased by 86% at Alum Creek. In 2012, BCHTTM dramatically improved the relief wells at Paint Creek Dam (Greenfield Levee). One well (W-4) was completely plugged prior to treatment. Following treatment, the *SC* increased from less than 1 gallon per minute per foot (gpm/ft) to approximately 25 gpm/ft.

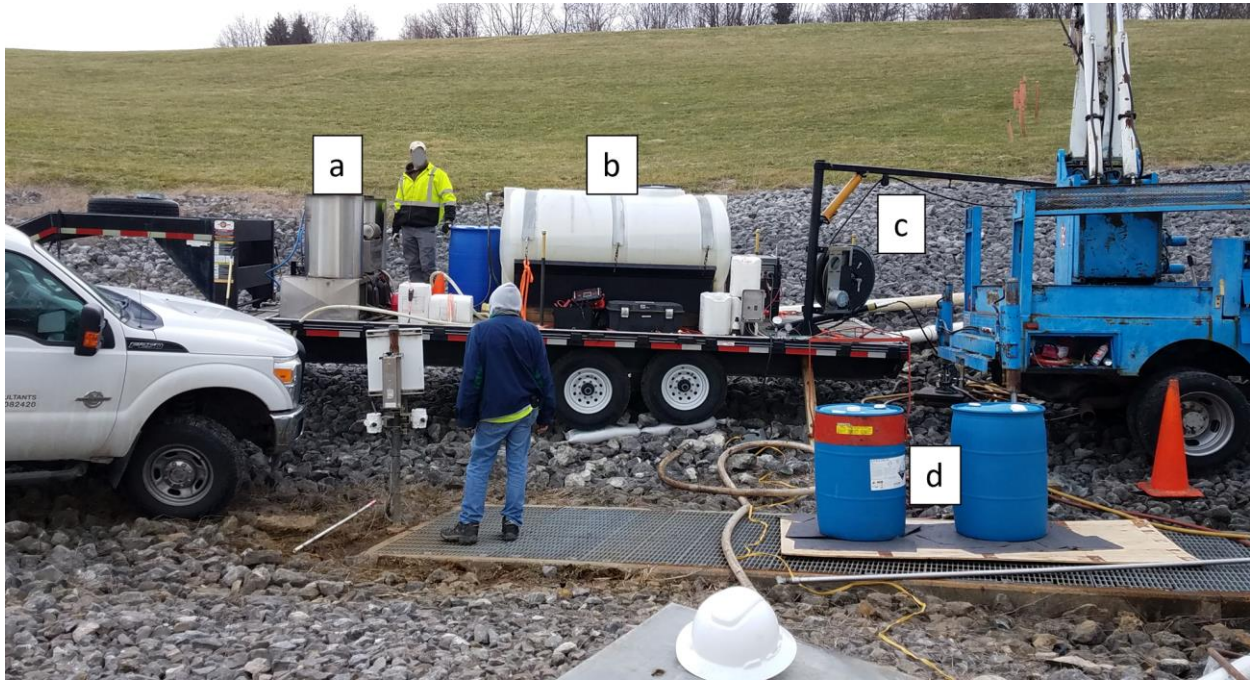


Figure 11–2. BCHTTM setup at a USACE project; major system components shown consist of heating units (a), water tank (b), boom (c), and acid (d) (North Branch Kokosing River Lake 2019)

- (3) *Brushing.* Brush the screen and well casing and screen to remove any biofilm.
- (4) *Surging and pumping.* Use air lifting and/or pumping to remove sand and any debris loosened during brushing.
- (5) *Shock phase.* Use a jetting procedure to inject heated (approximately 150 °F) chemicals into the well at approximately 1,100 pounds per square inch and initial line speed of 1 foot per second. Chemicals should always be used in volumes and concentrations specified by the manufacturer. A typical mixture is 5% hydroxyacetic acid, 5% sulfamic acid, 1% phosphate-free dispersant (PFD), and 1% penetrant by volume. PFD facilitates breakdown and the penetrant reduces the surface tension of water to allow better contact between cleansing agents and the well screen. The well is surged to facilitate penetration into the formation.
- (6) *Disruption phase.* Allow chemicals to soak in the well for 24 hours, then repeat the same injection and mixing procedure as before. Block-surge or air-lift the well repeatedly to facilitate penetration into the formation. Monitor the color and turbidity of discharge from the well.
- (7) *Removal phase.* Surging and pumping removes biomass and encrustation from the well. This phase is essentially redevelopment of the well. Low pH or severely turbid water may have to be containerized and/or treated depending on applicable state regulations. When the pH returns to 10% ambient, water may be discharged to the collector system.

Appendix A References

Section I

Required Publications

The single official repository for public documents originating from Headquarters USACE can be accessed at <https://www.publications.usace.army.mil/>. This includes the ERs, ECs, and EMs listed in this appendix. Unless otherwise noted, direct online links are provided below for referenced publications of the USACE Engineer Research and Development Center (ERDC) (formerly known as the U.S. Army Engineer Waterways Experiment Station [WES]). The general link for the ERDC library is <https://www.erdclibrary.usace.army.mil/Library/> and the link for the ERDC Knowledge Core site is <https://erdclibrary.erdclibrary.dren.mil/jspui/>.

Alford and Cullimore 1998

Alford, G. and Cullimore, R. 1998. *The Application of Heat and Chemicals in the Control of Biofouling Events in Wells*. CRC Press. Boca Raton, FL. p 208. (Available commercially from online sources)

American Society of Civil Engineers (ASCE) 2014

Hydraulics of Wells: Design, Construction, Testing, and Maintenance of Water Well Systems. Reston, VA: ASCE. (Available for purchase at <https://ascelibrary.org/doi/book/10.1061/9780784412732>.)

American Water Well Association (AWWA) 2016

Standard B100-16 Granular Filter Material. (Available for purchase at <https://store.awwa.org/AWWA-B100-16-Granular-Filter-Material>)

Barron 1947

Barron, R.A. 1947. "Discussion of 'Relief Wells'." *ASCE Transactions*. 112(1): 1372–1376. (Available at <https://ascelibrary.org/doi/epdf/10.1061/TACEAT.0005984>)

Barron 1948

Barron, R.A. 1948. "The Effect of a Slightly Pervious Top Blanket on the Performance of Relief Wells." *Proceedings of the 2nd International Conference on Soil Mechanics and Foundation Engineering*. Netherlands. (Available in CD/DVD format only: https://www.issmge.org/uploads/publications/1/43/1948_04_0060.pdf)

Barron 1978–1982

Barron, R.A. 1978–1982. "Unpublished reports concerning Mathematical Theory of Partially Penetrating Relief Wells." U.S. Army Engineer WES. Vicksburg, MS.

Bennett 1945

Bennett, P.T. 1945. "Comments on the design of relief wells." *Conference on Control of Underseepage, Cincinnati, OH, June 1944*. 95–101. U.S. Army Engineer WES. Vicksburg, MS. (Available at https://books.google.com/books?id=UhlNAAAAYAAJ&pg=RA1-PA45&source=gbs_toc_r&cad=2#v=onepage&q&f=false)

Bennett 1946

Bennett, P.T. 1946. "The Effect of Blankets on Seepage through Pervious Foundations." *ASCE Transactions*. 111(1): 248–252. (Available at <https://doi.org/10.1061/TACEAT.0005901>.)

Bennett 1947

Bennett, P.T. 1947. "Discussion of 'Barksdale on Relief Wells'." *ASCE Transactions*. 112: 1376–1384. (Available at <https://ascelibrary.org/doi/epdf/10.1061/TACEAT.0005984>)

Bennett and Barron 1957

Bennett, P.T. and Barron, R.A. 1957. "Design Data for Partially Penetrating Relief Wells." *Proceedings of the 4th International Conference on Soil Mechanics and Foundation Engineering. London, United Kingdom*. 2: 282–285. (Available at https://www.issmge.org/uploads/publications/1/41/1957_1,2,3.pdf)

Bennett et al. 1954

Bennett, P.T., Focht, J.A., and Jervis, W.H. 1954. "Discussion of 'Relief Well Systems for Dams & Levees'." *ASCE Transactions*. 119(1): 862–875. (Available at <https://doi.org/10.1061/TACEAT.0006975>)

Bierschenk and Basil 1963

Bierschenk, W.H. and Basil, F.E. 1963. "Determining Well Efficiency by Multiple Step-Drawdown Tests." *International Association of Scientific Hydrology*. 64: 493–507. (Available at <https://iahs.info/uploads/dms/064043.pdf>)

Cedergren 1989

Cedergren, H.R. 1989. *Seepage, Drainage, and Flow Nets*. Third edition. New York: John Wiley & Sons, Inc. p 496. (Available commercially from online sources)

Cooper and Jacob 1946

Cooper, H.H., and Jacob, C.E. 1946. "A Generalized Graphical Method for Evaluating Formation Constants and Summarizing Well Field History." *American Geophysical Union Transactions*. 27: 526–534. (Available at <https://doi.org/10.1029/TR027i004p00526>)

Dachler 1936

Dachler, R. 1936. *Grundwasserströmung*. Berlin, Germany. In German. (Available commercially from online sources)

Darcy 1856

Darcy, H. 1856. *Les Fontaines Publiques De La Ville De Dijon*. Paris, France. In French. English translation by Patricia Bobeck: *The Public Fountains of the City of Dijon by Henry Darcy*. Kendal/Hunt. Dubuque, IA. 2004. p 506, plus 28 plates. (Available commercially from online sources)

Driscoll 1986

Driscoll, F.G. 1986. *Groundwater and Wells*. Second Edition. Johnson Screens, St. Paul, MN. p 1089. (Available commercially from online sources)

Duncan et al. 2008

Duncan, J., Brandon, T., Wright, S., and Vroman, N. 2008. "Stability of I-Walls in New Orleans during Hurricane Katrina." *ASCE Journal of Geotechnical and Geoenvironmental Engineering*. 134(5): 681–691. (Available at [http://dx.doi.org/10.1061/\(ASCE\)1090-0241\(2008\)134:5\(681\)](http://dx.doi.org/10.1061/(ASCE)1090-0241(2008)134:5(681)))

Duncan et al. 2011

Duncan, J., O'Neil, B., Brandon, T., and VandenBerge, D. 2011. "Evaluation of Potential for Erosion in Levees and Levee Foundations." *Virginia Tech Center for Geotechnical Practice and Research Report*. 4: 40. (Available for purchase from <https://www.cgprapps.cee.vt.edu/index.php?do=list&item=publications>)

EC 1165-2-218

Levee Safety Program

EM 1110-1-1802

Geophysical Exploration for Engineering and Environmental Investigations

EM 1110-1-1804

Geotechnical Investigations

EM 1110-2-1602

Hydraulic Design of Reservoir Outlet Works

EM 1110-2-1901

Seepage Analysis and Control for Dams

EM 1110-2-1902

Conduits, Pipes, and Culverts Associated with Dams and Levee Systems

EM 1110-2-1905

Bearing Capacity of Soils

EM 1110-2-1908

Instrumentation of Embankment Dams and Levees

EM 1110-2-1913

Evaluation, Design, and Construction of Levees

EM 1110-2-2902

Conduits, Pipes, and Culverts associated with Dams and Levee Systems

EM 1110-2-3105

Mechanical and Electrical Design of Pumping Stations

ER 1105-2-100

Planning Guidance Notebook

ER 1110-1-1807

Drilling in Earth Embankment Dams and Levees

ER 1110-2-1156

Safety of Dams – Policy and Procedures

ER 1110-2-1942

Inspection, Monitoring, and Maintenance of Relief Wells

Fatherree 2006

Fatherree, B.H. 2006. "The History of Geotechnical Engineering at the Waterways Experiment Station, 1932-2000." Engineer Research and Development Center (Available at <https://hdl.handle.net/11681/46811>)

Ferris et al. 1962

Ferris, J.G., Knowles, D.B., Brown, R.H., and Stallman, R.W. 1962. "Theory of Aquifer Tests." *United States Geological Survey (USGS) Water Supply Paper 1536-E*. 113. (Available at https://pubs.usgs.gov/wsp/wsp1536-E/pdf/wsp_1536-E.pdf)

Forchheimer 1914

Forchheimer, P. 1914. *Hydraulik*. In German. (Available commercially from online sources)

Freeze and Cherry 1979

Freeze, R.A. and Cherry, J.A. 1979. *Groundwater*. Englewood Cliffs, NJ: Prentice-Hall, Inc. (Available at <https://fc79.gw-project.org/english/>)

French 1859

French, H.F. 1859. "Farm Drainage." Orange Judd & Company. (Available at <https://www.gutenberg.org/ebooks/23435>.)

GeoSlope 2007

SLOPE/W, Slope stability analysis program. (Available at <https://www.seequent.com/>)

Guy et al. 2014

Guy, E.D., Ider, H.M., and Darko-Kagya, K. 2014. "Several Relief Well Design Considerations for Dams and Levees." *Ohio River Valley Soils Seminar XLV: Geotechnical Aspects of Waterfront Development*. Cincinnati, OH. Pp 81–97 (Available at http://kgeg.org/wp-content/uploads/2017/10/ORVSS_45_Waterfront_development.pdf)

Guy et al. 2010

Guy, E.D., Nettles, R.L., Davis, J.R., Carter, S.C., and Newberry, L.A. 2010. "Relief Well System Design Approach: HHD Case Study." *Association of State Dam Safety Officials Proceedings, 2010, Charleston, WV*. 19. (Available at <https://www.semanticscholar.org/paper/RELIEF-WELL-SYSTEM-DESIGN-APPROACH-%3A-HHD-CASE-STUDY-Guy-Nettles/63d2b897036b252d14e62e6d89c8e72d90a76a1f>.)

Hadj-Hamou et al. 1990

Hadj-Hamou, T., Tavassoli, M.R., and Sherman, W.C. 1990. "Laboratory Testing of Filters and Slot Sizes for Relief Wells." *ASCE Journal of Geotechnical Engineering*. 116(9): 1325–1346. (Available at [https://doi.org/10.1061/\(ASCE\)0733-9410\(1990\)116:9\(1325\)](https://doi.org/10.1061/(ASCE)0733-9410(1990)116:9(1325)))

Harr 1962

Harr, M.E. 1962. *Groundwater and Seepage*. New York, NY: McGraw-Hill, Inc. (Available commercially from online sources)

Houben 2015

Houben, G. 2015. "Review: Hydraulics of Water Wells – Flow Laws and Influence of Geometry." *Hydrogeology Journal*. 23: 1633–1657. (Available at <https://link.springer.com/article/10.1007/s10040-015-1312-8>)

Houben and Kenrick 2022

Houben, G. and Kenrick, M. 2022. "Step-Drawdown Tests: Linear and Nonlinear Head Loss Components." *Hydrogeology Journal*. 30: 1315–1326. (Available at <https://doi.org/10.1007/s10040-022-02467-8>)

Houben and Treskatis 2007

Houben, G. and Treskatis, C. 2007. *Water Well Rehabilitation and Reconstruction*. New York, NY: McGraw-Hill, Inc. (Available commercially from online sources)

Huisman 1972

Huisman, L. 1972. *Groundwater Recovery*. MacMillan. p 336. (Available commercially from online sources)

Jacob 1947

Jacob, C. 1947. "Drawdown Test to Determine Effective Radius of Artesian Well." *ASCE Transactions*. 112(1): 1047–1064. (Available at <https://doi.org/10.1061/TACEAT.0006033>)

Jacob 1950

Jacob, C. 1950. "Flow of Groundwater." In *Engineering Hydraulics*, edited by H. Rouse. Horizon Pubs and Distributors. Chapter 5: 321–386. (Available commercially from online sources)

Jervis 1945

Jervis, W.H. 1945. "Design of relief well systems." In *Proceedings of Conference on Control of Underseepage, Cincinnati, Ohio, 1944*, p. 81-103. WES. Vicksburg, MS. (Print copies available from ERDC Library, use erdclibrary@chat.libraryh3lp.com)

Johnson 1947

Johnson, S.J. 1947. Discussion of Middlebrooks, T.A. and Jervis, W.H. "Relief Wells for Dams and Levees" in the Barksdale, H.C. 1947 article "Discussion on 'Barksdale on Relief Wells.'" *ASCE Transactions* 112(1): 1339–1398. (Available at: <https://ascelibrary.org/doi/epdf/10.1061/TACEAT.0005984>)

Johnstone 1797

Johnstone, J. 1797. *An Account of the Most Approved Mode of Draining Land, According to the System Practised by Mr. Joseph Elkington*. London, United Kingdom. (Available commercially from online sources)

Kasenow 2001

Kasenow, M. 2001. *Aquifer Test Data: Analysis and Evaluation*. Third edition. Highlands Ranch, CO: Water Resources Publications. (Available as hard copy and CD-ROM only: <https://www.wrpllc.com/books/atd.html>)

Keffer and Guy 2021

Keffer, A.M. and Guy, E.D. 2021. "Partial Penetration Relief Well Design Nomograms." *Proceedings from the 10th International Conference on Scour and Erosion (ICSE-10)*, Reston, VA, 2021. (Available at https://www.issmge.org/uploads/publications/108/109/Partial_Penetration_Relief_Well_Design_Nomograms.pdf)

Keffer and Guy 2023

Keffer, A.M. and Guy, E.D. 2023. "Relief Wells for Dams and Levees Considering Landward Head." *ASCE Journal of Geotechnical and Geoenvironmental Engineering*. 149(11): 1–13. (Available at <https://doi.org/10.1061/JGGEFK.GTENG-10671>)

Keffer et al. 2019

Keffer, A.M. Guy, E.D., and Chang, E.M. 2019. "Finite Element Modeling of Partial Penetration Well Uplift Factors." *Geo-Congress 2019. Geotechnical Special Publication No. 305*. 57–66. (Available at <https://ascelibrary.org/doi/epdf/10.1061/9780784482070.006>)

Keffer et al. 2023

Keffer, A.M., Guy, E.D., and Grote, K.R. 2023. "Finite line relief well system design for dams and levees." *In Geo-Congress 2023: Geotechnical Systems from Pore-Scale to City-Scale, Geotechnical Special Publication 343, Reston, VA, 2023.* (Available at <https://ascelibrary.org/doi/abs/10.1061/9780784484708.004>)

Khosla 1930

Khosla, A.N. 1930. *Paper No. 138, Hydraulic Gradients in Subsoil Water Flow in Relation to Stability of Structures Resting on Saturated Soils.* Pakistan Engineering Congress. (Available at <https://pecongress.org.pk/images/upload/books/P18-PAPER138.pdf>)

Kozeny 1933

Kozeny, J. 1933. *Theorie und Berechnung der Brunnen Wasserkraft und Wassenwirtschaft.* Volume 28. In German. (Available at <https://onlinelibrary.wiley.com/doi/10.1002/jpln.19330280104>)

Kruseman and de Ridder 2000

Kruseman, G.P., and de Ridder, N.A. 2000. "Analysis and Evaluation of Pumping Test Data." Second Edition. *ILRI Publication 47.* Institute for Land Reclamation and Improvement; Wageningen, Netherlands. (Available at <https://gw-project.org/books/analysis-and-evaluation-of-pumping-test-data/>)

Kyle 2015

Kyle, R.J. 2015. "Analysis and Evaluation of Aquifer Pumping Test Data, What Can We Learn and What is Relevant?" *AWWA Annual Fall Conference, Las Vegas, NV, 2015.* (Available at <https://ca-nv-awwa.org/CANV/downloads/2015/AFC15presentations/AquiferPumpingTests.pdf>)

Leonards 1962

Leonards, G.A. 1962. *Foundation Engineering.* John Wiley & Sons, Inc., Hoboken, NJ. p 514. (Available commercially from online sources)

Long and U.S. Army WES 1931

Long, H.T. and WES. 1931. "Preliminary Report on Investigation of Seepage in Levees." Vicksburg, MS. (Print copy available from ERDC Library, use erdclibrary@chat.libraryh3lp.com)

Mansur and Dietrich 1965

Mansur, C.I. and Dietrich, R.J. 1965. "Pumping Test to Determine Permeability Ratio." *Journal of the Soil Mechanics and Foundation Division. Proceedings of the ASCE.* 91(4): 151–183. (Available at <https://doi.org/10.1061/JSFEAQ.0000755.>)

Mansur and Kaufman 1962

Mansur, C.I. and Kaufman, R. 1962. "Dewatering." *Foundation Engineering. Edited by G.A. Leonards.* New York, NY: McGraw-Hill, Inc. (Available in selected public libraries: <https://search.worldcat.org/title/1048638653>)

Mansur et al. 2000

Mansur, C.I., and Postol, G., and Salley, J.R. 2000. "Performance of Relief Well Systems Along Mississippi River Levees." *ASCE Journal of Geotechnical and Geoenvironmental Engineering*. 727–738. (Available at [https://doi.org/10.1061/\(ASCE\)1090-0241\(2000\)126:8\(727\)](https://doi.org/10.1061/(ASCE)1090-0241(2000)126:8(727)).)

Mansur and Turnbull 1948

Mansur, C.I. and Turnbull, W. 1948. "Model Studies of Drainage Wells for Dams and Levees on Pervious Foundations." *Second International Conference on Soil Mechanics and Foundation Engineering. Paper No. 11.4*. (Available in print book format only: <https://www.worldcat.org/formats-editions/8932447>.)

McAnear and Trahan 1972

McAnear, C.L. and Trahan, C.C. 1972. "Three-Dimensional Seepage Model Study, Oakley Dam, Sangamon River, Illinois." WES Miscellaneous Paper S-72-3: Vicksburg, MS. (Available at <https://apps.dtic.mil/sti/citations/ADA033148>)

Middlebrooks 1948

Middlebrooks, T.A. 1948. "Seepage Control for Large Earth Dams." *Transactions of the Third International Congress on Large Dams, Stockholm, Sweden*. (Available in CD/DVD format only: https://www.icold-ciqb.org/GB/publications/congresses_proceedings.asp)

Middlebrooks and Jervis 1947

Middlebrooks, T.A. and Jervis, W.H. 1947. "Relief Wells for Dams and Levees." *ASCE Transactions*. 112(1): 1321–1338. (Available at <https://ascelibrary.org/doi/pdf/10.1061/TACEAT.0006047>)

Minnesota Department of Health (MDOH) 2021

Iron Bacteria in Well Water. (Available at <https://www.health.state.mn.us/communities/environment/water/wells/waterquality/ironbacteria.html>)

Mitronovas 1968

Mitronovas, F. 1968. Laboratory tests of relief well filters. WES Miscellaneous Paper S-68-4. Vicksburg, MS. (Available at <https://apps.dtic.mil/sti/citations/ADA036368>)

Muskat 1937

Muskat, M. 1937. *The Flow of Homogeneous Fluids through Porous Media*. New York, NY: McGraw-Hill, Inc. (Available commercially from online sources)

Neuman 1975

Neuman, S.P. 1975. "Analysis of Pumping Test Data from Anisotropic Unconfined Aquifers Considering Delayed Gravity Response." *American Geophysical Union*. 11(2): 329–342. (Available at <https://doi.org/10.1029/WR011i002p00329>)

Ohm 1827

Ohm, G. S. 1827. *Die Galvanische Kette, Mathematisch Bearbeitet*. Berlin, Germany. In German. (Available commercially from online sources)

Robbins and Griffiths 2022

Robbins, B.A., and Griffiths, D.V. 2022. “Quantifying the performance of piping mitigation measures with two-dimensional, adaptive finite element analysis.” *Proceedings of the 20th International Conference on Soil Mechanics and Geotechnical Engineering, Sydney, Australia, 2022*. (Available at https://www.issmge.org/uploads/publications/1/120/ICSMGE_2022-468.pdf)

Seed et al. 2008

Seed, R., Bea, R., Athanasopoulos-Zekkos, A., Boutwell, G., Bray, J., Cheung, C., Cobos-Roa, D., Ehrensing, L., Harder Jr., L., Pestana, J., Riemer, M., Rogers, J., Storesund, R., Vera-Grunauer, X., and Wartman, J. 2008. “New Orleans and Hurricane Katrina II: The 17th Street Drainage Canal.” *ASCE Journal of Geotechnical and Geoenvironmental Engineering*. 134(5): 740–761. (Available at [https://doi.org/10.1061/\(ASCE\)1090-0241\(2008\)134:5\(740\)](https://doi.org/10.1061/(ASCE)1090-0241(2008)134:5(740)))

Sharma 1974

Sharma, S.N.P. 1974. “Partially Penetrating Multiple-Well System in a Confined Aquifer with Application to a Relief Well Design.” *Journal of Hydrology*. 23: 1–37. (Available at [https://doi.org/10.1016/0022-1694\(74\)90021-3](https://doi.org/10.1016/0022-1694(74)90021-3))

Slichter 1945

Slichter, F.B. 1945. “Pressure relief wells at Fort Peck Dam.” *In Conference on Control of Underseepage, 13–14 June 1944; Cincinnati, OH, pp. 45–50*. U.S. Army Engineer WES. (Available at https://books.google.com/books?id=UhiNAAAAYAAJ&pg=RA1-PA45&source=gbs_toc_r&cad=2#v=onepage&q&f=false)

Smith 1998–2015

Smith, A. 1998–2015. Personal communication with Albert Smith from Johnson Well Screen on 8 September 2015.

Spaulding 1976

Spaulding. 1976. Personal notes regarding derivations of seepage equations. St. Paul District. U.S. Army Corps of Engineers. Unpublished. (Electronic copy provided to ERDC Library, June 2024, use erdclibrary@chat.libraryh3lp.com)

Talbot and Pabst 2006

Talbot, J. and Pabst, M. 2006. “Filters for Earth Dams: Gradation Design and Construction Guidance Used by Federal Agencies.” *The Journal of Dam Safety*. 4(4): 12. (Available at <https://damsafety.org/reference/filters-earth-dams>)

Terzaghi 1927

Terzaghi, C. 1927. “Wellpoint Method for Handling Excavation of Foundation Pit at New Sewage Pumping Station.” *Journal of the Boston Society of Civil Engineering*. XIV (7): 63–71. (Request copy from: bsces@engineers.org)

Theis 1935

Theis, C. 1935. "The Relation Between the Lowering of the Piezometric Surface and the Rate and Duration of Discharge of a Well Using Groundwater Storage." *American Geophysical Union Transactions*. 16: 519–524. (Available at <https://doi.org/10.1029/TR016i002p00519>)

Todd 1980

Todd, D.K. 1980. *Groundwater Hydrology*. New York, NY: John Wiley & Sons. (Available commercially from online sources)

Turnbull and Mansur 1954

Turnbull, W. and Mansur, C.I. 1954. "Relief Well Systems for Dams and Levees." *ASCE Transactions*. 119(1): 875–878. (Available at <https://doi.org/10.1061/TACEAT.0007104>)

Turnbull and Mansur 1959

Turnbull, W. and Mansur, C.I. 1959. "Construction and Maintenance of Underseepage Control Measures." *Proceedings of the ASCE*. 85 (6): 97–124. (Available at <https://ascelibrary.org/doi/epdf/10.1061/JSFEAQ.0000239>)

Turnbull and Mansur 1961

Turnbull, W. and Mansur, C.I. 1961. "Design of Control Measures for Dams and Levees." *Proceedings of the ASCE*. 126 (1): 1486–1521. (Available at <https://ascelibrary.org/doi/epdf/10.1061/TACEAT.0008149>)

U.S. Bureau of Reclamation (USBR) 2001

Water Measurement Manual (3rd edition). A Water Resources Technical Publication. U.S. Government Printing Office. Washington, DC. (Available at https://www.usbr.gov/tsc/techreferences/mands/wmm/WMM_3rd_2001.pdf)

USBR and USACE 2019

Best Practices in Dam and Levee Safety Risk Analysis: Joint publication by U.S. Department of the Interior, Bureau of Reclamation, and U.S. Army Corps of Engineers. Version 4.1. (Available at <https://www.usbr.gov/damsafety/risk/methodology.html>)

U.S. Army 1983

Dewatering and Groundwater Control. Departments of the Army, Navy, and Air Force. Washington D.C. (Available at <https://www.wbdg.org/ffc/army-coe/technical-manuals-tm/tm-5-818-5>). Note: Superseded by UFC 3-220-05 in 2004.

U.S. Department of Agriculture (USDA) 2012

Musselman, R. "Sampling Procedure for Lake or Stream Surface Water Chemistry." Rocky Mountain Research Station. Research Note RMRS-RN-49. Fort Collins, CO. (Available at <https://doi.org/10.2737/RMRS-RN-49>)

U.S. Department of Energy (DOE) 1993

Resonant Sonic Drilling: History, Progress and Advances in Environmental Restoration Programs. Prepared by Westinghouse Hanford Company. Presented at Environmental Remediation 1993. Augusta, GA. (Available at <https://www.osti.gov/servlets/purl/10109181>)

U.S. Environmental Protection Agency (EPA) 1983

“Methods for Chemical Analysis of Water and Wastewater.” Office of Research and Development, Washington D.C. EPA/600/4-79/020. (Available at https://www.wbdg.org/FFC/EPA/EPACRIT/epa600_4_79_020.pdf)

U.S. Geological Survey (USGS) 1997

Guidelines and Standard Procedures for Studies of Ground-Water Quality: Selection and Installation of Wells, and Supporting Documentation. Water-Resources Investigations Report 96-4233; Reston, VA. (Available at <https://doi.org/10.3133/wri964233>)

Ultimate Reengineering Services LLC (URS) 2015

“Guidance document for geotechnical analyses: Urban levee evaluations project.” Prepared for the California Department of Water Resources, Sacramento, CA. 980. (Available for download https://ferix.water.ca.gov/lep/service/download/downloadDocumentByFileName?fileName=20150427_guidancedoc.pdf)

United Facilities Criteria (UFC) 3-220-05

Dewatering and Groundwater Control (Available at <https://www.wbdg.org/ffc/dod/unified-facilities-criteria-ufc/ufc-3-220-05>)

USACE 1939a

The Efficacy of Systems of Drainage Wells for the Relief of Subsurface Hydrostatic Pressures (TM 151-1). (Available at <http://hdl.handle.net/11681/21376>)

USACE 1939b

Mississippi River Levees Underseepage Studies, Black Bayou Levee. East Bank in Mississippi, 440 M.B.C. Vicksburg District: Vicksburg, MS. (Availability: Electronic copy provided to ERDC Library, June 2024, use erdclibrary@chat.libraryh3lp.com)

USACE 1941

Investigation of Underseepage, Lower Mississippi River Levees. TM 184-1. WES: Vicksburg, MS. (Available at <http://hdl.handle.net/11681/21229>)

USACE 1942

Field and Lab, Investigation of Design Criteria for Drainage Wells. TM 195-1. WES: Vicksburg, MS. (Available at <https://usace.contentdm.oclc.org/digital/collection/p266001coll1/id/4762>)

USACE 1949

Relief Well Systems for Dams and Levees on Pervious Foundations: Model Investigation. TM 3-304. WES: Vicksburg, MS. (Available at <https://usace.contentdm.oclc.org/digital/collection/p266001coll1/id/1960/>)

USACE 1950

Investigation of Underseepage and Its Control by Relief Wells: Commerce and Trotters, MS. TM 3-316. WES: Vicksburg, MS. (Volume 1 available at <http://hdl.handle.net/11681/21234>. Volume 2 available at <http://hdl.handle.net/11681/21662>)

USACE 1952

Control of Underseepage by Relief Wells, Trotters, Mississippi. TM 3-341. WES: Vicksburg, MS. (Volume 1 available at <https://apps.dtic.mil/sti/tr/pdf/ADA012771.pdf>. Volume 2 available at <http://hdl.handle.net/11681/21306>)

USACE 1955

Relief Well Design (Civil Works Engineer Bulletin 55-11). (Available at <https://usace.contentdm.oclc.org/digital/collection/p266001coll1/id/9779/rec/1>)

USACE 1956a

Investigation of Underseepage and Its Control, Lower Mississippi River Levees. Volumes 1 and 2. TM 3-424. WES: Vicksburg, MS. (Volume 1 available at <http://hdl.handle.net/11681/3489>. Volume 2 not available electronic)

USACE 1956b

Investigation of Underseepage, Mississippi River Levees, Alton to Gale, IL. Volumes 1 and 2. TM 3-430. WES: Vicksburg, MS. (Volume 1 available at <http://hdl.handle.net/11681/21274>. Volume 2 available at <http://hdl.handle.net/11681/21289>)

USACE 1958

Analysis of Piezometer and Relief Well Data, Arkabutla Dam (TR No. 3-479). U.S. Army Engineer WES. (Available at <http://hdl.handle.net/11681/21485>)

USACE 1962

Missouri River Division Memorandum on 1962 Omaha Seepage Conference: Omaha, NE, 28 November 1962. (Electronic copy provided to ERDC Library, June 2024, use erdclibrary@chat.libraryh3lp.com)

USACE 1963

Three-Dimensional Electrical Analogy Seepage Model Studies, TM No. 3-619. WES: Vicksburg, MS. (Available at <https://usace.contentdm.oclc.org/digital/api/collection/p266001coll1/id/4055/download>)

USACE 1965

Banks, D.C. 1965. Three-Dimensional Electrical Analogy Seepage Model Studies; WES TR No. 3-619, Appendix B: Flow to a single Well Centered Inside a Circular Source, Series H.

USACE 1968

History of the Waterways Experiment Station. WES: Vicksburg, MS. (Available at the ERDC Knowledge Core site, use erdclibrary@chat.libraryh3lp.com)

USACE 1972

Montgomery, R.L. and WES. 1972. "Investigation of Relief Wells, Mississippi River Levees, Alton to Gale, Illinois." Miscellaneous Paper S-72-21. (Available at <http://hdl.handle.net/11681/20841>)

USACE 1976

Re-evaluation of Underseepage Controls Mississippi River Levees, Alton to Gale, IL. Phase I: Performance of Underseepage Controls During the 1973 Flood; St. Louis, MO. (Print copy of Volume 1 available from ERDC Library, use erdclibrary@chat.libraryh3lp.com)

USACE 1998

Engineering and Design, Soil Mechanics Data, Groundwater, and Seepage (Mississippi River Valley Division Regulation (DIVR) 1110-1-400). Unpublished. (Electronic copy provided to ERDC Library, June 2024, use erdclibrary@chat.libraryh3lp.com)

USACE 2002

Performance of Levee Underseepage Controls: A Critical Review (Engineer Research and Development Center/Geotechnical and Structures Laboratory [ERDC/GSL] TR-02-19) (Available at the ERDC Knowledge Core site, use erdclibrary@chat.libraryh3lp.com)

USACE 2016

Seepage and Piping through Levees and Dikes Using 2D and 3D Modeling Codes (ERDC/CHL TR-16-6). (Available at the ERDC Knowledge Core site, use erdclibrary@chat.libraryh3lp.com)

USACE 2018

Comparison of Levee Underseepage Analysis Methods Using Blanket Theory and Finite Element Analysis (ERDC/GSL TR-18-14). (Available at the ERDC Knowledge Core site, use erdclibrary@chat.libraryh3lp.com)

Van Beek et al. 2010

Van Beek, V.M., De Bruijn, H.T.J., Knoeff, J.G., Bezuijen, A., Förster, U. 2010. "Levee failure due to piping: a full-scale experiment." In: Burns, S.E., Bhatia, S.K., Avila, C.M.C., Hunt, B.E., editors. Proceedings of the Fifth International Conference on Scour and Erosion; 7–10 November 2010. San Francisco, CA. *ASCE Geotechnical Special Publication No. 210*. 283–292. Reston, VA. (Available at <https://ascelibrary.org/doi/epdf/10.1061/41147%28392%2927>)

Walshire et al. 2020

Walshire, L., Dunbar, J., and Corcoran, M. 2020. "A History of Relief Well Use and Current Practices in the U.S. Army Corps of Engineers." *Geo-Congress 2020, Geotechnical Special Publication No. 316*. 200–210. (Available at <https://ascelibrary.org/doi/epdf/10.1061/9780784482797>)

Walton 1960

Walton, W. 1960. "Leaky Artesian Aquifer Conditions in Illinois." *Report of Investigation 39*. Urbana, IL: Illinois State Water Survey. (Available at <https://www.isws.illinois.edu/pubdoc/RI/ISWSRI-39.pdf>)

Walton 1962

Walton, W. 1962. "Selected Analytical Methods for Well and Aquifer Evaluation." *Bulletin 49*. Urbana, IL: Illinois State Water Survey. (Available at <https://www.isws.illinois.edu/pubdoc/B/ISWSB-49.pdf>)

Williams 1985

Williams, D. 1985. "Modern Techniques in Well Design." *Journal of the American Water Works Association*. 77 (9): 68–74. (Available at <https://doi.org/10.1002/j.1551-8833.1985.tb05608.x>)

Wisconsin Department of Natural Resources (DNR) 1996

Karklins, S. and Lenon, J. 1996. "Groundwater Sampling Field Manual." Bureau of Drinking and Groundwater. PUBL-DG-038 96. (Available at <https://dnr.wisconsin.gov/sites/default/files/topic/DrinkingWater/Publications/DG038.pdf>)

Yanai 1963

Yanai, K. 1963. "Fundamental Problems Related to Relief Well. Soils and Foundations." *Japanese Geotechnical Society*. 3(2): 49–62. (Available at https://doi.org/10.3208/sandf1960.3.2_49)

Yeh et al. 2006

Yeh, G., Cheng, H., Zhang, F., Huang, G. 2006. A First-Principle, Physics-Based Watershed Model: WASH123D. (Available for download at https://www.researchgate.net/publication/228446073_A_first-principle_physics-based_watershed_model_WASH123D.)

Section II**Prescribed Forms****ENG Form 1836**

Drilling Log

ENG Form 6316

Relief Well Installation Report (replaces WES Form 797)

ENG Form 6317

Relief Well Pumping Test Report (replaces WES Form 796)

ENG Form 6318

Well Development Data

ENG Form 6319

Sand Infiltration Test

Section III

Measurement Conversion

Table A-1
Measurement conversion table

Measurement	To Convert From	Multiple By ¹	To Obtain
Length	inches (in)	25.4	millimeters (mm)
	feet (ft)	0.3048	meters (m)
	yards (yds)	0.9144	meters (m)
	mile (mi)	1609	kilometers (km)
Area	square inches (in ²)	645.16	square millimeters (mm ²)
	square feet (ft ²)	0.09290	square meters (m ²)
	square yards (yds ²)	0.83613	square meters (m ²)
Volume	cubic inches (in ³)	16.387	cubic centimeters (cm ³)
	cubic feet (ft ³)	0.02832	cubic meters (m ³)
	cubic yards (yd ³)	0.76456	cubic meters (m ³)
	gallon (gal)	3.7854	liters (l)
	acre-foot (ac-ft)	1233.5	cubic meters (m ³)
Permeability	feet/day	0.0003527	centimeters per second (cm/s)
Mass	pounds (lbs)	0.45359	kilograms (kg)
	ton (short tons, 2000 pounds)	0.90718	metric tons
Force	pounds force (lbf)	4.4482	newtons (N)
	pounds per square foot (psf)	47.880	Pascals (pa)
Velocity	feet per second (ft/sec)	0.3048	meters per second (m/sec)
Discharge	cubic feet per second (cfs)	0.02832	cubic meters per second (cms)
	cubic feet per second (cfs)	1.9835	acre-foot per day (ac-ft/day)
	gallons per minute (gpm)	0.00223	cubic feet per second (cfs)
	gallons per minute (gpm)	0.00006309	cubic meters per second (m ³ /s)
Temperature	degree Fahrenheit (°F)	(°F – 32) x 5/9	degree Centigrade (°C)
Density	pounds per cubic foot (pcf)	16.018	kilograms per cubic meter (kg/m ³)

¹ To reverse conversion of the from/to obtain units shown, divide by the conversion factor.

Appendix B List of Symbols

Symbol	Definition
a	Well spacing
B	Summation of B_1 , B_2 and B_3
B_1	Linear aquifer-loss coefficient caused by head losses in the aquifer
B_2	Linear well-loss coefficient caused by drilling damage to aquifer
B_3	Partially penetration loss coefficient
b	Aquifer thickness
C	Non-linear well loss coefficient
c	Landward factor for calculating effective seepage exit distance
C_u	Coefficient of uniformity
C^*	Partial-penetration factor
D	Total thickness of foundation
\bar{D}	Effective (transformed) foundation thickness
d	Thickness of pervious substratum
D_{10}	Grain size at which 10 percent by weight of sample is finer
D_{15}	Grain size at which 15 percent by weight of sample is finer
D_{50}	Grain size at which 50 percent by weight of sample is finer
D_{60}	Grain size at which 60 percent by weight of sample is finer
D_{85}	Grain size at which 85 percent by weight of sample is finer
E	Well efficiency
E -ratio	Ratio of current efficiency to the baseline efficiency
FS	Factor of safety
FS_{ves}	Vertical effective stress factor
FS_{vg}	Vertical gradient factor of safety
G_p	Ratio of flow from a partial-penetration well to that of a full-penetration well at the same drawdown
g	Acceleration due to gravity
H	Total net head on well system
h	Net head on the well system corrected for well losses
h_a	Allowable excess head
H_{av}	Average net head in vertical plane of wells
H_{ave}	Average net head along well line in plan view
h_{av}	Average net head in vertical plane of wells corrected for total well losses
h_{ave}	Average net head along well line in plan view corrected for total well losses
H_d	Maximum net head landward of wells
H_e	Entrance head loss

Symbol	Definition
H_{el}	Elevation head
H_f	Friction head loss
H_{HGL}	Hydraulic grade line elevation without wells
H_m	Net head midway between wells
h_m	Net head midway between wells corrected for total well losses
h_p	Head at point of interest
H_v	Velocity Head loss
H_w	Total well losses
h_w	Head at the radius of the well
h_x	Excess head at any distance, x , landward from the landside toe
h_{xx}	Excess head for each uplift factor
h_o	Excess head calculated at landside toe
i_c	Critical vertical gradient
i_{cr}	Critical vertical gradient
i_e	Vertical gradient at point of interest typically the embankment toe
i_h	Horizontal gradient
i_{vg}	Vertical gradient at point of interest
K	Hydraulic conductivity
k	Permeability
k_{bl}	Vertical permeability of landside blanket
k_{br}	Vertical permeability of riverside blanket
\bar{k}_e	Effective (transformed) permeability
k_f	Horizontal permeability of foundation
k_h	Horizontal permeability
L	Total distance from effective seepage entry to effective seepage exit
L_1	Distance from river to riverside levee toe
L_2	Base width of levee and berm
L_3	Length of foundation and top stratum beyond landside levee toe
L_p	Driscoll parameter
M	Slope of hydraulic grade line (at mid-depth of pervious stratum)
ΔM	Net seepage gradient toward the well line
N	Number of wells in the finite line
Q	Flow rate
Q_{max}	Maximum flow rate
Q_s	Quantity of seepage beneath a levee or dam
Q_{sw}	Seepage beyond well systems
Q_w	Quantity of flow to a single well

Symbol	Definition
Q_{wi}	Discharge from the i^{th} well
Q_{wp}	Flow from a partial-penetration well
R	Radius of influence of well
r	Radial distance from pumping well to observation well or to point at which head is calculated
r_0	Radius of influence determined from a semi-log plot of drawdown versus radial distance
r_o	Distance to the middle of a finite line source
R_i	Radius of influence of the i^{th} well
r_i	Distance from the i^{th} well to the point at which head is computed
r_w	Well radius
r_{we}	Effective radius
S	Distance from effective source of seepage entry into foundation to the landside embankment toe. Chapter 5: Distance from well line to effective seepage entrance
s_a	Drawdown in an ideal well subject only to aquifer losses
S_c	Specific capacity
$S_{c\ initial}$	Initial specific capacity
$S_{c\ new}$	Current specific capacity
s_{fp}	Drawdown in full-penetration well
s_{pp}	Drawdown in partial-penetration well
S_t	Storativity
s_t	Total drawdown in well
s_w	Drawdown attributable to well losses = $s_t - s_a$
Δs_{t-t}	Change in drawdown over one log cycle of time
Δs_{t-d}	Change in drawdown over one log cycle of radial distance
s_t/Q	Specific drawdown
SCR	Specific capacity ratio
T	Transmissivity
t	Time
V	Velocity of water in the riser pipe
W	Well screen length
\bar{W}	Effective well screen length
W_D	Well discharge elevation
W/D	Actual well penetration
\bar{W}/\bar{D}	Effective well penetration
x	Distance landward between landside toe and location x
x_1	Distance from effective seepage entry to riverside levee toe
x_3	Distance from the landside embankment toe to effective seepage exit

Symbol	Definition
z	Thickness of top stratum
z_b	Transformed thickness of top stratum for head computation
z_{bl}	Transformed thickness of landside top stratum
z_{br}	Transformed thickness of riverside top stratum
z_t	Transformed thickness of landside top stratum for uplift computation
z_t	Vertical distance to surface, typically the landside blanket thickness
γ'	Average effective (or buoyant) unit weight of overlying soil
γ_{sat}	Total, or saturated, unit weight of overlying soil
γ	Total, or saturated, unit weight of overlying soil
γ_w	Unit weight of water
θ_{av}	Average uplift factor
θ_d	Landward uplift factor
θ_m	Mid-well uplift factor
$\Delta\theta$	Change in uplift factor
$\theta_{mm}, \theta_{me},$ θ_{dm}, θ_{de}	Finite line uplift factors
θ_{de}	Uplift factor for calculating maximum head landward of the end of a finite well line
θ_{dm}	Uplift factor for calculating maximum head landward of the middle of a finite well line
θ_{me}	Uplift factor for calculating excess head at end of a finite well line
θ_{mm}	Uplift factor for calculating excess head at middle of a finite well line
θ_{xx}	General designation for an uplift factor in vicinity of a finite well line

Appendix C Mathematical Analysis of Underseepage and Substratum Pressure

C-1. Introduction

Designing seepage control measures is based on a seepage analysis. The information required for an analysis includes field measurements of piezometric data, seepage flow rates, and observations of performance during flood events. The mathematical analysis of underseepage and substratum pressure is covered in EM 1110-2-1901 and EM 1110-2-1913. This appendix contains a few fundamental concepts related to seepage analyses performed for dams, levees, or other foundations that are common to both EMs and have been used for decades throughout USACE.

C-2. Finite element method

FEM is a versatile and now widely used analysis method that evaluates levee seepage for any dam, levee, or other foundation stratigraphy. The approach is covered in detail in EM 1110-2-1901.

C-3. Blanket Theory

BT is a simple graphical approach to evaluate underseepage where the stratigraphy can be represented as a more pervious substratum (aquifer) underlying a less pervious top stratum (blanket). BT equations contained herein were developed during a study reported in WES TM 3-424 (USACE 1956a) of piezometric data and seepage measurements at levees along the Lower Mississippi River and confirmed by model studies.

a. General. A more complete description of BT is included in EM 1110-2-1913 and TM 3-424. Only a subset of the equations for various cases, entrance, and exit conditions are presented here to help the reader understand concepts related to relief well analysis and design. When used appropriately, the BT approach results in reasonable estimates of both the hydrostatic pressure at the landside toe of the embankment and the amount of seepage that would occur for actual conditions.

b. Blanket Theory assumptions. It is necessary to make certain simplifying assumptions before making any theoretical seepage analysis. The following is a list of such assumptions and criteria necessary to perform BT underseepage analysis.

- (1) All seepage is laminar, which is common to both BT and FEM.
- (2) Seepage may enter the pervious substratum at any point on the waterside; any waterside borrow pits that may be present (through the waterside top stratum) and riverine levees often have exposed aquifer sand in the riverbed.
- (3) Flow through the top stratum (blanket) is vertical.
- (4) Flow through the pervious substratum (aquifer) is horizontal.

(2) *Effective seepage entrance.* The effective source of seepage entry into the pervious substratum (point A in Figure C–1) is the hypothetical point along an impervious top stratum where a vertical boundary with total head equal to the waterside water level would approximate actual flow conditions through the waterside foundation. It is also defined as that line or point where the HGL beneath the embankment projected riverward with a slope M intersects the waterside water level.

Table C–1
Factors involved in Blanket Theory seepage analyses

Factor	Definition
d	Thickness of pervious substratum
H	Net head on levee
h_o	Head beneath top stratum at landside levee toe
h_x	Head beneath top stratum at distance x from landside levee toe
i_c	Critical gradient for landside top stratum
k_b	Vertical permeability of top stratum
k_{bl}	Vertical permeability of landside top stratum
k_{br}	Vertical permeability of riverside top stratum
k_f	Horizontal permeability of pervious substratum
L	Distance from effective seepage entry to effective seepage exit
L_1	Distance from river to riverside levee toe
L_2	Base width of levee and berm
L_3	Length of foundation and top stratum beyond landside levee toe
M	Slope of hydraulic grade line (at mid-depth of pervious stratum)
Q_s	Total amount of seepage passing beneath the embankment
S	Distance from effective seepage entry to landside toe of levee or berm
x_1	Distance from effective seepage entry to riverside levee toe
x_3	Distance from landside levee toe to effective seepage exit
z	Thickness of top stratum
z_b	Transformed thickness of top stratum for head computation
z_{bl}	Transformed thickness of landside top stratum
z_{br}	Transformed thickness of riverside top stratum
z_t	Transformed thickness of landside top stratum for uplift computation

(3) *Effective seepage exit.* The effective seepage exit (point B, Figure C–1) is the hypothetical point along an impervious top stratum where a vertical open drainage face would approximate actual flow conditions through the landside foundation. This point is

also defined as the point where the HGL beneath the levee projected landward with a slope M intersects the groundwater or tailwater.

(4) *Open entrances, exits, and seepage blocks.* Many types of geologic features can be incorporated in BT by treating a foundation feature as either a block in the aquifer or an opening in the blanket. For example, the thickened landside blanket in Figure C–1 can be represented as a blocked seepage exit where L_3 is the distance from the levee toe to the seepage block. A blocked exit results in a longer x_3 distance, while an open exit results in a shorter x_3 distance. These equations are provided in EM 1110-2-1913 and USACE 1956a.

(5) *Uplift beneath the blanket.* Points A and B in Figure C–1 define the HGL with slope M , and it is straightforward to evaluate the excess uplift pressure acting beneath the top stratum at the landside toe. Equations are also provided in EM 1110-2-1913 and USACE 1956a to determine excess uplift pressure beneath a semi-pervious blanket for any x -location landside of the embankment toe. It is helpful for understanding BT equations to recognize M can be expressed in terms of the effective entrance and exit points as shown in equation C–2. The excess head at the landside toe, h_o , is determined from equation C–3.

$$M = \frac{H}{x_1 + L_2 + x_3} \quad (\text{C-2})$$

$$h_o = H \left(\frac{x_3}{x_1 + L_2 + x_3} \right) \quad (\text{C-3})$$

(6) *Quantity of seepage.* The quantity of underseepage per unit length of embankment can be evaluated from equation C–4 and all four terms are defined in Table C–1. Note that equation C–3 is the general seepage equation based on Darcy’s Law. In BT terms, the quantity of underseepage per unit length of embankment is equation C–5.

$$Q_s = Mk_f d \quad (\text{C-4})$$

$$Q_s = k_f H \frac{d}{(x_1 + L_2 + x_3)} \quad (\text{C-5})$$

(7) *Blanket Theory cases.* Eight BT cases shown in Figure C–2 are presented in USACE 1956a and EM 1110-2-1913, but only the equations for a semipervious blanket of infinite length are presented below (Case 7 in Figure C–2). Other equations are used to consider open entrances, exits, and seepage blocks discussed in paragraph C–3c(7).

(8) *Infinite waterside blanket (for $L_1 = \text{infinite distance}$).* Equation C–6 can be used to calculate x_1 for the infinite waterside blanket case. For levees, the river is a source at finite distance L_1 and a slightly different equation for x_1 is used. Also, borrow pits are

common and treated as an open entrance as described in the previous paragraph. Consult USACE 1956a and EM 1110-2-1913 for equations appropriate for conditions other than the infinite blanket case.

$$x_1 = \frac{1}{c} = \sqrt{\frac{k_f z_{br} d}{k_{br}}} \quad (C-6)$$

Where c is a riverside factor (equation C-7):

$$c = \sqrt{\frac{k_{br}}{k_f z_{br} d}} \quad (C-7)$$

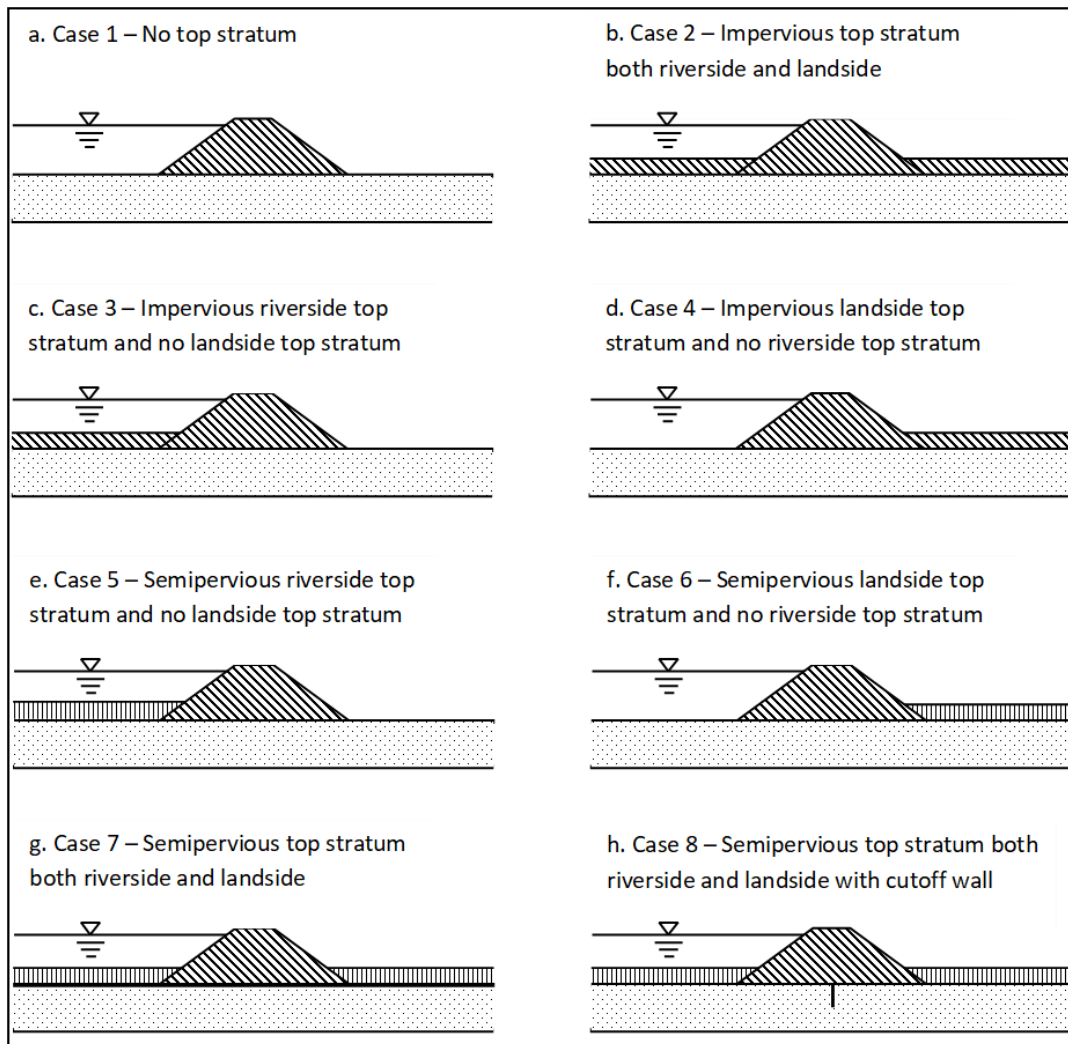


Figure C-2. The eight cases covered by the Blanket Theory

(9) *Infinite landside blanket (for $L_3 = \text{infinite distance}$).* Equation C–8 can be used to calculate x_3 for the infinite landside blanket case. Landside swales and drainage ditches are a common open exit that is described above. Also, levees often have a landside bluff, paved surfaces, or a thicker blanket at a known distance that creates a seepage block. Consult USACE 1956a and EM 1110-2-1913 for equations appropriate for conditions other than the infinite blanket case.

$$x_3 = \frac{1}{C} = \sqrt{\frac{k_f z_{bl} d}{k_{bl}}} \quad (\text{C-8})$$

where C is a landside factor (equation C–9):

$$c = \sqrt{\frac{k_{bl}}{k_f z_{bl} d}} \quad (\text{C-9})$$

(10) *No waterside or landside blanket.* Where no waterside or landside blanket is present and the aquifer is exposed at the toe of the embankment, the x_1 or x_3 distance is simply $0.43*d$.

d. Factors involved in Blanket Theory analysis with relief wells. Key factors from BT in Figure C–1 are included in Figure C–3 to describe the incorporation of relief wells in BT calculations. Parameters related to relief well analysis are described in Chapter 5, and many are listed here in Table C–2.

(1) *Change in hydraulic grade line at the line of wells, ΔM .* The presence of a line of relief wells at the toe of the levee creates two distinct HGLs of different piezometric slope. These two lines are: 1) the HGL on the entrance side of the well line, and 2) the HGL on the exit side of the well line (Figure C–3). The equation for ΔM is given in Chapter 5 of this manual and included here as equation C–10. This factor is simply the difference in the hydraulic grade line from the entrance side of the line of wells to the exit side as shown in Figure C–3.

$$\Delta M = \frac{H - H_{av}}{S} - \frac{H_{av}}{x_3} \quad (\text{C-10})$$

(2) *Excess head without well loss.* Excess head without well losses along well line, h_{av} , and midway between wells, h_m are shown in equations C–11 and C–12. The dimensionless well factors θ_{av} and θ_m are described in Chapter 5.

$$h_{av} = a (\Delta M)(\theta_{av}) \quad (\text{C-11})$$

$$h_m = a (\Delta M)(\theta_m) \quad (\text{C-12})$$

(3) *Excess head with well loss.* Excess head in the well line, with well losses, can be expressed as H_{av} , the average head, and H_m , the head midway between wells, as shown in equations C-13 and C-14. H_w is the total well loss, including elevation and efficiency, as described in Chapter 9.

$$H_{av} = H_w + h_{av} \quad (C-13)$$

$$H_m = H_w + h_m \quad (C-14)$$

(4) *Quantity of seepage with wells.* The quantity of flow to a single well, Q_w , is determined from equation C-15. The seepage for a reach with wells is equal to flow from the well system plus the seepage beyond the well system. Seepage beyond the well system, Q_{sw} , is computed by equation C-16, and similar in form to equation C-5.

$$Q_w = a (\Delta M) (\bar{k}_f) (\bar{D}) \quad (C-15)$$

$$Q_{sw} = \frac{\bar{k}_f \times \bar{D} \times H_{av}}{x_3} \quad (C-16)$$

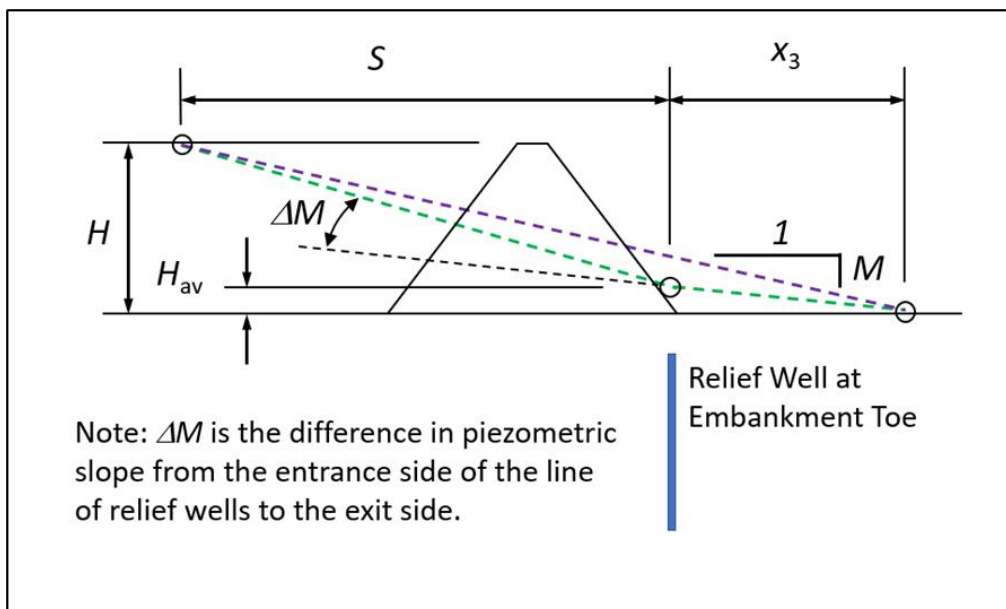


Figure C-3. Illustration of change in pressure due to line of relief wells

Table C-2
Additional factors to include in a Blanket Theory seepage analysis for an infinite line of relief wells

Factor	Definition
a	Well spacing
ΔM	Change in hydraulic grade line due to wells
H_{av}	Average excess head at the location of the well line including well losses
h_{av}	Average excess head at the location of the well line
H_m	Excess head midway between wells including well losses
h_m	Excess head midway between wells
H_w	Total well losses (including elevation and efficiency)
Q_w	The quantity of flow to a single well
Q_{sw}	Seepage beyond the well system

(5) *Steps to analyze or design an infinite line of wells.*

- (a) For design, start by selecting trial values for a , r_w , and W/D .
- (b) Determine θ_{av} and θ_m .
- (c) Assume H_{av} .
- (d) Calculate ΔM from equation C-10.
- (e) Calculate h_{av} from equation C-11.
- (f) Calculate Q_w from equation C-15.
- (g) Determine H_w from Q_w using the methods in Chapter 9.
- (h) Calculate H_{av} from equation C-13.
- (i) If H_{av} in paragraph (h) above differs from paragraph (c) above, return to step (c) using the value for H_{av} determined in step (h).
- (j) Calculate h_m from equation C-12.
- (k) Calculate H_m from equation C-14.
- (l) If H_m is larger than the target allowable head, try a different combination of a , r_w , and W/D .

Note. If W/D is less than 50% and x_3 is an order of magnitude larger than well spacing, a , the head downstream of the well line may be larger than the head midway between wells. In those cases, H_d and θ_d should be checked in addition to H_m and θ_m using equation 5-15 and Figure 5-6.

Appendix D Image Well Theory and Other Analytical Well Solutions

D–1. Applicability

Analytical procedures for determining well flows and head distributions adjacent to artesian relief wells using image well theory are presented below. By definition, relief wells signify artesian conditions, and equations for artesian flow are applicable. In cases where wells are pumped and gravity flow conditions exist, procedures for well analysis can be found in UFC 3-220-05.

D–2. Assumptions

It is assumed in the following analyses that all seepage flow is laminar and viscous (Darcy's Law is applicable). It is also assumed that steady-state conditions prevail; the rate of seepage and rate of head reduction have reached equilibrium and are not time dependent.

D–3. Flow from a circular source

Certain geologic or terrain conditions may require assuming a circular source of seepage.

a. *Single well.* Where there is a single well in a confined aquifer of infinite extent, this circular source is termed the radius of influence. The formulas for a full-penetration well located at the center of a circular source (see Figure D–1) are:

$$h_p = H - \frac{Q_w}{2\pi kD} \ln \frac{R}{r} \quad (\text{D-1})$$

$$h_w = H - \frac{Q_w}{2\pi kD} \ln \frac{R}{r_w} \quad (\text{D-2})$$

where:

H = gross head on the system

Q_w = discharge from the well

R = radius of influence of the well

k = permeability

D = thickness of aquifer

r = distance from the well to the point at which head is computed

h_p = head at point of interest, p

h_w = head at the radius of the well, r_w

Note. Equations D–1 and D–2 have the same general form and h_w in this equation does not represent well losses. Likewise, the head at any point, h_p , does not include well losses.

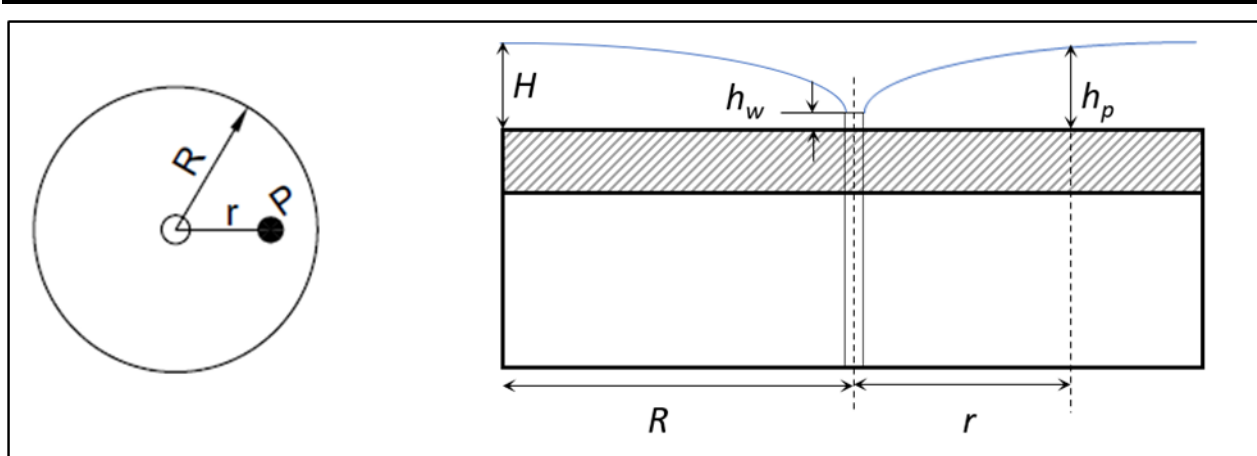


Figure D-1. Artesian flow to a single well with a circular source

b. *Multiple well systems.* In many applications, a system of pressure relief wells with wells located in various spatial arrangements is required. The head at any location, p , produced by a system of full-penetration wells was first determined by Forchheimer (1914). His general equation, as later modified by Dachler (1936), is:

$$h_p = H - \frac{1}{2\pi kD} \left(\sum_{i=1}^{i=n} Q_{wi} \ln \frac{R_i}{r_i} \right) \quad (D-3)$$

where:

H = gross head on the system

n = number of wells

k = permeability

D = depth of aquifer

Q_{wi} = discharge from the i^{th} well

R_i = radius of influence of the i^{th} well

r_i = distance from the i^{th} well to the point at which head is computed

h_p = head at point of interest, p

c. *Superposition.* The multiple well system equations are based on the principle of superposition. The head at a given well is the head resulting from the well flowing as if no other wells are present minus the head reduction caused by the other wells within the radius of influence. When wells are pumped, the values of Q_{wi} are known or assumed. When wells are used for pressure relief under artesian conditions, the flow from each well must be computed considering the discharge elevation of each well. The procedure requires either the solution of n simultaneous equations to determine individual well flows or the assumption of known head at each well location. If the head is assumed at each well location, it must be equal to the discharge elevation plus any well losses. This requires iterative calculations because well losses are a function of well flow.

d. *Multiple wells with a circular source, general case.* The general equations for a group of full-penetration wells subject to seepage from a circular source with radius, R , are shown in Figure D-2. The assumption for this case is that the radius, R , is large with respect to the distances between wells. Figure D-2 is drawn with h_w equal to the ground surface elevation. Other equations for special arrays of wells are included in UFC 3-220-05 but are outside the scope of this manual.

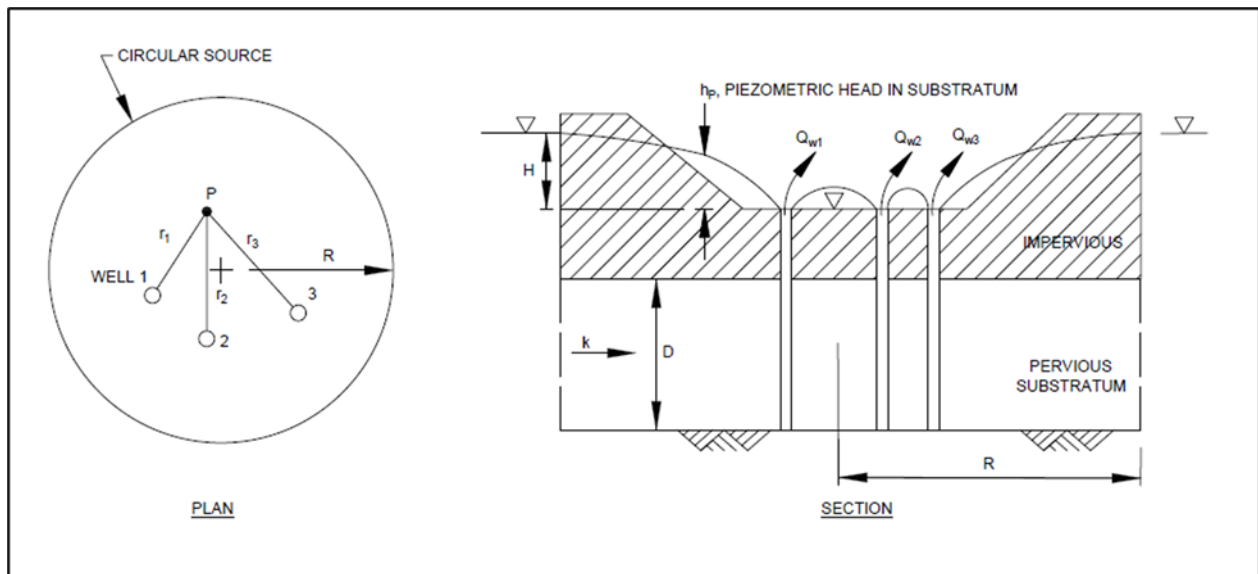


Figure D-2. Artesian flow to multiple wells with a circular source
(adapted from U.S. Army 1983)

e. *Noncircular source.* If geologic or terrain conditions indicate a non-circular source of seepage, the same equations can be used. The radius of influence, R , is simply replaced by A_c , defined as an effective average of the distance from the well center to the external boundary. For a rectangular boundary of sides $2a$ and $2b$, the value A_c is equation D-4:

$$A_c = \sqrt{\frac{4ab}{\pi}} \quad (D-4)$$

D-4. Line sources

Although the circular source is a common assumption for wells in general, most relief wells are used adjacent to a linear source. A usual case for dams and levees is to have multiple wells with a reservoir upstream of a linear dam or along a levee following a river. The river or lake opposite a well or multiple wells along the toe of a levee or dam may be approximated by a line source.

a. *Finite line source.*

(1) In cases where the length of the source of seepage is relatively small compared to its distance from the well, the source may be considered as a finite line source. The solution for a single well adjacent to a finite line source was developed by Muskat (1937). The formulas, which are available only in terms of head at the well, are shown in equations D-5 and D-6 using Figure D-3, where c is half the length of the line source.

$$h_w = H - \frac{Q_w}{2\pi kD} \ln \frac{4S}{r_w} \left[\frac{(c^2 - r_o^2)^2 + 4S^2c^2}{c^2r_o^2\sqrt{(c^2 - r_o^2)^2 + 4S^2c^2}} \right] \quad (D-5)$$

(2) For a well located on a perpendicular bisector, $r_o = S$, and this simplifies to:

$$h_w = H - \frac{Q_w}{2\pi kD} \ln \frac{2S}{r_w} \left(1 + \frac{S^2}{c^2} \right) \quad (D-6)$$

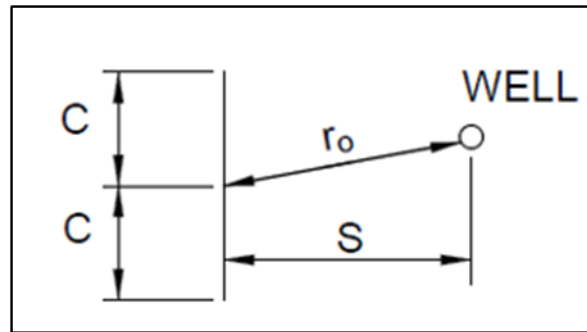


Figure D-3. Artesian flow to a single well with a finite line source

b. *Infinite line source.* Conditions may arise where the flow to the well originates from the bank of a river or canal reservoir or another body of water. In such cases, the bank or shoreline may act as an infinite line source of seepage. If leakage occurs through the top stratum, the effective distance to the infinite line source of seepage should be computed as discussed in Appendix C.

(1) *Single well.*

(a) Solutions for a single well adjacent to an infinite line source (see Figure D-4) is determined using the method of images described by Muskat (1937), Todd (1980), and EM 1110-2-1901. The formulas are equations D-7 and D-8:

$$h_p = H - \frac{Q_w}{2\pi kD} \ln \frac{r'}{r} \quad (\text{D-7})$$

$$h_w = H - \frac{Q_w}{2\pi kD} \ln \frac{2S}{r_w} \quad (\text{D-8})$$

(b) A solution for h_p is also presented in terms of x and y coordinates in equation D-9 and shown in Figure D-4.

$$h_p = H - \frac{Q_w}{2\pi kD} \ln \left[\frac{y^2 + (x + s)^2}{y^2 + (x - s)^2} \right]^{\frac{1}{2}} \quad (\text{D-9})$$

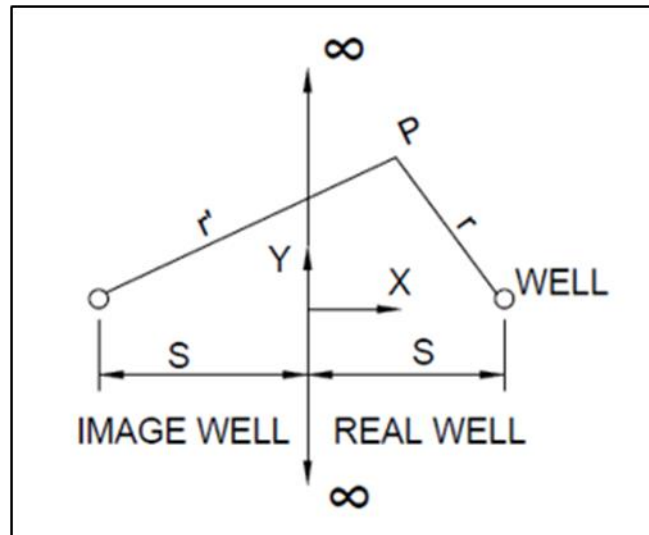


Figure D-4. Artesian flow to a single well with an infinite line source and variables to calculate head at point of interest, P

(2) *Image Well Method applied to multiple wells.* The method of images is an extremely powerful tool for developing solutions to wells for various boundary conditions. Solutions for various boundary conditions including barriers are presented by Ferris, Knowles, Brown, and Stellman (1962), Freeze and Cherry (1979), and Todd (1980).

(3) *Multiple wells with a linear source using image wells.* Where wells are located adjacent to a source that can be approximated by an infinite line source, and the pervious stratum is overlain by an impervious top stratum extending infinitely landward, a solution for heads and well flows using image wells is shown in Figure D-5. Equation D-10 is the general case where the flow from each well is variable. This approach can be used in combination with Blanket Theory as described in Chapter 6, with examples provided in Appendix I. Equations D-11 and D-12 can be used when the discharge for wells is equal.

$$h_p = H - \frac{1}{2\pi kD} \sum_{i=1}^{i=n} Q_{wi} \ln \frac{r_i}{r_i} \quad (D-10)$$

$$h_p = H - \frac{nQ_w}{2\pi kD} \sum_{i=1}^{i=n} \ln \frac{r_i}{r_i} \quad (D-11)$$

$$Q_w = \frac{2\pi kD (H)}{\ln \frac{2S_j}{r_w} + \sum_{i=1}^{i=n, i \neq j} \ln \frac{r_i}{r_i}} \quad (D-12)$$

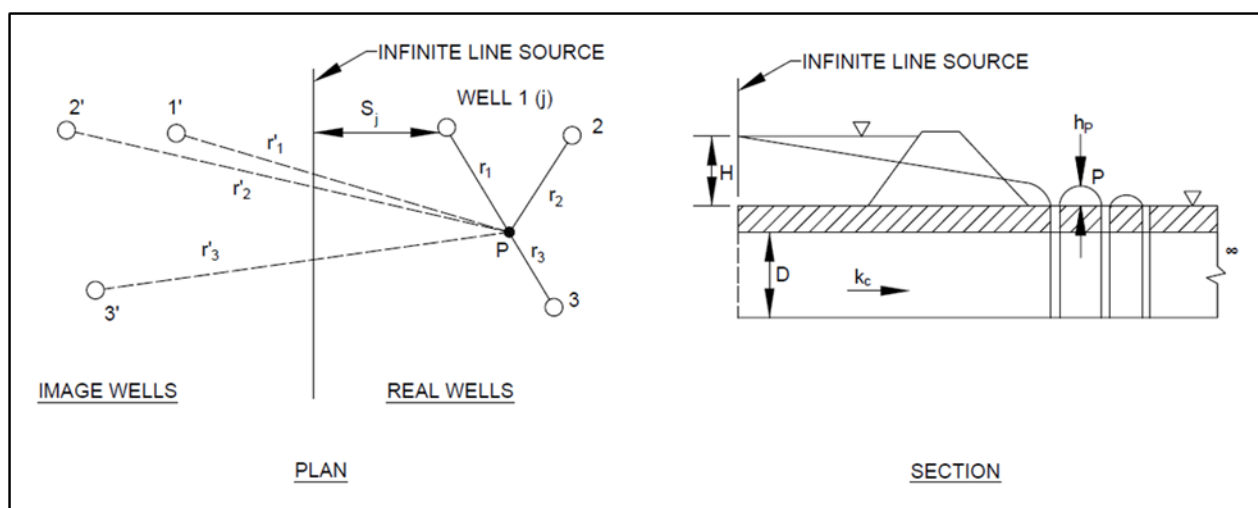


Figure D-5. Artesian flow to multiple wells with an infinite line source with variables shown for calculating head at point of interest, P

(4) *Infinite line source and infinite line sink.* The theoretical line sink, parallel to the infinite line source, is referred to as an infinite line sink. Barron (1948) developed a solution also based on the method of images, considering one of the infinite line sources as a sink.

(5) *Infinite line source and infinite line barrier.* Wells located between a river denoted by an infinite line source and a barrier such as a buried channel or rock bluff are another typical problem. In this case, the image well for the river would have a second image well with respect to the rock bluff, which, in turn, would have an image with respect to the river, and so on. Barron (1982) presented a solution for this case.

D-5. Complex boundary conditions

Geologic factors may impose conditions that are difficult to simulate using circular or line sources and barriers. These simple approaches do not include irregular aquifer thickness or blanket composition. In such cases, finite-element or finite-difference models are used as described in Chapter 6. Flow net analyses or electrical analogy

tests were used to advantage at many USACE projects that required 3D analyses. Mansur and Kaufman (1962) described the use of flow nets for designing well systems. USACE (1963), USACE (1965), and McAnear and Trahan (1972) all described methods for conducting 3D electrical analogy tests. These references are applicable to all three approaches.

Appendix E Partial-Penetration Wells and Stratified Aquifers

E-1. Well penetration

Unless otherwise indicated, most analyses assume wells penetrate the full thickness of the aquifer. For practical reasons, it is often necessary to use wells that only partially penetrate the aquifer. For aquifers with uniform permeability, the calculation of penetration percentage, W/D , is straightforward. For stratified aquifers, an aquifer transformation as described in paragraph E-1b(1) is required for this calculation.

a. Partial-penetration wells in a homogeneous aquifer.

(1) The ratio of flow from a partial-penetration artesian well, Q_{wp} , to that of a full-penetration well at the same drawdown, Q_w , is defined as G_p and is shown in equation E-1. Values of G_p based on the values in Table E-1 for an effective well radius, r_w , of 1.0 foot and a radius of influence, R , of 1,000 feet are plotted in Figure E-1.

$$\frac{Q_{wp}}{Q_w} = G_p \quad (\text{E-1})$$

or

$$Q_{wp} = G_p Q_w = \frac{2\pi kD(H - h_w)G_p}{\ln \frac{R}{r_w}} \quad (\text{E-2})$$

(2) An approximate value of G_p can be obtained from equation E-3 as developed by Kozeny (1933).

$$G_p = \frac{W}{D} \left(1 + 7 \sqrt{\frac{r_w}{2W}} \cos \frac{\pi W}{2D} \right) \quad (\text{E-3})$$

(3) Another estimate of G_p can be obtained by equation E-4, as developed by Muskat (1937), assuming a constant flow per unit length of well screen. In Muskat's equation, the partial-penetration well function, $G(\bar{T})$, is a function of W/D with approximate values from Harr (1962) given in Table E-1. Values of G_p based on Muskat's equation for a well with an effective radius (r_w) of 1.0 foot and a radius of influence (R) of 1,000 feet are plotted in Figure E-1.

$$G_p = \frac{\ln \frac{R}{r_w}}{\frac{D}{2W} \left[2 \ln \frac{4D}{r_w} - G(\bar{T}) \right] - \ln \left(\frac{4D}{R} \right)} \quad (\text{E-4})$$

Table E-1
Partial-penetration well function, $G(\bar{T})$ (Harr 1962)

W/D	$G(\bar{T})$
.1	6.4
.2	5.0
.3	4.3
.4	3.5
.5	2.9
.6	2.4
.7	1.9
.8	1.3
.9	0.7
1.0	0.0

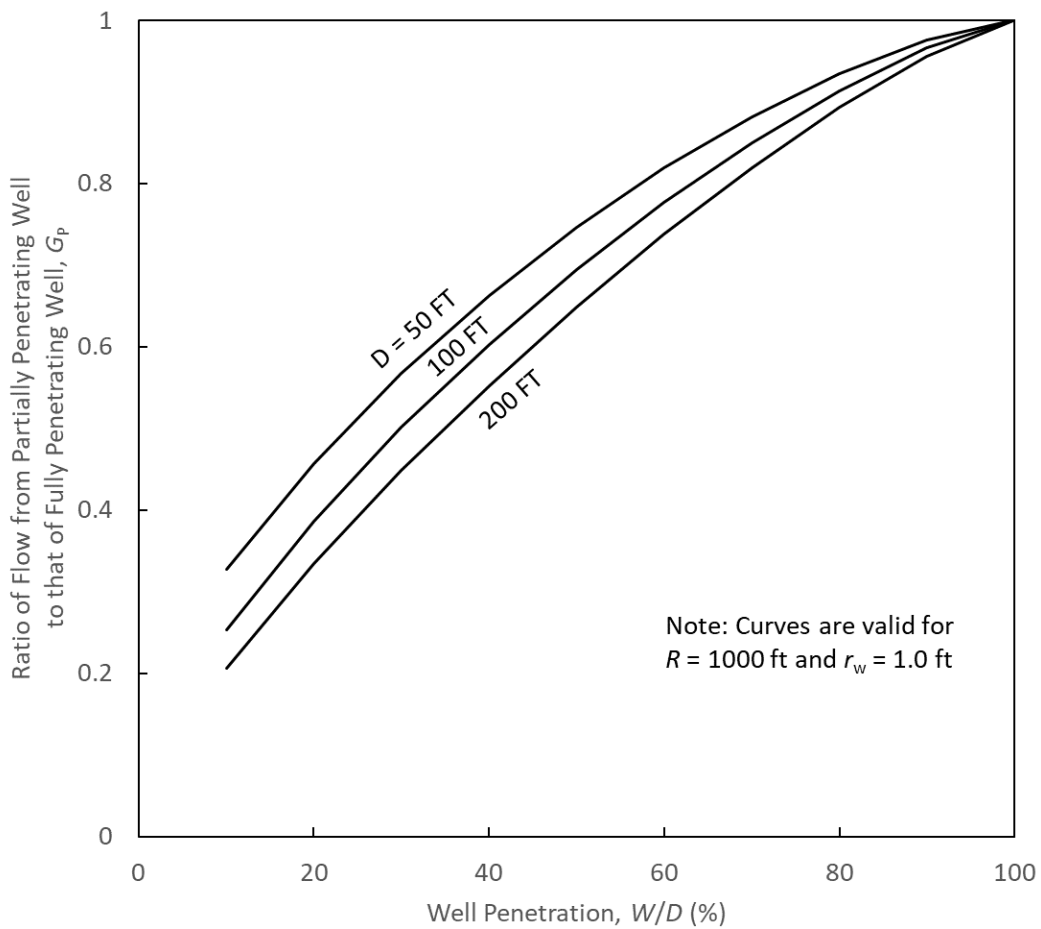


**Figure E-1. Flow to partial-penetration well (W/D versus G_p)
with circular source (after Harr 1962)**

b. *Effective well penetration in a stratified aquifer.*

(1) In a stratified aquifer, flow is concentrated in the more permeable layers. Therefore, the effective well penetration usually differs from the actual penetration, which is computed from the ratio of well screen length to total aquifer thickness. The effective penetration in a stratified aquifer is a function of the transformed aquifer thickness and effective screen length. An aquifer transformation allows a stratified aquifer to be represented as a single uniform layer as shown in equation E-5.

(2) The effective screen length, for an individual layer, \bar{w} , is the product of horizontal permeability, k_h , and layer thickness. The effective screen length for the aquifer, \bar{W} , is the sum of \bar{w} for all layers. The effective well penetration, \bar{W}/\bar{D} , is then the ratio of the effective screen length to the transformed aquifer thickness, \bar{D} , as shown in equation E-7. Figure E-2 illustrates the concept of transformed thickness and effective penetration. The following steps can be used to determine these parameters.

(3) A foundation often consists of one or more anisotropic strata. In such cases a transformation is required to use analytical methods, including BT, that assume a single isotropic layer. Transformation into an isotropic stratum is done according to equations E-5 and E-6. These equations are appropriate for transforming a stratified aquifer where the individual strata are either all isotropic or anisotropic, or some combination of both. In the case of isotropic strata, horizontal and vertical permeability (k) are equal in equation E-5 ($k_h = k_v$). The horizontal dimension of the problem remains unchanged in this transformation.

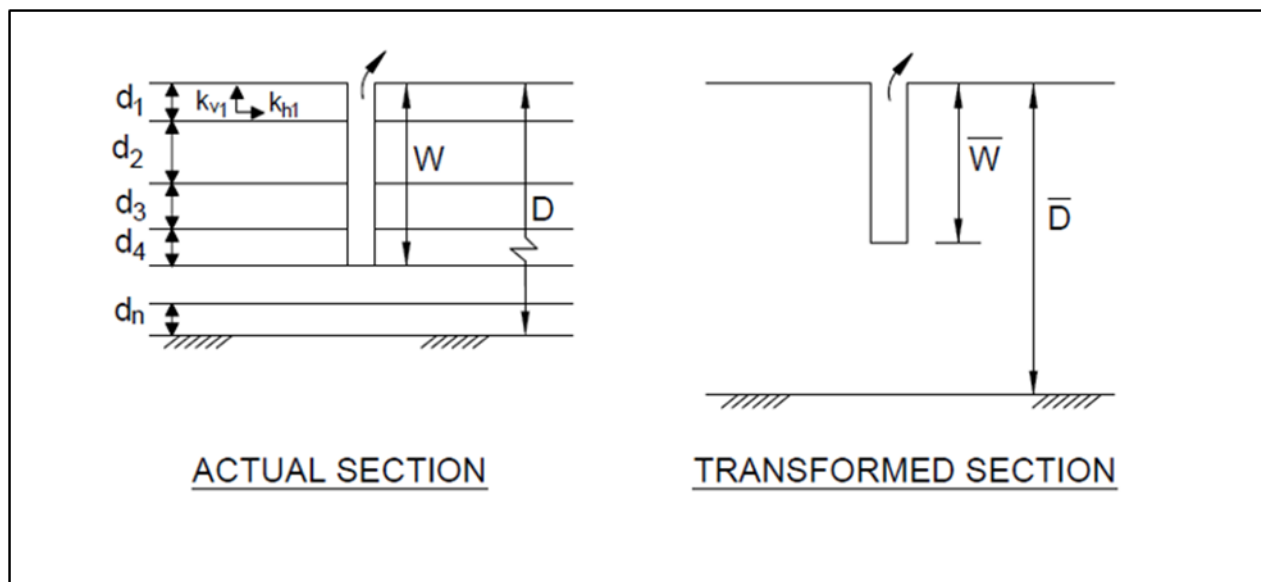


Figure E-2. Comparison of actual and effective well penetration

(4) Calculate the thickness of the equivalent homogeneous, isotropic aquifer, \bar{D} , using equation E-5. The number of strata, n , is numbered from top to bottom as shown in Figure E-2.

$$\bar{D} = \sqrt{\sum_{m=1}^{m=n} d_m k_{hm} \sum_{m=1}^{m=n} d_m / k_{vm}} \quad (\text{E-5})$$

(5) Calculate the effective permeability of the transformed aquifer, \bar{k}_e , using equation E-6.

$$\bar{k}_e = \sqrt{\frac{\sum_{m=1}^{m=n} d_m k_{hm}}{\sum_{m=1}^{m=n} d_m / k_{vm}}} \quad (\text{E-6})$$

(6) Calculate the effective well screen penetration into the transformed aquifer, \bar{W}/\bar{D} , using equation E-7.

$$\frac{\bar{W}}{\bar{D}} = \frac{\sum_0^W \bar{d}\bar{k}}{\int_{m=1}^{m=n} d_m k_m} = \frac{\sum_0^W \bar{d}\bar{k}}{\bar{D} \bar{k}_e} = \frac{\sum_0^W dk_h}{\sum_{m=1}^{m=n} d_m k_{hm}} \quad (\text{E-7})$$

(7) In many cases the designer initially determines the effective penetration needed to achieve the desired pressure relief. The approach above is then used iteratively to determine the actual well penetration required to reach the effective well penetration. This is most easily accomplished by various trials in an Excel spreadsheet.

(8) The stratified aquifer transformation generally assumes that the actual well penetration and effective penetration begin at the top of the aquifer. However, blank sections are sometimes for thin layers of low k at the top of the aquifer. These blank sections will not have a significant impact on the seepage results using an aquifer transformation and the effective penetration. However, Physical Model D in TM 3-304 demonstrated that when an aquifer is composed of two layers nearly equal in thickness, with the upper layer having substantially lower k than the base layer, blanking of the upper layer had a significant impact on seepage results. This impact was much larger than the change in effective penetration normally indicates. For this reason, where the upper blank sections of a well system are significant in length compared to the overall aquifer depth, evaluation using 3D FEM may be warranted.

E-2. Transformation example

TM 3-304 (USACE 1949) documents physical model studies performed at ERDC, formerly the WES, on various scaled uniform and stratified models. In this example, models A-a-1 and B-a from TM 3-304 are used to demonstrate the effects of aquifer transformation on effective well penetration when using the methods described above. Model A-a-1 simulated a uniform aquifer and Model B-a simulated a stratified aquifer. Each model assumed the same average k for the foundation and each had similar

boundary conditions. Therefore, comparison of these two models serves as a suitable case study. Schematics for each model are shown in Figure E-3 and Figure E-4.

a. Each model was evaluated with a range of well spacing (29, 58, 87, and 130 feet) and actual well penetrations of 100%, 50%, and 25%. Model A-a-1 assumes a uniform aquifer; thus, the effective and actual penetrations are equal. Model B-a was evaluated for physical penetrations of 100%, 50%, 25%, and 10%. Since Model B-a is a stratified aquifer with layers of varying thickness and permeability, an effective penetration must be used for each scenario. This is required when using analytical methods such as BT or image wells.

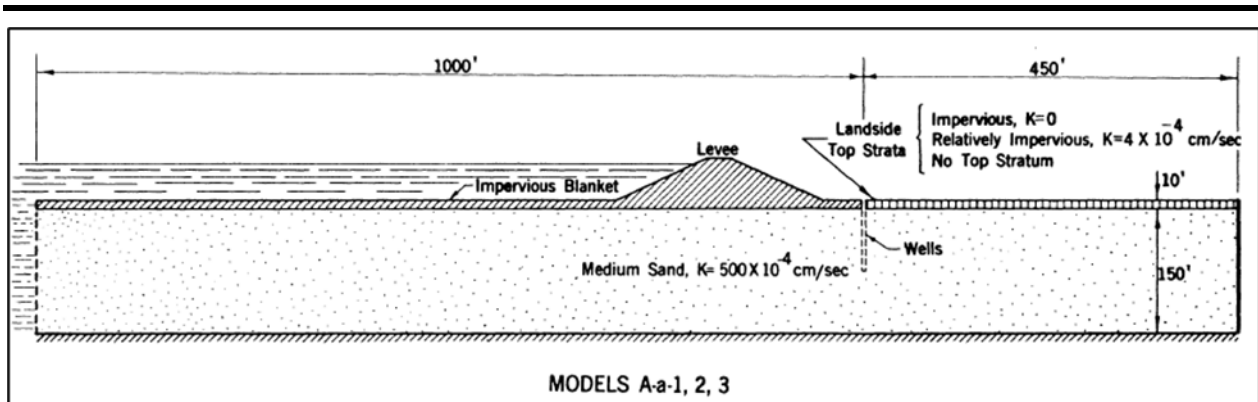


Figure E-3. Schematic of physical model test with a uniform sand aquifer

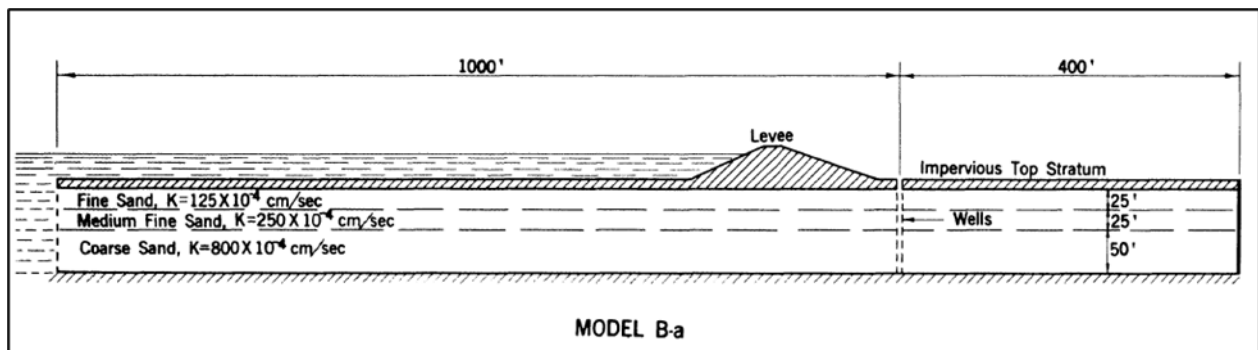


Figure E-4. Schematic of physical model test with a stratified sand aquifer

b. The results of the aquifer transformation for Model B-a are shown in Figure E-5. Since the lower portions of the aquifer have a higher k than the upper portions, they weigh more heavily on the formulated (\bar{k}_e) . Due to this, effective penetrations for partial-penetration wells in Model B-a (2.5% to 18.6%) are substantially less than the actual penetrations (10% to 50%). This result demonstrates the importance of understanding aquifer characteristics and analyzing partial-penetration wells in terms of effective penetration.

c. The relationship between effective penetration and the net foundation head predicted by BT for Model A-a-1 and Model B-a is shown in Figure E-5. The observed net head from both models aligns well when plotted against effective penetration (solid

lines). However, net head for Model B-a (dashed lines) differs significantly from that for Model A-a-1 when plotted against the actual penetrations. These differences demonstrate yet again the importance of transforming a stratified aquifer and using effective penetration for partial-penetration wells when applying an analytical solution.

d. Figure E–5 also illustrates that partial-penetration wells can dramatically reduce well system performance. The effects of partial penetration on head reduction are relatively minor at effective penetrations greater than 50%, especially for more closely spaced wells. However, between effective penetrations of 50% and 25%, the well system performance begins to be more sensitive to changes in effective penetration. For effective penetrations less than 25%, there are significant effects. Partial penetrations in this range introduce significant changes in effectiveness for small changes in effective penetration. Effective penetrations of less than 25% should be considered very carefully before they are used in practice. To reduce sensitivity of drawdown to small changes in effective penetration, effective penetrations greater than 50% are typically recommended.

e. BT was used to replicate the physical lab test for Model B-a. The range in relief well penetration and spacing shown in Table E–2 and Figure E–5 were considered. The impermeable plexiglass top used in the physical models was represented in BT as a low permeability layer (10^{-10} cm/second, or approximately 0.0315 mm/year). This mimicked a condition of negligible flow through the blanket. Results for this base case are described in the following paragraphs. Figure E–6 shows model constraints assumed for BT analysis and matching those of Model B-a. The aquifer in Figure E–6 is the transformed case, as required by BT.

Table E-2
Calculation of effective well penetration for Model B-a in Figure E-4

	k_h	k_v	k-ratio	Layer Thickness, d_m	Screen Length, w_m	\bar{k}	$d_m k_{hm}$	d_m/kv_m	$w_m k_{hm}$		
Soil	ft/d	ft/d	k_h / k_v	ft	ft	(ft/day)	(ft ² /day)	(day)	(ft ² /day)		
Sand 1	42.520	42.520	1.0	25	25	42.520	1,063.000	0.588	1,063.000		
Sand 2	81.638	81.638	1.0	25	25	81.638	2,040.950	0.306	2,040.950		
Sand 3	272.126	272.126	1.0	50	50	272.126	13,606.300	0.184	13,606.300		
				D= Σ =	100	W= Σ =	100	Σ =	16,710.250	1.078	16,710.250
						Effective Aquifer Depth	$\bar{D} =$	134.210	ft	Actual	
						Effective Aquifer Permeability	$\bar{k}_e =$	124.508	ft/day	Penetration	
						Effective Screen Length	$\bar{W} =$	134.210	ft	W/D	
						Effective Penetration	$\bar{W}/\bar{D} =$	100%	=	100%	
	k_h	k_v	k-ratio	Layer Thickness, d_m	Screen Length, w_m	\bar{k}	$d_m k_{hm}$	d_m/kv_m	$w_m k_{hm}$		
Soil	ft/d	ft/d	k_h / k_v	ft	ft	(ft/day)	(ft ² /day)	(day)	(ft ² /day)		
Sand 1	42.520	42.520	1.0	25	25	42.520	1,063.000	0.588	1,063.000		
Sand 2	81.638	81.638	1.0	25	25	81.638	2,040.950	0.306	2,040.950		
Sand 3	272.126	272.126	1.0	50	0	272.126	13,606.300	0.184	0.000		
				D= Σ =	100	W= Σ =	50	Σ =	16,710.250	1.078	3,103.950
						Effective Aquifer Depth	$\bar{D} =$	134.210	ft	Actual	
						Effective Aquifer Permeability	$\bar{k}_e =$	124.508	ft/day	Penetration	
						Effective Screen Length	$\bar{W} =$	24.930	ft	W/D	
						Effective Penetration	$\bar{W}/\bar{D} =$	18.6%	<	50%	

	k_h	k_v	k-ratio	Layer Thickness, d_m	Screen Length, w_m	\bar{k}	$d_m k_{hm}$	d_m/kv_m	$w_m k_{hm}$	
Soil	ft/d	ft/d	k_h / k_v	ft	ft	(ft/day)	(ft ² /day)	(day)	(ft ² /day)	
Sand 1	42.520	42.520	1.0	25	25	42.520	1,063.000	0.588	1,063.000	
Sand 2	81.638	81.638	1.0	25	0	81.638	2,040.950	0.306	0.000	
Sand 3	272.126	272.126	1.0	50	0	272.126	13,606.300	0.184	0.000	
				D= Σ =	W= Σ =	Σ =	16,710.250	1.078	1,063.000	
						Effective Aquifer Depth	\bar{D} =	134.210	ft	Actual
						Effective Aquifer Permeability	\bar{k}_e =	124.508	ft/day	Penetration
						Effective Screen Length	\bar{W} =	8.538	ft	W/D
						Effective Penetration	\bar{W}/\bar{D} =	6.4%	<	25%
	k_h	k_v	k-ratio	Layer Thickness, d_m	Screen Length, w_m	\bar{k}	$d_m k_{hm}$	d_m/kv_m	$w_m k_{hm}$	
Soil	ft/d	ft/d	k_h / k_v	ft	ft	(ft/day)	(ft ² /day)	(day)	(ft ² /day)	
Sand 1	42.520	42.520	1.0	25	10	42.520	1,063.000	0.588	425.200	
Sand 2	81.638	81.638	1.0	25	0	81.638	2,040.950	0.306	0.000	
Sand 3	272.126	272.126	1.0	50	0	272.126	13,606.300	0.184	0.000	
				D= Σ =	W= Σ =	Σ =	16,710.250	1.078	425.200	
						Effective Aquifer Depth	\bar{D} =	134.210	ft	Actual
						Effective Aquifer Permeability	\bar{k}_e =	124.508	ft/day	Penetration
						Effective Screen Length	\bar{W} =	3.415	ft	W/D
						Effective Penetration	\bar{W}/\bar{D} =	2.5%	<	10%

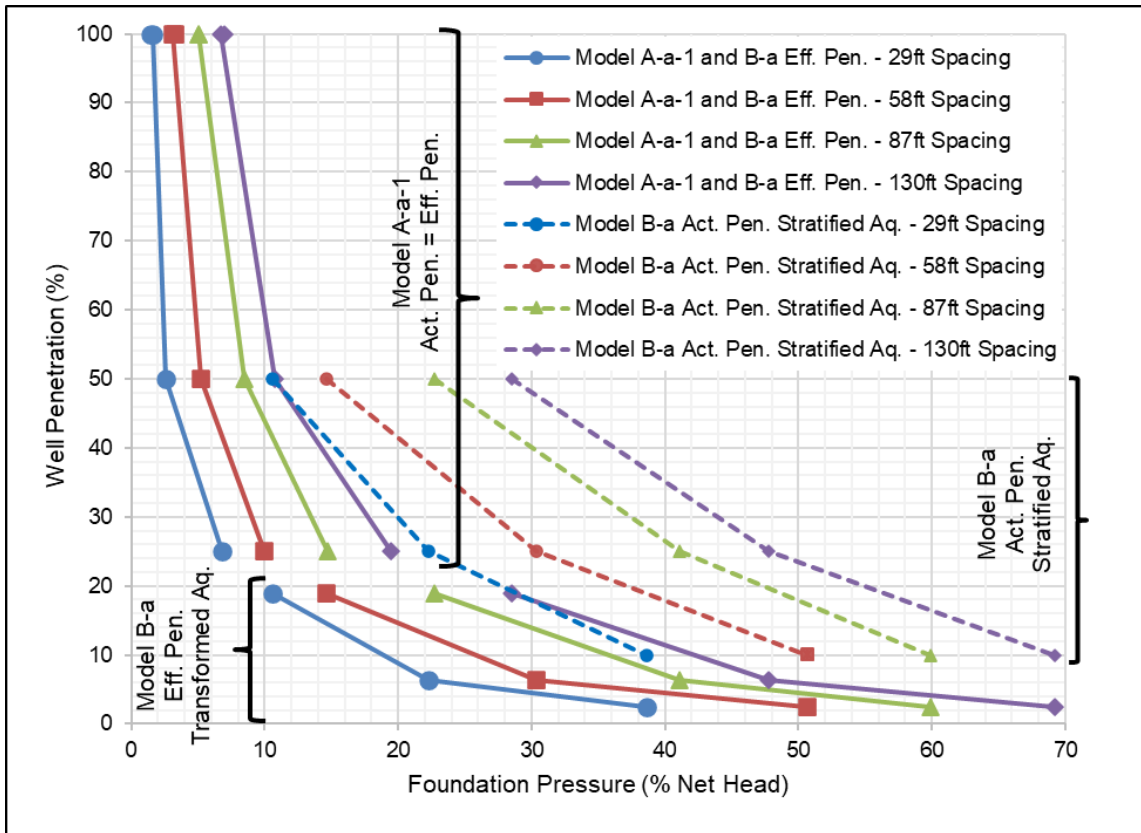
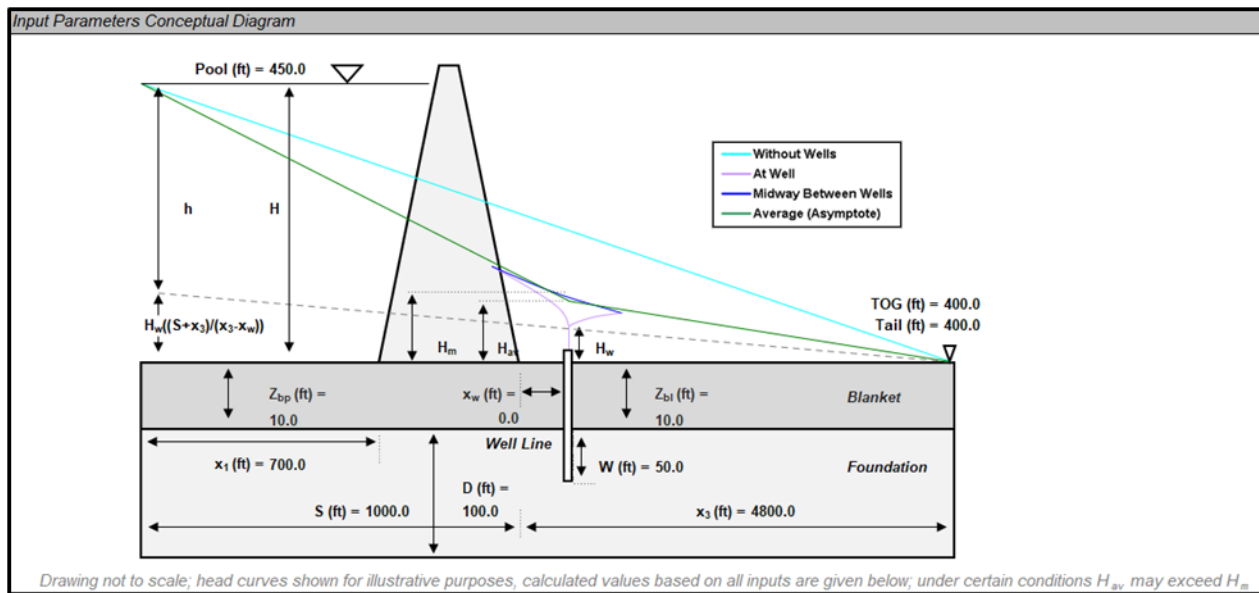


Figure E-5. Effective and actual well penetration versus observed pressure relief for Model A-a-1 and B-a (from Technical Memorandum 3-304)



Drawing not to scale; head curves shown for illustrative purposes, calculated values based on all inputs are given below; under certain conditions H_w may exceed H_m

Figure E-6. Blanket Theory input parameters for the 10^{-10} cm/second blanket condition

f. Mid-well head (H_m) was computed using BT and compared to results from Model B-a.

g. Results of the comparison between BT and Model B-a are shown in Table E-3 and Figure E-7. Results are in general agreement for the 100% W/D case. For scenarios where effective penetration is 19% or less, BT results in estimates of much lower mid-well head (H_m) values.

Table E-3
Comparison of results, Blanket Theory, and physical model, Model B-a

Penetration		Well Spring	Mid-well Head H_m (% H)	
Actual	Effective	(ft)	Physical Model	Blanket Theory
100%	100%	29	1.6	1.0
100%	100%	58	3.1	2.6
100%	100%	87	5.0	4.4
100%	100%	174	8.5	10.2
50%	19%	29	10.6	4.2
50%	19%	58	14.6	11.0
50%	19%	87	22.7	17.4
50%	19%	174	34.5	32.7
25%	6.3%	29	22.3	11.7
25%	6.3%	58	30.4	23.7
25%	6.3%	87	41.1	33.3
25%	6.3%	174	54.2	52.0
10%	2.5%	29	38.6	19.6
10%	2.5%	58	50.7	34.8
10%	2.5%	87	59.9	45.6
10%	2.5%	174	78.7	64.1

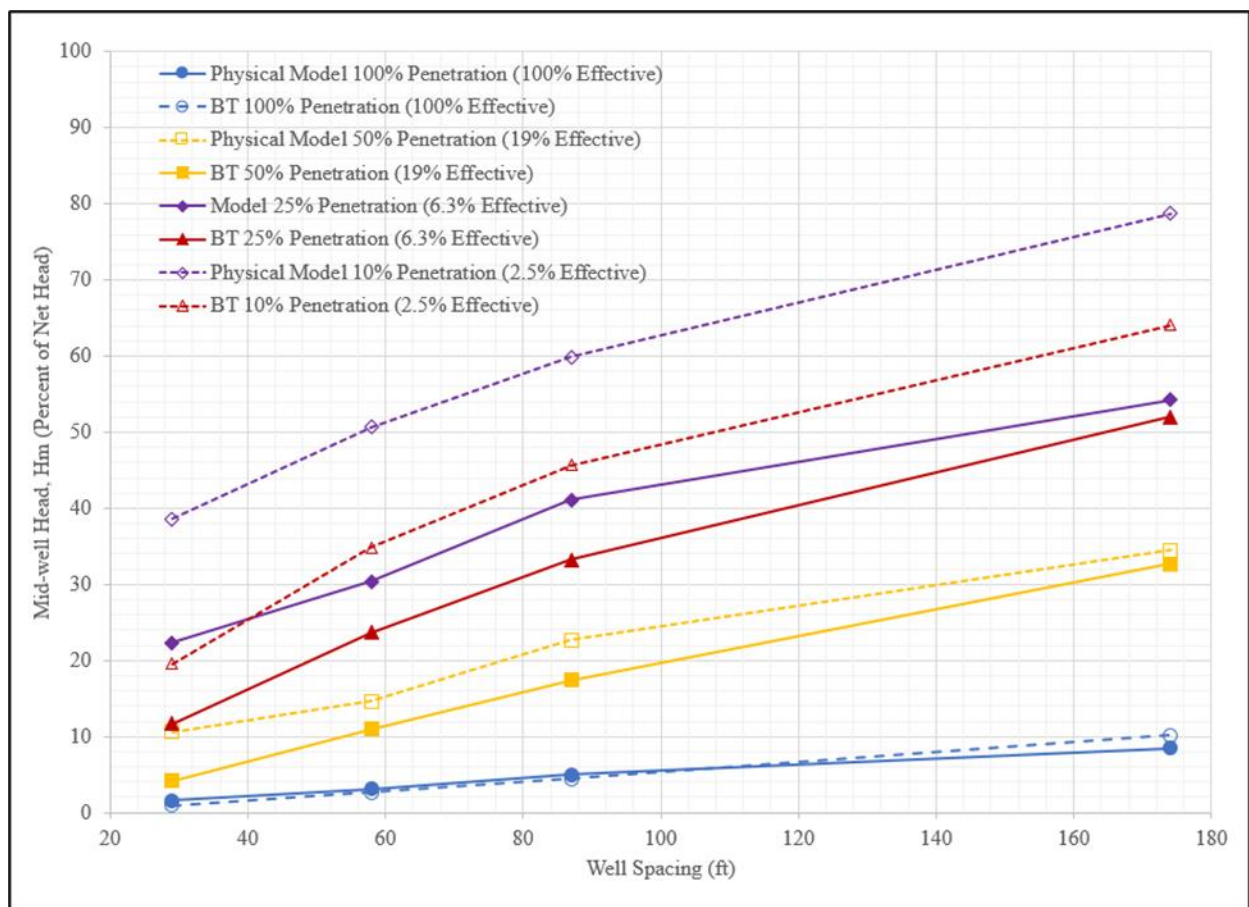


Figure E-7. Comparison of mid-well head, Blanket Theory versus physical model, Model B-a

h. Further comparisons between these BT results with physical model results and 3D seepage analyses are included in Appendix F. The 3D transformation example was modeled using the finite element WASH123D modeling code (Yeh et al. 2006). The primary purpose of the 3D FEM model of this stratified aquifer is to validate the partial-penetration approach described in this appendix. The results confirm using BT with aquifer transformation are reasonable when effective penetration is greater than 25%. It should be noted that the comparisons in Appendix F currently only account for a landside blanket permeability of 10^{-6} cm/second. The model documentation also provides a means for practitioners using 3D FEM software to confirm their approach.

i. Appendix F also includes 3D FEM simulations of features in Model B-a not evaluated in the 1950s physical lab testing. This was done to support the update in this manual. These features include the effects of well efficiency, blank sections at the top of the well above the screen, and a modeled defect representing a sand boil that allows flow through the confining blanket.

Appendix F Three-Dimensional, Finite Element Modeling of Relief Wells in a Transformed Aquifer

F–1. Introduction

A series of 3D numerical groundwater models was built to simulate seepage through pervious strata beneath dams or levees and assess the impact of relief wells on subsurface pressures. The model simulations were designed to replicate selected physical models documented in TM 3-304 (USACE 1949). Results were also compared with relief well flow and mid-well head calculated using BT. The final step was using the model to conduct a series of sensitivity studies, which included modeling a well efficiency of 80%, replacing the top 10 feet of screen in the fine sand with a blank section, and incorporating a 1.5-foot-diameter sand-filled hole to represent a sand boil.

F–2. Model setup

Three numerical groundwater models were constructed using the finite element WASH123D modeling code (Yeh et al. 2006). Each of the models was designed to simulate seepage through pervious foundation materials under a dam or levee and compare a series of relief well spacings and penetrations. Physical model B-a from TM 3-304 was the basis for the model. Features of the numerical model were then modified to demonstrate the impact (or lack of impact) on modeled relief well flow and mid-well head. The features that were manipulated included the downstream boundary and representation of the subsurface stratigraphy.

a. *Model #1: Reproduction of Physical Model B-a (TM 3-304).*

(1) A schematic of physical model B-a from TM 3-304 is shown in Figure F–1(a). In this model, which had a scale ratio of 1:50, the foundation consisted of three sand layers. In descending order, these layers were: a 25-foot fine sand layer, a 25-foot medium sand layer, and a 50-foot coarse sand layer. Each of the layers was isotropic with equal horizontal and vertical hydraulic conductivity (K). The K of these layers increased downward. The K values were 800×10^{-4} cm/second (227 feet/day) for the coarse sand, 250×10^{-4} cm/second (71 feet/day) for the medium sand, and 125×10^{-4} cm/second (35 feet/day) for the fine sand.

(2) The model was constructed in a steel flume where water could not enter or leave through the top, bottom, or sides, perpendicular and downstream of the levee. A plastic plate was used to model the impervious top stratum on both the landside and riverside of the levee. Relief wells were placed at the levee toe, a distance equivalent to 1,000 feet from the upstream boundary and 400 feet from the downstream boundary. The model was run with a range of relief well spacings of 29, 58, 87, and 174 feet, and a range of relief well penetrations of 10%, 25%, 50%, and 100%. Well diameters were equivalent to 2 feet.

(3) Numerical Model #1 was constructed to replicate the thickness and K of each of the permeable subsurface strata in physical model B-a. The distances of the relief wells from the upstream and downstream boundaries were also identical to the scaled physical model. A 10-foot-thick blanket was added above the aquifer in the numerical model and given a K of 0.01×10^{-4} cm/second (0.00283 feet/day). The ground surface coincides with the top of the blanket and was set at an elevation of 410 feet. The bottom of the model is at an elevation of 300 feet. Table F-1 summarizes the details of the modeled stratigraphic layers. A cross section through the numerical model is shown on Figure F-1(b). The horizontal width of the model (parallel to the levee) was set to 870 feet so that multiple relief wells could be modeled in three dimensions.

(4) The same relief well spacings, penetrations, and well diameter described above for the physical model were simulated in the numerical model, with the addition of 70% relief well penetration. Layout of the relief well spacings are shown in Figure F-2. Figure F-3 depicts the various relief well penetrations, and Table F-2 summarizes the modeled screen elevations. Relief wells were assumed to be fully efficient (no friction losses in the well or losses across the well screen).

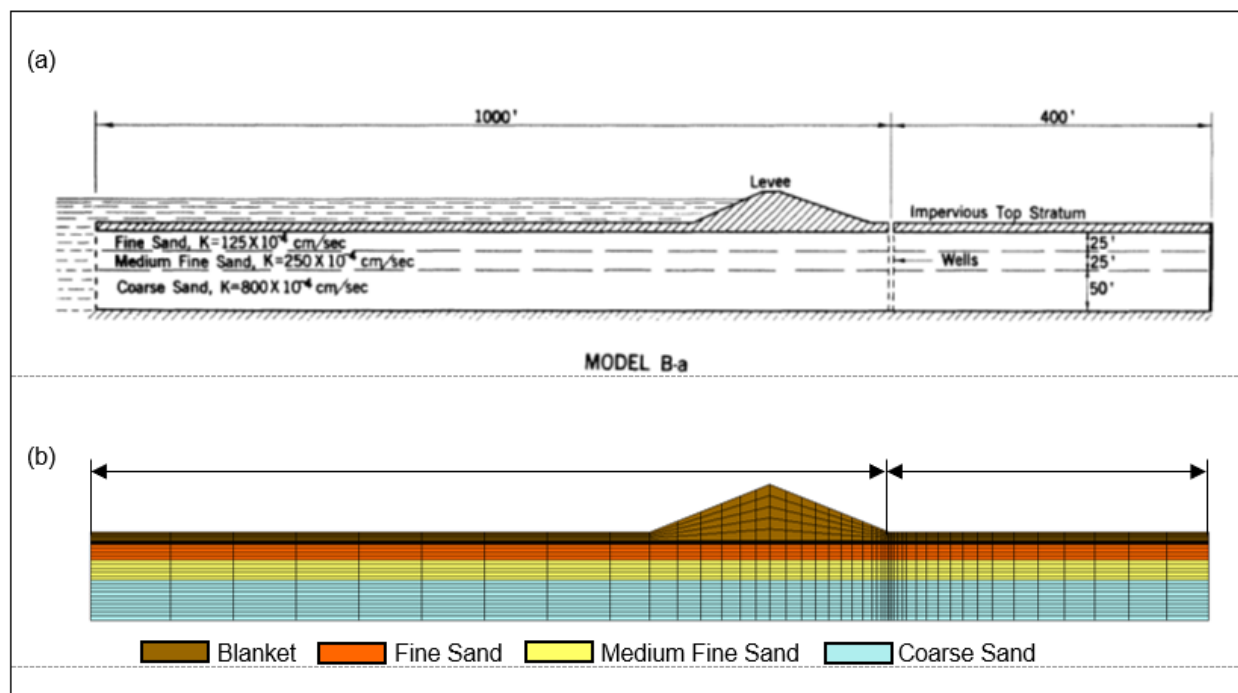


Figure F-1. Model cross sections; (a) schematic of physical model B-a from Technical Memorandum 3-304 (USACE 1949) and (b) cross section of WASH123D numerical seepage model

Table F-1
Modeled stratigraphy (Models #1 and #2)

Stratum	Top Elevation (ft)	Base Elevation (ft)	Thickness (ft)	K_h (cm/s)	K_h (ft/day)	K_h/K_v
Blanket	410	400	10	1.00E-06	0.00284	1.0
Fine Sand	400	375	25	1.25E-02	35	1.0
Medium Fine Sand	375	350	25	2.50E-02	71	1.0
Coarse Sand	350	300	50	8.00E-02	227	1.0

Notes:

K_h = Horizontal hydraulic conductivity

K_h/K_v = Ratio of horizontal to vertical hydraulic conductivity

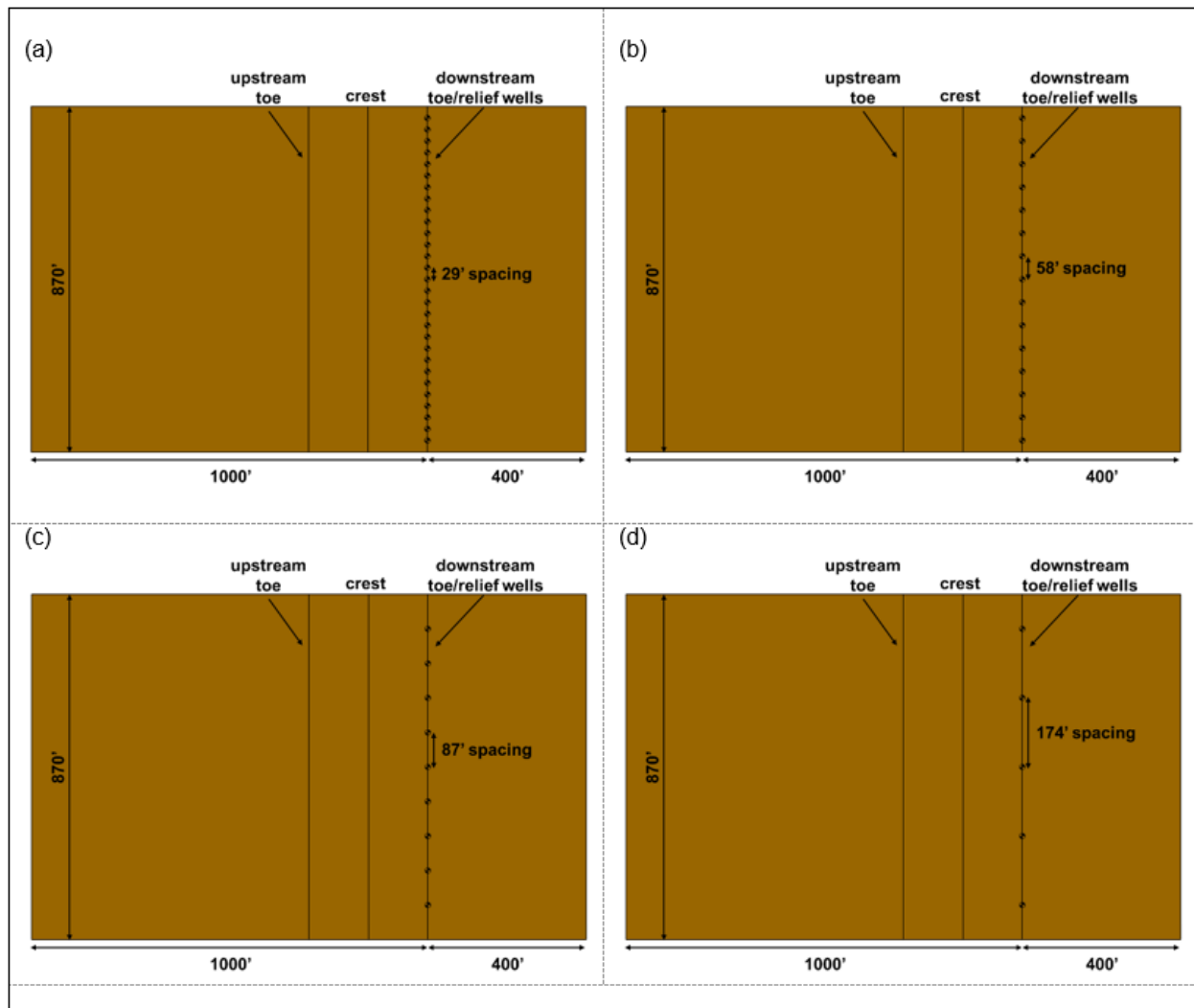


Figure F-2. Plan view of numerical model; (a) 29-foot well spacing, (b) 58-foot well spacing, (c) 87-foot well spacing, and (d) 174-foot well spacing

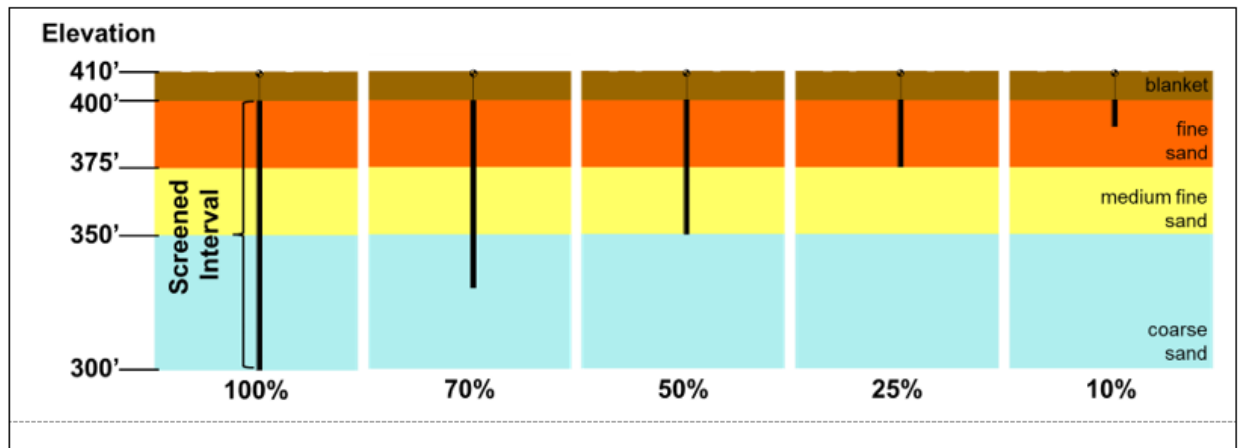


Figure F-3. Modeled relief well penetration

Table F-2
Relief well screen elevations at various penetrations

	Top (ft)	Base (ft)
100% Penetration	400	300
70% Penetration	400	330
50% Penetration	400	350
25% Penetration	400	375
10% Penetration	400	390

(5) The upstream vertical face of the model was assigned a head of 460 feet. The relief wells were allowed to discharge to the ground surface at 410 feet, creating a 50-foot difference in the headwater and tailwater conditions. The sides, top, bottom, and downstream face of the model served as no-flow boundaries. Water enters the model through the upstream face and leaves the model through the relief wells. There are no other sources or sinks of water in Model #1.

(6) WASH123D uses a finite element mesh for numerical computations. The horizontal node mesh spacing is approximately 2 feet at the line of relief wells. The spacing expands to a maximum of 100 feet at the upstream boundary. Figure F-4 shows the horizontal resolution of the mesh. Vertically, the WASH123D model has 29 layers of elements. Ten layers of 5-foot-thick elements represent the coarse sand. The medium fine sand is represented by five layers of 5-foot-thick elements. The fine sand is divided into nine layers. The bottom four layers are 5 feet thick. The top five layers are 1-foot thick for additional resolution at the top of the aquifer/well screen. The blanket is represented by five layers of 2-foot-thick elements.

(7) The vertical model layering can be seen in Figure F-1(b). The vertical layering was chosen to provide maximum flexibility for a variety of relief well penetrations.

Constructing numerous layers of thin elements may not be a best modeling practice in all situations but was appropriate for the goals of this modeling exercise.

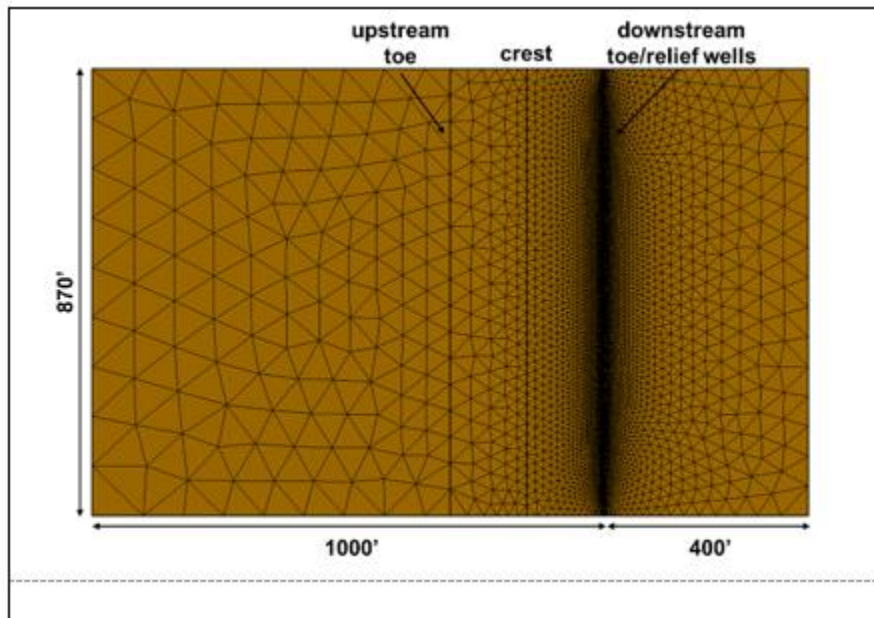


Figure F-4. Numerical Model #1 computational mesh, plan view

b. *Model #2: Extend Downstream Boundary.* In the second numerical model, the distance from the relief well line to the downstream boundary was extended from 400 to 4,800 feet (Figure F-5). This allowed evaluation of the impact of the downstream boundary. All other features of Model #2, including layering, K values, and relief well configurations, were retained from Model #1. The downstream boundary remained a no-flow boundary along with the sides, top, and bottom of the numerical model. The upstream vertical face of the model was again assigned a specified head of 460 feet, and relief wells were allowed to discharge to the ground surface at elevation 410 feet.

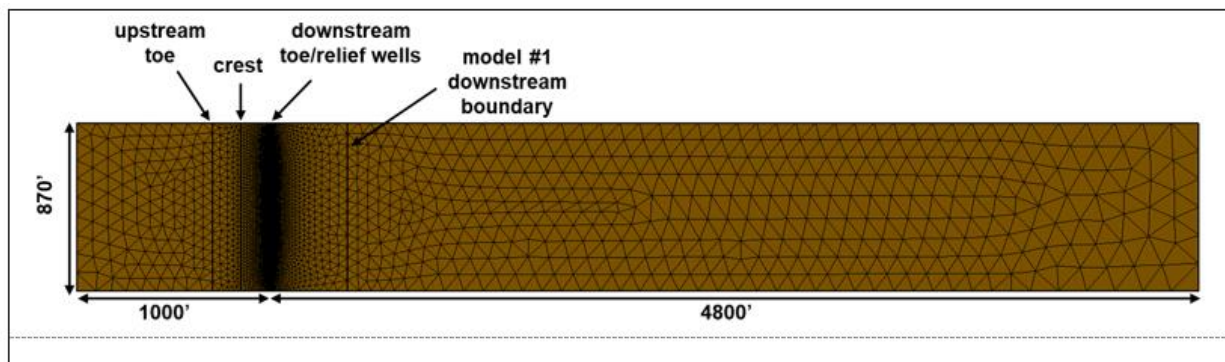


Figure F-5. Numerical Model #2 and Model #3 computational mesh, plan view

(1) *Model #2a: Specified Head Downstream Boundary.* Model #2a was a variation of Model #2. In Model #2a, a specified head of 410 feet was assigned to the vertical face of the model at the downstream boundary instead of the no-flow boundary used previously in Model #2. In Model #2a, water enters the model at the upstream boundary and can leave the model through the relief wells or through the downstream boundary.

(2) *Model #2b: Increased Blanket K.* Model #2b was a second variation of Model #2. This variation tested the sensitivity of the model to the blanket K . In Model #2b, the blanket K was increased by two orders of magnitude to 1.0×10^{-4} cm/second (0.284 feet/day). This simulation included a no-flow boundary at the surface of the model, as was previously modeled.

(3) *Model #2c and Model #2d: Flow to Surface.* The numerical models discussed thus far have included a no-flow boundary at the model surface (top of landside and riverside blanket). This boundary mimics the plastic plate used as the top boundary in the physical model. In Models #2c and #2d, water in the aquifer was allowed to flow upward through the landside blanket to the ground surface. Once water reached the surface, it was assumed to form surface runoff while the top of the model on the riverside remained a no-flow boundary. There was no ponding above ground surface in these models. Model #2c included a blanket hydraulic conductivity of 1.0×10^{-6} cm/second (0.00284 feet/day), while Model #2d included a blanket hydraulic conductivity of 1.0×10^{-4} cm/second (0.284 feet/day). Models #2c and #2d were run using relief well spacings of 29, 58, 87, and 174 feet, with well penetrations of 100%, 50%, 25%, and 10%.

c. *Model #3: Aquifer Transformation.* Model #3 uses the same horizontal dimensions as Model #2, but the foundation has been transformed into a single uniform layer. The transformed foundation thickness and K are equivalent to the stratified foundation represented in Models #1 and #2. Figure F-6 shows a cross section through Model #3. The transformed foundation thickness is 134 feet. Accordingly, ground surface was set to an elevation of 400 feet, and the base of the aquifer was set to an elevation of 266 feet. The effective K (horizontal and vertical) of the transformed aquifer is 3.69×10^{-2} cm/second (105 feet/day). This model does not include a confining blanket.

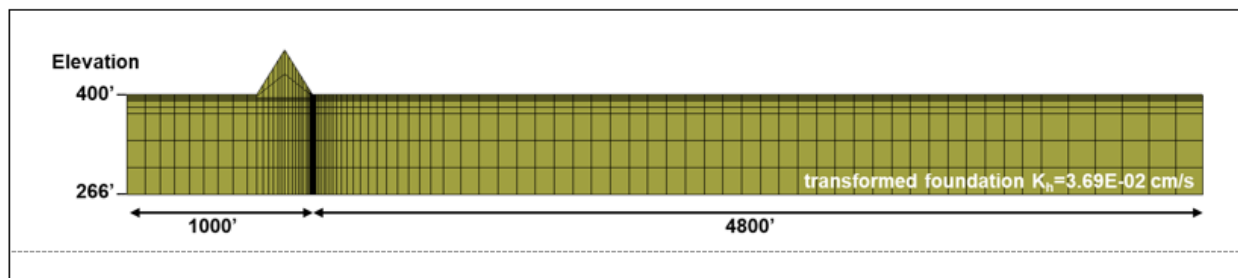


Figure F-6. Cross-sectional view of transformed aquifer model; vertical magnification = 4x horizontal

(1) The number of element layers in Model #3 was set to 9 since only one material type was present. The aquifer was subdivided so that layers of nodes would coincide with the top and bottom elevations of relief well screens. Layer thicknesses ranged from approximately 36 feet at the base of the aquifer to 2 feet at the top of the aquifer.

(2) Relief well spacings and penetrations previously modeled were used with the transformed foundation model. However, relief well penetrations were adjusted to reflect the effective penetrations in the transformed foundation. The transformed screen elevations are listed in Table F–3. The transformed aquifer parameters and effective relief well penetrations are provided in Appendix E.

Table F–3
Transformed relief well screen elevations

	Top (ft)	Base (ft)
100% Penetration (100% Effective)	400	266
70% Penetration (51% Effective)	400	331.7
50% Penetration (19% Effective)	400	374.5
25% Penetration (6% Effective)	400	392
10% Penetration (3% Effective)	400	396

(3) A specified head of 450 feet was applied to the upstream face of Model #3. All other model boundaries (top, sides, and downstream face) were no-flow, consistent with the setup of Model #1 and Model #2. Relief wells discharged to the ground surface elevation of 400 feet, making the difference between the headwater and tailwater conditions equal to 50 feet.

F–3. Model results

The four numerical models described in paragraph F–2 calculated head distribution within the foundation and relief well flow. These results were compared to those from the physical model (B-a from WES 1949) and BT. BT results are presented in Appendix E. Since headwater and tailwater elevations were not identical in each model, the percent of net head ($\%H$) was used to compare head calculated by the various models. This parameter is computed as:

$$\%H = \frac{\text{MidWell Head} - \text{Tailwater}}{\text{Headwater} - \text{Tailwater}} \times 100\%$$

a. Evaluation.

(1) Head was compared midway between two relief wells at the top of the aquifer. In models that included a 10-foot blanket, this location coincided with the interface between the aquifer and blanket. Since multiple relief wells were included in the numerical model, the head was taken midway between the center relief well and the neighboring well on either side. Head to either side of the center well was virtually

symmetrical. The influence of the side boundaries on the reported numerical model results had to be considered.

(2) To minimize this influence, reported relief well flow was an average of flow from the relief wells located in the center 348 feet of the model. This equated to the average flow from the center three wells for the 174-foot relief well spacing, the center five wells for the 87-foot spacing, the center seven relief wells for the 58-foot spacing, and the center 13 wells for the 29-foot spacing. The variation in flow from the subset of wells that was averaged was small (< 5 gpm).

b. Model #1 Results: Reproduction of Physical Model B-a (TM 3-304).

(1) Model #1 computed mid-well head and relief well flow (in gpm). Table F-4 summarizes these results as well as those from the physical model and BT. Figure F-7 shows mid-well head (%*H*) versus relief well spacing for each well penetration. In general, results from the numerical model and BT are in close agreement for relief well penetrations of 100%, 70% (51% effective) and 50% (19% effective).

(2) The 50% (19% effective) penetration case was a nearly perfect match to BT. Numerical model and BT results also compare closely to the physical model when relief wells fully penetrate the aquifer (100% effective penetration), but there are no results from the physical model for a well penetration of 70% (51% effective) for which to compare numerical model or BT results. At penetrations of 10% (2.5% effective), mid-well head calculated by BT are noticeably lower than those determined by the physical or numerical models. The physical and numerical models have a better agreement for well penetrations of 10% (2.5% effective) and 25% (6.3% effective) at most well spacings, but mid-well heads computed by the numerical model are noticeably lower than head determined by the physical model at a well spacing of 29 feet.

Table F-4
Model results of mid-well head and relief well flow

	Well Spacing (ft)	Mid-Well Head (%H)			Relief Well Flow (Q)		
		Physical Model	Blanket Theory	Numerical Model #1	Physical Model	Blanket Theory	Numerical Model #1
100% Well Penetration (100% Effective)	29	1.6	1.0	1.6	105	105	105
	58	3.1	2.6	3.7	210	207	204
	87	5.0	4.4	6.2	310	305	317
	174	8.5	10.2	12.8	590	579	563
70% Well Penetration (51% Effective)	29	N/A	1.4	2.2	N/A	103	103
	58	N/A	4.4	5.5	N/A	200	199
	87	N/A	7.6	9.4	N/A	291	308
	174	N/A	16.9	18.6	N/A	532	524
50% Well Penetration (19% Effective)	29	10.6	4.2	4.4	95	97	99
	58	14.6	11.0	11.1	180	182	183
	87	22.7	17.4	18.7	235	256	275
	174	34.5	32.7	33.0	460	429	430
25% Well Penetration (6.3% Effective)	29	22.3	11.7	13.1	85	91	84
	58	30.4	23.7	27.8	150	160	141
	87	41.1	33.3	41.3	185	215	193
	174	54.2	52.0	59.4	285	321	258
10% Well Penetration (2.5% Effective)	29	38.6	19.6	27.1	65	87	67
	58	50.7	34.8	47.5	105	143	100
	87	59.9	45.6	61.9	120	183	124
	174	78.7	64.1	76.7	130	251	147

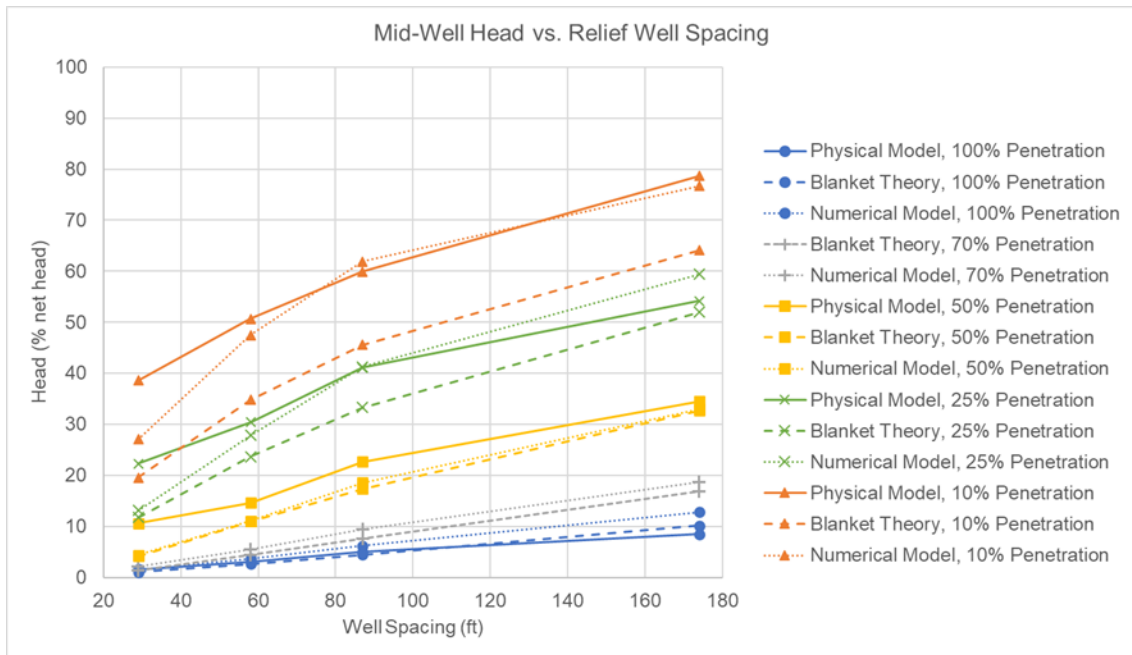


Figure F-7. Comparison of mid-well head from the physical model, Blanket Theory, and Model #1

(3) Figure F-8 shows relief well flow plotted as a function of well spacing for each well penetration. As with the mid-well head, the numerical model, physical model, and BT agree best for greater degrees of well penetration and at closer well spacings. At 10% penetration (2.5% effective), well flow determined with BT is significantly higher than those determined from the physical or numerical models.

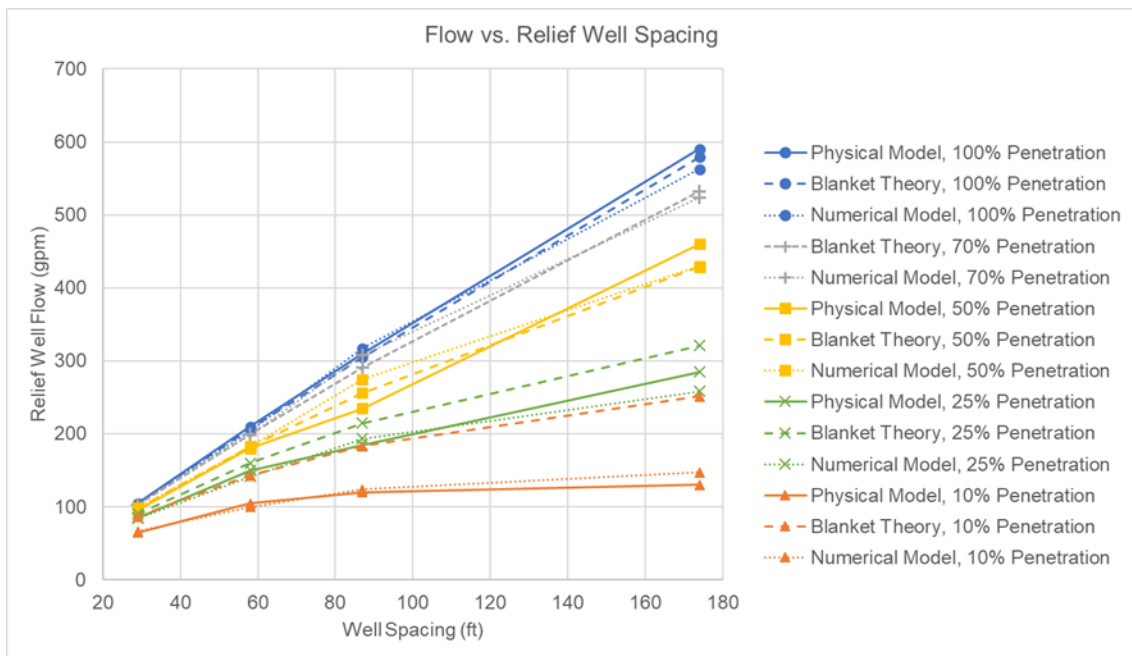


Figure F-8. Comparison of mid-well head from the physical model, Blanket Theory, and Model #1

(4) Figure F–9 compares equipotential lines ($\%H$) from Physical Model B-a to those from the numerical model for a relief well spacing of 29 feet. The top images (Figure F–9(a)) show results for full-penetration wells. Results shown in the bottom images (Figure F–9(b)) are for 25% penetration (6.3% effective). Overall, the head contours from the numerical model are similar to those determined by the physical model. Additional images of head results from Numerical Model #1 are included in Figure F–33 through Figure F–49. These images include total head contours in plan view as well as cross-sectional views through the center relief well. Also included are views perpendicular to the dam/levee and along the line of relief wells, parallel to the dam/levee.

c. *Model #2 Results: Extend Downstream Boundary.* The purpose of Model #2 was to explore the effect of the downstream boundary location on results. Specifically, Model #2 tested to determine if this boundary in Model #1 was sufficiently far from the relief wells. The boundary needed to be far enough from the relief wells that it did not influence well flow or mid-well head. In Model #2, the downstream boundary was extended from 400 feet beyond the line of relief wells to 4,800 feet. The downstream boundary remained a no-flow boundary in this model for the base-case scenario. The mid-well head and relief well flow determined by Model #2 were identical to those determined by Model #1.

(1) *Presentation of results.* Relief well flow and mid-well head can be found in Table F–4 or Table F–5. Figure F–10 and Figure F–11 compare total head contours at the top of the fine sand from Model #1 to Model #2. Figure F–10 depicts model results from the model simulation that included full-penetration relief wells every 174 feet. Figure F–11 shows results from the model simulation that included relief wells every 29 feet and 10% penetration (2.5% effective).

(2) *General results.* The results from Models #1 and #2 demonstrate that a boundary of 400 feet downstream of the relief wells does not influence the model results. This applies to model scenarios that include no-flow boundaries at the top, sides, and downstream end of the model. This conclusion may not hold true for different sets of boundary conditions (such as specified head boundary). Since practical applications of the 3D model often simulate more complex flow systems than these example models, it is critical to have a good understanding of the conceptual flow system when developing a 3D model so that defensible boundary conditions can be applied and model boundaries are selected such that they do not impact the simulation results.

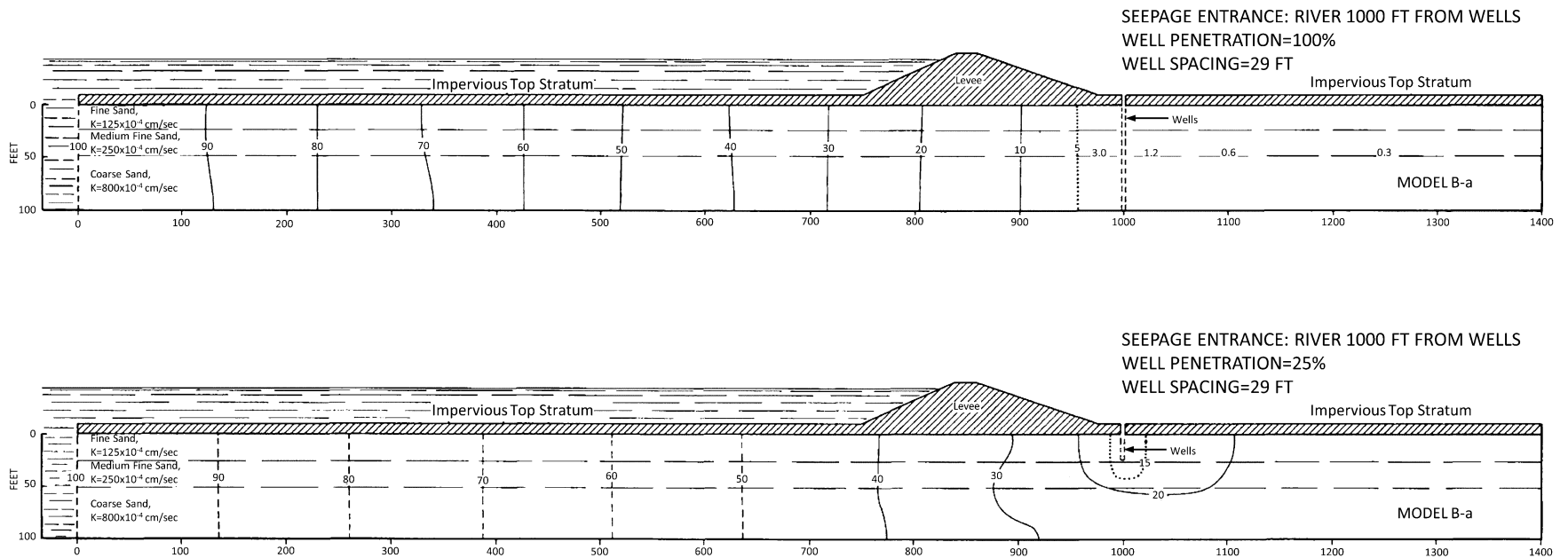


Figure F-9. Comparison of equipotential lines in percent of net head from Physical Model B-a (USACE 1949, Figure 30) and Numerical Model #1 for 29-foot well spacing and (a) 100% well penetration or (b) 25% penetration

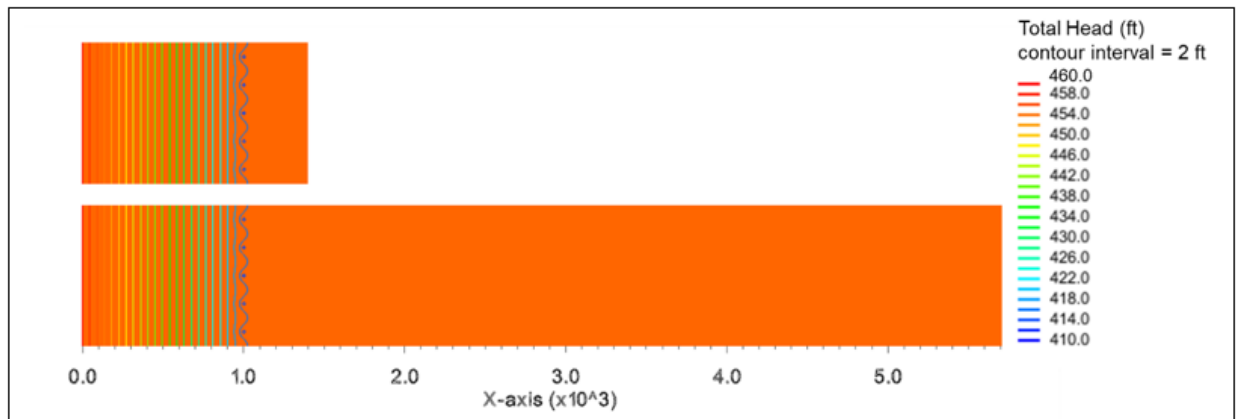


Figure F-10. Plan view of total head contours at the top of the fine sand aquifer for full-penetration wells every 174 feet. The top image shows results from Model #1 (downstream boundary located 400 feet from relief wells), and the bottom image shows results from Model #2 (downstream boundary located 4,800 feet from relief wells)

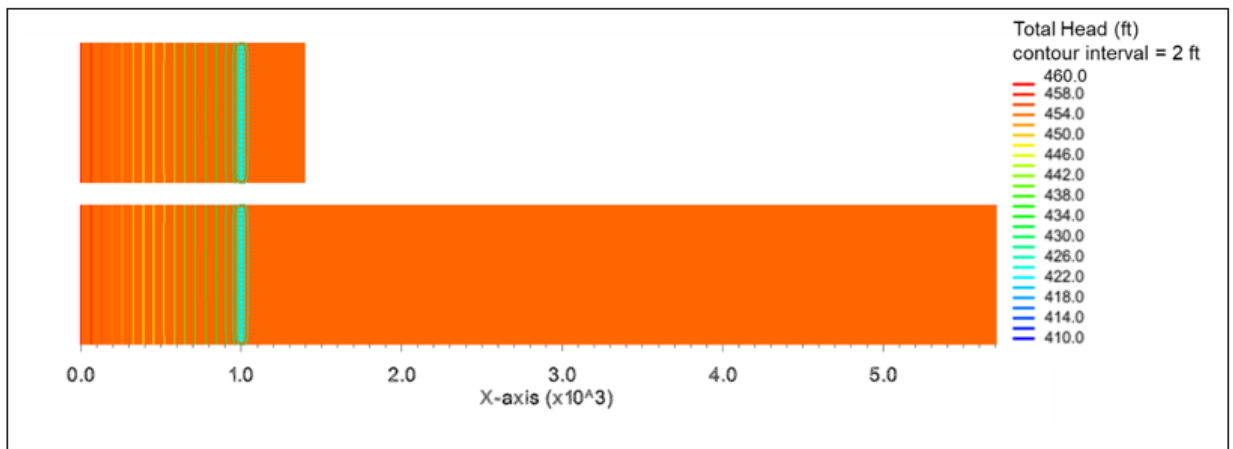


Figure F-11. Plan view of total head contours at the top of the fine sand aquifer for relief wells every 29 feet penetrating 10% (2.5% effective) of the aquifer. The top image shows results from Model #1 (downstream boundary located 400 feet from relief wells), and the bottom image shows results from Model #2 (downstream boundary located 4,800 feet from relief wells)

(3) *Model #2a Results: Specified Head Downstream Boundary.*

(a) In Model #2a, the downstream boundary in Model #2 (located at 4,800 feet from the relief wells) was changed from a no-flow boundary to a specified head boundary. The vertical face of the downstream boundary was assigned a head of 410 feet, which coincides with the ground surface and the elevation to which relief wells can discharge. Table F-5 compares mid-well head ($\%H$) and relief well flow from Model #2a to Model #2, the physical model, and BT.

(b) Table F-6 compares the difference in mid-well head and relief well flow between Model #2a and Model #2. Head in Model #2a was slightly lower than in

Model #2 but higher than those calculated using BT. Head from Model #2a was mostly lower than determined by the physical model. The exception was for full-penetration wells at spacings of 58, 87, and 174 feet. Relief well flow in Model #2a was lower than Model #2. However, these differences were mostly below 10%. Differences were greater than 10% for 25% penetration (6.3% effective) and a well spacing of 174 feet. Differences were also greater than 10% for 10% penetration and spacings of 58, 87, and 174 feet.

(c) Model #2a well flow was mostly lower than determined using the physical model. The exception was for flow from full-penetration wells every 87 feet and 50% penetrating (19% effective) wells every 29 and 87 feet. Model #2a well flow was within 10% of flow calculated by BT except for wells penetrating 25% of the aquifer (6.2% effective) at spacings of 58, 87, and 174 feet and wells penetrating 10% of the aquifer (2.5% effective) at all spacings (Table F-40).

Table F-5
Mid-well head as percent of net head (%H) and relief well flow results from Technical Memorandum 3-304, Blanket Theory, and Numerical Models #2 and #2a

	Well Spacing (ft)	Mid-Well Head (%H)				Relief Well Flow (Q)			
		Physical Model	Blanket Theory*	Model #2**	Model #2a	Physical Model	Blanket Theory*	Model #2**	Model #2a
100% Well Penetration (100% Effective)	29	1.6	1.2	1.6	1.6	105	105	105	104
	58	3.1	2.6	3.7	3.6	210	207	204	203
	87	5.0	4.4	6.2	6.1	310	305	317	314
	174	8.5	10.2	12.8	12.5	590	579	563	550
70% Well Penetration (51% Effective)	29	N/A	1.4	2.2	2.2	N/A	103	103	103
	58	N/A	4.4	5.5	5.4	N/A	200	199	196
	87	N/A	7.6	9.4	9.2	N/A	291	308	301
	174	N/A	16.9	18.6	18.0	N/A	532	524	506
50% Well Penetration (19% Effective)	29	10.6	4.2	4.4	4.4	95	97	99	97
	58	14.6	11.0	11.1	10.8	180	182	183	178
	87	22.7	17.4	18.7	17.9	235	256	275	264
	174	34.5	32.7	33.0	30.9	460	429	430	403
25% Well Penetration (6.3% Effective)	29	22.3	11.7	13.1	12.5	85	91	84	81
	58	30.4	23.7	27.8	26.0	150	160	141	132
	87	41.1	33.3	41.3	37.8	185	215	193	177
	174	54.2	52.0	59.4	52.9	285	321	258	230
10% Well Penetration (2.5% Effective)	29	38.6	19.6	27.1	25.1	65	87	67	62
	58	50.7	34.8	47.5	42.8	105	143	100	90
	87	59.9	45.6	61.9	54.5	120	183	124	109
	174	78.7	64.1	76.7	66.2	130	251	147	127

*BT results presented in this table are comparable to Numerical Model #2. BT results comparable to Model #2a are available in Table F-36 and Table F-39.

**Result of Model #2 were identical to the results of Model #1, which replicated the WES physical model and are comparable to the BT results reported in this table.

Table F-6
Comparison of mid-well head and relief well flow, Numerical Models #2 and #2a

	Well Spacing (ft)	Mid-Well Head (ft)			Relief Well Flow (gpm)		
		Model #2	Model #2a	Model #2a vs. #2 Head Difference	Model #2	Model #2a	Model #2a vs. #2 Percent Difference
100% Well Penetration (100% Effective)	29	410.8	410.8	0.0	105	104	-1.0%
	58	411.8	411.8	0.0	204	203	-0.5%
	87	413.1	413.1	0.0	317	314	-1.0%
	174	416.4	416.3	-0.1	563	550	-2.3%
70% Well Penetration (51% Effective)	29	411.1	411.1	0.0	103	103	0.0%
	58	412.7	412.7	0.0	199	196	-1.2%
	87	414.7	414.6	-0.1	308	301	-2.0%
	174	419.3	419.0	-0.3	524	506	-3.5%
50% Well Penetration (19% Effective)	29	412.2	412.2	0.0	99	97	-2.0%
	58	415.5	415.4	-0.1	183	178	-2.8%
	87	419.3	418.9	-0.4	275	264	-4.1%
	174	426.5	425.5	-1.0	430	403	-6.5%
25% Well Penetration (6.3% Effective)	29	416.5	416.3	-0.2	84	81	-3.6%
	58	423.9	423.0	-0.9	141	132	-6.6%
	87	430.7	428.9	-1.8	193	177	-8.6%
	174	439.7	436.4	-3.3	258	230	-11.5%
10% Well Penetration (2.5% Effective)	29	423.6	422.6	-1.0	67	62	-7.8%
	58	433.8	431.4	-2.4	100	90	-10.5%
	87	440.9	437.3	-3.6	124	109	-12.9%
	174	448.4	443.1	-5.3	147	127	-14.6%

Note:

A positive difference indicates that the Model #2a result is higher than the Model #2 result. A negative difference indicates that the Model #2a result is lower than the Model #2 result.

(4) *Model #2b Results: Increase Blanket Hydraulic Conductivity.* In Model #2b, the K of the blanket material was increased from the 0.01×10^{-4} cm/second used in Model #2 (0.00284 feet/day) to 1.0×10^{-4} cm/second (0.284 feet/day). Total head and relief well flow results were almost identical to the base-case scenario using the lower K (Model #2). This is likely due to the no-flow boundary at the surface of the model (top of the blanket). This condition was selected to be consistent with the physical model setup. Table F-7 compares the %H and relief well flow calculated by Model #2b to those from Model #2. Results are also given from the physical model and BT. Table F-8 compares the difference in mid-well head and relief well flow between Model #2b and Model #2.

Table F-7

Mid-well head as percent of net head (%H) and relief well flow results from Technical Memorandum 3-304, Blanket Theory, and Numerical Models #2, #2b, #2c, and #2d

	Well Spacing (ft)	Mid-Well Head (%H)						Relief Well Flow (gpm)					
		Physical Model*	Blanket Theory*	Model #2	Model #2b	Model #2c	Model #2d	Physical Model*	Blanket Theory*	Model #2	Model #2b	Model #2c	Model #2d
100% Well Penetration (100% Effective)	29	1.6	1.0	1.6	1.6	1.6	1.5	105	105	105	105	105	103
	58	3.1	2.6	3.7	3.7	3.7	3.5	210	207	204	204	204	196
	87	5.0	4.4	6.2	6.2	6.2	5.7	310	305	317	318	316	293
	174	8.5	10.2	12.8	12.8	12.7	10.9	590	579	563	563	557	486
70% Well Penetration (51% Effective)	29	N/A	1.4	2.2	2.2	2.2	2.1	N/A	103	103	103	103	99
	58	N/A	4.4	5.5	5.5	5.4	5.0	N/A	200	199	199	198	184
	87	N/A	7.6	9.4	9.4	9.3	8.2	N/A	291	308	308	305	270
	174	N/A	16.9	18.6	18.7	18.4	14.8	N/A	532	524	524	516	421
50% Well Penetration (19% Effective)	29	10.6	4.2	4.4	4.5	4.4	4.0	95	97	99	99	98	90
	58	14.6	11.0	11.1	11.1	11.0	9.2	180	182	183	183	181	155
	87	22.7	17.4	18.7	18.7	18.3	14.3	235	256	275	275	270	213
	174	34.5	32.7	33.0	33.00	32.1	22.4	460	429	430	430	418	295
25% Well Penetration (6.3% Effective)	29	22.3	11.7	13.1	13.1	12.8	10.0	85	91	84	84	83	64
	58	30.4	23.7	27.8	27.8	27.1	18.8	150	160	141	142	138	97
	87	41.1	33.3	41.3	41.3	39.8	25.1	185	215	193	194	186	118
	174	54.2	52.0	59.4	59.4	56.6	31.9	285	321	258	258	246	140
10% Well Penetration (2.5% Effective)	29	38.6	19.6	27.1	27.1	26.3	17.5	65	87	67	67	64	43
	58	50.7	34.8	47.5	47.5	45.5	27.0	105	143	100	100	96	57
	87	59.9	45.6	61.9	61.8	58.6	31.9	120	183	124	124	117	64
	174	78.7	64.1	76.7	76.7	72.1	36.3	130	251	147	148	138	70

Notes: (see next page)

*Physical model and BT results in this table are comparable to Numerical Models #1, #2, and #2b. BT results are also available for models #2c and #2d in Table F-36 and Table F-39.

1. Numerical Model #2: Downstream no-flow boundary extended from 400 ft beyond relief wells (Model #1) to 4800 ft from relief wells. No-flow boundary at model surface. Blanket hydraulic conductivity = 1.0×10^{-6} cm/second.
2. Numerical Model #2b: Blanket hydraulic conductivity increased from 1.0×10^{-6} cm/second to 1.0×10^{-4} cm/second. No-flow boundary at model surface.
3. Numerical Model #2c: No-flow boundary removed from model surface downstream of dam/levee. Blanket hydraulic conductivity = 1.0×10^{-6} cm/second.
4. Numerical Model #2d: No-flow boundary removed from model surface downstream of dam/levee. Blanket hydraulic conductivity = 1.0×10^{-4} cm/second.

Table F-8
Comparison of mid-well head and relief well flow, Numerical Models #2, #2b, #2c, and #2d

	Well Spacing (ft)	Mid-Well Head (ft)							Relief Well Flow (gpm)						
		Model #2	Model #2b	Model #2b vs. #2 Head Diff.	Model #2c	Model #2c vs. #2 Head Diff.	Model #2d	Model #2d vs. #2 Head Diff.	Model #2	Model #2b	Model #2b vs. #2 % Diff.	Model #2c	Model #2c vs. #2 % Diff.	Model #2d	Model #2d vs. #2 % Diff.
100% Well Penetration (100% Effective)	29	410.8	410.8	0.0	410.8	0.0	410.8	0.0	105	105	0.0%	105	-0.4%	103	-2.2%
	58	411.8	411.8	0.0	411.8	0.0	411.7	-0.1	204	204	0.0%	204	-0.2%	196	-4.2%
	87	413.1	413.1	0.0	413.1	0.0	412.8	-0.3	317	318	0.3%	316	-0.3%	293	-7.8%
	174	416.4	416.4	0.0	416.4	0.0	415.5	-0.9	563	563	0.0%	557	-1.0%	486	-14.7%
70% Well Penetration (51% Effective)	29	411.1	411.1	0.0	411.1	0.0	411.0	-0.1	103	103	0.0%	103	0.0%	99	-4.0%
	58	412.7	412.7	0.0	412.7	0.0	412.5	-0.2	199	199	0.0%	198	-0.5%	184	-7.8%
	87	414.7	414.7	0.0	414.7	0.0	414.1	-0.6	308	308	0.0%	305	-1.0%	270	-13.1%
	174	419.3	419.3	0.0	419.2	-0.1	417.4	-1.9	524	524	0.0%	516	-1.5%	421	-21.8%
50% Well Penetration (19% Effective)	29	412.2	412.2	0.0	412.2	0.0	412.0	-0.2	99	99	0.0%	98	-0.7%	90	-10.1%
	58	415.5	415.5	0.0	415.5	-0.0	414.6	-0.9	183	183	0.0%	181	-1.1%	155	-16.9%
	87	419.3	419.3	0.0	419.2	-0.1	417.2	-2.1	275	275	0.0%	270	-1.7%	213	-25.2%
	174	426.5	426.5	0.0	426.1	-0.4	421.2	-5.3	430	430	0.0%	418	-2.8%	295	-37.2%
25% Well Penetration (6.3% Effective)	29	416.5	416.5	0.0	416.4	-0.1	415.0	-1.5	84	84	0.0%	83	-1.6%	64	-26.3%
	58	423.9	423.9	0.1	423.5	-0.4	419.4	-4.5	141	142	0.7%	138	-2.4%	97	-37.3%
	87	430.7	430.6	0.1	429.9	-0.8	422.5	-8.2	193	194	0.5%	186	-3.5%	118	-47.9%
	174	439.7	439.7	0.1	438.3	-1.4	425.9	-13.8	258	258	0.0%	246	-4.8%	140	-59.4%
10% Well Penetration (2.5% Effective)	29	423.6	423.6	0.0	423.1	-0.5	418.7	-4.8	67	67	0.0%	64	-3.8%	43	-43.4%
	58	433.8	433.7	-0.1	432.7	-1.1	423.5	-10.3	100	100	0.0%	96	-4.5%	57	-54.8%
	87	440.9	440.9	0.0	439.3	-1.6	426.0	-14.9	124	124	0.0%	117	-5.5%	64	-63.5%
	174	448.4	448.4	0.1	446.0	-2.4	428.1	-20.3	147	148	0.7%	138	-6.0%	70	-70.9%

Notes: (see next page)

1. Numerical Model #2: Downstream no-flow boundary extended from 400 ft beyond relief wells (Model #1) to 4,800 ft from relief wells. No-flow boundary at model surface. Blanket hydraulic conductivity = 1.0×10^{-6} cm/second.
2. Numerical Model #2b: Blanket hydraulic conductivity increased from 1.0×10^{-6} cm/second to 1.0×10^{-4} cm/second. No-flow boundary at model surface.
3. Numerical Model #2c: No-flow boundary removed from model surface downstream of dam/levee. Blanket hydraulic conductivity = 1.0×10^{-6} cm/second.
4. Numerical Model #2d: No-flow boundary removed from model surface downstream of dam/levee. Blanket hydraulic conductivity = 1.0×10^{-4} cm/second.
5. Results for well penetrations of 50% and 25% were not computed for Models #2c and #2d.
6. A positive difference indicates that the Model #2"x" result is higher than the Model #2 result. A negative difference indicates that the Model #2 "x" result is lower than the Model #2 result.

(5) *Model #2c and Model #2d Results: Leaky Blanket.*

(a) Models #2c and #2d explored the impact of removing the no-flow boundary at the model surface downstream of the dam/levee. In these models, water is allowed to exit the model at both the surface and through the relief wells. Water discharging at the surface is assumed to run off and not accumulate. Models #2c and #2d were run for all relief well spacings and penetrations. In Model #2c, the K of the blanket was set to 0.01×10^{-4} cm/second (0.00284 feet/day). Relief well flow and mid-well head in these model variations were similar to those computed by the model with a no-flow boundary at the model surface. Results are reported in Table F–7 and Table F–8.

(b) Differences in $\%H$ were slightly greater for 10% penetration than for full-penetration wells. Removing the no-flow boundary resulted in a greater $\%H$ differential when the blanket K was increased to 1.0×10^{-4} cm/second (0.284 feet/day). This was the case with Model #2d. In this simulation, less water was discharged through the relief wells as more water was allowed to discharge to the surface through the leaky blanket. Differences in computed flow from the relief wells were significant when relief wells penetrated only 10% (2.5% effective) of the aquifer. Larger relief well spacings also resulted in greater differences in model results when compared to the model simulation with the no-flow boundary at the surface (Model #2). Results from Model #2d are reported in Table F–7 and Table F–8.

d. *Model #3 Results: Transformed Foundation.* The aquifer material of the foundation in Model #3 was represented by a single material. The thickness and K are transformed values equivalent to the stratified foundation in Model #1 and Model #2. Table F–9 compares mid-well head ($\%H$) and well flow from Model #3 to the physical model, BT, and Model #1. Table F–10 compares the difference in mid-well head and relief well flow from Models #1 and #3.

Table F-9
Mid-well head as percent of net head (%H) and relief well flow results from Technical Memorandum 3-304, Blanket Theory, and Numerical Models #1 and #3

	Well Spacing (ft)	Mid-Well Head (%H)				Relief Well Flow (Q)			
		Physical Model	Blanket Theory	Model #1	Model #3	Physical Model	Blanket Theory	Model #1	Model #3
100% Well Penetration	29	1.6	1.0	1.6	2.0	105	105	105	110
	58	3.1	2.6	3.7	4.3	210	207	204	215
	87	5.0	4.4	6.2	6.9	310	305	317	334
	174	8.5	10.2	12.8	13.6	590	579	563	590
70% Well Penetration	29	N/A	1.4	2.2	2.6	N/A	103	103	109
	58	N/A	4.4	5.5	5.8	N/A	200	199	209
	87	N/A	7.6	9.4	9.7	N/A	291	308	324
	174	N/A	16.9	18.6	18.8	N/A	532	524	552
50% Well Penetration	29	10.6	4.2	4.4	4.5	95	97	99	105
	58	14.6	11.0	11.1	10.1	180	182	183	197
	87	22.7	17.4	18.7	16.6	235	256	275	299
	174	34.5	32.7	33.0	29.6	460	429	430	477
25% Well Penetration	29	22.3	11.7	13.1	13.1	85	91	84	94
	58	30.4	23.7	27.8	25.7	150	160	141	161
	87	41.1	33.3	41.3	37.5	185	215	193	225
	174	54.2	52.0	59.4	54.3	285	321	258	310
10% Well Penetration	29	38.6	19.6	27.1	23.3	65	87	67	83
	58	50.7	34.8	47.5	39.7	105	143	100	130
	87	59.9	45.6	61.9	53.0	120	183	124	169
	174	78.7	64.1	76.7	68.5	130	251	147	213

**Table F–10
Comparison of mid-well head and relief well flow, Numerical Models #1 and #3**

	Well Spacing (ft)	Mid-Well Head (ft)			Relief Well Flow (Q)		
		Model #1	Model #3*	Model #3 vs. #1 Head Difference	Model #1	Model #3	Model #3 vs. #1 Percent Difference
100% Well Penetration (100% Effective)	29	410.8	411.0	0.2	105	110	4.7%
	58	411.8	412.1	0.3	204	215	5.3%
	87	413.1	413.5	0.4	317	334	5.2%
	174	416.4	416.8	0.4	563	590	4.7%
70% Well Penetration (51% Effective)	29	411.1	411.3	0.2	103	109	5.1%
	58	412.7	412.9	0.2	199	209	5.2%
	87	414.7	414.8	0.1	308	324	5.3%
	174	419.3	419.4	0.1	524	552	5.3%
50% Well Penetration (19% Effective)	29	412.2	412.3	0.1	99	105	5.9%
	58	415.5	415.0	-0.5	183	197	7.4%
	87	419.3	418.3	-1.0	275	299	8.4%
	174	426.5	424.8	-1.7	430	477	10.4%
25% Well Penetration (6.2% Effective)	29	416.5	416.5	0.0	84	94	11.2%
	58	423.9	422.8	-1.1	141	161	13.2%
	87	430.7	428.7	-2.0	193	225	15.3%
	174	439.7	437.1	-2.6	258	310	18.3%
10% Well Penetration (2.5% Effective)	29	423.6	421.7	-1.9	67	83	21.3%
	58	433.8	429.9	-3.9	100	130	26.1%
	87	440.9	436.5	-4.4	124	169	30.7%
	174	448.4	444.3	-4.1	147	213	36.7%

Notes:

*Head reported in this table for Model #3 is 10 ft higher than calculated by the model so that a direct comparison the Model #1 can be made, as headwater and tailwater conditions in Model #1 were 10 ft higher than in Model #3 to account for the blanket.

A positive difference indicates that the Model #3 result is higher than the Model #1 result. A negative difference indicates that the Model #3 result is lower than the Model #1 result.

(1) A comparison of mid-well head in Table F–10 shows that head computed in Model #3 is slightly higher than in Model #1 for penetrations of 100% (100% effective) and 70% (51% effective) but lower than in Model #1 for penetrations of 50% (19% effective, spacings of 58 feet, 87 feet, and 174 feet), 25% (6.2% effective), and 10% (2.5% effective). Figure F–12 illustrates Model #3 head is also slightly higher than in the physical model for full penetration. Model #3 head is the same or lower than the physical model for lower penetrations. This includes values of 50% (19% effective), 25% (6.3% effective), and 10% (2.5% effective). The physical model did not include a well penetration of 70% (51% effective). Model #3 head is higher than computed by BT

except for wells penetrating 50% of the aquifer (19% effective) at spacings of 58, 87, and 174 feet (Table F–9 and Figure F–12).

(2) Well flow computed by Model #3 is higher than Model #1 and the physical model for all well spacings and penetrations. Figure F–13 shows that this differential is greater for wells that are not full penetration. This can be attributed to the simplified representation of the aquifer. Flow computed by Model #3 is higher than computed by BT except for 10% penetration (2.5% effective) at all spacings and 25% penetration (6.2% effective) at a spacing of 174 feet. Model #3 flow more closely approximates BT for 10% penetration than Model #1.

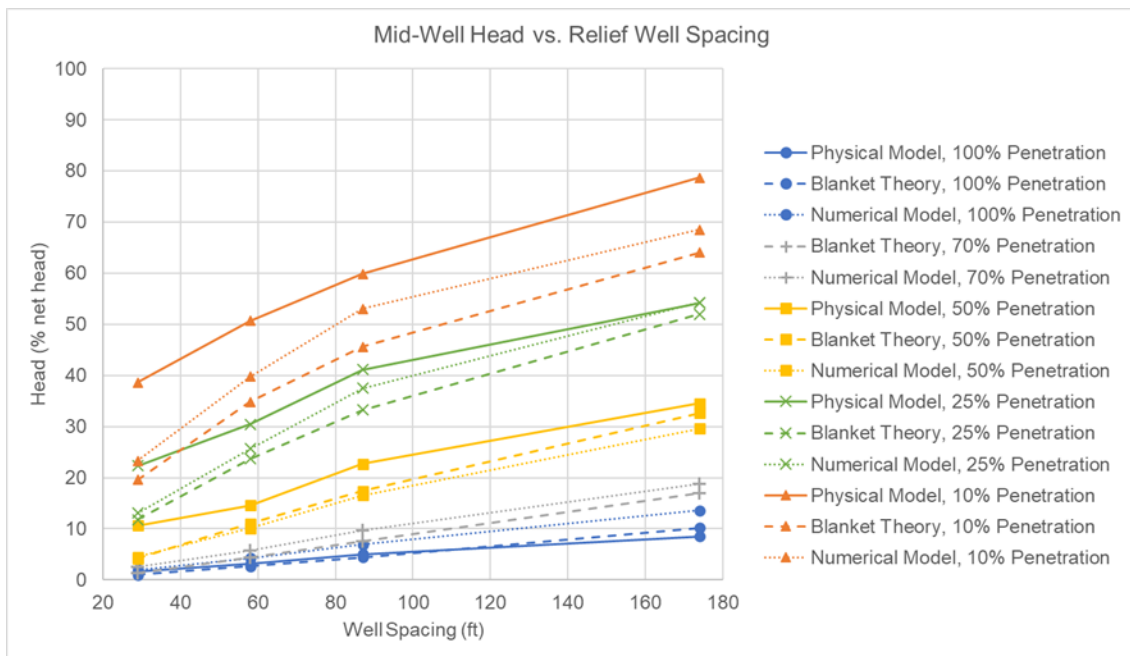


Figure F–12. Comparison of mid-well head from the physical model, Blanket Theory, and Model #3

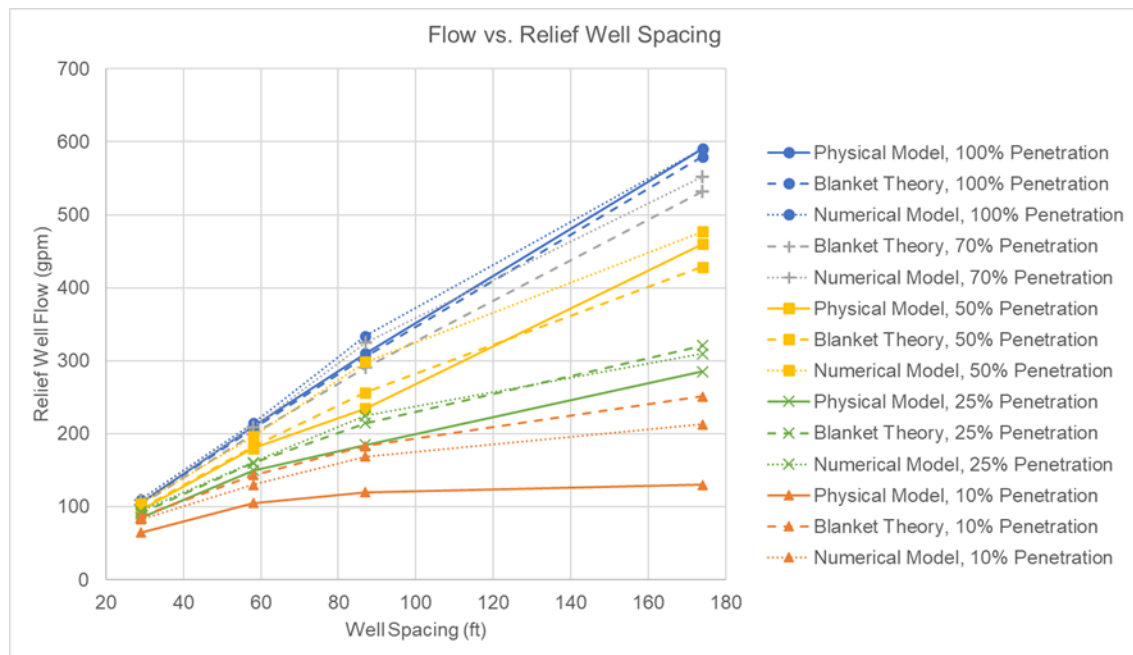


Figure F-13. Comparison of relief well flow from the physical model, Blanket Theory, and Model #3

F-4. Sensitivity studies

A series of sensitivity studies was performed to explore variations in selected features of the 3D numerical model. The sensitivity studies are variations of Model #2c (discussed in paragraphs F-2b(3) and F-3c(5)) unless otherwise noted. This model simulated a stratified aquifer overlain by a leaky blanket and a no-flow downstream boundary. The sensitivity studies included reducing the relief well efficiency to 80% and replacing the top 10 feet of screen in the fine sand with a blank section. Additional sensitivity studies included a blanket defect, which was a cylinder filled with sand to represent a sand boil.

a. Reduced well efficiency (80%).

(1) All previously discussed model scenarios included the assumption that friction losses in the well are negligible. In other words, relief wells were modeled as 100% efficient. In the sensitivity scenarios discussed in this section, friction losses were increased until well flow was approximately 80% of flow without friction losses. This had the effect of simulating relief wells operating at 80% efficiency (Table F-11).

(2) Relief wells with 80% efficiency were modeled at a spacing of 87 feet for penetrations of 100%, 70% (51% effective), 50% (19% effective), 25% (6.3% effective), and 10% (2.5% effective). Table F-12 shows mid-well head computed by the model at the base of the blanket. This table also includes a calculated estimate of mid-well head assuming relief wells operating at 80% efficiency. These estimates assume the wells are reducing head only 80% of that achieved at 100% efficiency. The results compare favorably with the 3D model results. Figure F-14 graphically shows the model

computed head mid-way between relief wells for the scenarios involving 100% and 80% efficient wells.

Table F-11
Three-dimensional model simulated relief well flow in gallons per minute 80% versus 100% efficiency

Well Penetration (Effective)	Calc. 80% Efficiency*	Modeled 80% Efficient	Modeled 100% Efficient
100% (100%)	252.7	252.0	315.9
70% (51%)	244.0	245.1	305.0
50% (19%)	216.2	217.2	270.2
25% (6.3%)	149.1	148.6	186.4
10% (2.5%)	93.9	94.3	117.4

Note:

*Calculated 80% efficient relief well flow was determined by multiplying the modeled 100% efficient well flow by 0.8. For the modeled 80% well efficiency case, modeled friction losses in the well were adjusted until the modeled relief well flow was close to the calculated 80% efficient flow.

Table F-12
Mid-well head summary – 80% versus 100% efficiency

Well Penetration (Effective)	Mid-Well Head (ft)			Mid-Well Head (%H)		
	80% Efficient Calc. Estimate*	3D Model Results		80% Efficient Calc. Estimate*	3D Model Results	
		80% Efficient	100% Efficient		80% Efficient	100% Efficient
100% (100%)	421.7	422.3	413.1	23.4	24.6	6.2
70% (51%)	423.0	422.9	414.7	25.9	25.8	9.3
50% (19%)	426.6	426.3	419.2	33.1	32.6	18.3
25% (6.3%)	435.1	435.2	429.9	50.3	50.3	39.8
10% (2.5%)	442.7	442.6	439.3	65.4	65.3	58.6
No Wells	456.1	456.1	456.1	92.2	92.2	92.2

Note:

Estimates of mid-well head for the scenario including 80% well efficiency were computed by the following calculations: 80% efficient calculated estimate = (3D-modeled mid-well head without relief wells) – (0.8[3D modeled mid-well head without relief wells – 3D modeled mid-well head with 100% efficient wells])

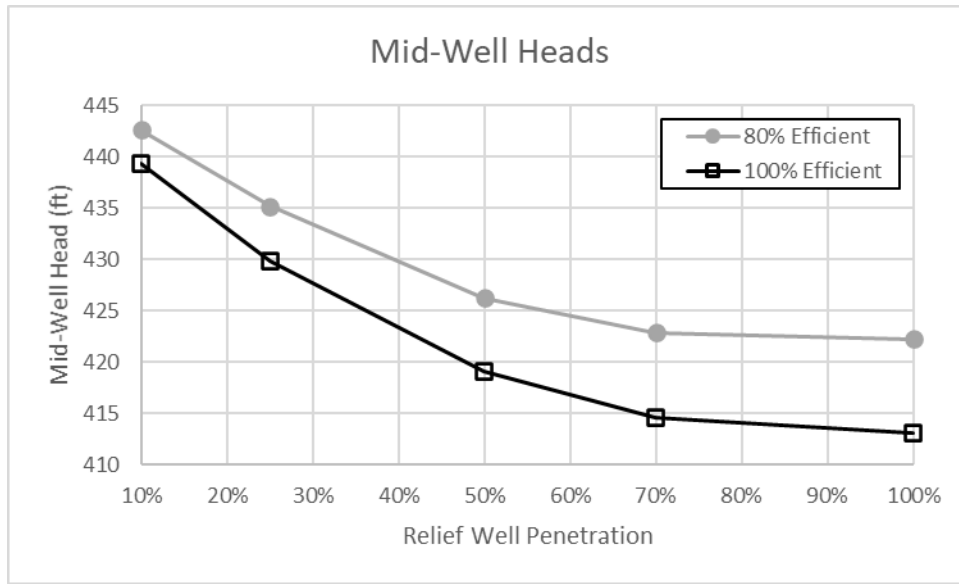


Figure F-14. Head computed mid-way between relief wells for 80% and 100% efficiency

b. Relief wells with 10-foot blank section.

(1) In this sensitivity study, the top 10 feet of each relief well screen was blocked. This cut off flow to the wells from the top 10 feet of fine sand underlying the blanket. A well spacing of 87 feet was used in these scenarios with well penetrations of 100%, 70% (51% effective), 50% (19% effective), and 25% (6.3% effective). Figure F-15 depicts the open screen intervals for these model simulations.

(2) Table F-13 and Table F-14 compare results from the model simulations, including the blank 10-foot section of screen, to simulations without the blank section in terms of mid-well head and relief well flow. Figure F-16 and Figure F-17 graphically show these results. Overall, the impact of blocking the upper 10 feet of each relief well screen was minimal for well penetrations of 100% and became slightly more pronounced as the well penetration decreased.

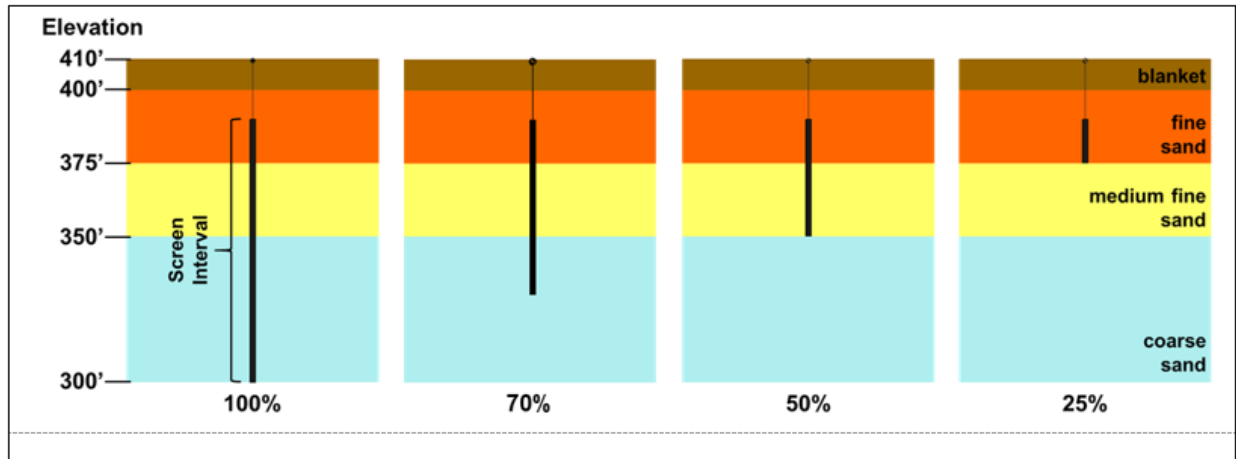


Figure F-15. Screen intervals with a 10-foot blank section at top of fine sand for penetrations of 25, 50, 70 and 100%

Table F-13

Mid-well head summary – relief wells with and without a 10-foot blank section of screen

Well Penetration (Effective) (Effective with Blank)	With 10-ft Blank Section		Without 10-ft Blank Section	
	Mid-Well Head (ft)	%H	Mid-Well Head (ft)	%H
100% (100%) (97.5%)	413.2	6.4	413.1	6.2
70% (51%) (48.9%)	414.9	9.7	414.7	9.3
50% (19%) (16%)	419.7	19.4	419.2	18.3
25% (6.3%) (3.8%)	432.1	44.2	429.9	39.8
No Wells	456.1	92.2	456.1	92.2

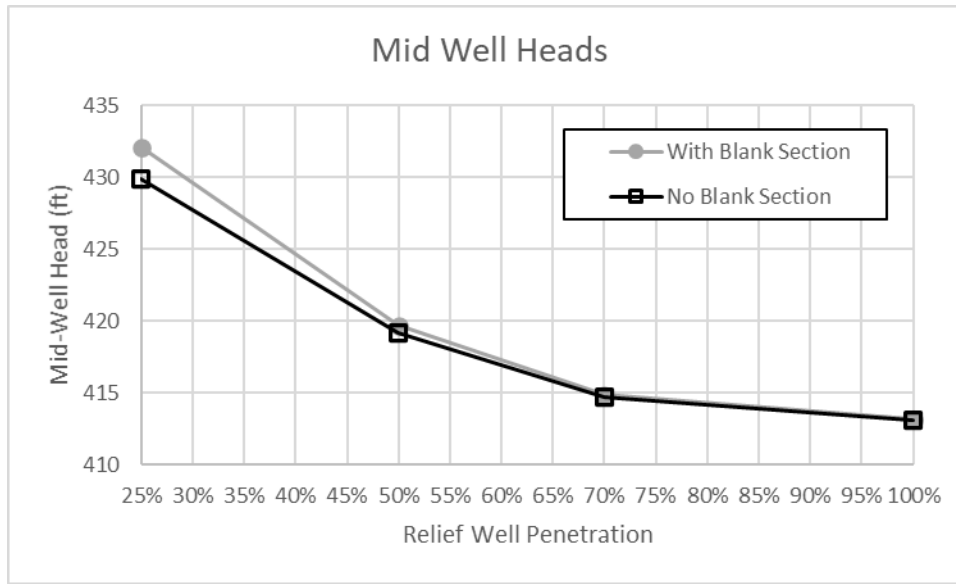


Figure F-16. Head computed mid-way between wells at the top of the aquifer/base of the blanket; relief wells with and without a 10-foot blank section of screen are compared

**Table F-14
Relief well flow in gallons per minute; relief wells with and without a 10-foot blank section of screen**

Well Penetration (Effective) (Effective with Blank)	With 10-ft Blank Section	Without 10-ft Blank Section
100% (100%) (97.5%)	316	316
70% (51%) (48.9%)	304	305
50% (19%) (16%)	268	270
25% (6.3%) (3.8%)	172	186

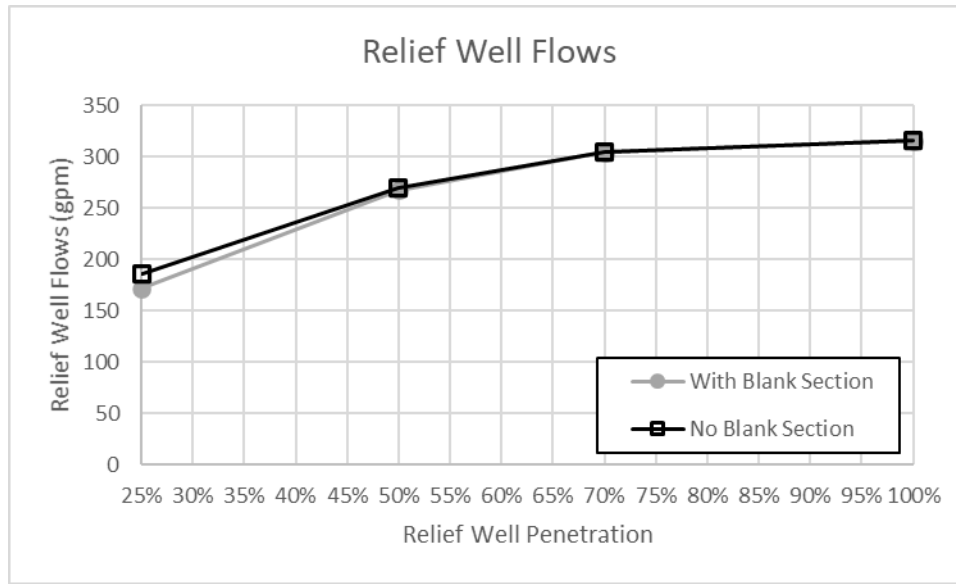


Figure F-17. Relief well flow with and without a 10-foot blank section of screen

c. *Blanket defect.* In this set of sensitivity studies, the model was modified to include a defect in the blanket. Seven defect locations were compared, with each model simulation including only one defect. These defects were named “A” through “G” as shown in Figure F-18. All defects were located midway between relief wells, which were spaced 87 feet apart. The locations were placed at varying distances upgradient and downgradient of the well line. Defect A was located 25 feet upgradient of the relief wells, and Defect B was located in line with the wells. Defects C through G were located 25, 50, 100, 200, and 300 feet downgradient of the well line, respectively. Only a portion of the model domain around the defects is shown in Figure F-18. The full extent of the model domain is similar to that pictured in Figure F-5.

(1) Due to the nature of the 3D mesh, there were minor differences in size and shape of the modeled defects. Defect surface areas ranged between 2.20 and 2.35 feet², which are equivalent to circular sand boils ranging from 1.4 feet to 1.5 feet in diameter. The surface areas of each defect are summarized in Table F-15. Defects were modeled by assigning a much higher K value (8.0×10^{-2} cm/second or 227 feet/day) than the surrounding blanket (1.0×10^{-6} cm/second or 0.00283 feet/day).

(2) The K of a coarse sand was selected to represent the defect since it was assumed that the sand in the defect would be in a loosened state. Defects were assumed to extend vertically the full 10-foot thickness of the blanket. The ground surface was modeled at an elevation of 410 feet at all defect locations, and defects were assumed to discharge to this elevation with no surface ponding. Model simulations were run with relief well penetrations of 100%, 70% (51% effective), 50% (19% effective), 25% (6.3% effective), and 10% (2.5% effective). Well spacing was simulated as 87 feet. A no-well simulation was also modeled.

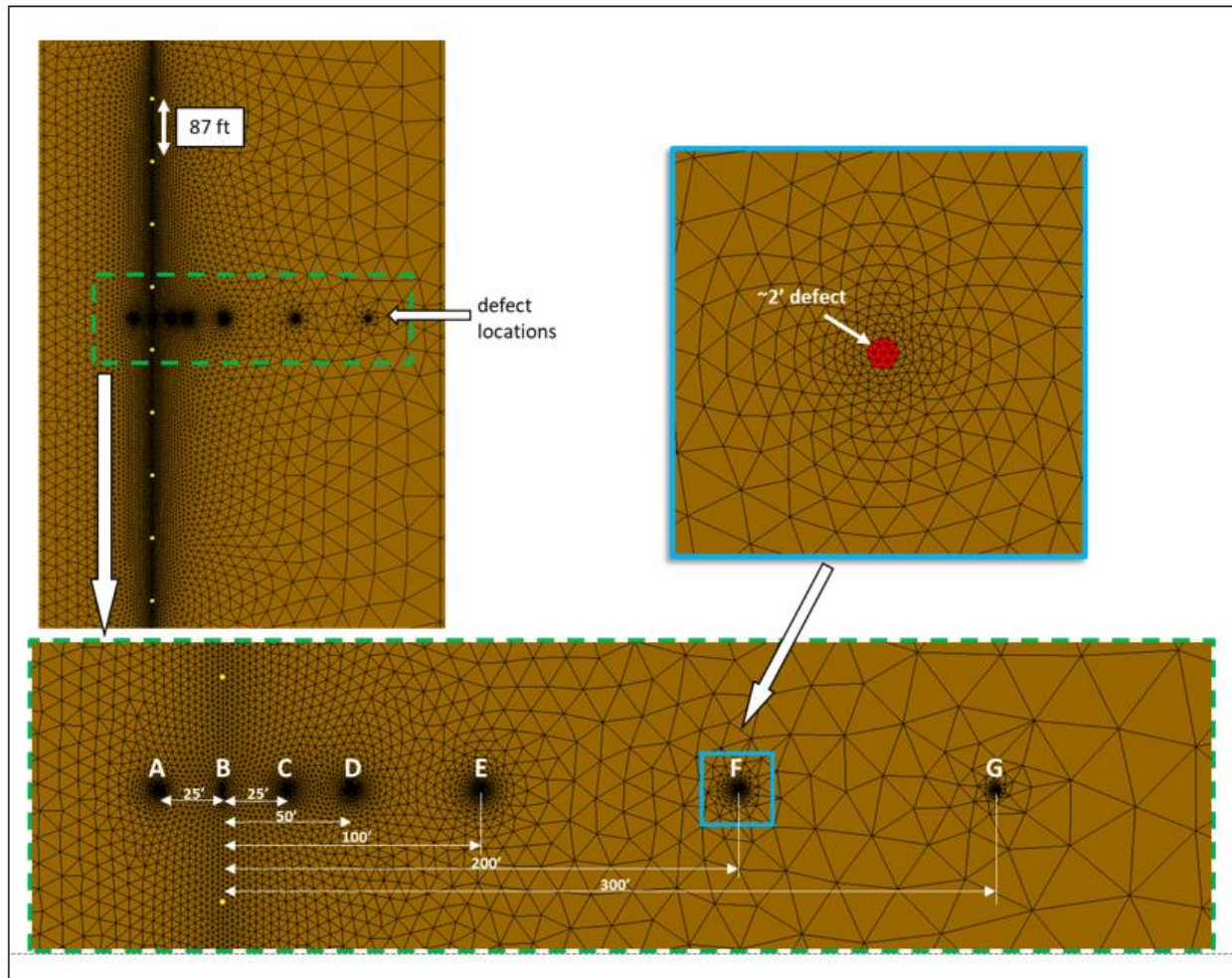


Figure F-18. Blanket defect model setup (full model domain not pictured)

Table F-15
Defect surface area

Defect Location	A	B	C	D	E	F	G
Surface Area (sq. ft)	2.25	2.20	2.25	2.25	2.25	2.25	2.35

(3) Model output from the defect simulations was compared based on multiple output parameters. This included flow to the ground surface, horizontal gradients computed outward from the defect center, and vertical gradients across the 10-foot blanket thickness. Since the surface areas of the defects varied slightly, defect flow was computed in terms of both gpm and gpm per square foot of defect surface area. These results are tabulated in Table F-16 and shown in Figure F-19.

(4) Horizontal gradients computed from the center of each defect to 100-foot upgradient are plotted in Figure F-20. The gradients computed over 5 feet from the center of the defect are summarized in Table F-17. Vertical gradients across the defect are summarized in Table F-18. Relief well flow was also extracted from the model and

summarized in Table F–19. The presence of defects had little impact on the simulated well flow.

Table F–16
Defect flow (87-foot well spacing)

Well Penetration (Effective)	Defect Location						
	A	B	C	D	E	F	G
Flow from Defect, gpm							
100% (100%)	0.49	0.38	0.34	0.33	0.34	0.34	0.36
70% (51%)	0.69	0.57	0.55	0.55	0.57	0.58	0.60
50% (19%)	1.25	1.14	1.12	1.16	1.20	1.21	1.25
25% (6.3%)	2.58	2.43	2.48	2.54	2.60	2.60	2.69
10% (2.5%)	3.71	3.53	3.63	3.68	3.73	3.71	3.83
No Wells	5.70	5.44	5.66	5.64	5.63	5.58	5.77
Flow from Defect, gpm per sq. ft							
100% (100%)	0.22	0.17	0.15	0.15	0.15	0.15	0.15
70% (51%)	0.31	0.26	0.24	0.25	0.25	0.26	0.26
50% (19%)	0.56	0.52	0.50	0.51	0.53	0.54	0.53
25% (6.3%)	1.15	1.10	1.10	1.13	1.15	1.15	1.14
10% (2.5%)	1.65	1.61	1.62	1.64	1.66	1.65	1.63
No Wells	2.53	2.47	2.51	2.51	2.50	2.48	2.45

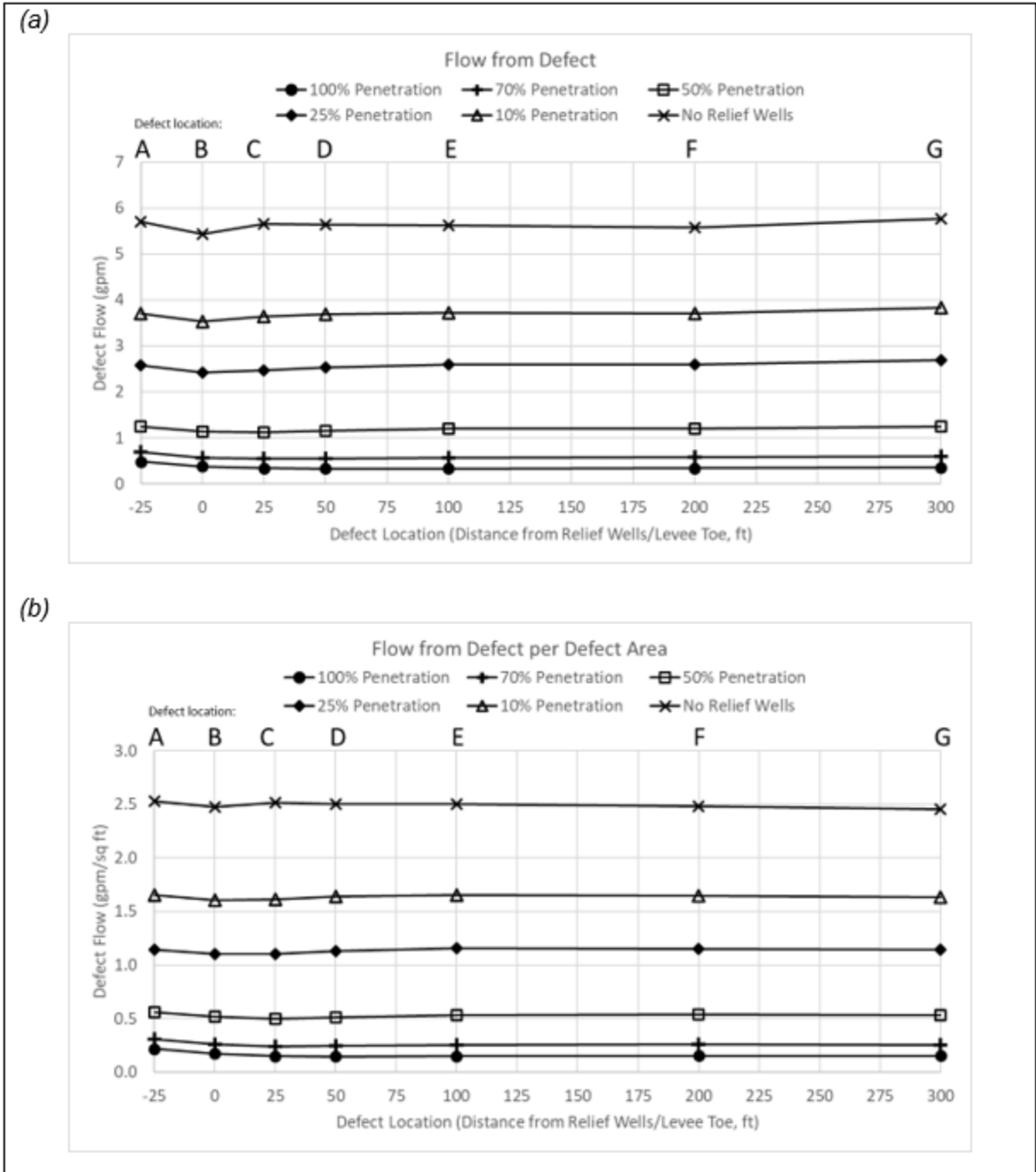


Figure F-19. Flow from defects to ground surface in (a) gallons per minute and (b) gallons per minute per square foot (87-foot well spacing)

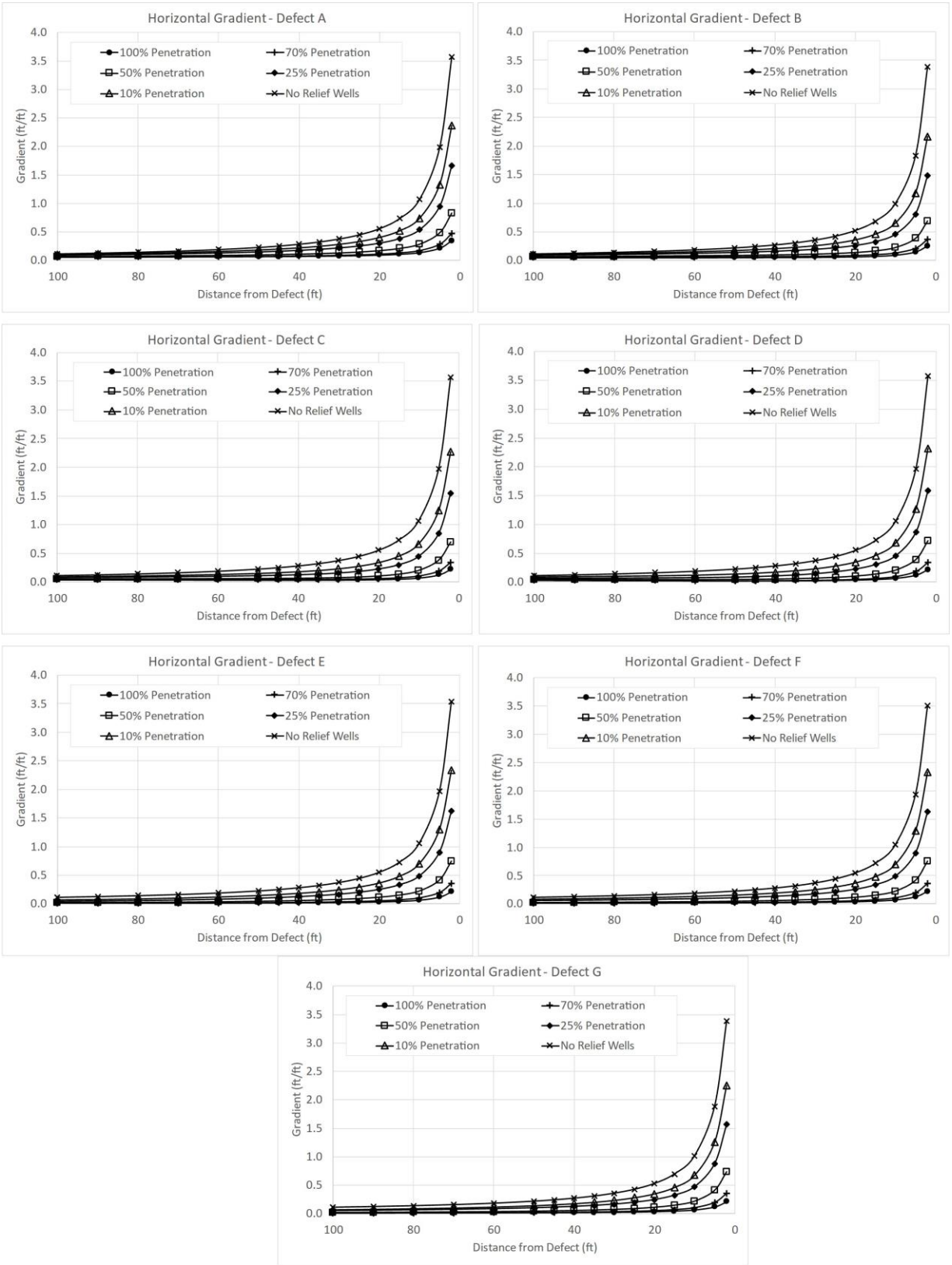


Figure F-20. Horizontal gradients computed from the center of each defect (87-foot well spacing)

Table F-17
Horizontal gradient computed over 5 feet from center of defect (87-foot well spacing)

Well Penetration (Effective)	Defect Location						
	A	B	C	D	E	F	G
100% (100%)	0.21	0.15	0.13	0.12	0.12	0.12	0.12
70% (51%)	0.28	0.21	0.19	0.19	0.20	0.20	0.20
50% (19%)	0.49	0.39	0.38	0.39	0.41	0.42	0.41
25% (6.3%)	0.95	0.81	0.84	0.87	0.90	0.90	0.88
10% (2.5%)	1.33	1.18	1.25	1.27	1.30	1.29	1.25
No Wells	1.99	1.83	1.97	1.97	1.96	1.94	1.89

Table F-18
Vertical gradient computed across 10-foot depth of defect (87-foot well spacing)

Well Penetration (Effective)	Defect Location						
	A	B	C	D	E	F	G
100% (100%)	0.30	0.24	0.21	0.20	0.20	0.21	0.21
70% (51%)	0.42	0.36	0.33	0.34	0.35	0.35	0.36
50% (19%)	0.76	0.71	0.69	0.71	0.73	0.74	0.74
25% (6.3%)	1.57	1.53	1.51	1.55	1.58	1.58	1.58
10% (2.5%)	2.26	2.25	2.22	2.25	2.27	2.26	2.26
No Wells	3.47	3.54	3.45	3.45	3.43	3.41	3.40

Table F-19
Relief well flow in gallons per minute for simulations including a blanket defect (87-foot well spacing)

Well Penetration (Effective)	Defect Location							
	None	A	B	C	D	E	F	G
100% (100%)	313	313	312	313	313	313	313	313
70% (51%)	302	302	302	302	302	302	302	302
50% (19%)	268	268	268	268	268	268	268	268
25% (6.3%)	185	185	185	185	185	185	185	185
10% (2.5%)	117	116	116	116	116	116	117	117

(5) Simulations were performed that included a relief well efficiency of 80% and a defect at location B (in-line with relief wells). Table F–20 compares the flow from Defect B with 80% and 100% efficient relief wells. Table F–21 compares horizontal and vertical gradients for the 80% and 100% scenarios. Table F–22 summarizes flow from the relief wells assuming 80% and 100% efficiency for scenarios with and without Defect B. Results are shown graphically in Figure F–21 through Figure F–23.

Table F–20
Defect B flow – 80% versus 100% relief well efficiency (87-foot well spacing)

Well Penetration (Effective)	Defect Flow, gpm		Defect Flow, gpm per sq. ft	
	80% Efficient	100% Efficient	80% Efficient	100% Efficient
100% (100%)	1.64	0.38	0.75	0.17
70% (51%)	1.74	0.57	0.79	0.26
50% (19%)	2.15	1.14	0.98	0.52
25% (6.3%)	3.35	2.43	1.52	1.10
10% (2.5%)	4.38	3.53	1.99	1.61
No Wells	5.44	–	2.47	–

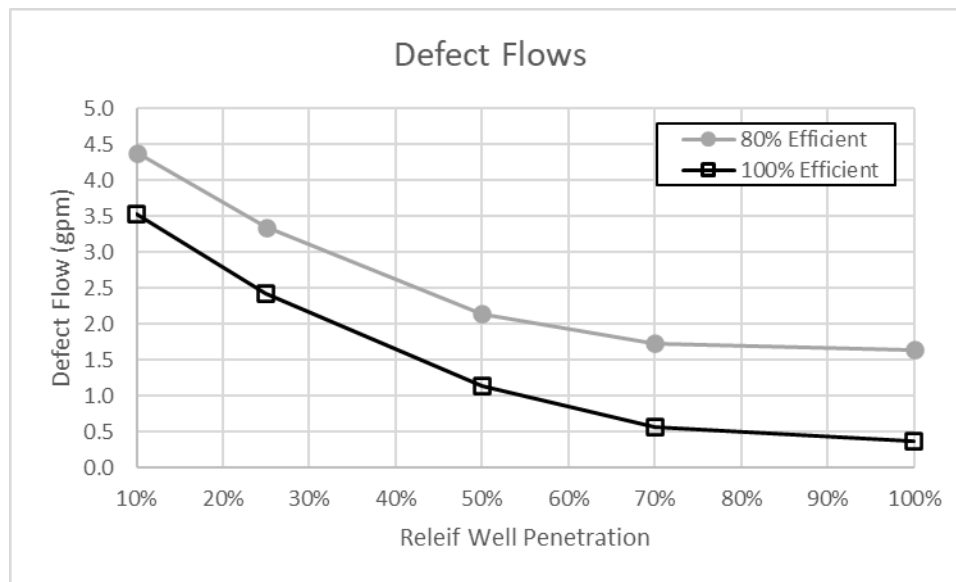


Figure F–21. Defect B flow – 80% efficiency versus 100% efficiency (87-foot well spacing)

Table F-21
Gradient summary (Defect B) – 80% versus 100% relief well efficiency (87-foot well spacing)

Well Penetration (Effective)	5-ft Horizontal Gradients		Vertical Gradients	
	80% Efficient	100% Efficient	80% Efficient	100% Efficient
100% (100%)	0.52	0.15	0.97	0.24
70% (51%)	0.55	0.21	1.02	0.36
50% (19%)	0.67	0.39	1.25	0.71
25% (6.3%)	1.01	0.81	1.94	1.53
10% (2.5%)	1.31	1.18	2.51	2.25
No Wells	1.58	–	3.04	–

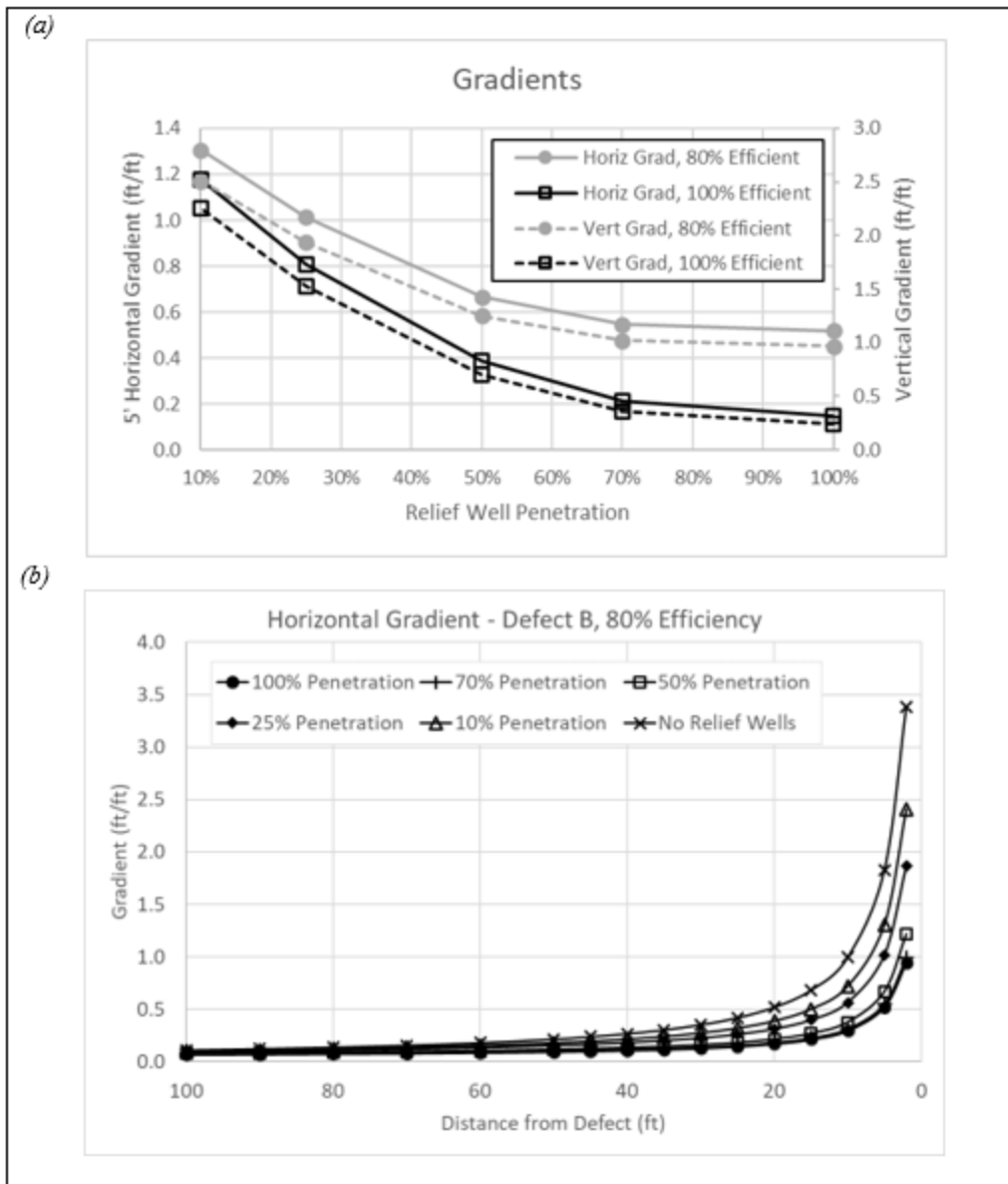


Figure F-22. Gradient summary (Defect B) – 80% well efficiency (87-foot well spacing): (a) horizontal gradient computed 5 feet from center of Defect B and vertical gradients across the defect, and (b) horizontal gradient computed from center of Defect B for simulations assuming relief well efficiency of 80%

Table F–22
Relief well flow in gallons per minute – 80% versus 100% relief well efficiency (87-foot well spacing)

Well Penetration (Effective)	No Defect		Defect B	
	80% Efficient	100% Efficient	80% Efficient	100% Efficient
100% (100%)	252	316	249	312
70% (51%)	245	305	244	302
50% (19%)	217	270	216	268
25% (6.3%)	149	186	148	185
10% (2.5%)	94	117	94	116

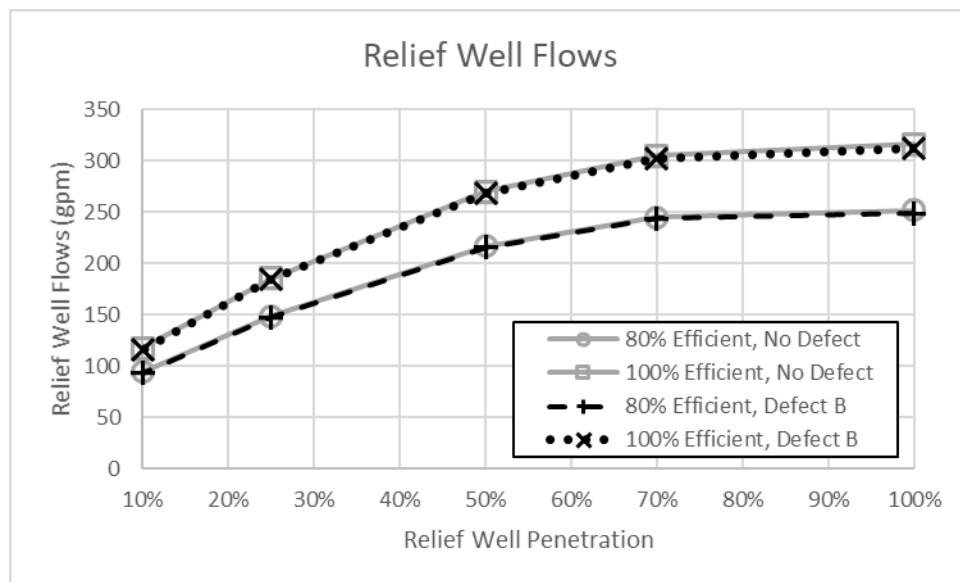


Figure F–23. Relief well flow – 80% versus 100% relief well efficiency (87-foot well spacing)

(6) Defect B was also modeled for the scenario in which the top 10 feet of each relief well screen was blocked. Table F–23 compares the flow from Defect B for simulations with and without a blank section of screen. The horizontal and vertical gradients were also compared for these two scenarios (Table F–24). Finally, Table F–25 summarizes flow from the relief wells with and without the defect and with and without the blank section of screen. Results are shown graphically in Figure F–24 through Figure F–26.

Table F-23
Defect B flow – relief wells with and without a 10-foot blank section of screen (87-foot well spacing)

Well Penetration (Effective) (Effective with Blank)	Defect Flow, gpm		Defect Flow, gpm per sq. ft	
	With 10-ft Blank Section	Without 10-ft Blank Section	With 10-ft Blank Section	Without 10-ft Blank Section
100% (100%) (97.5%)	0.44	0.38	0.20	0.17
70% (51%) (48.9%)	0.63	0.57	0.29	0.26
50% (19%) (16%)	1.25	1.14	0.57	0.52
25% (6.3%) (3.8%)	2.93	2.43	1.33	1.10
No Wells	5.44	–	2.47	–

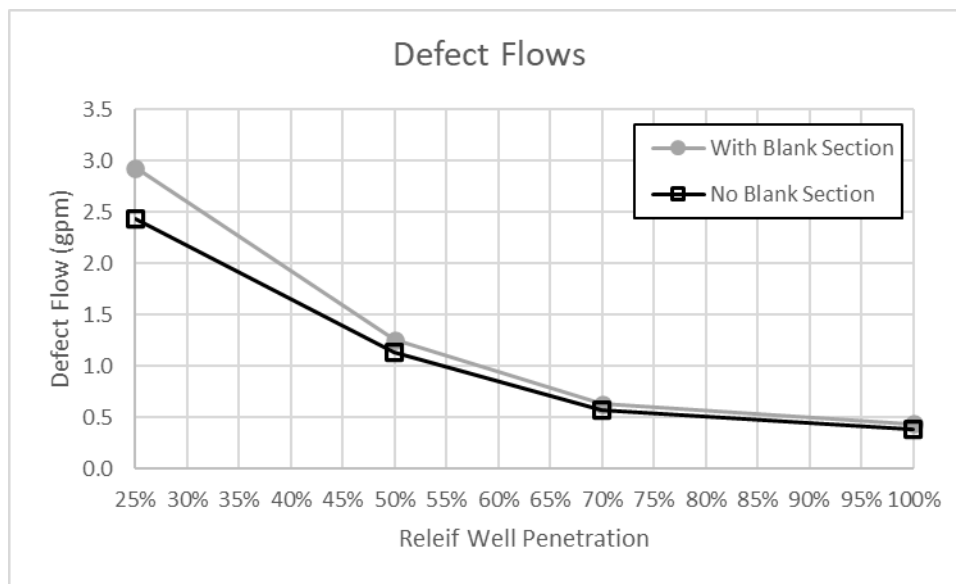


Figure F-24. Defect flow (location B) – relief wells with and without a 10-foot blank section of screen (87-foot well spacing)

Table F-24
Gradient summary (Defect B) – relief wells with and without a 10-foot blank section of screen (87-foot well spacing)

Well Penetration (Effective) (Effective with Blank)	5-ft Horizontal Gradients		Vertical Gradients	
	With 10-ft Blank Section	Without 10-ft Blank Section	With 10-ft Blank Section	Without 10-ft Blank Section
100% (100%) (97.5%)	0.15	0.15	0.25	0.24
70% (51%) (48.9%)	0.22	0.21	0.37	0.36
50% (19%) (16%)	0.41	0.39	0.75	0.71
25% (6.3%) (3.8%)	0.89	0.81	1.70	1.53
No Wells	1.83	–	3.54	–

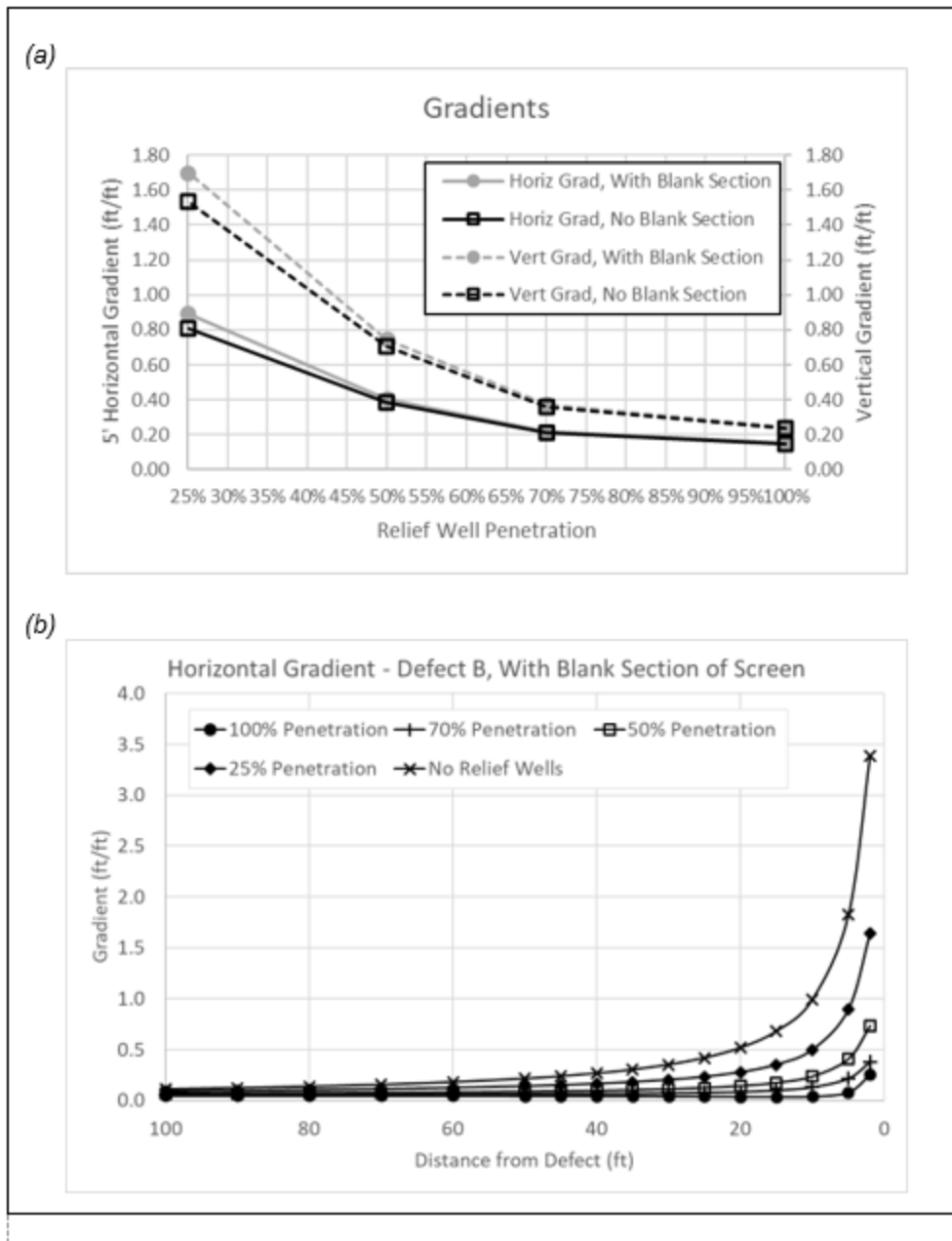


Figure F-25. Gradient summary (Defect B) – relief wells with 10-foot blank section of screen (87-foot well screen): (a) horizontal gradient computed 5 feet from center of Defect B and vertical gradients across the defect, (b) horizontal gradient computed from center of Defect B for simulations including 10-foot blank section of screen

Table F-25

Relief well flow in gallons per minute – relief wells with and without a 10-foot blank section of screen (87-foot well spacing)

Well Penetration (Effective) (Effective with Blank)	No Defect		Defect B	
	With 10-ft Blank Section	Without 10-ft Blank Section	With 10-ft Blank Section	Without 10-ft Blank Section
100% (100%) (97.5%)	316	316	312	312
70% (51%) (48.9%)	304	305	301	302
50% (19%) (16%)	268	270	265	268
25% (6.3%) (3.8%)	172	186	170	185

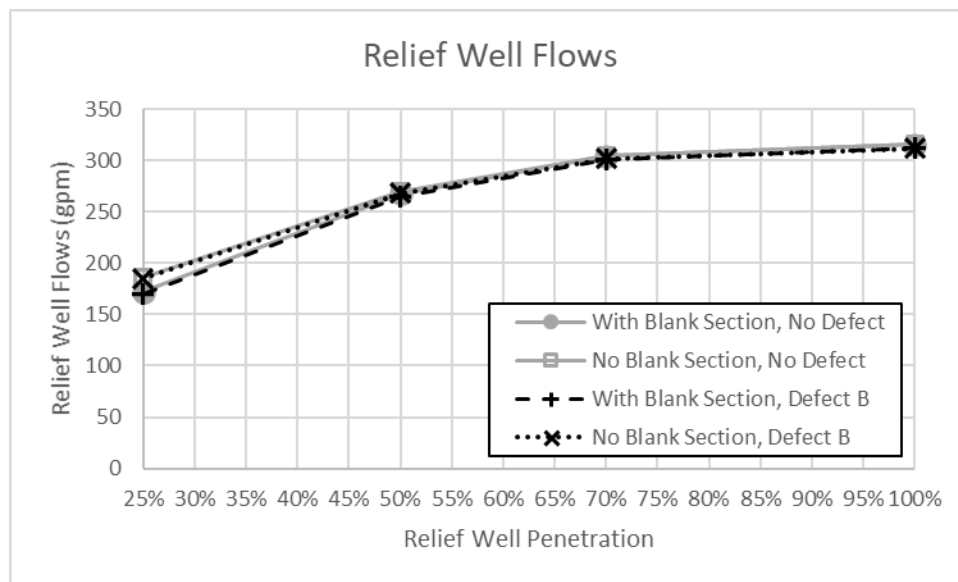


Figure F-26. Relief well flow – relief wells with and without a 10-foot blank section of screen (87-foot well spacing)

(7) Model simulations including a defect at location B were run with a relief well spacing of 261 feet. This spacing is 3 times that of the 87-foot spacing used in previous simulations of the defects. Simulations with the larger spacing were performed with and without a blank section of well screen (similar to runs discussed in paragraph F-4c(6)). Output parameters consist of flow from Defect B, horizontal and vertical gradients, and relief well flow. Table F-26 through Table F-28 compare results with and without the blank section of screen. Figure F-27 through Figure F-29 graphically show these results. The results indicate that the presence of the blank screen section had little effect on the output parameters.

Table F-26

Defect B flow – 261-foot relief well spacing; relief wells with and without a 10-foot blank section of screen

Well Penetration (Effective) (Effective with Blank)	Defect Flow, gpm		Defect Flow, gpm per sq. ft	
	With 10-ft Blank Section	Without 10-ft Blank Section	With 10-ft Blank Section	Without 10-ft Blank Section
100% (100%) (97.5%)	1.38	1.37	0.63	0.62
70% (51%) (48.9%)	1.88	1.90	0.85	0.87
50% (19%) (16%)	3.03	2.96	1.38	1.35
25% (6.3%) (3.8%)	4.74	4.54	2.16	2.06
10% (2.5%) (0%)	N/A	5.35	N/A	2.43
No Wells	5.44	–	2.47	–

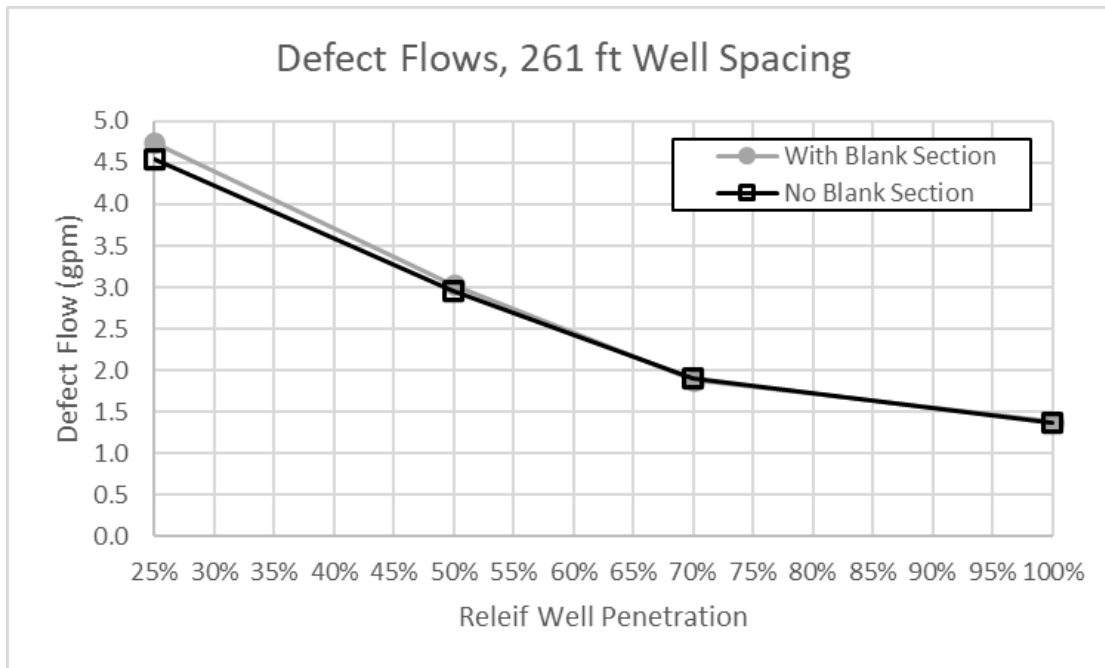


Figure F-27. Defect B flow – 261-foot relief well spacing

Table F-27**Gradient summary (Defect B) – 261-foot relief well spacing; relief wells with and without a 10-foot blank section of screen**

Well Penetration (Effective) (Effective with Blank)	5-ft Horizontal Gradients		Vertical Gradients	
	With 10-ft Blank Section	Without 10-ft Blank Section	With 10-ft Blank Section	Without 10-ft Blank Section
100% (100%) (97.5%)	0.44	0.44	0.82	0.81
70% (51%) (48.9%)	0.59	0.59	1.12	1.10
50% (19%) (16%)	0.92	0.90	1.76	1.72
25% (6.3%) (3.8%)	1.40	1.35	2.71	2.60
10% (2.5%) (0%)	N/A	1.58	N/A	3.04
No Wells	1.83	–	3.54	–

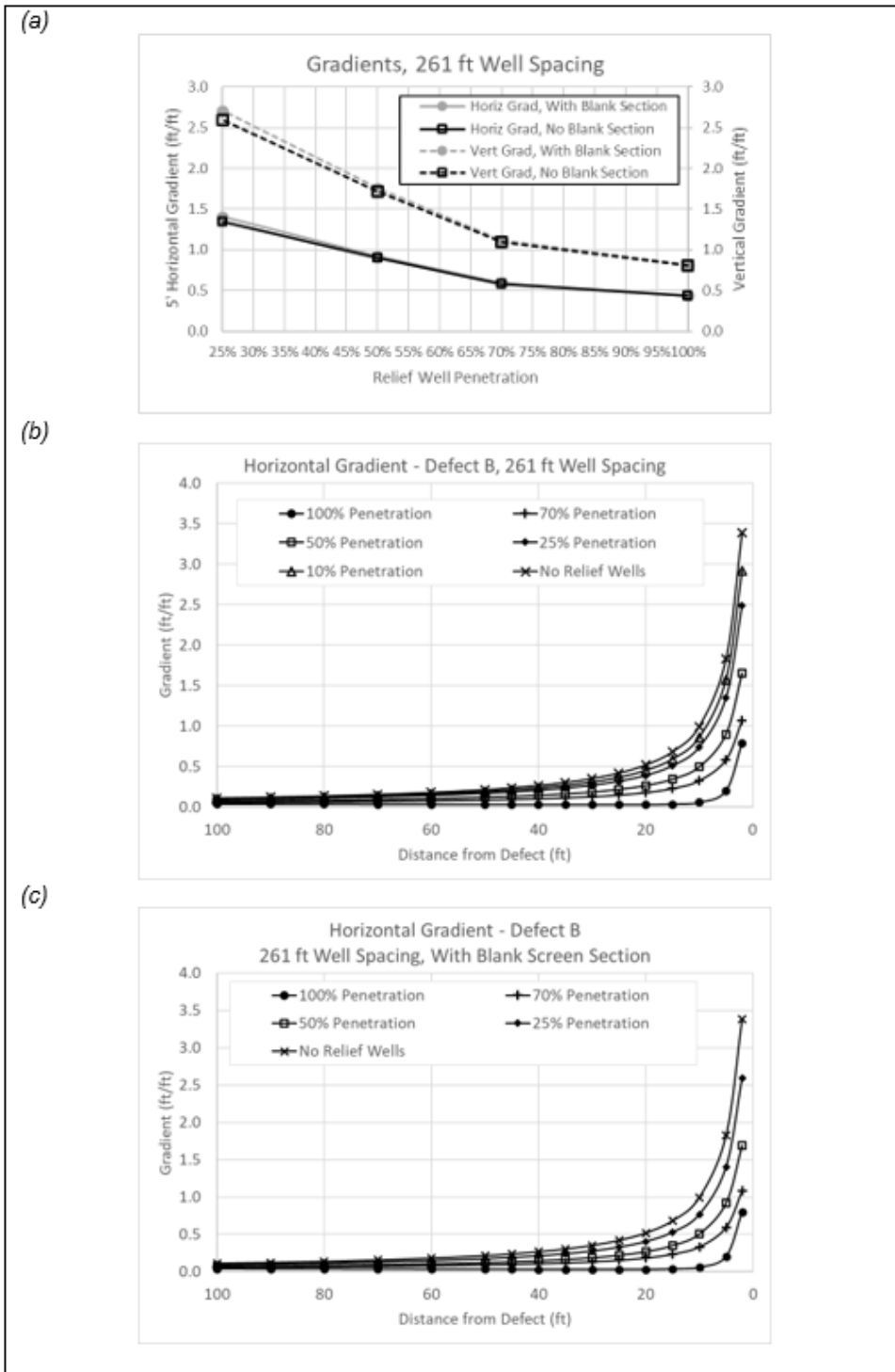


Figure F-28. Gradient summary – 261-foot relief well spacing: (a) horizontal gradient computed 5 feet from center of Defect B and vertical gradients across the defect; (b) horizontal gradient computed from center of Defect B, relief wells every 261 feet, no blank section of screen; and (c) horizontal gradient computed from center of Defect B, relief wells every 261 feet, blank section at top 10 feet of relief well screens

Table F-28

Relief well flow in gallons per minute – 261-foot relief well spacing; relief wells with and without a 10-foot blank section of screen

Well Penetration (Effective) (Effective with Blank)	With 10-ft Blank Section	Without 10-ft Blank Section
100% (100%) (97.5%)	798	800
70% (51%) (48.9%)	720	724
50% (19%) (16%)	537	549
25% (6.3%) (3.8%)	254	287
10% (2.5%) (0%)	N/A	151

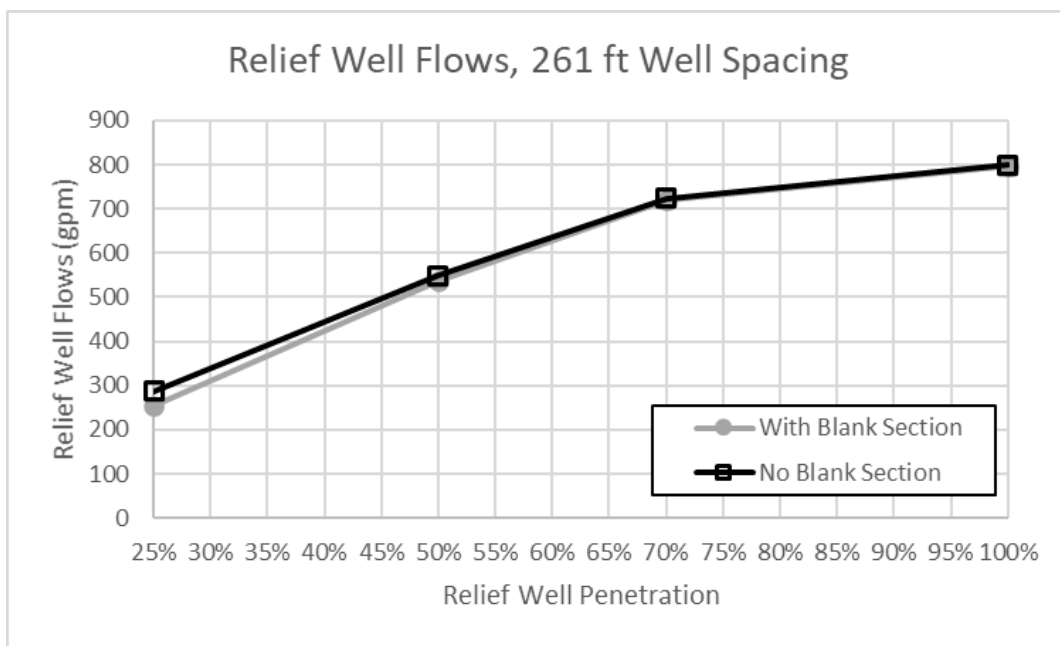


Figure F-29. Relief well flow – 261-foot well spacing

d. *Anisotropy.* The effects of anisotropy on Model #2 and Model #2d (paragraphs F-2b and F-2b(3)) were explored by reducing the vertical hydraulic conductivity (K_v) of the aquifer materials to be 25% of the horizontal hydraulic conductivity (K_h). The K_v of the blanket remained equal to the K_h for these scenarios. A relief well spacing of 174 feet was used for this sensitivity, along with well penetrations of 100%, 70% (51% effective), 50% (19% effective), 25% (6.3% effective), and 10% (2.5% effective). A transformed aquifer case was also modeled. The transformed aquifer was 268 feet thick with an effective K of 1.84×10^{-2} cm/second (52.2 feet/day). Well screen elevations for the transformed aquifer case are listed in Table F-29.

Table F–29
Transformed relief well screen elevations

Penetration (Effective)	Top (ft)	Base (ft)
100% (100%)	400	132.0
70% (51%)	400	263.3
50% (19%)	400	349.1
25% (6.3%)	400	383.1
10% (2.5%)	400	393.3

(1) Head calculated by the 3D numerical model is compared to BT in Table F–30. Results from the case including anisotropy are listed at the top of the table. Results from the isotropic case are listed at the bottom of the table for comparison. These results are also presented in Table F–31 in terms of %*H*. The addition of anisotropy to the stratified numerical model raised mid-well head by up to 0.3 foot in Model #2 and lowered head by up to 0.6 foot in Model #2d. The largest head difference between Numerical Model #2 and BT was observed for a well penetration of 10% (2.5% effective) for both the isotropic and anisotropic cases.

(2) Head computed by Numerical Model #2 was closest to those computed by BT for a well spacing of 50% (19% effective). Head computed by BT was in slightly better agreement with Model #2d than with Model #2. The differences between head computed by Model #2d and BT was less than 1 foot for all well penetrations, but, surprisingly, the largest difference in head (0.74 foot) occurred for a relief well penetration of 100%. Head results for models that included anisotropy are presented graphically in Figure F–30.

Table F-30
Mid-well head in feet

Well Penetration (Effective)	Model #2			Model #2d	
	BT	Stratified Numerical	Transformed Numerical*	BT	Stratified Numerical
$K_h: K_v = 4:1$					
100% (100%)	415.1	416.4	416.9	414.5	415.3
70% (51%)	418.4	419.4	419.3	416.7	417.2
50% (19%)	426.9	426.8	424.1	421.2	420.8
25% (6.3%)	437.9	439.9	434.8	425.3	425.3
10% (2.5%)	445.2	448.6	446.5	427.4	427.6
$K_h: K_v = 1:1$					
100% (100%)	415.1	416.4	416.8	414.5	415.5
70% (51%)	418.5	419.3	419.4	416.9	417.4
50% (19%)	426.3	426.5	424.8	421.2	421.1
25% (6.3%)	436.0	439.7	437.1	426.4	425.9
10% (2.5%)	442.0	448.4	444.3	428.7	428.1

Notes:

*Adjusted for headwater/tailwater conditions of 460 feet/410 feet, respectively.

Model #2 includes a no-flow boundary at the model surface. In Model #2d, water is allowed to discharge to the surface through the landside blanket ($K = 1.0 \times 10^{-4}$ cm/second).

Table F-31
Mid-well head in percent of net head (%H)

Well Penetration (Effective)	Model #2			Model #2d	
	BT	Stratified Numerical	Transformed Numerical*	BT	Stratified Numerical
$K_h: K_v = 4:1$					
100% (100%)	10.2	12.8	13.9	9.1	10.6
70% (51%)	16.7	18.8	18.5	13.4	14.3
50% (19%)	33.8	33.5	28.1	22.3	21.6
25% (6.3%)	55.9	59.7	49.6	30.7	30.7
10% (2.5%)	70.3	77.2	73.1	34.8	35.2
$K_h: K_v = 1:1$					
100% (100%)	10.2	12.8	13.6	9.1	10.9
70% (51%)	16.9	18.6	18.8	13.8	14.8
50% (19%)	32.7	33.0	29.6	22.4	22.4
25% (6.3%)	52.0	59.4	54.3	32.7	31.9
10% (2.5%)	64.1	76.7	68.5	37.3	36.3

Note:

Model #2 includes a no-flow boundary at the model surface. In Model #2d, water is allowed to discharge to the surface through the landside blanket ($K = 1.0 \times 10^{-4}$ cm/second).

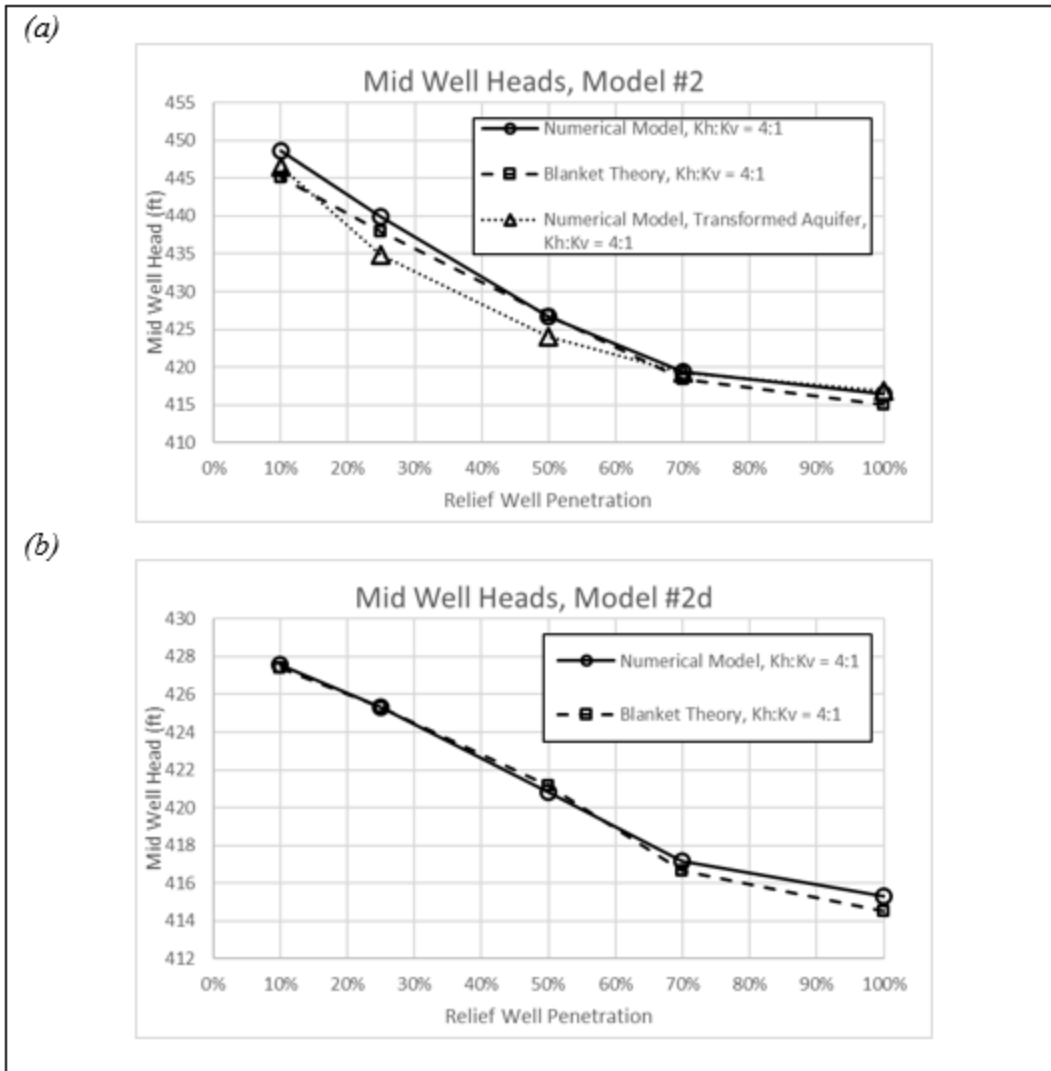


Figure F-30. Comparison of mid-well head calculated by the numerical model and Blanket Theory for an anisotropic aquifer: (a) results from Model #2, and (b) results from Model #2b

(3) Relief well flow calculated by the 3D numerical model are compared to BT in Table F-32. Results from the case including anisotropy are listed at the top of the table. Results from the isotropic case are listed at the bottom of the table for comparison. The addition of anisotropy to the stratified numerical model decreased relief well flow for wells that did not fully penetrate the aquifer for both Model #2 and Model #2d. Relief well flow from wells that fully penetrated the aquifer did not change in Model #2 and slightly increased in Model #2d. Relief well flow computed by Numerical Models #2 and #2d was in good agreement with flow computed by BT for penetrations of 50% (19% effective) or greater. Relief well flow for models that included anisotropy are presented graphically in Figure F-31.

Table F-32
Relief well flow in gallons per minute

Well Penetration (Effective)	Model #2			Model #2d	
	BT	Stratified Numerical	Transformed Numerical*	BT	Stratified Numerical
$K_h: K_v = 4:1$					
100% (100%)	579.2	562.7	573.9	517.3	488.5
70% (51%)	521.8	516.9	533.7	417.7	413.7
50% (19%)	403.3	409.8	459.3	266.1	276.4
25% (6.3%)	280.6	233.7	318.4	146.7	123.7
10% (2.5%)	197.7	128.6	169.9	89.0	59.7
$K_h: K_v = 1:1$					
100% (100%)	579.2	562.7	590.4	517.3	486.1
70% (51%)	531.7	524.0	552.5	433.5	421.2
50% (19%)	428.8	429.6	476.9	294.1	295.1
25% (6.3%)	320.8	258.2	309.8	140.1	139.8
10% (2.5%)	251.4	147.4	213.1	67.9	70.1

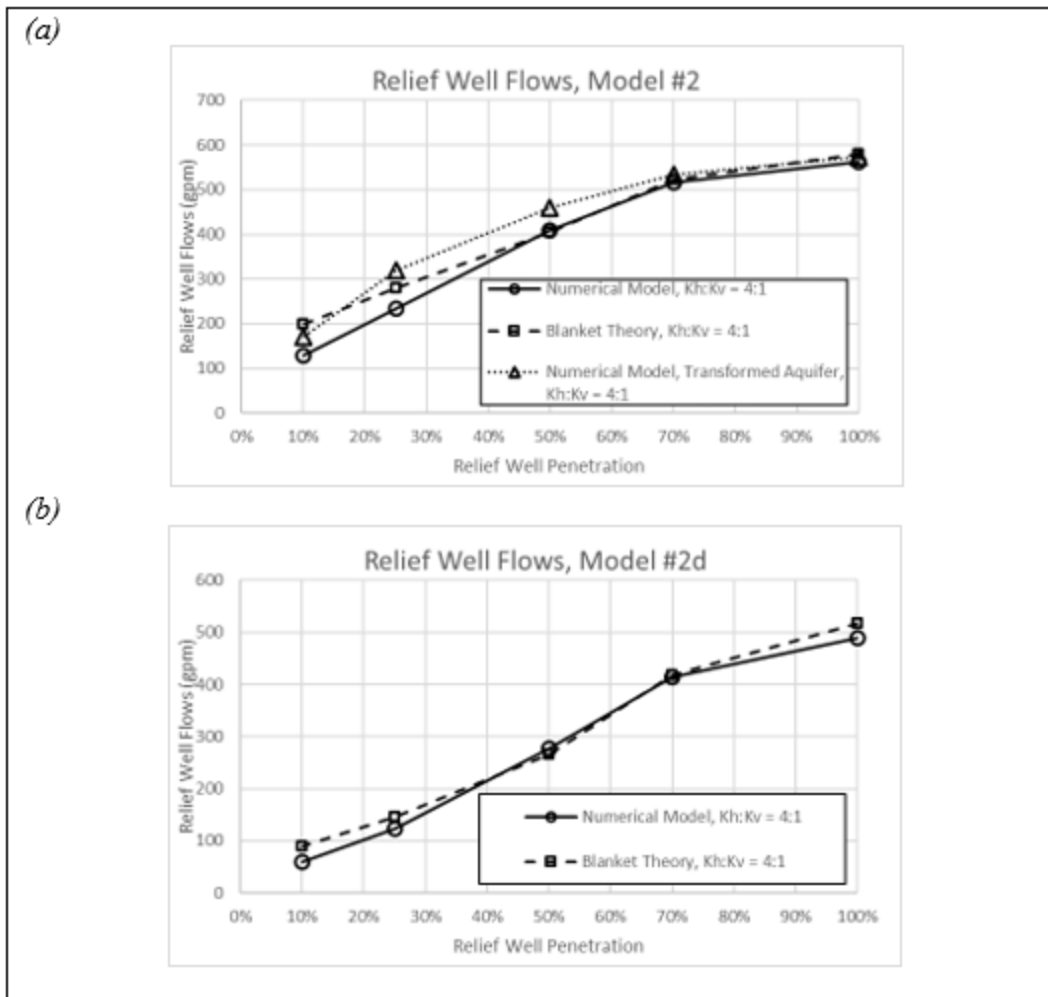


Figure F-31. Comparison of relief well flow calculated by the numerical model and Blanket Theory for an anisotropic aquifer: (a) results from Model #2, and (b) results from Model #2b

F-5. Summary

a. Physical model B-a from TM 3-304 was recreated using the WASH123D numerical modeling code. The numerical model was constructed to replicate the relief wells and boundary conditions of the physical model. Whereas the upper boundary of the physical model consisted of a glass plate, the numerical model simulated a 10-foot-thick, low-permeability blanket at the model surface. The numerical model calculated head and relief well flow. These results were compared to those from both the physical model and BT.

b. The numerical model and physical model produced similar results at most relief well spacings and penetrations. Larger differences between mid-well head in the two models was generally seen for smaller well spacings and smaller relief well penetrations while differences in relief well flow were greater for larger well spacings and smaller penetrations. BT also produced similar results to the numerical model for relief well

penetrations up to 50% (19% effective), but significant differences were seen at penetrations of 25% (6.2% effective) and 10% (2.5% effective).

Variations of selected model elements were also simulated numerically to assess their impact on the model results. Variations included extending the downstream boundary, applying a specified head to the downstream boundary, and increasing the K of the blanket. There was also variation in how the aquifer was simulated. In one case, it was modeled as a 3-layer system consistent with the physical model. In the other case, consistent with BT, it was modeled as an equivalent transformed aquifer consisting of uniform material with a single K value and a larger aquifer thickness. Model variations are summarized in Table F–33. Table F–36 through

c. Table F–40 includes summary tables of results from the series of numerical models and the results obtained from BT and the physical model.

d. Figure F–33 through Figure F–49 show contours of total head in cross section through a well location, plan view, and profile along the toe through the well line. Figure F–36 is the same as Figure F–35 with shading of the total head contours rather soil regions to better demonstrate average total head along the line of full-penetration wells. This plane is analogous to the average head along the well line, H_{av} , determined using BT using the well factor θ_{av} . A similar image for 51% effective penetration wells is included as Figure F–40.

Table F–33
Summary of numerical model features

Numerical Model	Downstream boundary distance from relief wells	Downstream boundary type	Surface boundary type downstream of dam/levee	Blanket hydraulic conductivity	Aquifer Type
Model #1	400 ft	No-flow	No-flow	1×10^{-6} cm/s	Stratified
Model #2	4,800 ft	No-flow	No-flow	1×10^{-6} cm/s	Stratified
Model #2a	4,800 ft	Specified head = 410 ft	No-flow	1×10^{-6} cm/s	Stratified
Model #2b	4,800 ft	No-flow	No-flow	1×10^{-4} cm/s	Stratified
Model #2c	4,800 ft	No-flow	Leaky Blanket	1×10^{-6} cm/s	Stratified
Model #2d	4,800 ft	No-flow	Leaky Blanket	1×10^{-4} cm/s	Stratified
Model #3	4,800 ft	No-flow	No-flow	N/A	Transformed

e. Model variations demonstrated that:

(1) A good understanding of the conceptual flow system is important when developing a 3D model so that defensible boundary conditions can be applied. Variations in boundary conditions may affect the conclusions.

(2) Extending the no-flow downstream boundary from 400 feet to 4,800 feet downstream of the relief well line did not impact model results. This comparison was conducted for simulations where no-flow boundaries were applied to the top boundary, side boundaries perpendicular to the levee, and downstream boundary. The distance of the downstream boundary may affect results if other boundary conditions are applied.

(3) Changing the downstream boundary located 4,800 feet from the relief wells from a no-flow boundary to a specified head boundary had only minor impacts on mid-well head. However, this variation had larger impacts on relief well flow, especially for larger well spacings and lower well penetrations. Relief well flow calculated by the model with the specified head downstream boundary was lower than calculated with the no-flow boundary.

(4) Increasing the K of the blanket while maintaining a no-flow boundary at the ground surface had only minor impacts on model results.

(5) The no-flow boundary forming the model surface downstream of the levee was removed and water was allowed to discharge to the surface through a “leaky blanket.” The impact of this variation was to reduce relief well flow and mid-well head. These differences are relatively minor when the K of the blanket was set to 1.0×10^{-6} cm/second (0.00284 feet/day) but increase as the K of the blanket increases.

(6) Representing the aquifer as a single material instead of a stratified foundation resulted in differences in both mid-well head and relief well flow compared to the physical model. These differences were significant only for wells that penetrated 10% (2.5% effective) of the aquifer. This indicates that aquifer transformations may not be appropriate for small, effective penetrations.

f. A series of sensitivity studies were also performed by modifying Numerical Model #2c. These sensitivity studies explored the impact of reducing the relief well efficiency to 80% and using blank pipe in the top 10 feet of the well screen. Also evaluated were incorporating a defect in the blanket and increasing the well spacing. In most instances, the impacts from these modifications were more apparent for smaller well penetrations. The sensitivity studies also demonstrated the following:

(1) Reducing the well efficiency to 80% resulted in the expected head beneath the blanket based on the model with 100% efficient wells and the model without wells.

(2) The 10-foot blank section at the top of the well did not reduce the effective well penetration significantly, except for the 25% (6.3% effective) (3.8% effective with blank) penetration. Including the blank section resulted in commensurate increases in head and gradient compared to the change in effective penetration.

(3) For the cases with a defect representing a sand boil through the blanket, the presence of wells decreased flow as well as gradient in and around the defect, regardless of defect location.

(4) To test the impact of anisotropy, vertical conductivities of the aquifer materials in Model #2 and Model #2d were reduced so that $K_h:K_v$ was 4:1. Head and relief well flow results from Model #2 were closest to BT for well penetrations of 50% (19% effective) and above. Head results from Model #2d were less than 1 foot for all well penetrations, with the largest difference occurring for a well penetration of 100%. Relief well flow results from Model #2d were closest to BT for well penetrations of 50% (19% effective) and above.

F–6. Additional considerations

a. The WASH123D 3D models in this appendix result in similar values as measured in physical models that contributed to BT relief well equations still in use today. These results both validate the 3D modeling approach and demonstrate BT provides reasonable results for an infinite line of wells for a range of well penetration. The 3D model was adapted incrementally from a replication of the lab test in Case 1 to better reflect typical field conditions in the models that constitute Case 2.

(1) The boundary conditions for these cases are summarized in Table F–29. In practice, relief wells are typically used where a leaky landside blanket exists with a permeability somewhere between values used for the landside blanket in Models #2c and #2d. The BT approach for this example includes an aquifer transformation to account for the stratified aquifer. A transformed aquifer with a single isotropic sand was modeled in Case 3 to evaluate the transformation equations presented in Appendix E.

(2) 2D, 3D, and BT models without wells result in identical total head beneath the blanket. The head at any distance landward from the landside toe is calculated using BT equation 6–3 in the main report. This equation is for an infinite landside blanket. An adjusted BT equation is included in EM 1110-2-1913 to calculate the head and any distance when there is a landside block. That version of the BT equation exactly matches 2D and 3D model results with a landside no-flow boundary at 4,800 feet (Figure F–32).

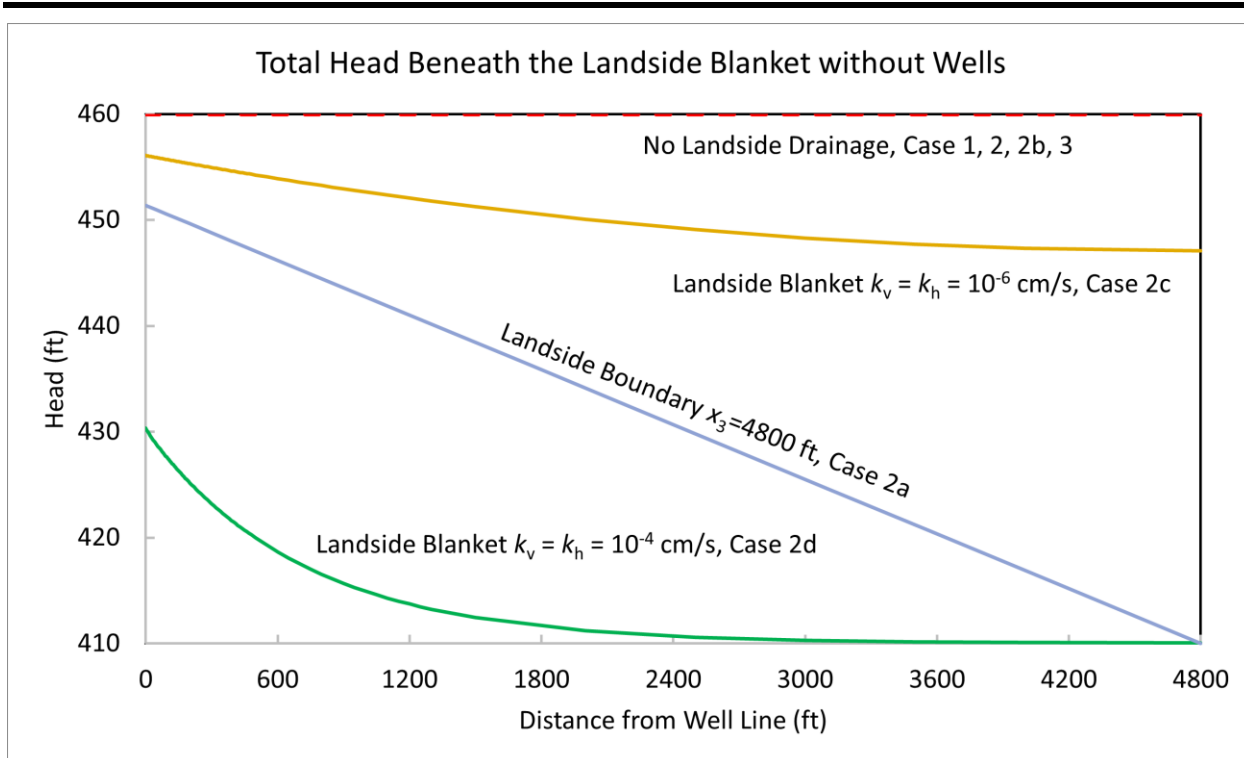


Figure F-32. Total head beneath the landside blanket without wells

(3) An intermediate well penetration of 70% was added to all 3D models performed. Although not included in the original TM 3-304 physical models, this results in an effective penetration of 51%. This is a more typical well penetration considering the aquifer stratigraphy than the three shallow well scenarios used in the physical model. It is common practice to design relief wells so that they effectively penetrate at least half the aquifer.

(4) Table F-4, Figure F-7, and Figure F-8 demonstrate both 3D models and BT equations reasonably approximate physical well flow and piezometric head midway between wells. The 3D models provide a good match with physical models for all cases. BT underpredicted head and overpredicted flow for the two cases with 25% and 10% penetration (6.3% and 2.5% effective penetration). Although BT equations apply to wells that effectively penetrate at least 25% of the aquifer, the beneficial effects of wells diminish for shallow wells. The exact stratigraphy of aquifer permeability is difficult to assess and estimates of the effective penetration are never precise. The results from all models demonstrate the sensitivity to well penetration when wells do not effectively penetrate at least half of the aquifer.

(5) Table F-9, along with Figure F-12 and Figure F-13, show very similar results for the transformed 3D model. Since BT calculations for this stratified foundation include an aquifer transformation, the single set of BT results are comparable with both Case 1 and Case 3 results. Results are in generally good agreement between the three approaches for both Case 1 and Case 3.

(6) As described in paragraph F–3d, 3D results are not identical between the stratified aquifer model (Case 1) and the transformed aquifer model (Case 3). The aquifer transformation results in lower mid-well head for wells that do not effectively penetrate half the aquifer. The physical model and 3D models result in higher mid-well head than BT for these shallow wells. Case 3 results in higher flow than Case 1 for the 3D models. Case 1 well flow results are in good agreement with BT for reasonable values of well penetration. Case 3, which includes an aquifer transformation, was in better agreement with BT for the shallow well scenarios.

(7) 3D models for full-penetration wells at large spacing result in higher mid-well head than either the physical model or BT. These physical model test results may have been considered when BT well equations were developed. This would explain why BT seems to be a better match with the physical model where differences do exist with 3D model results.

(8) There are two common approaches to account for the loss in well efficiency over time, to either factor the reduction in head due to the presence of relief wells or to reduce well flow in the model. Table F–12 demonstrates either approach results in the same calculation of head midway between wells for a 20% loss in well efficiency.

(9) Each of the soil layers were assumed to be anisotropic in several of the models with the vertical permeability reduced to one-quarter of the horizontal value. This was done to double the transformed depth of the aquifer, which has a small effect on BT results. Although changing the vertical permeability does not change the effective well penetration, aquifer depth is a secondary input for BT well factors.

(10) Anisotropy does not change BT results for full-penetration wells. Table F–30 and Table F–31 show reducing vertical permeability results in minimal changes to mid-well head in either BT or 3D models. Where drainage through the landside blanket is allowed in Model 2d, anisotropy resulted in slightly lower mid-well head in all cases except the full-penetration BT results, which are unchanged. Similarly, Table F–32 shows the reduced vertical permeability results in lower well flow values in most cases. For the transformed aquifer, the decrease in vertical permeability results in a small increase in well flow for the small well penetration cases (6.3% and 2.5% effective). This unexpected increase is seen in both the 3D transformed aquifer for Case 2 and in the BT results for Case 2d. While interesting and unexpected, these small penetration wells would not be used in practice.

b. Including a defect through the blanket at a range of distances from the levee toe demonstrates that relief wells improve conditions even where a sand boil is present. BEP is a function of many factors and is difficult to predict in natural soil deposits. One primary consideration is the seepage flow and hydraulic gradient to an advancing BEP erosion path. In addition to flow through the defect, gradient is measured horizontally at the base of the blanket across 5 feet to the center of the defect in these models.

(1) There has been consensus that wells reduce the likelihood of a BEP erosion pipe to progress toward the source from a boil landward of the well line. Table F–16

shows a significant reduction in flow and horizontal gradient (Table F–17) for defect “location A.” This demonstrates the potential for relief wells to also reduce the likelihood of progression for boils closer to the source than the well line. Flow and gradient values at location A reduced by an order of magnitude with full-penetration wells. There is a similar reduction with wells that effectively penetrate half the aquifer and a factor of 5 reduction for wells with only 19% effective penetration.

(2) Additional sensitivity studies demonstrate well efficiency reduces the positive effect on conditions around a boil. Flow and gradient of 80% efficient full-penetration wells happen to be about the same as for 100% effective wells that effectively penetrate half the aquifer. Replacing 10 feet of screen with a 10-foot blank section at the top of the well has almost no impact of flow and gradient in and around the defect.

(3) These models with a defect at various locations through the confining blanket included a well spacing of 87 feet. A much larger spacing of 261 feet was used to verify this positive effect relief wells have on flow and gradient around a boil. The reduction in flow and gradient is approximately a factor of 4 for full-penetration wells and a factor of 2 for wells with 19% effective penetration.

c. Additional sensitivity studies were used to investigate a blank well section in the intermediate fine sand layer. This topic is discussed in Chapter 2 and illustrated with Figure 2–2. Table F–13 and Figure F–16 show the 10-foot blank section has minimal effect on mid-well head beneath the blanket. Note that this case includes isotropic soils and the upper fine sand in Figure 2–2 is denoted as anisotropic.

(1) Additional models were performed both with and without the 10-foot blank section for both isotropic and anisotropic aquifer soils. Defect “B” was included in the blanket at the landside toe midway between relief wells spaced of 261 feet. Case 2c, with both full-penetration wells and the 51% effective penetration wells, was included at the relatively large relief well. Results are shown in Table F–34.

Table F-34

Flow and gradient for Case 2c with 261-foot relief well spacing and a sand boil at defect location "B"

With full screen		$W/D = 100\%$	$W/D = 100\%$	(51.4% effective)	(51.4% effective)
$k_h/k_v =$		1	4	1	4
Q_w	(gpm)	800	800	724	710
Q_{boil}	(gpm)	1.37	1.17	1.88	1.67
$i_{h \text{ over } 5'}$	-	0.44	0.59	0.59	0.82
$i_{v,boil}$	-	0.81	0.70	1.10	0.98
With 10' blank section		$W/D = 100\%$	$W/D = 100\%$	(51.4% effective)	(51.4% effective)
$k_h/k_v =$		1	4	1	4
Q_w	(gpm)	798	798	720	705
Q_{boil}	(gpm)	1.38	1.19	1.90	1.70
$i_{h \text{ over } 5'}$	-	0.44	0.60	0.59	0.83
$i_{v,boil}$	-	0.82	0.71	1.12	1.00

(2) Anisotropy results in less flow and a lower vertical gradient through the defect because the vertical permeability of the three sand layers in the aquifer is reduced. However, anisotropy does result in a larger horizontal gradient beneath the blanket to the defect. For each scenario included in Figure F-35 the presence of the 10-foot blank section had a negligible effect on flow and gradient around the defect.

d. This example was replicated using the Finite Element program SEEP/W from GeoSlope International. The model was created using the same approach as the generalized levee cross section in paragraph I-3d. A line of relief wells was included in this model using the procedures described in Appendix G. These procedures are demonstrated using that example in paragraph I-3d(6). Results of these 2D FEM analyses are presented in Table F-35, along with results from 3D, BT, and the physical model tests discussed elsewhere in this appendix. Shading is used for total head midway between wells in this table to differentiate between effective penetration ratio for the various models.

Table F-35
Comparison of Blanket Theory, Physical Model, 2D, and 3D model results

		W/D=100%		(51.4% eff)		(19.0% eff)	
$k_h/k_v =$		1	4	1	4	1	4
Case 1,2,2b with 174-ft spacing							
Blanket Theory	H_m (ft)	415.1	415.1	418.5	418.3	426.3	426.9
	Q_w (gpm)	579.2	579.2	531.7	521.8	428.8	403.3
Physical Model	H_m (ft)	414.3	–	N/A	–	427.3	–
	Q_w (gpm)	590.0	–	N/A	–	460.0	–
2D FEM	H_m (ft)	417.0	417.0	420.5	420.4	427.8	427.4
	Q_w (gpm)	637.0	632.9	581.7	575.0	463.7	452.5
3D FDM	H_m (ft)	416.4	416.4	419.3	419.4	426.5	426.8
	Q_w (gpm)	562.7	562.7	524.0	516.9	429.6	409.8
Case 3 with 174-ft spacing							
3DT - 134'	H_m (ft)	416.8	416.9	419.4	419.3	424.8	424.1
	Q_w (gpm)	590.4	573.9	552.5	533.7	476.9	459.3
2DT - 134'	H_m (ft)	416.1	416.1	419.3	419.2	426.4	425.8
	Q_w (gpm)	557.1	557.1	510.1	504.4	406.8	393.8
2DT - 268'	H_m (ft)	416.1	–	419.0	–	426.4	–
	Q_w (gpm)	556.1	–	505.0	–	386.5	–
Case 2a with 174-ft spacing							
Blanket Theory	H_m (ft)	415.0	–	418.2	–	425.3	–
	Q_w (gpm)	569.3	–	514.7	–	401.8	–
2D FEM	H_m (ft)	416.0	416.0	418.9	418.8	425.1	424.7
	Q_w (gpm)	541.9	541.9	493.5	490.6	391.0	383.5
3D FDM	H_m (ft)	416.3	–	419.0	–	425.5	–
	Q_w (gpm)	549.9	–	505.8	–	402.6	–
Case 2c with 174-ft spacing							
Blanket Theory	H_m (ft)	415.1	–	418.3	–	426.6	–
	Q_w (gpm)	575.1	–	524.7	–	408.4	–
2D FEM	H_m (ft)	416.0	416.0	419.1	419.0	425.6	425.3
	Q_w (gpm)	550.1	550.1	505.0	502.2	407.3	399.6
3D FDM	H_m (ft)	416.3	–	419.2	–	426.1	–
	Q_w (gpm)	557	–	516	–	418	–
Case 2d with 174-ft spacing							
Blanket Theory	H_m (ft)	414.5	414.5	416.9	416.7	421.2	421.2
	Q_w (gpm)	517.2	517.2	433.4	417.7	294.1	266.1
2D FEM	H_m (ft)	416.1	416.1	418.4	418.3	422.3	422.0
	Q_w (gpm)	539.6	539.0	456.4	452.4	313.6	305.0
3D FDM	H_m (ft)	415.5	415.3	417.4	417.2	421.2	420.8
	Q_w (gpm)	486.1	488.5	421.2	413.7	295.1	276.3

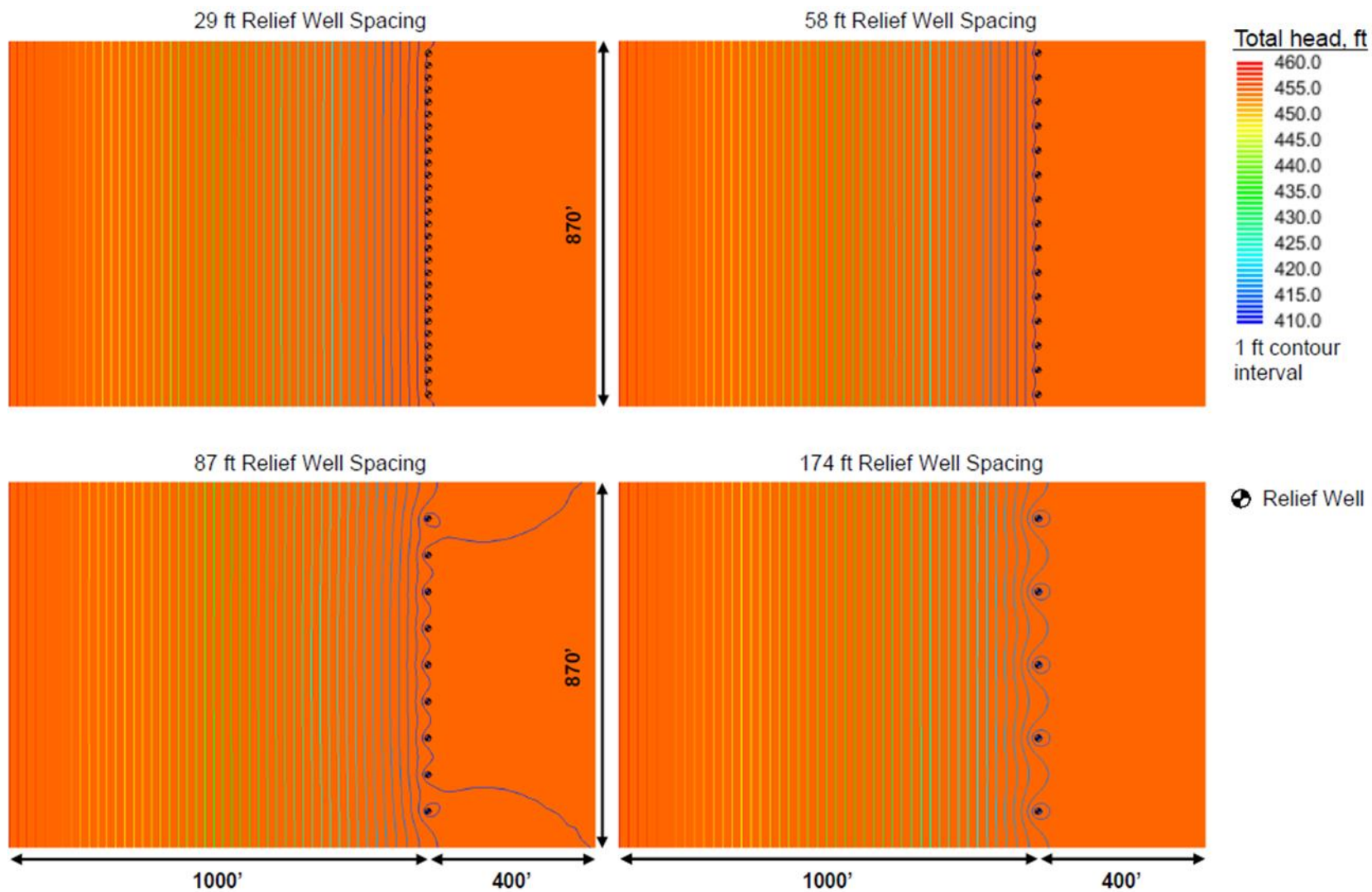


Figure F-33. Model #1 total head results, top of fine sand 100% relief well penetration (100% effective)

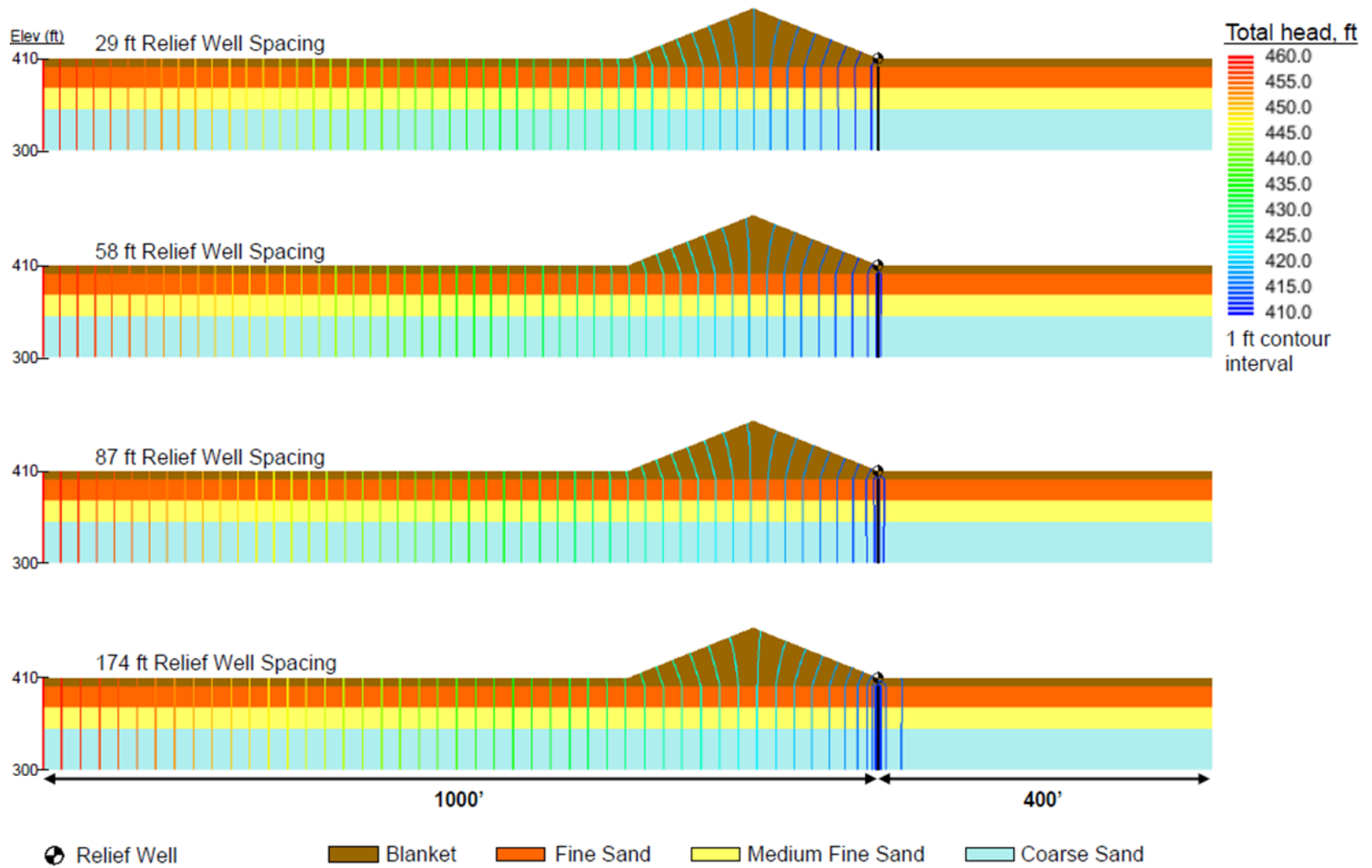


Figure F-34. Model #1 total head results, cross section through center relief well, 100% relief well penetration (100% effective)

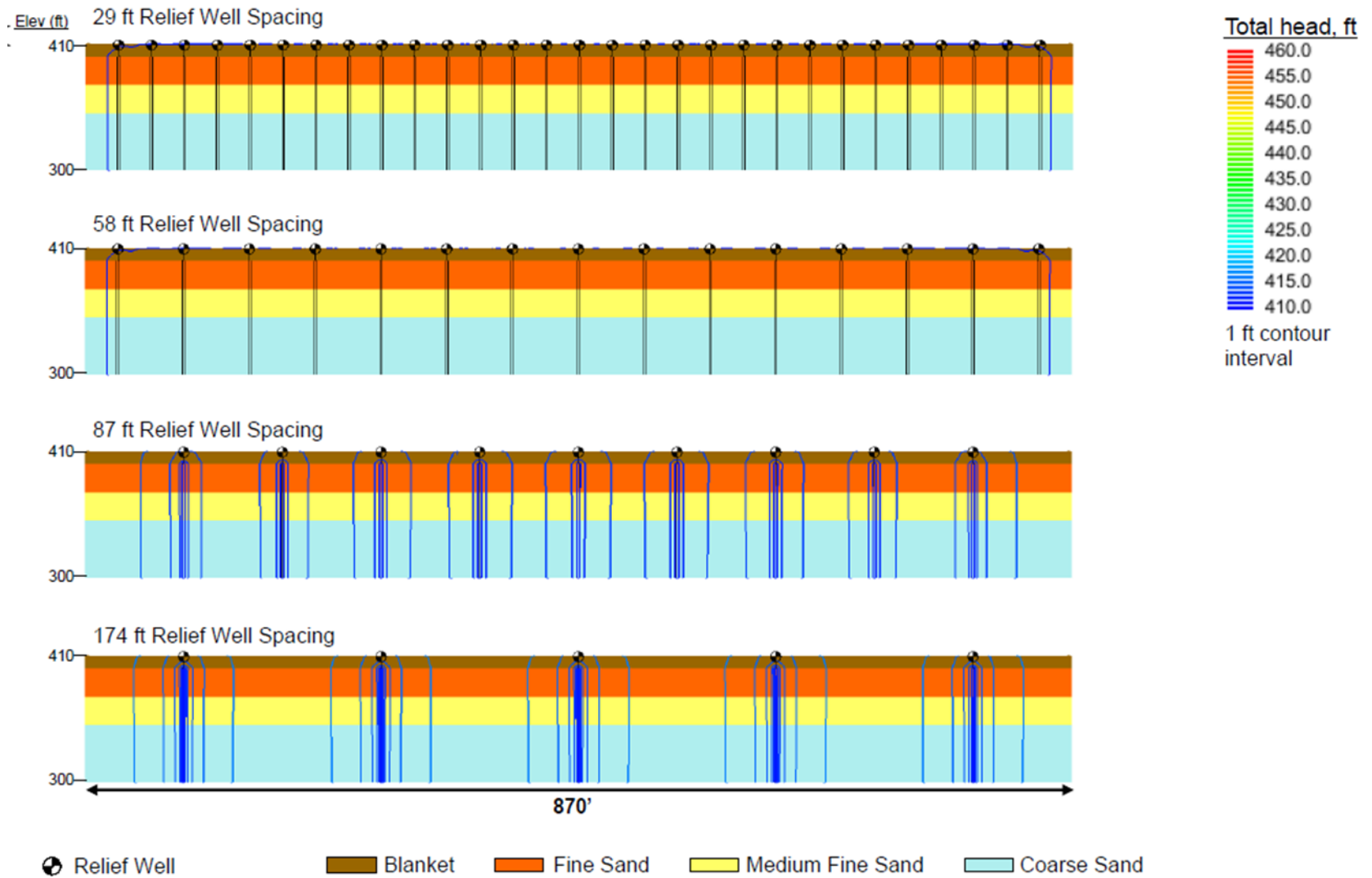


Figure F-35. Model #1 total head results, cross section through relief well line, 100% relief well penetration (100% effective)

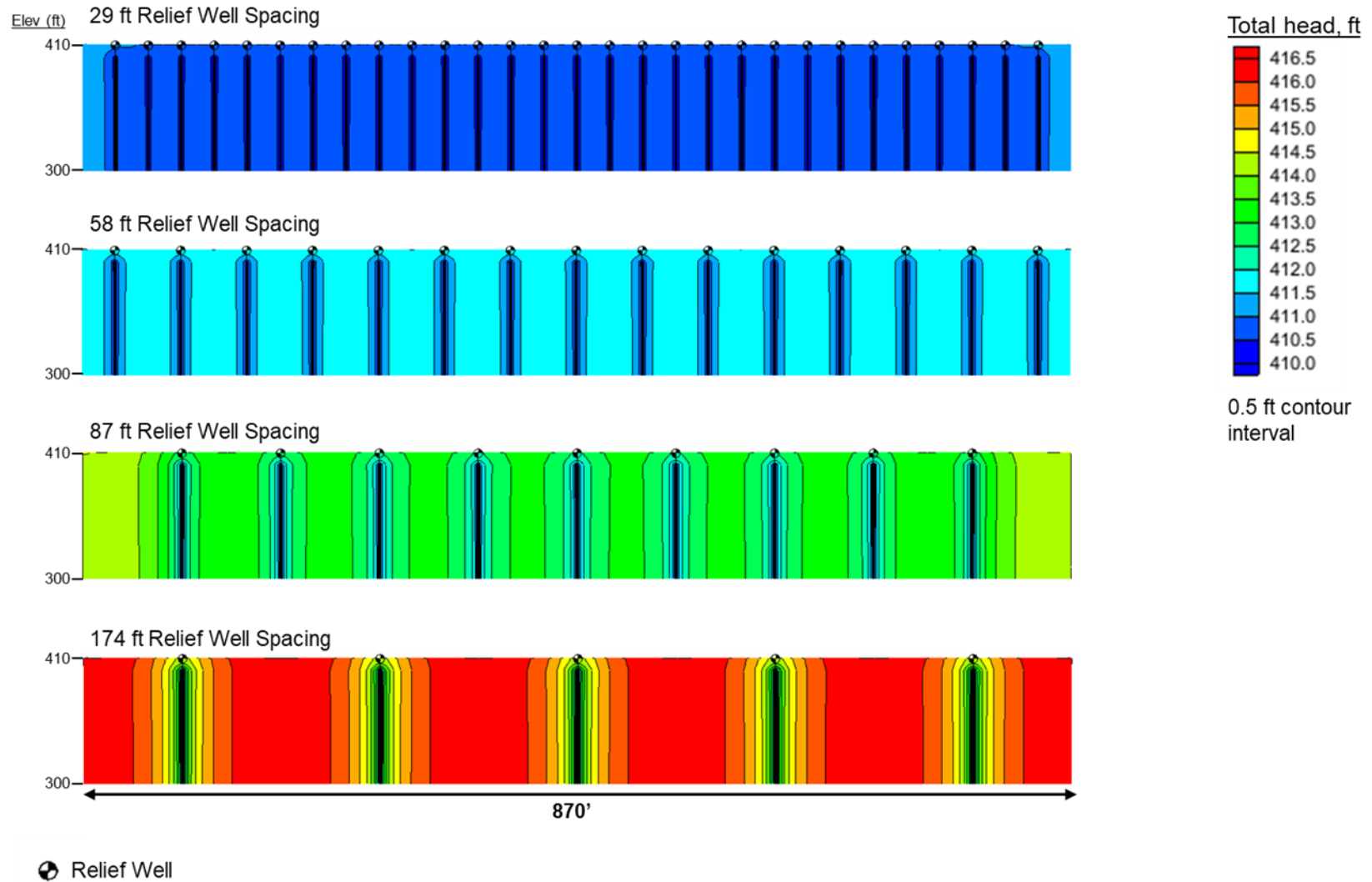


Figure F-36. Model #1 total head results contoured from 410 feet to 416.5 feet, cross section through relief well line, 100% relief well penetration (100% effective)

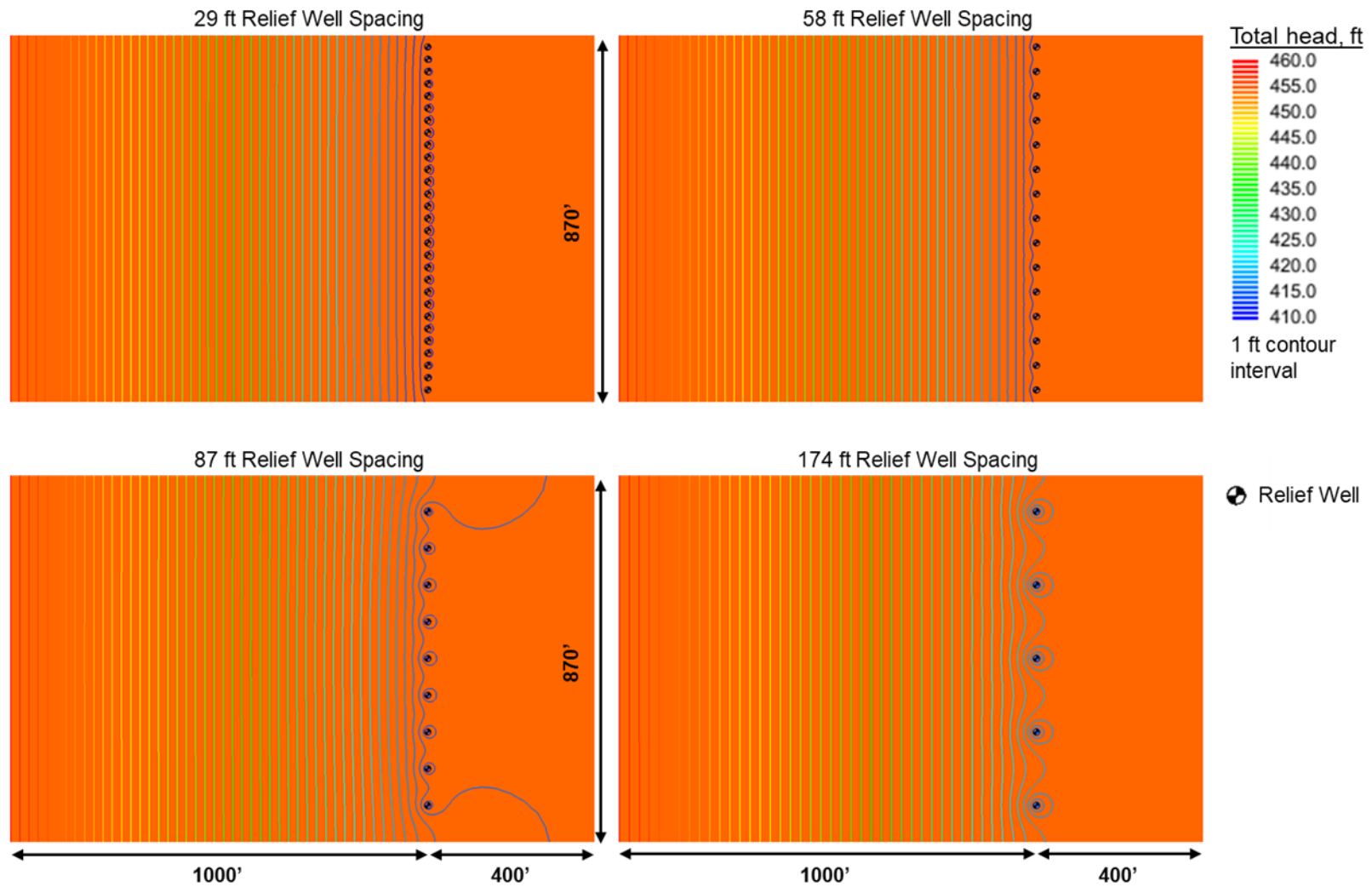


Figure F-37. Model #1 total head results, top of fine sand, 70% relief well penetration (51% effective)

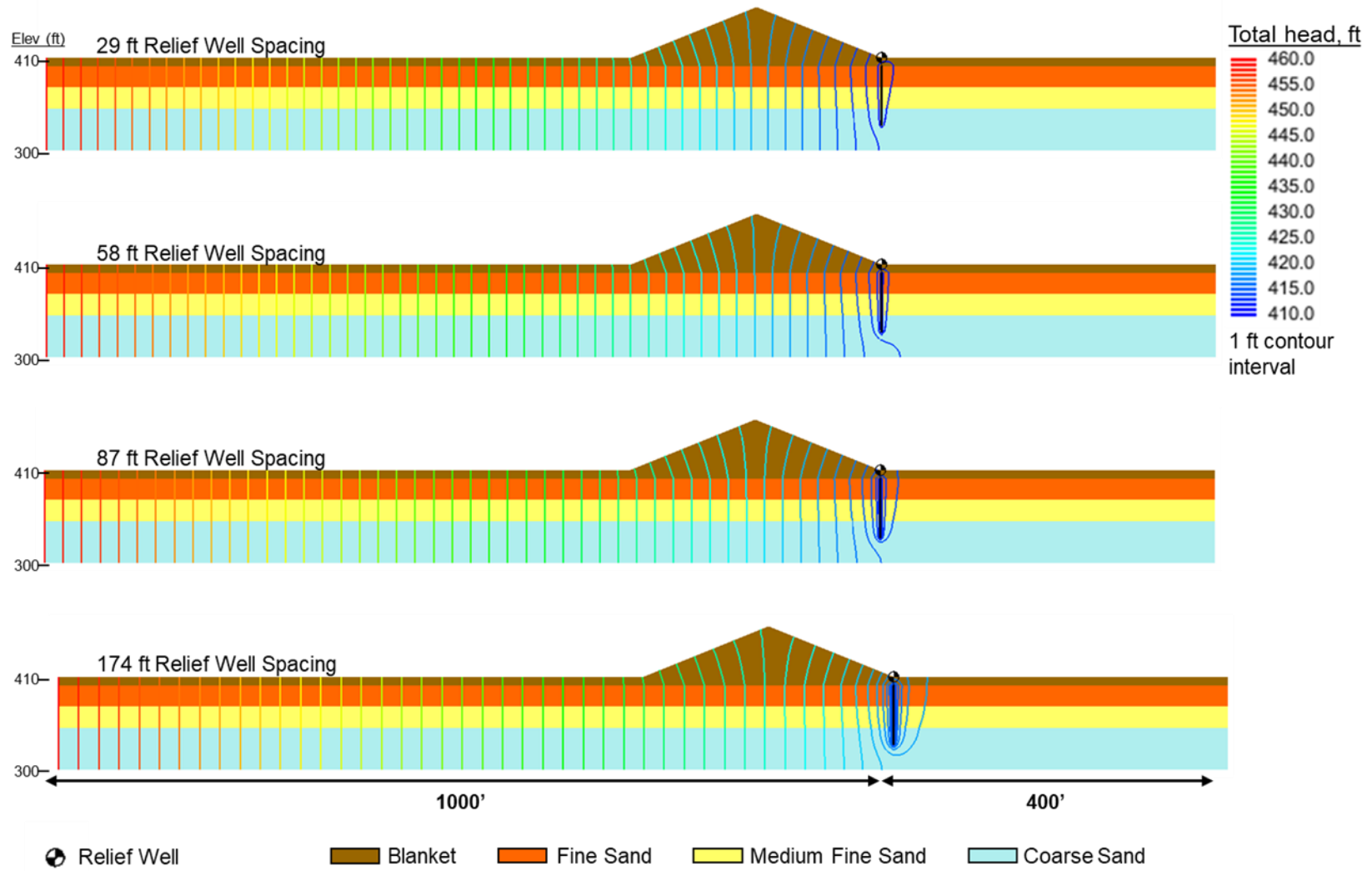


Figure F-38. Model #1 total head results, cross section through center relief well, 70% relief well penetration (51% effective)

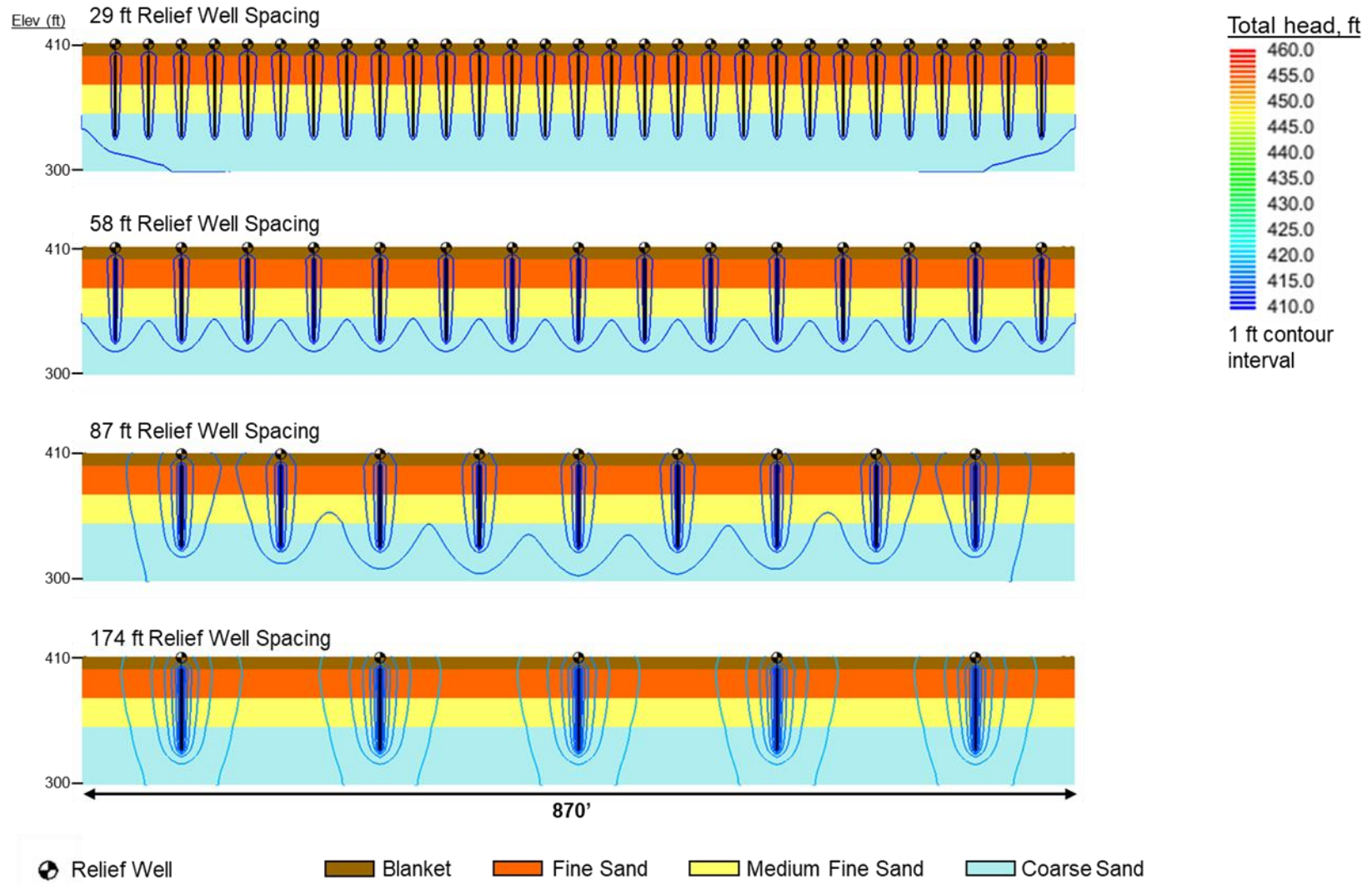


Figure F-39. Model #1 total head results, cross section through relief well line, 70% relief well penetration (51% effective)

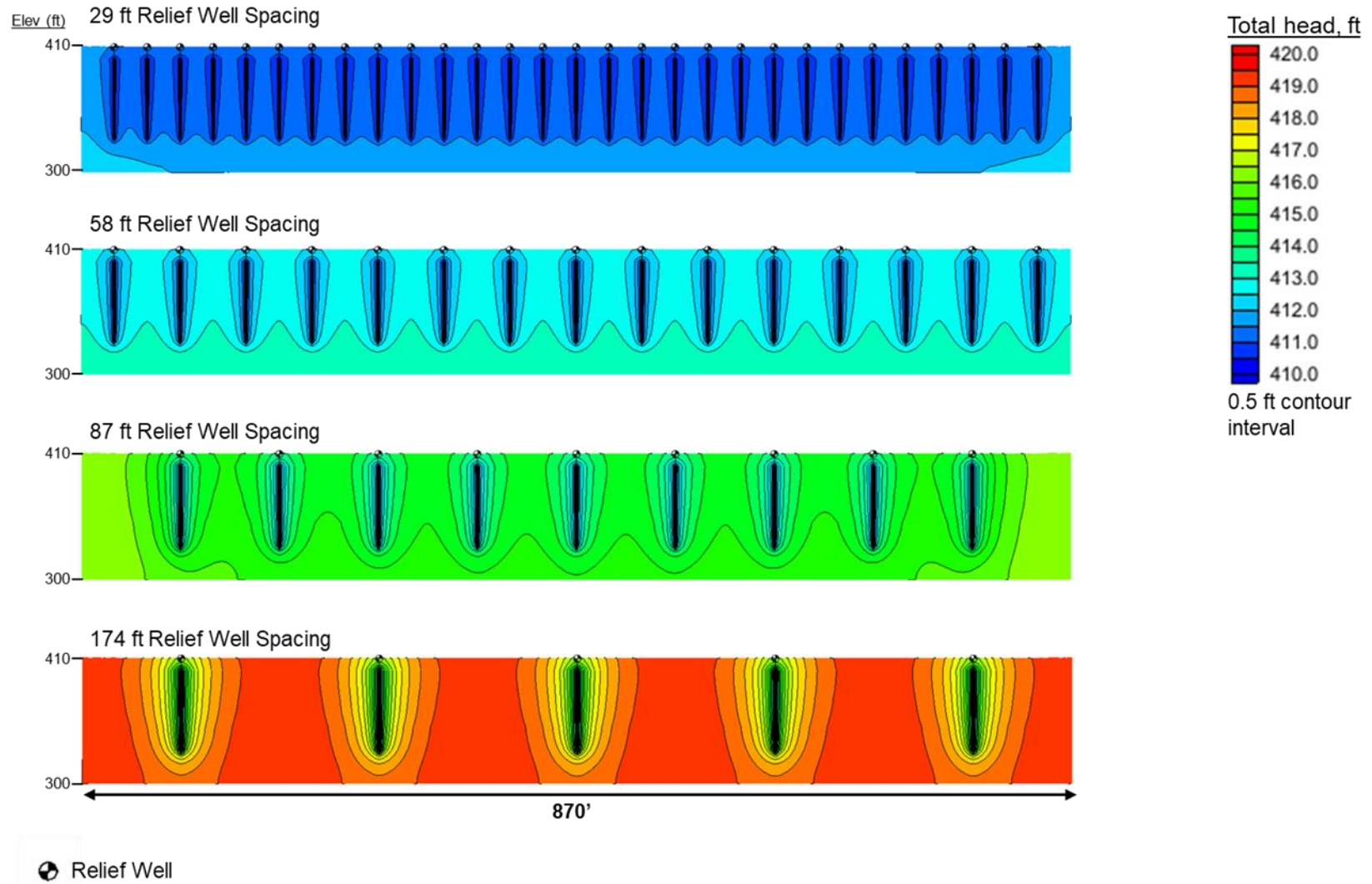


Figure F-40. Model #1 total head results contoured from 410 feet to 420 feet, cross section through relief well line, 70% relief well penetration (51% effective)

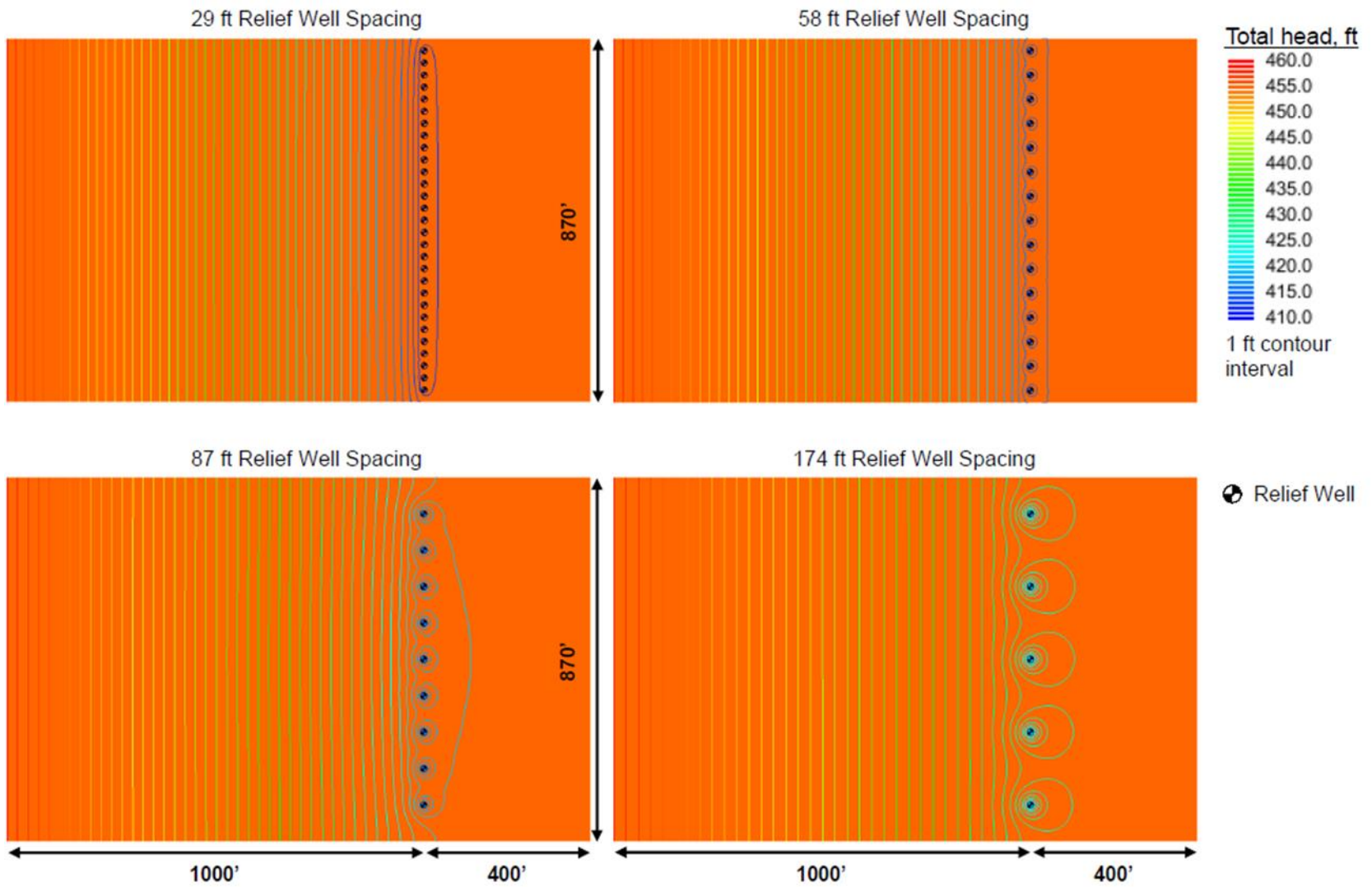


Figure F-41. Model #1 total head results, top of fine sand, 50% relief well penetration (19% effective)

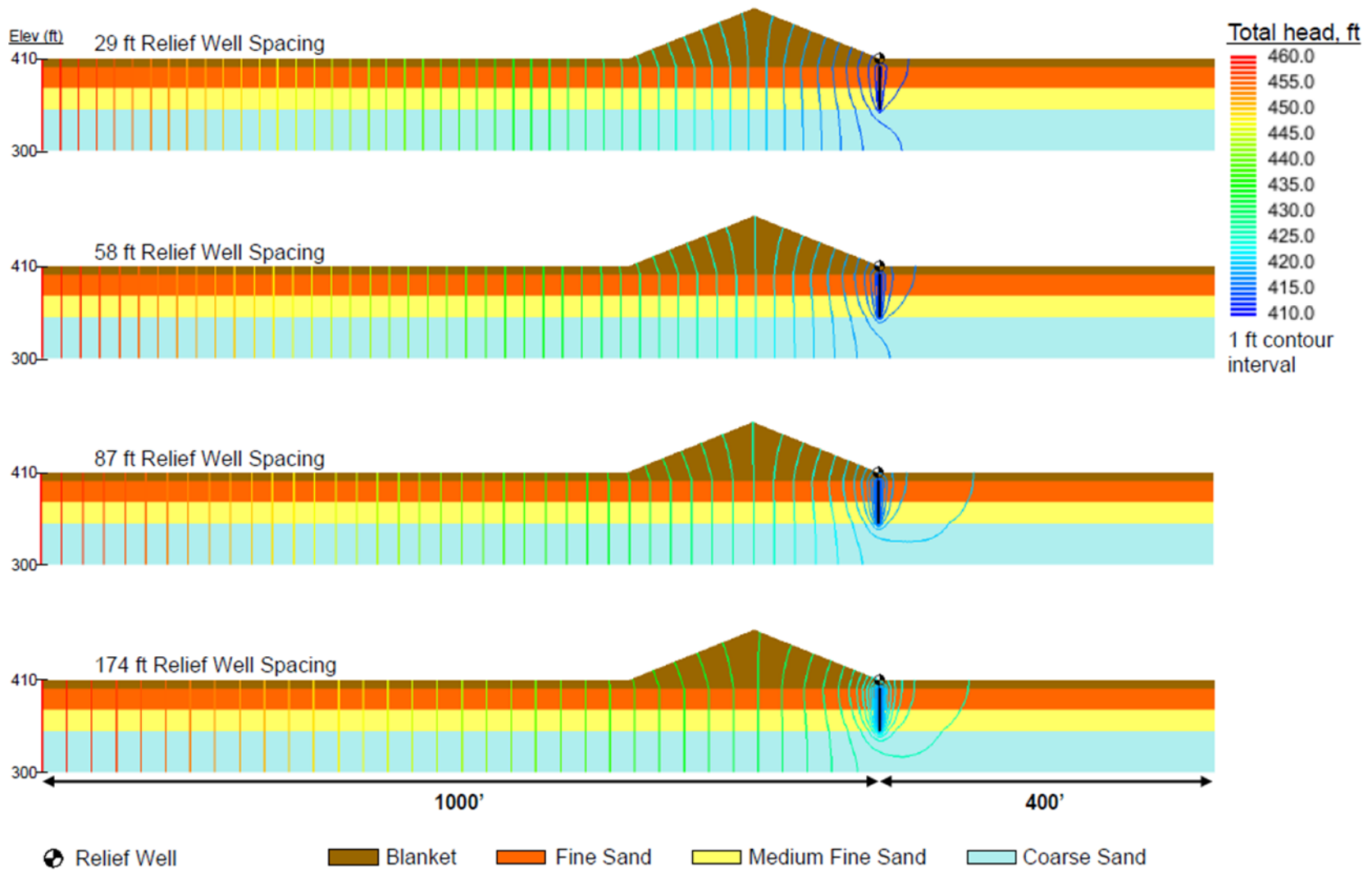


Figure F-42. Model #1 total head results, cross section through center relief well, 50% relief well penetration (19% effective)

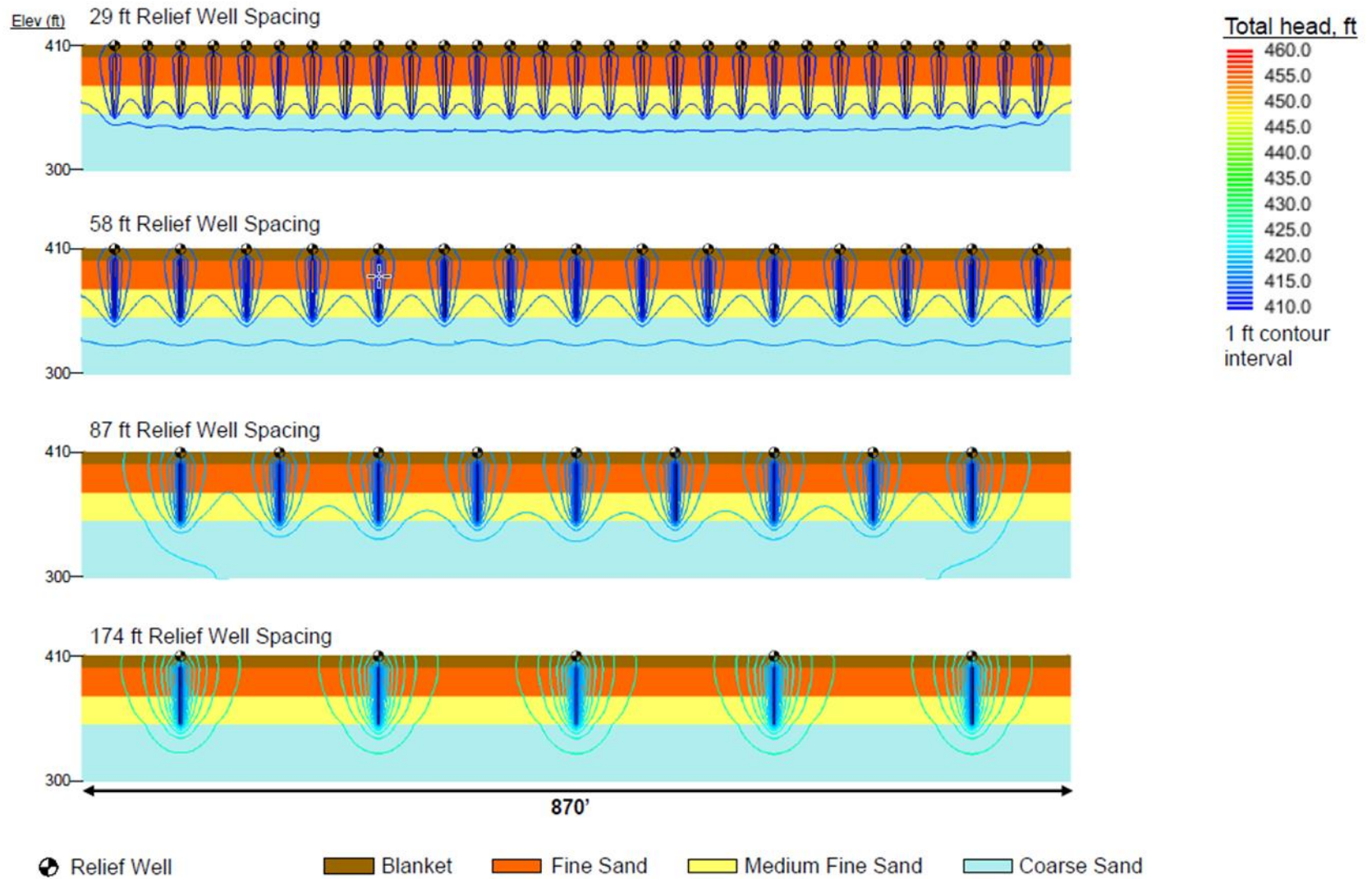


Figure F-43. Model #1 total head results, cross section through relief well line, 50% relief well penetration (19% effective)

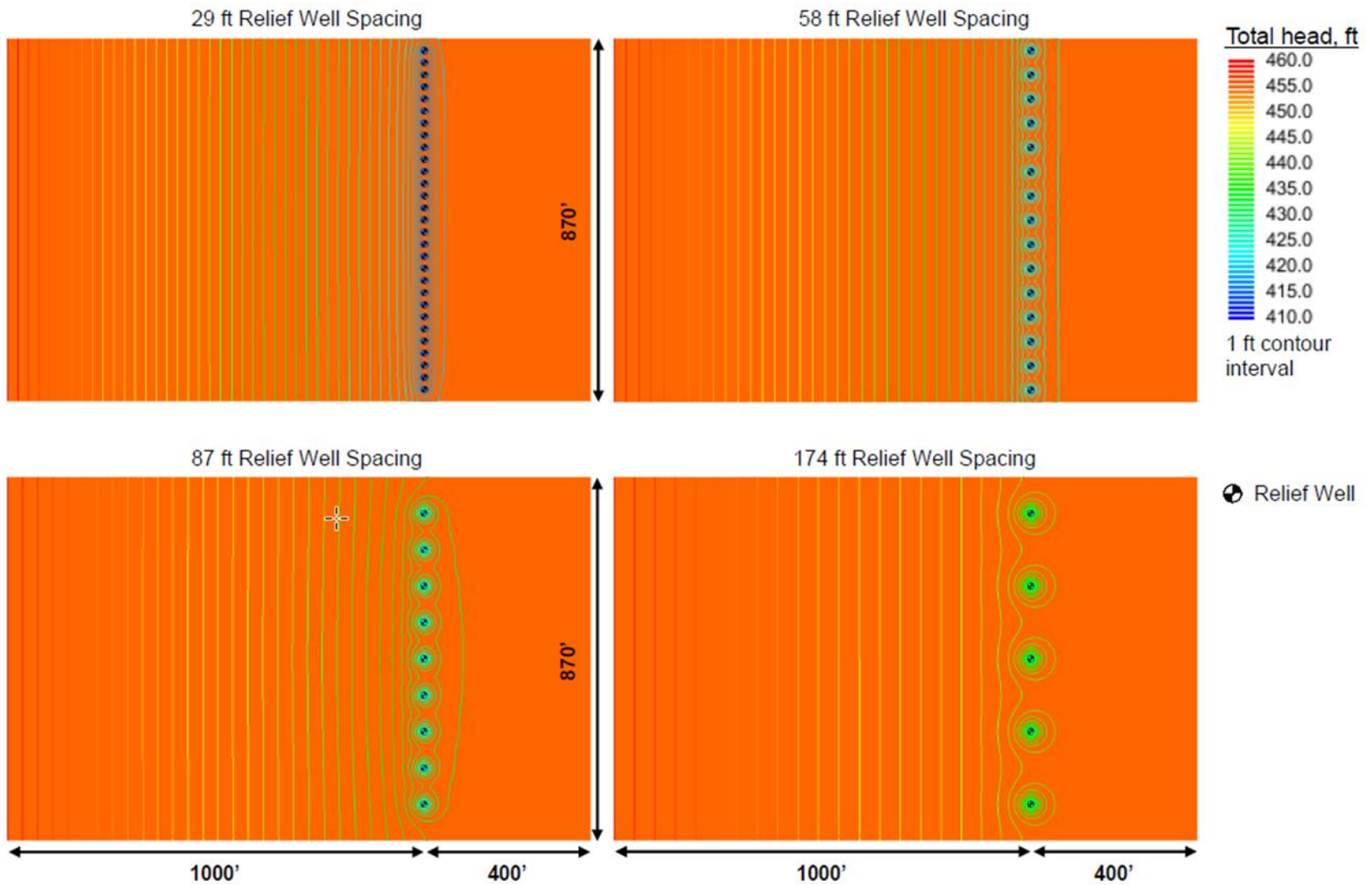


Figure F-44. Model #1 total head results, top of fine sand, 25% relief well penetration (6.2% effective)

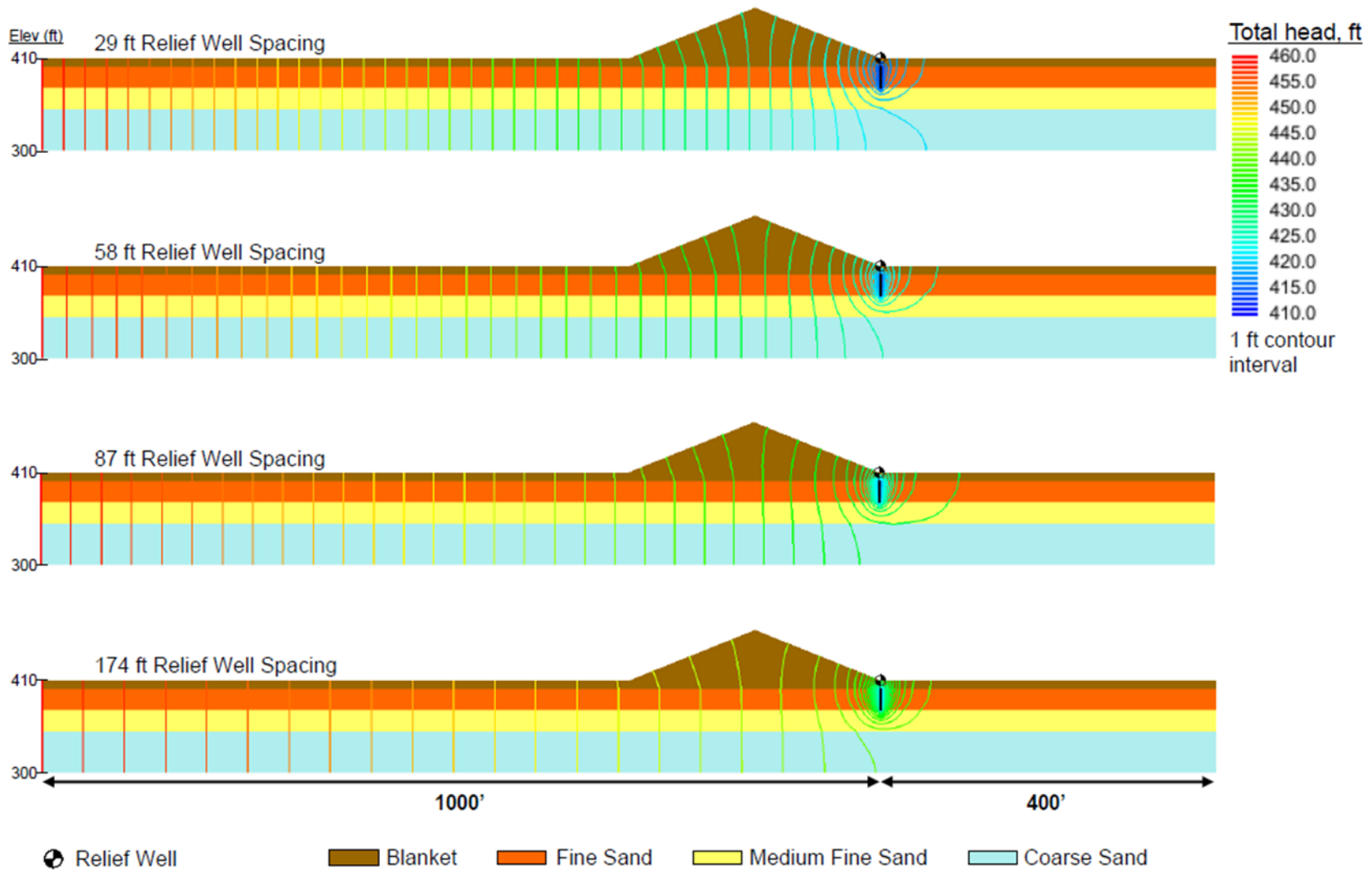


Figure F-45. Model #1 total head results, cross section through center relief well, 25% relief well penetration (6.2% effective)

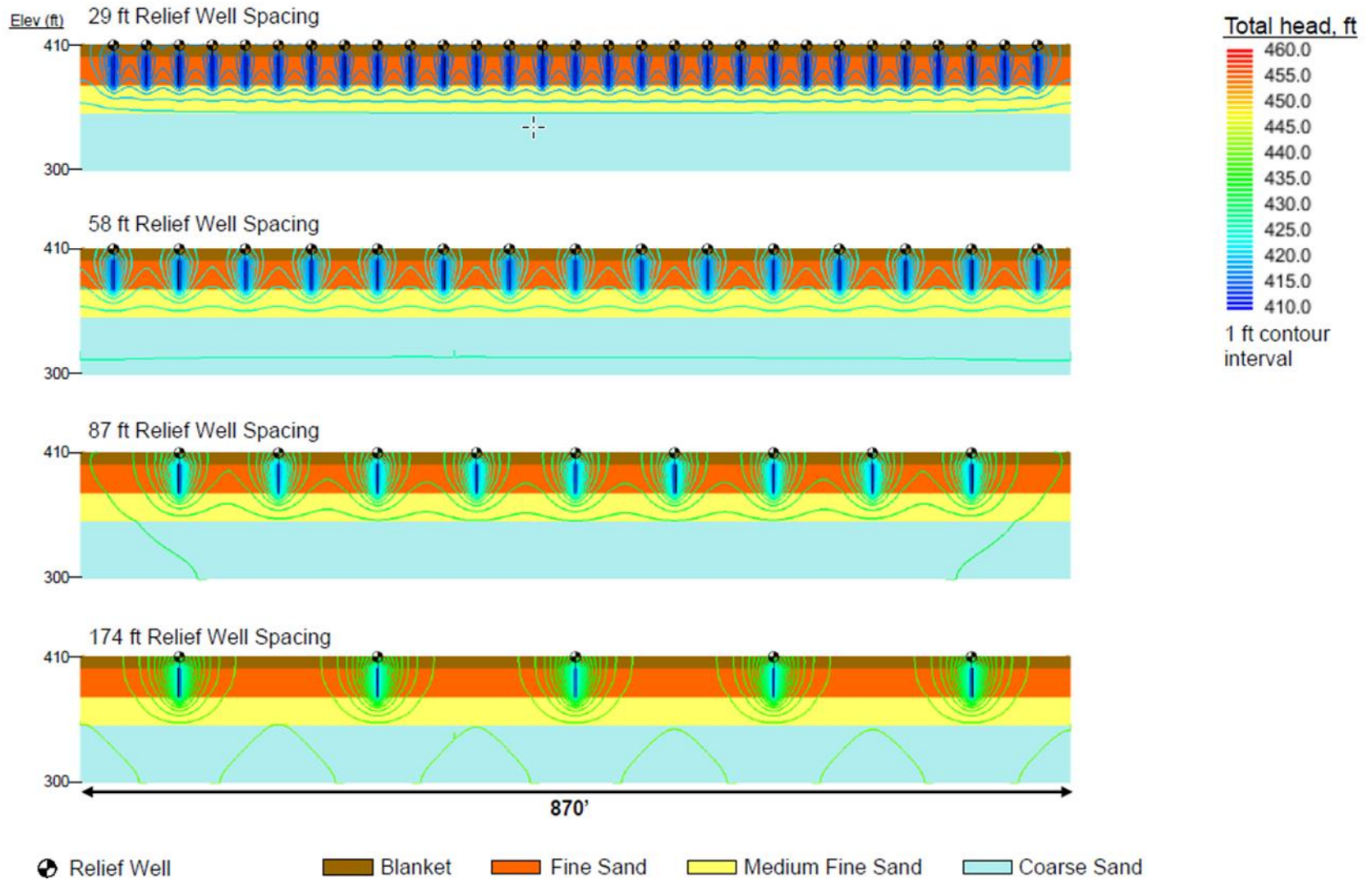


Figure F-46. Model #1 total head results, cross section through relief well line, 25% relief well penetration (6.2% effective)

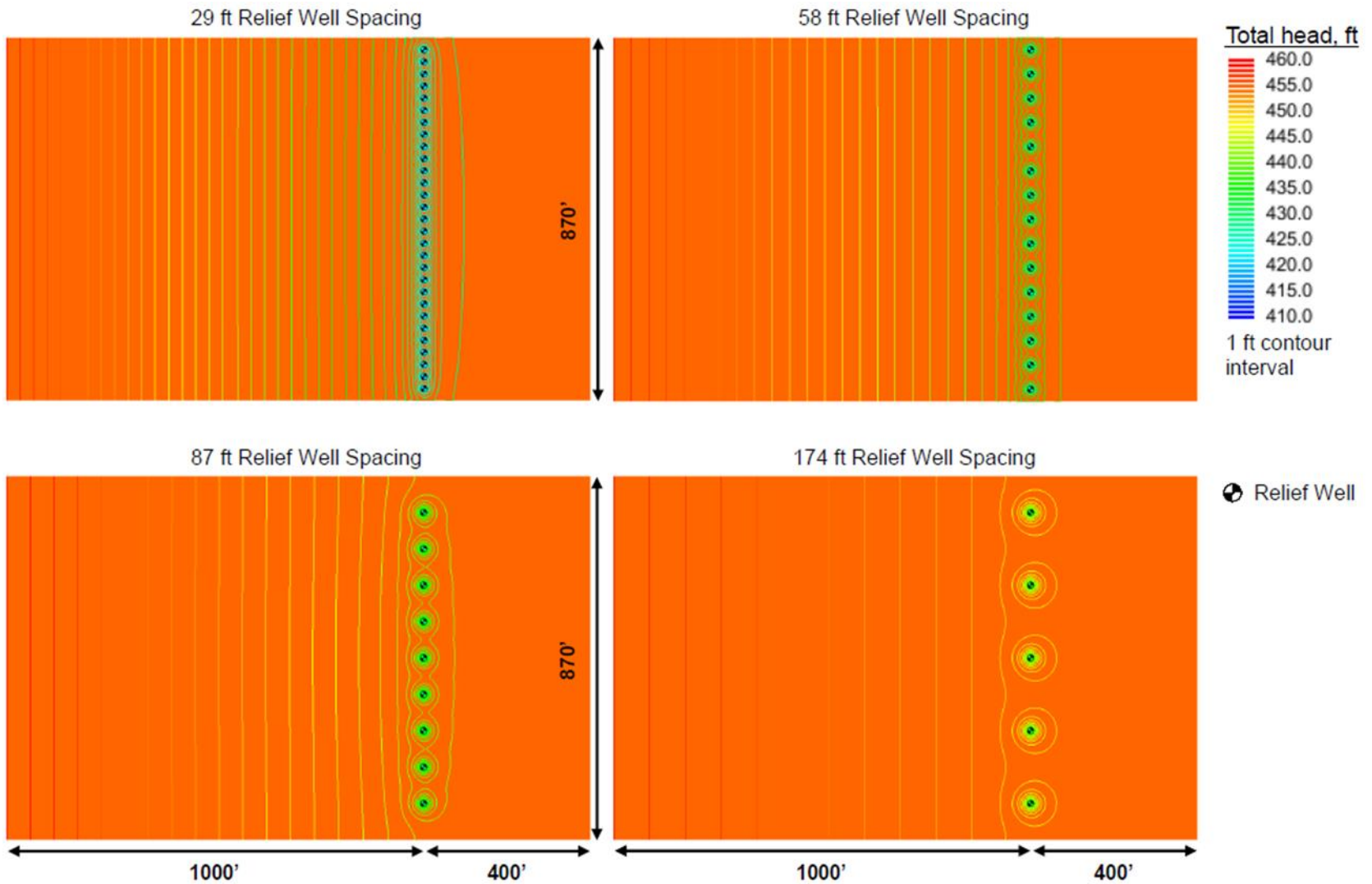


Figure F-47. Model #1 total head results, top of fine sand, 10% relief well penetration (2.5% effective)

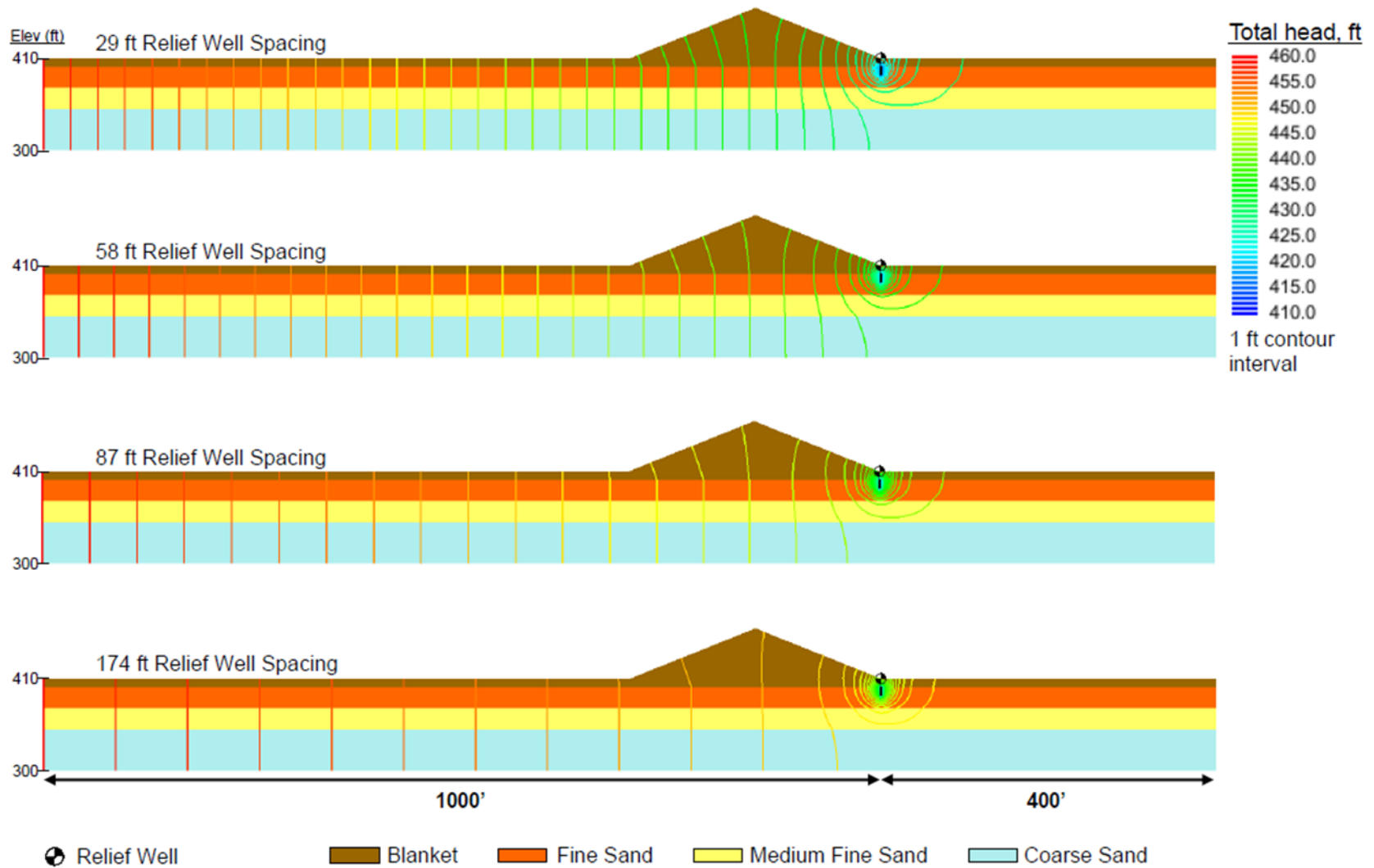


Figure F-48. Model #1 total head results, cross section through center relief well, 10% relief well penetration (2.5% effective)

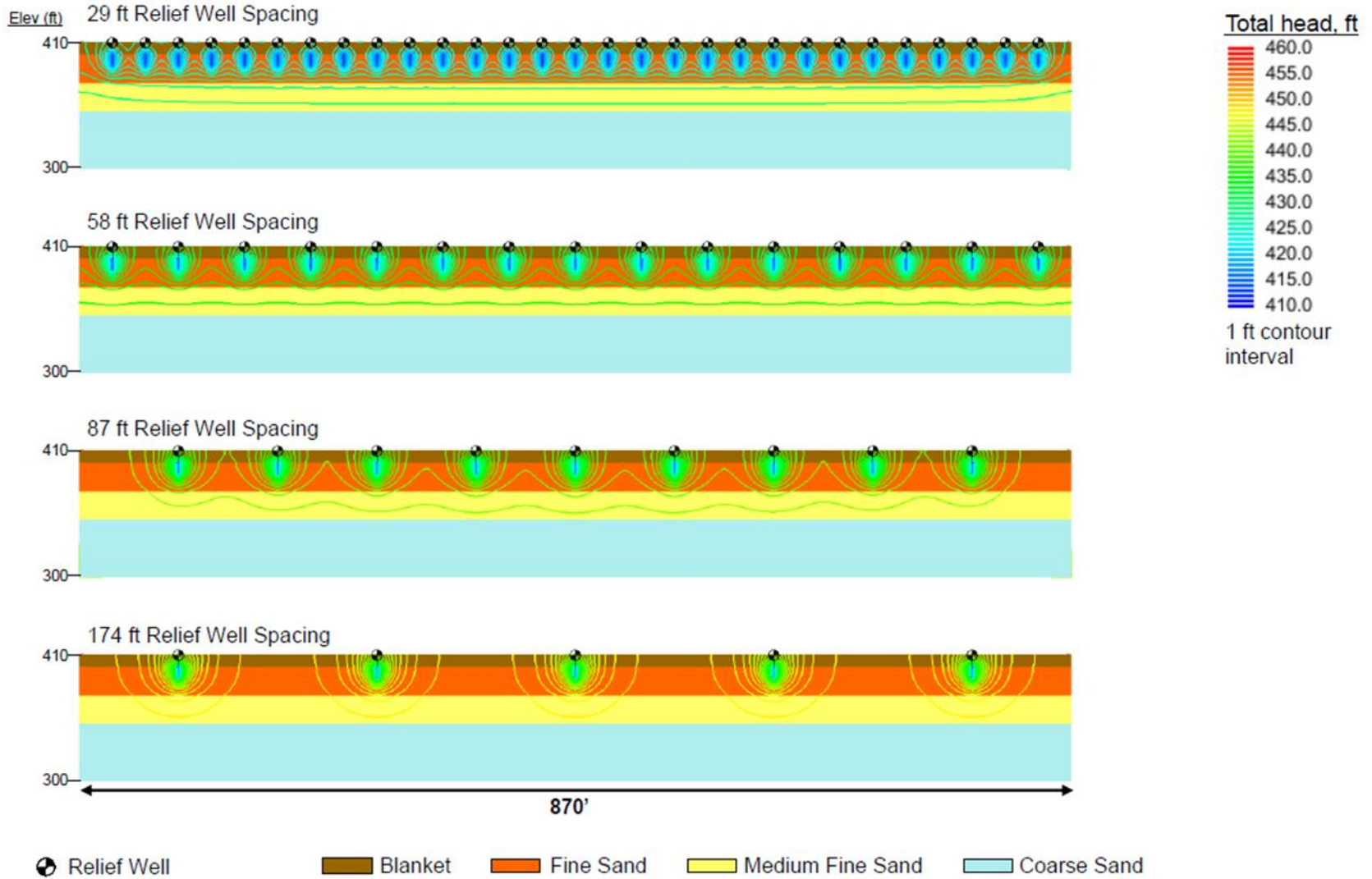


Figure F-49. Model #1 total head results, cross section through relief well line, 10% relief well penetration (2.5% effective)

Table F-36
Summary of mid-well head results in percent of net head (%H)

	Well Spacing (ft)	Physical Model	Blanket Theory					Numerical Models					
			#1/#2	#2a	#2b	#2c	#2d	#1/#2	#2a	#2b	#2c	#2d	#3
100% Well Penetration (100% Effective)	29	1.6	1.0	1.0	1.0	1.0	1.0	1.6	1.6	1.6	1.6	1.5	2.0
	58	3.1	2.6	2.6	2.6	2.6	2.6	3.7	3.6	3.7	3.7	3.5	4.3
	87	5.0	4.4	4.4	4.4	4.4	4.2	6.2	6.1	6.2	6.2	5.7	6.9
	174	8.5	10.2	10.0	10.2	10.1	9.1	12.8	12.5	12.8	12.7	10.9	13.6
70% Well Penetration (51% Effective)	29	N/A	1.4	1.4	1.4	1.4	1.3	2.2	2.2	2.2	2.2	2.1	2.6
	58	N/A	4.4	4.3	4.4	4.4	4.1	5.5	5.4	5.5	5.4	5.0	5.8
	87	N/A	7.6	7.5	7.6	7.5	6.8	9.4	9.2	9.4	9.3	8.2	9.7
	174	N/A	16.9	16.4	16.9	16.7	13.8	18.6	18.0	18.7	18.4	14.8	18.8
50% Well Penetration (19% Effective)	29	10.6	4.2	4.1	4.2	4.1	3.8	4.4	4.4	4.5	4.4	4.0	4.5
	58	14.6	11.0	10.7	11.0	10.9	9.2	11.1	10.8	11.1	11.0	9.2	10.1
	87	22.7	17.4	16.7	17.4	17.1	13.7	18.7	17.9	18.7	18.3	14.3	16.6
	174	34.5	32.7	30.6	32.7	33.1	22.4	33.0	30.9	33.0	32.1	22.4	29.6
25% Well Penetration (6.2% Effective)	29	22.3	11.7	11.4	11.7	16.8	12.7	13.1	12.5	13.1	12.8	10.0	13.1
	58	30.4	23.7	22.5	23.7	29.2	20.7	27.8	26.0	27.8	27.1	18.8	25.7
	87	41.1	33.3	31.0	33.3	38.8	26.0	41.3	37.8	41.3	39.8	25.1	37.5
	174	54.2	52.0	46.9	52.0	55.3	32.7	59.4	52.9	59.4	56.6	31.9	54.3
10% Well Penetration (2.5% Effective)	29	38.6	19.6	18.7	19.6	31.9	23.7	27.1	25.1	27.1	26.3	17.5	23.3
	58	50.7	34.8	32.3	34.8	45.2	30.0	47.5	42.8	47.5	45.5	27.0	39.7
	87	59.9	45.6	41.6	45.6	54.4	33.4	61.9	54.5	61.8	58.6	31.9	53.0
	174	78.7	64.1	56.5	64.1	68.3	37.3	76.7	66.2	76.7	72.1	36.3	68.5

Table F-37
Summary of mid-well head results in feet

	Well Spacing (ft)	Physical Model	Blanket Theory*					Numerical Models					
			#1/#2	#2a	#2b	#2c	#2d	#1/#2	#2a	#2b	#2c	#2d	#3*
100% Well Penetration (100% Effective)	29	410.8	410.5	410.5	410.5	410.5	410.5	410.8	410.8	410.8	410.8	410.8	411.0
	58	411.6	411.3	411.3	411.3	411.3	411.3	411.8	411.8	411.8	411.8	411.7	412.1
	87	412.5	412.2	412.2	412.2	412.2	412.1	413.1	413.1	413.1	413.1	412.8	413.5
	174	414.3	415.1	415.0	415.1	415.1	414.5	416.4	416.3	416.4	416.4	415.5	416.8
70% Well Penetration (51% Effective)	29	N/A	410.7	410.7	410.7	410.7	410.7	411.1	411.1	411.1	411.1	411.0	411.3
	58	N/A	412.2	412.2	412.2	412.2	412.0	412.7	412.7	412.7	412.7	412.5	412.9
	87	N/A	413.8	413.7	413.8	413.8	413.4	414.7	414.6	414.7	414.7	414.1	414.8
	174	N/A	418.5	418.2	418.5	418.4	416.9	419.3	419.0	419.3	419.2	417.4	419.4
50% Well Penetration (19% Effective)	29	415.3	412.1	412.1	412.1	412.1	411.9	412.2	412.2	412.2	412.2	412.0	412.3
	58	417.3	415.5	415.4	415.5	415.4	414.6	415.5	415.4	415.5	415.5	414.6	415.0
	87	421.4	418.7	418.4	418.7	418.6	416.9	419.3	418.9	419.3	419.2	417.2	418.3
	174	427.3	426.3	425.3	426.3	426.6	421.2	426.5	425.5	426.5	426.1	421.2	424.8
25% Well Penetration (6.2% Effective)	29	421.2	415.9	415.7	415.9	418.4	416.3	416.5	416.3	416.5	416.4	415.0	416.5
	58	425.2	421.9	421.2	421.9	424.6	420.4	423.9	423.2	423.9	423.5	419.4	422.8
	87	430.6	426.6	425.5	426.6	429.4	423.0	430.7	428.9	430.6	429.9	422.5	428.7
	174	437.1	436.0	433.5	436.0	437.7	426.4	439.7	436.4	439.7	438.3	425.9	437.1
10% Well Penetration (2.5% Effective)	29	429.3	419.8	419.3	419.8	425.9	421.9	423.6	422.6	423.6	423.1	418.7	421.7
	58	435.4	427.4	426.2	427.4	432.6	425.0	433.8	431.4	433.7	432.7	423.5	429.9
	87	440.0	432.8	430.8	432.8	437.2	426.7	440.9	437.3	440.9	439.3	426.0	436.5
	174	449.4	442.0	438.3	442.0	444.1	428.7	448.4	443.1	448.4	446.0	428.1	444.3

Note: *Head calculated by BT and Numerical Model #3 was increased by 10 feet from their original values so that they could be directly compared to the results of other models presented in this table. BT and Model #3 used headwater and tailwater conditions of 450 feet and 400 feet, respectively, but numerical models that incorporated a 10-foot blanket used headwater and tailwater conditions that were 10 feet higher. BT results are presented in Appendix E and Model #3 is discussed in paragraphs F-2c and F-3c.

Table F-38

Difference between numerical model and Blanket Theory calculated mid-well heads (in feet)

	Well Spacing (ft)	Numerical Model #1/#2	Numerical Model #2a	Numerical Model #2b	Numerical Model #2c	Numerical Model #2d
100% Well Penetration (100% Effective)	29	0.27	0.27	0.27	0.27	0.25
	58	0.51	0.51	0.52	0.51	0.45
	87	0.88	0.86	0.89	0.88	0.72
	174	1.32	1.26	1.32	1.30	0.91
70% Well Penetration (51% Effective)	29	0.40	0.40	0.40	0.40	0.38
	58	0.54	0.53	0.54	0.54	0.46
	87	0.92	0.89	0.92	0.90	0.68
	174	0.86	0.81	0.86	0.84	0.48
50% Well Penetration (19% Effective)	29	0.14	0.14	0.14	0.14	0.12
	58	0.03	0.04	0.04	0.03	0.01
	87	0.62	0.57	0.63	0.60	0.29
	174	0.15	0.15	0.16	-0.51	-0.03
25% Well Penetration (6.2% Effective)	29	0.67	0.57	0.68	-1.99	-1.36
	58	2.06	1.79	2.06	-1.05	-0.94
	87	4.01	3.38	4.01	0.49	-0.45
	174	3.71	2.97	3.70	0.62	-0.41
10% Well Penetration (2.5% Effective)	29	3.78	3.23	3.77	-2.79	-3.11
	58	6.34	5.25	6.32	0.15	-1.49
	87	8.12	6.47	8.10	2.14	-0.76
	174	6.33	4.81	6.32	1.88	-0.52

Note:

A positive value indicates that head calculated by the numerical model was higher than head calculated using BT.

A negative value indicates that head calculated by BT was higher than head calculated by the numerical model.

Table F-39
Summary of relief well flow results in gallons per minute

	Well Spacing (ft)	Physical Model	Blanket Theory					Numerical Models					
			#1/#2	#2a	#2b	#2c	#2d	#1/#2	#2a	#2b	#2c	#2d	#3
100% Well Penetration (100% Effective)	29	105	105	105	105	105	104	105	104	105	105	103	110
	58	210	207	206	207	206	201	204	203	204	204	196	215
	87	310	305	303	305	304	291	317	314	318	316	293	334
	174	590	579	569	579	575	517	563	550	563	557	486	590
70% Well Penetration (51% Effective)	29	N/A	103	102	103	102	99	103	103	103	103	99	109
	58	N/A	200	197	200	199	185	199	196	199	198	184	209
	87	N/A	291	286	291	289	261	308	301	308	305	270	324
	174	N/A	532	515	532	525	433	524	506	524	516	421	552
50% Well Penetration (19% Effective)	29	95	97	96	97	97	88	99	97	99	98	90	105
	58	180	182	177	182	180	153	183	178	183	181	155	197
	87	235	256	247	256	252	202	275	264	275	270	213	299
	174	460	429	402	429	408	294	430	403	430	418	295	477
25% Well Penetration (6.2% Effective)	29	85	91	88	91	82	67	84	81	84	83	64	94
	58	150	160	152	160	139	99	141	132	142	138	97	161
	87	185	215	200	215	179	116	193	177	194	186	118	225
	174	285	321	290	321	255	140	258	230	258	246	140	310
10% Well Penetration (2.5% Effective)	29	65	87	83	87	66	43	67	62	67	64	43	83
	58	105	143	133	143	103	57	100	90	100	96	57	130
	87	120	183	167	183	127	62	124	109	124	117	64	169
	174	130	251	222	251	165	68	147	127	148	138	70	213

Table F-40

Percent difference between numerical model and Blanket Theory calculated relief well flow

	Well Spacing (ft)	Numerical Model #1/#2	Numerical Model #2a	Numerical Model #2b	Numerical Model #2c	Numerical Model #2d
100% Well Penetration (100% Effective)	29	0.3%	-0.2%	0.0%	-0.1%	-0.9%
	58	-1.3%	-1.4%	-1.1%	-1.3%	-2.6%
	87	3.8%	3.5%	4.0%	3.8%	0.9%
	174	-2.8%	-3.4%	-2.9%	-3.1%	-6.2%
70% Well Penetration (51% Effective)	29	0.7%	0.7%	0.7%	0.7%	0.5%
	58	-0.4%	-0.5%	-0.4%	-0.5%	-0.7%
	87	5.6%	5.2%	5.6%	5.5%	3.5%
	174	-1.5%	-1.7%	-1.4%	-1.6%	-2.9%
50% Well Penetration (19% Effective)	29	1.7%	1.6%	1.6%	1.6%	2.0%
	58	0.5%	0.5%	0.5%	0.5%	1.2%
	87	7.0%	6.7%	7.0%	6.8%	5.5%
	174	0.3%	0.2%	0.2%	2.4%	0.4%
25% Well Penetration (6.2% Effective)	29	-7.6%	-8.6%	-7.3%	0.8%	-3.7%
	58	-12.6%	-13.5%	-12.2%	-0.8%	-2.9%
	87	-10.6%	-12.3%	-10.3%	4.2%	2.2%
	174	-21.7%	-23.0%	-21.6%	-3.5%	-0.2%
10% Well Penetration (2.5% Effective)	29	-25.5%	-29.0%	-26.0%	-1.6%	0.4%
	58	-35.5%	-38.6%	-35.6%	-7.9%	-0.7%
	87	-38.6%	-41.9%	-38.6%	-7.6%	3.5%
	174	-52.4%	-54.3%	-52.0%	-17.6%	3.2%

Note:

A positive percent difference indicates that flow calculated by the numerical model is higher than flow calculated by BT. A negative percent difference indicates that flow calculated by the numerical model is lower than flow calculated by BT.

Appendix G Seepage Analysis Using the Finite Element Method for Relief Wells

G-1. Introduction

Although this appendix was written for levees, the approach is also applicable to dams or other structures with an infinite line of wells. It presents a conservative yet practical means to include a line of wells in 2D FEM models. A total head boundary condition determined using well factors from BT is applied to the location of the well screen. The well factors already incorporate effects of partial penetration, so this boundary is conservative with respect to calculated excess head. However, applying the boundary to only the screen rather than the full depth of the aquifer tends to underpredict well flow. This practical approach provides a means to evaluate complex foundation conditions.

a. Seepage analysis using FEM is a common approach for engineers to assess seepage pressures at the base of the blanket and evaluate if under-seepage control features are required. FEM allows designers and engineers more variability in boundary conditions and material properties versus using closed-form solutions. Variations of layer thickness, hydraulic conductivity, levee geometry, and ground surface profile can be easily incorporated in FEM compared to closed-form solutions that rely on simplified assumptions.

b. 3D seepage analysis using FEM is a powerful tool that can include wells as described in Chapter 6 of this manual. Since it is difficult to implement and not as readily available to many engineers, 2D seepage analysis using FEM is often performed. Closed-form solutions are simple and effective if the required simplifying assumptions do not deviate too far from real-world conditions. 2D FEM is also effective, and often more practical, for complex levee seepage analysis.

c. Levees located along rivers and streams are commonly founded on stratified alluvium deposits with a relatively impervious blanket of clays and silts underlain by a more pervious substratum of sands and gravels. Rivers and streams often cut through the relatively impervious blanket and are hydraulically connected to the pervious substratum. Thus, for levees founded on these deposits, analyses discussed in EM 1110-2-1913 are necessary to evaluate the potential for a seepage exit occurring landward of the levee. The upper, relatively impervious blanket typically confines the pervious substratum.

d. Assuming the impervious blanket is intact and without defects, the potential for a seepage exit from the pervious substratum through the blanket landward of the levee is based on development of seepage pressures beneath the blanket. If seepage pressures beneath the blanket become artesian, the seepage could exit through the blanket via existing defects, cracks, or rupture of the blanket caused by the seepage pressures if FS_{vg} is exceeded. Of concern to levee integrity is the resulting unfiltered seepage exit, which could lead to internal erosion and piping of the foundation soils beneath the levee, leading to breach.

e. To mitigate for unacceptable seepage pressures beneath the relatively impervious blanket, the engineer may consider under-seepage control features such as seepage berms, cut-off walls, drains, and relief wells. These control features can be included in the seepage analysis using FEM as part of the design. Seepage berms and cut-off walls can be considered as a continuous feature in 2D seepage analysis using FEM.

f. Since levees are often long and continuous structures, closed-form solutions for relief wells provided in Chapter 5 assume the well line is comprised of equally spaced wells infinite along the levee. There is no clear approach to modeling an infinite well line in a 2D seepage analysis using FEM. To model an infinite well line in a 2D seepage analysis using FEM, adjustments in the 2D analysis are required to account for the 3D well flow regime. With these adjustments, the 2D seepage analysis can provide accurate solutions that can be used for design of infinite relief well lines.

g. A levee seepage analysis example is also provided to demonstrate how the results of this approach compare to other seepage analysis methods for relief wells. Another example of the method applied to a general levee cross section is included in Appendix I.

G-2. General well design and assumptions

Wells along a levee are typically referred to as relief wells. The relief wells relieve seepage pressures in the pervious substratum. The wells flow due to the hydraulic gradient in the pervious substratum driven by the difference between the waterside static hydraulic head from the river or stream and static hydraulic head at the well (assuming no head losses through the well screen, the well filter materials, and the well riser). For levees, the static hydraulic head at the well is controlled by the discharge elevation of the well and the well losses. Often, the discharge elevation is at or near the landside ground surface near the well.

a. The relief well design for levees is based on achieving an acceptable seepage pressure beneath the relatively impervious blanket, typically evaluated using the effective stress/vertical critical gradient factor of safety criteria. The factor of safety is achieved by varying the well spacing, well radius, well depth, and well discharge elevation. The wells can either fully penetrate or partially penetrate the substratum depending on the required seepage pressure reduction and cost effectiveness.

b. In a 2D seepage analysis model, a drainage slot is used to represent an infinite line of full- or partial-penetration relief wells. A drainage slot is a slot with infinite length along the levee and is represented by a line with assigned boundary conditions. Given the proper boundary conditions are assigned to the drainage slot, seepage flow into a drainage slot will be approximately the same as an infinite line of relief wells and seepage pressures beneath the levee can be determined. The theory on using a drainage slot to represent an infinite line of relief wells and proper boundary conditions for the drainage slot will be provided in the subsequent sections of this appendix.

c. For these 2D analyses, the following conditions are assumed:

- (1) Levee and underlying foundation conditions and properties are continuous infinitely along the levee alignment.
- (2) The relief wells are uniformly spaced and infinite along the levee alignment.
- (3) The waterside and landside boundary conditions are continuous infinitely along the levee alignment.

G-3. Full-penetration wells

A general plan view flow net of a full-penetration drainage slot and full-penetration well is shown in Figure G-1. When examining flow to a slot, the flow is directly to the drainage slot. For flows to an infinite line of relief wells evenly spaced at a distance a , the flow path is longer; therefore, the resistance to flow for a well is greater. USACE (1939b) and Middlebrooks and Jervis (1947) introduce the term “extra length” when discussing infinite well lines, and it is a reference to the longer flow path for the well.

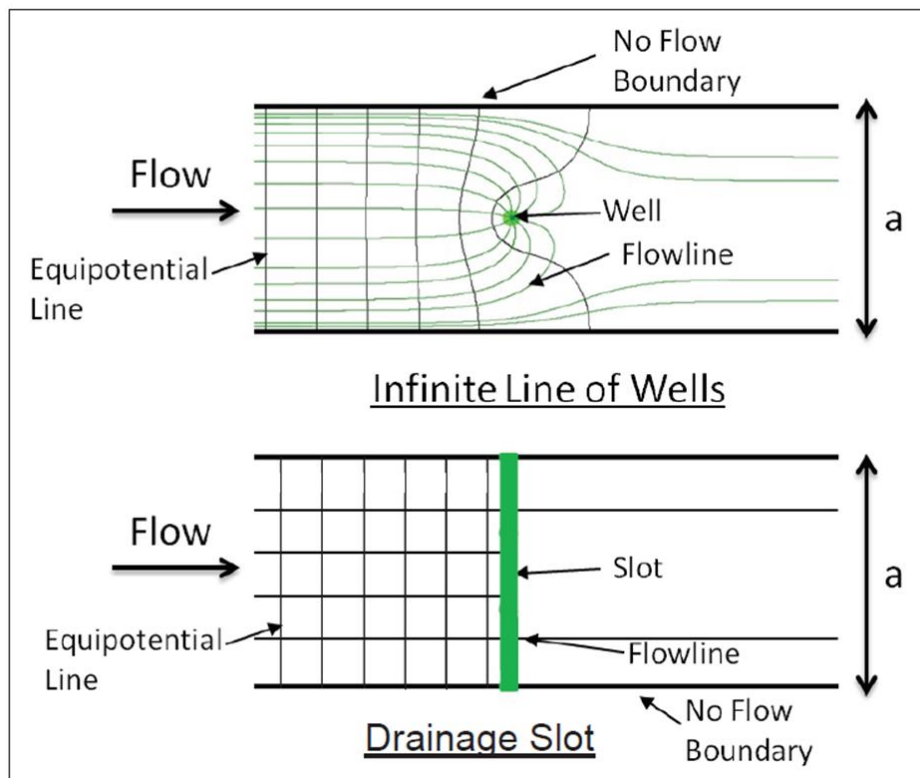


Figure G-1. General plan view flow net of a full-penetration infinite well line and a full-penetration drainage slot; flow is from a line source located a distance L from the well or drainage slot

a. Figure G-1 also illustrates another key concept for an infinite well line. The equipotential lines for the well line are similar to the drainage slot near the line source.

Therefore, the well line can be represented by an equivalent drainage slot having the same flow as the well line. To produce an equivalent drainage slot, the constant head boundary condition at the drainage slot has to be increased by the additional head loss ($h_{\Delta L}$) due to the “extra length” of the flow path to the well. Although not included in this discussion, additional hydraulic head loss in the well is also typically included as explained in Chapter 9 and in paragraph G–7c. The head potential for the wells can be defined as equation G–1:

$$H - h_w = H - h_s + h_{\Delta L} \quad (\text{G-1})$$

where:

H = total head of the line source

h_w = the total head of the well

h_s = total head of the equivalent drainage slot

b. Muskat (1937) provided a closed-form solution for infinite line of relief wells. This solution is for a completely impervious top stratum of infinite length landward of the well, isotropic pervious substratum, and an infinite line source. Equation G–2 is the flow per well (Q_w) in the well line from Muskat’s formulation.

$$Q_w = \frac{2\pi k D (H - h_w)}{\ln\left(\frac{a e \frac{2\pi L}{a}}{2\pi r_w}\right)} = \frac{2\pi k D (H - h_w)}{\frac{2\pi L}{a} + \ln\left(\frac{a}{2\pi r_w}\right)} \quad (\text{G-2})$$

where:

k = pervious substratum horizontal hydraulic conductivity

D = pervious substratum thickness

a = well spacing

L = distance of the line source from the well line

r_w = radius of the well

c. The flow to a drainage slot (Q_s) for this condition can be computed using Darcy’s Law as equation G–3 where the variables have the same definition as for equations G–1 and G–2:

$$Q_s = k i A = k \left(\frac{H - h_s}{L}\right) (D a) \quad (\text{G-3})$$

d. The additional head loss ($h_{\Delta L}$) shown in equation G–1 can be evaluated by equating the flow of the equivalent drainage slot equal to the flow of the infinite well line. Thus, the additional head loss ($h_{\Delta L}$), which is equivalent to the average excess head for an infinite well line (h_{av}) can be defined as equation G–4:

$$h_{\Delta L} = \frac{Q_s \ln\left(\frac{a}{2\pi r_w}\right)}{2\pi k D} \quad (\text{G-4})$$

Note. An equivalent drainage slot can be used to represent the well line if the boundary condition at the drainage slot is increased by $h_{\Delta L}$ to account for the additional head loss to the well.

e. A generalized total head profile along the well line is shown in Figure G-2. Using an equivalent drainage slot in the analysis, the total head profile will be constant along the well line. However, Figure G-2 shows that the head for the equivalent drainage slot is higher than the actual head at the well and lower than the actual head near the midpoint between the wells. Given the shape of the head profile along the line of the wells, the total head profile line of the equivalent drainage slot intersects the total head profile curve for the well at a distance of approximately $a/6$ from the well.

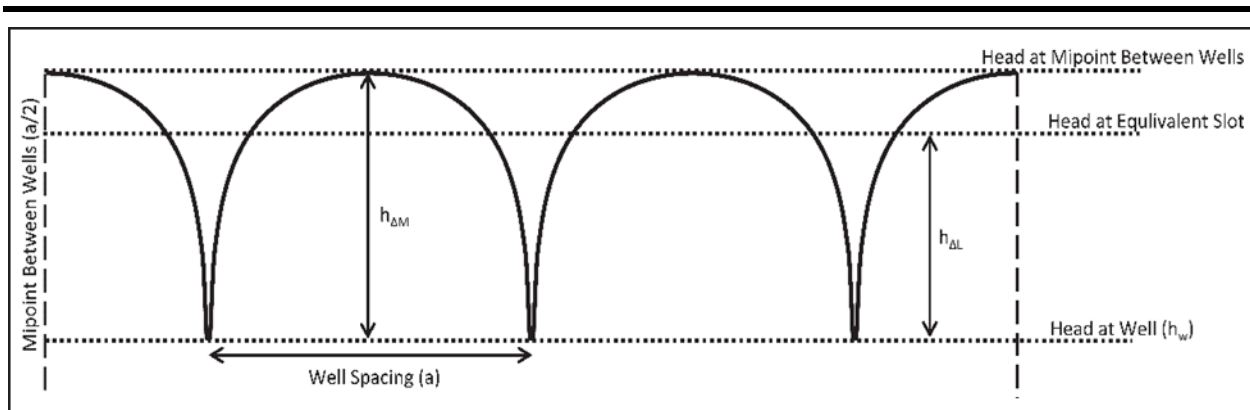


Figure G-2. General total head profile along the well line at the base of an impervious blanket; $h_{\Delta M}$, $h_{\Delta L}$, and h_w are shown to demonstrate the comparison between the variables

f. Figure G-2 also shows that the maximum total head between the wells occurs at the midpoint or $a/2$ from the well, which will always occur for full-penetration wells. The maximum total head between the wells is higher than the total head represented by the equivalent drainage slot. Mansur and Kaufman (1962) provide a solution for computing the maximum total head between the wells ($h_{\Delta M}$), which is equivalent to mid-well excess head (h_m) as follows in equation G-5:

$$h_{\Delta M} = \frac{Q_s \ln\left(\frac{a}{\pi r_w}\right)}{2\pi k D} \quad (\text{G-5})$$

Note. This equation can be derived from Muskat's formulation (Muskat 1937) of the pressure distribution along the infinite well line. The difference between $h_{\Delta M}$ and $h_{\Delta L}$

represents the additional head at the midpoint between the wells for the equivalent drainage slot and is shown as follows in equation G-6:

$$h_{\Delta M} - h_{\Delta L} = \frac{Q_w}{2\pi k D} \ln(2) \quad (\text{G-6})$$

G-4. Partial-penetration relief wells

A similar process can be used for an infinite line of partial-penetration wells. The well line can be modeled using an equivalent partial-penetration drainage slot. The drainage slot would be modeled at the same location and same width, but full penetration. The equivalent slot is modeled as partial penetration as a conservative measure, but average head in the plane of the wells would be overestimated, and well discharge would be underestimated when compared with results of the Chapter 5 method. As with full-penetration well lines, the boundary condition at the equivalent drainage slot should be increased by $h_{\Delta L}$ to account for the additional head loss to the wells.

a. The additional head loss ($h_{\Delta L}$) and head between the wells ($h_{\Delta M}$) for partial-penetration wells is more complex to evaluate than for full-penetration wells. The equation for additional head loss ($h_{\Delta L}$ or h_{av}) (equation G-7) and head between the wells ($h_{\Delta M}$ or h_m) (equation G-8) is similar to the equation for full-penetration wells except it includes θ_{av} and θ_m factors, respectively, as follows (from Mansur and Kaufman 1962):

$$h_{\Delta L} = \frac{Q_s \theta_a}{k D} \quad (\text{G-7})$$

$$h_{\Delta M} = \frac{Q_s \theta_m}{k D} \quad (\text{G-8})$$

b. There were several efforts to develop the θ_{av} and θ_m factors. Bennett and Barron (1957) developed a nomograph that gave values of θ_{av} and θ_m for various well penetration ratios (W/D), the well spacing to well radius ratio (a/r_w), and the pervious substratum thickness to well spacing ratio (D/a). This nomograph is shown in Figure 5-3. The nomograph was based on equations G-9 and G-10:

$$\theta_{av} = \frac{1}{2\pi} \left[\ln\left(\frac{a}{2\pi r_w}\right) + \left(\frac{D}{W} - 1\right) \ln\left(\frac{4D}{r_w}\right) - \frac{D}{2W} \ln(F(I)) + B \right] \quad (\text{G-9})$$

$$\theta_m = \theta_{av} + \frac{1}{2\pi} [\ln(2) - B_m] \quad (\text{G-10})$$

Note. $F(\Gamma)$ is a gamma function provided by Muskat (1937, page 274, equation 6). B and B_m values were evaluated from electrical analogy models (Bennett and Barron 1957). The equation includes both theoretical results and empirical data.

c. Barron (1978–1982) developed a mathematical theory for partial-penetration relief wells. However, a final published version that included comparisons to 3D electrical analogy models could not be found. Figure H–5 and Figure H–6 in Appendix H show comparisons of Barron’s theoretical model with the electrical analogy models. However, since Barron’s final paper could not be found, it is difficult to evaluate the validity of this comparison. A comparison of θ_{av} and θ_m values between the engineer manual nomograph and Barron theoretical model was made. The values from the nomograph generally compare within 5% to values from Barron’s theoretical model.

d. The purpose of providing equations G–9 and G–10 is to illustrate the relationship of the θ_{av} and θ_m factors for various well and pervious substratum parameters. The θ_{av} and θ_m factors are not affected by flow rate (Q_w) or pervious substratum hydraulic conductivity (k). The θ_a factor is affected by the geometric relationships of the well radius (r_w), well spacing (a), well penetration (W), and pervious substratum thickness (D). Generally, the θ_{av} factor increases as the ratio of well spacing to well radius (a/r_w) increases, as the ratio of pervious substratum thickness to well spacing increases (D/a), and generally as the well penetration to pervious substratum thickness ratio decreases (W/D).

e. The θ_m factor becomes less than the θ_{av} factor for D/a generally greater than 1 for well penetrations less than 75%. This represents a situation where the total head for the equivalent drainage slot will be higher than the total head at the midpoint between the wells. The increase in total head between the equivalent drainage slot and well line can be evaluated by taking the ratio of θ_{av} to θ_m . Since the equivalent drainage slot will produce the same flow as the infinite line of relief wells, the equipotential lines will be the same at distances from the well line equal to the well spacing or greater (similar to Figure G–1). However, a plan view seepage analysis or a 3D analysis may be needed to verify the seepage pressures along the well line.

f. Similar to full-penetration wells, the difference between $h_{\Delta M}$ and $h_{\Delta L}$ represented the additional head at the midpoint between the wells for the equivalent drainage slot. For a partial-penetration drainage slot, the difference is shown as follows in equation G–11:

$$h_{\Delta M} - h_{\Delta L} = \frac{Q_w}{k D} (\theta_m - \theta_a) \quad (\text{G-11})$$

G–5. Two-dimensional seepage analysis using the finite element method procedure

a. As shown in the previous sections, an equivalent drainage slot can be used to represent an infinite line of wells. For 2D analyses, incorporating the equivalent

drainage slot with the appropriate θ_{av} and θ_m factors can be accomplished. The procedure for modeling an infinite line of wells in a 2D seepage analysis using FEM is an iterative process. A well spacing, well penetration, and well discharge elevation is selected prior to performing the analysis. The analysis will be used to evaluate the effective stress/vertical critical gradient factor of safety and the flow rate per well.

b. The following steps are provided to obtain an analysis solution for an infinite line of relief wells at a selected well spacing, well penetration, and well discharge elevation. Note that the well spacing, well penetration, and well discharge elevation is kept constant throughout the steps provided below. Refer to Appendix D in EM 1110-2-1913 for general guidelines in performing seepage analyses using FEM.

(1) *Step 1 – Initial two-dimensional seepage analysis using the finite element method.*

(a) The analysis is performed using the initial boundary conditions for the equivalent drainage slot. The boundary condition (noted as BC in equation G–12) for the equivalent drainage slot is assigned as a constant total head boundary condition as defined in equation G–12. Recall that $h_{\Delta L} = h_{av}$:

$$\text{Equivalent Drainage Slot BC} = \text{Discharge Elev.} + h_{av} + H_w \quad (\text{G–12})$$

(b) Where the discharge elevation is the discharge elevation of the well line, h_{av} is the average excess head in a line of wells and is equal to $h_{\Delta L}$, which is the additional head loss determined from equation G–4 for full-penetration wells or equation G–7 for partial-penetration wells, and H_w is the well losses due to hydraulic losses through well screen, filter, and other well components. Chapter 9 discusses well losses.

(c) The boundary condition for the equivalent drainage slot is full penetration, so is assigned across the full foundation depth. The drainage slot boundaries can be represented by a line in the seepage analysis using FEM, and the boundary condition for the drainage slot can be assigned to that line. Since h_{av} and H_w are based on the flow rate of the equivalent drainage slot, these values can be initially assumed or taken as zero.

(d) It is important to note that mesh size used in the analysis has a substantial impact on the seepage flows estimated from the analysis. A fine mesh should be used at the well line. A general practice includes setting an area of finer, uniform mesh extending a distance, upstream and downstream, at least equal to the well spacing. Mesh elements should be sized such that at least two elements fit into each geometry layer. A sensitivity analysis by varying the size of the mesh should be performed to ensure that the seepage flows estimated from the analysis are accurate and not influenced by irregular elements.

(2) *Step 2 – Update equivalent drainage slot boundary condition.* The results of the initial analysis are used to compute the flow rate for the equivalent drainage slot. The flow rate for the equivalent drainage slot (Q_s) is computed as the total flow along

the boundary of the drainage slot representing the screened portion of the well multiplied by the well spacing. Note that the total flow is the flow rate entering the drainage slot minus the flow rate exiting the drainage slot. The values for h_{av} and H_w will be computed using the flow rate for the equivalent drainage slot (Q_s) determined from the initial analysis.

(3) *Step 3 – Two-dimensional seepage analysis using the finite element method with updated equivalent drainage slot boundary condition.*

(a) The analysis should be performed with the updated equivalent drainage slot boundary conditions. The equivalent drainage slot boundary condition should be updated with the computed h_{av} and H_w values determined from Step 2. The results from the revised seepage analysis will be used to update the equivalent drainage slot boundary condition similar to Step 2 (paragraph G–5b(2)).

(b) Several iterations of updating the equivalent drainage slot boundary condition and subsequent analyses will be needed until the updated equivalent drainage slot boundary condition is essentially unchanged between iterations. The analysis results from the last iteration where the equivalent drainage slot boundary condition is unchanged is the considered the final solution for the 2D seepage analysis using FEM with an infinite line of relief wells.

(4) *Step 4 – Compute final well flows.* The final well flows are computed from the final solution for the analysis determined from Step 3 (paragraph G–5b(3)). The final well flow is the total flow along the boundary of the drainage slot representing the screened portion of the well multiplied by the well spacing.

(5) *Step 5 – Determine head between wells.*

(a) The maximum seepage pressures often exist at the midpoint between the wells. The analysis results from Step 3 (paragraph G–5b(3)) do not estimate the seepage pressures between the wells and are considered an average of the seepage pressures along the well line. In some configurations where the well penetration is less than 75%, the maximum seepage pressures is appropriately estimated with the average seepage pressures along the well line and the seepage pressures can be determined directly from the analysis solution in Step 3. This occurs when the θ_{av} factor is equal to or higher than the θ_m factor. However, where the maximum seepage pressures exist at the midpoint between the wells, another analysis is needed to estimate the pressures between wells.

(b) The analysis solution determined from Step 3 will be revised such that the equivalent drainage slot boundary condition is computed using h_m , which is equal to $h_{\Delta M}$ in equation G–12. h_m is computed using equation G–5 for full-penetration wells and equation G–8 for partial-penetration wells. When computing h_m , the flow rate for the equivalent drainage slot (Q_s) will be the flow rate determined from Step 4 (paragraph G–5b(4)). The analysis should be performed with the equivalent drainage slot boundary condition using h_m instead of h_{av} . The seepage analysis results from this analysis

provide an estimate of the seepage pressure between the wells and the associated effective stress/vertical critical gradient factor of safety.

G-6. Levee seepage analysis example and comparison with other methods

A comparison of seepage analysis methods was conducted for a generalized levee shown in Figure G-3 with full-penetration wells. This was performed to compare the results of modeling infinite well lines as an equivalent drainage slot in the 2D analysis with the results of a plan view seepage analysis of the same geometry and properties. The 2D analysis was performed using the steps provided in the previous section.

a. Since the pervious substratum is confined by an impervious blanket along the top and bottom, a plan view seepage analysis can be used to provide an accurate solution for comparison. In the plan view seepage analysis, the relief wells are modeled as a circular drain with the same diameter as the relief well. The constant head boundary on the left side of the model represents the line source (river) and has a value of 30 feet. The constant head boundary on the right side of the model represents the far field landside boundary condition and is equal to the ground surface elevation of zero feet. The wells have a discharge elevation of 1 foot above the ground surface and fully penetrate the pervious substratum.

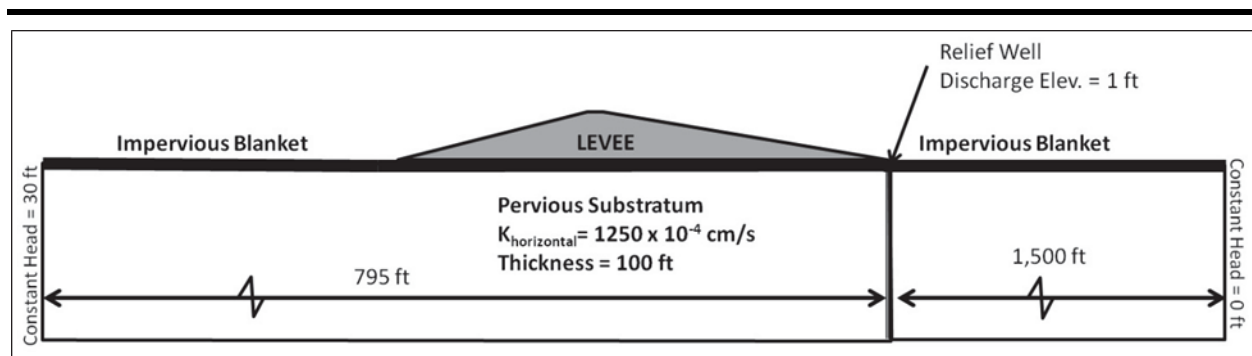


**Figure G-3. Generalized levee; seepage analysis cross section (not to scale).
Ground surface elevation is assumed to be Elevation 0.**

b. The impervious blanket and levee have a hydraulic conductivity of zero (completely impervious). The pervious substratum has a thickness of 100 feet and a hydraulic conductivity of $1,250 \times 10^{-4}$ cm/second. The drainage slot has a thickness of 1 foot.

c. The plan view analysis is shown in Figure G-4. The wells have a diameter of 1 foot.

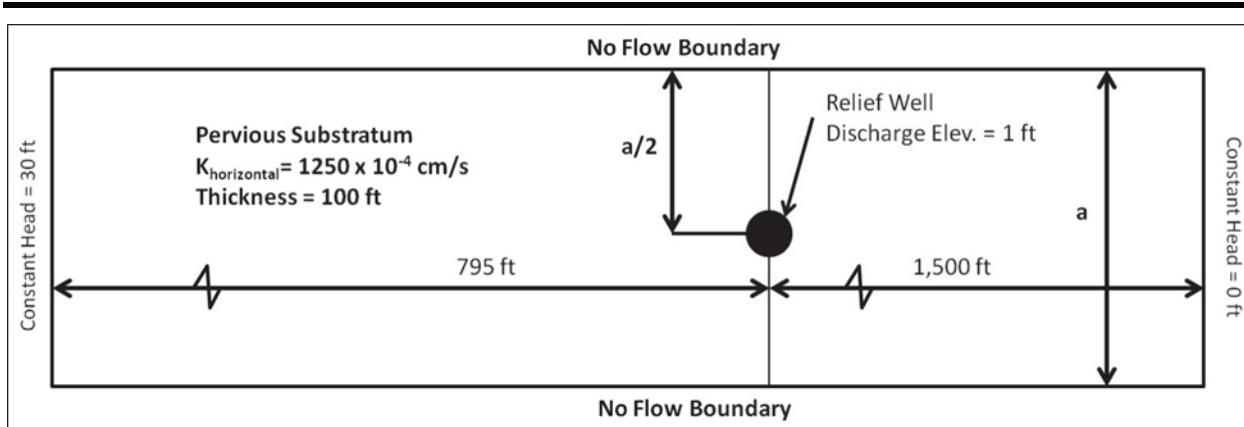


Figure G-4. Generalized levee; plan view analysis section (not to scale)

d. The results of the analyses are shown in Table G-1. The flow per well for the 2D analysis was evaluated by taking the difference of the flow into the drainage slot and flow out of the drainage slot and multiplying the difference by the well spacing.

Table G-1
Results of generalized levee comparison

Well Spacing (ft)	Q (gpm) per Well		h_{av} (ft) for 2D Seepage Analysis using FEM	Total Head at Midpoint Between Wells (ft)	
	Plan View Seepage Analysis using FEM	2D Seepage Analysis using FEM		Plan View Seepage Analysis using FEM	2D Seepage Analysis using FEM
100	597.3	596.1	1.78	3.04	3.14
200	1062.2	1051.2	3.78	5.25	5.41
300	1413.3	1392.9	5.49	7.16	7.33

e. Table G-1 indicates that the flow per well computed by the 2D and plan view analysis agree within 2%. For the total head at the midpoint between the wells, the 2D and plan view analysis agree within 3% with the flow per well computed by 2D analysis results slightly higher than by plan view analysis. Note that the h_{av} was computed using equation G-4 for the 2D analysis. The differences (in percentage terms) between the 2D and plan view analysis were not appreciably affected by the well spacing. Thus, the differences may be due to slight modeling errors (due to element size, mesh layout, model convergence) in the 2D and plan view analysis. However, this demonstrates that the full-penetration relief wells can be modeled in a 2D analysis using an equivalent drainage slot with reasonable accuracy.

f. The flow passing the well line from the 2D and the plan view analysis were compared. Table G-2 shows this comparison and indicates that the analyses agree. For the 2D analysis, the flow passing the well line was evaluated as the flow out of the drainage slot multiplied by the well spacing.

Table G-2
Flow passing the well line comparison

Well Spacing (ft)	Q (gpm) Passing the Well Line	
	Plan View Seepage Analysis using FEM	2D Seepage Analysis using FEM
100	32.9	34.2
200	113.9	117.2
300	232.3	239.0

g. The results of the total head at the base of the impervious blanket toward the line source and the landside far-field boundary are compared between the 2D and plan view analysis. The head comparison was made along two alignments in the model—a line perpendicular to the well line crossing through the center of a well, and a line perpendicular to the well line crossing through the midpoint between the wells. Both alignments are lines of symmetry in the problem. In theory, the line of symmetry between the wells will be a no-flow boundary (flow is parallel only at the boundary). As stated earlier, the well line can be replaced by an equivalent drainage slot with the same flow because the equipotential lines are equal at a distance from the well line. Therefore, the 2D FEM analysis conducted should equate to the same head distribution beneath the impervious blanket at a distance landward and toward the waterside of the well line.

h. Figure G-5 compares the total head distribution at the base of the impervious blanket along a line perpendicular to the well line through the well. This figure shows that the actual drawdown at the well (from the plan view analysis) is higher, resulting in lower total heads at the base of the impervious top stratum in the vicinity of the well. Thus, the difference in total head between the equivalent drainage slot and well at the well line is equal to h_{av} as shown in equation G-1. The 2D analysis produces a close approximation at roughly one-half the well spacing ($a/2$) landward of the well line and one-third ($a/3$) riverward of the well line. Beyond a distance of half the well spacing, the 2D analysis and plan view analysis results have the same total head profile at the base of the impervious blanket.

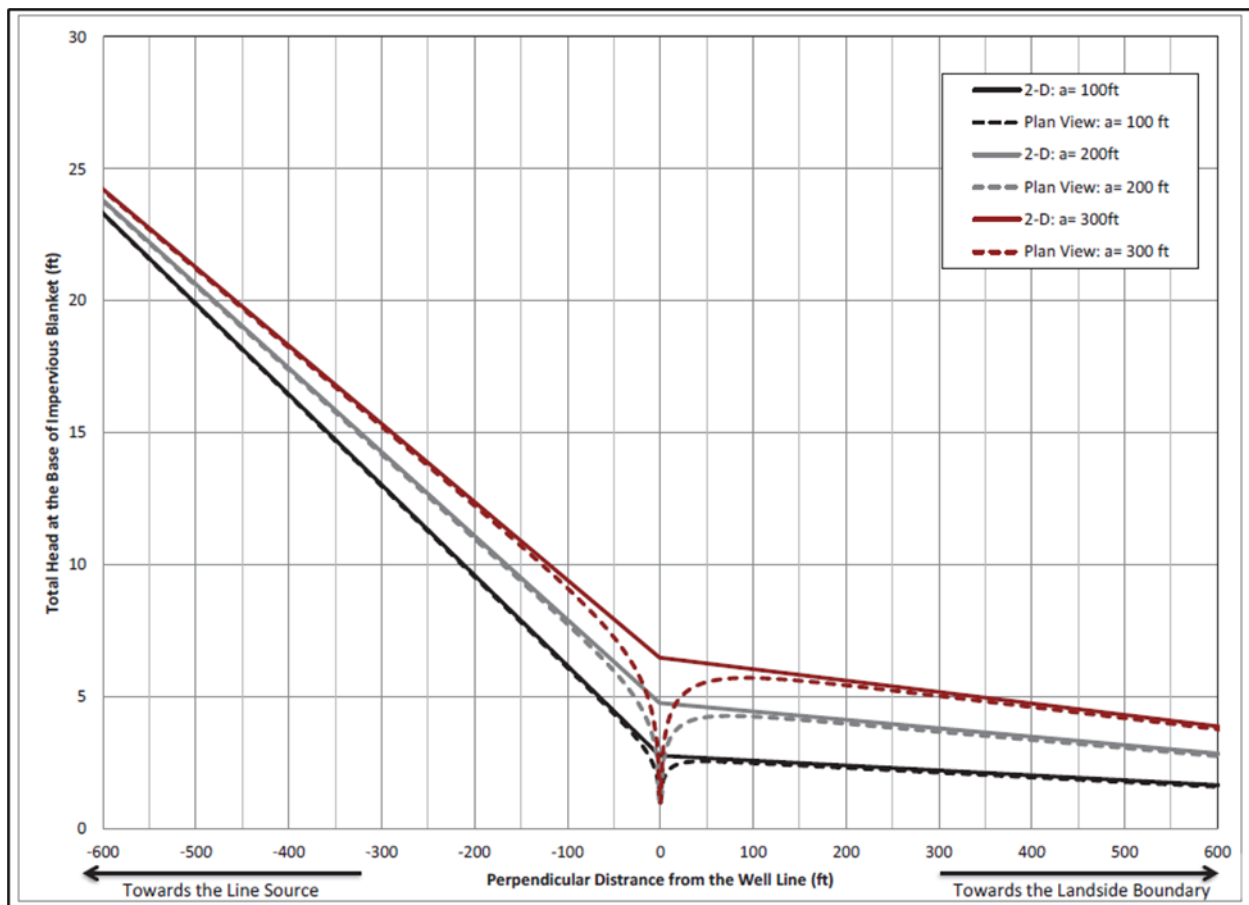


Figure G-5. Total head at the case of the impervious blanket for line perpendicular to the well line through the well

i. Figure G-6 shows the comparison of the total head beneath the impervious blanket at a line perpendicular to the well through the midpoint between the wells. The total head from the 2D analysis is equal to the total head from the plan view analysis at the well line. However, the total head profile beneath the impervious blanket upstream and downstream of the well line is higher in the 2D analysis. The total head profile was determined using Step 5 (paragraph G-5b(5)) in the 2D analysis procedure. The seepage analysis results from Step 5 from the procedure will generally overestimate the seepage pressures at distances upstream and downstream of the well line and are considered conservative.

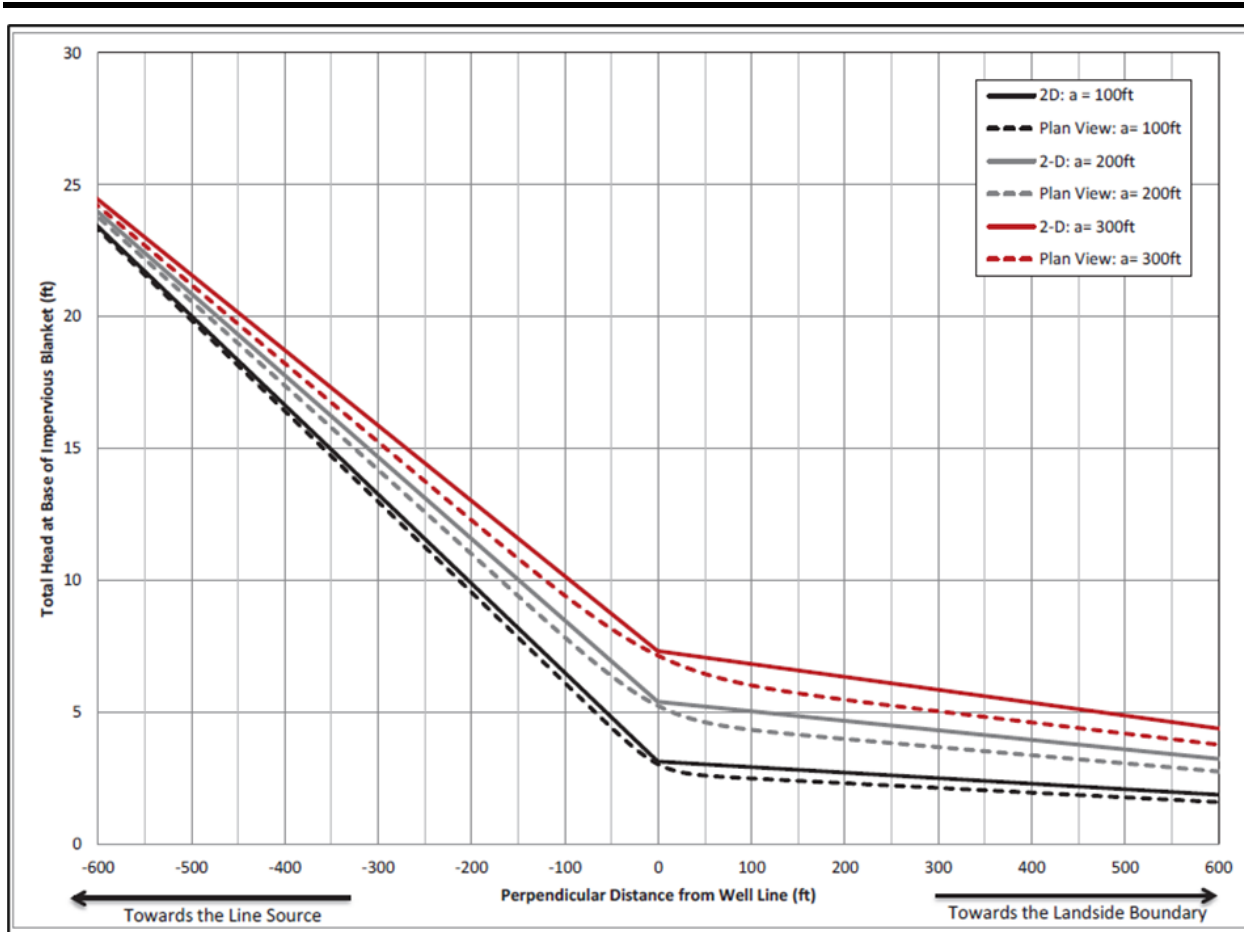


Figure G-6. Total head at the base of the impervious blanket for line perpendicular to the well line through the midpoint between wells

G-7. Additional considerations

The approach for modeling infinite well lines in a 2D seepage analysis using FEM presented in this appendix are for a set of ideal conditions. Actual conditions for the levee and well line design often vary from these idealized conditions. The conditions encountered may include a finite well line length, flow around the end of the well line, stratification of the pervious substratum, and well losses due to flow through the well filter and screen. The impacts of these conditions on the 2D analysis are discussed in the following paragraphs.

a. Finite versus infinite well line.

(1) For a well line to be considered infinite along the levee alignment, the well line must extend to the boundary of the pervious substratum along the levee alignment. The boundary of the pervious substratum should be impervious. For some levees, the pervious substratum extends beyond the well line and 3D flow around ends of the well line can impact well flows, seepage pressures between the wells, and seepage pressures landward of the well line. Using the 100-foot spacing example for a

generalized levee presented in this appendix, a plan view analysis was performed using a well line of length 1,500 feet with the ends of the well line also 1,500 feet from the boundary of the pervious substratum.

(2) Figure G–7 shows the total head profile along the well line compared to the infinite well line solution. As shown in the figure, the head between wells is higher than computed from the infinite well line solution. The head between the wells is lower at the center of the well line and gradually increases near the end of the well line. Figure G–8 shows the flow for each well along the well line and the flow per well for an infinite well line. The well flows for the finite well line are higher than for the infinite well line. The flow per well gradually increases from the center of the well line toward the end of the well line. The 3D flow regime of a finite well line cannot be accounted for in the 2D analysis. Chapter 6 offers a method to adjust the closed-form solution for finite well lines.

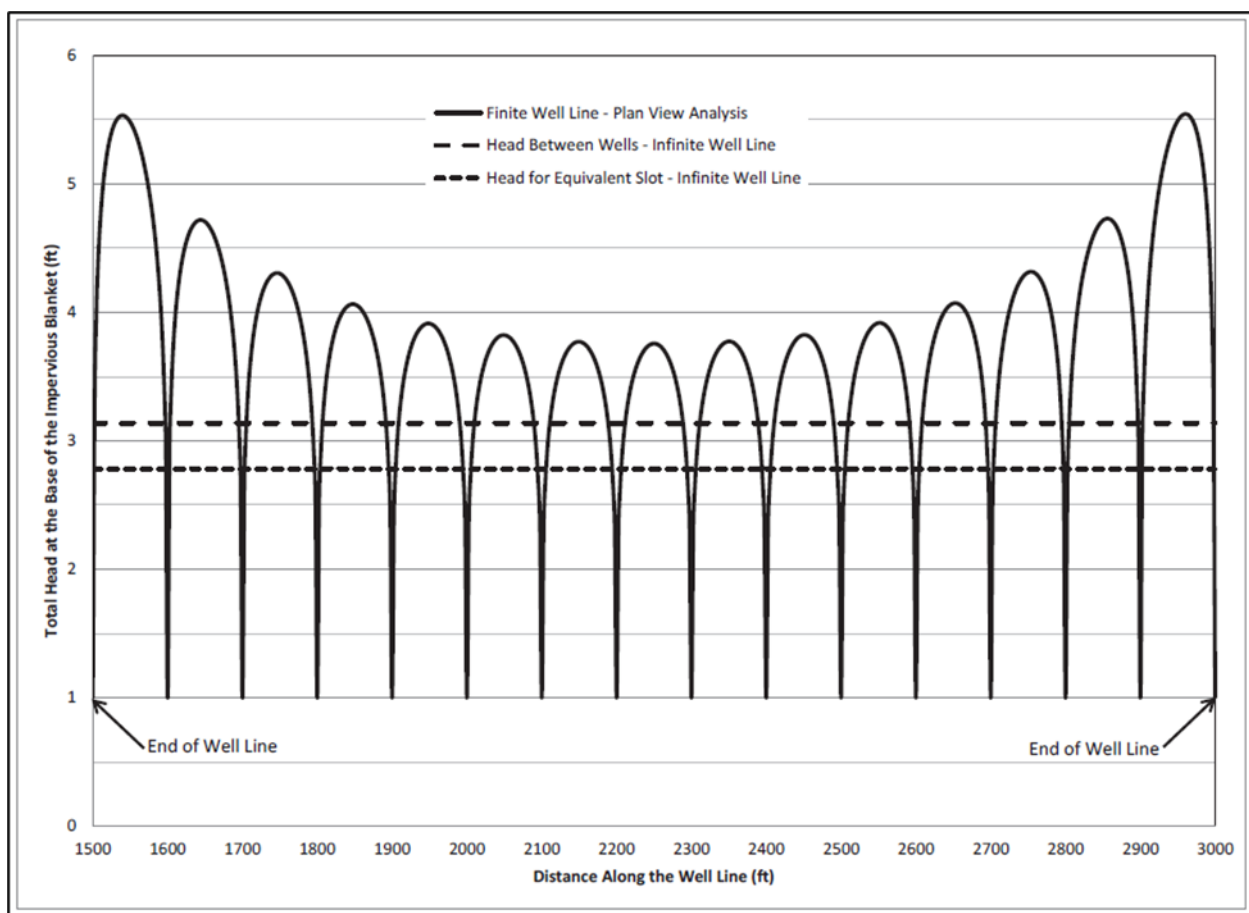


Figure G–7. Total head at the case of the impervious blanket along well for a finite well line and an infinite well line

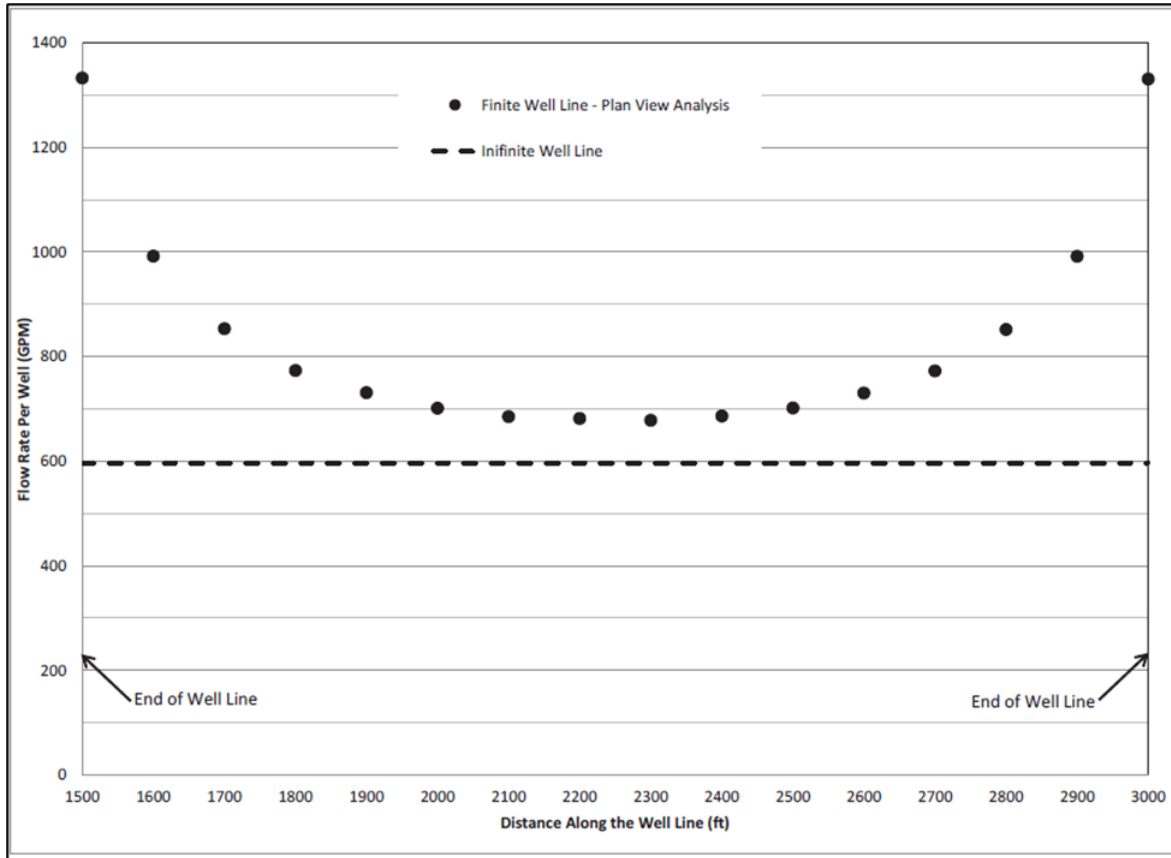


Figure G-8. Well flows for a finite and an infinite well line

b. *Stratified pervious substratum.*

(1) In most situations, the pervious substratum is stratified and not a homogenous, isotropic unit as assumed in the closed-form solutions and equations presented in this appendix. This becomes an issue when computing h_{av} and h_m for full-penetration wells and partial-penetration wells. If the flow in the pervious substratum is generally horizontal, a reasonable approximation of these factors may be obtained by converting the stratified pervious substratum into a uniform pervious substratum of isotropic hydraulic conductivity (k) and thickness (D). Appendix E provides an approach from TM 3-424 (USACE 1956a) for converting the stratified pervious substratum into a uniform pervious substratum.

(2) For partial-penetration wells in a stratified pervious substratum, the effective penetration and transformed aquifer thickness should be used when determining the θ_{av} and θ_m factors. A method for computing the effective penetration of the well is also provided in Appendix E. Note that the 2D analysis should incorporate the stratified pervious substratum, but the θ_{av} and θ_m factors should be based on the converted, uniform pervious substratum properties.

c. *Well head losses.* Head losses due to flow through the well components (well filter, screen, and riser) affect the performance of the well. These head losses should be included in the 2D or 3D analysis. Often these head losses are based on the velocity through the well filter, screen, and riser (Chapter 9). The 2D analysis can be performed initially assuming no head loss through the well components. The flow per well evaluated from the initial 2D analysis can then be used to estimate the head loss. The calculated head loss should then be added to the boundary condition of the equivalent drainage slot. Note that this assumes that the head losses through the well components are the same for every well.

G–8. Summary

a. Seepage analysis using the FEM is a common approach for assessing seepage pressures beneath a levee. Seepage analysis using FEM allows the designer more flexibility to consider more complex boundary conditions than closed-form solutions. Relief wells are often considered solutions for under-seepage remediation for levees. There are closed-form solutions given in Chapter 5 for computing the well flow and seepage pressures for an infinite well line.

b. An infinite well line can be represented by a full-penetration equivalent drainage slot in a 2D analysis given the drainage slot has the same flow as the well line. This can be accomplished by increasing the total head boundary condition at the equivalent drainage slot by h_{av} (given as $h_{\Delta L}$) in equation G–4 for full-penetration wells and equation G–7 for partial-penetration wells. The increase in head is to account for the extra length in the flow path to a well versus the drainage slot.

c. Beyond a certain lateral distance from the well, the seepage pressures determined using an equivalent drainage slot in the 2D analysis are generally equivalent to the seepage pressures determined for a line of wells in a plan view analysis. In the vicinity of the well, the equivalent drainage slot will estimate seepage pressures higher than the actual drawdown of the well. At the midpoint between the wells, the equivalent drainage slot may estimate seepage pressures lower than the actual well line. At the well line, the seepage pressures from the equivalent drainage slot can be increased by the difference between h_m and h_{av} ($h_{\Delta M}$ and $h_{\Delta L}$) as shown in equation G–6 (full-penetration well) and G–11 (partial-penetration well) to estimate the head between the wells.

d. For the generalized levee example used in this appendix, the seepage pressures evaluated from the 2D analysis (using an equivalent drainage slot) gave essentially the same seepage pressures beyond a distance $a/2$ for a line perpendicular to the well line through the well and a distance $a/3$ for a line perpendicular to the well line through the well midpoint. However, within these distances of the well line, the seepage pressures evaluated from the 2D analysis using an equivalent drainage slot are not correct and the understanding of well theory is needed to make proper adjustments.

e. Actual conditions for the levee and well line design often vary from the idealized conditions presented in this appendix. The conditions may include a finite well line length with flow around the end of the well line, stratification of the pervious substratum, or well losses due to flow through the well components. For finite wells, the 3D flow around the ends of the well line cannot be accounted for accurately in a 2D analysis. For stratified pervious substratum, h_m and h_{av} can be estimated by converting the substratum to a uniform pervious substratum of isotropic hydraulic conductivity (k) and thickness (D). Well losses due to flow through the well components should be added to the boundary condition of the equivalent drainage slot.

Appendix H

History of Well Factors for an Infinite Line of Partial-Penetration Relief Wells

H-1. Historic use of wells to reduce substratum pressure

a. Wells have historically been used for agricultural seepage control (Johnstone 1797; French 1859), for reducing uplift pressures on hydraulic structures (Khosla 1930), and for construction dewatering (Terzaghi 1927). Floods during the late 19th to early 20th centuries caused detrimental underseepage, sand boils, and at least six Mississippi River levee failures due to internal erosion (Fatherree 2006). Underseepage research was subsequently accelerated by the Mississippi River Commission, the USACE Vicksburg Engineer District, and (WES, now ERDC). Since the 1930s, USACE has researched and used pressure relief wells for flood protection structure seepage control (USACE 1939a, b, c).

b. Field studies in the late 1920s (Long and U.S. Army WES 1931), adaptation of approaches from the petroleum industry (Muskat 1937), and model and theoretical work (USACE 1939a, b, c) led to the development of an initial nomogram and formulas for partial-penetration relief well systems design by the late 1930s. This design process, sometimes referred to as the Muskat-Jervis approach, employed the theoretical, infinite, full-penetration well line solution by Muskat and electric analog-based partial-penetration solutions developed by USACE. Muskat (1937) contained an approach for evaluating head distribution and flows for fully penetration infinite well lines. The text included discussion on calculating flows for partial-penetration wells but not head distribution.

c. When wells do not fully penetrate a pervious aquifer or foundation, vertical flow components (absent for full-penetration wells) increase flow path distances and head losses leading to reduced well discharges and increased foundation uplift pressures. USACE recognized a need to analyze situations in which wells partially penetrated the foundation of structures. Partial (versus full) penetration wells may sometimes offer technical or economic advantages for dam and levee applications. However, in the 1930s, a mathematical formulation for an infinite line of wells, parallel to a line source and partially penetrating a homogeneous, isotropic (either natural or transformed) pervious foundation did not exist.

(1) Using the analogous nature of Darcy's Law (Darcy 1856) to Ohm's Law (Ohm 1827), electrical current can be substituted for seepage flow rate, electromotive force for net seepage head, and conductance of the electrolytic medium for hydraulic conductivity of the aquifer. Figure 2-1 shows the original USACE electrical analogy model setup (USACE 1939b), where line sources and sinks (vertical flow surface boundary conditions) were applied via copper plates and wells were simulated by copper wires inserted to various depths. Measuring the voltage (total head) drop through the aquifer solution allowed calculation of gradient and flow quantity. These measurements were taken along the edge of the tank and midway between wells at the top of the aquifer.

(2) From these experiments, the “extra length factor” was introduced as a design parameter to represent the additional resistance relative to a continuous slot as groundwater flow converges to a line of wells. In addition to the energy loss due to the increased horizontal flow path lengths, partial-penetration wells have an increased vertical flow path. The “head factor” was also introduced as a design parameter on charts and was the measured head at the midpoint between wells in experiments. The extra length factor and head factor concepts are still used today in the calculation of design flows and uplift for relief well design. Today these factors are referred to as the average and mid-well uplift factors.

H–2. Nomogram prior to 1955

a. An initial nomogram (USACE 1939b) was developed that employed the extra length concept. Unfortunately, an error was introduced in the head factor chart (Appendix 2, Plate 10, Chart 1) of USACE (1939b). This error can cause an over-prediction of pressure relief in certain cases. Erroneous charts from USACE (1939b) work were also reproduced by USACE (1941), USACE (1944), Middlebrooks and Jervis (1947), Yanai (1963), and the analogy results of USACE (1939b). These charts were superseded by the publication of a corrected single design chart in 1955, the nomogram still in use today described in paragraph H–3.

(1) During the 1940s to early 1950s, several versions of a similar nomogram were published with different appearances and, in some cases, different axis labels, but all yielded similar solutions (USACE 1941 and 1942; Jervis 1945; Middlebrooks and Jervis 1946, 1947; Mansur and Turnbull 1948; USACE 1949). Each made use of the Muskat-Jervis solutions. A design nomogram (Middlebrooks and Jervis 1947) generally representative of those published before 1955 is shown as Figure H–1.

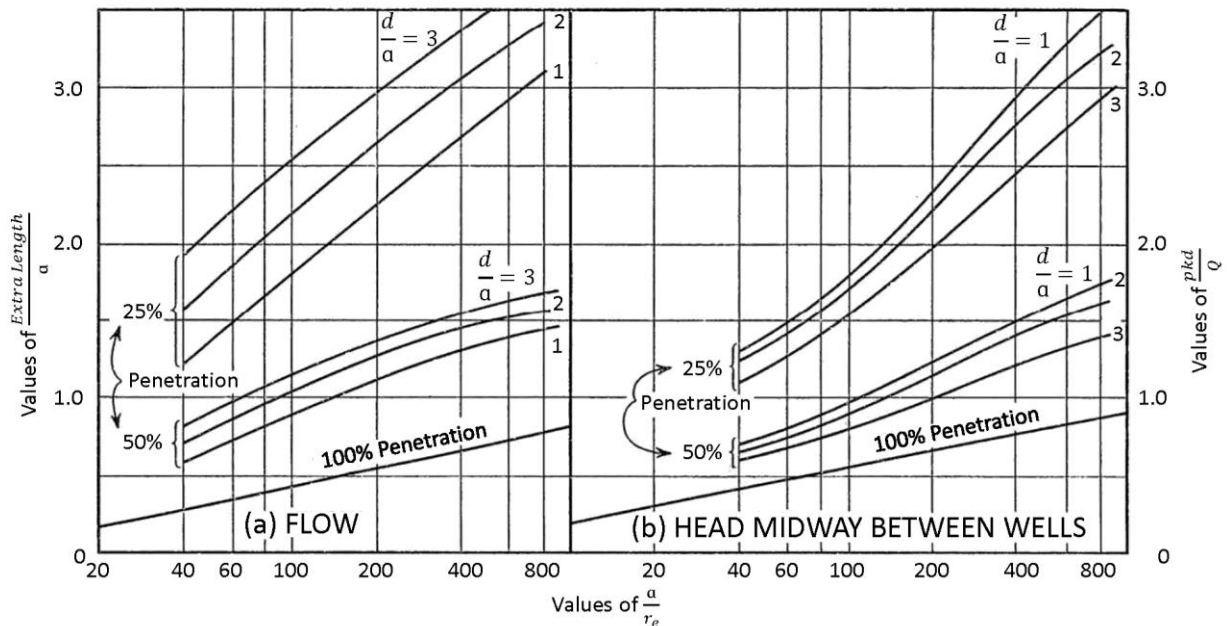


Figure H-1. Relief well design nomogram from Middlebrooks and Jervis (1947)

(2) For input parameters of percent well penetration, well spacing, effective well radius, and pervious foundation thickness, solutions could be read on the left side chart in Figure H-1 for the extra length factor. Before 1955, nomogram outputs were used to calculate well discharge, which was then used with the mid-well factor reading derived from the right side chart in Figure H-1 (today known as θ_m) to calculate the net head midway between wells.

b. Underseepage problems along Mississippi River levees during the 1937 flood and similar concerns elsewhere led to continued relief wells research during the 1940s (USACE 1968).

(1) USACE conducted physical modeling to further evaluate the design and performance of partial-penetration relief wells. The USACE (1949) physical model tests were conducted in a steel flume measuring 8.5 meters (28 feet) long, 1.2 meters (4 feet) tall, and 1.1 meters (3.5 feet) wide. Turnbull and Mansur (1959) also published these model tests. One side of the flume was tapped with piezometers to measure pressures at the base of the top stratum and in the foundation, and the other side was made of glass for viewing of flow lines indicated by injection of dye tracer. Relief wells were modeled as 1.3-centimeter (0.5-inch) diameter wells landward of the levee toe, and different well spacings were obtained by plugging different wells for each test. The penetration was adjusted by partially filling the full-penetration screens with sand.

(2) Further studies led to methods capable of considering flow landward of a well line and the presence of a semi-pervious top stratum (USACE 1941; Bennett 1945, 1946, and 1947; Barron 1947 and 1948). Formulas were extended to allow consideration of landward flow using source-side and exit-side gradients with the

average head concept. The average net head in the plane of (and landward of) the well line was not previously considered. While prior approaches had assumed a completely impervious top stratum extending landward to infinity, in practice a semi-pervious top stratum may exist, or an impervious top stratum may extend landward a finite distance.

c. Approaches were therefore developed to allow conversion of a semi-pervious top stratum to an equivalent finite length of impervious top stratum. Work in the 1940s contributed to BT (closed-form solutions for seepage pressures and flows) as introduced in the 1950s (USACE 1956a) and then documented further by EM 1110-2-1913 and USACE (2018). Pool and tailwater boundary conditions were incorporated into BT design equations in Bennett (1946). A solution for a line of wells between an infinite line source and line sink was developed by Barron (1948) and shown in Figure H-2.

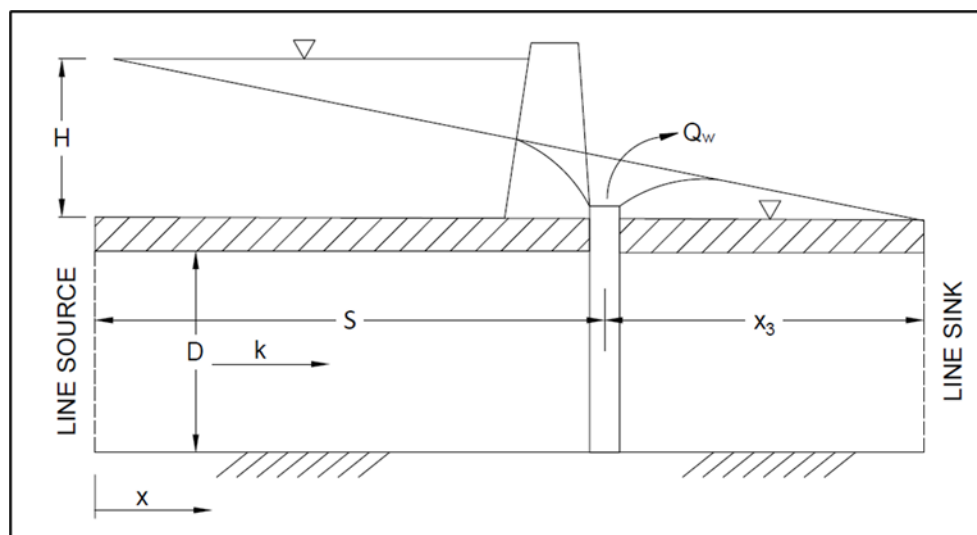


Figure H-2. Drawdown for well between infinite line source and downstream sink (after Barron 1948)

d. There is a special case in which there is no landside top stratum, as shown in Figure H-3. The flow is a combination of artesian and gravity flow. Johnson (1947) provides equations that may be used to estimate flow and head for this special case. It is unclear if this approach has been used in practice.

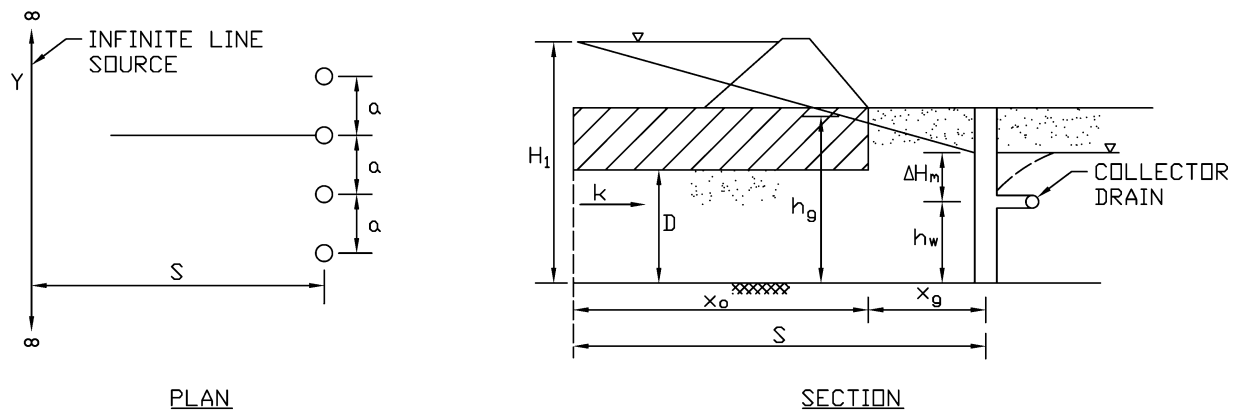


Figure H-3. Infinite line of full-penetration wells, combined gravity, and artesian flow

H-3. Introduction to the modern (post-1955) nomogram and well factors (θ_{av} and θ_m)

a. Results of electrical analog models, physical models, and theoretical studies were used to develop a nomogram for the design of partial-penetration relief well systems (USACE 1955). The nomogram (Figure H-4) allows the design of an infinite line of equally spaced relief wells penetrating a homogeneous, isotropic (either natural or transformed) pervious foundation overlain by an impervious top stratum. The development of the well factors (also known as uplift factors) included in the nomogram was described as “experimental and theoretical.” The nomogram provides a graphical solution for uplift factors used in design (and back-analysis) computations of discharge and foundation uplift pressures for a given well system.

b. Relief wells research continued in the 1950s including further field (USACE 1950, 1952) and experimental data analysis (Turnbull and Mansur 1954; Bennett et al. 1954). In USACE (1955), a revised relief well design nomogram was published (Figure H-4) and it was stated (without explanation) that the prior nomograms were in error. Bennett and Barron (1957) suggest that a review of model data coupled with limited additional theoretical study found the initial partial-penetration design curves to be in error.

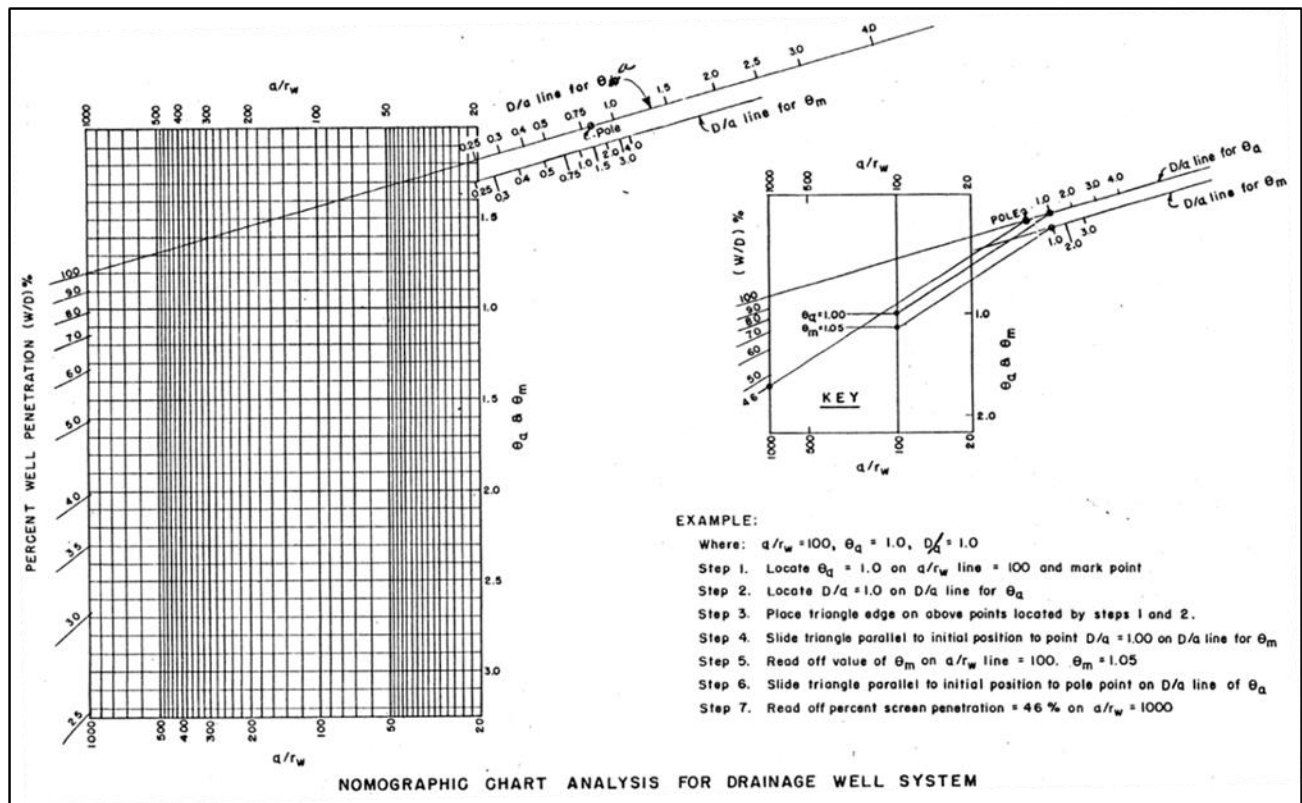


Figure H-4. Relief well design nomogram from USACE (1955)

(1) USACE (1955) established that the maximum head (the greater of the average and mid-well) would now control design, whereas previously only the mid-well uplift was considered. In some partial-penetration cases, head landward of the well line exceeds head midway between the wells, and so the average head governs uplift (Spaulding 1976). Therefore, the pre-1955 process could underestimate uplift and lead to non-conservative systems. Equations for computing well discharge, average head, and mid-well head were also formulated in terms of net seepage gradient and finite impervious top stratum length. For a case of an infinite impervious top stratum, these equations provide the same solutions as prior ones; however, they also allow consideration of a landward impervious top stratum of finite length (length to a natural sink or equivalent semi-pervious top stratum).

(2) Theta notations (originally θ_a and θ_m , today known as θ_{av} and θ_m) were also introduced for both the average and mid-well (uplift) factors in USACE (1955). These dimensionless values, obtained from the nomogram in Figure H-4, represent the effects of nomogram parameters separately from the effects of source and landward boundary conditions. Similar to earlier approaches, the uplift factors obtained from this nomogram are used to compute well discharge and mid-well head and, in addition to earlier approaches, the 1955 nomogram output and equations are used to compute the net seepage gradient toward the well line and then the average net head in the plane of the wells.

(3) The BT method of analysis for underseepage problems (USACE 1956a) incorporated the 1955 nomogram for well system design purposes; the nomogram in USACE (1956a) changed the original 1955 uplift factor notation from θ_a to θ_{av} . Theoretical work from Bennett and Barron (1957) helped explain the origins of the 1955 nomogram and relation among inputs and provided formulas for approximate uplift factor solutions.

c. The nomogram introduced a method for calculating θ_{av} and θ_m using inputs of foundation thickness (D), well spacing (a) and radius (r_w), and well penetration (W/D). Figure 3-38 of Leonards (1962) presents a nomogram constructed from the USACE (1955) design chart with equations to calculate well flow (Q_w), h_m , and h_{av} .

d. Following its initial release in 1955, the USACE design nomogram was later published in other references. TM No. 3-424 (USACE 1956a) includes the nomogram with additional discussion on the incorporation of well losses into design computations. Bennett and Barron (1957) also include equations describing the uplift factors. However, direct use of their “approximate solutions” is limited as they rely on corrections from test data that are not published. Mansur and Kaufman (1962) provide useful design charts based on Civil Works Engineer Bulletin #55-11 (USACE 1955). Equations 5–16 through 5–19 and Table 5–1 in this manual are “more theoretically exact” uplift factor solutions by Barron in the years following development of the original “approximate” solutions.

e. While Barron’s theoretical approach has not been fully traceable or illustrated to date, it is evident he successfully developed one. Barron performed extensive research on the topic over several decades (with numerous published and unpublished papers). Figure H–5 and Figure H–6 show the theoretical solutions closely agree electrical analogy test results.

f. Modern 3D FEM analyses also validate Barron’s approach. Figure H–7 shows that results from the various uplift factor approaches (electrical analogy, physical modeling, analytical, and FEM) are very similar. Keffer et al. (2019) describe the error in the original 1939 nomogram from Jarvis that is evident for lower penetration percentages in this plot. Figure H–7 also includes the Sharma analytical approach that is described in paragraph H–5.

g. In Chapter 5, there are equations for calculating θ_{av} and θ_m for full-penetration wells. For partial well penetrations, theoretical values for θ_{av} and θ_m are obtained from Table 5–1, Figure 5–5, equation 5–15, equation 5–16, and/or the nomogram in Figure 5–3. The Figure 5–4 nomogram was originally published in CW-EB #55-11 (USACE 1955) and is based on the results of electrical analog and physical models and theoretical studies. Note that the nomogram has been often republished with several errors listed in Appendix L and described in Guy et al. (2014). One significant error is the required “pole” point on the D/a line for θ_{av} is missing from some versions. A relatively new landward uplift factor (θ_a) can be obtained from Figure 5–6.

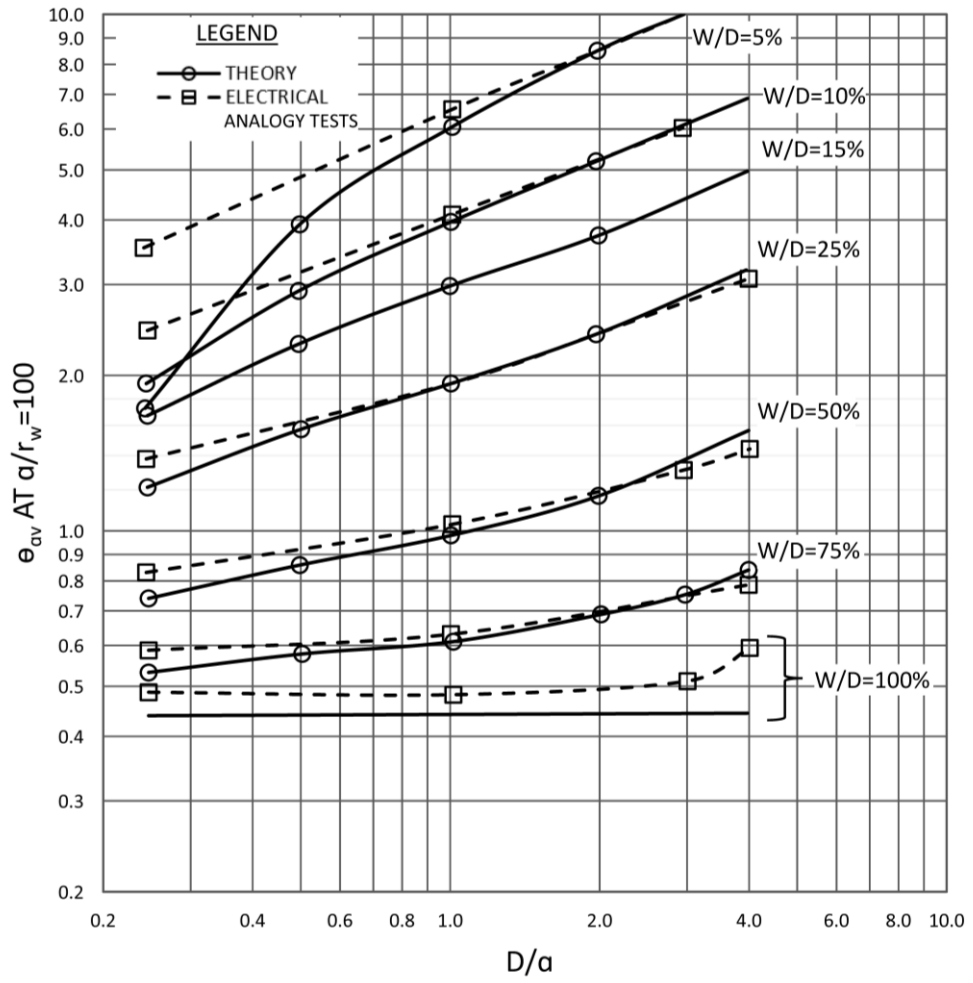


Figure H-5. Theoretical values of average uplift factor (after Barron 1978-1982)

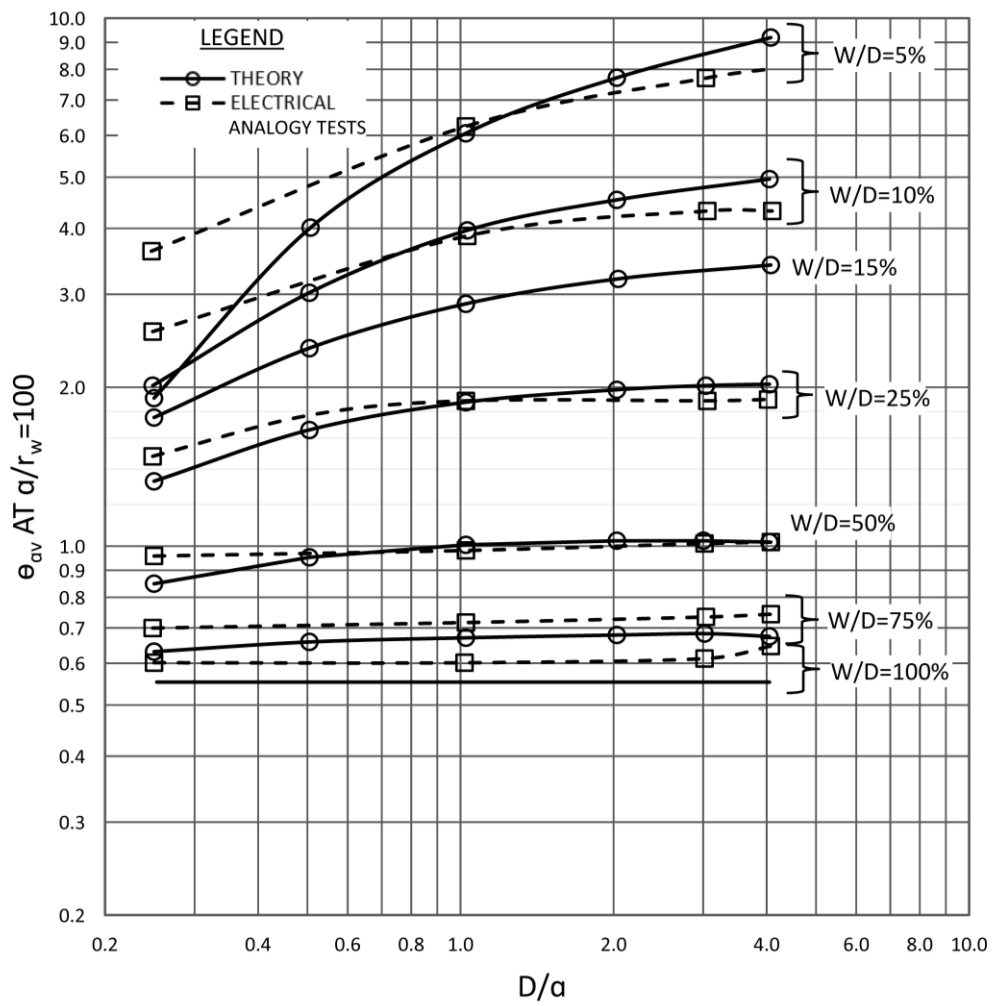


Figure H-6. Theoretical values of mid-well uplift factor (after Barron 1978-1982)

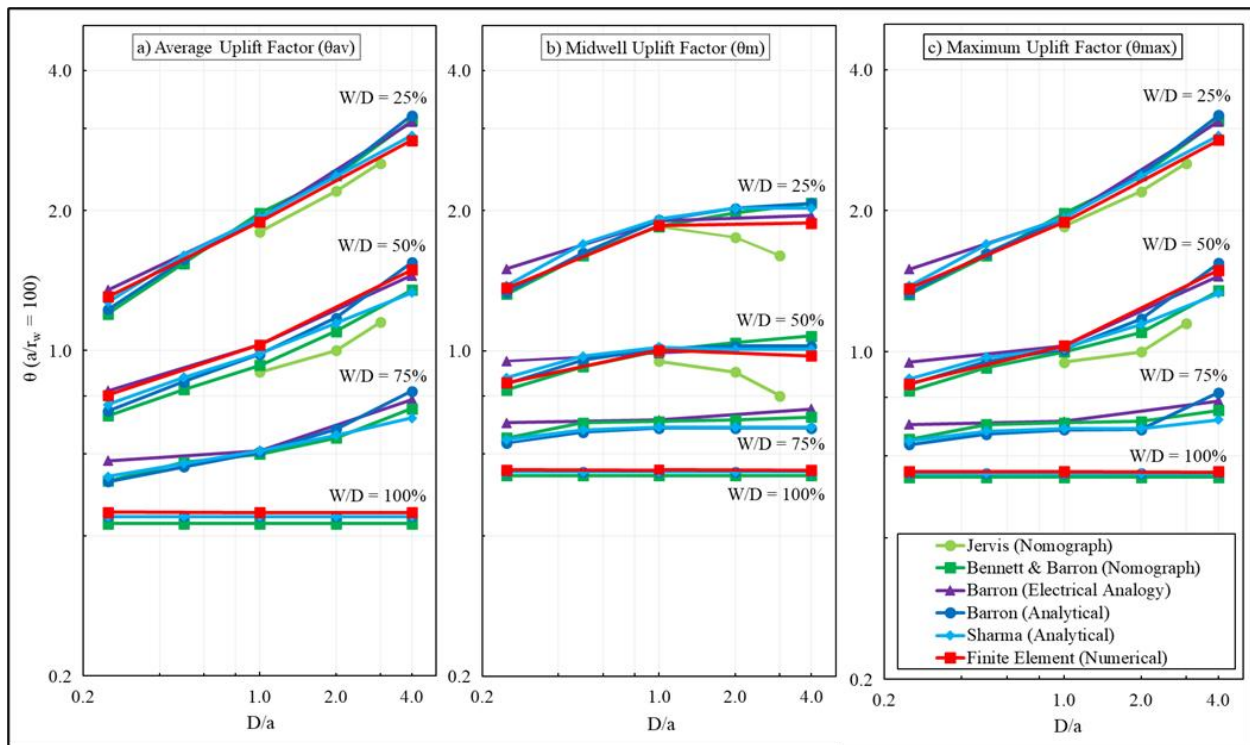


Figure H-7. Well factor determined from various methods (figure adapted from Keffer et al. 2019)

h. USACE (1955) also introduced the concept of designing well systems against the greater of the average and mid-well heads. For certain partial-penetration cases θ_{av} can exceed θ_m , and in these cases θ_{av} should be used for not only flow but also design head (uplift) computation. The significance of an error in pre-1955 nomograms, coupled with use of the average rather than mid-well uplift factor in some cases for computing maximum uplift, is documented, and a correction factor for rectifying the original error is given.

i. For input parameters of percent well penetration (W/D), well spacing (a), effective well radius (r_w), and pervious foundation thickness (D), solutions can be obtained for the average and mid-well uplift factors (θ_{av} and θ_m). These dimensionless factors represent the effects of the nomogram's input parameters separately from the effects of source and landward boundary conditions.

j. These factors are used with the seepage entry and exit distances, material properties, and well losses to compute discharge and foundation uplift pressures for a given infinite line of relief wells, as shown in Figure 5-1. The θ_{av} is used to compute the average net head in the plane of the wells, the net seepage gradient toward the well line, and the well discharge. The θ_m is used to compute the net head midway between the wells (at the base of the impervious top stratum). The importance of using the effective rather than actual well penetration in these calculations is noted throughout this manual.

k. There were other required corrections to relations shown in Figure 5–1 from historically published versions of the nomogram as given in Guy et al. (2014). θ_{av} exceeds θ_m for some partial-penetration well line scenarios as indicated by Figure H–4. Keffer and Guy (2021b) refers to the greater of average and mid-well uplift factors as θ_{max} .

(1) In practice, the design of infinite relief well lines has often relied on uplift factor solutions obtained from directly reading the nomogram, computer simulation of the nomogram, or Barron’s theoretical uplift factors (Guy et al. 2010). Due to the complex nature of operating the nomogram, and for general efficiency, some have automated its function.

(2) As shown in paragraph H–5, the theoretical work of Sharma (1974) can be employed to determine uplift factors using an analytical approach. The significance of Sharma’s work, in terms of historical importance and practical application, appears generally unrecognized to date. As the analytical solutions closely agree with the nomogram, both approaches are further validated for use.

l. Since 1955 there have been no significant revisions to the relief well nomogram or accompanying design formulas, although the nomogram was adapted to another form using the same data (Mansur and Kaufman 1962; U.S. Army 1983) and reproduced with slight differences in Turnbull and Mansur (1961), EM 1110-2-1901, and the 1992 version of this manual. Not widely recognized to date, an analytical method for computing uplift factors was independently developed during this era by Sharma (1974). Further documentation of BT was also compiled (Spaulding 1976). USACE refined and further verified uplift factors estimation with mathematical theory and electric analog tests (Barron 1978–1982).

m. In Guy et al. (2014), a few corrections are noted for the nomogram related to theoretical uplift factors and the head and flow equations in the original version of this manual. In Keffer et al. (2019), FEM was used to independently compute uplift factors that were found to agree with those of the 1955 nomogram, post-1955 USACE theoretical studies, and uplift factors computed by adapting Sharma (1974).

n. Lastly, another unique relief well design nomogram was developed by Keffer and Guy (2021) by considering historical research and completing FEM and analytical computations. It provides solutions that are similar to and further verify post-1955 USACE solutions. This new nomogram provides the maximum uplift factor for design, improves visualization of the uplift factor solutions behavior, and can be used for manual verification of automated solutions.

o. Finite lines of relief wells have historically been addressed by either including additional wells at the ends of the line or using a factor to increase mid-well head. Figure H–8 from USACE (1956a) is further explained in Turnbull and Mansur (1961) and is an example of this increase in mid-well head. A more complete set of well penetration ratio, spacing, and finite length have been considered in Keffer et al. (2023).

This updated approach to estimate head both between wells and landward of a finite well line is included in Chapter 6.

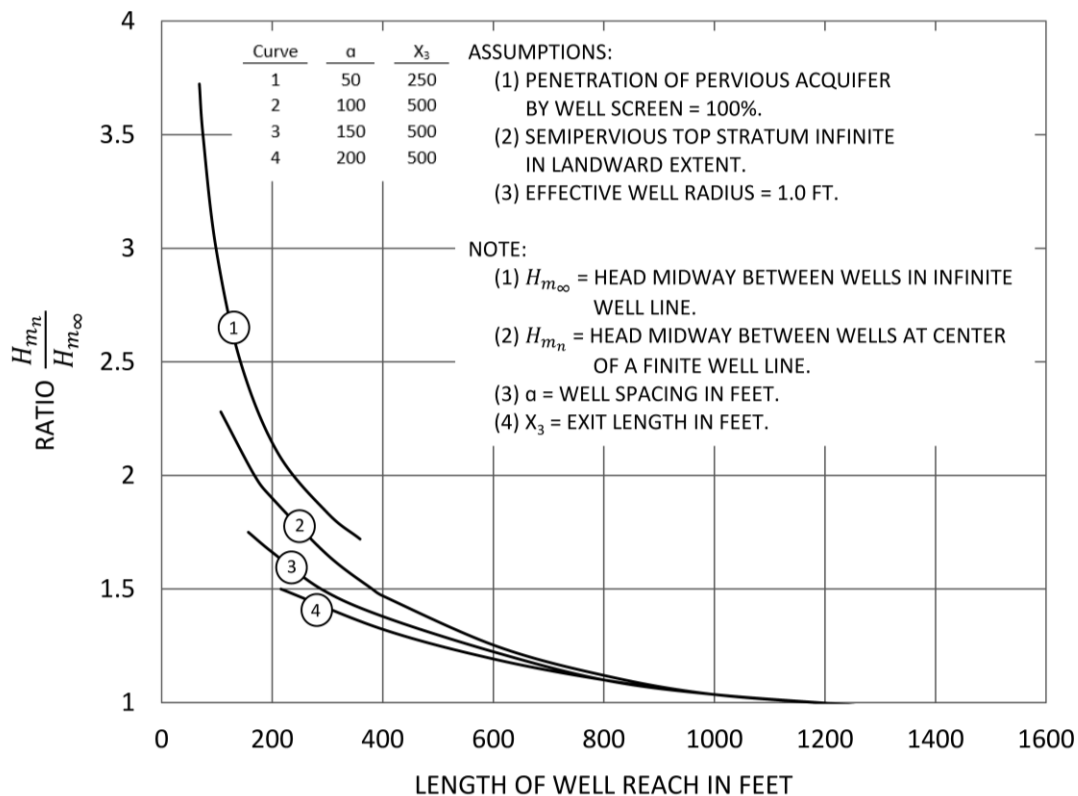


Figure H-8. Ratio of head midway between relief wells at center of a finite well system to head midway between wells in an infinite system (after USACE 1956a)

H-4. Design equations history

a. *Design evolution.* As the relief well design nomogram has evolved, so have equations that use the uplift factors from it to compute discharge and heads. The origins of some nomogram axes and design equations are not entirely documented in the historical literature. A few missing links are provided herein that help clarify key historical differences in the design process ranging from the original formulas (USACE 1939b, 1941).

b. *Equations.* Equivalent forms of the below equations are presented in chronological order of publication, for conditions with infinite impervious top stratum followed by finite impervious top stratum (actual or equivalent). Equations for the finite case are also applicable to the infinite case because the equations are equivalent if the effective seepage exit distance is very large (infinite). Notation h , h_{av} , and h_m used below are for uplift heads that have been corrected for well losses (such as efficiency).

(1) If well losses (H_w) are assumed zero, these symbols can be used interchangeably with H , H_{av} , and H_m found in literature. In practice, well flow and uplift

head are computed with this assumption, then well losses are estimated, and an iterative approach is used to balance losses with discharge (USACE 1956a). Well losses are explained in Chapter 9 and are added to h_{av} and h_m to get H_{av} and H_m . Losses are extrapolated to the effective seepage entrance and added to h to get H as shown in Figure 5–1.

(2) Equations H–1 to H–7 use original notation followed by modern notation from left to right. The equations improve understanding by showing the relationships between solutions for each parameter and the introduction of new parameters (such as θ_{av} , θ_m , x_1 , S , x_3) over time. Modern notations for the equations are summarized in Table H–1 and the historic notation equivalencies are also noted.

c. *Prior to 1955.* After multiplying the left chart output in Figure H–1 by well spacing, equation H–1 is used to calculate well discharge. It is shown with historic (USACE 1941) and modern notation, for an infinite impervious top stratum. Output from the right chart of Figure H–1 allows equation H–2 to be solved for mid-well head as shown by equation H–3. Substitution of well discharge (in terms of extra length factor) from equation H–1 results in equation H–3 for mid-well head, shown in terms of the extra length factor and modern notation for an infinite impervious top stratum. Equation H–4 defines average head for an infinite impervious top stratum in a similar manner.

$$Q_w = \frac{KhaD}{d + EL} = \frac{k_f Dha}{S + a\theta_{av}} \quad (\text{H-1})$$

$$\theta_m = \frac{pkd}{Q} = \frac{h_m k_f D}{Q_w} \quad (\text{H-2})$$

$$h_m = \frac{\theta_m Q_w}{k_f D} = \frac{h\theta_m}{\frac{S}{a} + \frac{EL}{a}} = \frac{h\theta_m}{\frac{S}{a} + \theta_{av}} \quad (\text{H-3})$$

$$h_{av} = \frac{\theta_{av} Q_w}{k_f D} = \frac{h\theta_{av}}{\frac{S}{a} + \theta_{av}} \quad (\text{H-4})$$

d. *1955 to present.*

(1) USACE (1955) established the use of equations H–5 to H–7 for a finite impervious top stratum. This refinement allowed for wells to be designed for a wide range of cases that are assessed with BT, described in Appendix C. Equations H–1 through H–4 for an infinite impervious top stratum have been used without modification since 1955. However, the equations for the unique case with x_3 equal to infinity are no longer necessary.

(2) Equation H–5 (which is equation 5–1 in this manual) uses the relationship between net gradient (equation H–8; equation 5–8) toward the wells and well flow from

Bennett (1947, 1954). The final term of equation H-5 is derived through substitution of the net gradient and uses modern notation (equation 5-2).

(3) Bennett et al. (1954) gives the relationship between extra length and net gradient shown in equation H-6 where average head is calculated in modern notation (equation 5-10) and by substitution for net gradient (equation 5-7).

(4) The mid-well head is shown in terms of net gradient in the first term of equation H-7 (equation 5-12), and substitution for net gradient yields the final term in modern notation (equation 5-11).

(5) Equations H-5 through H-7 provide corrected equations from historically published versions. Unfortunately, θ_{av} was misinterpreted to be an exponent rather than a multiplier in the USACE (1955) equations.

$$Q_w = a(\Delta M)(k_f)(D) = \frac{hk_f D}{\frac{S}{a} + \theta_{av} \left(\frac{S + x_3}{x_3} \right)} \quad (\text{H-5})$$

$$h_{av} = EL(\Delta M) = a(\Delta M)(\theta_{av}) = \frac{h\theta_{av}}{\frac{S}{a} + \theta_{av} \left(\frac{S + x_3}{x_3} \right)} \quad (\text{H-6})$$

$$h_m = a(\Delta M)(\theta_m) = \frac{h\theta_m}{\frac{S}{a} + \theta_{av} \left(\frac{S + x_3}{x_3} \right)} \quad (\text{H-7})$$

$$\Delta M = \frac{h - h_{av}}{S} - \frac{h_{av}}{x_3} \quad (\text{H-8})$$

Table H-1
Modern notation for relief well design equations

Notation*	Definition
a	Well spacing
D	Thickness of isotropic, homogeneous pervious foundation (actual or transformed)
EL	Extra length
EL/a	Extra length factor
H	Net head on well system
h	Net head on well system, corrected for well losses
H_{av}	Average net head in plane of wells
h_{av}	Average net head in plane of wells, corrected for well losses
H_m	Net head midway between wells
h_m	Net head midway between wells, corrected for well losses
H_w	Total well losses (elevation and hydraulic: entrance, friction, and velocity)
k_f	Effective hydraulic conductivity of pervious foundation
ΔM	Net seepage gradient toward the well line
Q_w	Discharge from single well
S	Distance from effective seepage entrance to landside embankment toe
W	Length of well screen (actual or transformed)
W/D	Effective penetration of well screen into pervious foundation
x_3	Distance from landside embankment toe to effective seepage exit
θ_{av}	Average uplift factor
θ_m	Mid-well uplift factor
θ_{max}	Maximum uplift factor, greater of θ_{av} and θ_m

Note:

The following clarifies different notation used today in practice and in this manual with respect to those found in the historical literature: $D = d$, $h_m = p = P$, $k_f = K = k$, $S = d = L_s$, $x_3 = L_e$, $Q_w = Q$, $\theta_{av} = \theta_a = EL/a$, and $\theta_m = \theta$.

H-5. Sharma analytical approach

a. S.N.P. Sharma conducted his doctoral research on well hydraulics in the Civil Engineering Department of the Indian Institute of Technology. After his passing in 1973, a paper detailing some of his extensive work on the derivation of discharge and drawdown expressions for partial-penetration well systems was published (Sharma 1974). He developed approaches for analyzing various well array and boundary

condition circumstances (including an infinite line of equally spaced wells with an infinite line source) by employing the concept of average pressure around a well along with the theory of images and the principle of superposition.

b. Sharma recognized that existing methods for evaluating these factors were either “unwieldy or very approximate,” and thus worked to develop explicit expressions applicable for confined aquifer steady-state conditions. His philosophy, relevant to the design of well systems and underseepage analyses in general, was “considering the uncertain knowledge of soil and the non-homogeneity of aquifers, great accuracy of calculation may not be warranted. However, it is natural to try to develop approximate analytical methods that are simple and at the same time estimate the effect of various factors entering the problem with sufficient accuracy.”

c. Without a copy of CW-EB #55-11 (USACE 1955) but with awareness of Mansur and Kaufman (1962), Sharma (1974) provides analytical expressions for θ_{av} and θ_m , while showing a limited but positive agreement of his results and the relief well system design charts in Figure 3-38 of Mansur and Kaufman. While Sharma’s methods are shown below to have “sufficient accuracy,” whether or not Sharma’s methods are “simple” perhaps depends on perspective. To aid in implementation, Sharma’s expressions are provided herein using the nomenclature of the USACE nomogram.

d. Uplift factors for partial penetration obtained using the Sharma approach agree with those of the widely employed design nomogram. As they have unique origins, the agreement between the solutions further validates both methods for determining the uplift factors. The Sharma analytical approach requires the same input parameters as the nomogram, and solutions are provided in a chart that is useful for design. Following the work of Sharma (1974), an analytical approach is presented for determining the average (θ_{av}) and mid-well (θ_m) uplift factors that are often used in the design of relief well systems for water retention structures.

(1) The expressions below have been slightly shortened from their original presentation in Sharma in that the distance of the well array from the line source is set as a constant equivalent to the well spacing. In terms of practical application, uplift factor solutions are not sensitive to variations in this parameter across the range of realistic field scenarios; in addition and as mentioned above, the source and landward boundary conditions are accounted for separately in design analyses (along with material properties and well losses) to estimate discharge and foundation uplift pressures.

(2) With these modifications, the Sharma (1974) analytical expressions for θ_{av} and θ_m are presented below as equations H-9 and H-10 (via equations H-11, H-12, and H-13).

$$\theta_{av} = \frac{1}{2\pi} \left[\ln \frac{1}{4\pi} + \alpha_S' + 2 \sum_{i=1}^{\infty} \left\{ S \left(\frac{W}{D}, \frac{ia}{D} \right) - S \left(\frac{W}{D}, \frac{\sqrt{a^2(i^2 + 4)}}{D} \right) \right\} \right] \quad (\text{H-9})$$

$$\theta_m = (\theta_{av} + 0.11) - \frac{1}{\pi} \sum_{i=0}^{\infty} \left\{ S \left(\frac{W(2i+1)a}{D}, \frac{a}{D} \right) - S \left(\frac{W}{D}, \frac{\sqrt{(2i+1)^2(a/2)^2 + 4a^2}}{D} \right) \right\} \quad (\text{H-10})$$

where:

$$\alpha_S' = \ln \left[\left(\frac{\pi}{2} \times \frac{W}{D} \times \frac{D}{r_w} \right)^{\frac{1}{(W/D)}} \times \frac{a}{D} \right] - S \left(\frac{W}{D}, \frac{2a}{D} \right) \quad (\text{H-11})$$

and:

$$S \left(\frac{W}{D}, \frac{2a}{D} \right) = \frac{2}{\pi^2 \left(\frac{W}{D} \right)^2} \sum_{n=1}^{\infty} \frac{1}{n^2} K_o \left(n\pi \times \frac{2a}{D} \right) \sin^2 \left(n\pi \times \frac{W}{D} \right) \quad (\text{H-12})$$

and:

$$S' \left(\frac{W}{D}, \frac{2a}{D} \right) = \frac{2}{\pi \left(\frac{W}{D} \right)} \sum_{n=1}^{\infty} \frac{1}{n} K_o \left(n\pi \times \frac{2a}{D} \right) \sin \left(n\pi \times \frac{W}{D} \right) \quad (\text{H-13})$$

(3) The nomenclature is as follows. Note that a , D , r_w , and W have units of length:

θ_{av} = average uplift factor

θ_m = mid-well uplift factor

a = well spacing

D = pervious foundation (aquifer) thickness

r_w = effective well radius

W = well penetration

W/D = percent well penetration

α_S' = penetration factor for line source; for full-penetration wells
($W/D = 1$), $\alpha_S' = 2a/r_w$

K_o = zero order modified Bessel function of second kind; BESSELK() function in Microsoft Excel

$S(W/D, 2a/D)$ = penetrative corrective function of (W/D) and $(2a/D)$ for average pressure; note this S function is not to be confused with distance to the effective seepage entrance

$S'(W/D, 2a/D)$ = penetrative corrective function for pressure at the base of the top blanket; note this S function is not to be confused with distance to the effective seepage entrance

(4) Equations H-12 and H-13 are basic forms of the penetrative corrective functions. Other forms of the functions, as shown in equations H-9 and H-10, are solved in practical application by substituting for $2a/D$ (in equations H-12 and H-13), with either ia/D , $\sqrt{a^2(i^2 + 4)}/D$, $(2i + 1)a/2D$, or $\sqrt{(2i + 1)^2(a/2)^2 + 4a^2}/D$ (from equations H-9 and H-10), as appropriate.

e. For the case of well spacing greater than or equal to aquifer thickness ($a \geq D$), equations H-9 and H-10 simplify to equations H-9a and H-10a.

$$\theta_{av} = \frac{1}{2\pi} \left(\ln \frac{1}{4\pi} + \alpha_S' \right) \quad (\text{H-9a})$$

$$\theta_m = (\theta_{av} + 0.11) - \frac{1}{\pi} S' \left(\frac{W}{D}, \frac{a}{2D} \right) \quad (\text{H-10a})$$

f. A comparison of uplift factor solutions using equations H-9 through H-10a with those obtained by hand using the USACE nomogram (Figure H-9) is presented in Figure H-10. Using $i = 1$ to 4 in equation H-9 and $i = 0$ to 4 in equation H-10 in the summation terms is adequate. The range of solutions plotted in Figure H-10 covers the range of the nomogram in terms of a/r_w and W/D values, and the range of D/a values for which θ_m exceeds θ_{av} ($D/a = 0.25$ and 1.00). The uplift factors can be compared for different input parameter cases, and their magnitude differences can be viewed along the central y-axes of the plots.

g. From a practical standpoint, the nomogram and analytical uplift factor solutions in Figure H-10 appear to agree well. As Turnbull and Mansur (1954) remark, "precise solutions are neither possible nor necessary since landside conditions and distribution of pressure and flow are too variable" and in general, this is why underseepage control designs must be adjusted to account for critical field locations and geologic features.

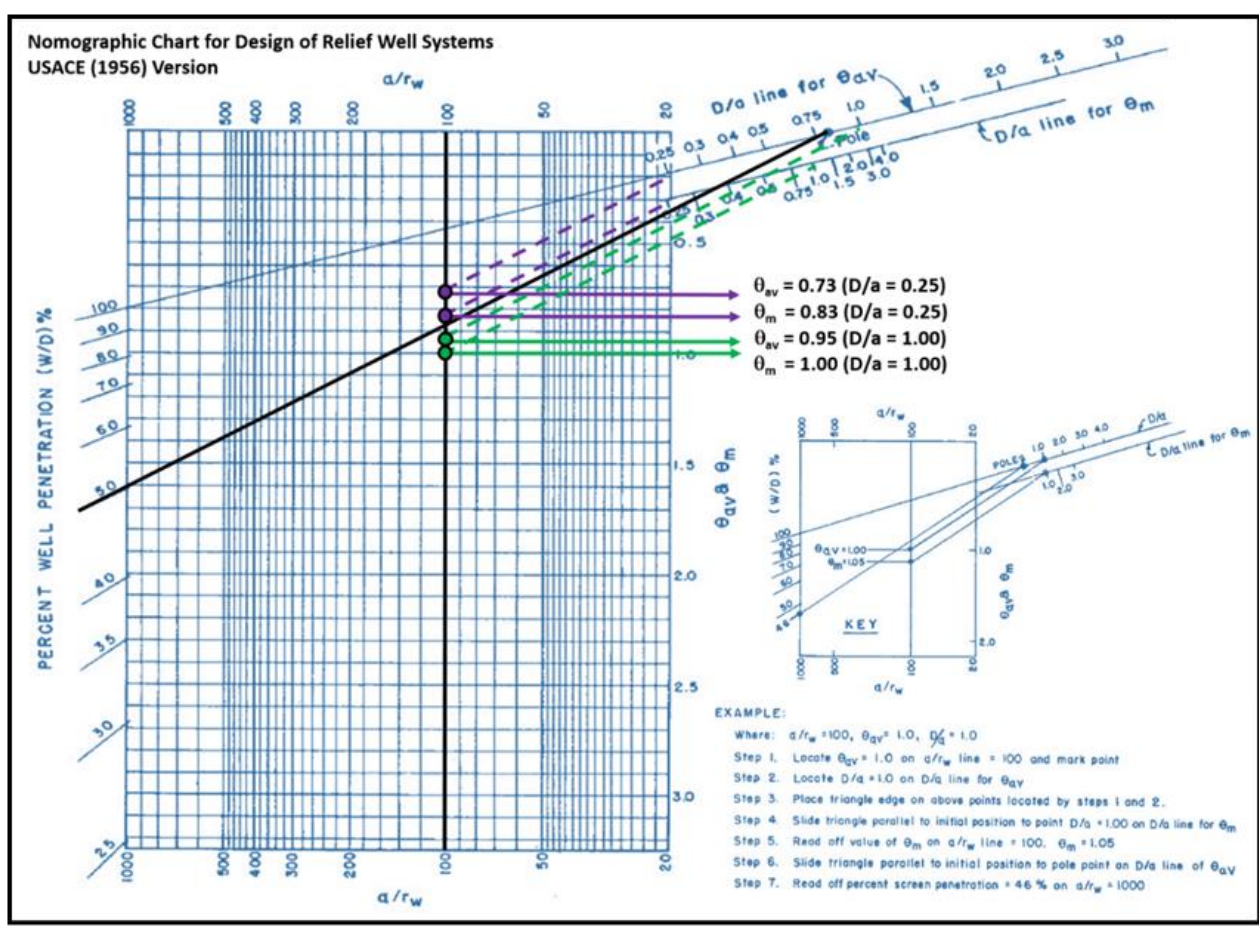


Figure H-9. Example uplift factor solutions (for $W/D = 50\%$ and different D/a values) using the USACE design nomogram

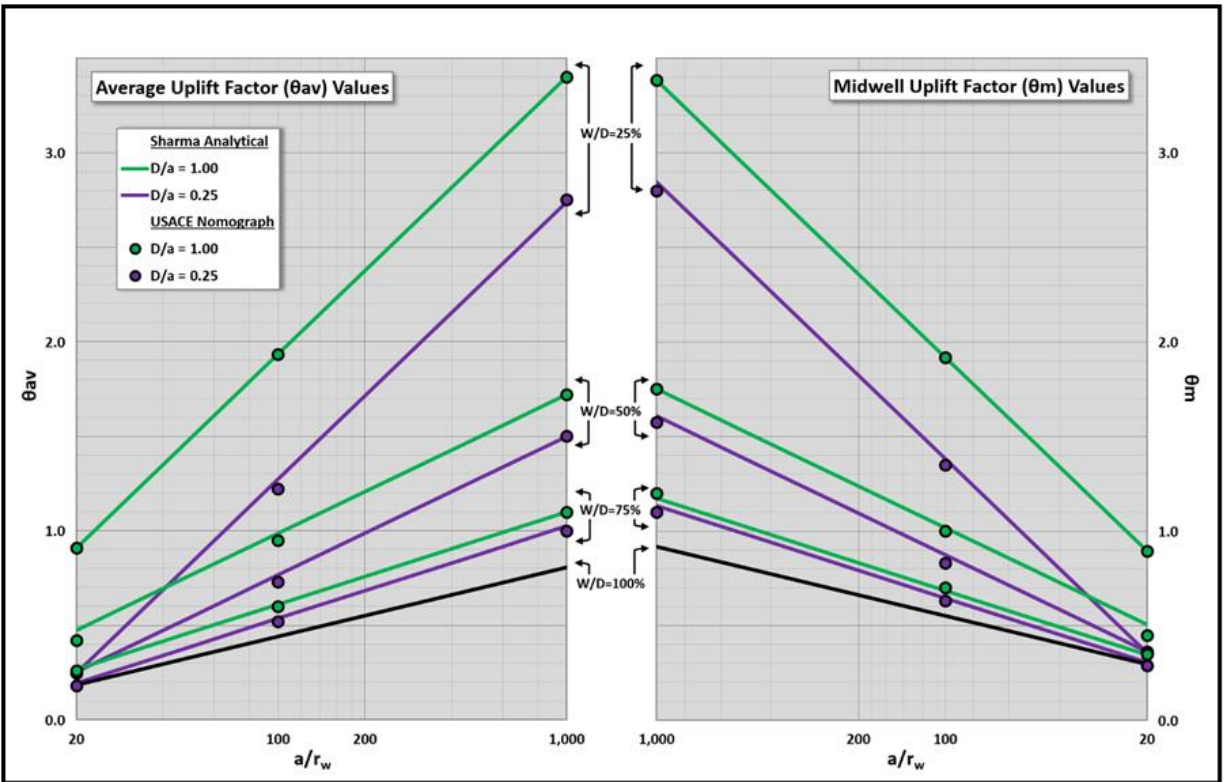


Figure H-10. Comparison of uplift factor solutions from the Sharma analytical approach and the USACE nomogram (Figure H-9)

h. Using equations H-9 through H-10a, uplift factor solutions were also plotted for the full range of the USACE nomogram conditions as shown in Figure H-11 ($D/a = 0.25, 0.50, 1.00, 2.00,$ and 4.00). As mentioned in paragraph H-3b(1), the greater of the average and mid-well heads will typically have an allowable design value, and the θ_{max} values (equivalent to the greater of θ_{av} and θ_m) plotted in Figure H-11 represent the maximum uplift factor. When θ_{max} is greater than θ_{av} (discernable from results along the central y-axes) it is equivalent to θ_m , and the mid-well head controls design. Alternatively, when θ_{max} is equal to θ_{av} for a given input parameter case, the average head controls design.

i. Similar uplift factor solutions can be obtained from Figure H-11, as can be obtained for any conditions represented by the USACE nomogram. As solutions are often automatically provided by computer programs, a benefit of Figure H-11 may be to provide a recommended hand check on automated solutions, or to help visualize the behavior of the uplift factor solutions as a function of equation and nomogram input parameters.

j. The significance of Sharma's theoretical work, in terms of historical importance and practical application, appears generally unrecognized by the profession to date. As illustrated, Sharma (1974) provides a mathematical basis and analytical approach for determining the uplift factors that are often used in the design of relief well systems.

Solutions from this approach agree with those of the frequently employed USACE design nomogram (USACE 1955), which was based on the results of electrical analog and theoretical studies and is still widely used in practice. This agreement further validates both uplift factor determination methods. Therefore, Figure H–11, which illustrates the analytical expressions or their solutions plotted across the range of nomogram input parameters, can be used to obtain or check the uplift factors θ_{av} and θ_m for the design of a partial-penetration, infinite line of relief wells.

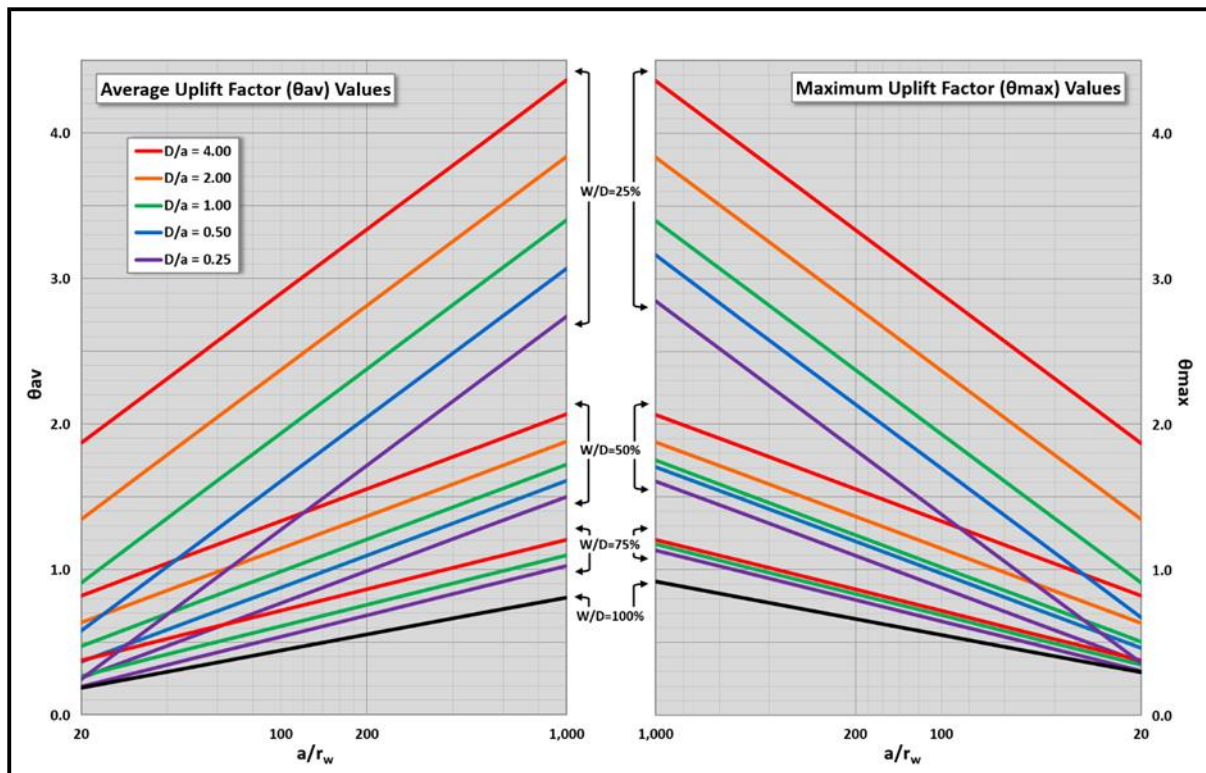


Figure H–11. Uplift factor solutions obtained using the Sharma analytical approach for the full range of the USACE design nomogram (Figure H–9) input parameters

k. There are two points to note when using the Sharma approach.

(1) While any percent of well penetration can be evaluated with the analytical expressions, Sharma (1974) recommends that for W/D less than 20%, the uplift factor solutions should be considered “approximate” because of a significant contribution of the spherical flow at the bottom of well. This design caution is consistent with prior USACE electrical analog modeling results (Middlebrooks and Jervis 1947) that show that head rises rapidly as W/D drops below 25%; as a result of such findings, the lowest W/D value on the USACE nomogram is 25%.

(2) As another caution, Bennett and Barron (1957) noted that “serious errors develop in applying the results of an infinite line of wells to the design of a finite line, because of the increased well discharges and uplift pressures midway between the wells.” Thus, while the computed uplift factor solutions may be obtained using the

Sharma analytical approach with “sufficient accuracy,” there are other important conditions relevant to the theory and application of the uplift parameter solutions, such as relief well efficiency (Chapter 9) and effects of a finite line of wells (Chapter 6), which must be appreciated for successful application.

Appendix I Example Relief Well Calculations

I-1. Introduction

This appendix contains examples to calculate well flow and head beneath the blanket using BT, IWM, and simple 2D FEM models. The primary goal of the examples is to evaluate the same conditions with different methods to demonstrate that the methods generally provide similar results. Two main examples are used: the Harrisonville Levee and a general levee cross section.

a. Site characterization. Pressures in the substratum are strongly influenced by the contrast between transmissivity of the aquifer and the vertical permeability and thickness of a confining blanket. The calculated heads with any method that incorporates relief wells are not significantly affected by aquifer permeability. However, the calculated well flow depends directly on the aquifer permeability used in any model. Practitioners understand permeability is a difficult parameter to determine and that some of these models tend to underpredict well flow. It is common practice to assign aquifer permeability based on the most pervious layers in the aquifer, which tends to offset underestimated well flow in some of the calculation methods.

b. Well head loss.

(1) Components of well head loss, H_w , and the loss in well efficiency over time are described in detail in Chapter 9. Three common approaches are used to incorporate the loss in well efficiency over time in well calculations. The first approach is to combine an estimate of the loss in efficiency over time with the other components in the H_w term. The second approach is to estimate a zero or non-zero value of initial H_w , then reduce well flow to account for well degradation. This reduction in flow may be achieved by increasing the H_w term. A third approach is to estimate initial head loss, H_w , and then adjust the calculated head to account for well degradation. The third approach is described with the Harrisonville example in paragraph I-2.

(2) The second and third approaches are applied with the general levee cross-section example in paragraph I-3. The term “efficiency” to account for well degradation over time in some of these example calculations is a misnomer and should not be confused with well efficiency described in Chapter 9.

c. Example 1, Harrisonville Levee. The line of relief wells along the toe of this levee is first analyzed using the simple BT approach presented in Appendix C. Practitioners new to well design are encouraged to replicate the spreadsheet calculations in this simple example. The Harrisonville Levee demonstrates how to perform design well calculations from an existing levee using background data readily available for many projects. The intent is to describe parameters used in design in the simplest manner possible. This example is also analyzed using IWM and results from the two approaches are compared to measurements taken during a flood event.

d. *Example 2, General Levee Cross Section.* This example first uses the FEM approach in Appendix G to analyze an infinite line of wells. A 2D model is created for this typical levee cross section adapted from TM 3-424 (USACE 1956a), and a slot is added to represent a continuous line of wells. Sometimes described as the “hybrid” approach, theta values from Chapter 5 are used to incorporate 3D effects of isolated wells. BT calculations are included for this example using several scenarios to allow for comparison with other methods. These scenarios include finite lines of 5 and then 20 wells using either partial- or full-penetration wells using the methods in Chapter 6. IWM and a plan view FEM analysis are included and comparable with the full-penetration well cases.

I-2. Harrisonville Levee example

a. *Infinite line of relief wells example using Blanket Theory.* TM 3-430 (USACE 1956b) used charts to design relief wells that predate the nomogram and well factors used in this manual. However, this TM is readily accessible and clearly documents the design of seepage control measures for 157 miles along the Mississippi River. An example taken from the TM is herein analyzed using BT with well factors to calculate the head reduction and flow from wells. This example also demonstrates how to interpret design data from similar historical archives. Practitioners are advised to enter the few equations and create this simple example spreadsheet themselves to understand this approach. BT equations for relief well analysis used here are presented in Appendix C.

b. *Geologic profile.* The geologic profile, relief well, and piezometer locations for Harrisonville Levee District from STA 810 to 841 are included as Plate 87 in TM 3-430, Vol 2 (USACE 1956b). This profile is also included in this manual as Figure 3–7, which includes Relief Wells 76 through 84.

c. *Original design data.* All pertinent design data for Relief Wells 1 through 95 are included in Plate 96 in TM 3-430 Vol 2. This data is also included in rows 2 through 10 in Figure I–1 for the 3,100-foot reach that includes Relief Wells 76 through 92. These parameters are defined in Table I–1. Note that blanket parameters z and k_b are labeled without subscript because it is understood they are landside. The riverside entrance distance is described by the parameter s . The data needed for this example is replicated in rows 13 through 21 of Figure I–1 along with parameters described in the next section.

d. *Calculations.* The equations presented in the following sections are shown in blue font in Figure I–1. The calculation for h_o in cells J15 to J21 is unnecessary because results match data from the TM in cells L4 to L10.

Stationing	To	Net Grade	Ground	Tailwater	Net Head	Main (M)	Distance	s	Ratio	z	h ₁	h ₂	h ₁ -h ₂	a ₁	d	k _i	Q _w /H	Q _w	Reach L	H _{int} /H _{int}	a ₁	a ₂	Design STA	Final #	Well Numbers	Standpipe		
810	817	410.5	390.5	390.5	20.0	M	3900	800	400	6.0	7.1	4.0	3.1	155	80	1200	19.7	394	3100	1	155	150	810.5	815	4	76	79	1.5
817	820	410.5	392.0	392.0	18.5	M	4100	800	400	6.5	6.7	4.3	2.4	185	85	1300	27.2	503.2	3100	1	185	200	816.5	818.5	2	80	81	1.5
820	826	410.0	390.0	390.0	20.0	M	4200	800	1000	8.5	10.1	5.7	4.4	205	85	1500	34.5	690	3100	1	205	200	821	825	3	82	84	2
826	831	410.0	388.5	388.5	21.5	M	4100	800	1000	9.0	11.0	6.0	5.0	200	70	1500	28.6	614.9	3100	1	200	200	826.5	830.5	3	85	87	2
831	836	410.0	390.0	390.0	20.0	M	4000	800	1000	10.0	10.5	6.7	3.8	250	60	1650	31.2	624	3100	1	250	250	833	833.5	2	88	89	2
836	840	410.0	390.0	390.0	20.0	M	3800	800	1000	7.5	9.8	5.0	4.8	175	60	1550	32.4	648	3100	1	175	175	837.75	839.5	2	90	91	2
840	841	410.0	389.5	389.5	20.5	M	3800	800	1000	7.0	9.9	4.7	5.2	155	65	1100	15.7	321.85	3100	1	155	150	841	841	1	92	92	2

Black font are TM 3-424 data, green font are input (from below), blue font are calculations

Stationing	To	Tailwater	Net Head	x3	x3	s	Ratio	z	ho	ha	d	k _i	Q _w	a ₁	θ _{av}	θ _m	ΔM	H _w	hav	Hav	hm	Hm	Q _w	Q _w
810	817	390.5	20	438.2	440.3	800	400	6	7.1	4	80	1200	394	150	1.05	1.14	0.0109	0.75	1.72	2.47	1.87	2.62	0.516	231.4
817	820	392	18.5	470.1	454.2	800	400	6.5	6.7	4.3	85	1300	503.2	200	1.1	1.21	0.0083	0.97	1.82	2.79	2.00	2.97	0.601	269.6
820	826	390	20	850.0	816.2	800	1000	8.5	10.1	5.7	85	1500	690	200	1.1	1.21	0.0109	1.41	2.40	3.80	2.64	4.04	0.911	408.9
826	831	388.5	21.5	793.7	838.1	800	1000	9	11.0	6	70	1500	614.9	200	1.07	1.18	0.0122	1.22	2.61	3.83	2.88	4.10	0.842	377.7
831	836	390	20	774.6	884.2	800	1000	10	10.5	6.7	60	1650	624	250	1.08	1.19	0.0090	1.24	2.44	3.68	2.69	3.93	0.735	329.7
836	840	390	20	670.8	768.6	800	1000	7.5	9.8	5	60	1550	648	175	1.03	1.14	0.0122	1.30	2.21	3.51	2.44	3.74	0.654	298.4
840	841	389.5	20.5	674.5	747.2	800	1000	7	9.9	4.7	65	1100	321.85	150	1.02	1.12	0.0135	0.63	2.06	2.69	2.26	2.89	0.474	212.6

Sharma θ_{av} and θ_m for rw=0.9

Stationing	To												
810	817	817	820	820	826	826	831	831	836	836	840	840	841
d	a	d	a	d	a	d	a	d	a	d	a	d	a
80	150	85	200	85	200	70	200	60	250	60	175	65	150

Parameter	Value	Parameter	Value	Parameter	Value	Parameter	Value	Parameter	Value	Parameter	Value	Parameter	Value
a	150	a	200	a	200	a	200	a	250	a	175	a	150
D	80	D	85	D	85	D	70	D	60	D	60	D	65
r _w	0.9	r _w	0.9	r _w	0.9	r _w	0.9	r _w	0.9	r _w	0.9	r _w	0.9
W/D	0.5	W/D	0.5	W/D	0.5	W/D	0.5	W/D	0.5	W/D	0.5	W/D	0.5
a/r _w	166.6666667	a/r _w	222.2222222	a/r _w	222.2222222	a/r _w	222.2222222	a/r _w	277.7777778	a/r _w	194.4444444	a/r _w	166.6666667
D/a	0.5333333333	D/a	0.425	D/a	0.425	D/a	0.35	D/a	0.24	D/a	0.342857143	D/a	0.4333333333
θ _{av}	1.05	θ _{av}	1.10	θ _{av}	1.10	θ _{av}	1.07	θ _{av}	1.08	θ _{av}	1.03	θ _{av}	1.02
θ _m	1.14	θ _m	1.21	θ _m	1.21	θ _m	1.18	θ _m	1.19	θ _m	1.14	θ _m	1.12
θ _{max}	1.14	θ _{max}	1.21	θ _{max}	1.21	θ _{max}	1.18	θ _{max}	1.19	θ _{max}	1.14	θ _{max}	1.12

Figure I-1. Design data and calculations for first iteration of relief well example

(1) *Seepage exit distance, x_3* . One critical parameter missing from the TM 3-430 (USACE 1956b) tables is the seepage exit distance, x_3 . This could be calculated using equation C-8 for an infinite landside blanket. From inspection of Figure C-1, x_3 could also be determined from H , h_o without wells, and S using similar triangles. Simple rearrangement of terms in the relationship presented as equation I-1a results in equation I-1b used to back-calculate x_3 . Note the slight difference between values in columns E and F in Figure I-1. The back-calculated x_3 value in column F was used for this example.

$$\frac{x_3}{h_o} = \frac{x_3 + S}{H} \quad (I-1a)$$

$$x_3 = \frac{h_o S}{H - h_o} \quad (I-1b)$$

(2) *Change in hydraulic grade line due to wells, ΔM* . The equation for ΔM is given in Chapter 5 of this manual, explained in Appendix C, and included here as equation I-2. The average head in the plane of the wells, H_{av} , can be assumed to be the allowable head along the well line, h_a in TM 3-430 (USACE 1956b). This value for h_a is only an initial estimate for H_{av} . The subsequent iteration would use the values in cells U15 through U21 for H_{av} .

$$\Delta M = \frac{H - H_{av}}{S} - \frac{H_{av}}{x_3} \quad (I-2)$$

(3) *Well head loss, H_w* . Chapter 9 includes tables and figures to determine well head loss for a range of well sizes. TM 3-430 Vol 1 (USACE 1956b) includes Figure 22 (Head Loss in 8-inch (ID) Wood Stave Well with 6-inch Gravel Filter) to determine H_w (in feet) based on Q_w (in gpm). The curve for H_w has since been fitted to equation I-3.

$$H_w = 0.33 + 0.0000205 * Q_w^{1.6628} \quad (I-3)$$

(4) *Average uplift factor, θ_{av} , and mid-well uplift factor, θ_m* . The well factors account for much of the complexity in the analysis of partial-penetration wells. They can be determined from the nomogram, figures in Chapter 5, or the Sharma spreadsheet (discussed in Appendix H). In this example, results from the Sharma spreadsheet are included in Figure I-1. They are simply pasted as images for recordkeeping and manually entered in cells P13 to Q21. Well factors are a function of well spacing (a), penetration ratio (W/D), and assumed aquifer depth (D). This example uses the assumed design effective penetration ratio of 50%. Well factors remain constant and are not influenced by the loss in well performance over time.

(5) *Applicable equations.*

(a) Excess head without well losses along well line, h_{av} , and midway between wells, h_m are shown in equations I-4 and I-5.

$$h_{av} = a (\Delta M)(\theta_{av}) \quad (I-4)$$

$$h_m = a (\Delta M)(\theta_m) \quad (I-5)$$

(b) Excess head with well losses, H_{av} , and midway between wells, H_m are shown in equations I-6 and I-7.

$$H_{av} = H_w + h_{av} \quad (I-6)$$

$$H_m = H_w + h_m \quad (I-7)$$

(c) Well flow, Q_w is shown in equation I-8.

$$Q_w = a (\Delta M)(\bar{k}_e)(\bar{D}) \quad (I-8)$$

(6) *Multiple iterations increase precision.* Flow through the wells results in hydraulic well losses and reduces piezometric head in the foundation. The first iteration of this example assumes flow through the wells and piezometric head are equal to values listed in TM 3-430 (USACE 1956b) Plate 96. The second iteration perform calculations using the flow and piezometric head from the first iteration. There are multiple ways to plug the resulting H_{av} and Q_w back into a spreadsheet to generate subsequent iterations. Results are presented for this example with five iterations using a simple manual iteration process.

(7) *Future performance loss.* As described in paragraph I-2a, TM 3-430 used design curves rather than the equations presented in this manual. In the maintenance section of TM 3-430, pumping tests are recommended to verify wells have at least 80% of their installed specific capacity. Although not explicitly described in the original design, results suggest head calculations may include some conservatism to account for performance loss over time. Therefore, wells in this example are assumed to have 80% of the design performance for head calculations. However, flow is not factored to account for future performance loss. In design, relief well flow is used to size collector systems that must have adequate discharge capacity. Performance loss based on pumping test data should be considered when back-analyzing collected flow data from high-water events.

e. *Results.*

(1) The primary results of interest are H_m in cells W15 to W21 and Q_w in cells Y15 to Y21 of Figure I-1. These parameters are also shown in Figure I-2 and Figure I-3,

respectively, along with design values in TM 3-430. H_m results, including the 80% factor, are essentially the same as the original design values. Where piezometer and well flow data are available, those values could be used for H_m and Q_w to evaluate performance. Flood data could be used to adjust assumed seepage entrance or exit distance, permeability, or evaluate well performance loss.

(2) Simple linear projections of H_m and Q_w based on measurements during the 1993 flood are included in Figure I-2 and Figure I-3. Calculations of Q_w , including the 80% factor, are not used to size discharge or storage during design but should be considered in the evaluation of field data as shown in Figure I-4. Although these simple comparisons with flood data are useful, note that the relationship between H_m and Q_w with flood height is non-linear for relief wells. In this case, with measurements taken during the 1993 flood within 90% of the design height, differences due to non-linearity are small.

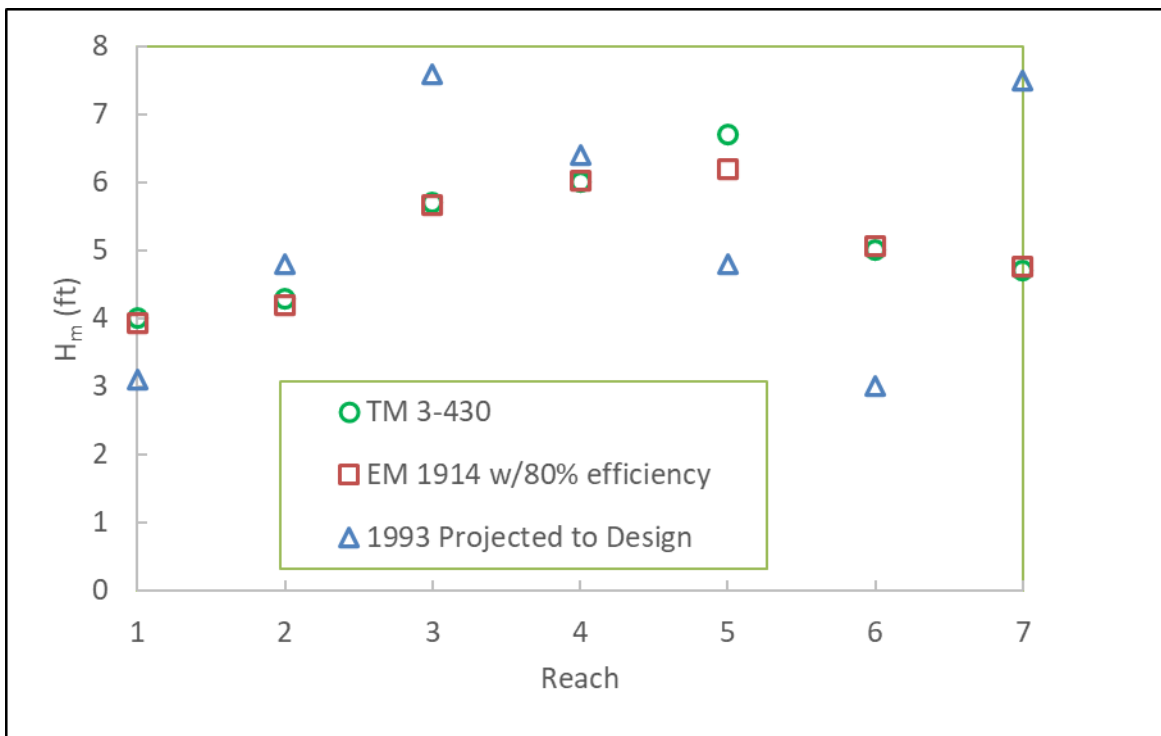


Figure I-2. H_m for each well reach compared with original design and field measurement

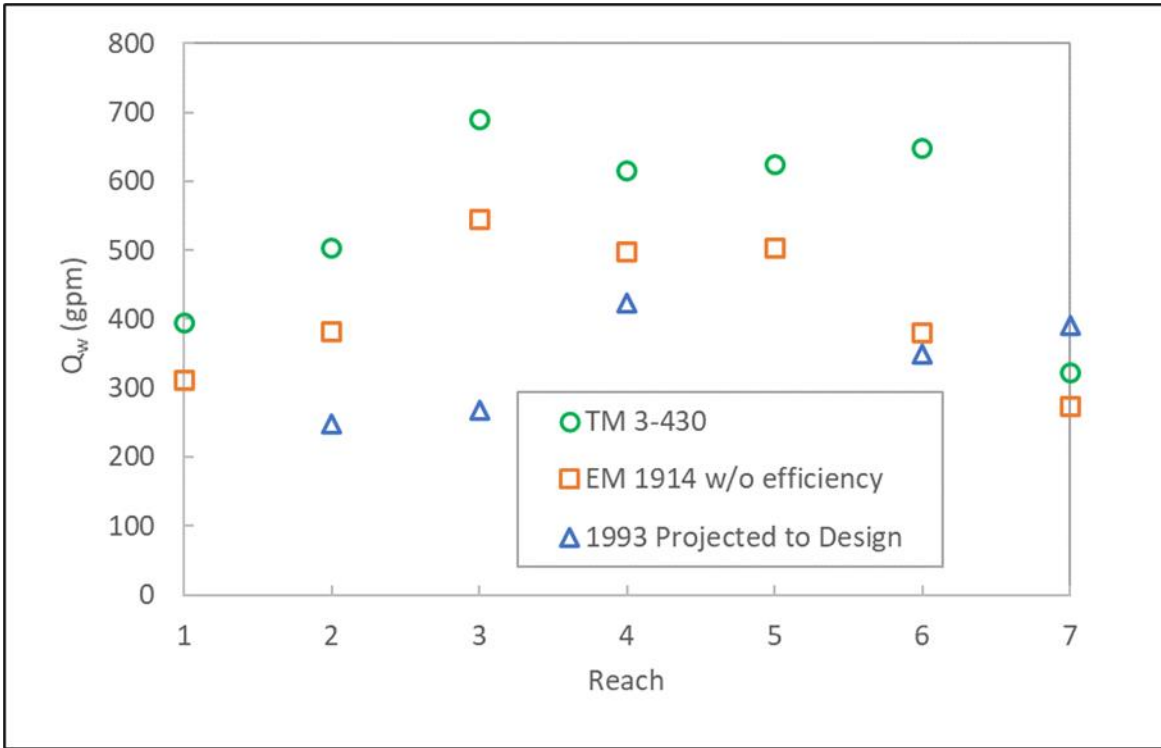


Figure I-3. Q_w compared with original design and field measurement

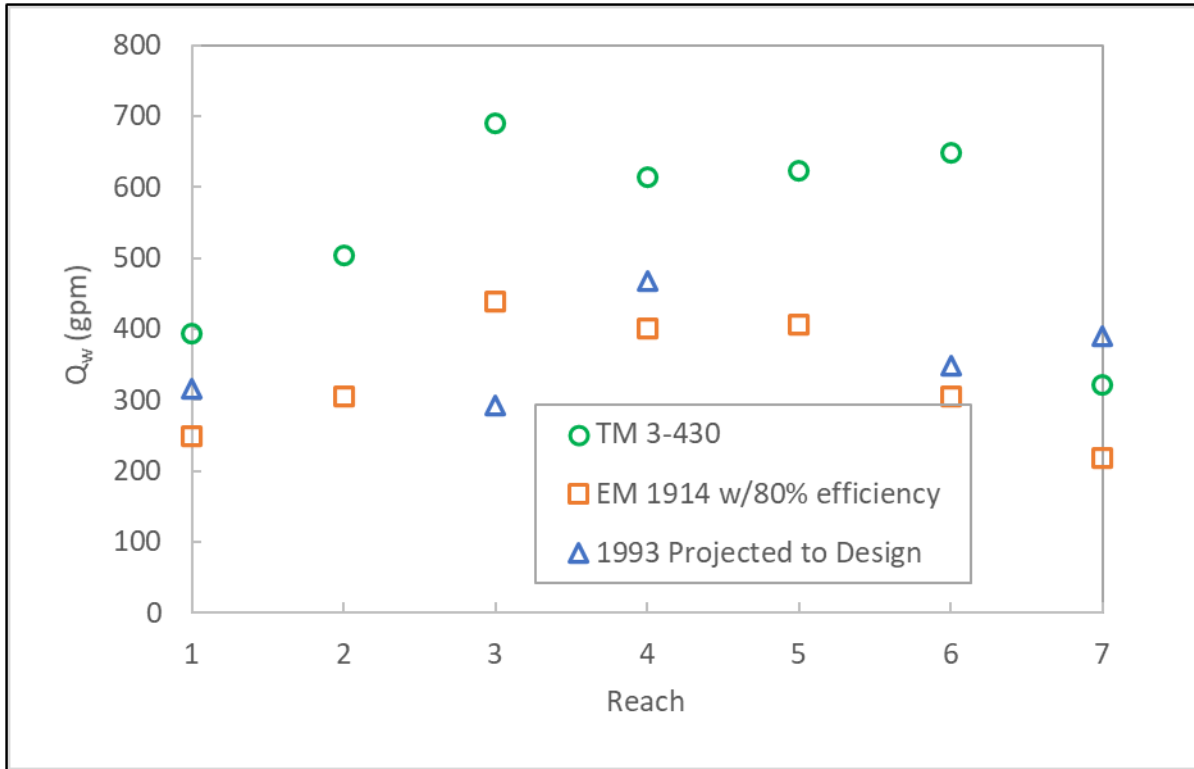


Figure I-4. Q_w factored for performance loss (80%) compared with original design and field measurement (Note: Reaches 2 and 5 have no well flow information)

f. *Image Well Method with Blanket Theory adaptation.* Image well theory is described in Appendix D and the application of IWM to relief well analysis by using BT is further explained in Chapter 6. The reaches between Stations 810+00 and 841+00 at the Harrisonville Levee were analyzed using the IWM with BT adaptation. All wells between stations 810+00 and 841+00 were included in the analysis of each individual reach. Had all wells within the zone of influence for each reach been considered, the calculated heads would have been higher. The results are shown in Figure I-5 with comparison to results included in Appendix C, calculated using the BT infinite well solution. There is good agreement between IWM with BT adaptation and the BT infinite well solution for calculated heads. The IWM with BT adaptation generally calculated lower well flows for most reaches.

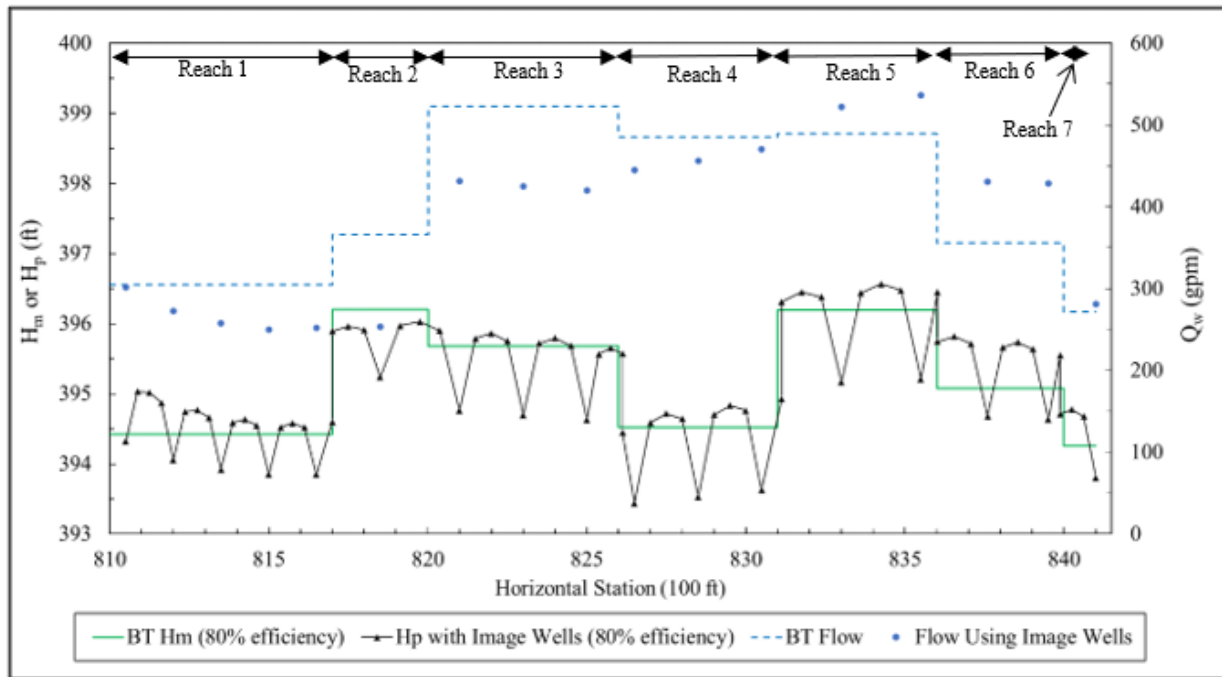


Figure I-5. Example of Image Well Method compared with Infinite Well Approach (Chapter 5)

g. *Back-analysis using Image Well Method with Blanket Theory adaptation.*

(1) The Harrisonville Levee has piezometers for measuring foundation aquifer pressure to monitor the relief well system. The levee experienced floods in 1973 and 1993, and piezometer readings were obtained for known river levels. The IWM with BT adaptation was used to predict piezometer readings for comparison with the observed data. The relief wells, based on reduced specific capacities observed in 1996, were assumed to be operating at 80% of the installed performance level. This was modeled in the analysis by reducing the calculated flow by 80%. The results are shown in Table I-1.

(2) The predicted piezometric levels based on the analysis were, on average, 0.3 foot lower than the observed levels. Most predicted values were within 1.0 foot of the observed values, and the maximum deviation was 2.0 feet. The agreement between predicted and observed values is considered reasonable. One reason for the discrepancies between observed and predicted values could be due to the time lag between the flood peak and piezometer responses. Time lag would result in predicted piezometer elevations being higher than observed piezometer elevations. Other possible factors include over-simplification of the project geology, assumptions inherent in the calculations, and unknown boundary conditions. Additional explanations are potentially inaccurate piezometer readings and the use of the *SCR* to reduce the flows used to calculate head.

Table I-1

Observed piezometer readings compared with prediction using the Image Well Method with Blanket Theory adaptation

Piezometer	Station	Piezometer Location	Flood	River Elevation ¹ (ft)	Piezometer Elevation ¹ (ft)	Image Well PZ Prediction ²	Image Well PZ – Measured PZ (feet)
P-46	815+82	Landside Toe	April 1973	404.4	393.6	393.5	-0.1
			July 1993	407.7	393.2	394.1	0.9
P-47	815+88	Landside Toe	April 1973	404.6	394.5	393.5	-1.0
			July 1993	407.9	394.7	394.1	-0.6
P-48	822+00	Landside Toe	April 1973	404.5	392.3	394.3	2.0
			July 1993	407.9	396.7	395.3	-1.4
P-49	827+45	Landside Toe	April 1973	404.5	393.8	393.2	-0.6
			July 1993	407.8	394.3	394.1	-0.2
P-50	838+67	Landside Toe	April 1973	404.2	394.4	394.1	-0.2
			July 1993	407.4	396.5	395.0	-1.5
						AVERAGE	-0.3

Notes:

¹ Average of 2 to 4 days data at assumed flood peak.

² Assumed 80% *SCR* for all wells. Average *SCR* from 1996 Pump Tests was 83%.

I-3. Analysis of a general levee cross section

a. *Introduction.* As described in paragraph I-1d, several methods are used to evaluate wells at the landside toe of a levee in this example. This example is first evaluated without wells in a typical plain-strain 2D FEM model, and then wells are included using the procedures in Appendix G. (The application of FEM without wells is described in more detail in EM 1110-2-1901 and for levees in EM 1110-2-1913). BT calculations are performed to replicate the FEM model both with and without wells. Additional BT calculations are performed for comparison purposes with other analysis methods or approaches, including IWM. Finally, a plan view 2D FEM model is performed that includes a well that represents an infinite line of wells at the landside toe of this example levee.

b. *Background.* An evaluation was performed of the generic levee cross section shown in Figure I-6. This figure, from TM 3-424 (USACE 1956a), illustrates many factors considered in the application of BT to design levee underseepage control measures: (1) a thin, less pervious blanket overlying a deep aquifer of more pervious sands and gravels, (2) flow from the riverbed, (3) flow from windows in the riverside blanket such as borrow pits, (4) a leaky landside blanket, and (5) piezometer measurements or a calculated energy grade line that account for all the above. The steps required to generate an FEM model of a levee cross section are described in the following paragraphs. In paragraph I-3d, evaluation of the same levee cross section using BT is described.

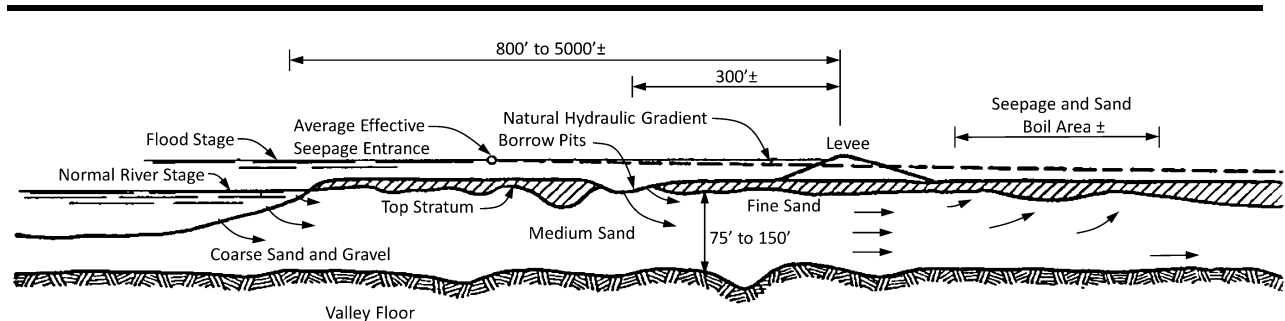


Figure I-6. Generalized levee cross section
(adapted from USACE 1956a as shown in Manseur et al. (2000))

c. *Seepage design approach.* The design methods in USACE 1956a are based on an evaluation of vertical gradient, i_v , through the top stratum landside of the levee toe. This is typically done by comparison with a critical vertical gradient, i_{cv} , and expressed as the vertical gradient factor of safety, FS_{vg} , which is i_{cv}/i_v . Calculations of i_v and FS_{vg} are then compared to field performance observations as illustrated in Figure I-7, leading to “performance-based” factors of safety (such as $FS_{vg} > 1.6$ at levee toe). Seepage analyses to support levee design focus primarily on pore pressure beneath a blanket to prevent heave due to vertical seepage and are predicated on eliminating concentrated seeps such as sand boils landward of the levee. By preventing heave, flotation, uplift,

etc., BEP in the horizontal direction due to horizontal seepage in the underlying aquifer is also prevented.

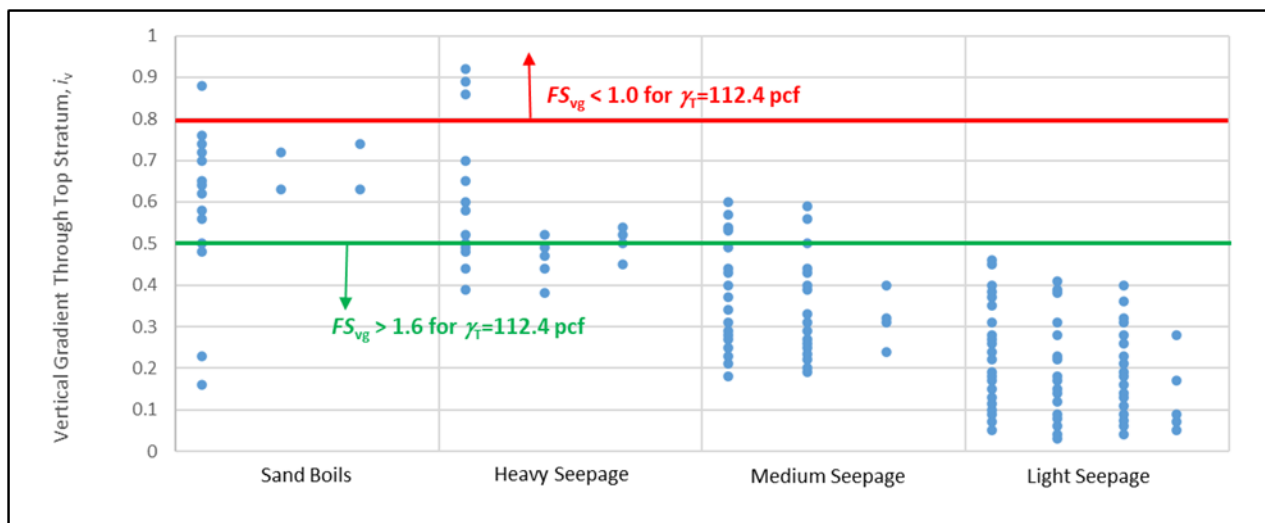


Figure I-7. Comparison of vertical gradient through a landside confining layer with observed performance (adapted from USACE 1956a)

(1) *Analysis methods.*

(a) In practice, BT has generally been replaced by FEM as the tool to evaluate i_v and the associated vertical gradient factor of safety (FS_{vg}) because there are limitations with the simple BT approach. For example, USACE (2002) recognized the significance of an intermediate silty sand or sandy silt layer that is not properly accounted for with the 2-layer BT approach. FEM can better handle the presence of an intermediate layer and other site-specific complexities in the foundation, and 3D FEM analyses can further account for bends in levee alignment and known features of limited extent.

(b) Despite this change in analytical tools, the USACE approach for assessing blanket performance will continue to be based on Terzaghi's heave calculation and the critical values for vertical gradient that were determined based on field observations of performance. BT can provide a valuable check for FEM analyses and it is useful for both parameter studies and the rapid evaluation of numerous levee reaches that have similar dimensions and foundation conditions.

(2) *Observational approach.* For foundations similar to Figure I-6, poor performance with levee underseepage is more often attributed to unknown foundation conditions rather than the method of analysis. Practicing geotechnical engineers supplement analytical tools with observation and judgment to address uncertain foundation conditions and limitations inherent to methods of analysis and design. Using the observational method, performance expectations from design are compared to actual field performance. If observed performance is worse than expected, a number of actions may be warranted depending on the risk of breach. These include additional investigations, new subsurface interpretation and analysis models, reliability

assessments, and additional mitigation structural and non-structural alternatives may be considered and implemented.

(3) *Progression of backward erosion piping.* USACE has vast collective experience modeling either relatively impermeable or leaky blankets that overlie pervious aquifers similar to Figure I–6. These models inform estimates of the probability of heave/uplift due to vertical seepage through the blanket. The models are sometimes also used to inform estimates of BEP progression once a defect in a landside-confining blanket forms. The horizontal gradient, i_h , is considered a refinement over the simple average or “global” horizontal gradient across the structure. Unfortunately, the evaluation of performance once a defect has formed rarely considers concentrated flow through the defect. Such flow may drastically change i_h in the region of the defect or advancing pipe head. Chapter 4 provides more information on risk-informed design.

d. *FEM model of generalized levee cross section.*

(1) *Cross section.* The generic levee cross section shown in Figure I–6 was modeled using the finite element program SEEP/W from GeoSlope International. There are other equivalent seepage analysis packages available. The structure includes a 30-foot-high levee sitting on a 10-foot confining blanket overlying a 100-foot sand aquifer. Similar to minimum distances indicated in Figure I–6, the borrow pit is 380 feet, and the river is 850 feet, from the levee centerline, as shown in Figure I–8. These distances are measured from the most landward point where the riverside blanket is compromised, and foundation sands are exposed.

(2) *Mesh.* For seepage analyses with a confining blanket, such as the example herein, a somewhat coarser mesh can be used, as the presence of a confining blanket helps to avoid numerical sensitivity experienced at the levee toe in the no-blanket situation. In addition to mesh size, for programs where the user has control over mesh dimensions, element aspect ratios (width to height) closer to unity are preferred. For more information on mesh refinement, see EM 1110-2-1901, EM 1110-2-1913, Ultimate Reengineering Services LLC (URS) 2015, and Duncan et al. (2011).

(3) *Boundary conditions.*

(a) In this example (Figure I–8), the analysis water level is 28 feet above the riverside and landside blanket. This boundary is applied to the entire riverside ground surface, including the riverbed, blanket, borrow pit, and levee. A no-flow, vertical boundary is used at the left edge of the model. Such a boundary is commonly used for levee analyses to represent the flow conditions at the middle of a river. In most programs, the edge of a region along the perimeter of the model is a no-flow boundary unless it is specified otherwise. Potential seepage face boundaries are used to model the landside ground surface, including the levee landside slope and blanket. An appropriate boundary for the extreme landside edge of the model is often difficult to determine for many levee analyses.

(b) Analysts should consider many conditions that may affect seepage flow, including seepage blocks, seepage exits, and variations in the regional groundwater table. These may be affected by multiple other sources. If the landside boundary is located a great distance from the levee, it begins to approximate an infinite boundary condition. For this example, the foundation landside edge is modeled as a vertical no-flow boundary located 0.5 miles from the levee centerline. At this distance, replacing the no-flow boundary with a constant-head boundary equal to the ground surface elevation would not change the model results.

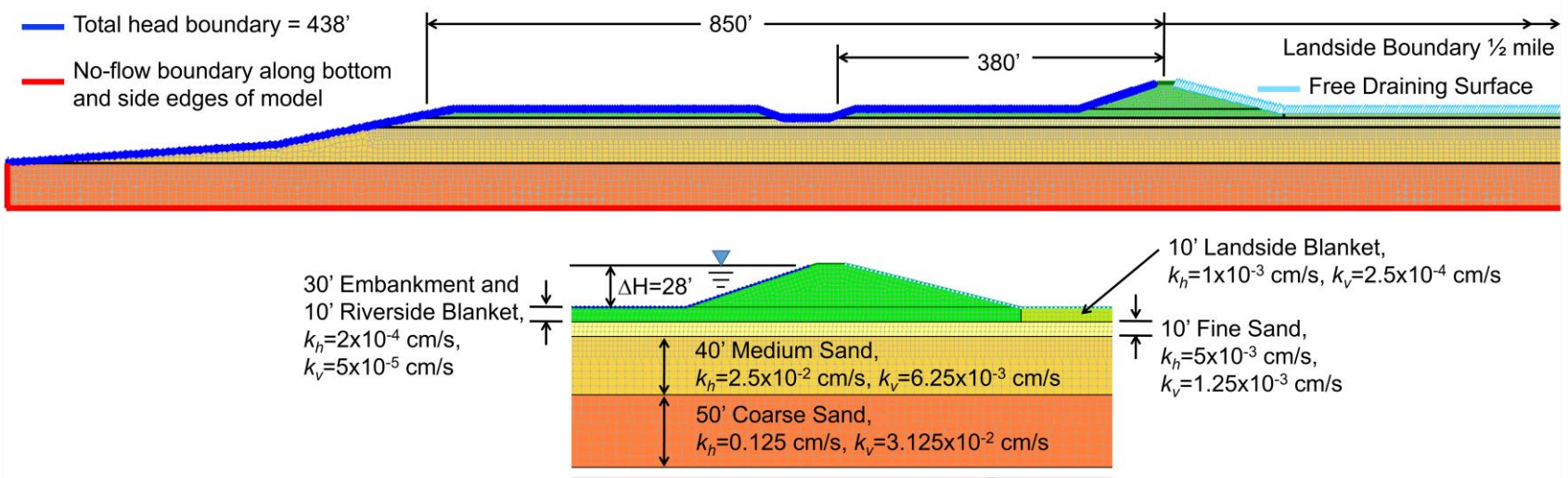


Figure I-8. SeepW model based on cross section in Figure I-6

(4) *Material properties.* Soil permeability values used in these analyses are listed in Table I–2. The values of k_h listed in Table I–2 are not meant to represent any particular location. However, the selected values are typical of soils in the Mississippi Valley based on values in Division Regulation (DIVR) 1110-1-400 (USACE 1998) that match historical piezometer measurements. Often, sites in the Mississippi Valley have an in situ blanket material k_v that is higher than laboratory measurements. This is due to the presence of defects and other heterogeneities with higher values than those listed in Table I–2. Historically, most relief wells have been designed with the assumption that soils are isotropic, although that may be partially due to limitations with BT. The higher conductivity ratio used in this example illustrates the influence of aquifer transformation and anisotropy in relief well calculations.

Table I–2
Saturated permeability values for general levee example

Soil	k_h (10^{-4} cm/s)	k_h (ft/s)	Conductivity Ratio (k_v/k_h)
Levee and Waterside Blanket	2	6.56E-06	0.25
“Leaky” Landside Blanket	10	3.28E-05	0.25
Fine sand	50	1.64E-04	0.25
Medium Sand	250	8.20E-4	0.25
Coarse Sand	1,250	0.00410	0.25

(5) *Results without relief wells.* Results from the model shown in Figure I–9 include total head contours and total flow beneath the levee, q_{total} . Also shown are flow lines depicting eight paths of equal flow, i_v measured across the blanket at the landside levee toe, and i_{cv} beneath the blanket at the toe. Total head beneath the blanket represents how high water would rise in a piezometer. The excess head above the ground surface, h_o , shown in Figure I–9, is used in conjunction with blanket thickness to calculate i_v . Note that the model extends further to the right than is shown in Figure I–9 (see Figure I–8). Total head contours for this case are also shown in a larger image around the levee toe in Figure I–10

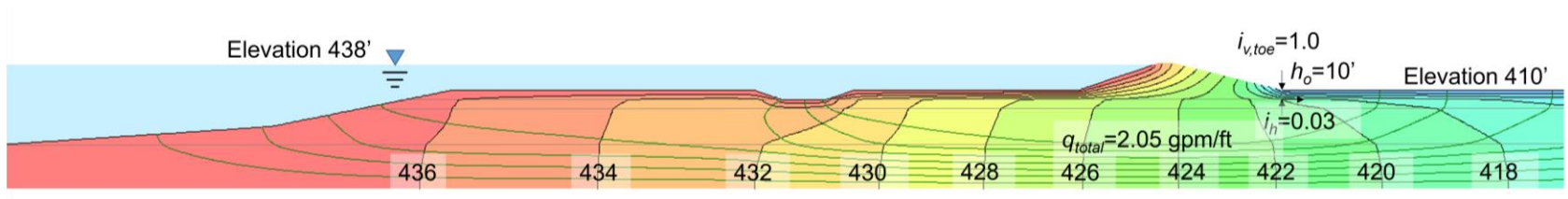


Figure I-9. Output total head contours, flow, and the excess head and gradient at location where FS_{vg} is measured

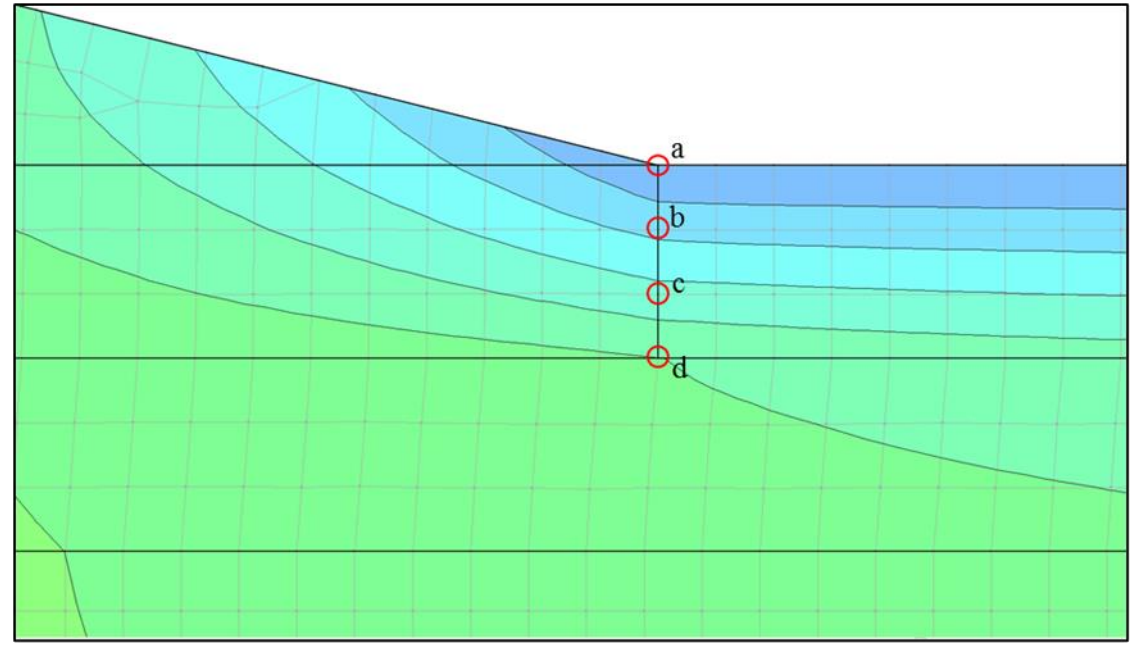


Figure I-10. Landside levee toe and points used to assess various measures of vertical gradient and to calculate vertical gradient factors of safety

(a) Vertical gradient factor of safety, FS_{vg} .

1. Figure I–10 shows how FS_{vg} can be measured across the base of the 10-foot-thick blanket at the landside toe of the levee. The excess head is the difference between total head from the FEM model at point (d) and the total head at point (a). At this location there is 10 feet of excess head, h_o , through the blanket. Assuming a soil total unit weight of 112.4 pcf of the blanket, $i_{cv} = 0.8$ and $FS_{vg} = 0.8$ for this example.

2. The critical gradient formulation can be used to calculate the factor of safety in situations where the vertical flow emerges at the ground surface. For this case, the average vertical gradient across the blanket is 1.0. For a soil with a total unit weight of 112.4 pcf, $i_{cv} = 0.8$, and $FS_{vg} = 0.8$, giving essentially the same result. Subtle changes in gradient lead to subtle variations in factors of safety through the blanket. To demonstrate this, nodal information on total head is extracted from four points indicated in Figure I–10 and is used to calculate excess head, h_o . The resulting value, along with the associated FS_{vg} , is shown in Table I–3.

3. Due to the low FS_{vg} , the blanket would be expected to experience significant seepage. This flow would likely be concentrated through both existing defects and sand boils that are likely to form. These unfiltered seepage exits may become vulnerable to BEP in the underlying aquifer materials. In addition, because of associated low effective stresses in the aquifer sands, there may also be instability of the landside slope, particularly if the levee is narrow and the landside slope is steep (Duncan et al. 2008 and Seed et al. 2008).

Table I–3
Example calculations for FS_{vg}

Point	h_o (ft)	Z_t (ft)	nodal i_v	γ_w (pcf)	γ_{sat} (pcf)	γ' (pcf)	i_v	i_c	FS_{vg}
(a)	0	0	0.97*	62.4	112.4	50	N/A	N/A	N/A
(b)	3.52	3.33	1.00	62.4	112.4	50	1.056	0.801	0.759
(c)	6.65	6.67	0.98	62.4	112.4	50	0.998	0.801	0.803
(d)	10.03	10	0.56*	62.4	112.4	50	1.003	0.801	0.799

Note:

*In general, nodal i_v values listed in most seepage programs are estimated based on averages of gradients in the elements connected to the node and may not represent gradients through a single material, such as at a material contact or at the boundary of a model. In general, the analysts should use gradients measured over a prescribed distance, not nodal gradients, to calculate factors of safety.

(b) *Mitigation alternatives.* The model shown in Figure I–8 can be adapted to include mitigation features presented in EM 1110-2-1901 or EM 1110-2-1913. These include landside berms, drainage/pressure relief features, upstream blankets, and cut-off walls. Various combinations of these features have been used to allow drainage from the pervious substratum while reliably preventing the removal of foundation soils.

(6) *Relief wells.* A line of relief wells located along the levee toe is included in the model. These wells discharge to the ground surface at an elevation of 410 feet. Screens are present from elevations 380 to 320 feet, a length of 60 feet. The line of relief wells is simulated in the FEM as a total head boundary applied along a thin, vertical box at the well screen location. Note the width of this box was set to 2 feet to avoid numerical instability with the seepage program used. The value of total head applied to this boundary is determined through an iterative process that accounts for head loss. Head losses are functions of well flow, well spacing, aquifer depth, and well penetration of the aquifer. The iterative process used here to determine head loss is described in paragraph I–3d(6). The steps below follow the guidance in Appendix G for simulating relief wells in a FEM.

(a) *Well penetration.* An effective well penetration of 61.6% was calculated for this example, with 30 feet of screen in the medium sand and 30 feet of screen in the coarse sand. This can be determined using the approach in Appendix E for a transformed aquifer. The same result may be determined by summing the product of screen length and horizontal permeability in each layer, then dividing by the aquifer transmissivity.

(b) *Design head loss.* Hydraulic head loss for flow into the well (H_w) is determined for this well from Figure 61 in TM 3-424 (USACE 1956a). This is the same curve described for the Harrisonville example in paragraph I–2d(3). The components of head loss are for the same well (8-inch diameter, 60-foot-long screen, 30-foot riser) as this example. Other combinations of screen diameter, length, and riser length can be determined from the series of charts in paragraph 7–9g. All the values for entrance loss (H_e) were developed for wood screens. However, they are typically used for all screen types because H_e is relatively small. H_e is expected to be even smaller for the modern stainless-steel screens commonly used for relief wells today.

(c) *Well design factors.* The additional head loss ($h_{\Delta L}$) and head between the wells ($h_{\Delta M}$) is calculated using equations G–7 and G–8, respectively. Although the process is iterative, the well factors do not change for each iteration. For well spacing of 150 feet, $\theta_{av} = 0.843$ and $\theta_m = 0.931$ using the Sharma (1974) approach described in Appendix H. This is for an aquifer thickness of 100 feet with average permeability of 730×10^{-4} cm/second, penetration ratio of 61.6%, and an assumed well radius of 1 foot. As discussed in the various BT solutions of this problem below, the well factors would be different using a transformed aquifer depth and permeability according to Appendix E. A transformed aquifer thickness of 342 feet with effective permeability of 215×10^{-4} cm/second, penetration ratio of 61.6%, and an assumed well radius of 1 foot results in $\theta_{av} = 0.999$ and $\theta_m = 0.903$.

(d) *Iterative procedure.* The initial trial value of total head is the well discharge elevation of 410 feet. Flow per unit length is determined from the FEM model using a flux line drawn around the boundary representing the well screen. This unit length flow is manually converted to a well flow, q_w , to calculate head loss through the well, H_w . The well flow is also used to calculate head loss midway between wells, h_m , and average head loss along the well line in plan view, h_{av} . These head losses are added to the discharge elevation to get total head midway between wells, H_m , and average total

head, H_{av} . H_{av} determined from each iteration is used as the total head applied to the flux line to start the next iteration. This process is repeated until the difference between input and output head loss is acceptably small.

(e) *Future performance loss.* A reduced relief well performance to 80% of the no-loss condition was assumed for this example. This accounts for biofouling of the screen and filter that typically occurs over time. The well performance is used in the calculation of i_v at the landside embankment toe. A gradient value is determined that is intermediate between results with and without wells. In the case with 150-foot well spacing, the well performance of 80% results in an increase in total head beneath the blanket from 413.7 to 415.0 feet, still considerably less than the 420.0 feet without wells. This increase due to an assumed performance of 80% that is included in the calculations presented in the following section.

(f) *Results with relief wells.* According to Appendix G, the final step is to apply total head at the well screen set to the value midway between wells. For this example, $TH_{well-m} = 413.86$ feet from the final iteration. This process was repeated for several values of well spacing as shown in Figure I-11 to select a spacing of 150 feet. The calculated well flow is 365 gpm (2.44 gpm/feet), which results in the target $FS_{vg} = 1.6$ through the blanket at the toe of the levee midway between wells. Flow from these wells reduces pore pressures in the aquifer and results in the flow paths and total head contours shown in Figure I-12 for the 100-foot aquifer. Table I-4 lists the head loss calculations for each iteration in the case with 150-foot well spacing. FS_{vg} is calculated based on total head beneath the blanket at the landside toe.

(g) *Summary.* A comparison between Figure I-9 and Figure I-12 shows the effect relief well flow has on seepage through the foundation. Since i_v at the landside embankment toe is reduced, sand boils or other seepage-related defects are less likely. Also shown in these two figures is the horizontal gradient, i_h , which is often used in risk assessment. Since the i_h increases with wells in place (from $i_h = 0.03$ to 0.047 in this example) it was previously thought wells could worsen BEP progression. Note that the model described here includes an intact blanket with no sand boils. As described in Chapter 4, it is now better understood that because wells lessen flow through any defect in the blanket, they reduce the likelihood of BEP progression.

Table I-4
Iterative relief well head loss calculations with 150-foot well spacing

TH_{well} (ft)	q_{slot} (gpm/ft)	Q_w (gpm)	H_w (ft)	$H_m (h_{\Delta M})$ (ft)	$H_{av} (h_{\Delta L})$ (ft)	TH_{well-m} (ft)	$TH_{well-av}$ (ft)
410	3.49	523	1.01	4.52	4.10	415.53	415.11
412.55	2.73	410	0.78	3.54	3.21	414.33	413.99
413.27	2.52	378	0.73	3.27	2.96	413.99	413.68
413.48	2.46	368	0.71	3.18	2.88	413.89	413.59
413.53	2.44	366	0.71	3.17	2.87	413.87	413.57
413.55	2.44	365	0.70	3.16	2.86	413.86	413.56

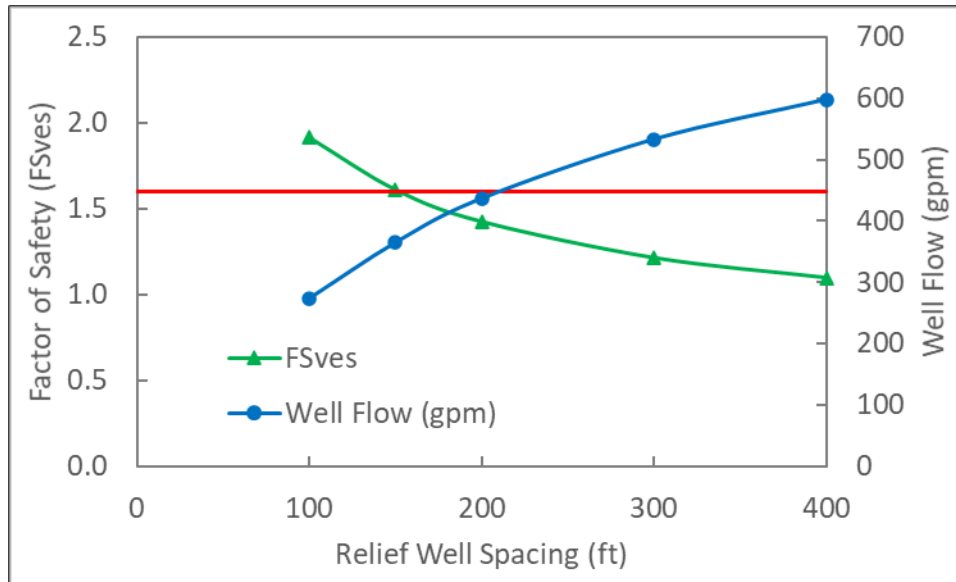


Figure I-11. FS_{vg} versus relief well spacing to achieve target value of $FS_{vg} = 1.6$

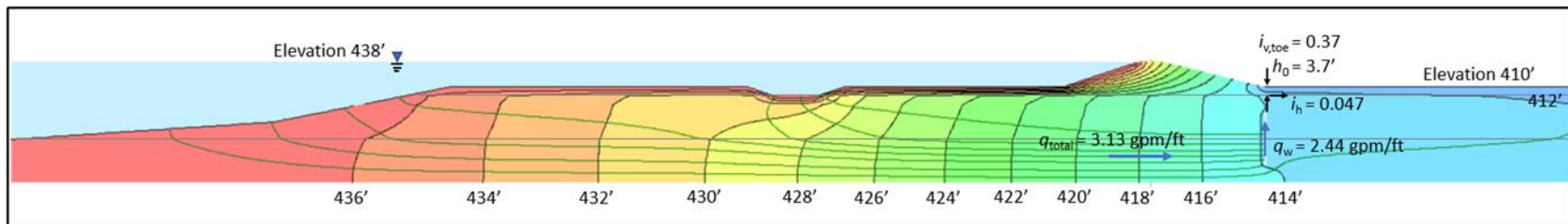


Figure I-12. Total head pressure contours, total flow, well flow, and flow lines for the case with a line of relief wells at 150-foot spacing

e. *Simple Blanket Theory calculations for the generalized levee cross section.*

(1) *Approach.* BT was applied to this problem using two different approaches commonly used in USACE for relief well design and analysis.

(a) The first approach, presented below, is to assume a single isotropic aquifer permeability. This approach is presented to illustrate basic BT calculations. A simple spreadsheet assembled in the same manner as described for the example in paragraph I-2 is used for this purpose. Initially, this is done without wells. Then, an infinite line of wells every 150 feet is included to compare with FEM results presented above.

(b) The second approach, described in paragraph I-3f, is to properly incorporate aquifer transformation according to Appendix E. A spreadsheet (Guy et al. 2010) that originated in Huntington District (LRH) is used to facilitate these calculations, herein referred to as the LRH spreadsheet.

(c) A comparison of results for the two approaches is also included in paragraph I-3g. Calculations for a finite line of wells every 170 feet are also performed in paragraph I-3h to demonstrate the application of the finite line of wells method in Chapter 6. The IWM with BT adaptation described in Chapter 6 was also applied to the generalized levee cross section and is discussed in paragraph I-3i.

(2) *Input parameters.* The same input parameters used in the FEM analysis for the generalized levee cross section (paragraph I-3c) were also used in the simplified BT analysis. The BT parameters are explained in Appendix C and listed along with results from the BT calculations in Table I-5 through Table I-7.

(a) *Dimensions.* The width of the levee, L_2 , and infinite landside boundary, L_3 , condition is straightforward. Determining the entrance distance, L_1 , requires some judgment. Three cases are listed in Table I-5; an infinite entrance distance, an entrance at the borrow pit, and an entrance at the river. In this example, blanket thickness, z_{br} and z_{bl} , and depth of aquifer, d , are selected to be the same as in the FEM model.

(b) *Permeability values.* Permeability of the riverside blanket, k_{br} , and landside blanket, k_{bl} , are derived from those listed in Table I-2. These values represent the vertical permeability and are reduced from the horizontal permeability by the anisotropy. The permeability of the aquifer is a weighted average of the horizontal permeability in each of the three sand layers. In this case, the weighted average results in $k_h = 730 \times 10^{-4}$ cm/second (0.0024 feet/second). As discussed in paragraph I-1a, many designers would assign a permeability closer to the value for the more pervious coarse sand for the aquifer in this example.

(3) *Results without wells.* The calculated excess head, h_o , and flow per unit length, q_s are listed in Table I-5 for each of the three assumed entrance conditions (river, borrow pit, and flow through the blanket). Case 3, with an assumed entrance at the river, is the best match with FEM results in paragraph I-2c. There is little

contribution of seepage from the exposed fine sand beneath the borrow pit in this example compared to the coarse sand with a direct connection to the river. Sensitivity studies with the FEM model could be used to better understand the contribution from each source of seepage.

(4) *Results with an infinite line of wells with 150-foot spacing.* The BT approach was repeated with wells for all three cases described above. An effective well penetration of 61.6% and 150-foot well spacing, a , were the same as in the FEM approach presented earlier. The dimensionless well factors, $\theta_{av} = 0.843$ and $\theta_m = 0.931$, are the same values used in that example rather than $\theta_{av} = 0.999$ and $\theta_m = 0.903$ if a transformed aquifer thickness were used. Initially, the BT calculations are performed with only hydraulic well losses, H_w , based on the relationship with flow. Similar to the FEM example, a reduced relief well performance, 80% of the initial condition, was then incorporated using the approach described in paragraph I-3d(6)(e). Results are shown in Table I-6.

(5) *Results with an infinite line of wells with 170-foot spacing.* A line of wells at 170-foot spacing for Case 3 was also considered for comparison with the IWM models in paragraph I-3i. Calculations were performed for both $W/D = 61.6\%$ and $W/D = 100\%$ (full penetration). Since the full-penetration wells are more effective than the $W/D = 61.6\%$, a larger spacing satisfies design criteria. BT results are shown in Table I-7 for both full and partial-penetration wells.

Table I-5
Blanket theory parameters and results without wells

	ΔH	k_f	d	z_{br}	k_{br}	L_1	x_1	L_2	L_3	z_{bl}	k_{bl}	x_3	h_o	i_{vg}	q_s	q_s
Case	ft	ft/s	ft	ft	ft/s	ft	ft	ft	ft	ft	ft/s	ft	ft		ft ³ /s	gpm/ft
1	28	730	100	10	0.50	Infinite	1208.5	230	Infinite	10	2.50	540.4	7.65	0.765	0.0034	1.52
2	28	730	100	10	0.50	280	275.1	230	Infinite	10	2.50	540.4	14.47	1.447	0.0064	2.88
3	28	730	100	10	0.50	750	666.5	230	Infinite	10	2.50	540.4	10.53	1.053	0.0047	2.09

Table I-6
Blanket theory parameters and results with an infinite line of wells every 150 feet

	ΔH	x_3	S	z	h_o	d	k_f	a	θ_{av}	θ_m	H_{av} guess	ΔM	H_w	h_{av}	H_{av}	h_m	H_m	Q_w	Q_w	SCR	H_m^*
Case	ft	ft	ft	ft	ft	ft	10 ⁻⁴ cm/s	ft	-	-	-	-	ft	ft	ft	ft	ft	ft ³ /s	gpm	%	ft
1	28	540	1438	10	7.6	100	730	150	0.843	0.931	2.24	0.0138	0.49	1.74	2.23	1.92	2.42	0.494	221.9	80	3.46
2	28	540	505	10	14.5	100	730	150	0.843	0.931	5.46	0.0345	1.08	4.37	5.45	4.82	5.91	1.240	556.6	80	7.62
3	28	540	897	10	10.5	100	730	150	0.843	0.931	3.36	0.0213	0.67	2.69	3.36	2.97	3.64	0.764	342.9	80	5.02

Note:

* H_m is shown including reduced well performance to correspond with a specific capacity ratio (SCR) = 80%

Table I-7
Blanket theory parameters and results for Case 3 with an infinite line of wells every 170 feet

	ΔH	x_3	S	z	h_o	d	k_f	a	θ_{av}	θ_m	H_{av} guess	ΔM	H_w	h_{av}	H_{av}	h_m	H_m	Q_w	Q_w	SCR	H_m^*
Pen %	ft	ft	ft	ft	ft	ft	10 ⁻⁴ cm/s	ft	-	-	-	-	ft	ft	ft	ft	ft	ft ³ /s	gpm	%	ft
100	28	540	897	10	10.5	100	730	170	0.525	0.635	2.84	0.0228	0.80	2.04	2.83	2.46	3.26	0.929	416.8	80	4.71
61.6	28	540	897	10	10.5	100	730	170	0.863	0.958	3.70	0.0203	0.71	2.97	3.69	3.30	4.01	0.825	370.2	80	5.31

Note:

* H_m is shown including reduced well performance to correspond with a specific capacity ratio (SCR) = 80%

f. *LRH spreadsheet Blanket Theory calculations for the generalized levee cross section.* The second approach to BT analysis used in this example is incorporated into the LRH spreadsheet. Figure I–13 is a screen shot of input parameters in the LRH spreadsheet. Values in red represent user input, black indicates values calculated by the spreadsheet from the user input. The specific values shown correspond to Case 3 for the example presented below.

	A	B	C	D	E	F	G	H	I	J	K
1	Relief Well System Design and Analysis Program										
2	Project	EM 1914 -- Appendix I - Classic Section									
3	Program is Applicable for Blanket Aquifer Foundation Case with an Infinite Line of Wells Parallel to an Infinite Line Source										
4	Parameter	Expected Value	Units	Definition							
5	Load and Underseepage Geometric Parameters										
6	Pool	438.00	ft	Pool elevation							
7	Tail	410.00	ft	Landside tail water elevation							
8	H	28.00	ft	Net head on well system							
9	TOG	410.00	ft	Landside top of ground elevation							
10	L ₁	750.0	ft	Distance from poolside embankment toe to an open seepage entrance; enter "NA" if not applicable							
11		NA	ft	Distance from poolside embankment toe to a seepage block; enter "NA" if not applicable							
12	L ₂	230.0	ft	Base width (total) of embankment							
13		115.0	ft	Base width of embankment U/S of centerline							
14		115.0	ft	Base width of embankment D/S of centerline							
15	L ₃	NA	ft	Distance from landside embankment toe to an open seepage exit; enter "NA" if not applicable							
16		NA	ft	Distance from landside embankment toe to a seepage block; enter "NA" if not applicable							
18	x ₁	667.0	ft	Distance from poolside embankment toe to effective seepage entry							
19		NA	ft	x ₁ estimated from aquifer foundation piezometric data or another approach; enter "NA" if not applicable							
20	S	897.0	ft	Distance from effective source of seepage entry into foundation to the landside embankment toe (fig. 11, TM 3-424)							
21	x ₃	540.0	ft	Distance from landside embankment toe to effective seepage exit							
22		NA	ft	x ₃ estimated from aquifer foundation piezometric data or another approach; enter "NA" if not applicable							
23	Blanket Strata Parameters										
24	Z _{top-1}	10.0	ft	Actual thickness of poolside blanket stratum 1 Classification: <i>Levee and Waterside Blanket</i>							
29	Z _{top}	10.0	ft	Total actual thickness of poolside blanket strata							
30	K _{top-1}	1.4E-01	ft/d	K _v (vertical hydraulic conductivity) of poolside blanket stratum 1							
35	K _{top}	1.4E-01	ft/d	Effective K _v of poolside blanket strata (eq. 3, TM 3-424)							
36	C _{top}	0.00083		Constant for poolside blanket strata (eq. B-4, EM 1110-2-1914)							
37	Z _{sl-1}	10.0	ft	Actual thickness of landside blanket stratum 1 Classification: <i>Leaky Landside Blanket</i>							
42	Z _{sl}	10.0	ft	Total actual thickness of landside blanket strata							
43	K _{sl-1}	7.1E-01	ft/d	K _v (vertical hydraulic conductivity) of landside blanket stratum 1							
48	K _{sl}	7.1E-01	ft/d	Effective K _v of landside blanket strata (eq. 3, TM 3-424)							
49	C _{sl}	0.0019		Constant for landside blanket strata (eq. B-4, EM 1110-2-1914)							
50	γ _{sat sl-1}	112.4	pcf	Saturated unit weight (γ _{sat}) of landside blanket stratum 1 (changed from 115)							
55	γ _{sat sl}	112.4	pcf	Effective saturated unit weight of landside blanket strata							
56	γ _{bu sl}	50.0	pcf	Effective buoyant unit weight (γ _b) of landside blanket strata							
57	Aquifer Foundation Strata Parameters										
58	D ₁	10.0	ft	Actual thickness of foundation stratum 1				Classification: <i>Fine Sand</i>			
59	D ₂	40.0	ft	Actual thickness of foundation stratum 2				Classification: <i>Medium Sand</i>			
60	D ₃	50.0	ft	Actual thickness of foundation stratum 3				Classification: <i>Coarse Sand</i>			
68	D	100.0	ft	Total actual thickness of foundation strata							

Figure I–13. Screen shot of input in Huntington District spreadsheet for Case 3

(1) *Input parameters.* Input values used in the LRH analysis are the same as in the simple BT approach described in paragraph I–3e with one important difference: the anisotropy of the three sand layers, each with a set of k_h and k_v values, is incorporated using the spreadsheet. These values, along with the aquifer thickness, d , are used to perform an aquifer transformation as described in Appendix E.

(a) For this example, the resulting transformed thickness, \bar{D} , is equal to 342 feet.

(b) The resulting transformed permeability of the aquifer is an effective permeability ($\overline{k_e}$). In this case, $\overline{k_e} = 215 \times 10^{-4}$ cm/second (7.05×10^{-4} feet/second).

(c) The transformed thickness, \overline{D} , and the effective permeability (k_e) were used with the simple approach from paragraph I-3e for comparison purposes.

(d) An effective well penetration of 61.6% and 150-foot well spacing, a , were the same as in the FEM model.

(e) The dimensionless well factors defined above in equations I-4 and I-5 were calculated using the Sharma (1974) method. The current version of the LRH spreadsheet can calculate well factors for effective well penetrations of 25, 50, 75 and 100%. For other values of partial penetration, the well factors must be calculated using the Sharma (1974) method or by other means. This requires manually entering the well factors into the spreadsheet.

(2) *Results without wells.* Table I-8 shows the excess head, h_o , and flow per unit length, q_s , calculated by the LRH spreadsheet.

(3) *Results with an infinite line of wells.* Initially the BT evaluations considered results without any well losses. Well losses were then incorporated into subsequent evaluations.

(a) *Results with no well losses.* Results with wells and no well losses are shown for the LRH spreadsheet in Table I-9.

(b) *Results with well losses.* Results with wells and well losses are shown in Table I-10 for the LRH approach. Using the LRH spreadsheet, the value of the well loss term (H_w) was adjusted to obtain flows 80% of those for the no-loss condition. The resulting values range from 2.11 to 5.27 feet for the three cases. This procedure had the effect of simulating a 20% decline in well performance over time relative to the base condition. The base condition in this instance is assumed to be 100%. Figure I-14 is a screen shot of output from the LRH spreadsheet for Case 3.

(4) *Comparison of results from FEM and both Blanket Theory approaches.* For the assumed entrance at the river, Case 3, BT results again match well with FEM results presented above. BT for Case 3 resulted in an excess head of 10.5 feet without relief wells. BT including wells with 80% performance resulted in 4.7 feet of excess head and 5.0 feet in the simple BT approach. FEM for Case 3 resulted in an excess head of 10.0 feet without relief wells, including wells with 80% performance resulted in 5.0 feet of excess head. Well flow was also similar, either 343 or 349 gpm for the BT approaches compared with 365 gpm for FEM. These values do not include the 80% performance adjustment.

Table I-8**Blanket Theory parameters and results from Huntington District spreadsheet with no wells – Huntington District spreadsheet**

	ΔH	k_e	d	\underline{D}	z_{br}	k_{br}	L_1	x_1	L_2	L_3	x_3	z_{bl}	k_{bl}	h_o	i_{vg}	q_s	q_s
Case	ft	10^{-4} cm/s	ft	ft	ft	10^{-4} cm/s	ft	ft	ft	ft	ft	ft	10^{-4} cm/s	ft	–	ft ³ /s/ft	gpm/ft
1	28	215	100	342	10	0.50	Infinite	1208.5	230	Infinite	540	10	2.50	7.64	0.764	0.0034	1.53
2	28	215	100	342	10	0.50	280	275.1	230	Infinite	540	10	2.50	14.47	1.447	0.0065	2.90
3	28	215	100	342	10	0.50	750	666.5	230	Infinite	540	10	2.50	10.53	1.053	0.0047	2.11

Table I-9**Blanket Theory parameters and results with wells and no well losses (150-foot spacing) – Huntington District spreadsheet**

	h_o	d	\underline{D}	k_e	a	θ_{av}	θ_m	ΔM	H_w	h_{av}	H_{av}	h_m	H_m	Q_w	Q_w
Case	ft	ft	ft	ft/s	ft	–	–	–	ft	ft	ft	ft	ft	ft ³ /s	gpm
1	7.64	100	342	7.05E-04	150	0.999	0.903	0.0141	0.00	2.111	2.111	1.908	1.908	0.5063	227.2
2	14.47	100	342	7.05E-04	150	0.999	0.903	0.0352	0.00	5.277	5.277	4.770	4.770	1.2657	568.0
3	10.53	100	342	7.05E-04	150	0.999	0.903	0.0216	0.00	3.238	3.238	2.927	2.927	0.7766	348.6

Table I-10**Blanket Theory parameters and results with wells and well losses (150-foot spacing) – Huntington District spreadsheet**

	h_o	d	\underline{D}	k_e	a	W/D'	θ_{av}	θ_m	ΔM	H_w	h_{av}	H_{av}	h_m	H_m	Well Cond	Q_w	Q_w
Case	ft	ft	ft	ft/s	ft	–	–	–	–	ft	ft	ft	ft	ft	%	ft ³ /s	gpm
1	7.64	100	342	7.05E-04	150	62%	0.999	0.903	0.0113	1.52	1.69	3.21	1.53	3.05	80.0	0.406	182.0
2	14.47	100	342	7.05E-04	150	62%	0.999	0.903	0.0282	2.90	4.22	7.12	3.81	6.71	80.0	1.012	454.2
3	10.53	100	342	7.05E-04	150	62%	0.999	0.903	0.0173	2.10	2.59	4.69	2.34	4.44	80.0	0.622	279.0

	A	B	C	D	E	F	G	H	I	J	K
199	Well Spacing Parameters										
200	$\theta_{approximate}$	245.0	ft	Well spacing predicted from automated trials to approximately meet $FS_{required}$ (if prediction result is an error, increase W/D)							
201	a	150	ft	Final design well spacing, enter value which yields adequate $FS_{uplift-a}$ and reliability if designing a new well system							
202	a/r_w	150.8		Ratio used for determination of θ_{av} and θ_m parameters							
203	D/a	2.28		Ratio used for determination of θ_{av} and θ_m parameters							
204	θ_{av}	0.999		Average uplift parameter (derived from table 5-1, EM 1110-2-1914; based on theoretical well factors solutions)							
210	H_w	2.10	ft	Hydraulic well losses (e.g. entrance, friction, and velocity) for Q_w , excluding potential partial penetration losses							
211	Q_w	279.0	gpm	Discharge from a single well with hydraulic well losses (derived from eq. 7-7, EM 1110-2-1914)							
212	H_w	2.10	ft	Total well losses (elevation and efficiency)							
213	h	22.41	ft	Net head on well system corrected for total well losses							
214	h_{av}	2.59	ft	Average net head in plane of wells corrected for total well losses (derived from fig. 5-4b, eq. 5-23, EM 1110-2-1914)							
215	H_{av}	4.69	ft	Average net head in plane of wells (eq. 43, TM 3-424)							
216	Δm	0.017		Net seepage gradient toward the well line (derived from eq. 7-6, EM 1110-2-1914; Darcy's law eq.)							
217	θ_m	0.903		Midwell uplift parameter (derived from table 5-1, EM 1110-2-1914; based on theoretical well factors solutions)							
218	h_m	2.34	ft	Net head midway between wells corrected for total well losses (derived from fig. 5-4b, eq. 5-22, EM 1110-2-1914)							
219	H_m	4.44	ft	Net head midway between wells (eq. 45, TM 3-424)							
220	$> H_{2w}, H_m$	414.69	ft	Total head elevation equivalent of the greater of H_{2w} and H_m at well line resulting from well spacing (a)							
221	Relief Well System Design and Analysis Program beta vs 12.10.15										
222	Deterministic Design Results										
223	$FS_{uplift-a}$	1.71		Effective stress factor of safety against uplift at well line resulting from well spacing (a)							
224	Check to ensure $FS_{uplift-a}$ is \geq to $FS_{required}$, if not well system design is inappropriate and should be adjusted										
225	$h_{excess-a}$	4.69	ft	Excess head above TOG (or tail water elevation if $>$ than TOG) at well line							
226	i_{2w-a}	0.47		Vertical gradient through blanket at well line							
227											
228											
229											
230											
231											
232											
233											
234											
235											
236											
237											
238											
239											
240											
241											
242											
243											
244											
245											
246											
247											

Figure I-14. Screenshot of output in Huntington District spreadsheet for Case 3

g. *Replication of Huntington District spreadsheet using simplified Blanket Theory approach.* A proper comparison of the two BT approaches presented above requires they use the same set of assumptions. There are two significant differences: (1) aquifer transformation incorporated with the LRH spreadsheet, and (2) incorporation of well head loss.

(1) *Aquifer transformation.* Without wells, the simple average of horizontal permeability yields the same result as the proper aquifer transformation. Note h_o and q_s are the same for all three cases considered in Table I-5 and Table I-8. Effective well penetration is also the same using either approach (61.6%). However, in addition to W/D the dimensionless well factors include the variable D/a . When partial-penetration wells are included, the transformed D should be used to determine θ_{av} and θ_m . The

original well factors of $\theta_{av} = 0.843$ and $\theta_m = 0.931$ based on $D = 100$ feet are changed to $\theta_{av} = 0.999$ and $\theta_m = 0.903$ based on $\bar{D} = 342$ feet for results in Table I-11.

(2) *Well head loss.* In the simple BT approach, initial hydraulic well losses are included with the H_w term. Then, any reduction in well performance is included by adjusting the resulting H_m value. This is why two values of H_m are listed in Table I-11 (without and then with the $SCR = 80\%$ adjustment). In the LRH spreadsheet, both hydraulic well loss and deterioration are included in the H_w term. The spreadsheet is initially used with $H_w = 0$, then H_w is increased until flow reduces to the target value. In this example, the target value is 80% of the initial flow. For comparison with the LRH spreadsheet, the initial hydraulic head loss from Table I-11 was changed to $H_w = 0$ for all three cases to produce Table I-12.

(3) *Comparison of results with $H_w = 0$.* Values for H_{ave} (2.11 feet, 5.28 feet, and 3.24 feet) and H_m (1.91 feet, 4.77 feet, and 2.93 feet) are identical in Table I-9 and Table I-12 for all three cases considered. Well flow is also identical between the two tables (227 gpm, 568 gpm, and 349 gpm) for all three cases.

(4) *Comparison of results with wells at 80% of the no-loss condition.* Values for H_m (3.05 feet, 6.71 feet, and 4.45 feet) are identical in Table I-10 and Table I-12 for all three cases considered. Also note that well flow in Table I-10 (182 gpm, 454 gpm, and 279 gpm) is 80% of the well flow in Table I-12 for all three cases. There is no meaningful comparison for H_{ave} because it is not adjusted from the no-loss condition in Table I-12.

(5) *Discussion of various Blanket Theory approaches.* This example demonstrates the simple BT approach can match the more rigorous aquifer transformation if the dimensionless well factors are based on \bar{D} . Then the two approaches agree when well losses (both hydraulic and due to deterioration) are included in the same manner. For this example, using \bar{D} rather than D results in a value of H_{ave} that is larger than H_m . Unless additional calculations are used to determine H_d as shown in Chapter 5, designers use H_{max} as the maximum of H_{ave} or H_m . The adjustment in Table I-11 to account for well deterioration should have been performed on H_{ave} that is larger than H_m . Then H_{max} would be essentially the same in Table I-6 and Table I-11, with Q_w approximately 5% less when using \bar{D} rather than D for this example.

h. Calculations with a finite line of wells at 170-foot spacing. Procedures in Chapter 6 of this manual are employed to determine flow and head for a finite number of wells. The method uses four new theta values to account for end effects from seepage around wells. Excess head is determined along the well line and a line landside (downstream) of the well line. Each theta represents excess head at either the middle or ends of one of those lines. Input and results from the infinite line of wells analysis shown in Table I-7, are used to demonstrate this method.

(1) *Determining theta values for finite well lines.* The same procedure was used four times to determine the four theta values for the case with five wells. This requires interpolation between charts in Figure 6-5 through Figure 6-8 as summarized in Table

I-13. Green font represents values that are included or calculated from values in Table I-7. Blue font represents values that are found from the four figures in Chapter 6. Red font are values determined using linear interpolation and used to calculate excess head in the following paragraph. Table I-14 is a summary of this procedure for the case with 20 wells.

Table I-11

Blanket theory parameters and results with an infinite line of wells every 150 feet and well factors based on a transformed aquifer thickness of $\bar{D} = 342$ feet

	ΔH	x_3	S	z	h_o	d	k_f	a	θ_{av}	θ_m	H_{av} guess	ΔM	H_w	h_{av}	H_{av}	h_m	H_m	Q_w	Q_w	SCR	H_m^*
Case	ft	ft	ft	ft	ft	ft	10^{-4} cm/s	ft	-	-	-	-	ft	ft	ft	ft	ft	ft ³ /s	gpm	%	ft
1	28	540	1438	10	7.6	100	730	150	0.999	0.903	2.46	0.0132	0.48	1.98	2.46	1.79	2.27	0.474	212.9	80	3.35
2	28	540	505	10	14.5	100	730	150	0.999	0.903	5.92	0.0328	1.02	4.91	5.93	4.44	5.46	1.177	528.2	80	7.26
3	28	540	897	10	10.5	100	730	150	0.999	0.903	3.68	0.0203	0.64	3.04	3.69	2.75	3.39	0.730	327.6	80	4.82

Table I-12

Blanket theory parameters and results with an infinite line of wells every 150 feet with a transformed aquifer thickness of $\bar{D} = 342$ feet and $H_w = 0$

	ΔH	x_3	S	z	h_o	d	k_f	a	θ_{av}	θ_m	H_{av} guess	ΔM	H_w	h_{av}	H_{av}	h_m	H_m	Q_w	Q_w	SCR	H_m^*
Case	ft	ft	ft	ft	ft	ft	10^{-4} cm/s	ft	-	-	-	-	ft	ft	ft	ft	ft	ft ³ /s	gpm	%	ft
1	28	540	1438	10	7.6	100	730	150	0.999	0.903	2.12	0.0141	0.00	2.11	2.11	1.91	1.91	0.505	226.8	80	3.05
2	28	540	505	10	14.5	100	730	150	0.999	0.903	5.28	0.0352	0.00	5.28	5.28	4.77	4.77	1.265	567.7	80	6.71
3	28	540	897	10	10.5	100	730	150	0.999	0.903	3.24	0.0216	0.00	3.24	3.24	2.93	2.93	0.777	348.6	80	4.45

Table I-13
Interpolation of Chapter 6 figures to determine theta values for five wells

$S/a = 5.274$						
$x_3/a = 3.179$						
$\theta_{mm} = 0.47$	for $\theta_m = 0.29$ and $N = 5$ from Figure 6.5			$\theta_{dm} = 0.26$	for $\theta_{av} = 0.18$ and $N = 5$ from Figure 6.7	
$\theta_{mm} = 2.28$	for $\theta_m = 1.92$ and $N=5$ from Figure 6.5			$\theta_{dm} = 2$	for $\theta_{av} = 1.93$ and $N = 5$ from Figure 6.7	
$\theta_{mm} = 0.85$	$\theta_m = 0.635$	100% penetration		$\theta_{dm} = 0.60$	$\theta_{av} = 0.525$	100% penetration
$\theta_{mm} = 1.21$	$\theta_m = 0.958$	61.6% penetration		$\theta_{dm} = 0.94$	$\theta_{av} = 0.863$	61.6% penetration
$\theta_{me} = 0.58$	for $\theta_m = 0.29$ and $N = 5$ from Figure 6.6			$\theta_{de} = 0.45$	for $\theta_{av} = 0.18$ and $N = 5$ from Figure 6.8	
$\theta_{me} = 2.47$	for $\theta_m = 1.92$ and $N = 5$ from Figure 6.6			$\theta_{de} = 2.2$	for $\theta_{av} = 1.93$ and $N = 5$ from Figure 6.8	
$\theta_{me} = 0.98$	$\theta_m = 0.635$	100% penetration		$\theta_{de} = 0.79$	$\theta_{av} = 0.525$	100% penetration
$\theta_{me} = 1.35$	$\theta_m = 0.958$	61.6% penetration		$\theta_{de} = 1.13$	$\theta_{av} = 0.863$	61.6% penetration

Table I-14
Interpolation of Chapter 6 figures to determine theta values for 20 wells

$S/a = 5.274$						
$x_3/a = 3.179$						
$\theta_{mm} = 0.29$	for $\theta_m = 0.29$ and $N = 20$ from Figure 6.5			$\theta_{dm} = 0.18$	for $\theta_{av} = 0.18$ and $N = 20$ from Figure 6.7	
$\theta_{mm} = 1.92$	for $\theta_m = 1.92$ and $N = 20$ from Figure 6.5			$\theta_{dm} = 1.5$	for $\theta_{av} = 1.93$ and $N = 20$ from Figure 6.7	
$\theta_{mm} = 0.63$	$\theta_m = 0.635$	100% penetration		$\theta_{dm} = 0.44$	$\theta_{av} = 0.525$	100% penetration
$\theta_{mm} = 0.96$	$\theta_m = 0.958$	61.6% penetration		$\theta_{dm} = 0.70$	$\theta_{av} = 0.863$	61.6% penetration
$\theta_{me} = 0.48$	for $\theta_m = 0.29$ and $N = 20$ from Figure 6.6			$\theta_{de} = 0.35$	for $\theta_{av} = 0.18$ and $N = 20$ from Figure 6.8	
$\theta_{me} = 2.18$	for $\theta_m = 1.92$ and $N = 20$ from Figure 6.6			$\theta_{de} = 1.9$	for $\theta_{av} = 1.93$ and $N = 20$ from Figure 6.8	
$\theta_{me} = 0.84$	$\theta_m = 0.635$	100% penetration		$\theta_{de} = 0.66$	$\theta_{av} = 0.525$	100% penetration
$\theta_{me} = 1.18$	$\theta_m = 0.958$	61.6% penetration		$\theta_{de} = 0.95$	$\theta_{av} = 0.863$	61.6% penetration

(2) *Results for a finite line of wells at 170-foot spacing.* The four theta values determined in the preceding section are used to determine excess head for a finite number of wells. In this example, theta values are higher along the well line than values landside (downstream) of the well line. The same equation 6–2 is used to determine excess head for each location, but only the higher values along the well line are presented here. Results are shown in Table I–15 for Case 3 with 5 wells and in Table I–16 with 20 wells. Also included in these tables is an estimate of well flow. A ratio of the excess head for the finite line of wells over the excess head for the infinite line of wells is a reasonable estimate for the increase in flow to a finite number of wells.

Table I–15
Results with five wells at 170-foot spacing for Case 3

	θ_{mm}	θ_{me}	Q_w	Q_w	H_w	h_{mm}	H_{mm}	h_{me}	H_{me}	Efficiency	H_{mm}	H_{me}
Pen (%)	–	–	ft ³ /s	gpm	ft	ft	ft	ft	ft	%	ft	ft
100	0.853	0.980	1.340	601.6	1.19	3.31	4.49	3.80	4.99	80	5.70	6.10
61.6	1.211	1.354	1.105	495.8	0.95	4.17	5.12	4.66	5.61	80	6.20	6.60

Note:

Q_w is factored by the average of θ_{mm} and θ_{me} over θ_m

Table I–16
Results with 20 wells at 170-foot spacing for Case 3

	θ_{mm}	θ_{me}	Q_1	Q_w	H_w	h_{mm}	H_{mm}	h_{me}	H_{me}	Efficiency	H_{mm}	H_{me}
Pen (%)	–	–	ft ³ /s	gpm	ft	ft	ft	ft	ft	%	ft	ft
100	0.635	0.840	1.078	484.0	0.93	2.46	3.39	3.26	4.18	80	4.82	5.45
61.6	0.958	1.176	0.919	412.4	0.79	3.30	4.09	4.05	4.84	80	5.37	5.98

i. Image Well Method with Blanket Theory adaptation. The IWM with BT adaptation described in Chapter 6 was repeated with four different scenarios for Case 3 above, also assuming an *SCR*, or efficiency ratio, of 80%. The relief well discharge elevation (410 feet) was increased by 0.33 foot to account for well riser stickup above the ground surface. The first two scenarios were with a five-well IWM with BT spreadsheet for partial-penetration wells (61.6% effective penetration) and full-penetration wells (100% effective penetration). The third and fourth scenarios were calculated with a similar but much larger 20-well spreadsheet.

(1) *Image Well Method with Blanket Theory adaptation for five wells.* The spreadsheet inputs and results for the five-well case and 61.6% penetration are shown in Figure I–15. The calculation tables supporting the determination of the flow from each well and the head at each point of interest for Figure I–15 are shown in Figure I–16 as an example of how to set up a calculation table.

(2) *Image Well Method with Blanket Theory adaptation for 20 wells.* Results are shown for the 20-well scenario with 61.6% penetration in Figure I–17. Only the head

along the line of relief wells is included because of the large size of the input and calculation tables required to include 20 wells. The 5-well and 20-well IWM with BT adaptation analysis results for wells every 170 feet with 61.6% penetration and 100% penetration are shown in Table I-17. Well flows are shown for 100% *SCR* for consistency with the other examples.

(3) Comparison *of results*. The difference in results between the 5-well and 20-well systems are attributable to the superposition principles used in the IWM with BT adaptation method that considers the number and spacing of wells in the well system. The drawdown for 61.6% effective penetration wells was 80% of the drawdown calculated for 100% effective penetration wells for the 20-well system and 89% for the 5-well system. This further reinforces the discussion from Chapter 3 regarding effective penetrations greater than 50% resulting in nearly as much drawdown as wells with full penetration. The IWM with BT adaptation method results in similar heads as the other examples, but the calculated flows were lower.

RELIEF WELL ANALYSIS

Aquifer k_{fs} =	0.0024	ft/s
Aquifer D =	100	ft
h_0 =	10.53	ft
Top of Structure EL =	438	ft elevation
Tailwater or Landside GSE =	410.0	ft elevation
Bottom Blanket =	400	ft elevation
blanket =	10.0	ft
z, Landside Toe =	896.02	ft
Well Radius, r_w =	1	ft
Riser radius for Hw calc =	0.333	ft

γ_{sat} =	112.4	pcf
i_c =	0.80	
FS _{well} =	1.80	
Design SCR or E-ratio	0.80	Applied to all wells
100% Eff. Total Flow =	3.91	cfs

toe locator for analysis = X 1 + L2
 typical bore hole radius is 8-12 inches (0.667 - 1.0 feet)
 typical riser radius is 4 - 6 inches (0.3333 - 0.5 feet)

(Use Individual Well Efficiency OR Bio Factor)
 Discharge Losses (DL) for elbows, T's, flaps, etc based on calculated Q_w. Manual iteration required.

h _a at well x-coord from Base Analysis (ft)	real well locations											Individual Well Bio Efficiency Factor	image well locations			Q _w (cfs) at specified efficiency. Useful for back analysis when using individual well efficiencies
	well number	x-coord (toe offset)	y-coord (station)	discharge el (ft)	Effective Penetration (%)	Penetration Factor, G	effective disch el (ft)	Q _w (cfs) 100% e ff.	v _w (ft/s)	H _w (ft)	Discharge Losses (ft)		well	x'	y'	
10.53	1	896.00	170	410.33	61.6	0.84	410.77	0.823	2.36	0.44	0.00	1.00	1	-896	170	0.658
10.53	2	896.00	340	410.33	61.6	0.84	410.72	0.760	2.18	0.39	0.00	1.00	2	-896	340	0.608
10.53	3	896.00	510	410.33	61.6	0.84	410.70	0.744	2.13	0.37	0.00	1.00	3	-896	510	0.595
10.53	4	896.00	680	410.33	61.6	0.84	410.72	0.760	2.18	0.39	0.00	1.00	4	-896	680	0.608
10.53	5	896.00	850	410.33	61.6	0.84	410.77	0.823	2.36	0.44	0.00	1.00	5	-896	850	0.658
											0.41	AVG Hw (ft)				

Change x-coord and y-coord in this table to change stationing of HGL Plot Parallel to Levee

Point of Interest	x-coord (toe offset)	y-coord (station)	H _{HGL} (ft)	Drawdown (ft)	h _p (ft)	h _a (ft)	Hw AVG	i	Fsi	h _p (ft) elevation	HGL (ft) elevation	h _a (ft) elevation
1	896.00		10.5	3.0	7.9	5.01	0.41	0.79	1.01	417.94	420.53	415.01
2	896.00	127.5	10.5	4.0	6.9	5.01	0.41	0.69	1.16	416.91	420.53	415.01
3	896.00	170.0	10.5	6.3	4.6	5.01	0.41	0.46	1.74	414.60	420.53	415.01
4	896.00	212.5	10.5	4.4	6.5	5.01	0.41	0.65	1.23	416.50	420.53	415.01
5	896.00	255.0	10.5	4.4	6.5	5.01	0.41	0.65	1.23	416.51	420.53	415.01
6	896.00	297.5	10.5	4.7	6.3	5.01	0.41	0.63	1.28	416.27	420.53	415.01
7	896.00	340.0	10.5	6.7	4.3	5.01	0.41	0.43	1.88	414.27	420.53	415.01
8	896.00	382.5	10.5	4.8	6.1	5.01	0.41	0.61	1.31	416.12	420.53	415.01
9	896.00	425.0	10.5	4.7	6.2	5.01	0.41	0.62	1.29	416.22	420.53	415.01
10	896.00	467.5	10.5	4.9	6.1	5.01	0.41	0.61	1.32	416.06	420.53	415.01
11	896.00	510.0	10.5	6.8	4.2	5.01	0.41	0.42	1.92	414.18	420.53	415.01
12	896.00	552.5	10.5	4.9	6.1	5.01	0.41	0.61	1.32	416.06	420.53	415.01
13	896.00	595.0	10.5	4.7	6.2	5.01	0.41	0.62	1.29	416.22	420.53	415.01
14	896.00	637.5	10.5	4.8	6.1	5.01	0.41	0.61	1.31	416.12	420.53	415.01
15	896.00	680.0	10.5	6.7	4.3	5.01	0.41	0.43	1.88	414.27	420.53	415.01
16	896.00	722.5	10.5	4.7	6.3	5.01	0.41	0.63	1.28	416.27	420.53	415.01
17	896.00	765.0	10.5	4.4	6.5	5.01	0.41	0.65	1.23	416.51	420.53	415.01
18	896.00	807.5	10.5	4.4	6.5	5.01	0.41	0.65	1.23	416.50	420.53	415.01
19	896.00	850.0	10.5	6.3	4.6	5.01	0.41	0.46	1.74	414.60	420.53	415.01
20	896.00	892.5	10.5	4.0	6.9	5.01	0.41	0.69	1.16	416.91	420.53	415.01

Figure I-15a. Image Well Method with Blanket Theory adaptation inputs for analysis, results for well flow, and results for heads around five-well system with well spacing of 170 feet, partial-penetration wells

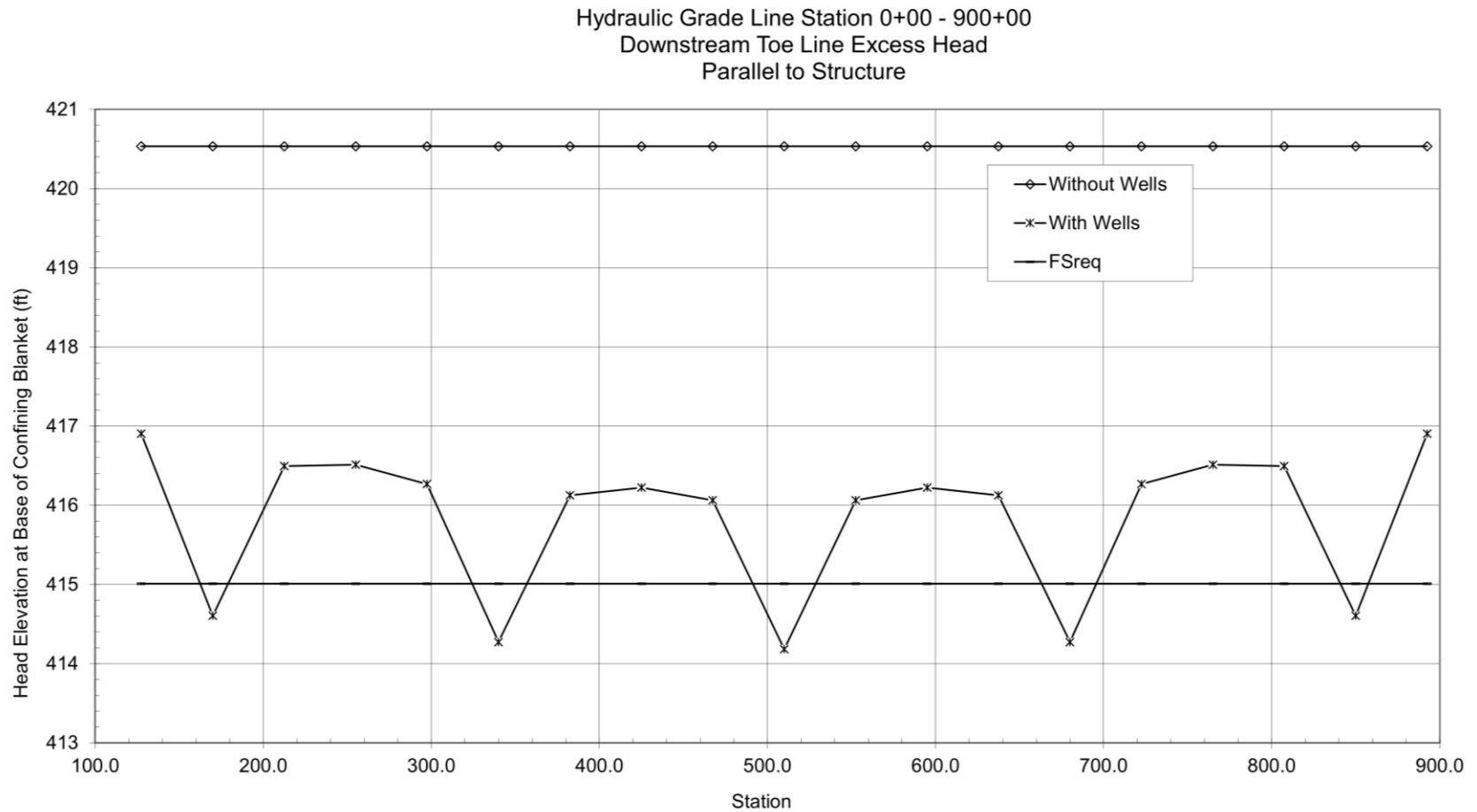


Figure I-15b. Image Well Method with Blanket Theory adaptation inputs for analysis, results for well flow, and results for heads around five-well system with well spacing of 170 feet, partial-penetration wells

USED TO CALCULATE Q_w FOR EACH WELL																
	n (ft)	r_1 (ft)	$\ln r_1/r_1$	r_2 (ft)	r_2 (ft)	$\ln r_2/r_2$	r_3 (ft)	r_3 (ft)	$\ln r_3/r_3$	r_4 (ft)	r_4 (ft)	$\ln r_4/r_4$	r_5 (ft)	r_5 (ft)	$\ln r_5/r_5$	SUM $\ln r/r$
	1.00	1792.00	7.49	170.00	1800.05	2.38	340.00	1823.97	1.68	510.00	1883.16	1.30	680.00	1916.68	1.04	13.86
	170.00	1800.05	2.38	1.00	1792.00	7.49	170.00	1800.05	2.38	340.00	1823.97	1.68	510.00	1883.16	1.30	15.19
	340.00	1823.97	1.68	170.00	1800.05	2.38	1.00	1792.00	7.49	170.00	1800.05	2.38	340.00	1823.97	1.68	15.57
	510.00	1883.16	1.30	340.00	1823.97	1.68	170.00	1800.05	2.38	1.00	1792.00	7.49	170.00	1800.05	2.38	15.19
	680.00	1916.68	1.04	510.00	1883.16	1.30	340.00	1823.97	1.68	170.00	1800.05	2.38	1.00	1792.00	7.49	13.86
TABLE USED TO CALCULATE DRAWDOWN FOR EACH POINT OF INTEREST FOR PARALLEL PLOT																
x_{CAL} (ft)	n (ft)	r_1 (ft)	$Q_{w1} * \ln r_1/n$	r_2 (ft)	r_2 (ft)	$Q_{w2} * \ln r_2/r_2$	r_3 (ft)	r_3 (ft)	$Q_{w3} * \ln r_3/r_3$	r_4 (ft)	r_4 (ft)	$Q_{w4} * \ln r_4/r_4$	r_5 (ft)	r_5 (ft)	$Q_{w5} * \ln r_5/r_5$	$\Sigma Q_{wi} * \ln r/r$
0.0	170.00	1800.05	2.08	340.00	1823.97	1.36	510.00	1883.16	1.03	680.00	1916.68	0.84	850.00	1983.37	0.75	4.85
0.0	42.50	1792.50	3.30	212.50	1804.56	1.74	382.50	1832.37	1.24	552.50	1875.24	0.99	722.50	1932.17	0.87	6.51
0.0	1.00	1792.00	6.61	170.00	1800.05	1.91	340.00	1823.97	1.33	510.00	1883.16	1.05	680.00	1916.68	0.91	9.46
0.0	42.50	1792.50	3.30	127.50	1796.53	2.15	297.50	1816.53	1.43	467.50	1851.98	1.12	637.50	1902.02	0.96	7.17
0.0	85.00	1794.01	2.69	85.00	1794.01	2.47	255.00	1810.05	1.55	425.00	1841.71	1.19	595.00	1888.20	1.02	7.14
0.0	127.50	1796.53	2.34	42.50	1792.50	3.04	212.50	1804.56	1.70	382.50	1832.37	1.27	552.50	1875.24	1.08	7.53
0.0	170.00	1800.05	2.08	1.00	1792.00	6.08	170.00	1800.05	1.87	340.00	1823.97	1.36	510.00	1883.16	1.14	10.03
0.0	212.50	1804.56	1.89	42.50	1792.50	3.04	127.50	1796.53	2.10	297.50	1816.53	1.47	467.50	1851.98	1.22	7.76
0.0	255.00	1810.05	1.73	85.00	1794.01	2.47	85.00	1794.01	2.42	255.00	1810.05	1.59	425.00	1841.71	1.29	7.61
0.0	297.50	1816.53	1.60	127.50	1796.53	2.15	42.50	1792.50	2.97	212.50	1804.56	1.74	382.50	1832.37	1.38	7.86
0.0	340.00	1823.97	1.48	170.00	1800.05	1.91	1.00	1792.00	5.94	170.00	1800.05	1.91	340.00	1823.97	1.48	10.19
0.0	382.50	1832.37	1.38	212.50	1804.56	1.74	42.50	1792.50	2.97	127.50	1796.53	2.15	297.50	1816.53	1.60	7.86
0.0	425.00	1841.71	1.29	255.00	1810.05	1.59	85.00	1794.01	2.42	85.00	1794.01	2.47	255.00	1810.05	1.73	7.61
0.0	467.50	1851.98	1.22	297.50	1816.53	1.47	127.50	1796.53	2.10	42.50	1792.50	3.04	212.50	1804.56	1.89	7.76
0.0	510.00	1883.16	1.14	340.00	1823.97	1.36	170.00	1800.05	1.87	1.00	1792.00	6.08	170.00	1800.05	2.08	10.03
0.0	552.50	1875.24	1.08	382.50	1832.37	1.27	212.50	1804.56	1.70	42.50	1792.50	3.04	127.50	1796.53	2.34	7.53
0.0	595.00	1888.20	1.02	425.00	1841.71	1.19	255.00	1810.05	1.55	85.00	1794.01	2.47	85.00	1794.01	2.69	7.14
0.0	637.50	1902.02	0.96	467.50	1851.98	1.12	297.50	1816.53	1.43	127.50	1796.53	2.15	42.50	1792.50	3.30	7.17
0.0	680.00	1916.68	0.91	510.00	1883.16	1.05	340.00	1823.97	1.33	170.00	1800.05	1.91	1.00	1792.00	6.61	9.46
0.0	722.50	1932.17	0.87	552.50	1875.24	0.99	382.50	1832.37	1.24	212.50	1804.56	1.74	42.50	1792.50	3.30	6.51

Figure I-16. Calculation tables to support results shown in Figure I-15 (a and b)

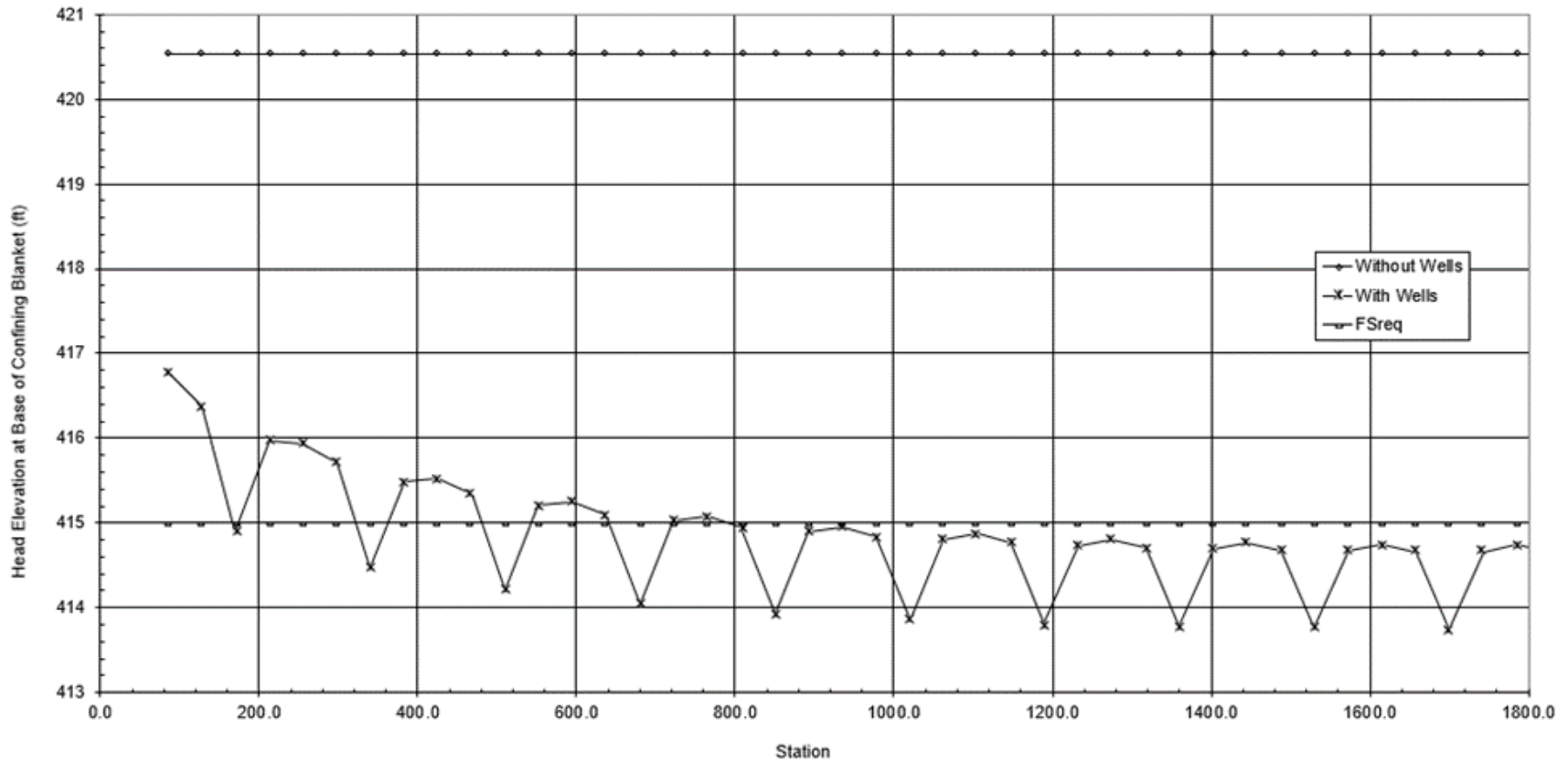


Figure I-17. Image Well Method with Blanket Theory adaptation analysis results for heads around 20-well system with well spacing of 170 feet, partial-penetration (61.6%) wells

Table I-17

Image Well Method with Blanket Theory adaptation analysis results for 5-well and 20-well systems with 170-foot spacing for 100% and 61.6% penetration

Pen (%)	Number of Wells	$Q_{w\text{-middle}}$	$Q_{w\text{-end}}$	$Q_{w\text{-AVG}}^*$	$H_{m\text{-middle}}$	$H_{m\text{-end}}$
		(gpm)	(gpm)	(gpm)	(ft)	(ft)
100	5	420	467	443	5.2	5.6
61.6	5	357	397	376	6.0	6.3
100	20	253	347	279	3.7	5.1
61.6	20	213	293	234	4.7	5.9

Note:

* $Q_{w\text{-AVG}}$ is average calculated flow of all wells.

j. FEM plan view model. An alternate approach described in Chapter 6 is to perform a plan view FEM model to estimate well flow and head beneath the blanket. This is much simpler than full 3D FEM analyses, and readily available to more practitioners. An example is included here based on the values in Table I-7.

(1) *Model input.* The well location is set at the origin (0, 0) in this example. The riverside (left) and landside (right) boundary conditions are set at the effective entrance and effective exit locations. A total head boundary of $TH = 438$ feet is at $x = -897$ feet and $TH = 410$ feet is at $x = 540$ feet. Based on H_w in Table I-7, a $TH = 410.8$ feet is applied to the well. The top and bottom are no-flow boundaries set midway between wells, $y = -85$ feet and 85 feet for the spacing of 170 feet. These boundaries are shown in Figure I-18. The average aquifer permeability of $k_f = 730 \times 10^{-4}$ cm/second is applied to the model.

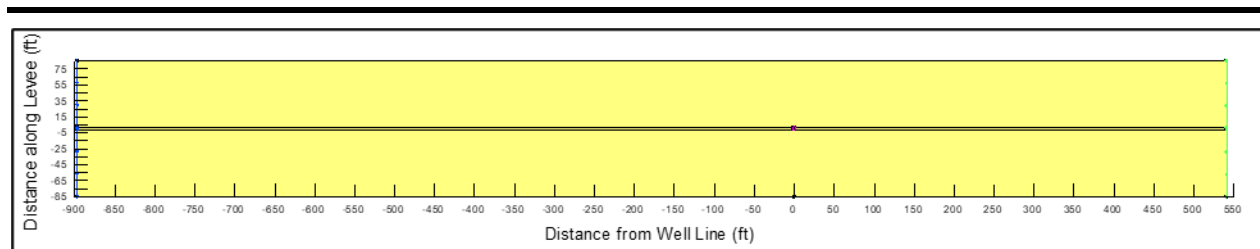


Figure I-18. Boundaries used in plan view model of the generalized levee cross section

(2) *Model output.*

(a) Total head contours in Figure I-19 illustrate the reduction in head across the model due to relief wells. Total head midway between wells is the measured at $x = 0$ feet on the either lower (0 feet, -85 feet) or upper boundary (0, 85 feet), with nodal information for the lower boundary midway point shown in Figure I-20. The excess head of 3.25 feet is effectively equal to the value of $H_m = 3.26$ feet in Table I-7. Similar to the cross-section FEM model in paragraph I-2c, flow to the well is determined by

calculating the sum of all water flux through a boundary around the modeled well location.

(b) When using a steady-state model, the relationship between flow versus time should be used to determine the sum of flow into the well given that time is theoretically infinite in this scenario, yielding a singular value. Although the method of flux measurement depends on the software used for relief well analysis, the concept is shown in Figure I–21 using a plot of total water flow across the circular well boundary. The resulting total flow out of the well of $Q_w = 421.0$ gpm is, again, very close to the value of $Q_w = 416.8$ gpm in Table I–7.

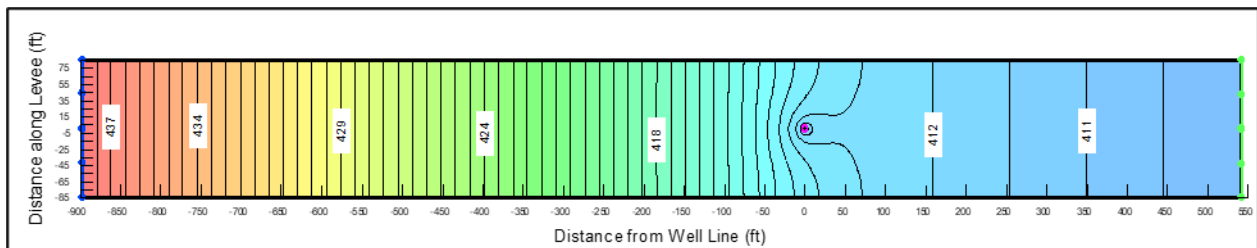


Figure I–19. Total head contours in a plan view model of the generalized levee cross section

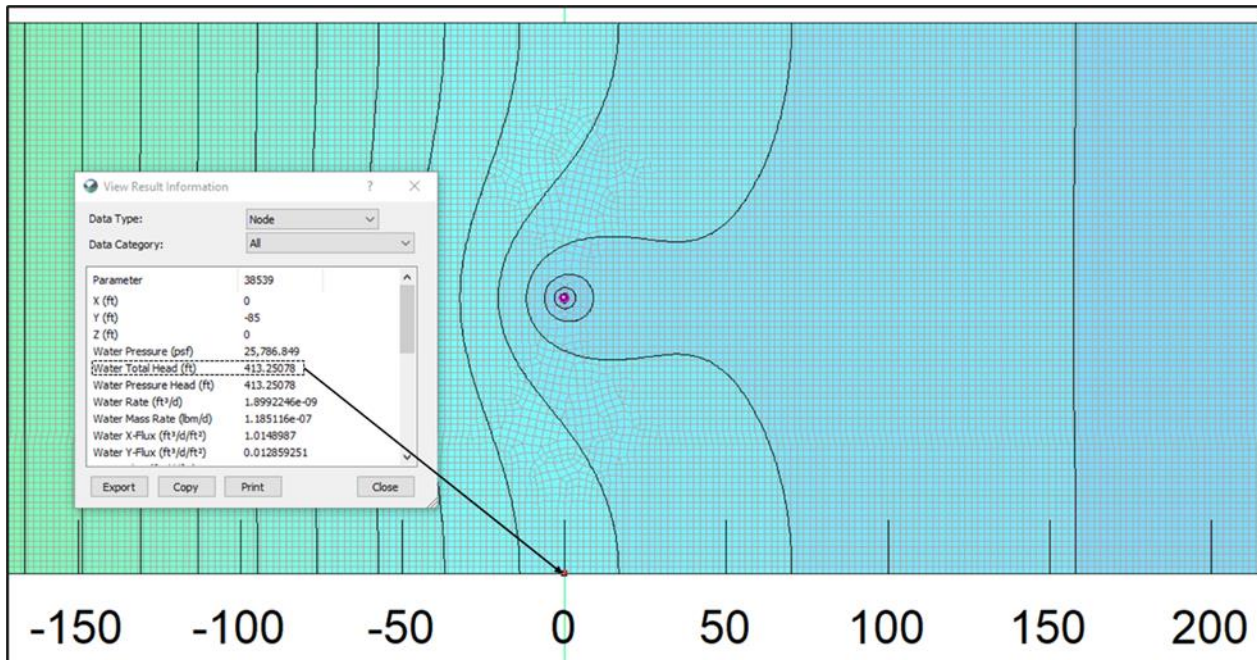


Figure I–20. Total head determined from node midway between wells

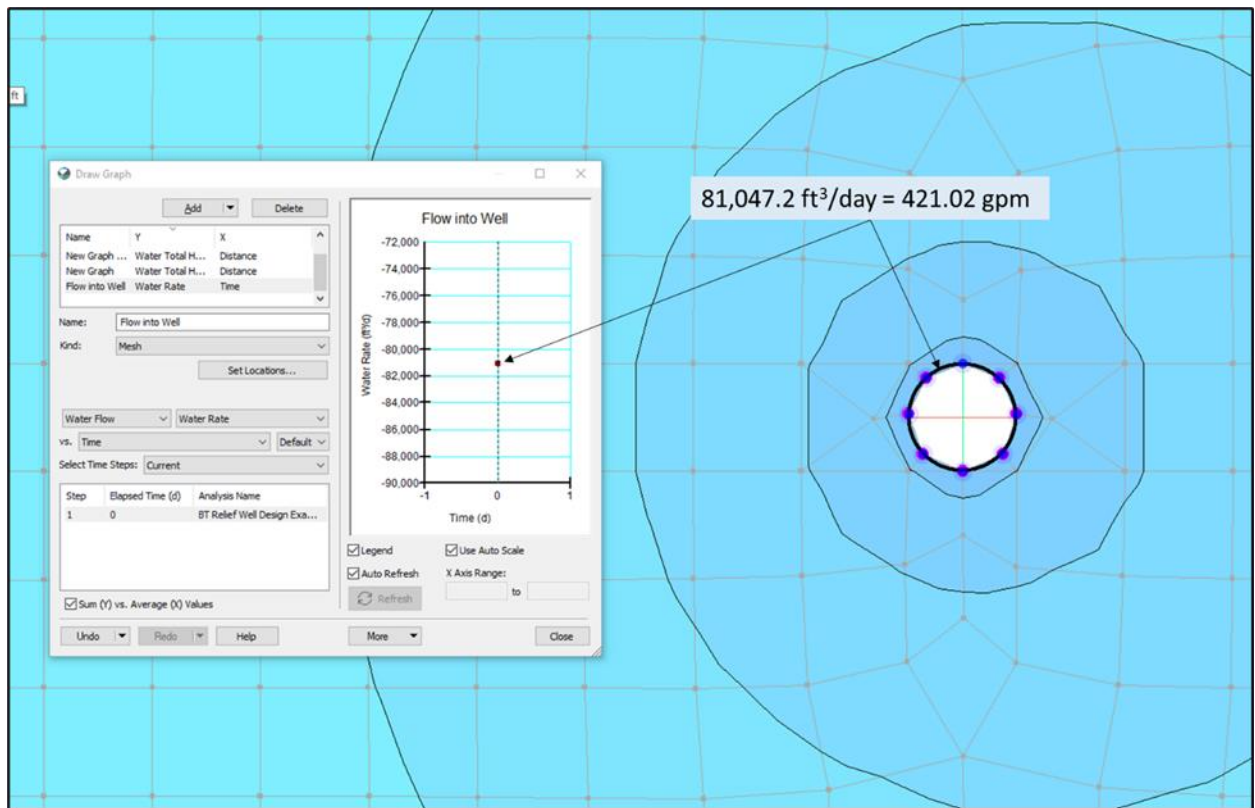


Figure I-21. Flux through a boundary used to determine flow to the well

Appendix J Application of Pumping Test Data for Relief Well Evaluation

J-1. Introduction

Appendix J demonstrates methods for the evaluation of relief well condition given pumping test data. In this appendix, common methods of analysis are presented with examples for evaluating relief well condition based on either *SCR* or relief well efficiency (*E*). Additionally, examples are presented to illustrate risk-informed decision-making in relief well evaluation. Finally, general relief well evaluation conclusions and recommendations for the application of pumping test data are presented.

a. ER 1110-2-1942 paragraph 10.a. states: “The values obtained from measurement of piezometric levels and flow quantities should be extrapolated to predict the values that would be produced by a maximum design reservoir level or river stage. If the specific capacities or the efficiencies of the wells are less than 80% of the values that were obtained at the time of installation of the wells or if these values are greater than those for which the structure was designed or, more critically, if these are above limits associated with reasonable predictions of satisfactory performance, then additional investigations and evaluations should be performed to determine the cause of the inadequacies and appropriate rehabilitation programmed. Reduced well efficiency will result in hydrostatic heads greater than those anticipated in the design. Wells that remain below 80% of original may require replacement or augmentation by additional wells to fulfill underseepage design requirements and provide satisfactory performance of the associated features during high pool level or river stage events.”

b. In practice, language in paragraph J-1a is often interpreted to mean rehabilitation or replacement for wells where pumping tests indicate that the specific capacity is less than 80% of that at the time of installation. More critically, an evaluation is often needed to determine if reduced well efficiency will result in hydrostatic heads greater than those anticipated in the design. This appendix provides examples of how differing criteria (efficiency versus *SCR*) may support evaluation.

c. A risk-based approach, according to ER 1110-2-1942 is recommended when applying pumping test data to the evaluation of relief well acceptability.

J-2. Constant rate pumping tests

The constant rate pumping test is the most common and least complex method of pumping tests for relief wells. The constant rate pumping test provides a basis for the calculation of specific capacity. The constant rate pumping test allows the estimation of aquifer properties if drawdown is recorded with time and can be further refined if adjacent piezometric levels are also measured. A single flow and stabilized drawdown are measured to calculate the specific capacity of well at a given point in time, as shown in Figure J-1. Specific capacity is calculated as the ratio of discharge flow to the measured drawdown (equation J-1):

$$SC = \frac{Q}{s_t} \quad (J-1)$$

where:

SC = specific capacity (gpm/ft)

Q = pumped flow rate (gpm)

s_t = drawdown (ft)

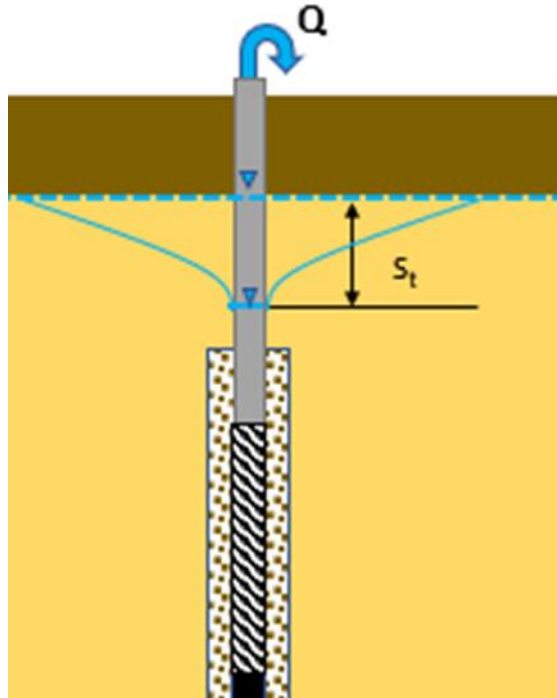


Figure J-1. Illustration of specific capacity variables

J-3. Application of constant rate test data for evaluation

Assessment of constant rate pumping test data is a straightforward process of evaluating the change in specific capacity or efficiency over time. Baseline relief well specific capacities should be established with a step drawdown pumping test, with subsequent constant rate tests used for comparison at one of the baseline pumping rates to determine the percent loss of specific capacity over time as described in Chapter 9.

J-4. Example 1: Specific capacity ratio

a. The calculated SCR is used to determine whether the historical USACE criteria for relief well testing of a recommended SCR between 80% and 100% is met. For example, a history of pumping tests for Levee District No. 1 – Relief Well 1 (RW1) are presented below in Table J-1. These pumping test data include installation test results

in 2000 and subsequent assessments on 5-year intervals, with rehabilitation of the relief well taking place in 2015.

b. The two tests in 2015 indicate pre- and post-rehabilitation results. For RW1, the baseline specific capacity, $SC_{baseline}$, is calculated as 80.6 gpm/ft, with a flow, Q , of 500 gpm and drawdown, s_t , of 6.2 feet. When RW1 is next tested in 2005, a flowrate of 500 gpm is used, and the resulting measured drawdown is 6.5 feet. Therefore, the updated specific capacity, $SC_{current}$, is 76.9 gpm/ft. The well is tested subsequently every 5 years, with the SCR falling below the required 80% threshold in 2015 to 69.7%. After rehabilitating the well, SCR returns to an acceptable value of 87.3%.

Table J-1
Levee District No. 1 constant rate pumping test results

Levee District No. 1	Date	Q (gpm)	s_t (ft)	SC (gpm/ft)	SCR
RW1	6/1/2000	500	6.2	80.6	–
	7/2/2005	500	6.5	76.9	95.4%
	7/5/2010	500	7.2	69.4	86.1%
	6/30/2015	500	8.9	56.2	69.7%
	8/10/2015	500	7.1	70.4	87.3%

J-5. Step-drawdown pumping tests

a. The step-drawdown pumping test is a common test that uses multiple flow rates, or “steps,” to assess a single relief well. Like the constant rate pumping test, if flow and drawdown are measured with time during the test and other piezometric measurements are taken, then aquifer parameters can be established. Where SCR is used as the defining evaluation criteria for relief wells, having multiple steps tested allows a wider range of comparison against previous tests. This can lead to a more reliable assessment where initial test conditions are more likely to be replicated.

b. The key difference between constant rate and step-drawdown tests for relief well evaluation is that using multiple flow rates (such as Q_1 , Q_2 , Q_3 in Figure J-2) generates a relationship that can be used to estimate a relief well’s loss components with coefficients, thus well efficiency, in addition to specific capacity. So, the step-drawdown test is often recommended for monitoring relief well performance without adding significant complexity to the pumping test. The following section will demonstrate the use of step-drawdown data to estimate efficiency using the Bierschenk (1963) method.

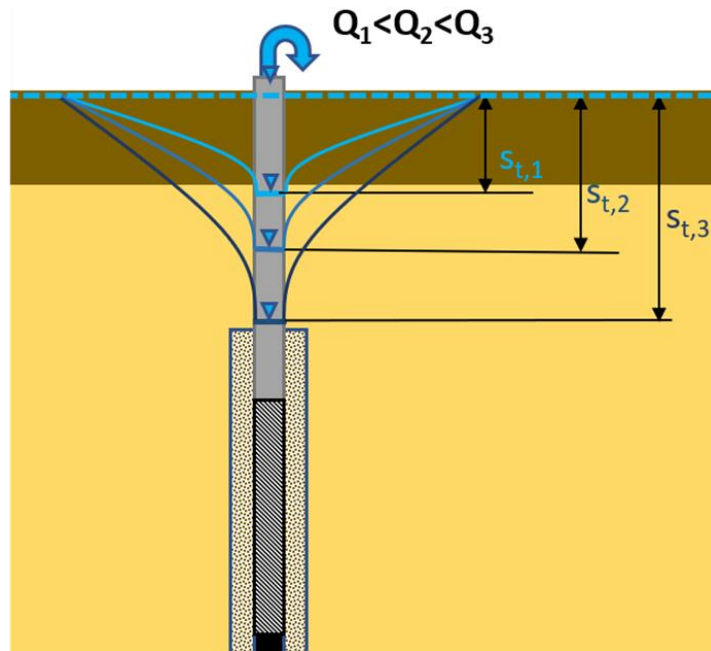


Figure J-2. Illustration of variables for step-drawdown testing

J-6. Application of step-drawdown test data for evaluation

Step-drawdown pumping test data can be used to define specific capacity, well condition, and efficiency for individual wells. Evaluation of step-drawdown pumping test data builds on the specific capacity calculations derived from measurements taken from each step of the test.

a. To qualitatively assess relief well condition and quantitatively estimate relief well efficiency, further steps are required to analyze the pumping test data. Evaluating well efficiency requires discretization of the components of an individual drawdown measurement, of which each are referred to as “head losses,” or simply “losses.” In simple terms, the head losses consist of linear, or laminar, components and a non-linear, or turbulent, component. The laminar components refer to aquifer loss, well loss, and partial-penetration loss. The turbulent component refers to the non-linear flow nearest the drawdown surface. These components are further described in Chapter 9.

b. As discussed in Chapter 9, head loss components can be simplified to consider two types of losses: aquifer losses and well losses, as shown in Figure J-3. This relationship is represented by equation J-2:

$$s_t = s_a + s_w \quad (J-2)$$

where:

s_t = total drawdown (ft)

s_a = aquifer loss (ft)

s_w = well loss (ft)

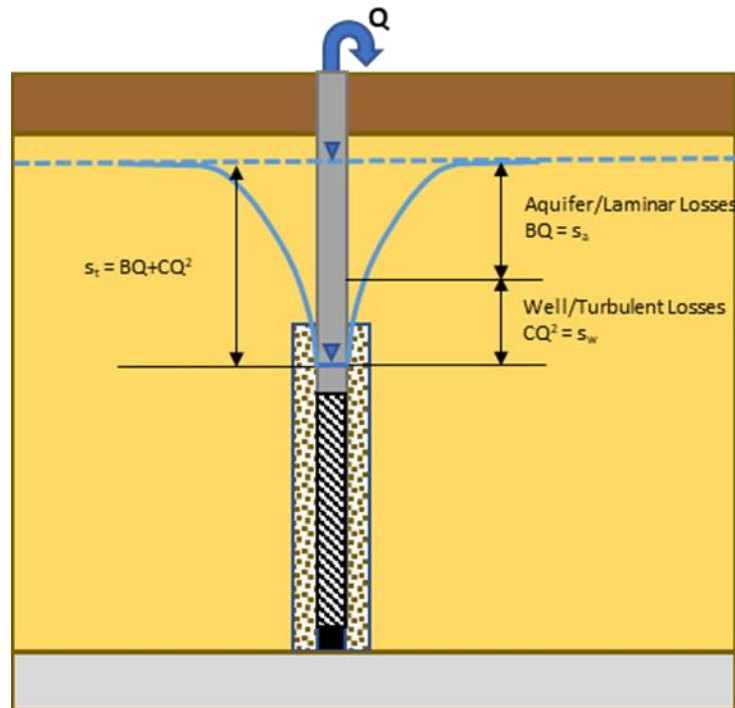


Figure J-3. Simplified head loss components

J-7. Example 2: Bierschenk method for relief well efficiency estimation

Using the Bierschenk (1963) method for analysis of a step-drawdown test, both aquifer loss, s_a , and well loss, s_w , can be determined using a linear regression of the plotted flow versus the corresponding inverse of specific capacity, allowing the calculation of the B and C coefficients. After determining the B and C coefficients, the well efficiency, E , can be calculated. The loss of well efficiency with time can be determined by comparing subsequent pumping tests to the baseline pumping tests.

a. This method assumes full penetration of the aquifer by the relief well. Consideration of effects from partial aquifer penetration are further discussed later in this section. To evaluate the condition and efficiency of a relief well using the step-drawdown method, the specific drawdown, $1/SC$ (or s_t/Q), for each step of the test must first be calculated. Once s_t/Q is known for each step, the relationship of s_t/Q versus Q is plotted, as shown, in Figure J-4. Example data for Figure J-4 are provided in Table J-2.

Table J-2
Levee District No. 1 step-drawdown pumping test data

Step	Q (gpm)	Drawdown (ft)	SC (gpm/ft)	s_t/Q (ft/gpm)
1	125	1.5	83.3	0.0120
2	250	3.3	75.8	0.0132
3	375	5.1	73.5	0.0136
4	500	7.1	70.4	0.0142
5	625	9.2	67.9	0.0147

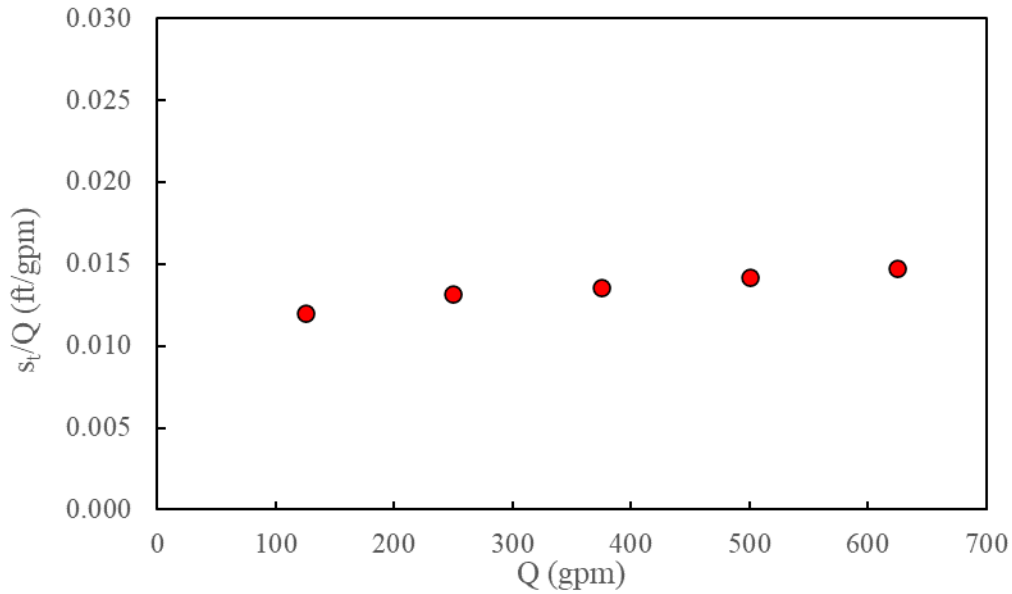


Figure J-4. Example step-drawdown base data

b. Using this data, a linear trendline is then generated to determine the slope and vertical intercept of the line passing approximately through each point, as shown in Figure J-5. From this relationship, the combined linear coefficient, B , can be estimated as the intercept of the line and the non-linear coefficient, C , can be estimated as the slope of the line as shown in equation J-3:

$$\frac{1}{S_c} = B + CQ \quad (J-3)$$

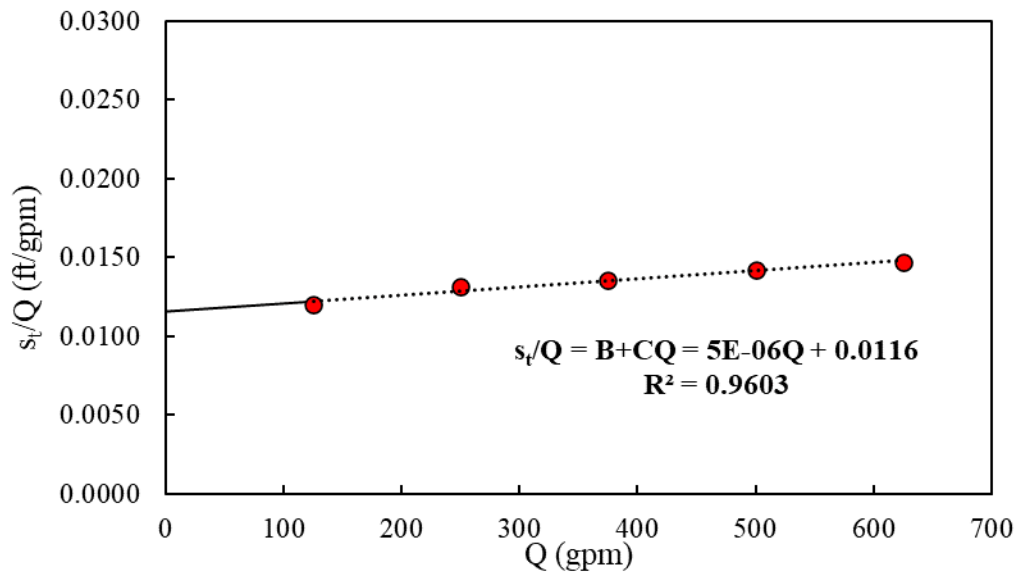


Figure J-5. Example step-drawdown base data with B - C relationship trendline

c. These terms can then be used to calculate the total theoretical drawdown and each of the two loss components, s_a and s_w , using equation J-4.

$$s_t = s_a + s_w = BQ + CQ^2 \quad (\text{J-4})$$

where:

- s_t = total drawdown (ft)
- Q = pumped flow (gpm)
- B = time dependent linear head loss coefficient
- C = time dependent non-linear well loss coefficient
- $BQ = s_a =$ aquifer loss (ft)
- $CQ^2 = s_w =$ well loss (ft)

d. With the individual well loss terms B and C now estimated, the well efficiency can be calculated with the following relationship in equation J-5:

$$E(\%) = \frac{s_a}{s_t} \times (100\%) = \frac{BQ}{BQ + CQ^2} \times (100\%) \quad (\text{J-5})$$

Note. Equation J-6 can simplify to:

$$E(\%) = \frac{BQ}{BQ + CQ^2} \times (100\%) = \frac{B}{B + CQ} \times (100\%) = \frac{(\text{Intercept})}{(\text{Intercept}) + (\text{Slope}) * Q} \times (100\%)$$

e. With the B and C coefficients known, relief well efficiency can be calculated for a target flow rate. For this example, the design flow rate is assumed to be 425 gpm at critical project flood loading, therefore:

$$E(\%) = \frac{0.0116}{(0.0116 + (5 \times 10^{-6} * 425 \text{ gpm}))} \times (100\%) = 85\% @ 425 \text{ gpm}$$

Note. The efficiency can then be compared to the baseline efficiency to determine the efficiency loss with time.

J-8. Qualitative considerations for relief well evaluation using step-drawdown data

Table J-3 presents qualitative descriptions to determine the condition of a relief well based on the non-linear well loss coefficient, C , as proposed by Kasenow (2001). C , as determined using the previously described Bierschenk (1963) method, is the slope of the s/Q versus Q line. This method serves as an additional check on relief well condition based on step-drawdown pumping test results and can be considered in combination with previously described analytical assessment. To demonstrate, if using the data from Example 2, the condition of RW1 is considered “properly constructed and developed” with C being equal to 0.000005.

Table J-3
Relation of well loss coefficient to well condition (from Kasenow 2001)

C (ft/gpm ²)	Condition of Well
< 0.000025	Properly constructed and developed
0.000025-0.000050	Mild deterioration or clogging
0.000050-0.00020	Severe clogging or deterioration
> 0.00020	Difficult to restore to original yield

J-9. Considerations for partial penetration

Where a relief well does not significantly penetrate the aquifer (less than 85 to 90%), considerations for additional well losses due to partial penetration should be considered. This is because head losses increase due to the flow dynamics of full-penetration wells versus partial-penetration wells. Where flow to full-penetration wells is generally completely horizontal to the well screen, flow to partial-penetration wells is horizontal for most of the well screen with sharper, curving flow paths near the top and bottom of the screen. This is illustrated in Chapter 9.

a. To account for the effects of partial penetration, the additional drawdown caused by the well not fully penetrating the aquifer needs to be added to the total theoretical drawdown (equation J-6):

$$s_p = s_t + s_{pp} \tag{J-6}$$

where:

- s_p = total drawdown of partial-penetration well (ft)
- s_t = total theoretical drawdown of full-penetration well (ft)
- s_{pp} = additional drawdown due to partial-penetration effects (ft)

b. The additional drawdown due to partial-penetration effects can be calculated with the following relationship developed by Huisman (1972). The Huisman relationship requires some knowledge or estimation of the aquifer hydraulic conductivity and effective thickness of the aquifer in the vicinity of the well being assessed. This method assumes a confined, generally uniform, and homogeneous/isotropic aquifer of practical infinite extent. Additionally, this method assumes steady-state flow (equation J-7).

$$s_{pp} = \frac{Q_n}{2\pi kb} \frac{(1 - \frac{L}{b})}{(\frac{L}{b})} \ln \left[\frac{(1 - \frac{L}{b})L}{r_{we}} \right] \quad (\text{J-7})$$

where:

- s_{pp} = additional drawdown from partial penetration (ft)
- Q = pumped flow rate at step n ($\frac{ft^3}{s}$)
- L = well depth (ft)
- b = aquifer thickness (ft)
- k = aquifer hydraulic conductivity (ft/s)
- r_{we} = effective well radius (ft)

c. Alternatively, the additional drawdown effects from partial penetration can be estimated using the Kozeny (1933) method where the ratio of drawdown expected for a full-penetration well to drawdown expected with a partial-penetration well, C^* , is modeled with an empirical relationship (equation J-8). If this method is used, careful evaluation of C^* is necessary. C^* should not exceed a value of 1. If C^* exceeds 1, the previously discussed Huisman method should be used to estimate additional drawdown. This method assumes the same aquifer conditions as the Huisman method described in paragraph J-9b. Additionally, this method should be limited to scenarios where the percentage of aquifer penetration is less than or equal to 50%.

$$C^* = \frac{s_{fully\ penetrating}}{s_{partially\ penetrating}} = \alpha \left[1 + 7 \sqrt{\frac{r_w}{2\alpha b}} \cos\left(\frac{\alpha\pi}{2}\right) \right] \quad (\text{J-8})$$

where:

- α = percent of aquifer penetration by well screen (such as 45% = 0.45)
- b = aquifer thickness (ft)
- r_w = well radius (ft)

d. With C^* calculated, the additional drawdown attributed to partial penetration can be calculated as equation J-9:

$$s_{pp} = s_a \left(\frac{1}{C^*} - 1 \right) \quad (\text{J-9})$$

e. Applying the additional drawdown using either method to estimate the additional contributions from partial-penetration effects, s_p is used in lieu of s_t to calculate efficiency for partial-penetration wells (equation J-10):

$$E(\%) = \frac{s_a}{s_p} \times (100\%) = \frac{s_a}{s_t + s_{pp}} \times (100\%) = \frac{BQ}{BQ + CQ^2 + s_{pp}} \quad (\text{J-10})$$

J-10. Example 3: Consideration of partial penetration – Levee District No. 1

In this example, the Huissmann and Kozeny methods are applied to the RW1 step-drawdown test data from Example 2. Figure J-6 shows an example cross section for evaluation of partial-penetration effects.

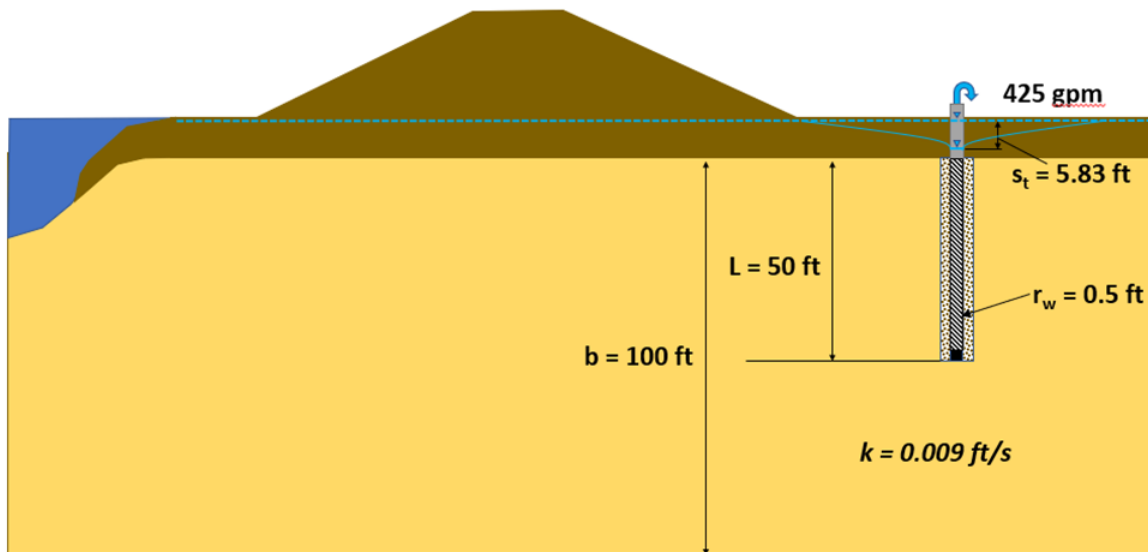


Figure J-6. Typical cross section for Example 3

a. First, well efficiency in this scenario is calculated using the Huisman method. From equation J-7 we know that:

$$s_{pp} = \frac{Q_n}{2\pi kb} \frac{(1 - \frac{L}{b})}{(\frac{L}{b})} \ln \left[\frac{(1 - \frac{L}{b})L}{r_w} \right]$$

$$s_{pp} = \frac{425 \text{ gpm}}{2\pi(0.009 \frac{\text{ft}}{\text{s}})(100 \text{ ft})} \frac{(1 - \frac{50 \text{ ft}}{100 \text{ ft}})}{(\frac{50 \text{ ft}}{100 \text{ ft}})} \ln \left[\frac{(1 - \frac{50 \text{ ft}}{100 \text{ ft}}) 50 \text{ ft}}{0.5 \text{ ft}} \right] = 0.66 \text{ ft}$$

$$E(\%) = \frac{s_a}{s_t + s_{pp}} = \frac{BQ}{BQ + CQ^2 + s_{pp}} = \frac{4.93 \text{ ft}}{4.93 \text{ ft} + 0.9 \text{ ft} + 0.66 \text{ ft}} = 0.76 \text{ (76\%)}$$

Using the Kozeny method, we can calculate efficiency with equation J-9:

$$C^* = \frac{s_{t, \text{fully penetrating}}}{s_{t, \text{partially penetrating}}} = \alpha \left[1 + 7 \sqrt{\frac{r_w}{2 \alpha b}} \cos \left(\frac{\alpha \pi}{2} \right) \right]$$

Therefore,

$$C^* = 0.5 \left[1 + 7 \sqrt{\frac{0.5 \text{ ft}}{2(0.5)(100 \text{ ft})}} \cos \left(\frac{0.5\pi}{2} \right) \right] = 0.75$$

$$s_{pp} = s_a \left(\frac{1}{C^*} - 1 \right) = (BQ) \left(\frac{1}{C^*} - 1 \right) = (4.93 \text{ ft}) \left(\frac{1}{0.75} - 1 \right) = 1.64 \text{ ft}$$

$$E(\%) = \frac{s_a}{s_t + s_{pp}} = \frac{BQ}{BQ + CQ^2 + s_{pp}} = \frac{4.93 \text{ ft}}{4.93 \text{ ft} + 0.9 \text{ ft} + 1.64 \text{ ft}} = 0.66 \text{ (66\%)}$$

b. Given the example pumping test data, with RW1 penetrating 50% of the aquifer, efficiency is estimated to be between 66% and 76%. Note that when using the Kozeny method, well penetration ratio (L/b in this formulation) should be limited to 50%. For penetrations exceeding this ratio, Huisman should be used. This example illustrates that care should be used when choosing the appropriate method for analysis. Furthermore, this example shows the need for accurate parameter estimation when conducting relief well analysis.

J-11. Distance-drawdown method

The distance-drawdown method employs multiple piezometric readings taken during a pumping test, either constant rate or step-drawdown, to estimate relief well efficiency. This method can be used only where reliable piezometric data can be obtained during the pumping test (observation wells, static bodies of water). As the name suggests, distance and drawdown are the critical components for analysis. This includes drawdown depths at various distances from the well, and an estimate of the distance where drawdown from resulting from the pumped well is zero ($s_{t,4}$ in Figure J-7).

Example 4 illustrates how the distance-drawdown method can be used to estimate relief well efficiency.

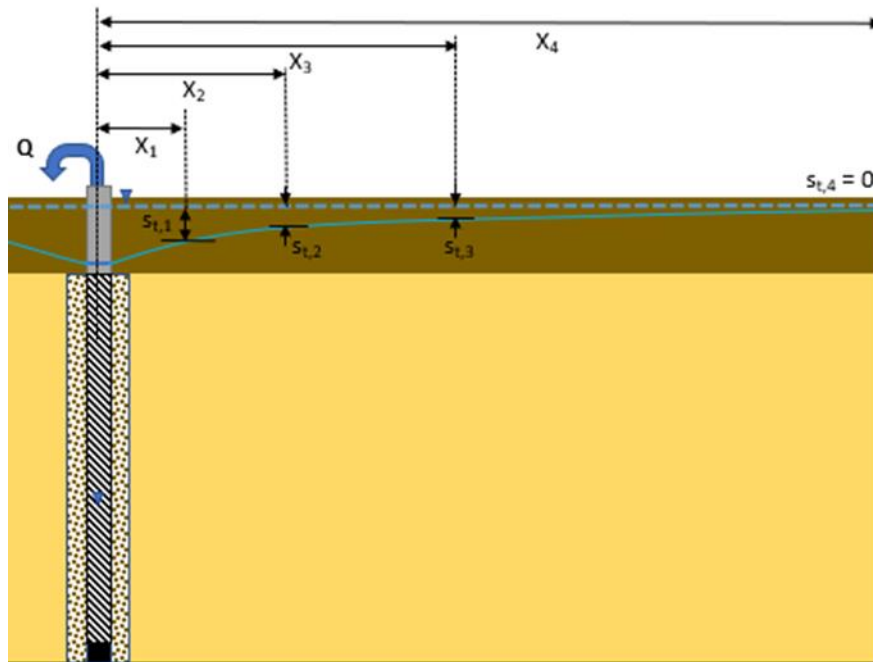


Figure J-7. Illustration of distance-drawdown method

J-12. Example 4: Distance-drawdown method for efficiency calculation

Levee System No. 1, RW1 is tested during installation, with piezometric readings take at three adjacent locations (at distances X_1 , X_2 , and X_3). The static water level is assumed at a distance 2,300 feet from the well being tested. Table J-4 summarizes drawdown readings at the series of locations. The flow rate during the pumping test for RW1 was 500 gpm and the measured drawdown inside the well was 7.1 feet.

Table J-4
Distance-drawdown measurements: Relief Well 1

Point	Distance, X_i (ft)	s_t (ft)
0	0	7.1
1	25	3.4
2	100	2.4
3	500	1.1
4	2,300	0.0

a. The first step in evaluating the distance-drawdown data is to plot distance (x-axis) versus drawdown (y-axis), where distance is represented on a log scale. For the given pumping test, this plot is shown in Figure J-8. Using this method, drawdown components can be estimated, where total drawdown is measured in the well ($s_{t,0}$) and

theoretical aquifer drawdown, s_a , is estimated to be the Y-intercept of the lognormal regression equation. With this in mind, we know that: $s_a = 5.85$ feet and $s_t = 7.10$ feet. Using equation J-5, we can estimate the well efficiency with the following:

$$E(\%) = \frac{s_a}{s_t} \times (100\%) = E(\%) = \frac{5.85 \text{ ft}}{7.10 \text{ ft}} \times (100\%) = 82.4\%$$

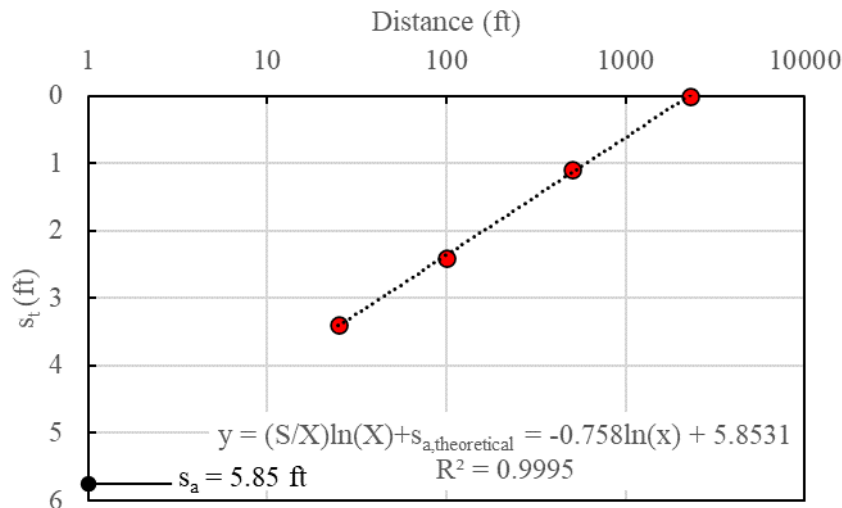


Figure J-8. Distance-drawdown plot

b. Additionally, Kasenow’s method for qualitative assessment of well condition can be used where C is assumed to be equal to s_w/Q^2 . Knowing $s_w = s_t - s_a$, we can calculate C as:

$$C = \frac{s_w}{Q^2} = \frac{7.1 \text{ ft} - 5.85 \text{ ft}}{(500 \text{ gpm})^2} = 0.000005$$

Where the calculated C indicates that the well is “properly constructed and developed” (Table J-3).

J-13. Risk-informed decision-making for relief well management

Various methods of relief well condition and efficiency evaluation have been presented. These methods may be used in determining well acceptance (requiring 80% efficiency or SCR); however, risk-informed decision-making may also be applied using the calculated efficiency values to create a more project-specific criteria. Two examples are presented that show two potentially different outcomes when looking at relief well efficiency through a risk-based lens. Each example considers a typical cross section of interest that is assessed for varying loading conditions and efficiencies for a levee system whose relief well is evaluated using infinite well system methods. From this level

of analysis, efficiency values from pumping tests can be used to make relief well maintenance or management decisions.

J-14. Example 5: Upper Mississippi levee system parametric study

A typical regional cross section was used to show the general effects of relief well efficiency on the effective stress factor of safety. The typical cross section for this study, shown in Figure J-9, was developed for a parametric study using the following assumed constraints: 75% aquifer penetration; aquifer hydraulic conductivity of 0.00492 ft/s (1500×10^{-4} cm/second); 8" inner diameter well; 100 feet spacing between wells; 5 feet landside clay blanket thickness, 50 feet aquifer depth.

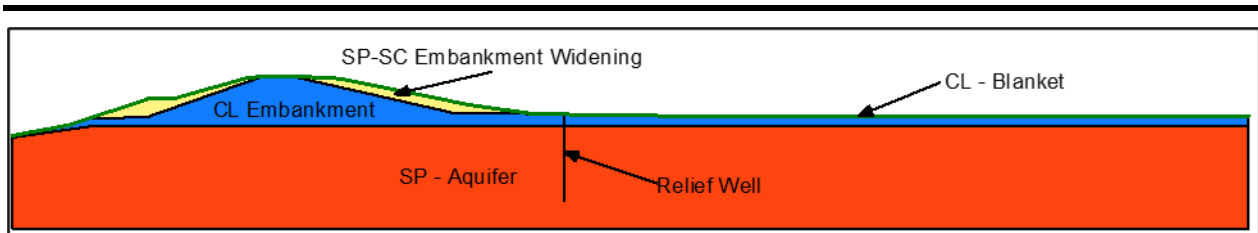


Figure J-9. Typical cross section – Upper Mississippi levee example

a. Detailed underseepage analysis of this cross section was completed for hydraulic loading events ranging from a 10-year (10% annual exceedance probability [AEP]) event to the top of levee loading condition, with results presented in Table J-5 and Figure J-10. This study accounts for relief well efficiencies ranging from 0% (no well present) to 100% (a well with no head losses). Each condition analysis presents a vertical gradient factor of safety, or the factor of safety against the initiation of failure via piping. It should be noted that no well is installed at the 100% efficiency condition due to various unavoidable head losses such as friction loss from a riser pipe or entrance loss at the well screen. Therefore, the 100% efficiency is theoretical, assuming for this example a minimum head loss.

Table J-5
Summary of factors of safety (Example 5)

Top of Levee Loading							
Efficiency	100%	90%	80%	75%	50%	25%	0%
H_m (ft)	1.75	2.22	2.69	2.93	4.12	5.30	6.49
$FS_{vg} \approx$	2.38	1.87	1.54	1.42	1.01	0.78	0.64
0.2% AEP							
Efficiency	100%	90%	80%	75%	50%	25%	0%
H_m (ft)	1.66	2.08	2.50	2.71	3.75	4.80	5.84
$FS_{vg} \approx$	2.50	2.00	1.66	1.54	1.11	0.87	0.71
1% AEP							
Efficiency	100%	90%	80%	75%	50%	25%	0%
H_m (ft)	1.58	1.95	2.32	2.51	3.43	4.35	5.27
$FS_{vg} \approx$	2.62	2.13	1.79	1.66	1.21	0.95	0.79
2% AEP							
Efficiency	100%	90%	80%	75%	50%	25%	0%
H_m (ft)	1.45	1.74	2.02	2.17	2.88	3.59	4.31
$FS_{vg} \approx$	2.86	2.39	2.05	1.92	1.44	1.16	0.96
10% AEP							
Efficiency	100%	90%	80%	75%	50%	25%	0%
H_m (ft)	1.16	1.39	1.62	1.73	2.29	2.86	3.43
$FS_{vg} \approx$	3.57	2.99	2.57	2.40	1.81	1.45	1.21

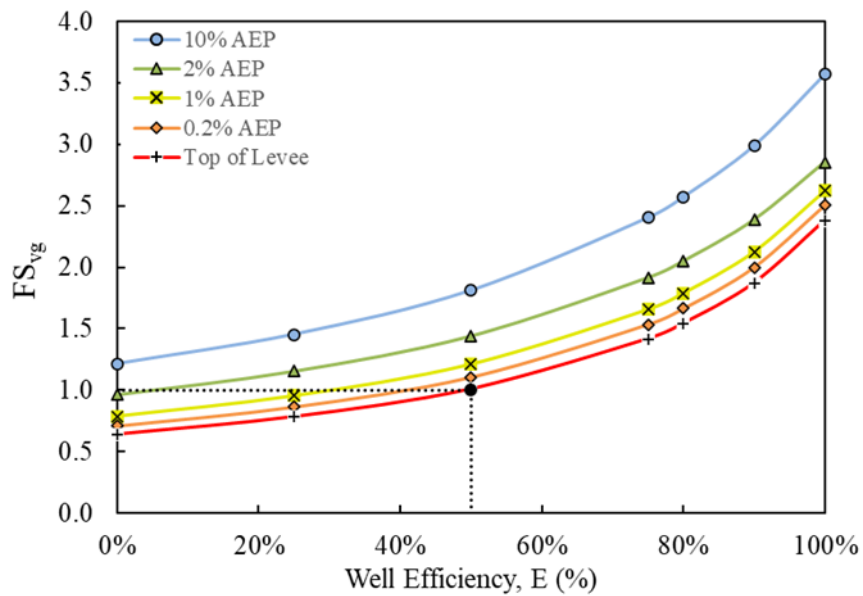


Figure J-10. Factor of safety (heave) versus well efficiency (Example 5)

b. Where the relief well is operating at 80% efficiency, the minimum factor of safety is 1.54 for the top of levee condition. This condition would likely be accepted in design, depending on the designer's interpretation of acceptable factors of safety. However, when considering the levee system with a risk-based approach, the probability of failure initiation increases to a likely scenario where the factor of safety decreases below a level of satisfactory performance. That is, initiation of the piping failure mode becomes likely where the factor of safety is below 1.0 for an intact blanket.

c. For the presented example, this occurs at top of levee loading where the relief well efficiency is less than 50%. Therefore, it may be practical to consider an acceptable relief well efficiency below 80% for this location. General consideration should be given to the potential of unknown blanket defects. Preferably determined through site-specific risk assessment, this example might warrant an acceptable minimum efficiency between 50% and 80%.

J-15. Example 6: Sid Simpson Levee System – South Beardstown segment

A typical cross section for the South Beardstown segment of the Sid Simpson Levee System was used to best show the general effects of relief well efficiency on the effective stress factor of safety. The typical cross section for this study, shown in Figure J-11, assumed constraints: 60-foot well screen, penetrating ~92% of the aquifer; Aquifer hydraulic conductivity of 0.0002 ft/s (60×10^{-4} cm/second); 12" inner diameter well; 200-foot well spacing; 5-foot landside clay blanket thickness, 77-foot aquifer depth.

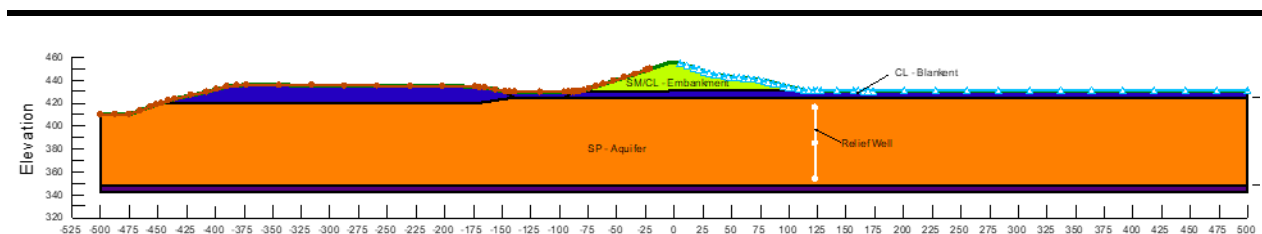


Figure J-11. South Beardstown typical section

a. A detailed underseepage analysis of this cross section was completed for hydraulic loading events ranging from an event loading 50% of the levee (elevation 436.3 feet) to the maximum theoretical loading, which is approximately 90% of the levee (elevation 452.6 feet). At this location, maximum loading is dictated by the incipient overtopping location lower in the system. This is a key consideration in assessing the range of loading for this type of analysis when using a risk-based approach. Results are presented in Table J-6 and Figure J-12. This example accounts for relief well efficiencies ranging from 50% to 100%. Each condition analysis presents a vertical gradient factor of safety.

Table J-6
Summary of factors of safety (Example 6)

90% Loading (Maximum Loading Case)						
Efficiency	100%	90%	80%	50%	25%	0%
H_m (ft)	5.15	6.06	6.96	9.67	11.93	14.20
$FS_{vg} \approx$	1.67	1.42	1.24	0.89	0.72	0.61
79% Loading (Design Case)						
Efficiency	100%	90%	80%	50%	25%	0%
H_m (ft)	4.65	5.42	6.20	8.52	10.45	12.38
$FS_{vg} \approx$	1.85	1.59	1.39	1.01	0.82	0.70
50% Loading						
Efficiency	100%	90%	80%	50%	25%	0%
H_m (ft)	3.39	3.83	4.27	5.60	6.71	7.81
$FS_{vg} \approx$	2.54	2.25	2.02	1.54	1.28	1.10

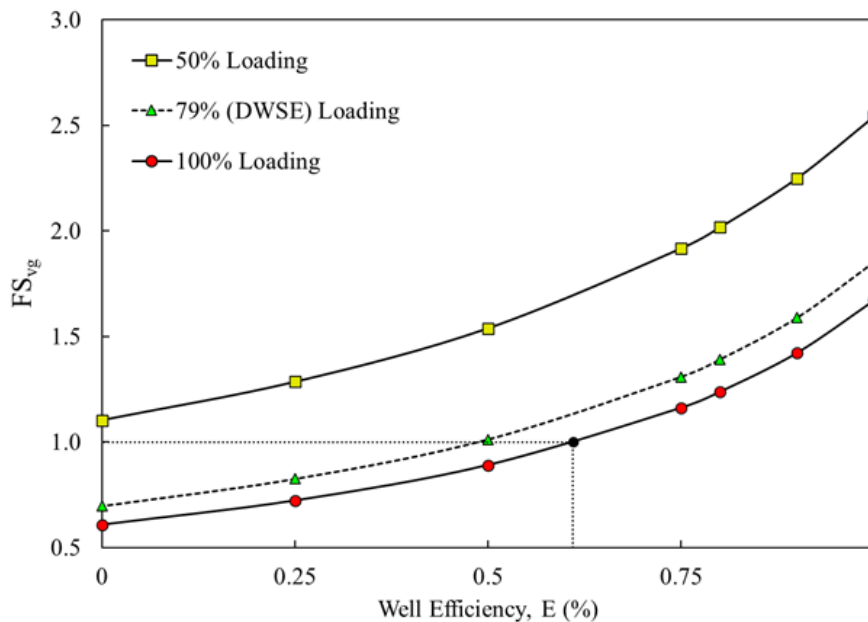


Figure J-12. Factor of safety (vertical gradient) versus well efficiency (Example 6)

b. For this example, where the relief well is operating at 80% efficiency, the minimum factor of safety is 1.24 for the maximum loading condition. This condition would likely not be accepted in design, and spacing of the relief wells would likely be reduced. However, when considering the levee system with a risk-based approach, the probability of initiation increases to a likely scenario where the factor of safety decreases below a level of satisfactory performance. That is, initiation of the piping failure mode becomes likely where the factor of safety is below 1.0 for an intact blanket.

c. For the presented example, this occurs at maximum levee loading where the relief well efficiency is less than 61%. It may be practical to consider an acceptable relief well efficiency between 61% and 80% for this location, with an increase over to minimum efficiency added to the $FS = 1.0$ condition to account for potential unknown blanket defects through site-specific risk assessment.

J-16. Relief well condition and testing frequency requirements

The risk of heave and formation of sand boils (piping) increases when hydrostatic pressures are not reduced, which can lead to failure as a levee becomes unstable. Relief wells in poor condition that show signs of being incapable of relieving excess hydrostatic pressures that may lead to unsatisfactory performance will likely need to be re-tested, rehabilitated, or replaced.

a. *Data considerations for condition assessment.* A risk-informed approach to relief well management should consider all available information when making engineering decisions. When assessing well condition and maintenance options, it is important to consider not only design history and updated analysis, but also past performance. The tools available to assess various systems have improved with the evolution of practice; however, the observational method still holds significant value. Relief well evaluations should consist of the following items where possible.

(1) *Calculation of specific capacity and/or well efficiency from pumping test data.* Well performance and changes with time should be assessed using the method most suitable for a given project or reach.

(2) *Analysis to determine the effect of reduced well performance on seepage risk.* Generally, the SCR or ratio of current efficiency to baseline efficiency is assumed to directly reduce the original design drawdown (BT and 2D FEM) or the original design well flow (3D FEM or image well BT adaptation). This effort can be scaled to conditions of concern for a given project or reach. For example, if there is only one load case that is concerning, then only one load case might need to be assessed.

(3) *Observations of past performance.*

(a) Qualitative observation data can help inform and/or interpret analysis. Since relief well performance tends to decrease with time, recent observational data is more valuable than historical observational data. Further, performance under loads nearer the design load require less data extrapolation than performance under low loads. Knowing that no issues were noted during a particular flood event can help build confidence (or skepticism) in analysis. Flow rates from wells and piezometric readings adjacent to or between wells can help provide calibration of analysis.

(b) Analysis of relief wells often leads to critical total head estimates at locations between wells (midpoint between wells), so having measurements at these locations during flood events can be the most valuable assessment of well condition as it affects a given system. As such, it is recommended that newly installed relief well systems

include appropriate instrumentation (piezometers) installed along the well system at the midpoint between wells where possible. Often, this includes wells near the middle and ends of the system, and potentially at different depths in the aquifer. Additional piezometers beyond the extents of the system, at a distance of one-half of the spacing of the nearest two wells, should be considered to evaluate end effects.

b. Pumping test frequency. Pumping tests should be performed at intervals of no greater than 5 years between tests to assess relief well performance. When using pumping tests to assess relief well performance, conditions of the baseline test should be replicated where possible for future tests, especially if using only a single flow rate (constant rate pumping test). The pumped flow rate and groundwater boundary conditions are primary drivers in the comparison of tests from one cycle to the next and should match previous tests where possible. Even though groundwater boundary conditions cannot be controlled, an effort should be made to conduct pumping tests at normal river conditions. Replication of baseline testing conditions allows a more reliable comparison of conditions.

Appendix K Numeric Analyses of Physical Tank Tests

K-1. Introduction

a. A series of axisymmetric and plan view FEM models were performed with SeepW (GeoSlope 2007) and compared with results of physical tank tests. The original purpose of these models was to better understand friction or head loss from flow through well screens and the surrounding filter.

b. These simple models demonstrate how to perform axisymmetric and plan view FEM models. Axisymmetric models lend themselves to pumping tests of a single well. Plan view models are used to model full-penetration wells. Practitioners that started with these examples were able to extend the concepts to other applications, both with and without relief wells to evaluate problems that many thought required more complex 3D FEM modeling.

c. As mentioned in Appendix C and described in EM 1110-2-1901, one of the underlying assumptions behind Darcy's Law to enable seepage modeling is that flow through soils is laminar. This appendix demonstrates how turbulence may be included in seepage analyses using permeability correction factors. One complication for this approach is a reduction in filter permeability due to turbulence would result in higher head loss and gradient in the filter. The higher gradient suggests more turbulence in the region around the screen and this may be an iterative process.

d. There is more potential for head loss with screens that have fewer, discrete slots than the continuous, wire-wound, stainless-steel slots commonly used today. Flow has a slightly larger path to the slot and the convergence of flow to discrete slots could lead to turbulence. However, the physical model tests show head loss in both older wood-stave and newer stainless steel well screens to be small. Flow appears to remain laminar and the response linear with flow rates typical for relief wells.

K-2. Background

a. USACE has been interested in well head loss for decades. Although head loss through the screen itself is negligible, head loss could occur as radial flow to the well, resulting in increasing velocity as the seepage flow approaches the well screen. There may be additional head loss with legacy wood-stave well screens with relatively small open area compared with modern, continuous-wire, stainless steel screens. Concentrated flow to a discrete number of slots in wood-stave well screens may result in turbulence when the flow changes direction to enter the well screen openings (Smith 1998–2015). Turbulence adds resistance to flow through soil, effectively reducing soil transmissivity or permeability. Turbulence increases with increasing velocity of flow to the well.

b. Lab testing to quantify head losses through well screens was performed to support TM 3-341 (USACE 1952); however, very little information is available from the original tank tests. From lab tests performed as part of that TM, a flow rate of 5 gpm/ft

resulted in head loss through the screen of 0.15 foot, and through the filter and screen of 0.24 foot. After surging, head loss through the well for the same flow rate reduced to 0.05 foot and 0.13 foot. These results support the statement in Chapter 9 that initial head loss amounted to only 0.1 to 0.25 foot for a flow through the screen of 10 gpm per foot of screen. This range is based on field piezometer measurements with wood-stave wells and initial entrance losses for wire-wrapped screens should be even less.

c. Physical model testing of wood-stave relief well screens at the WES and in the field in the 1940s identified well losses in various types of well screen (wood, brass, perforated corrugated metal pipe, perforated steel) and the filter pack surrounding the well screen. Subsequent tests completed by Tulane University and others on modern well screen (continuous-wrap stainless steel) measured losses in the surrounding filter pack and found very little head loss through the well screen.

d. To better understand head losses, axisymmetric and plan view FEM model results of tank tests were performed with SeepW (GeoSlope 2007). FEM model results supplement physical model test results and demonstrate where turbulent flow could result in a significant source of well loss in the filter pack near the cylindrical surface of the well screen. Although Darcy's Law and the Laplace Equation assume laminar flow, turbulence can be represented in FEM models using charts based on testing by Cedergren (1989) that are also presented in EM 1110-2-1901. These charts link turbulent flow to effective particle size and either flow velocity or gradient, and are used to reduce the permeability in portions of the gravel pack. The FEM analyses presented in this appendix demonstrate where turbulent seepage flow into a relief well screen could result in higher well head loss.

K-3. Tank test apparatus

a. The tank shown in Figure K-1 was used on at least three separate occasions to test various well screen and filter combinations as documented in three separate reports: TM 3-341 (USACE 1952), Mitronovas (1968), and Hadj-Hamou et al. (1990) performed at Tulane University.

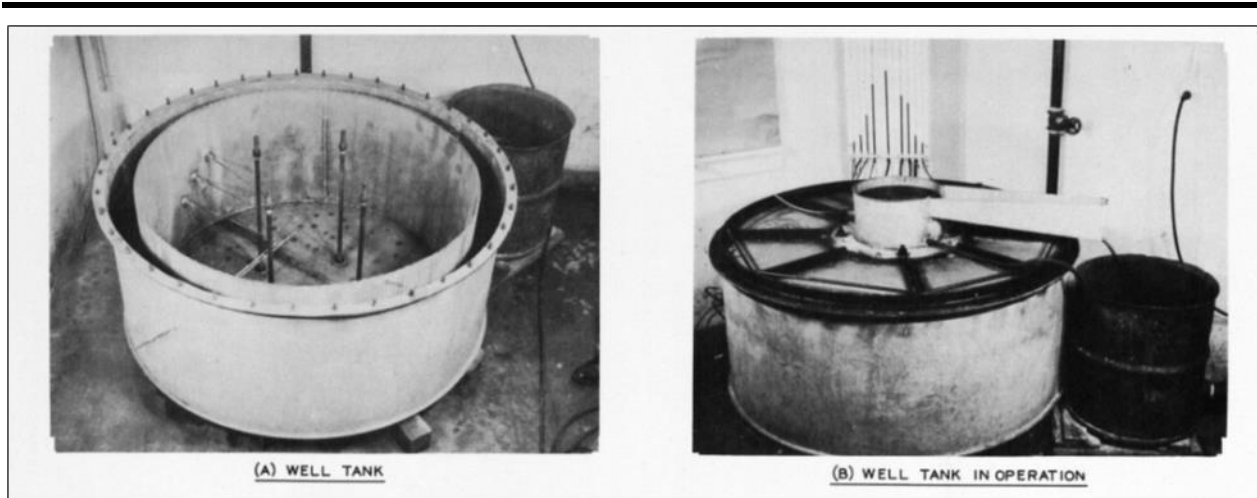


Figure K-1. Tank used for relief well tests per Technical Memorandum TM 3-341 (USACE 1952)

b. TM 3-424 (USACE 1956a) describes the tank tests in five pages of text in Volume 1, Appendix A. This gives general dimensions and a summary of the tank tests that mostly references Plate A-1. Plate A-1 includes photos of the tank, included here as Figure K-1 and Figure K-2, a grain size curve for sand and filter material used in the test, and a plot of head loss versus well flow. The testing apparatus was used to test a base sand and filter for a 2-foot length of well screen placed as shown in Figure K-2. It appears the four steel rods used to hold the well during placement of sand and filter in Figure K-2 are also used to secure the lid to the apparatus in Figure K-1(B).



Figure K-2. Tank used for relief well tests per Technical Memorandum TM 3-341 (USACE 1952)

c. Mitronovas (1968) included a detailed description of his testing that modified the tank to accommodate an 8-inch ID wood-stave well screen, as opposed to the original 6-inch ID. The side-view cross section of the testing apparatus shown in that report is included here as Figure K-3. Hadj-Hamou et al. (1990) adapted the tank again to test two types of stainless-steel well screen and also included a side view cross section of the tank, shown here as Figure K-4.

d. Although these three references are separate, stand-alone documents, all three together help to understand full details of the test procedure. Hadj-Hamou et al. (1990) list additional details of their testing, including a calculation of the effective well radius for each screen and filter combination they investigated. The effective radius is that radius for which there would be no hydraulic entrance loss, and in practice is taken to be the outside radius of the well screen plus one-half the thickness of the filter.

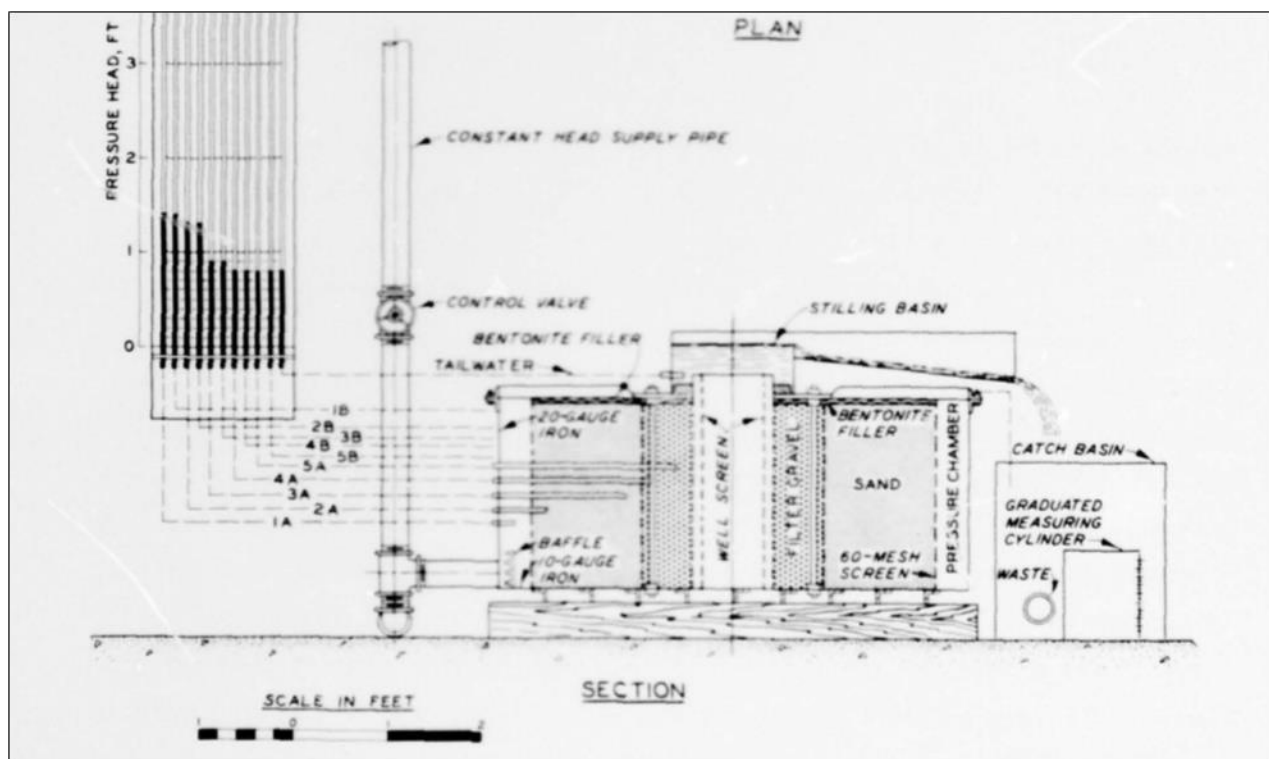


Figure K-3. Testing apparatus (Mitronovas 1968)

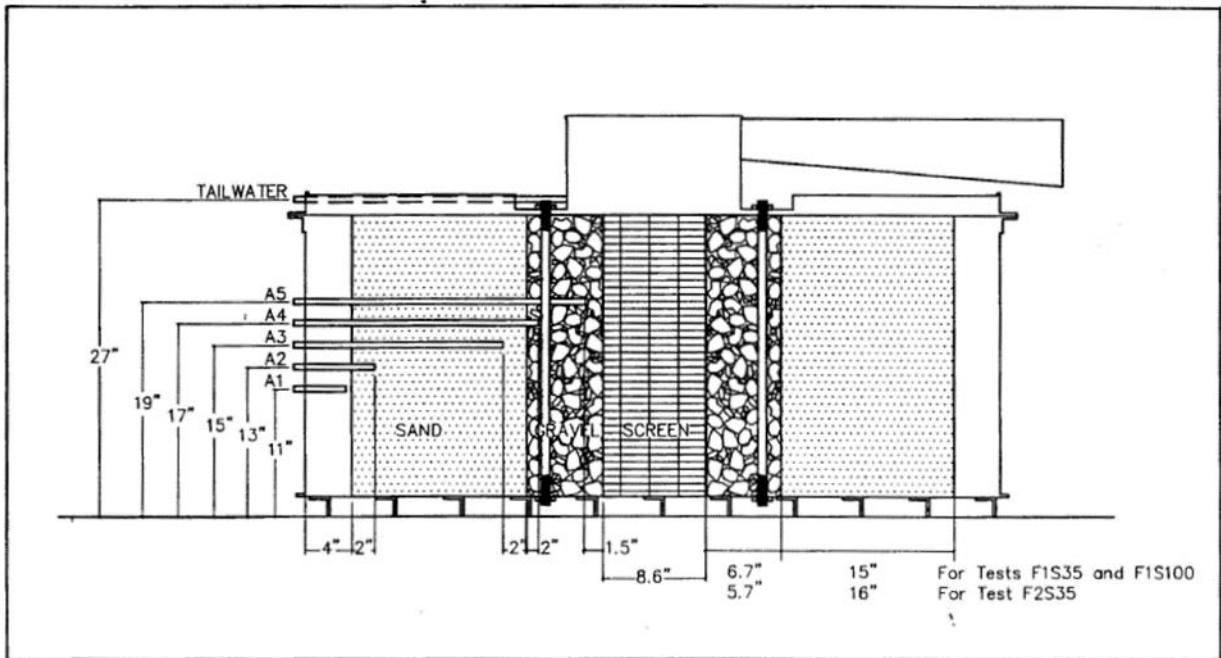


Figure K-4. Testing apparatus showing piezometer elevations (Hadj-Hamou et al. 1990)

K-4. Comparison of tank tests performed in 1968 and 1988

a. Tests on wood-stave well screens described in Mitronovas (1968) are very similar to tests performed with stainless steel well screens in Hadj-Hamou et al. (1990). Both series of tests included a “typical” filter sand used in the Mississippi Valley Division, and the two filters had nearly identical grain size distribution. A comparison of these tests showed more head loss occurred in the filter for the stainless steel well, which was not the expected result. The head loss measured across the filter and screen in the 1968 tests are very small. However, the 1988 tests had a slightly coarser base sand, resulting in a larger flow rate for a given differential head with a high portion of the head loss occurring in the filter. Differences in these tests are described in detail later in this appendix.

b. Results in Mitronovas (1968) are presented in tabular form along with plots of flow versus head loss and plots with head versus radial distance from the well, which were used to back-calculate permeability of the sand and filter based on the head loss measured across each region. Results are presented without surging and after each of three rounds of mechanical surging.

c. Hadj-Hamou et al. (1990) replicated earlier research and used an 8.5-inch diameter stainless steel well screen rather than 10.25-inch OD wood-stave well screen used by Mitronovas (1968). The radius of the filter pack was reduced from 11.5 inches to 11 inches. The grain-size distribution for filter 1 (labeled F1 with either the S35 or S100 screen) in the tests is nearly identical to filter 1 from Mitronovas (1968). The base sand in the 1988 testing is slightly coarser than the earlier testing, although the

permeability back-calculated by the authors of this later testing is slightly lower (107 x 10⁻⁴ cm/second versus 150 x 10⁻⁴ cm/second).

d. Both studies used the same equation to relate flow, permeability, and head loss over distance between piezometers to calculate permeability. Hadj-Hamou et al. (1990) present the equation for radial flow to the well, included here as equation K-1. Mitronovas (1968) rearranged this equation to calculate *k* in the form presented here as equation K-2.

$$Q = \frac{2\pi k D (H_1 - H_2)}{\ln\left(\frac{r_1}{r_2}\right)} \quad (\text{K-1})$$

$$k = \frac{Q \ln\left(\frac{r_2}{r_3}\right)}{2\pi D (h_2 - h_3)} \quad (\text{K-2})$$

e. Due to many factors, it is difficult to make conclusions about head losses due to turbulent flow by comparing the 1968 tests on a wood-stave well screen to the 1988 tests on a stainless-steel well screen. The focus of these earlier works was on the migration of sand into and through the filter and screen, and both sets of authors were interested in the potential change in filter permeability that would result from changes to sand and filter gradation. Any investigation into turbulent flow into the well screen requires an understanding of the migration of finer particles toward the well screen because turbulent flow and particle migration would each result in non-linear head loss across the filter. Hadj-Hamou et al. (1990) is not included in the FEM modeling below because the physical model experienced a significant amount of seepage between the soil and the tank lid.

K-5. SeepW models of tank tests

a. To better understand head losses through both filter packs and well screens, axisymmetric and plan view FEM models of tank tests were performed with SeepW using the information provided in Mitronovas (1968). The axisymmetric modeling is described in paragraph K-6 and the plan view modeling is described in paragraph K-7.

b. Figure K-5 and Figure K-6 show the plan view and the cross-sectional side view used for FEM SeepW models, and material properties for both models are indicated on the axisymmetric mesh in Figure K-7. As shown in Figure K-8, Figure K-9, and Figure K-10, flow and head loss across the Test 1 sand filter in Mitronovas (1968) are nearly identical to both axisymmetric and plan view models. Given that the permeability values were calculated from those tests, this is expected.

c. The plan view SeepW model is shown in Figure K-9. Figure K-10 is one of several similar plots of head loss versus distance in Mitronovas (1968) overlain with SeepW results shown in red. The flow of 8.58 gpm/ft in the 1968 lab test is shown in Figure K-10, and matches well with 8.65 gpm/ft in SeepW. The total slot area is 65.8 in²

per 24 inches, so $v_{\text{slot}} = 0.084$ ft/s. This velocity meets the general guideline that the open area of a well screen should be sufficiently large to maintain a low entrance velocity of less than 0.1 ft/s.

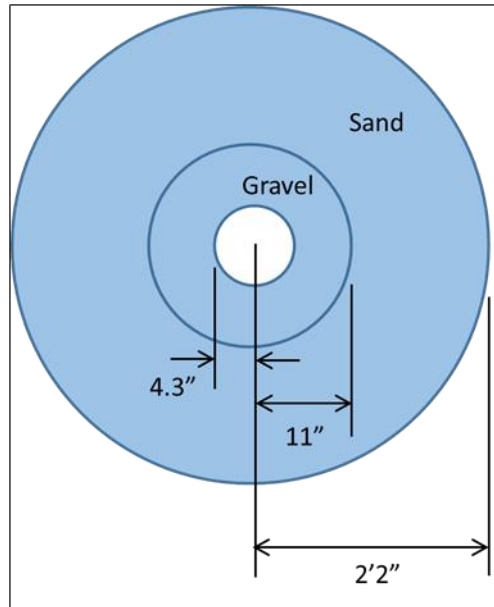


Figure K-5. Plan view of Mitronovas (1968) model used in the finite element model

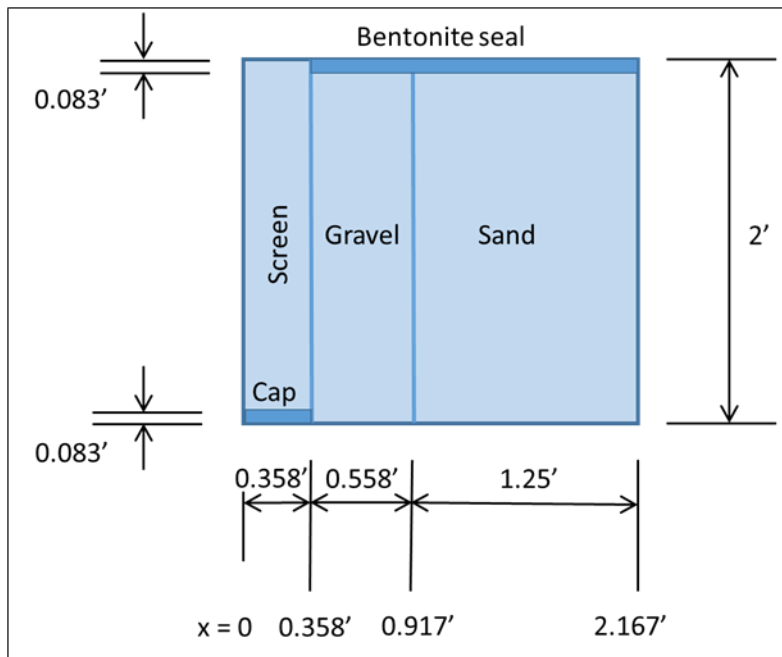


Figure K-6. Axisymmetric view of Mitronovas (1968) model used in the finite element model

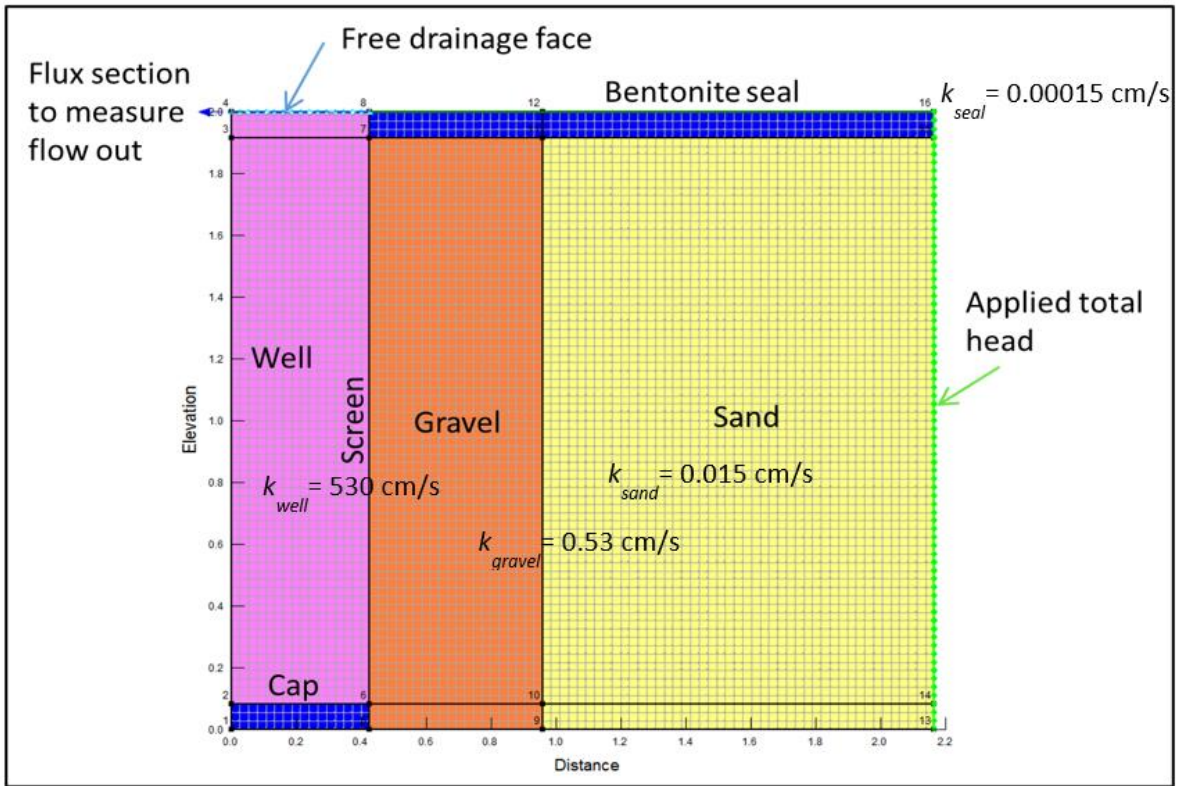


Figure K-7. Axisymmetric model mesh for Mitronovas (1968)

$Q_{well} = 8.65 \text{ gpm/ft}$ (versus 8.58 gpm/ft in lab)

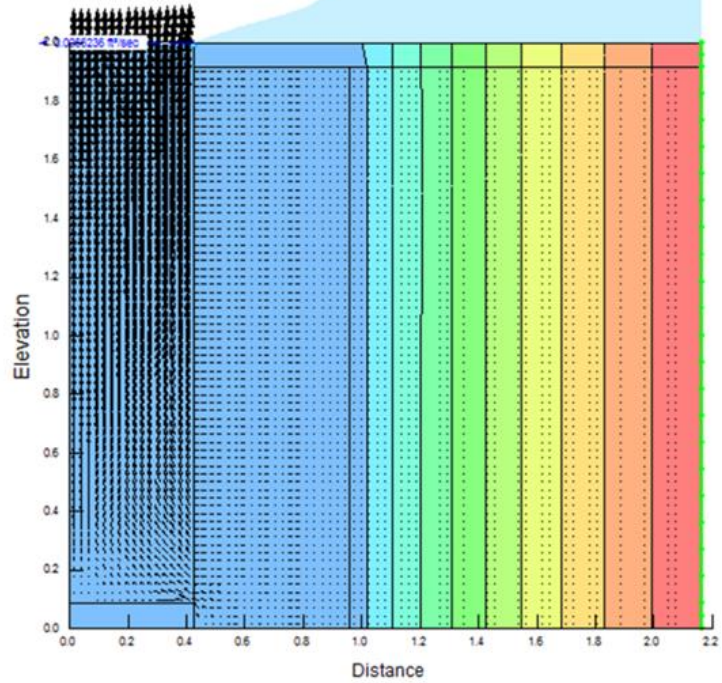


Figure K-8. Axisymmetric model results for Mitronovas (1968)

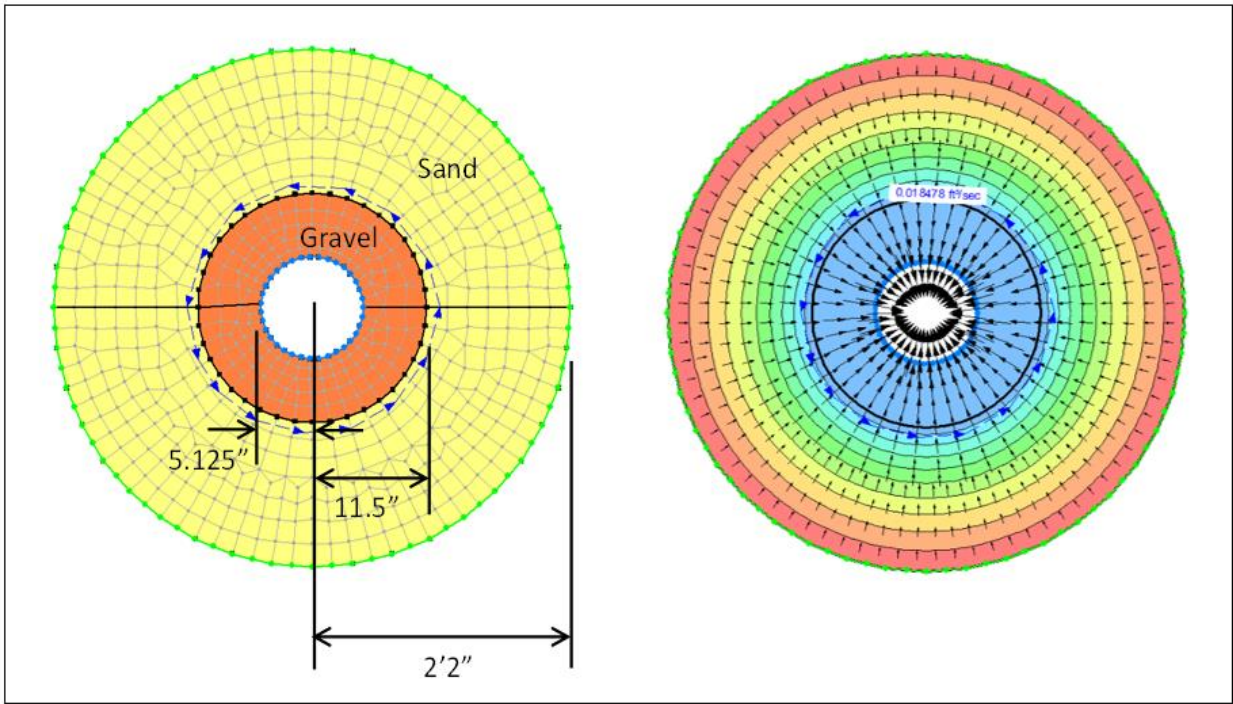


Figure K-9. Input and output of simple plan view model of Mitronovas (1968) Test 1

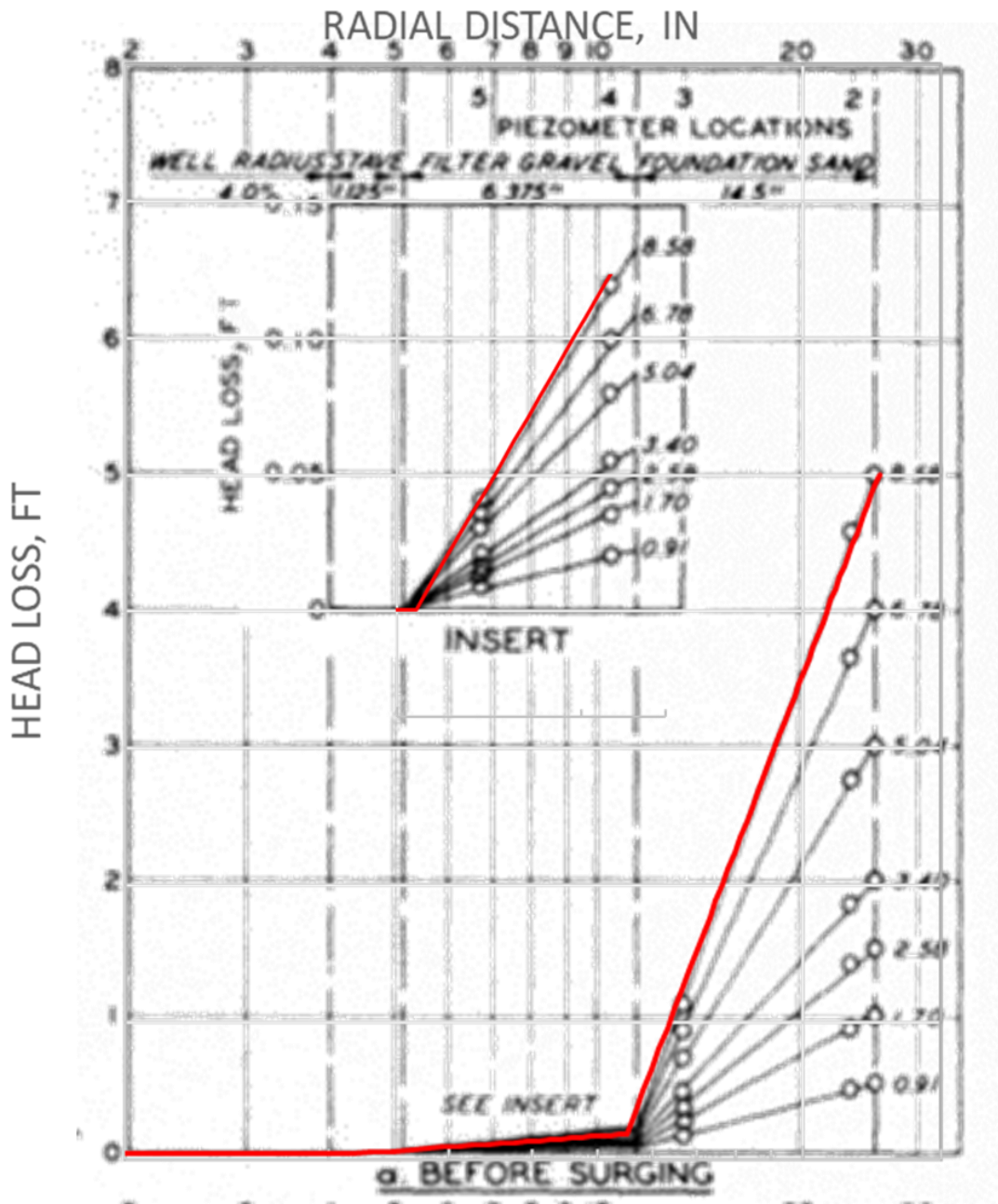


Figure K-10. SeepW results for the Mitronovas (1968) test plotted with lab results

d. The model created to match Mitronovas (1968) was adjusted to replicate tests performed in Hadj-Hamou et al. (1990). This required only minor changes in test dimensions and permeability of the sand. Unlike previous testing in the 1950s and 1960s, the Hadj-Hamou et al. (1990) authors did not estimate permeability for the filter. However, the filter gradation F1 in 1988 was nearly identical to the gradation of the Test 1 filter in 1968, and the same value was used in this model for the filter permeability.

e. Both axisymmetric and plan view FEM models result in the same flow as for the 1988 physical model. However, as shown in Figure K–11, there is significantly more head loss through the filter in these lab tests than the FEM modeling. This additional head loss in the filter is likely due to problems with the upper seal that allowed some flow to bypass the foundation sand. This illustrates the difficulty in performing these types of lab tests and that the clay seal used in the original testing was more effective.

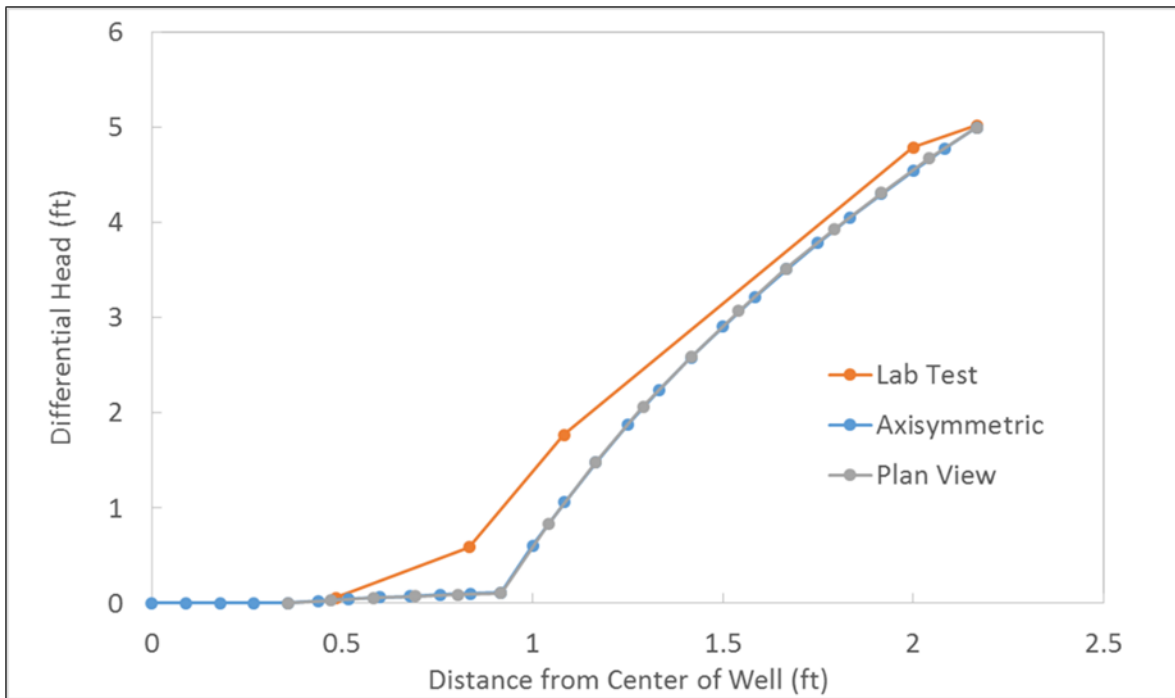


Figure K–11. SeepW results for the Hadj-Hamou et al. (1990) test plotted with lab results

K–6. Axisymmetric model including slots through the screen

a. The axisymmetric model was adapted to include a low-permeability region that represents the screen in the physical tests and concentrates flow through widely spaced regions of high permeability that represent discrete slots. The relatively large horizontal slots in Figure K–12 are based on slot size (3/16-inch) and open area (8.6%) of the wood-stave well screen used in Mitronovas (1968). Displacement vectors in Figure K–13 help visualize flow through the gravel pack to the slot, and nodal values are shown for velocity through the slot ($v_{\text{slot}} = 0.087$ ft/s). Including the screen in the model reduces flow from 8.65 to 8.58 gpm/ft of screen. Figure K–13 includes four vertical, colored lines where nodal velocity values were recorded and plotted in Figure K–14.

b. The blue line, located 4.2 inches from the well screen, is not shown in Figure K–13 since it is beyond the portion of the mesh shown. Inspection of Figure K–13 and Figure K–14 reveals very high velocity in nodes near the slot, and a decrease in velocity values with increasing distance from the slot. Based on the average grain size of the filter of 2.5 mm, Figure K–15 shows that flow is turbulent where velocity is greater than 0.5 cm/second and laminar where velocity is below 0.04 cm/second. At velocities

between 0.04 cm/second and 0.5 cm/second, flow is transitional between laminar and turbulent.

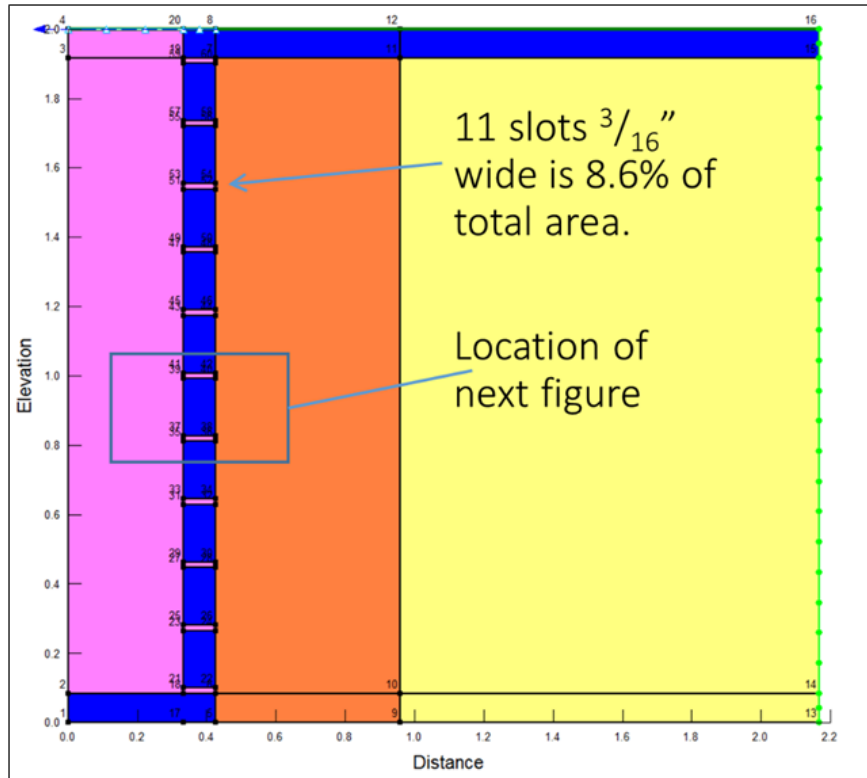


Figure K-12. Axisymmetric SeepW model with discrete slots through a low permeability screen

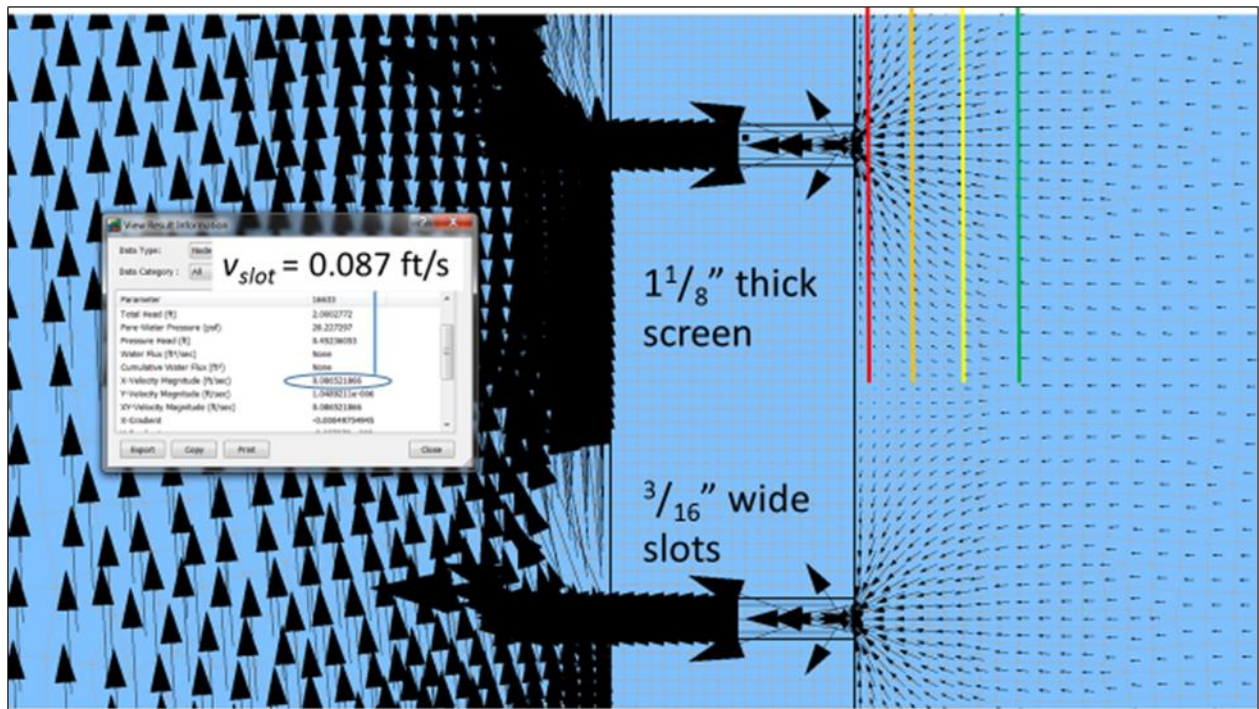


Figure K-13. Axisymmetric SeepW model with discrete slots through a low permeability screen, increased detail

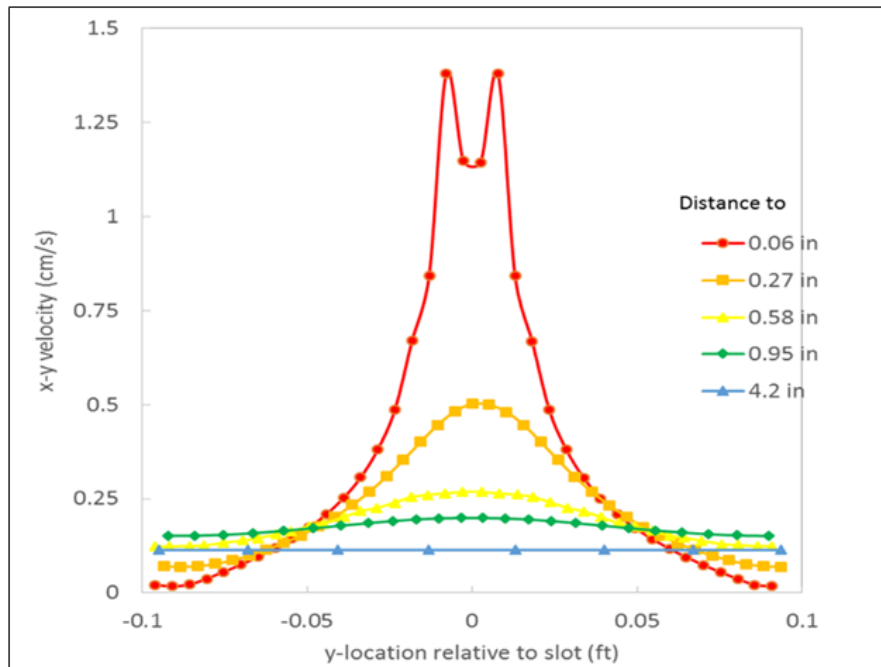


Figure K-14. Nodal velocity measured along five vertical lines outside of screen slot

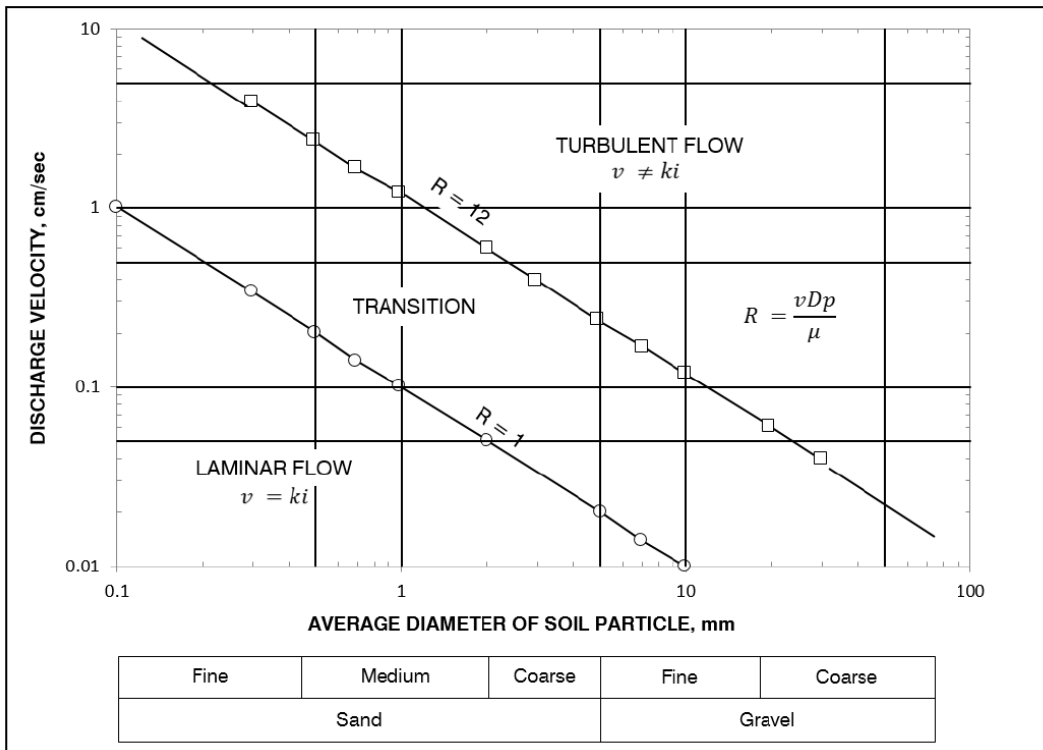


Figure K-15. Approximation for estimating reduction in permeability for turbulent flow (adapted from EM 1110-2-1901)

c. Cedergren (1989) accounts for turbulent flow with a reduction in soil permeability based on average soil particle size and gradient. Figure K-16, similar to Figure K-14, shows gradient recorded from nodes along the colored lines in Figure K-13. Nodal gradient values are very high near the slot and decrease away from the slot. The approximation in Figure K-17 could be used with this nodal gradient information to decrease permeability values used in portions of the filter in the FEM model to include the effect of turbulence. This approach was used to adjust filter permeability in regions adjacent to slots in the plan view model in paragraph K-7.

d. The plan view model presented in paragraph K-7 provides a more accurate depiction for vertical slots than the axisymmetric model in this section. Axisymmetric modeling lends itself to modeling screens with horizontal slots such as stainless-steel continuous-wire wrap, although the small slot size would require an extremely fine mesh. For investigations of flow into continuous-wire-wrapped screens, it would be more practical to model a very thin horizontal slice of the test rather than the full 2-foot height of the tank in the model here.

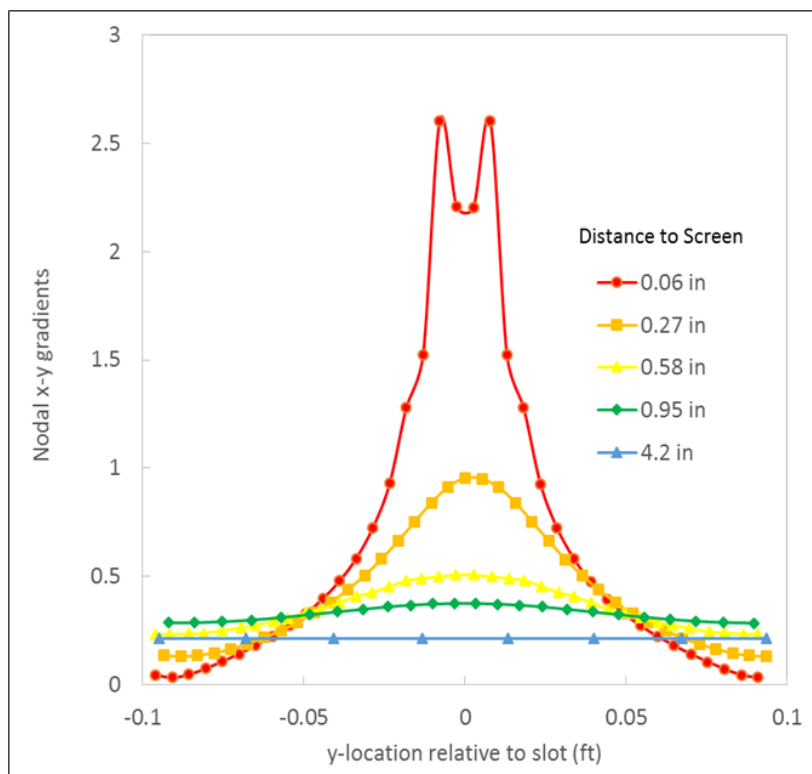


Figure K-16. Nodal gradient measured along five vertical lines outside of screen slot

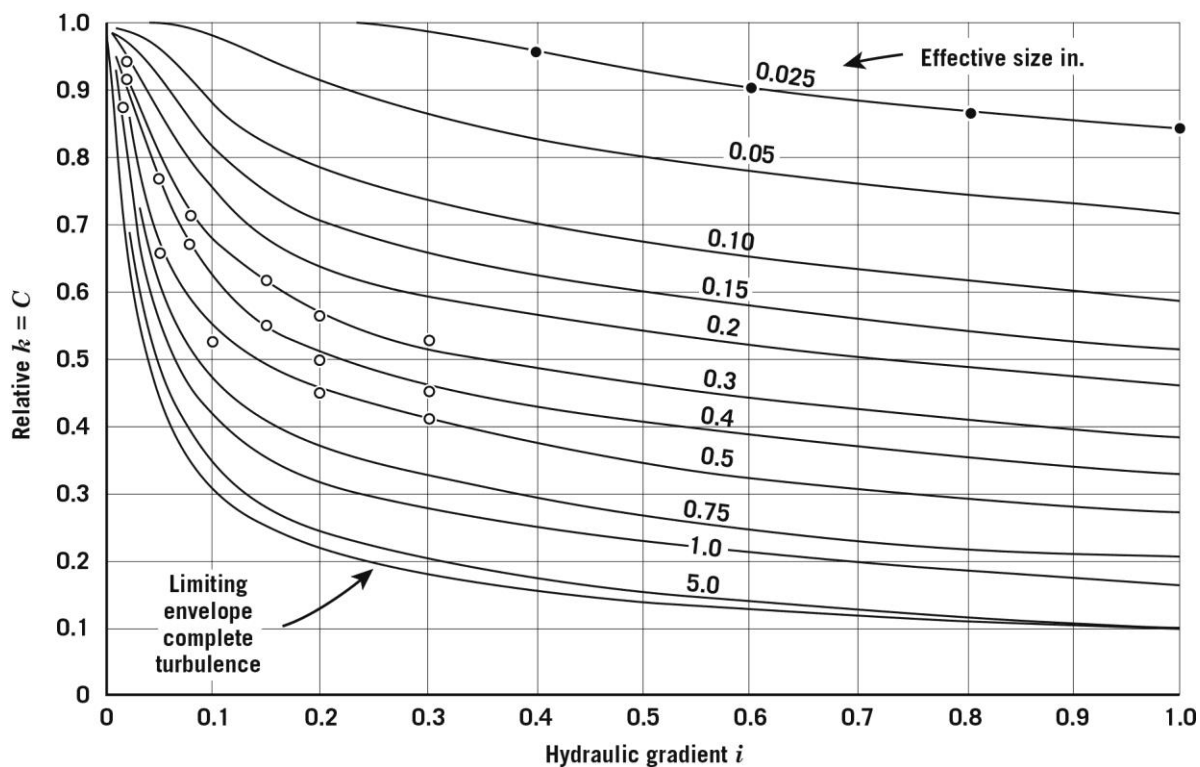


Figure K-17. Approximate reduction in permeability for turbulent flow (from EM 1110-2-1901)

K-7. Plan view model including slots through the screen

a. The plan view mesh was refined to include slots through a boundary that represents the physical wood-stave well screen as shown in Figure K-18. Plan view seepage models are well suited to model vertical slots, such as slots through wood-stave well screens.

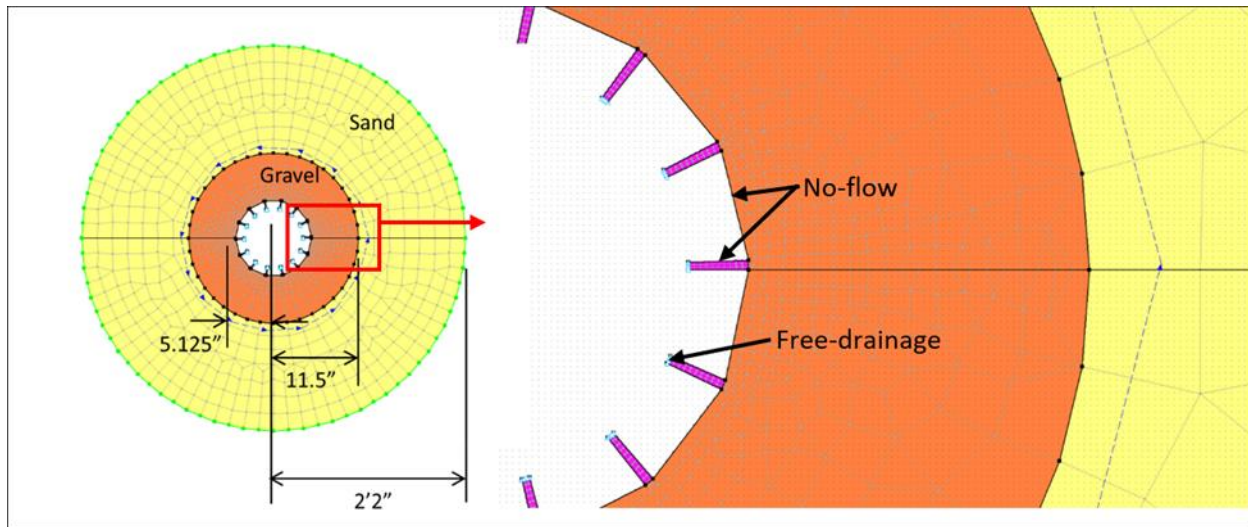


Figure K-18. Screen included in the model as a no-flow boundary, with free-drainage boundaries at every slot

b. Based on Figure 8-10 in EM 1110-2-1901 (included in this appendix as Figure K-18), a series of plan view models were created with reduced permeability, high gradients, and potentially turbulent flow. The d_{50} for the filter was set at about 0.10 inch. The results, shown in Figure K-19, show the average gradient adjacent to the slot is about 0.75 in the outer region, and about 2 in the inner region. The maximum gradient on the plot in Figure K-17 is 1.0 but extrapolating the 0.10-inch line to a gradient of 2 would indicate that permeability would be about one-third of the laminar value.

c. From Figure K-17, the permeability would be 63% of the laminar value for a gradient of 0.75 for an effective size of 0.10 inch. Given the original filter $k = 0.0174$ ft/sec (100%), the outer region k becomes 0.011 ft/s (63%), and the inner region k becomes 0.0058 ft/s (33%) due to turbulence. These permeability values are included in the model as shown in Figure K-20. Note that Figure K-17 is based on uniform sands, where the standard well filter modeled here is well graded.

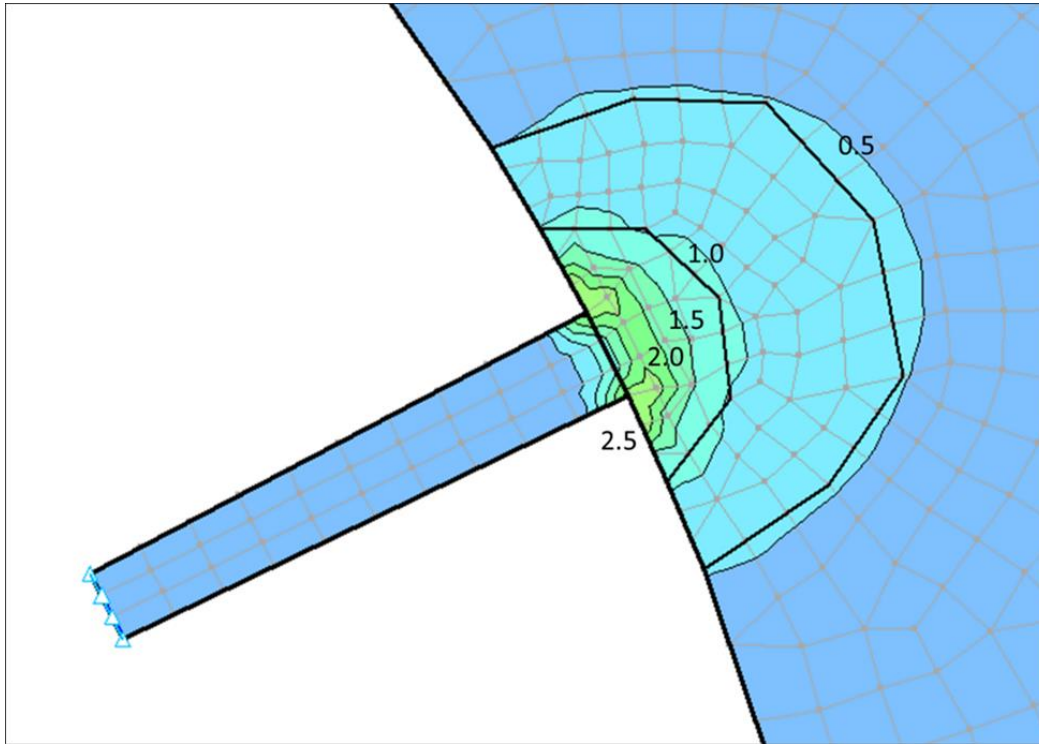


Figure K-19. Separate regions created along contours of high x-y gradient

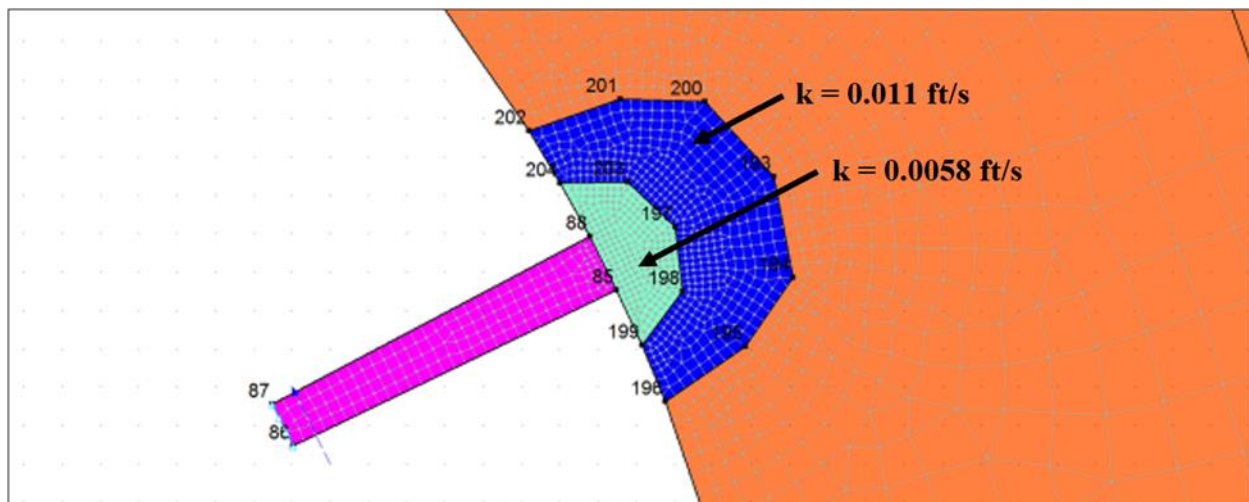


Figure K-20. Lower permeability assigned to regions around one of the slots

d. Two separate significant observations resulted from a series of models for this case: (1) the use of gradient to account for turbulence would need to be an iterative process of updating permeability based on gradient, solving to find the gradient in this region, and updating the permeability again; and (2) mesh refinement in the region around the slot has a significant effect on the quantity of flow through the slot. Increasing mesh refinement from 12 to 16 elements across the slot width resulted in a noticeable change in flow through the slot, even when modeling discrete slots in laminar

soils. The presumption is that mesh refinement would be more significant if turbulent flow warrants a reduction in permeability in the region around the slot.

K-8. Summary

a. The scope of any further lab testing performed on relief well screens and filters should be informed by tank tests that have been performed previously. Simple models as described in this appendix could also help determine the most useful lab tests. It is thought that head losses through the screen in the previous tests were measured by running the tank with the screen and no surrounding soil. This understanding is supported in Mitronovas (1968), which states screen losses are estimated using photos of screens to determine a percent of clogging and then are related to tests performed previously. Unfortunately, this approach would not account for head loss from the longer flow paths through the filter.

b. FEM model results match the tank test and can be used to investigate flow to wells through the filter and screen. The 1968 tests in particular are nearly identical to FEM results. However, if head loss does occur with flow through the filter to reach the slot, higher values of filter permeability may be needed in these models than the back-calculated value that did not account for flow to the slots. FEM models illustrate how turbulence described by Smith (1998–2015) would result in head loss. However, entrance losses are small in both the lab tests and recommended design values based on field pumping tests. The head loss due to turbulence outside the well screen appears to be negligible for typical relief well flow rates.

Glossary of Terms

Section I

List of Acronyms

Term	Definition
ABS	Acrylonitrile-Butadiene-Styrene
AEP	Annual Exceedance Probability
ASCE	American Society of Civil Engineers
ATR	Agency Technical Review
AWWA	American Water Well Association
BCHTTM	Blended Chemical-Heat Treatment
BEP	Backward Erosion Piping
BFA	Biodegradable Drilling Fluid Additives
BT	Blanket Theory
Cl ₂	Chlorine Gas
CL	Chlorides
CO ₂	Carbon Dioxide
CW-EB	Civil Works Engineer Bulletin
DA	Department of the Army
DEQ	Department of Environmental Equality
DIPP	Drilling and Invasive Program Plan
DIVR	Division Regulation
DNR	Department of Natural Resources
DOE	Department of Energy
DWSE	Design Water Surface Elevation
EC	Engineer Circular
EM	Engineer Manual
EPA	Environmental Protection Agency
ER	Engineer Regulation
ERDC	Engineer Research and Development Center
FC	Fort Chartres Levee District (Well Label)
FDM	Finite Difference Method
FEM	Finite Element Method
FOSM	First-Order Second-Moment
FS	Factor of Safety
H ₂ O ₂	Hydrogen peroxide
H ₂ S	Hydrogen Sulfide
HDPE	High-Density Polyethylene
HGL	Hydraulic Grade Line
HSA	Hollow-Stem Augers

Term	Definition
ID	Inner Diameter
IWM	Image Well Method
LLC	Limited Liability Company
LPE	Liquid Polymer Emulsion
LPE	Liquid Polymer Emulsion
LRH	Bolivar Dam Project in Huntingdon District
MDOH	Minnesota Department of Health
NSF	National Sanitation Foundation
OD	Outside Diameters
PDT	Project Development Team
PFD	Phosphate-Free Dispersant
PFM	Potential Failure Mode
PFMA	Potential Failure Mode Analysis
PI	Periodic Inspection
PVC	Polyvinyl Chloride
PZ	Piezometer
RMC	Risk Management Center
RST	Rossum Sand Tester
RW	Relief Well
SCR	Specific Capacity Ratio
STA	Station
TM	Technical Memorandum
U.S.	United States
UFC	United Facilities Criteria
URS	Ultimate Reengineering Services LLC
USACE	U.S. Army Corps of Engineers
USBR	U.S. Bureau of Reclamation
USDA	U.S. Department of Agriculture
USGS	United States Geological Survey
W/D	Well Penetration Ratio
WES	Waterways Experiment Station

Section II

Terms

Aquifer

The pervious foundation strata that provide a conduit for transmitting groundwater. In this manual, the aquifer is considered as confined with respect to all equations and methods.

Artesian

A permeable layer beneath a less-permeable layer that has excess head. Artesian conditions are necessary for relief wells to function.

Blanket

A low-permeability top strata, generally comprised of clays, silts, and fine sands, that overlies a more pervious layer.

Blanket Theory

A simple form of underseepage analysis where the foundation can be characterized as two layers: a pervious aquifer and an overlying blanket.

Excess head

The height above the surrounding ground surface that water will rise in a piezometer at a specific location.

Permeability

A measure of the ability of a porous material to allow fluids to pass through it. The permeability of a foundation is related to the soil porosity, the shape and size of the pores, and their interconnectivity.

Piezometer

As presented in this manual, a pipe with a screen near the bottom and open to atmosphere at the top. These devices are used to monitor piezometric head (see below) in the foundation layer. Open-standpipe piezometers, observation wells, and other types of piezometers are described in EM 1110-2-1908.

Piezometric head

The height above a datum that water will rise in a piezometer at a specific location.

Total head

From Bernoulli's Equation, the sum of the elevation head, velocity head, and pressure head. This is the same as piezometric head in this manual.

Waterside and landside

Waterside and landside delineate the two sides of a water-retaining structure. For levees, these have historically been called "flood side" and "protected side." "Upstream" and "downstream" are still used for dams, but these terms have a different meaning for riverine levees. Rivers flow from upstream to downstream.